KILOWATT ISOTOPE POWER SYSTEM PHASE II PLAN VOLUME II FLIGHT SYSTEM CONCEPTUAL DESIGN (FSCD)

KIPS

Sundstrand Energy Systems
ROCKFORD ILLINOIS 61101
A unit of Sundstrand Corporation

SUNDSTRAND

C00-4299-025

DISCLAIMER

KILOWATT ISOTOPE POWER SYSTEM

PHASE II PLAN

VOLUME II
FLIGHT SYSTEM CONCEPTUAL DESIGN (FSCD)

To

DEPARTMENT OF ENERGY

From

SUNDSTRAND ENERGY SYSTEMS
4747 HARRISON AVENUE
ROCKFORD, ILLINOIS 61101

NOTICE

"This document was prepared as an account of work sponsored by the United States Government. Neither the United States nor the United States Department of Energy nor any of their employees, nor any of their contractors, subcontractors, or their employees, make any warranty, express or implied, or assumes any legal liability or responsibility for the accuracy, completeness or usefulness of any information, apparatus, product or process disclosed, or represents that its use would not infringe privately-owned rights."

C00-4299-025
15 MARCH 1978

TABLE OF CONTENTS

LIST OF FIGURES

LIST OF TABLES

SECTION 2.0

FLIGHT SYSTEM CONCEPTUAL DESIGN

2.1 FOREWORD

This report was written to satisfy the requirement of Task 10.0 of the Statement of Work to Sundstrand Energy Systems under the Department of Energy Contract Number EN-77-C-02-4299. The report is contained in five volumes:

Volume I	–	Phase II Program Plan
Volume II	–	Flight System Conceptual Design (FSCD)
Volume III	–	Ground Demonstration System (GDS) FSCD vs. GDS Comparison Evaluation Criteria Comments
Volume IV	–	Teledyne FSCD and GDS
Volume V	–	Safety Quality Assurance Reliability

2.2 INTRODUCTION

This section describes the Kilowatt Isotope Power System (KIPS) Flight System Conceptual Design (FSCD). Included in this section are a background, a description of the flight system conceptual design, configuration of components, flight system performance, Ground Demonstration System test results, and advanced development tests.

2.3 BACKGROUND

The Flight System Conceptual Design (FSCD) is the result of several steps in the KIPS Phase I Program. Preliminary flight designs were created and reviewed with the Department of Energy. From the results of these designs a development system and major components were fabricated and tested. Test results and further analysis were used to refine the flight design and GDS hardware. The FSCD design is documented in this section. The GDS, which demonstrates the feasibility of the FSCD, is presented in Section 3.0 of this report.

2.4 DESCRIPTION OF FLIGHT SYSTEM CONCEPTUAL DESIGN CONFIGURATION

The KIPS Flight System Conceptual Design (FSCD) is illustrated in Figure 2.4-1.

The heat source assembly is located asymmetrically around the power conversion system and at the base of the radiator assembly which is mounted to the spacecraft bulkhead as shown in Figure 2.4-1.

The major subsystems are:

- Power Conversion System (PCS)
  - Combined Rotating Unit (CRU) - turbine, alternator, pump and bearings
  - Electrical and fluid controls
  - Regenerator and jet condenser
  - Filters, check valve, orifices
- Heat Source Assembly (HSA)
  - Heat source - MHW (plutonium oxide)
  - Boiler and auxiliary cooler
  - Emergency Heat Dump System (EHDS)
  - Structure/Insulation system
- Radiator Assembly (RA)
  - Radiator
  - Auxiliary cooler
  - Bypass valve

Key features of the KIPS design are radioisotope heat source assemblies, a supersonic axial impulse turbine, homopolar inductor alternator, centrifugal pump, working fluid (Dowtherm A – high purity eutectic of biphenyl and phenyl ether) lubricated fluid film bearings, once-through radiantly heated boiler, jet condenser, liquid working fluid pumped radiator, and electronic controller.

Figure 2.4-2 is a schematic of the KIPS. The KIPS uses an organic working fluid in a rankine thermodynamic cycle. It consists of two working circuits, the power loop and the heat rejection loop.

In the first loop, three radioisotope heat source assemblies provide energy to Dowtherm working fluid. This energy preheats and boils the fluid, creating a vapor which drives the turbine. The alternator, mounted directly on the turbine shaft, provides electrical power for the spacecraft. After the vapor leaves the turbine, it passes through a regenerator where the remaining superheat is used to preheat the liquid which is entering the heat source assemblies (boilers). The desuperheated vapor then passes through a condenser, changing to a liquid, and then to the pump, which pressurizes the liquid to the point necessary to complete the cycle.

In the heat rejection loop, a liquid circuit transfers the heat of condensation to the radiator, where the heat is rejected to space. This liquid then returns to the condenser, where the cold liquid

SYSTEM MECHANICAL ARRANGEMENT FLIGHT

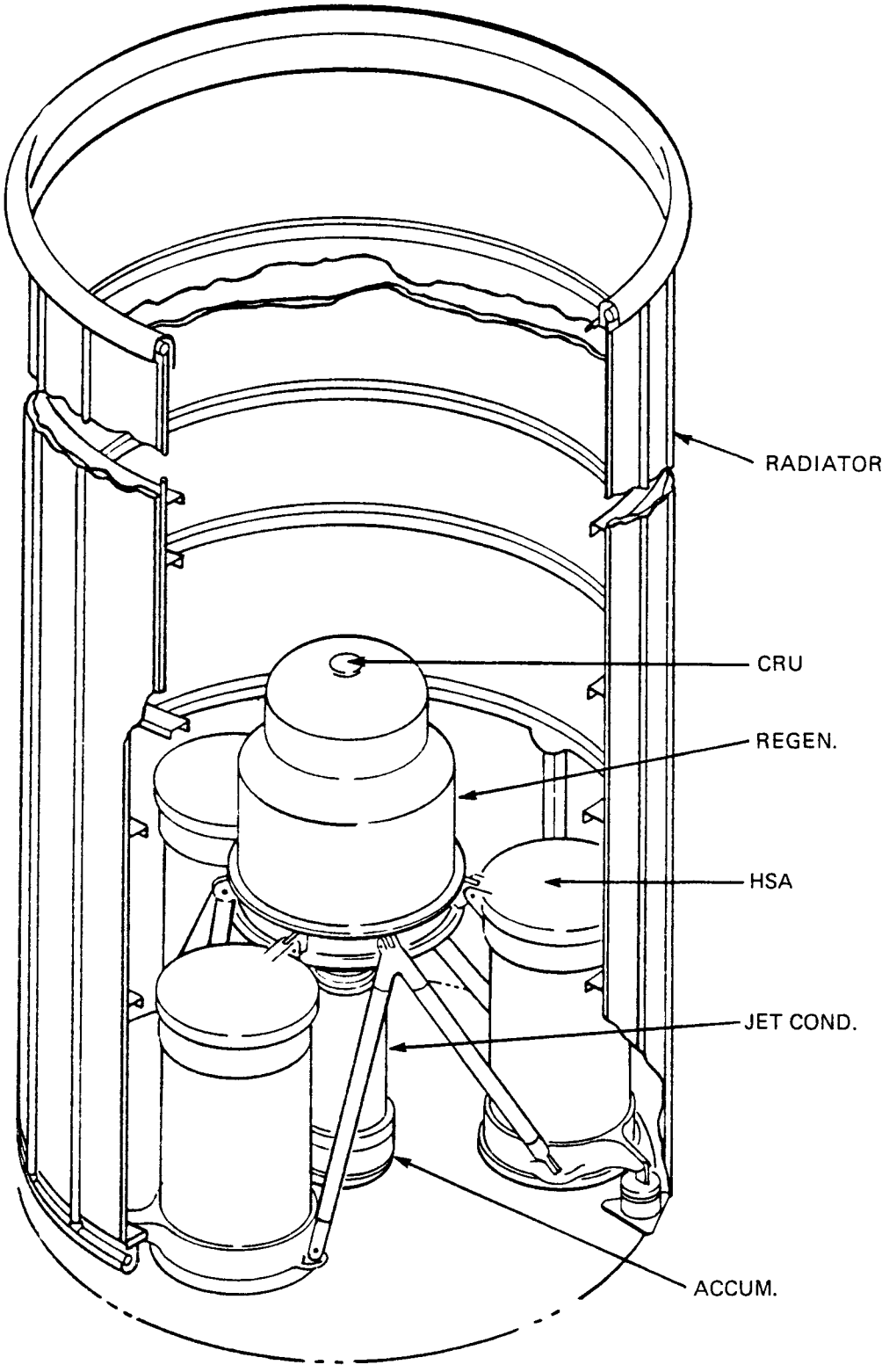

Figure 2.4-1 KIPS Baseline Flight System

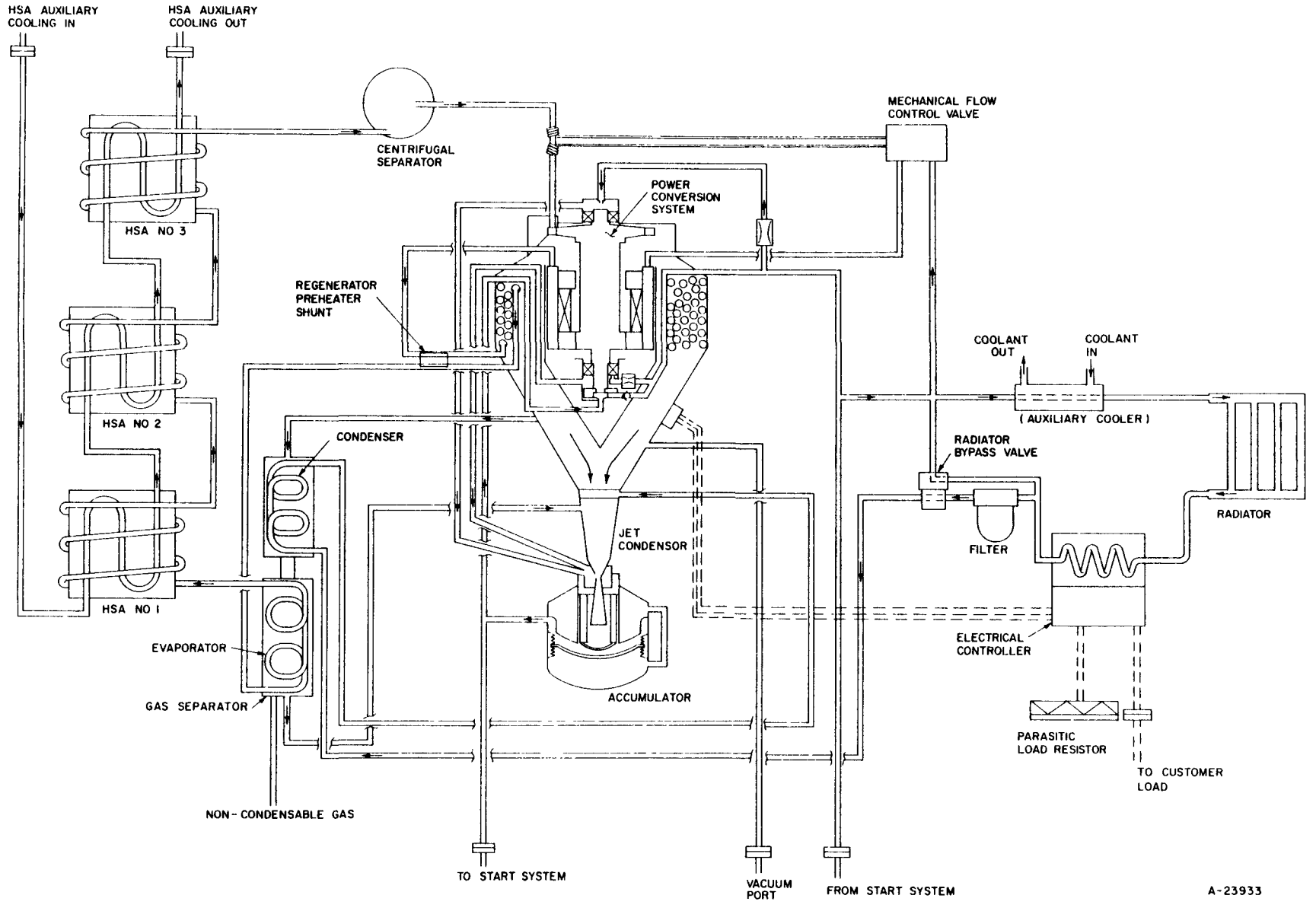

Figure 2.4-2 FSCD Schematic

provides the heat sink for the vapor condensation to take place in the jet condenser. The liquid of this circuit is mixed with the power loop fluid in the jet condenser before passing through the system pump.

The controls of the system are simple. A flow control valve maintains constant temperature at the turbine inlet as the radioisotope decays slightly over the seven year lifetime; a radiator bypass valve maintains a constant temperature of the liquid into the jet condenser as the spacecraft cycles from light to dark conditions in the space environment; the electronic controller provides voltage and speed controls as the electrical load demand on the KIPS is changed.

Three units of ground support equipment will be used. The start module is used to start the power system either for a ground start or a space start. The preferred mode of operation is a ground start. In this case, the start module would be disconnected prior to launch and the KIPS would be operating and producing partial power as required during launch and orbit transfer. The heater temperature control support module is used for cooling during the period between heat source assembly and power system startup. It is also used as emergency cooling for the heat source while the system is in the Space Shuttle. This cooling is supplied by a ground module for the Titan III and the launch vehicle for the Space Shuttle. The heat rejection support module is used for on the pad cooling prior to launch for Titan III applications and continuously while in the Shuttle bay. These support modules are decoupled after performing their function and are not part of the KIPS/Spacecraft system that is injected into operational orbit.

Figure 2.4-3 is a block diagram of the system illustrating typical operating conditions. As described above, the liquid outlet from the pump is split into two loops. The power loop passes liquid through the regenerator to extract energy from the turbine exhaust vapor. At the energy source, additional heat is transferred to the working fluid which is vaporized to drive the turbo-pump alternator. The cooling loop passes liquid flow through the radiator to reject waste heat and then to the jet condenser to condense the vapor emanating from the regenerator. The combined liquid is returned through the accumulator to the pump. As indicated in Figure 2.4-3 the organic Rankine cycle KIPS has a maximum power conversion system temperature of only 650°F which allows design with common materials as presented in this section.

Table 2.4-A is a summary of performance indicating the overall characteristics of the KIPS for the seven year life and five year mean mission duration. Total wet weight is 475 pounds. This system has not yet been fully weight optimized. The 450 pound goal is considered to be realistic for KIPS. A comprehensive weight reduction effort is planned for Phase II. For 1300 watts of electrical power at beginning of mission, the overall efficiency of the 28 VDC ± 2% system is 18.1%. Overall dimensions are 52" diameter by 96" long which is the result of optimizing the radiator as a function of liquid side delta P and weight. These dimensions can be changed to accommodate booster or spacecraft constraints. The KIPS is designed to be operating and generating power during launch, parking orbit and orbital transfer to final orbit.

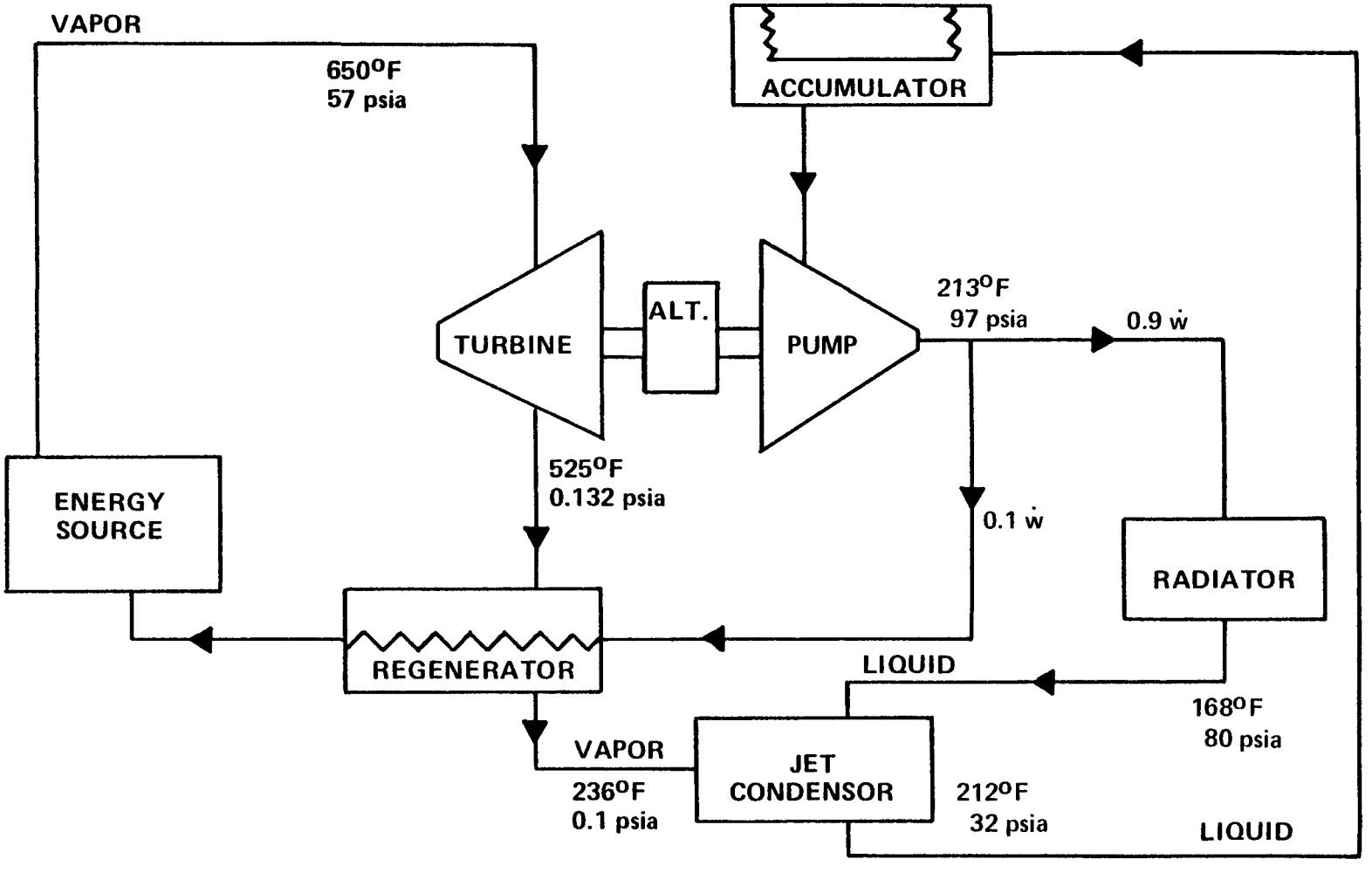

Figure 2.4-3 Typical Operating Conditions

Table 2.4-A KIPS Characteristics

Rated Output Power	1300W(e) BOM
Optional Ratings	500 to 2000W(e)
Input Power @1300W(e) BOM	7200(t)
Overall Thermal Efficiency (1)	18.1% rectified to 28 VDC
Peak Working Fluid Temperature	650°F
Total Weight(2)	475 pounds
Envelope Dimensions for 1300W(e) BOM(3)	52 inches Diameter 96 inches Length
Design Point Output Voltage	28 VDC ± 2%
Response - Variable Output Power - 0 to 100%	Milliseconds
Partial Output Power Capability	On Pad Launch to Parking Orbit Orbital Transfer to Final Orbit
Output Power Capability -0 to 100%	Spin Stabilized Spacecraft
Lifetime	7 years

Capable of Stable Operation with Unbalanced Solar Input

Resistant to Natural & Induced Radiation

(1) With RTG topping, system efficiency can be increased to 22.1% or higher. See Appendix A of Volume IV.

(2) Based on updated flight system design utilizing conventional materials, weight reductions such as alternate radiator configuration and CPU housing machining, to approach the 450 pound goal will be studied in the Phase II design phase.

(3) Flexible in design for both size and shape to fit the specific spacecraft.

2.5 CONFIGURATION OF COMPONENTS

The following paragraphs describe the individual subsystems and components of the FSCD. Appropriate discussions are included to describe trade-offs with alternate approaches, materials used, fabrication methods, stress and performance analysis approaches, and critical characteristics. Results of the development system component testing are included as necessary to explain the sizing and performance of these components and system.

2.5.1 HEAT GENERATION SYSTEM

Refer to Volume IV, Teledyne FSD and GDS, for a description of the heat generation system.

2.5.2 HEAT TRANSFER SYSTEM

2.5.2.1 Introduction

This section describes in detail the components necessary for energy absorption, regeneration and rejection by the system, the components required for transporting the working fluid around the system and the stability and compatibility of the selected working fluid with the components.

2.5.2.2 Summary

Thermal energy is absorbed by the KIPS in three boilers, one for each HSA. These boilers receive radiant energy in fin tube heat exchangers, which vaporize the liquid working fluid before passing to the turbine.

Superheat is removed from the turbine exhaust vapor in the regenerator and transferred to the liquid before it passes to the boiler. The amount of heat transferred in the regenerators is almost 50% of that absorbed in the boilers. The regenerator comprises a stack of helically wound finned tube bundles arranged in an overall counterflow configuration.

Vapor condensation takes place in the jet condenser. This is accomplished by accelerating the vapor stream and passing it over the surface of multiple, subcooled liquid jets emanating from a nozzle assembly. The liquid stream surface area is sufficient to condense all the vapor.

System heat is rejected from the jet condenser outlet liquid flow in a space radiator. This is a cylindrical fin-tube heat exchanger with multiple, parallel, axial, liquid tubes connected by headers.

The working fluid in the vapor phase is transported through ducting from the turbine to the regenerator, and regenerator to jet condenser. A transition bellows is located between the jet condenser vapor funnel and the liquid accumulator to compensate for differential expansion.

The complete system is covered with thermal insulation to minimize heat losses, both to improve system performance and to minimize thermal interaction with the spacecraft.

The selection of the working fluid is based upon satisfactory chemical stability, both thermally and radiolytically, for the total mission life with no adverse compatibility effects of the components with which it comes into contact.

2.5.2.3 Heat Transfer Fluid

The fluid selected for the KIPS was based on the following requirements:

Thermodynamic properties giving high efficiency, small system size, and low weight

High thermal stability

Low freezing point

Non-toxic

Non-flammable

Non-corrosive and compatible with materials commonly used in construction of power conversion equipment

While no single fluid is optimum for all the above requirements, Sundstrand's past experience and the broad data base available led to the selection of the eutectic mixture of biphenyl (23.5% by weight) and biphenyl-ether (73.5%) as the best available working fluid.

Some of the more important physical and transport properties of the fluid are presented in Tables 2.5.2-A and 2.5.2-B and in Figures 2.5.2-1 through 2.5.2-3.

2.5.2.4 Ducting, Bellows, Valves, Transitions

2.5.2.4.1 SYSTEM ACCUMULATOR

The system accumulator is located between the jet condenser and system pump. It provides a reference back pressure for the jet condenser and, hence, establishes the dynamic head recovery. It also provides adequate inlet head to the system pump.

During overspeed operation, the amount of fluid in the regenerator, radiator, vaporizer, and lines will be different than in steady state normal speed operation of the system. The accumulator accommodates this fluid inventory transfer among the system components by acting as an expansion compensator.

TRADE-OFFS: The following configurations were considered. A brief description of how each configuration would work follows.

Redundant Bellows (Figure 2.5.2-4): In this configuration two identical bellows are used. A partition is welded between the bellows to isolate the system fluid from the precharged gas. The space between the bellows OD and the housing ID is partially filled with system fluid. A small ullage space is left in this space to allow for thermal expansion of fluid. The ullage space is evacuated and sealed. The gas side is charged with a proper amount of nitrogen so that when the system attains steady state operation, the accumulator will set the required reference pressure at the jet condenser outlet and also hold the required amount of inventory. With this design, if the bottom bellows develops a crack, only a small amount of N_2 ends up on the ullage but the system continues operation without noticeable change in performance. If the top bellows develops a leak, a small amount of the working fluid ends up in the ullage space, but the system continues operation without noticeable change in performance. All other welds in this configuration are static joints.

Gas Filled: This configuration can be visualized by removing the lower bellows of the redundant bellows configuration. There is no buffer zone around the bellows between the charge pressure and system fluid. In normal operation this configuration would work in the same manner as the redundant bellows configuration. However, if the bellows develops a crack, the system fluid and charged gas would be able to interact and cause eventual system shutdown. The advantages that this configuration offers are that it is easier to fabricate and lighter.

Vented: This configuration is the same as the configuration described above except the gas filled side is vented to the low pressure zone of the system. The reference pressure needed is developed by compression of the bellows. In this design, if the bellows develops a small leak (0.002 diameter orifice), it can be fed back to the system and the system would continue operation. However, if the leak rate gets higher, there will be accumulation of fluid in the vented cavity and the system would

Table 2.5.2-A Physical Properties of Dowtherm A

Property	English Units	Metric Units
Atmospheric Boiling Point	494 8°F	257 1°C
Freezing Point	53 6 F	12 0°C
Flash Point, c o c	255°F	123 9 C
Fire Point, c o c	275°F	135 0 C
Auto Ignition Temp , A S T M	1150°F	621 1 C
Density at 75°F	66 0 lb /ft ^{3}	1 056 gm /cc @ 25°C
	8 82 lb /gal	
Volume Contraction Upon Freezing	6 63%	
Volume Expansion Upon Melting	7 10%	
Heat of Fusion	42 2 Btu/lb	23 4 Cal /gm
Specific Resistivity	1 2 x 10^{12} ohm cm @ 32°F	
	6 4 x 10^{11} ohm cm @ 68°F	
	3 9 x 10^{11} ohm cm @ 104°F	
Dielectric Constant at 75°F		
frequency 10^3	3 26	
frequency 10^4	3 27	
frequency 10^5	3 27	
Dissipation Factor at 75°F		
frequency 10^3	0 0012	
frequency 10^4	0 0001	
frequency 10^5	0 0001	
Dielectric Strength at 75°F	530 volts/mil	
Surface Tension in Air	40 1 Dynes/cm @ 68°F	
	37 6 Dynes/cm @ 104°F	
	35 7 Dynes/cm @ 140°F	
Critical Temperature	927°F	497°C
Critical Pressure	30 93 Atm	31 96 kg/cm^2
Critical Volume	0 0508 ft ^{3}/lb	3 17 cm ^{3}/gm
Heat of Combustion	14,000 Btu/lb	7,778 cal /gm

*c o c Cleveland open cup

Table 2.5.2-B Saturation Properties of Dowtherm A

TEMPERATURE		VAPOR PRESSURE		ENTHALPY			SPECIFIC HEAT	DENSITY		SPECIFIC GRAVITY
		Absolute	Gauge	Liquid	Latent	Vapor	Liquid	Liquid	Vapor	Liquid
°F	°C	lb /in ²	Vacuum in Hg	Btu/lb			Btu/(lb) (°F)	lb /ft ³		1/25°C
53 6	12 0	0 000	29 92	0 0	175 2	175 2	0 371	66 54	0 0000	1 069
60	15 6	0 000	29 92	2 4	174 4	176 8	0 374	66 37	0 0000	1 066
70	21 1	0 000	29 92	6 1	173 2	179 3	0 377	66 10	0 0000	1 062
80	26 7	0 001	29 92	9 9	172 0	181 9	0 381	65 82	0 0000	1 057
90	32 2	0 001	29 92	13 8	170 7	184 5	0 385	65 55	0 0000	1 053
100	37 8	0 001	29 92	17 6	169 6	187 2	0 388	65 27	0 0000	1 049
110	43 3	0 002	29 92	21 5	168 4	189 9	0 392	65 00	0 0001	1 044
120	48 9	0 003	29 92	25 5	167 2	192 7	0 396	64 72	0 0001	1 040
130	54 4	0 005	29 92	29 5	166 0	195 5	0 400	64 44	0 0001	1 035
140	60 0	0 007	29 91	33 5	164 9	198 4	0 403	64 16	0 0002	1 031
150	65 6	0 010	29 91	37 5	163 8	201 3	0 407	63 88	0 0003	1 026
160	71 1	0 014	29 90	41 6	162 7	204 3	0 411	63 60	0 0004	1 022
170	76 7	0 020	29 89	45 7	161 6	207 3	0 414	63 32	0 0005	1 017
180	82 2	0 027	29 87	49 9	160 4	210 3	0 418	63 03	0 0007	1 013
190	87 8	0 037	29 85	54 1	159 4	213 5	0 422	62 75	0 0009	1 008
200	93 3	0 051	29 83	58 3	158 3	216 6	0 426	62 46	0 0012	1 003
210	98 9	0 068	29 79	62 6	157 2	219 8	0 429	62 17	0 0016	0 999
220	104 4	0 091	29 74	66 9	156 2	223 1	0 433	61 88	0 0021	0 994
230	110 0	0 120	29 69	71 3	155 1	226 4	0 437	61 59	0 0027	0 990
240	115 6	0 16	29 60	75 7	154 0	229 7	0 440	61 30	0 0034	0 985
250	121 1	0 20	29 52	80 1	153 0	233 1	0 444	61 00	0 0044	0 980
260	126 7	0 26	29 40	84 5	152 0	236 5	0 448	60 71	0 0055	0 975
270	132 2	0 33	29 26	89 0	151 0	240 0	0 451	60 41	0 0069	0 971
280	137 8	0 41	29 09	93 6	149 9	243 5	0 455	60 11	0 0086	0 966
290	143 3	0 51	28 89	98 1	148 9	247 0	0 459	59 81	0 0106	0 961
300	148 9	0 63	28 65	102 7	147 9	250 6	0 463	59 50	0 0129	0 956
310	154 4	0 78	28 34	107 4	146 8	254 2	0 466	59 20	0 0157	0 951
320	160 0	0 96	27 97	112 1	145 8	257 9	0 470	58 89	0 0191	0 946
330	165 6	1 17	27 55	116 8	144 8	261 6	0 474	58 59	0 0229	0 941
340	171 1	1 41	27 06	121 5	143 8	265 3	0 477	58 28	0 0274	0 936
350	176 7	1 70	26 47	126 3	142 8	269 1	0 481	57 96	0 0326	0 931
360	182 2	2 03	25 80	131 2	141 7	272 9	0 485	57 65	0 0385	0 926
370	187 8	2 42	25 00	136 0	140 8	276 8	0 488	57 33	0 0454	0 921
380	193 3	2 86	24 11	140 9	139 8	280 7	0 492	57 02	0 0532	0 916
390	198 9	3 37	23 07	145 9	138 7	284 6	0 496	56 70	0 0620	0 911
400	204 4	3 96	21 87	150 9	137 6	288 5	0 500	56 37	0 0720	0 906
410	210 0	4 62	20 52	155 9	136 6	292 5	0 503	56 05	0 0833	0 901
420	215 6	5 37	19 00	160 9	135 6	296 5	0 507	55 72	0 0959	0 895
430	221 1	6 22	17 27	166 0	134 5	300 5	0 511	55 39	0 1100	0 890
440	226 7	7 18	15 31	171 1	133 5	304 6	0 514	55 06	0 1258	0 885
450	232 2	8 25	13 13	176 3	132 4	308 4	0 518	54 72	0 1432	0 879
460	237 8	9 44	10 71	181 5	131 3	312 8	0 522	54 38	0 1626	0 874
470	243 3	10 77	8 00	186 7	130 3	317 0	0 526	54 04	0 1840	0 868
480	248 9	12 24	5 01	192 0	129 1	321 1	0 529	53 70	0 2076	0 863
490	254 4	13 86	1 71	197 3	128 0	325 3	0 533	53 35	0 2335	0 857
494 8	**257 1**	**14 70**	**psig 0 00**	**199 9**	**127 4**	**327 3**	**0 535**	**53 18**	**0 2470**	**0 854**
500	260 0	15 65	0 95	202 7	126 9	329 5	0 537	53 00	0 2618	0 851
510	265 6	17 62	2 92	208 1	125 7	333 8	0 541	52 65	0 2929	0 846
520	271 1	19 78	5 08	213 5	124 5	338 0	0 545	52 29	0 3267	0 840
530	276 7	22 14	7 14	219 0	123 3	342 3	0 549	51 93	0 3636	0 834
540	282 2	24 71	10 01	224 5	122 1	346 6	0 554	51 56	0 4037	0 828
550	287 8	27 51	12 81	230 1	120 8	350 9	0 558	51 20	0 4472	0 823
560	293 3	30 55	15 85	235 7	119 5	355 3	0 562	50 82	0 4943	0 816
570	298 9	33 83	19 13	241 4	118 2	359 6	0 567	50 45	0 5452	0 811
580	304 4	37 38	22 68	247 1	116 9	364 0	0 571	50 06	0 6003	0 804
590	310 0	41 21	26 51	252 8	115 5	368 3	0 575	49 68	0 6597	0 798
600	315 6	45 34	30 64	258 6	114 1	372 7	0 579	49 29	0 7237	0 792
610	321 1	49 76	35 06	264 4	112 7	377 1	0 582	48 89	0 7926	0 785
620	326 7	54 51	39 81	270 2	111 3	381 5	0 586	48 49	0 8667	0 779
630	332 2	59 59	44 89	276 1	109 8	385 9	0 589	48 08	0 9464	0 772
640	337 8	65 03	50 33	282 0	108 3	390 4	0 593	47 67	1 032	0 766
650	343 3	70 82	56 12	288 0	106 8	394 8	0 596	47 25	1 124	0 759
660	348 9	77 00	62 30	294 0	105 2	399 2	0 599	46 82	1 223	0 752
670	354 4	83 57	68 87	300 0	103 6	403 7	0 602	46 38	1 328	0 745
680	360 0	90 56	75 86	306 1	102 0	408 1	0 605	45 94	1 442	0 738
690	365 6	97 97	83 27	312 2	100 3	412 5	0 608	45 49	1 564	0 731
700	371 1	105 8	91 10	318 3	98 6	416 9	0 611	45 03	1 695	0 723
710	376 7	114 2	99 50	324 5	96 8	421 3	0 615	44 56	1 836	0 716
720	382 2	123 0	108 30	330 7	95 0	425 8	0 619	44 08	1 988	0 708
730	387 8	132 3	117 60	337 0	93 1	430 2	0 623	43 59	2 151	0 700
740	393 3	142 1	127 40	343 4	91 2	434 6	0 628	43 09	2 327	0 692
750	398 9	152 5	137 80	349 7	89 2	438 9	0 633	42 57	2 517	0 684
760	404 4	163 4	148 70	356 2	87 1	443 3	0 640	42 04	2 723	0 675
770	410 0	174 9	160 20	362 7	84 9	447 6	0 647	41 49	2 946	0 667
780	415 6	187 1	172 40	369 3	82 6	451 8	0 655	40 93	3 190	0 658
790	421 1	199 8	185 10	375 9	80 1	456 0	0 664	40 34	3 456	0 648
800	426 7	213 3	198 60	382 7	77 6	460 2	0 675	39 74	3 749	0 638

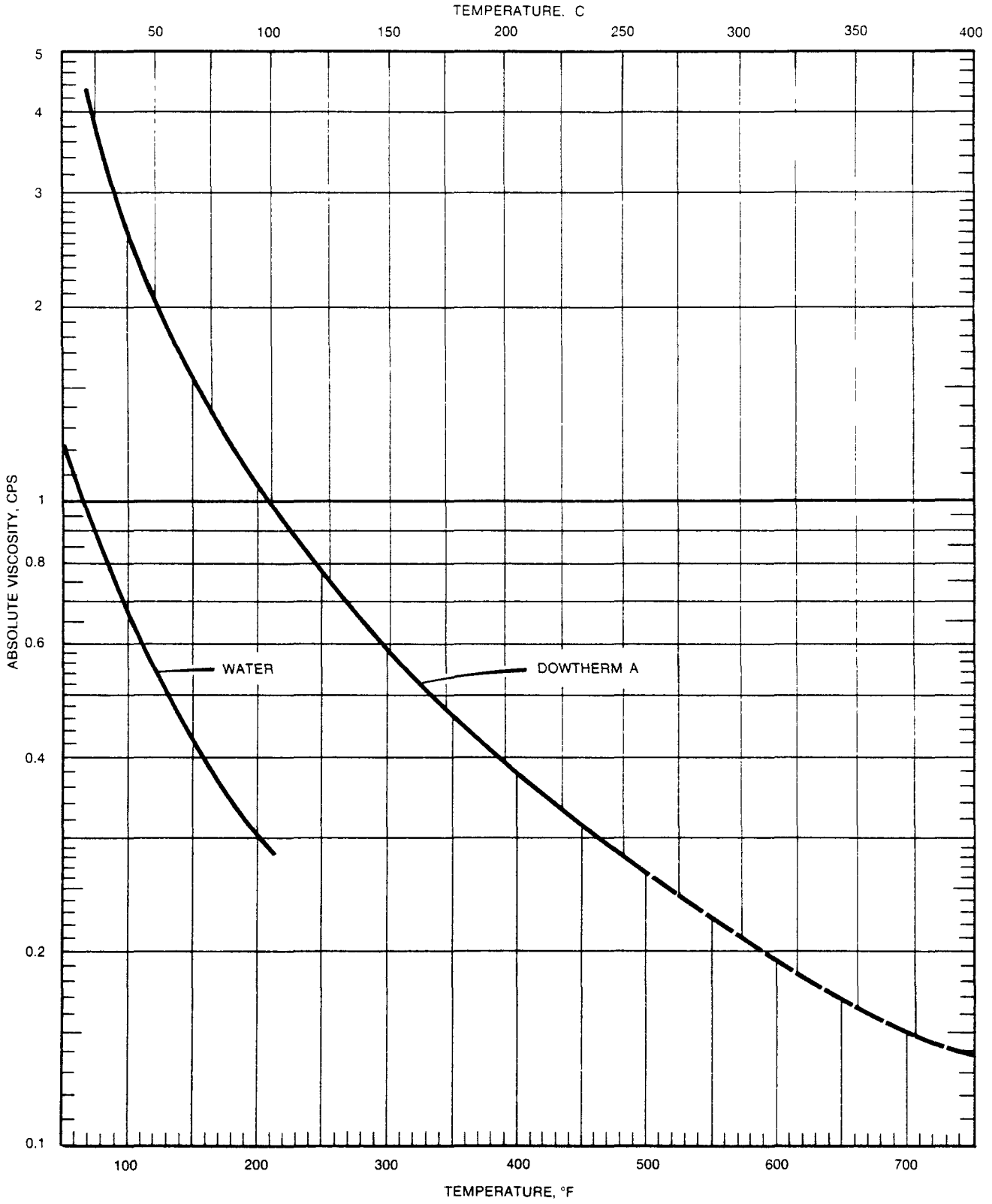

Figure 2.5.2-1 Liquid Viscosity of Dowtherm A

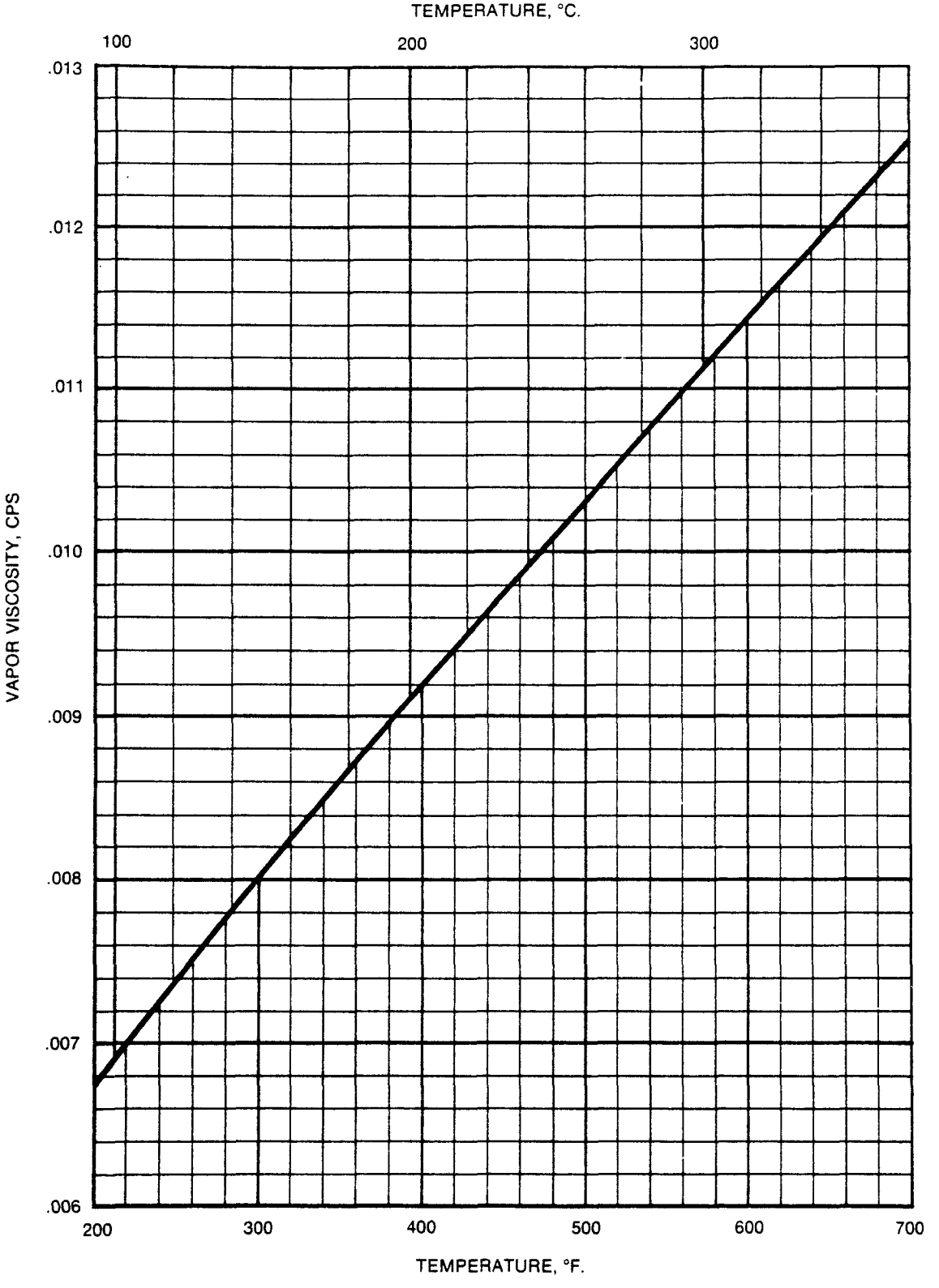

Figure 2.5.2-2 Vapor Viscosity of Dowtherm A

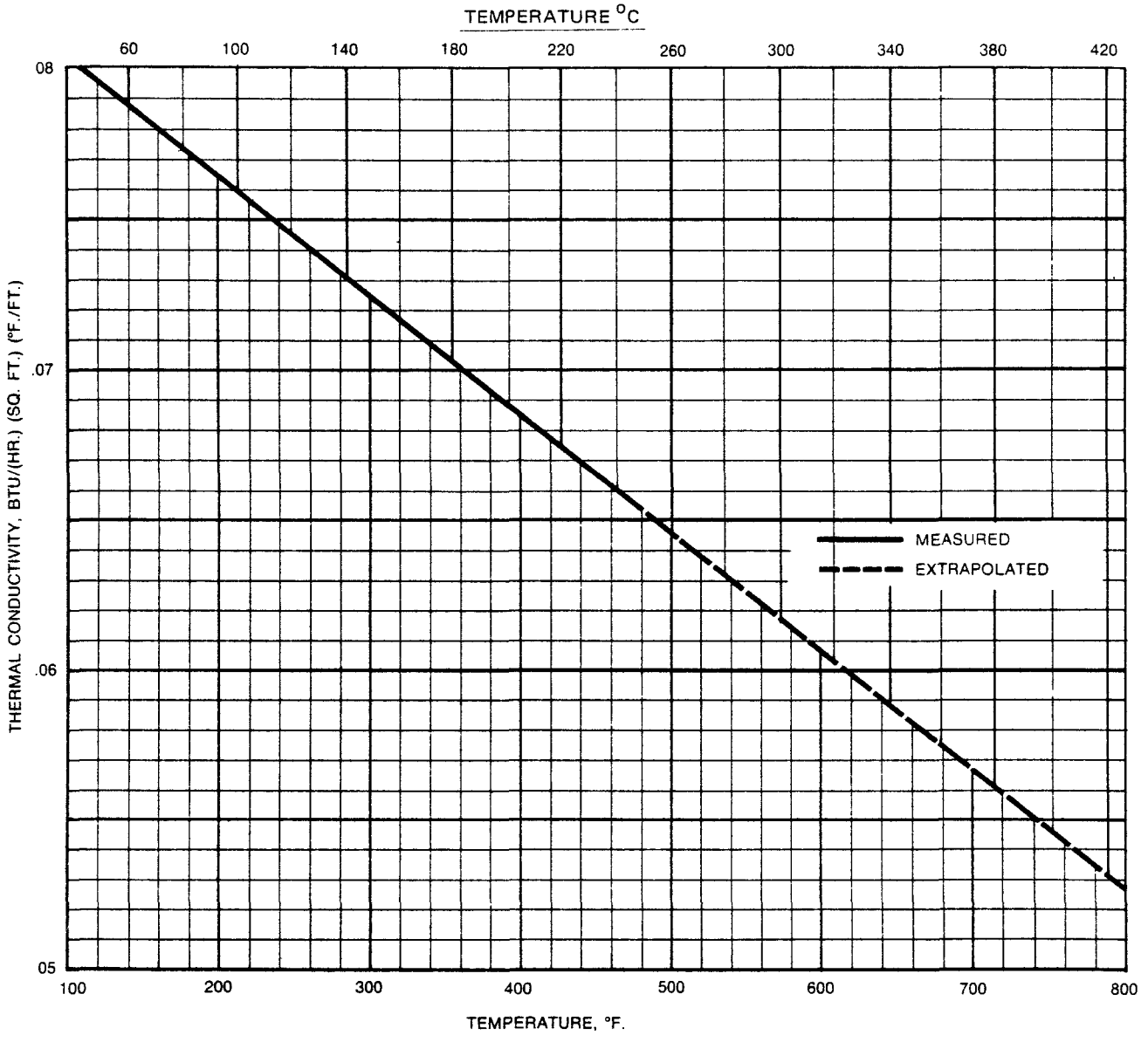

Figure 2.5.2-3 Liquid Conductivity of Dowtherm A

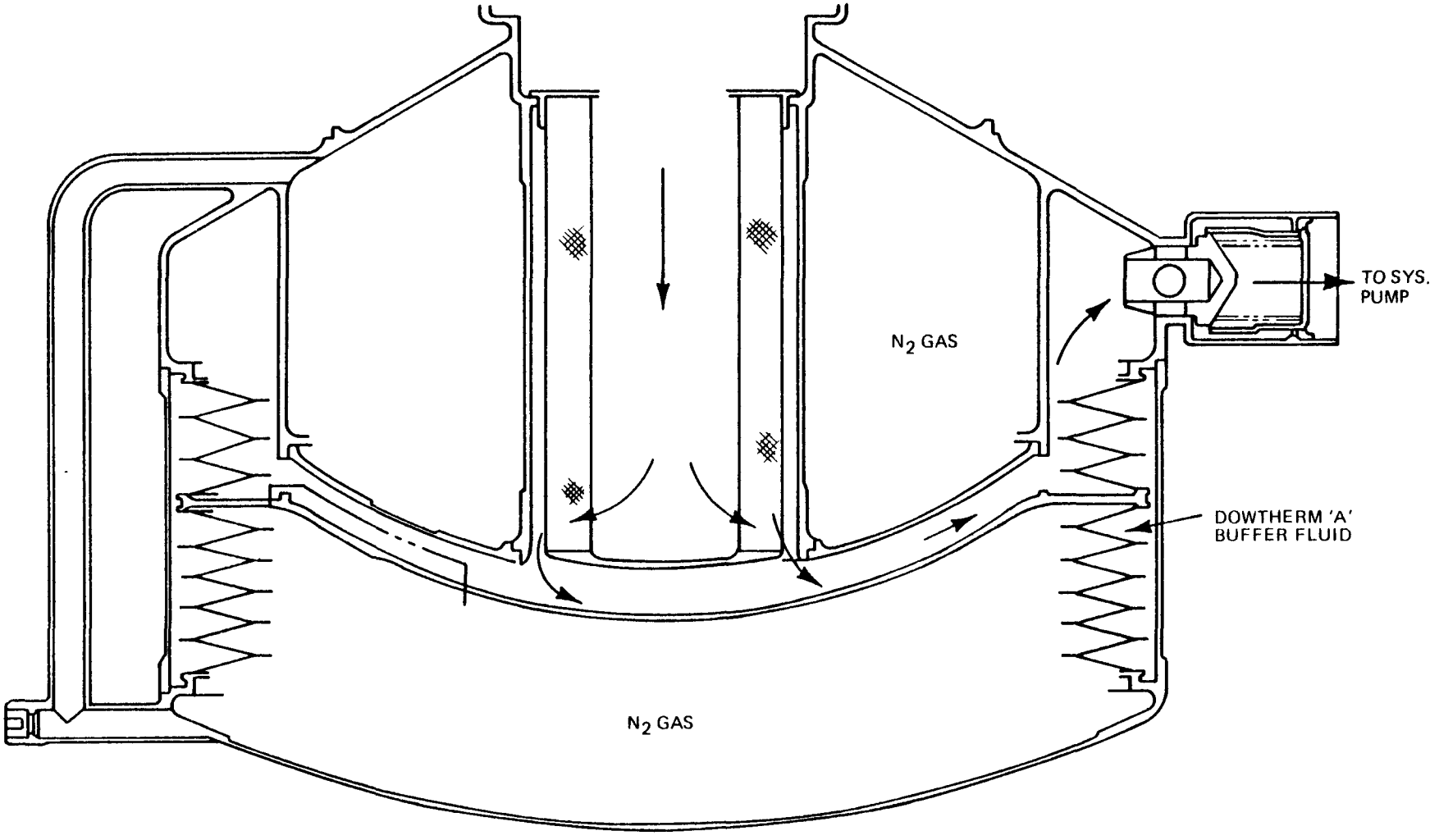

Figure 2.5.2-4 Redundandt Bellows Configuration

eventually shut down. Using the bellows as a spring to set the reference pressure results in a long stroke and thicker laminations. The vent connection would require two additional penetrations in the system.

Two Bellows: This configuration consists of two bellows of different effective area. The jet condenser inlet pressure is supplied to a small area to develop the force needed to set the jet condenser out pressure which is being exerted on the OD of the external bellows. Thus, in this configuration, all the force required to resist the jet condenser out pressure does not have to be developed by making the bellows stiffer. Also in this configuration during an overspeed operation (launch condition) since the jet condenser inlet pressure will rise, the accumulator pressure will rise proportionally. This means the pump size can be smaller and bearings can be lubricated from the pump inlet. The net effect is less power consumption for the pump. The disadvantages of this configuration are that the higher accumulator pressure during overspeed means high jet condenser recovery and this is undesirable for launch acceleration and vibration conditions. This configuration would require more penetrations. If the bellows develops a leak, the effect of leakage would be the same as for the vented configuration.

Valved: This configuration consists of a bellows similar to the gas filled configuration for taking up volumetric changes in the system and a second spring loaded bellows used to set the reference pressure for the jet condenser outlet. Both bellows' cavities are vented to a low pressure zone in the system. The advantage this configuration offers is that the volume compensating bellows does not set the reference pressure and so could be as light as the gas filled configuration bellows. This configuration, like the vented configuration, can handle a small leak through the bellows. The disadvantages are that this configuration needs additional penetrations like the two bellows configuration. Also there is continuous flow through the valve which is attached to spring loaded bellows and has to be drained through the bearing scavenge.

Others Considered: Piston, elastomeric bladder, and metallic bladder type of configurations were also considered. These configurations were rejected because of either limited life or excessive leakage limitations.

All configurations described in the previous paragraphs were considered for the following aspects:

Reliability and Safety: The redundant bellows configuration allows system operation with failure of one of the bellows. The gas filled bellows has the lowest ΔP across the bellows but a bellows failure would cause system shutdown.

Performance: During launch accelerations, it is desirable to have higher bearing flow. With the two bellows configuration this can be achieved by lubricating the bearings from the pump inlet and, thus, save on pump work. All other configurations require bearing lubrication to be done from the pump outlet to achieve higher bearing flow during overspeed (launch condition).

Risk: Construction of all bellows configurations is within the present state-of-the-art. However, redundant bellows configuration can operate with one bellows failure.

Weight: Since the ΔP across the gas filled bellows is the lowest, it would result in the lightest configuration. The valved configuration would result in the next lightest configuration while the vented configuration would be the heaviest.

Producibility: All configurations considered are producible with state-of-the-art manufacturing procedures.

Design Operation Flexibility: The redundant and gas filled configurations provide flexibility in design. The jet condenser recovery can be changed very easily without changing the fluid inventory in the system by varying gas charge pressure. The jet condenser outlet pressure in the valved configuration can be changed by changing the preload on one of the bellows. All 3 of these configurations can be used for multipower level systems. For a given bellows assembly, the jet condenser recovery can be changed only by changing system fluid inventory for the vented and two bellows configuration.

Based on this rationale, the redundant bellows configuration was selected for the FSCD.

ACCUMULATOR SIZING

Since the FSCD has a noncondensible gas removal device, the amount of fluid in the accumulator has to be just enough to provide a reference to the jet condenser at all times. It is not required to serve as a liquid reservoir to minimize the concentration of noncondensible gases. In the event that the bellows between the system fluid and ullage space failed, $\approx$ 2.2 cubic inches of system fluid will enter the ullage space. The accumulator displaceable fluid at normal operating condition is 7.2 cubic inches and thus provides a safety margin of greater than 2.

An inventory summary of the system fluid in various parts of the loop during normal speed and overspeed has been calculated (Table 2.5.2-C). This number may change slightly after all the inventory in interconnecting plumbing is estimated. Based on this table, it can be seen that during an overspeed, the system fluid will require 5 cubic inches of additional space which will be provided by compression of the bellows inside the accumulator. In the design of the accumulator, provision has been made to accept 15 cubic inches volumetric displacement and thus provide a safety factor of 2.

SYSTEM FILTER SIZING

In order to minimize system weight, this filter element is located in the accumulator, thereby eliminating a separate filter housing.

The function of the filter is to remove particles of sufficient size to score the bearing surfaces. During launch conditions, the minimum bearing film thickness is calculated to be approximately 0.00017 inch. The inner diameter of the bearing pads is plated with 0.0004 minimum silver plating thickness, hence, the absolute filtration level of retaining all particles larger than 0.00057 inch (14 microns) is desirable. The filter selected has a nominal rating of 2 microns and absolute rating of 10 microns. The filter area is equivalent to the AN6235-3A element (6 gpm) so at normal operating conditions, the pressure drop through the filter is low, as system flow is 2.28 gpm.

A 6 KW Sundstrand system was tested for more than 3000 hours and all hardware was visually inspected after termination of testing. No corrosion or erosion was observed in these areas and no evidence of particulate matter in the filter was apparent. The filter used had a nominal rating of 0.5 micron and absolute rating of 3 micron. Based on this experience, it is felt that no filter bypass is necessary.

RELIABILITY, STRESS, MARGIN OF SAFETY

The accumulator housings have been stressed to ensure that their failure probabilities are less than 1×10^{-9}.

Table 2.5.2-C Inventory Summary

COMPONENT	DESIGN	OVERSPEED
Boiler & Conn. Tubes	.927	.908
Regen to Boiler	.274	.263
Regen	3.766	3.687
Alternator to Regen.	.028	.028
Alternator	.334	.329
FCV to Alternator	.056	.055
Pump to Radiator	.750	.741
Radiator	1.956	1.931
Radiator to JC	.645	.636
Bypass Valve	.942	.929
Acc. to Pump	.468	.463
	10.146 LBS	9.970 LBS
Accumulator	.716 LBS	.892 LBS
Total	10.862 LBS	10.862 LBS
Accumulator Vol. (cu. in.)	20	25

It is our intention to procure the bellows assembly from Metal Bellows Corporation, who fabricated the GDS bellows and who has built many other bellows assemblies for space applications. The requirements for the bellows assembly will be as follows, with failure probability of less than 1×10^{-9}.

Number of full expulsion cycles = 20
(Estimated total number of starts)

Number of partial cycles = 2500 (once a day for 7 years)

Proof pressure = 60 psid minimum (1.5 x maximum accumulator pressure)

Burst pressure = 80 psid minimum (2.0 x maximum accumulator pressure)

Tables 2.5.2-D and 2.5.2-E show the materials being used in the accumulator and critical characteristics, respectively.

Table 2.5.2-D Materials

Item	Material
Accumulator Housing	AMS 5511, 5647 (304L)
Bellows Laminations	AMS 5548 (AM 350)
Remaining Parts of Bellows Assembly	AMS 5511, 5647 (304L)
System Filter	304 Stainless Steel
Check Valve	See para 2.5.2.4

Table 2.5.2-E Critical Characteristics

Characteristic	Location	Value	Comment
Filtration	System filter	2 μ nominal 10 μ absolute	Protects bearings. The largest particle allowed is smaller than minimum film thickness and plating thickness.
Material Conditions	Bellows assembly. Bellows heat treatment	SCT 1000	This affects the cycle life of the bellows.
Leakage	Complete assembly	1×10^{-8} SCC/Sec helium at 1 atmos.	Air leakage into the system would cause jets in jet condenser to defocus and cause floodout. Also, more tarry substance will be generated in vaporizer.

The accumulator assembly will be constructed as shown in Figure 2.5.2-4. The shell will be fabricated from 304L stainless steel and EB welded. All welds in the shell will be penetrant inspected and either ultrasonic or X-ray inspected. Some of the welds that are internal in the final assembly will also be helium leak tested prior to completion of final assembly. The weld between the filter and housing will not be ultrasonic or penetrant inspected to eliminate any possible contaminants from being trapped in filter mesh.

The bellows diaphragms after welding will be heat treated to SCT 1000 condition. The verification of the bellows joint will be done by metallurgical examination of the weld samples prior to and after completion of welding the actual part. This is an accepted practice in the bellows industry. To date, no other means of bellows weld inspection is available. Sandia Labs feel that the eddy current method may work but would need development.

Some samples from the GDS bellows were submitted to Oak Ridge and Sandia. After examining the configuration they concurred that the weld sampling process is acceptable.

Sandia Labs has procured several thousand welded bellows assemblies from the same vendor's plant

in Sharon, Massachusetts, using a tight material specification for AM-350. They destructive tested some of the bellows from a production run. To date this procedure has ensured satisfactory parts, as no failures of the bellows assemblies have occurred in the field.

In lieu of this NDT examination upon completion of assembly, it will be subjected to proof pressure test, helium leak test, limited cycle test, and another helium leak test. Development of the eddy current method may also be pursued for the FSCD as an added inspection tool.

2.5.2.4.2 CHECK VALVES

The FSCD has two check valves. Their function is to allow system startup with the use of a start module. Once the system is in operation, the check valves remain open.

TRADE-OFFS: The four configurations listed below were considered for this application (see Figure 2.5.2-5):

1. Ball type
2. Kepner cartridge
3. Circle seal C-200 cartridge
4. Circle seal C-2900 cartridge

Sundstrand has built and tested ball type check valves for various turbine systems. The valves were used in 1200°F gas lines and performed well. However, for liquid flow application, the design is not suitable since it requires a high reverse flow to close the valve. Because of this, ball type valves were rejected from further consideration.

In Configurations 3 and 4, the flow path is such that any contaminants will be washed out while in Configuration 2 it can be trapped and cause poppet hang-up.

Because of the type of design, Configurations 3 and 4 are able to close with low delta P in the reverse direction (2-4" of water). This is a desirable feature of check valves. Configuration 2 takes a higher delta P to move the poppet to the closed position.

Configuration 2 takes higher flow in reverse direction to close. Configuration 4 closes with low flow in the reverse direction, but once closed, surface tension holds it closed so a problem may occur when draining the system for a restart. Configuration 3 also closes with a low flow in the reverse direction but the construction is such that the system may be drained satisfactorily.

Configuration 3 has been used by the Air Force without a spring and is also being qualified for Space Shuttle LOX and LN2 system. Configuration 4 has not been tried without a spring, and Configuration 2 takes too high a reverse flow rate, both of which are risk statements.

Configuration 4 is lightest, with 3, then 2 weighing more.

All valves are off-the-shelf components. With minor modification of the springs, the valves are suitable for the FSCD.

After considering all the above factors and trade-offs, Configuration 3 was selected.

SIZING: Under normal operation, the fluid will flow through the check valves. Hence, it is desirable to have a high C_V. The valve selected has a C_V of 3.0.

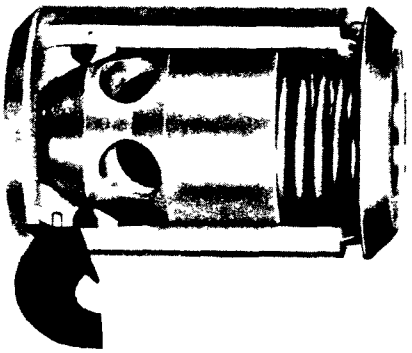

Configuration 2 Kepner Cartridge

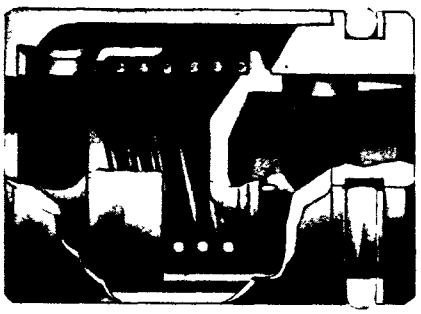

Configuration 3 Circle Seal C-200 Cartridge

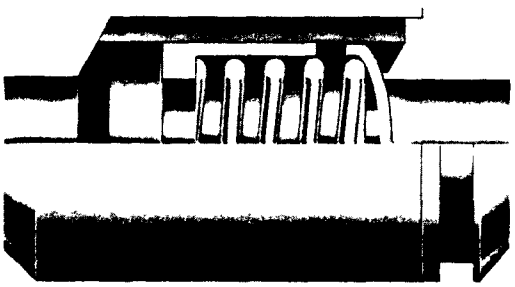

Configuration 4 Circle Seal C-2900 Cartridge

Figure 2.5.2-5 Check Valve Configurations

After completing initial ground tests, the system may have to be drained of working fluid (for a restart, for example). It will then be necessary that the check valve at the accumulator outlet remain partially open. This can be accomplished by designing the free height of the spring such that it results statically in a partial opening of the valve. Any flow reversal delta P will cause the poppet to close and stop the reversed flow.

In order to save weight, the internal components of the check valve will be installed in an existing PCS housing rather than using a cartridge.

RELIABILITY AND STRESS: The configuration selected has very low stresses. The flow path is such that it is self-cleaning and, hence, poppet hang-up is not likely. As mentioned earlier, once the system is in operation the valves are fully open and, hence, do not affect the reliability of the system.

MATERIALS: The poppet is made from 6061 alloy and anodized. The spring is made from 302 or 304 stainless steel.

CRITICAL CHARACTERISTICS

Characteristic	Location	Value	Comments
Surface finish	Poppet face and housing seal	32	Good finish results in low leakage in reverse flow direction during startup.
Reserve closing pressure	Check valve	2-4 in. of water	Allows maximum use of system fluid for startup.

2.5.2.4.3 EXPANSION BELLOWS

This bellows permits differential thermal expansion between the jet condenser and accumulator and the housing supporting these two subassemblies.

The bellows assembly consists of two concentric bellows welded to common flanges. The assembly is of redundant construction so that, if one of the bellows fails, it will not cause a system failure. The cavity between the bellows is evacuated.

TRADE-OFF: Formed bellows, diaphragms and welded bellows were considered for this application. The formed bellows concept was rejected because of inability to evacuate between the bellows. The diaphragm concept was rejected because of size and stress limitations. The welded redundant bellows configuration met the design requirements and, therefore, was selected.

SIZING: The diameter of the inner bellows is sized to fit over the diffuser of the jet condenser. The outer bellows is sized so it can be assembled over the inner bellows. The number of convolutions is based on deflection requirements.

RELIABILITY AND STRESS: The construction of the assembly is such that if one of the bellows fails, it will not cause system shutdown. The stress levels in the bellows will be maintained low enough such that it meets failure probability requirements of less than 1×10^{-9}.

MATERIALS: The materials of construction will be AM-350 for the laminations and 304L for the flanges. The laminations will be heat treated after welding. The completed assembly will be proof pressure tested, helium leak checked, and then the cavity between the bellows will be evacuated and sealed.

2.5.2.5 Regenerator

CONFIGURATION

The regenerator is an overall counterflow, spirally wound, finned tube configuration, mounted coaxially around the CRU. It consists of fourteen coils stacked one upon the other with liquid transfer to adjacent coils occurring at the ID and OD of the coil via a 180° return bend. This configuration results in a serpentine cross-flow of the liquid from coil to coil.

The coils are spaced and supported by baffles inserted between each coil. These baffles also ensure correct vapor flow through the regenerator. The entire assembly is held together with six tie bolts.

TRADE-OFFS

In the investigation of an appropriate regenerator design to meet the requirements of performance, reliability, and weight, several different heat exchanger types were considered. Since any configuration can be designed to meet the required effectiveness, the performance considerations are basically those of liquid and vapor side pressure drops and weight. In particular, the vapor side pressure drop is critical in determining turbine back pressure, hence, system performance as can be seen in Figure 2.5.2-6. Liquid side pressure drop is not as critical as can be seen in the performance sensitivity subsection 2.6.4.

Since the system flow rate is low and high effectiveness is required, high fin densities become a necessity. The inherently higher heat transfer characteristics of the liquid mean that the vapor side controls the heat transfer.

It was decided early in the program that, from a weight and packaging basis, an integrated CRU/regenerator/jet condenser was advantageous. This leads to a minimum number of joints in duct work and minimizes vapor flow passage transition ducting. Consequently, the regenerator needs to be designed to fit into the annular space around the CRU or into the volume between the CRU and jet condenser.

Three basic configurations have been considered: plate fin, sheet fin, and circular finned tube, with variations of each of these designs.

The typical plate fin design is built up of alternating layers of fins for liquid and vapor side, separated by thin plates and arranged in a general counterflow multipass configuration, with an appropriate header system to distribute the flow. This type of heat exchanger is typically the most compact type available but has many joints which are difficult to leak check.

In addition, the construction method employing flat plates essentially eliminates the potential for using aluminum construction because the stresses are too high at the hot end, although one potential way to solve this would be to use aluminum in the cold end only. Nickel is the preferred alternate material, having relatively good conductivity but high density. The trade-off analyses done for the plate fin, therefore, considered various fin configurations in nickel only. The plate fin construction lends itself to mechanical integration in that it forms a relatively rigid structure.

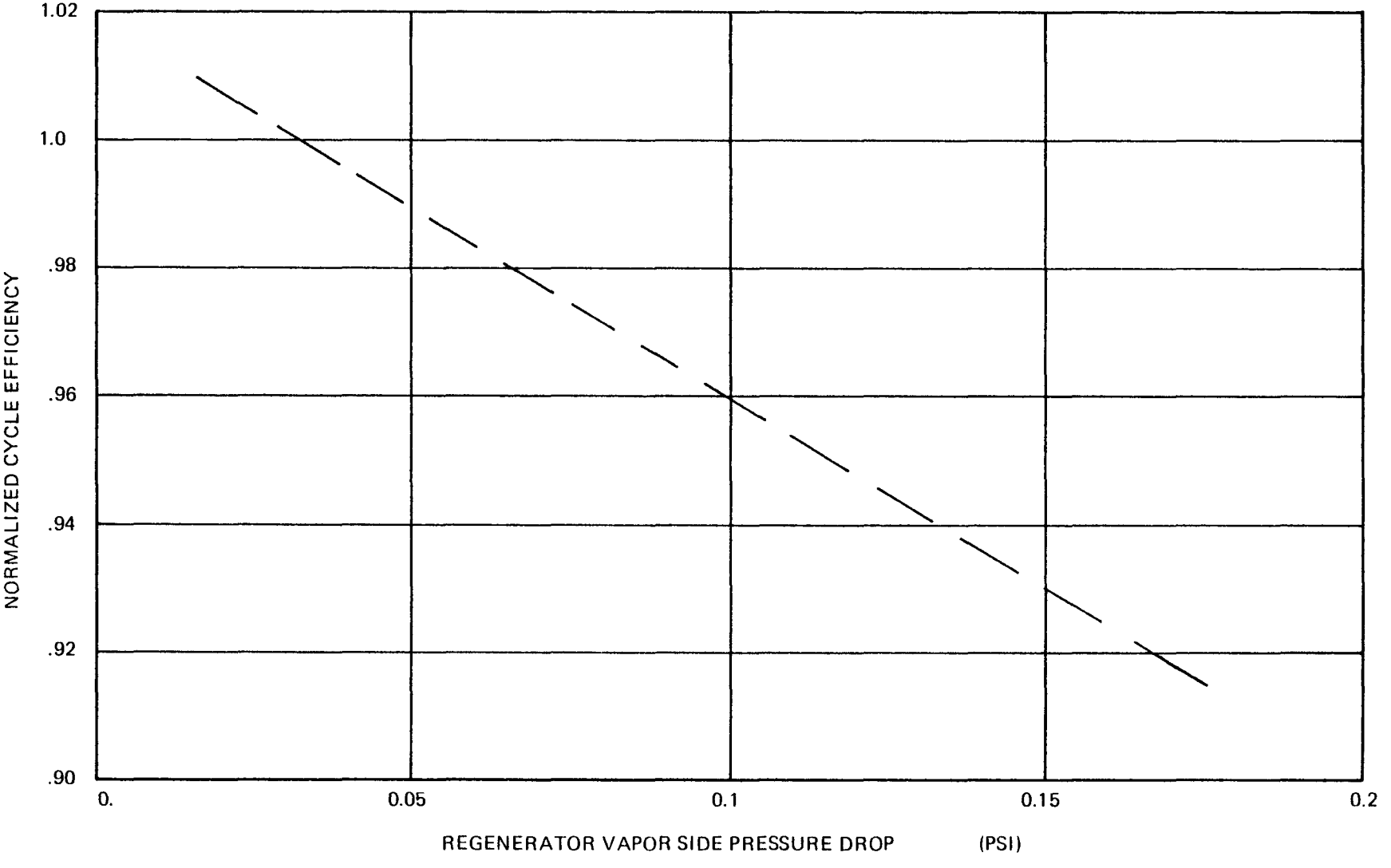

Figure 2.5.2-6 Cycle Efficiency vs. Regenerator Vapor ΔP

The sheet fin design comprises a series of tubes assembled through holes in a stack of thin sheets forming an extended surface. This is the type of heat exchanger used in automobile radiators and air conditioning equipment. Aluminum sheets can be used with aluminum tubes or even stainless steel tubes, though the latter construction leads to difficulties with the fin/tube joint. Even in the hot sections, the aluminum tubing could withstand the stresses imposed by the liquid pressure. This construction also has a relatively rigid construction but typically has relatively low fin density and a large number of joints associated with the interconnections between individual tubes. One version of this configuration has been investigated and is included in the trade-off.

The third configuration is the circular finned tube. This can have relatively high fin density and, because of the annular shape of the package, can be wound as a series of spiral tubes with interconnecting joints. The low number leads to relatively high reliability. As with the sheet fin configuration, the use of a tube to carry the high pressure liquid means that aluminum can be used throughout the construction. Two types of finned tubes were investigated, one with fins brazed to an aluminum tube, and the other a one-piece construction. The one-piece construction eliminates all the fin/tube braze joints. Table 2.5.2-F summarizes the basic configurations considered for a qualitative trade-off.

Table 2.5.2-F Regenerator Configurations

Configuration No. 1:	Plate fin – nickel Liquid side: lanced offset, hard way 0.100 inch plate separation, 12 FPI (fins per inch) Vapor side: laced offset, easy way 0.301 inch plate separation, 23 FPI Weight: 17.5 lbs.
Configuration No. 2:	Sheet fin Aluminum fin: 8 FPI Aluminum tube: 0.402 inch O.D. Weight: 35 lbs.
Configuration No. 3:	Finned tube – fin brazed to tube Aluminum fin: 14 FPI – 0.015 fin thickness Aluminum tube: 5/16 tube O.D. Weight (including baffles and support): 21 lbs.
Configuration No. 4:	Finned tube – integral construction Aluminum fin: 14 FPI – 0.022 fin thickness Aluminum tube: 5/16 tube O.D. Weight (including baffles and support): 24 lbs.

The following characteristics were evaluated for each configuration. The number of joints used is one of the most important factors in determining heat exchanger reliability. It should be noted that an internal leak from the liquid side to vapor side is not as critical as an external leak but would result in a degradation of performance; i.e., available output power. The plate fin construction has the greatest number of joints and a sheet fin would have the least number.

All types of heat exchangers could be built with the same effectiveness, but the pressure drops and weight are different for each type. Therefore, weight and ΔP, not effectiveness, are the important factors in the evaluation.

Extrapolation of existing design data is needed to correlate the vapor side heat transfer coefficients. To vary heat exchanger size is extremely difficult for the plate fin or sheet fin configurations, whereas addition or subtraction of coils is easy for the finned tube type. A test rig with variable size was built and used to confirm the design of the finned tube configuration used in the GDS. It should be noted that the FSCD retains the same regenerator size for all power levels, with minimal effect on performance.

The sizing of the finned tube version could be modeled most easily. It is configured to be the lowest risk design.

On a weight basis, the plate fin constructed from nickel is about the same weight as the all aluminum, brazed finned tube design and has a smaller volume. The plate fin has a somewhat awkward shape, however, from a packaging standpoint since it is basically rectangular in form, which would probably lead to the necessity for two separate heat exchanger cores to fit into an annular package.

The lower fin density for the sheet fin design leads to higher weights. The sheet fin design is the most common type used commercially, in automobile radiators and air conditions. The finned tube is relatively easy to produce but the winding into coils and joining of the individual sections involves a somewhat complicated process. The plate fin is the most difficult and expensive to manufacture because of all the braze joints that have to be made and the somewhat complex nature of the header system.

The result of the trade-off analysis was the selection of the finned tube configuration. The annular package is best fitted by a spirally wound finned tube with interconnecting joints. The integral finned tube version has distinct advantages over the brazed fin type; namely, it eliminates the problems of obtaining a good braze joint and cleaning the joint after brazing. Both brazed and integral finned tube configurations were fabricated for the GDS. Based upon this experience, the integral type was selected for the FSCD despite the slight weight penalty.

The tube configuration was selected from readily available sizes. The ID was sized to maintain the liquid side pressure drop within limits set by the radiator flow loop, without seriously affecting heat transfer. This can be done since the liquid side heat transfer coefficient is much larger than the vapor side coefficient. Tube pitch, both axial and radial, and fin OD were selected based on performance data available from Kays and London.[1]

PERFORMANCE ANALYSIS

The basic design objectives were as follows:

Minimize vapor side pressure drop.

Allow easy gas flow from the turbine diffuser into the heat exchanger and, hence, to the jet condenser.

Minimize weight.

[1] Compact Heat Exchangers. Kays and London. McGraw Hill.

Keep liquid side pressure drops less than 10 psi.

Achieve the 0.95 effectiveness which is essential for good system performance (see subsection 2.6.4 for system performance).

The effectiveness is defined as:

$$E = \frac{C_{Hot}}{C_{Min}} \left(\frac{T_{Hot\ In} - T_{Hot\ Out}}{T_{Hot\ In} - T_{Cold\ In}} \right)$$

where

C_{Hot} = capacity rate hot side = $(m\ C_p)_{Hot}$

C_{Cold} = capacity rate cold side = $(m\ C_p)_{Cold}$

C_{Min} = smaller of the two capacity rates

The regenerator configuration is basically counterflow with cross flow within each coil. Therefore, initial preliminary analyses were performed using NTU/effectiveness information for this type of heat exchanger, where the "Number of Transfer Units" is defined by:

$$NTU = \frac{-\ln \left(\frac{1 - E}{1 - EC} \right)}{1 - C}$$

where $C = \frac{\text{min capacity rate}}{\text{max capacity rate}}$

For KIPS, the capacity rate ratio, C, is 0.825 which combined with a required effectiveness E, of 0.95 leads to NTU = 8.37.

The vapor side heat transfer and pressure drop analysis was based on data presented in Kays and London and reproduced in Figure 2.5.2-7, with extrapolation for the lower Reynold's numbers. Liquid side analysis was performed using standard Dittus-Boelter correlations.

From a packaging and system dynamics standpoint, the regenerator housing length needs to be minimized. The inner regenerator housing is fixed by the size of the electrical generator, and various outer housing diameters were investigated to satisfy vapor side pressure drop and packaging constraints.

For a given geometry, the heat transfer coefficients were calculated for liquid and vapor sides leading to the required area:

$$A_L = \frac{(NTU)\ C}{U_L}$$

where U_L = overall heat transfer coefficient referred to liquid side

Finned circular tubes, surface CF-7.34.

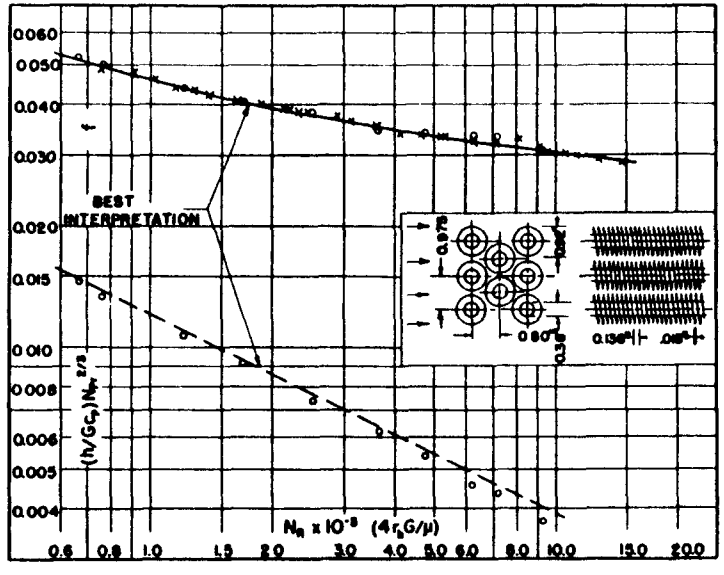

Tube outside diameter = 0.38 in.

Fin pitch = 7.34 per in.

Flow passage hydraulic diameter, $4r_h = 0.0154$ ft

Fin thickness (average)* = 0.018 in., aluminum

Free-flow area/frontal area, $\sigma = 0.538$

Heat transfer area/total volume, $\alpha = 140\ ft^2/ft^3$

Fin area/total area = 0.892

Note: Experimental uncertainty for heat transfer results possibly somewhat greater than the nominal ±5% quoted for the other surfaces because of the necessity of estimating a contact resistance in the bi-metal tubes.

* Fins slightly tapered.

Finned circular tubes, surface CF-8.72.

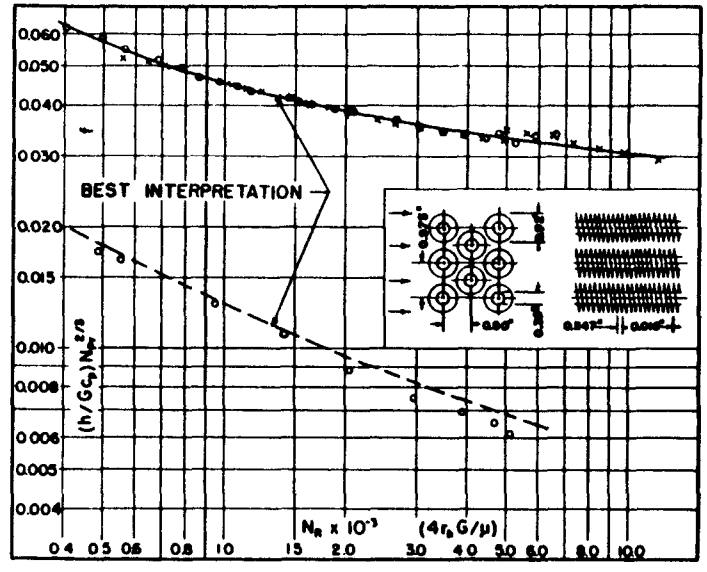

Tube outside diameter = 0.38 in.

Fin pitch = 8.72 per in.

Flow passage hydraulic diameter, $4r_h = 0.01288$ ft

Fin thickness (average)* = 0.018 in., aluminum

Free-flow area/frontal area, $\sigma = 0.524$

Heat transfer area/total volume, $\alpha = 163\ ft^2/ft^3$

Fin area/total area = 0.910

Note: Experimental uncertainty for heat transfer results possibly somewhat greater than the nominal ±5% quoted for the other surfaces because of the necessity of estimating a contact resistance in the bi-metal tubes.

* Fins slightly tapered.

Figure 2.5.2-7 Basis of Heat Transfer - Pressure Drop Calculations

A second, more accurate analysis was performed using a computer program to model the annular geometry. This allowed for the incorporation of local values of fluid properties rather than average the means. The Kays and London data set was used as the basis for the geometric configuration and for the heat transfer and pressure drop characteristics. The analysis procedure did not use NTU effectiveness relations, but rather an energy balance was performed starting from the hot end and working towards the cold end.

The heat transferred, Q, is given by:

$$Q = h_i A_i (T_w T_l) = h_o A_o (T_g - T_w)$$

where:

h_i and h_o are inside and outside heat transfer coefficients
A_i and A_o are inside and outside area
T_w = tube wall temperature
T_l = liquid temperature
T_g = gas temperature

then:

$$Q = hA\,(T_g - T_1)$$

If $\alpha = A_{hot}/V$
$\alpha i = A_{inside}/V$

$$\alpha fin = A_{fin}/V$$

$$\text{then } \frac{1}{hA} = \frac{1}{\alpha V}\left[\frac{1}{\frac{\alpha i}{\alpha_o}\,h_i} + \frac{1}{h_o\left(1 - \frac{\alpha_{fin}}{\alpha}(1 - \eta f)\right)}\right]$$

where ηf = fin efficiency
V = volume

For purposes of analysis, the tube was divided into angular elements as shown in Figure 2.5.2-8. It was assumed that uniform flow occurred on the gas side and that all the liquid flowed through the liquid side.

$$\text{Then } \delta Q = m_l C_{pl} (T_{le} - T_{li}) = \delta_{mg} C_{pg} (T_{gi} - T_{ge})$$

$$= h_i A_i (T_w - T_l) = h_o A_o (T_g - T_w)$$

$$= hA\,(T_g - T_l)$$

$$= \left(\frac{hA}{2}\right)(T_{gi} + T_{ge} - T_{li} - T_{le})$$

where

T_{gi} = gas temperature into element

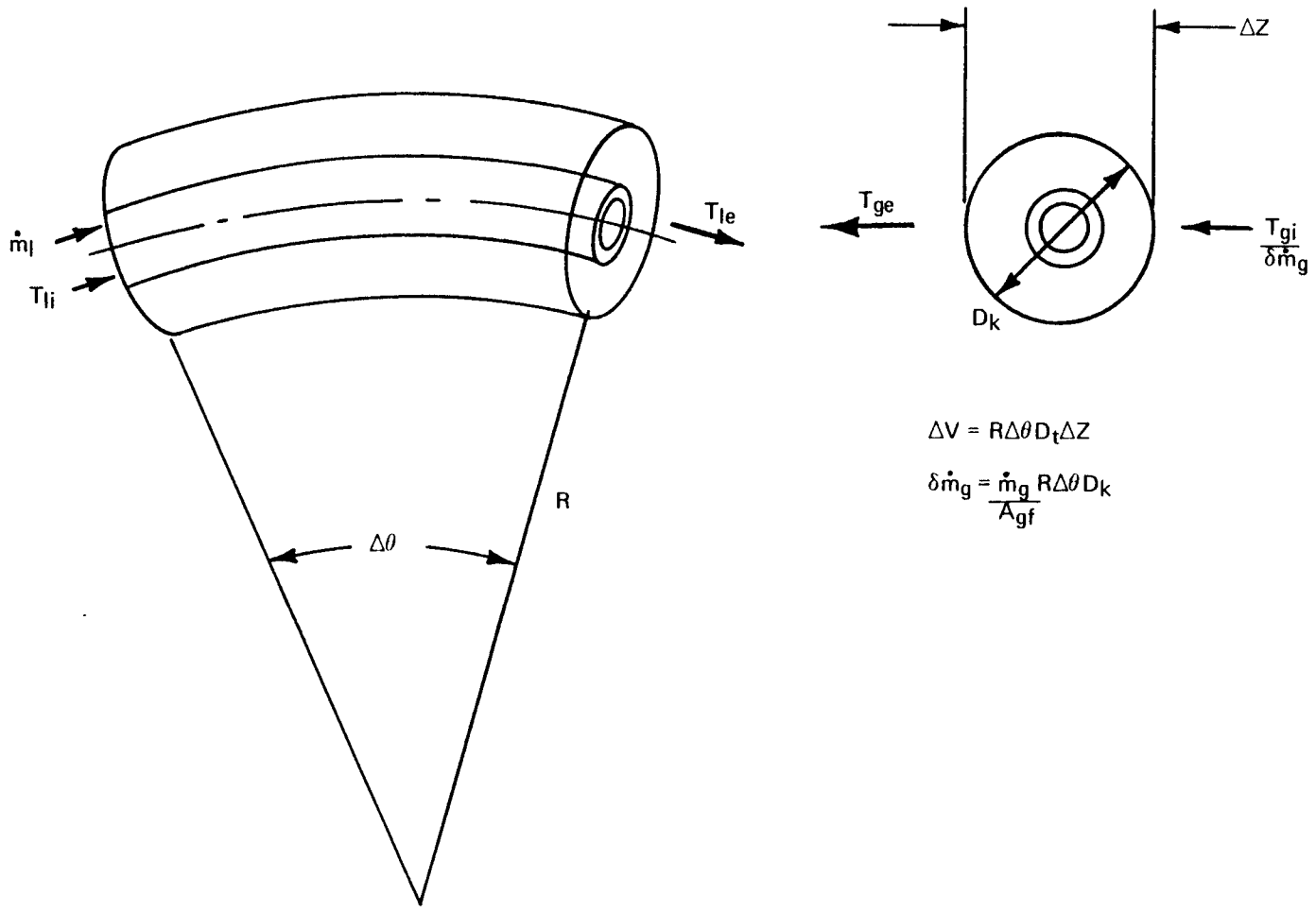

Figure 2.5.2-8 Regenerator Tube Angular Segments

T_{ge} = gas temperature out of element
T_{li} = liquid temperature into element
T_{le} = liquid temperature out of element

Heat transfer coefficients for inside and outside were determined by methods similar to those used in the previous analysis but using the elemental average temperatures. Hence, starting from the hot end of the heat exchanger and knowing the vapor inlet temperature and liquid outlet temperature, values for the liquid inlet temperature and vapor exit temperature were calculated. The resultant liquid outlet temperature was used for the inlet liquid temperature for the succeeding element. For each coil, the vapor inlet temperature was assumed the same for every element, and the exit temperatures were averaged for all elements to give the inlet temperature to the next adjacent coil.

By this method, the variation in temperature along the length of the coil was determined and the length adjusted until the required vapor outlet and liquid inlet temperatures were reached.

This analysis was based on a concentric tube arrangement, whereas in actuality, the tubes are spirally wound, making each coil slightly shorter and the overall heat exchanger length slightly larger for a required total tube length. The total tube length was conserved and the effect found to be negligible from testing.

The approximate analysis procedure and the computer analysis outlined above agree within approximately 10% for required heat exchanger size. It should be noted that certain extrapolations of the given data are present in the final design, i.e., the vapor side Reynold's number is outside of the data correlation, but the results of the test data indicate that these extrapolations are within reasonable limits.

The computer program allows multipower analysis to be readily performed since the effect of mass flow on temperatures for a given size can be calculated. These results are presented in Table 2.5.2-G.

Table 2.5.2-G Effect of Power Level on Regenerator Performance

Power Level (watts)	Mass Flow (lb/sec)	Regenerator Effectiveness
500	0.0146	0.955
1300	0.0306	0.95
2000	0.0451	0.934

Additional analyses have been performed to investigate the effect of axial conduction. The effect of this is minimal on the regenerator performance.

The effect of maldistributed flow at the exit of the turbine diffuser, entering the regenerator, for the 500 W or 1300 W designs, is difficult to analyze. The ratio of regenerator pressure drop to absolute pressure level is reasonably high (10%), so the flow should redistribute sufficiently well. The results of the GDS testing confirm this.

The pressure drop through the vapor side of the FSCD can be seen in Figure 2.5.2-9. The jet condenser showerhead vapor side pressure drop is discussed elsewhere, while the values for the

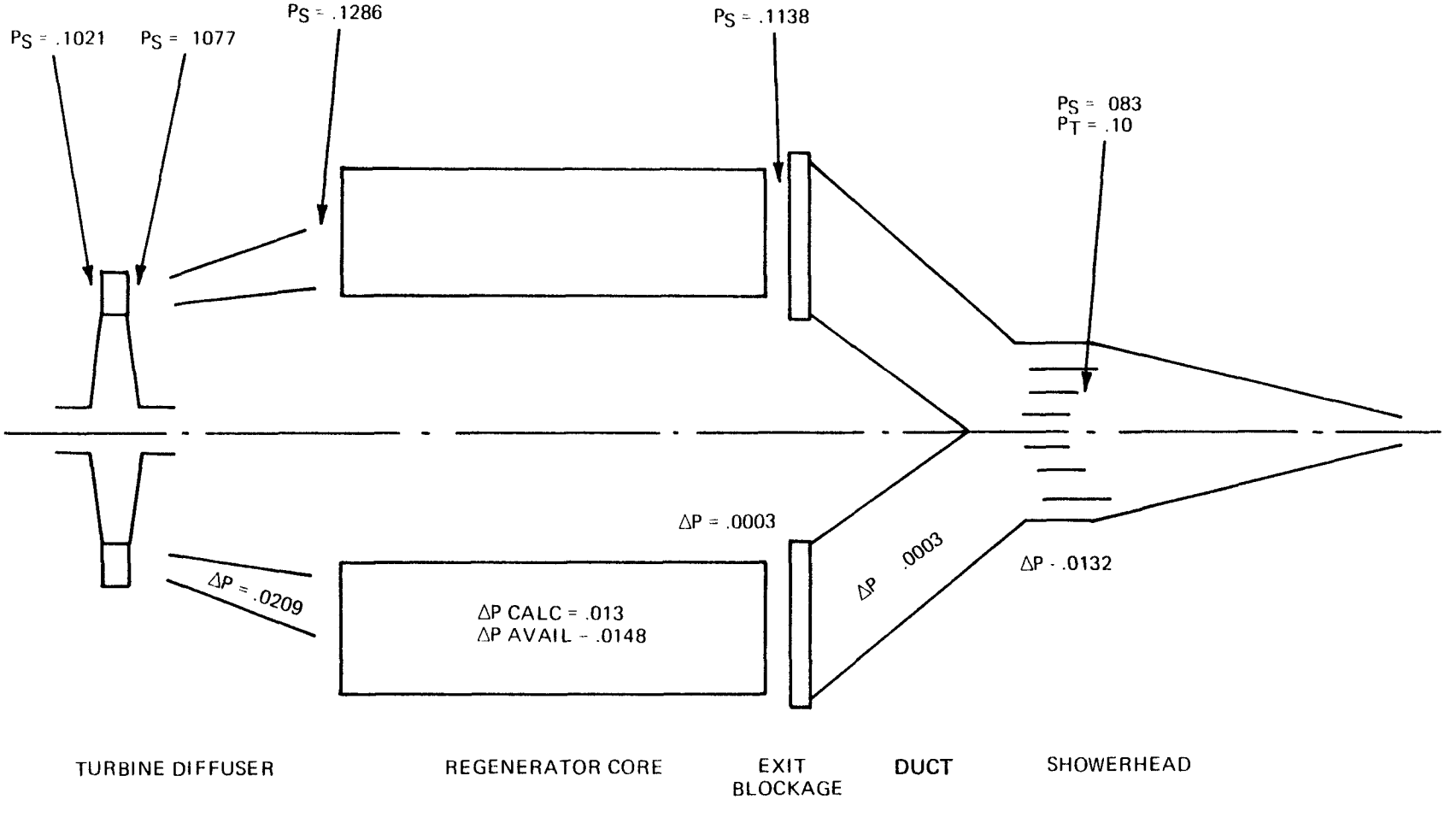

Figure 2.5.2-9 Vapor-Side Pressures

sudden expansion of leaving the core and the contraction, expansion losses associated with the support struts have been calculated and are shown in the figure. As can be seen, the regenerator core has a good pressure drop match compared to the design turbine back pressure conditions.

In order to prevent condensation of vapor on the first cold row of the regenerator core, a regenerator preheater has been incorporated to raise the liquid temperature above the local saturation conditions. This requires approximately a $2^{o}F$ increase in liquid inlet temperature and a heat transfer of 100 BTU/hr. The heat input is obtained by routing the inlet and outlet plumbing tubes side by side and thermally shunting them together with a stainless steel block brazed to both tubes.

MECHANICAL CONSTRUCTION

The regenerator is a spirally wound finned tube configuration, mounted coaxially around the CRU (reference Figure 2.5.2-10). This packaging arrangement was selected out of several alternative configurations to give the most compact arrangement for the KIPS system and to eliminate potential ducting.

Mounting of the coil in the housings and securing the individual coils have been studied to avoid damage to the coils during launch environments. Other considerations in the mechanical construction were proper tube spacing to maintain performance, minimum restrictions in the vapor flow path, avoidance of possible thermal shunts through the regenerator, alleviation of thermal stresses due to tube growth, limitation of stresses to assure high reliability, and inspectability of the parts and joints after final assembly.

The regenerator coils are made from 6061 aluminum tubing extruded to form an integral fin/tube construction. The fin/tubes are coiled into pancakes (approximately 12 foot lengths) and the end stripped for preparation of the U-bend weld.

The coils of the regenerator are separated from and supported by each other by means of 0.018 stainless steel (304L) baffle plates. The baffle plate assemblies are made by stamping the inner and outer plates and then joining the plates together using six equally spaced channels and welding them to the inner and outer plates. Each baffle plate is fabricated to ensure correct vapor flow through the regenerator.

As each regenerator coil is stacked up, a baffle plate is inserted between coils. Six grooves 0.125 inch wide are machined in each coil on each side to match the baffle plate spokes and, thus, the plates nest between fins. This ensures that at least six fins are contacting coil to coil through the assembly. Nesting of the baffle plate struts into the fins gives a keying effect that allows the coils to expand radially but eliminates torsional motion.

To constrain the regenerator, stiffer plates are needed at each end, and the coils are attached to the housings for axial constraint with preload on the coils.

A stiffer plate was made at the turbine end by adding six "T" sections to the baffle plate. Stiffness on the opposite end was obtained by utilizing the existing support structure frame and adding three smaller struts. The total coil assembly is mounted to the transition housing by means of six tie bolts which preload the assembly.

Excessive torsional distortion is prevented by keying the turbine end baffle plate to the outer

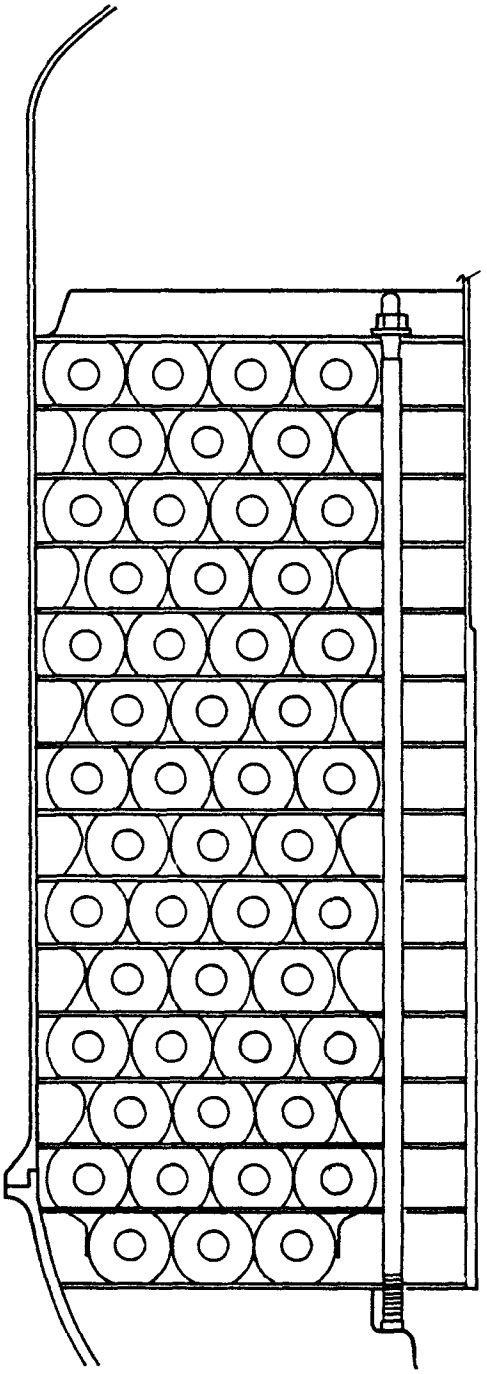

Figure 2.5.2-10 FSCD Regenerator Configuration

housing. Radial support is maintained by making the baffle plates a close conforming slip fit to the inner diameter of the outer regenerator housing.

The integral finned tubing is inherently more reliable because it has fewer, more accessible joints and is conductive to standard fabrication and inspection techniques. The flexibility in packaging reduces the number of joints in the duct work which leads to increased system reliability. In addition, the integral construction is inherently cleaner than the brazed construction because no braze flux is used. The potential presence of braze flux is a risk statement from a corrosion and fluid degradation standpoint.

STRESS

The stress analysis shows that the regenerator coils will withstand the thermal, shock, and vibration inputs without failure provided proper support is maintained. Based on the vibration level inputs, it was determined that six evenly spaced contacts were required between the coil fins to support the loads. With this support, the natural frequencies of the regenerator internal hardware are sufficiently higher than the natural frequencies of its mounting system, thus minimizing transmissibility through the struts.

FABRICATION AND INSPECTION

The individually-coiled finned tubes are stacked one upon the other with prebent aluminum U-bend welded to the ends of the coils. As the assembly is built, each weld joint is X-ray inspected and helium mass spectrometer leak checked to 1×10^{-8} scc/sec leak rate or better.

The fabrication, processing, and inspection of the regenerator are described in Figure 2.5.2-11.

Characteristic	Location	Value	Comment
Weld Joints	Tube Connections	——	Hermetic
Clearance	O.D. & I.D. of Baffles to Housings	0.030 I.D.	Performance
Finned Tube Contact	Fin to Baffle	6 Fins Minimum	Dynamics

TRANSITION TO JET CONDENSER

The transition section between the regenerator and the jet condenser resulted from an aerodynamic design study. This study optimized the vapor flow for minimum pressure losses and to provide for uniform mixing prior to introduction to the jet condenser.

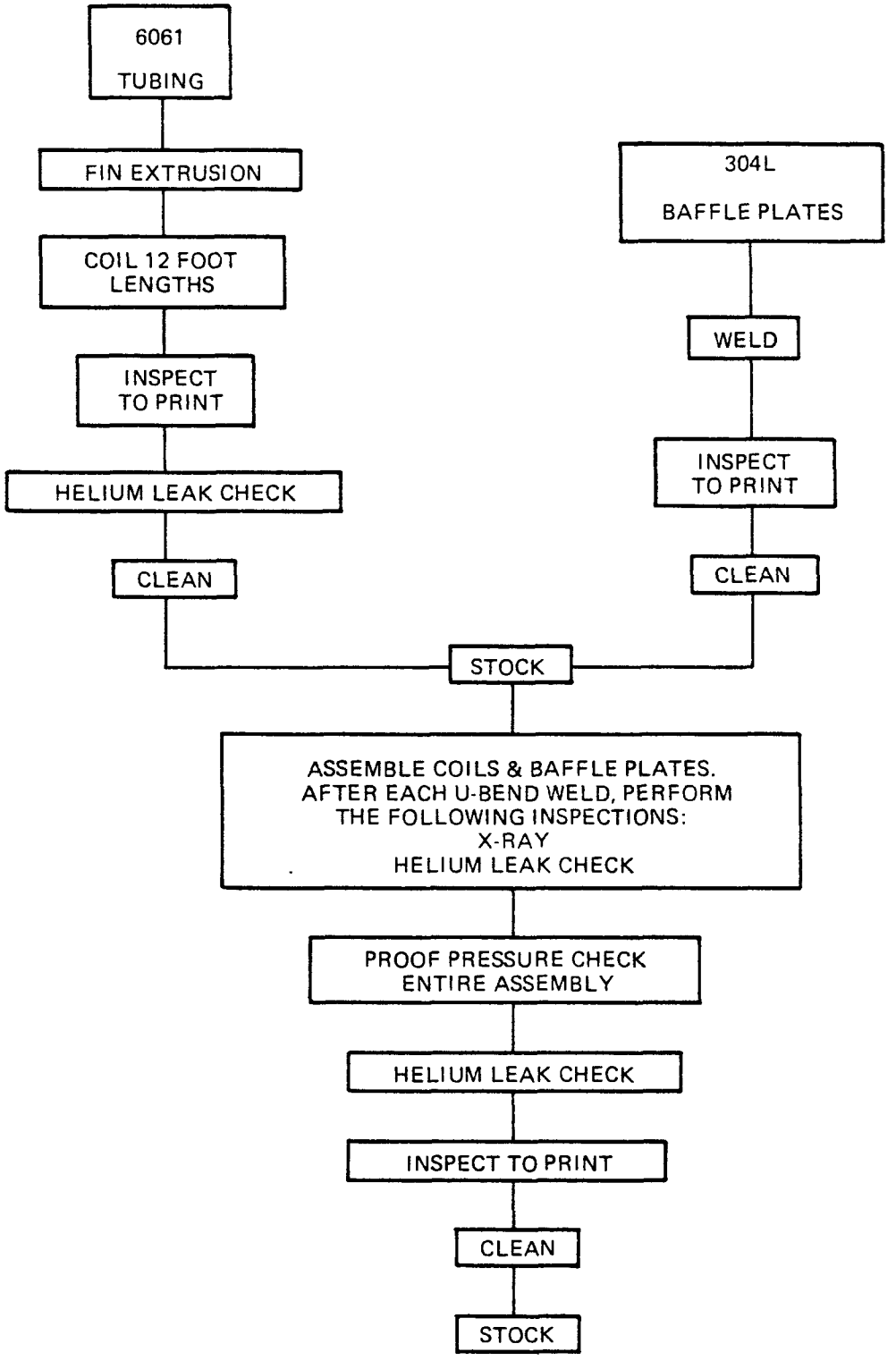

Figure 2.5.2-11 Regenerator Assembly

2.5.2.6 Flight System Radiator

Refer to Volume IV, Teledyne FSD and GDS, for a description of the flight system radiator.

2.5.2.7 Condensing Heat Exchanger

CONFIGURATION

The jet condenser consists of three major sections: the liquid injector, the vapor funnel, and the throat/diffuser.

The liquid injector is comprised of three hollow concentric rings supported by three equi-spaced elliptical hollow radial struts (see Figures 2.5.2.7-1 through 2.5.2.7-3). These form the liquid supply header system. Arranged upon the concentric rings are ninety orifice elements; forty-two in the outer ring, thirty in the middle ring, and eighteen in the inner ring. The orifice elements and ring header end cap form a single piece part for each ring. Each orifice element is of 0.010 inch inside diameter with an L/D of five. The orifice inlet has a one diameter lead-in radius.

The vapor funnel provides a boundary for the mixing/condensation process. The first section provides a rounded, smooth transition channelling vapor from the injector to the subsequent converging sections. The second and third sections are simple conical funnels.

The throat/diffuser has a constant diameter throat with a 0.010 inch gap in the middle through which bearing scavenge flow is ported. This is followed by a compound diffuser: the primary diffuser 0.700 inch long with a 2^{o} included angle and the secondary diffuser 2.900 inch long with a 6^{o} included angle.

TRADE-OFF STUDIES

Four types of condensing heat exchangers were considered for incorporation in the system and were evaluated on their performance, reliability, fabricability, weight, and ability to survive the launch environment as well as function in zero g.

Three of the configurations studied were surface condensers. A significant characteristic of all surface condensers is that a large vapor pressure drop is required to keep the condensate moving in the proper direction. Unless relatively high vapor pressure drops are used, various types of flow instabilities can occur when even slight acceleration fields operate in the direction opposite to flow. The result of these instabilities is either a large pressure fluctuation which is detrimental to system performance or, in the case of severe instability, depriming of the system pump resulting in system shutdown.

The first configuration is a condensing/subcooling radiator. In addition to the large pressure drop required, as the passages are larger, a greater amount of armor to prevent micrometeroid penetration would be required. The flexibility of this configuration is limited due to the required orientation. To allow the radiator thermal inertia to provide cooling during launch requires that the expander inlet be 100 to 150^{o}F superheated in normal operation causing a reduction in system performance. The condensing/subcooling radiator is very sensitive to unbalanced solar radiation which could result in pump depriming and system shutdown.

A surface condenser/subcooler with a pumped liquid radiator configuration is somewhat better than the radiating condenser although it still suffers from some of the same problems. A large vapor pressure drop is still required. The additional flow loop adds another pump and power conditioning equipment at a penalty to system performance and reliability. The smaller radiator tubes will lead

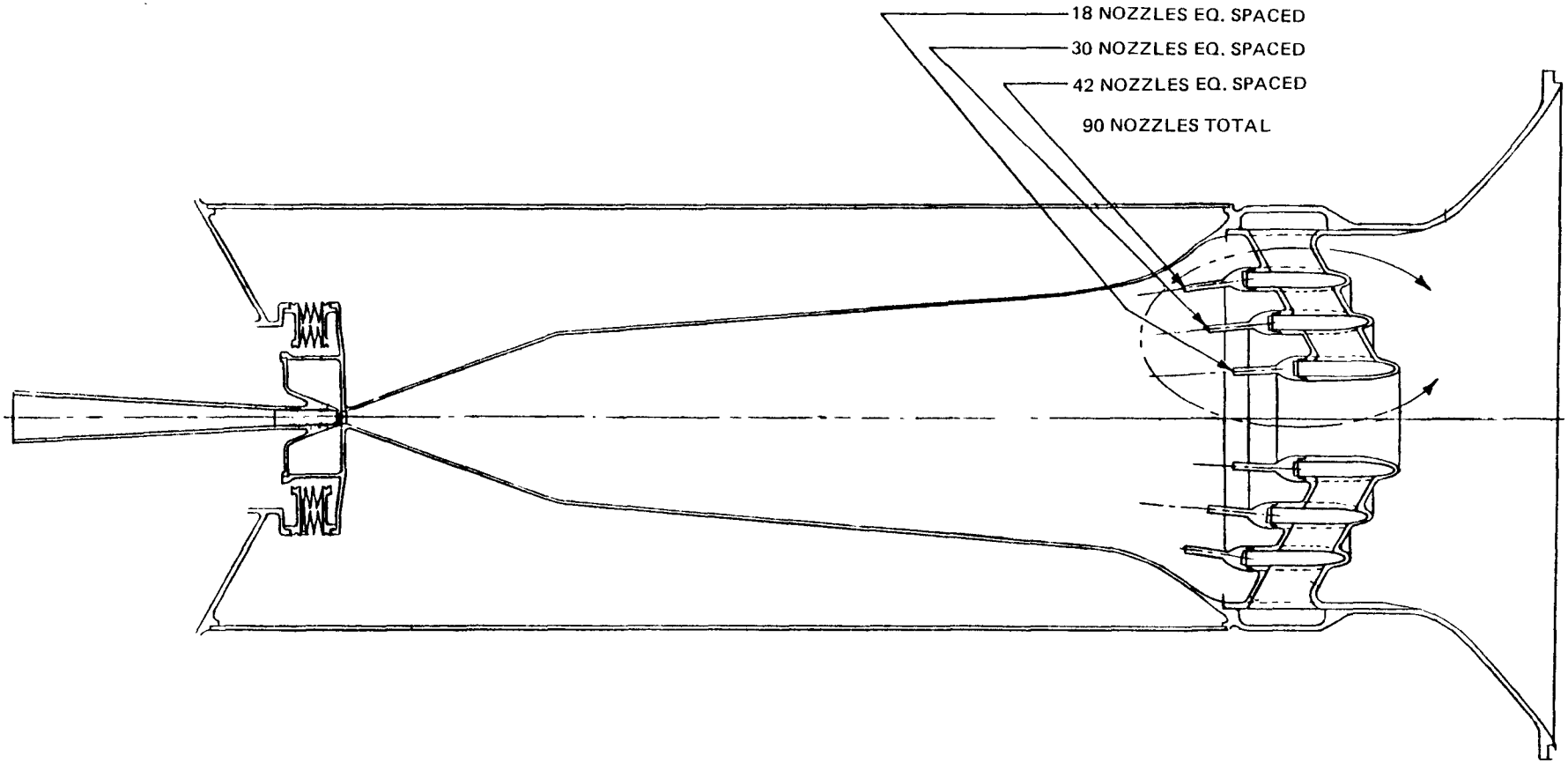

Figure 2.5.2.7-1 Jet Condenser

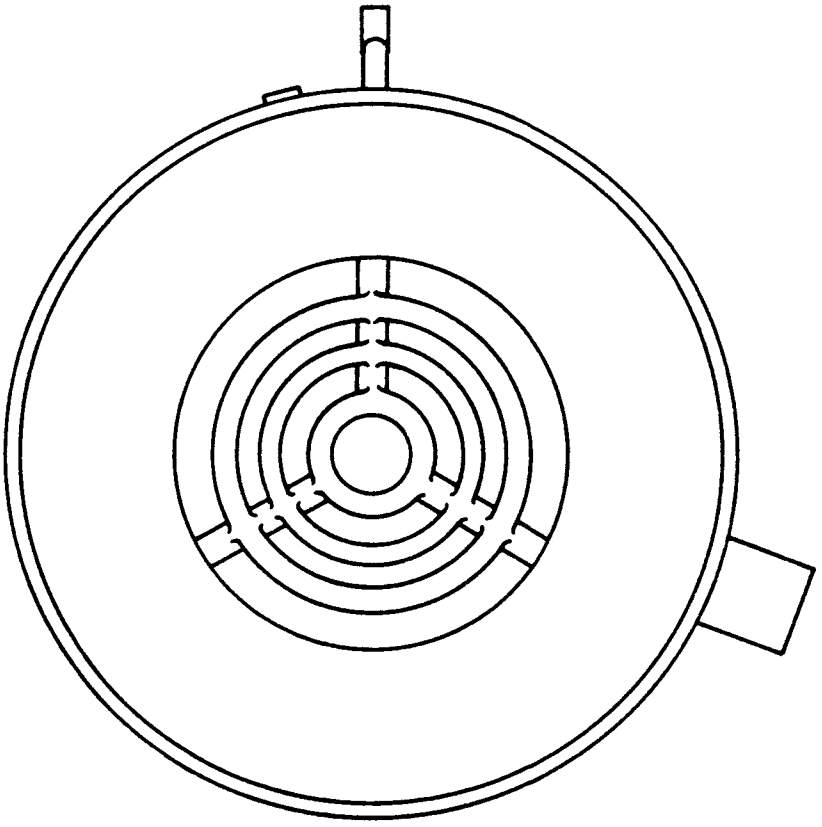

Figure 2.5.2.7-2 Internal View of Jet Condenser Injector Passages

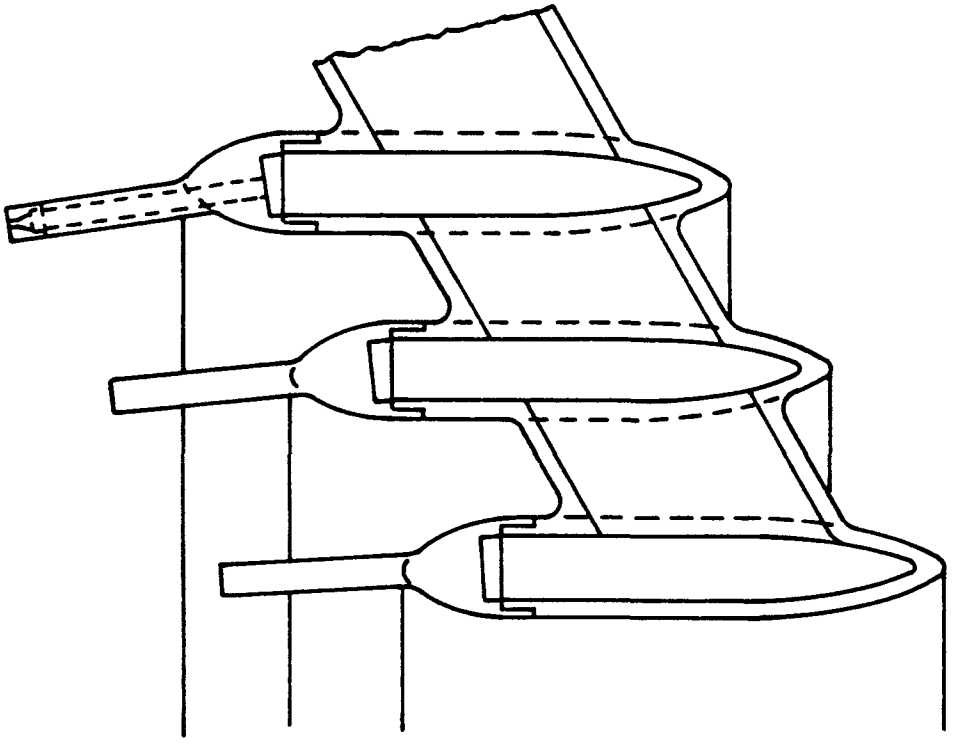

Figure 2.5.2.7-3 Jet Condenser Orifice Tubes

to a reduction in armor weight and greater integration flexibility. By varying the liquid flow through the radiator, the cooling required during launch could be supplied without requiring an inordinate amount of superheat during normal operation. Also, the radiator would be insensitive to unbalanced solar radiation.

With a wicking surface condenser, high g levels and vibration can cause the wick structure to dry out. It could be coupled with a pumped liquid radiator with the trade-offs as described above.

The jet condenser is a device in which low pressure vapor is ducted into a funnel coaxially with liquid jets of subcooled working fluid. The liquid jets are injected into the vapor with a high dynamic pressure and aimed at the throat of the vapor funnel. The vapor condenses on the subcooled liquid jets and the combined liquid jet passes through a throat into a diffuser. The high dynamic pressure liquid jet undergoes expansion in the diffuser to fill the entire cross section. In the sudden expansion, there is a loss of total pressure but a gain in static pressure of the liquid stream. Further recovery of static pressure occurs in passing through the diffuser. The behavior of the liquid jet in the diffuser is identical to that which occurs in the diffuser of a cavitating venturi. Thus, the outlet pressure from the diffuser can vary from essentially zero up to about 55-70% of inlet pressure depending on where the jet expands to fill the diffuser. This characteristic is used for inventory control in a jet condenser system by plumbing the diffuser outlet to a pressure controlled accumulator/reservoir.

Since the operation of the jet condenser is based on liquid momentum, the vapor pressure at the inlet can be very low as there is no requirement for a significant vapor pressure drop as is the case for surface condensers. Thus, a very low turbine back pressure can be used to improve turbomachinery volumetric flows (increase specific speed) and to increase isentropic head, hence increasing system efficiency.

Since the jet condenser relies on injected liquid momentum, it obviously can work in zero g. Even more important is that, with suitably high liquid injection velocities and moderately short jet lengths, it is quite insensitive to launch acceleration levels as well as vibrations.

The jet condenser is slightly less sensitive to noncondensable gases than the surface condensers, as some will be reabsorbed into the fluid at the throat but a gas removal system will still be incorporated to ensure long term performance and reliability.

The jet condenser could also be coupled with a pumped liquid radiator with the trade-offs as described above.

The additional flow for the jet condenser subcooled liquid requires a larger system pump than the previous condenser configurations. However, the jet condenser configuration has distinct advantages as a surface condensed system would required an additional jet pump to provide adequate NPSH for the system pump. The jet pump would have a flow ratio of about 1.5. The system pump specific speed would be 400 and a pump efficiency of approximately 40% results. With a jet condensed system no jet pump is required as the recovery provides the necessary NPSH to the system pump. The jet condenser flow ratio is 9. This raises the pump specific speed and the pump efficiency will be 65%. Therefore, a jet condensed system requires about 75% more pump power. This increased pump power is more than offset by the ability to run at a very low vapor pressure, hence turbine back pressure, for improved turbine and system efficiency.

With the attributes of 1) allowing low back pressure operation yielding high system efficiency, and 2) being less sensitive to launch acceleration and vibration, zero g operation and the space environment, the jet condenser does not have any of the liabilities that other types have, so it is the logical best choice for the KIPS condenser.

PERFORMANCE AND SIZING ANALYSIS

The basic design objectives were as follows:

1. Minimize vapor side pressure drop and eliminate flow separation.
2. Provide uniform vapor distribution about each orifice element.
3. Minimize weight.
4. Keep liquid side pressure drops less than 3 psi.
5. Minimize joints to assure reliability.

The jet condenser performance can be broken into two separate attributes, pressure recovery and thermal performance. The latter corresponds directly to mixing chamber pressure.

The pressure recovery directly determines the pressure rise needed by the system pump and, hence, pump work. Therefore, the recovery needs to be as high as possible considering both the steady state normal operation and launch (overspeed) modes. The transient condition of operation at design speed, immediately after operating at overspeed, when fluid inventory temperatures are high and a larger amount of fluid is held in the system accumulator must also be considered. For a jet condenser capable of a maximum recovery of 50%, the design operating recovery is reduced to 40% to account for this and to give adequate margin.

The jet condenser mixing chamber pressure has a large effect on system performance. The mixing chamber pressure is directly related to the turbine back pressure and thus the effect of a change in pressure is charged directly to system efficiency. The sensitivity analysis indicates a rise in pressure from 0.1 psia to 0.2 psia causes the cycle efficiency to drop by 2.6 percentage points.

Extensive rig testing on a Dowtherm working fluid loop with which the jet condenser state points could be accurately controlled and on a single nozzle loop with water/steam as the working fluid facilitated the formation of a jet condenser mathematical model. With the model it is possible to accurately predict the thermal performance (mixing chamber pressure) of a chosen jet condenser configuration.

This method was utilized to select and fabricate a GDS jet condenser configuration. The GDS configuration differs from the rig configuration only in those ways which do not invalidate the fabricability, inspectability and reliability demonstrated in the rig tests, but which facilitate improved performance. Model analysis indicates performance could be further improved. However, to assure the integrity of the predicted performance, the FSCD configuration was selected to be identical to the GDS except for minor changes in manufacturing which do not adversely affect performance, fabricability, inspectability or reliability. Refer to subsection 3.5.2.7 and Appendix A for a more detailed presentation of rig test results, model development and configuration analysis.

Jet condenser state points and mechanical configuration are described in Table 2.5.2.7-A.

The intra-jet condenser states are illustrated in Figure 2.5.2.7-4. Vapor flow rate, pressure and velocity as well as liquid surface and bulk temperatures are shown as functions of funnel axial location. These data are from the mathematical model analysis. It is interesting to note that approximately 50% of the vapor is condensed in the first 20% of the length. At 4 inches the condensation rate becomes limited by the intra-jet heat transfer. At that point the jet surface (TSL) has achieved saturated liquid conditions.

MECHANICAL CONSTRUCTION

All parts are machined from 304 stainless steel.

The liquid injector body is EDM'd on both internal and external surfaces. This allows maximum cross section liquid sections with rounded intersections for minimum liquid pressure drop while facilitating aerodynamic shaping and fairing of the external surfaces to minimize vapor side pressure drop.

The orifices are made an integral part of the ring header end caps to enhance the reliability. This eliminates 90 joints, which would be present if the orifices were made individually. It also allows aerodynamic shaping between the orifices and fairing of the header-to-orifice interface, which aids in minimizing vapor pressure drop. The orifices are machined into the three rings such that they are nominally focused at the throat. They are machined into tubes of 0.125 inch diameter and 0.500 inch length to facilitate fine tune focusing of the injector by slightly bending individual tubes to focus on a common focal point at the center of the throat. This fine tuning of the focus allows maximum hydraulic performance, minimum feedback to the bearing scavenge system and minimum effect from the launch dynamic environment.

The orifice end rings are fluxless furnace brazed to the injector body to minimize distortion and eliminate contamination of the injector body. The joint was designed to provide ample safety margins on stress in all operating modes (including overspeed pressure superimposed on the launch dynamics) and to be fully inspectable after completion of the brazing.

The completed injector assembly is then similarly brazed to the vapor funnel.

The vapor funnel is penetrated in one location midway through the shallow funnel to allow porting of the noncondensable gas separator vapor return.

The upstream half of the throat and the outer shell of the bearing scavenge annuli form an integral part of the vapor funnel.

The throat/diffuser section is a single part and also encompasses the inner shell and dividers for the bearing scavenge annuli.

This configuration minimizes the number of joints and eliminates external joints with the exception of tubing connecting the liquid inlet, bearing scavenges and noncondensable gas separator vapor return.

Table 2.5.2.7-A Jet Condenser Geometry and Performance

State Points:

Location	Mass Flow (lbm/sec)	Temperature (^{o}F)	Pressure (psia)
Liquid In	0.275	169	80.0
Vapor In	0.030	239	0.1
Bearing In	0.009	211	2.75
Liquid Out	0.314	211	32.0

Length	L	= 10 in.
Mixture chamber pressure	P_{mix}	= 0.083 psia
Number of nozzles	N	= 90
Orifice diameter	D_o	= .0100 in.
Effective vapor diameter at the liquid injector	D_{mix}	= 3.14 in.
Diameter at liquid injector	D_l	= 4.00 in.
Number of rings	n	= 3

Distribution	No. of Nozzles	Diameter (In.)	Angle to Axis (degrees)
Outer	42	2.808	8^{o} 12′
Middle	30	1.932	5^{o} 31′
Inner	18	1.014	2^{o} 49′

Vapor velocity at liquid injector	V_v	= 278.3 ft/sec (M=.6)
Liquid velocity	V_l	= 103.0 ft/sec (Re_D=8140)
Throat diameter	d_t	= 0.133 in.

Diffuser	Length (In.)	Half Angle (degrees)
Primary	0.700	1
Secondary	2.900	3

Pressure recovery	= 40%
Liquid side pressure drop	= 1.9 psid

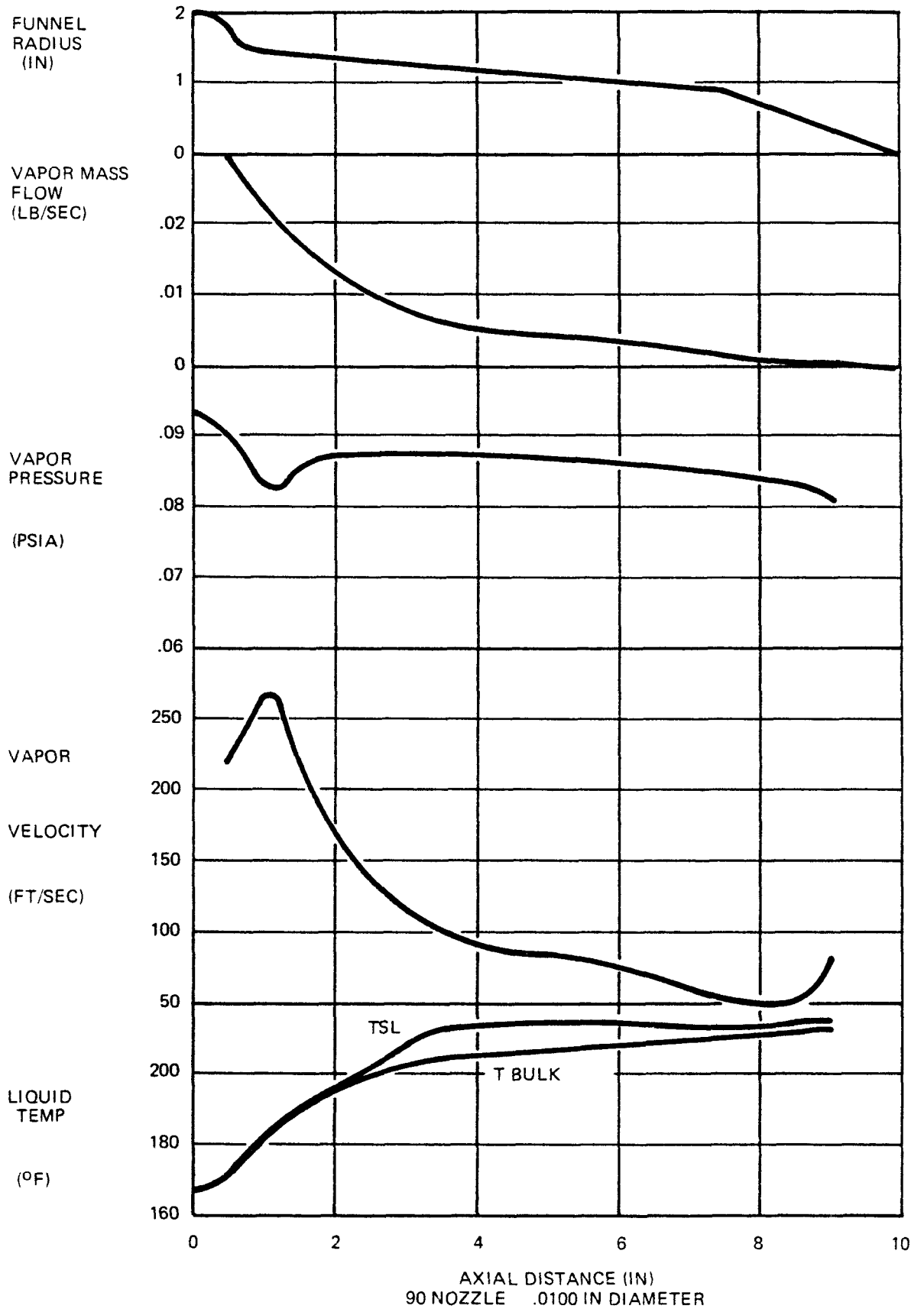

Figure 2.5.2.7-4 Jet Condenser Operating Characteristics

RELIABILITY

The selected configuration, with only tube porting joints as external joints and with the integral orifices, is inherently an extremely reliable configuration.

The fluxless braze assures that cleanliness can be maintained.

In order to minimize the impact of lateral inputs from shock or random excitation upon the deflection of the injected liquid streams relative to the throat it is necessary to reduce the structural response frequency to as low a value as possible. An analysis was performed to determine the worst case relative deflection between the injected liquid stream and the throat as described in subsection 2.5.5.3. This worst case relative deflection is 0.086 inch due to the response of the optimized structure.

A trade-off was performed to find the configuration which minimized the impact of this relative deflection. The configurations considered were: 1) hard mounts and open the throat to accept the worst case deflections (approximately 0.250 in), 2) shock mounts and open the throat, if required, as determined by test, and 3) shock mounts maintaining the throat at 0.133 in. and designing the throat to dynamically track jet deflections by counterweighting the jet condenser independently at the throat and nozzle.

Configuration 1) has the fewest number of parts and a simple jet condenser, however, it may lead to a more complex system due to the potential for pump cavitation at low jet condenser recovery and the need for strength in all other system components to survive the launch environment. Configuration 2) indicates a simple jet condenser but benefits also accrue in the design of other system components due to reduced structural loading from the launch environment. Configuration 3) is very complex requiring many more parts but has the potential of totally eliminating dynamic environment impacts.

Hydraulic performance is improved in each more complex configuration. Configuration 1) may lead to cavitation of the system pump during launch due to the reduced pressure recovery capability.

Essentially no development risk is involved in utilization of configurations 1) and 2). Configuration 2) requires determination of tolerance to impingement under the launch environment. This determination may be easily made under static test conditions. Tuning of the shock mounts may be required if the system dynamic response is not as predicted. Configuration 3) requires significant development of techniques to design the structure and liquid streams to vibrate in phase.

Configuration 2) leads to minimum system weight due to fewer effects on other components. Configuration 3) incurs maximum jet condenser and overall system weight.

Configurations 1) and 2) utilize proven manufacturing techniques and are fully inspectable. The third configuration utilizes unknown manufacturing techniques and inspectability. It is probable that many parts will be involved and a complex assembly sequence will result.

For the above reasons the configuration chosen is one in which shock mounts are incorporated to reduce the impact of the launch loads upon the total structure (second configuration). Static deflection tests (see subsection 3.5.2.7 and Appendix A) indicate that the current throat diameter is

not quite large enough to accomodate the predicted worst case deflection. However, the throat has been maintained at 0.133 in. diameter and if subsequent dynamic tests whow any problem the throat can be enlarged as necessary. The nonimpinging diameter under worst case loading has been determined to be approximately 0.165 inch (refer to subsection 2.5.2.9). This, then, is the upper limit of throat diameter.

STRESS

Stress analyses of the jet condenser injector, vapor funnel and diffuser are complete. Sizing and analysis was done following the reliability guidelines established to correlate stress levels and material capabilities. Stress analysis results are presented in subsection 2.5.5.

FABRICATION AND INSPECTION

The fabrication, processing and inspection of the KIPS FSCD jet condenser are described by Figure 2.5.2.7-5. The jet condenser is 100% inspectable throughout the manufacturing process.

The injector body rings and struts are rough machined on the outside and inside. The outside contours are then EDM'd to their final configuration. Then the internal passages in the struts are final EDM'd and the ring IDs are final machined. Full inspection of all internal and external dimensions follows.

The end cap/orifice rings are rough machined on the outside and inside. The outside surfaces and orifice feed diameter are final machined. The orifice diameter bore is then EDM'd in each orifice tube. Due to erosion of the electrode in this small size some taper develops. This taper is removed and gross surface erregularities are corrected by a subsequent machining operation. With a special tool which centers on the orifice diameter the inlet radius to the orifices are machined. Utilizing a fixture and test stand each orifice is then flow checked to assure that the proper flow for the assembly will be achieved at design pressure drop. Assessment can also be made as to locational stability and brooming resistance. Any orifices which do not meet the design requirements are reworked or replaced. The orifice rings are then cleaned using a technique developed by Sandia.

The injector body and orifice rings are now furnace brazed together. After inspection the completed injector assembly is installed in a test fixture which incorporates a target orifice at the throat plane. All nozzles but one are capped and, by bending, the nozzle is aligned so that the stream passes precisely through the target orifice. This is repeated for each nozzle.

All of the manufacturing, inspection and test techniques have been developed and demonstrated on the GDS. Refer to TP-404 for further information on focusing.

The vapor funnel and diffuser are conventionally machined and then welded together.

The jet condenser assembly is then completed by brazing the injector assembly into the vapor funnel after a final flow check to verify the focus the assembly is cleaned per CP 14.57-01 and helium leak checked.

CRITICAL CHARACTERISTICS

The cricital characteristics of the jet condenser are described in Table 2.5.2.7-B: It should be noted that all critical characteristics are assured to be within tolerance by at least one inspection test or

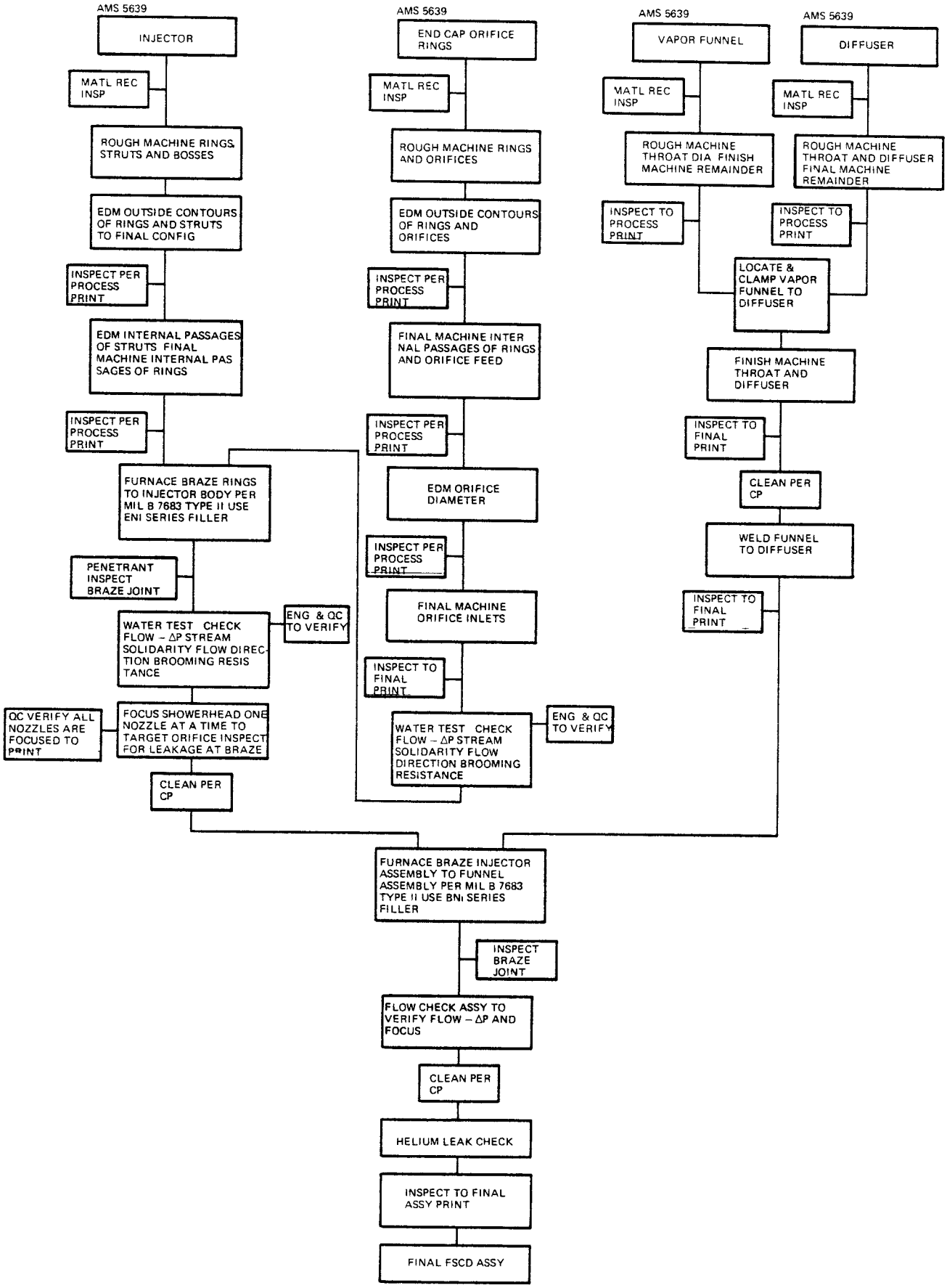

Figure 2.5.2.7-5 FSCD Jet Condenser Manufacturing Block Diagram

Table 2.5.2.7-B Jet Condenser Critical Characteristics

CHARACTERISTIC	DIMENSION	CHECKS TO ASSURE INTEGRITY	COMMENTS
Orifice Diameter	.0100 in. ± .0003	Dimensional Inspection Flow Tests	Increase Pump Work if too Large
Orifice Exit Corner Breaks	.001 max corner break	Dimensional Inspection Flow Tests	Severely Misdirected Jet Gives Low Orifice C_D And C_V Resulting In Reduced Recovery if Not Sharp
Throat Diameter	.1330 in. $^{+.001}_{-.000}$	Dimensional Inspection Flow Test	Throat Not Able To Swallow Injected Flow if Too Small
Injector Vapor Side Surface Finish	64 $\surd$	Inspect	Projects Through Boundary Layer if Too Rough
Throat and Primary Diffuser Surface Finish	32 $\surd$	Inspect	Slight Decrease In Pressure Recovery if Too Rough
Concentricity of Throat In Vapor Funnel To Throat In Diffuser	concentric within .0005 in.	Inspect	Throat Not Able To Swallow Injected Flow if Too Large

test operation and if within tolerance should produce no discernable effect upon jet condenser performance. The orifice diameter and corner break characteristics, which are the most critical in assuring design performance and reliability, are verified by a final inspection and four distinct flow tests (refer to Figure 2.5.2.7-5).

2.5.2.8 Thermal Insulation Stability

2.5.2.8.1 FOIL INSULATION

Refer to Volume IV, Teledyne FSD and GDS, for a description of the foil insulation.

2.5.2.8.2 FIBROUS INSULATION

Refer to Volume IV, Teledyne FSD and GDS, for a description of the fibrous insulation.

2.5.2.8.3 PCS INSULATION

TRADE-OFFS: Trade-off studies were conducted to determine the type of insulation to be used to insulate the PCS components. The selected insulation must satisfy these requirements:

Low thermal conductivity

Low mass density

The ability to maintain its desirable characteristics over a period of 7 years

Because of the rather low operating temperatures of the PCS components (650°F maximum), numerous insulation materials are available and were considered for this application. Table 2.5.2.8-A summarizes the properties of some of the candidate materials.

The most important factor to be considered in the selection of the insulation is the product of thermal conductivity and density since this will give the lowest weight for a required heat loss. It is obvious from the table that though Min K has very low conductivity, the $K\rho$ product is very high due to the high density. On the other hand, Microlite "AA" has an extremely low density and lowest $K\rho$ value, but its current availability is questionable. Multifoil insulation has a very low effective conductivity in vacuum but a relatively high value in air and is difficult to apply.

Trade-off studies were performed between Microlite "AA", TG15000, and multifoil insulation using aluminum foils with zirconium oxide separator. The effects of additional radiation barriers on the outside of the bulk insulation are included, using individual foil emissivity values of 0.04. As the number of these foils increases, the effective emissivity decreases, and the relative thermal resistance between the bulk insulation and the radiation barriers decreases allowing reduced amounts of bulk insulation for the same heat loss in a vacuum environment. However, heat losses for ground operation do increase with the reduced amount of bulk insulation.

The results of these trade-offs are presented in Table 2.5.2.8-B for the plumbing and regenerator turbine shells.

Table 2.5.2.8-A Fibrous Insulation Materials

Material	Effective Thermal Conductivity (BTU-FT/FT^2-HR-^{o}F) Air	Vacuum	Density LB_m/FT^3	$(K\varphi)_{vac}$	Max Operating Temp ^{o}F
Microlite "AA" (J-M)* (silicone binder)	.0483	.0243	0.6	.0146	750
Microfibre Felt (J-M)	.0308	.0092	4.0	.0367	–
Micro-quartz (J-M)	.033	.010	3.5	.035	2000
Min K – 1301 (J-M)	.018	.011	20	.217	1300
Min K – F182 (J-M)	.018	.011	16	.176	–
TG 15000 (HITCO)	.0354	.0078	3.0	.0234	800
Fibre Frax Lo Con (CARB)**	.0317	.011	4.0	.044	–
Multi-foil (AL-Z_rO_2)	–	.0000463	–	–	1000

* Johns-Manville
** Carborundum

Table 2.5.2.8-B Summary of Insulation Thermal Analysis

	High Temp Plumbing		Regenerator and Turbine Shells	
	Heat Loss (BTU/hr)	Weight (lb)	Heat Loss (BTU/hr)	Weight (lb)
2" thick Microlite + (1) Al. foil	139	0.99	66	0.81
2" thick Microlite + (2) Al. foils	—	—	38	0.93
2" thick Microlite + (3) Al. foils	48	1.23	24	1.05
2" TG15000 + (1) Al. foil	63	4.56	30	3.73
.65" TG15000 + (1) Al. foil	—	—	66	1.15
.65" TG15000 + (3) Al. foils	50	1.85	24	1.51
2" TG15000 + (3) Al. foils	22	4.8		
.032" multi-foil .062" multi-foil	9 5	0.89 1.98	16 8	1.74 4.9

ANALYSIS: The critical areas of the Power Conversion System where heat loss must be minimized are the turbine and regenerator shells and the high temperature fluid plumbing lines. The jet condenser and accumulator are not as important from a system performance standpoint since heat has to be rejected from fluid at this location anyway. However, to keep heat input to the spacecraft to an acceptable level, some insulation will be used to cover these components.

Based on these analysis results 0.65 inches of TG15000 plus 3 aluminum foils were selected for the PCS bulk insulation giving a heat loss of 24 BTU/hr in vacuum and a weight of 1.51 pounds. Also, 0.032 inch of multifoil has been selected for the plumbing with a heat loss of 9 BTU/hr in vacuum and a weight of 0.89 pound. Since the conductivity of the multifoil is not currently well documented, experiments will be necessary to determine whether this insulation will be acceptable from the standpoint of exposed surface temperature. The back-up insulation would be 2" TG15000 with a heat loss of 22 BTU/hr and a weight of 4.8 pounds, a weight penalty of almost 4 pounds.

All these analyses were performed for vacuum operation with an average radiator temperature of 180°F, with radiation being the only mode of heat transfer. Air operation will increase heat losses due to convection and increased bulk insulation conductivity. The heat losses under these conditions will increase at least one order of magnitude.

A thin layer of insulation will be applied to the jet condenser accumulator surfaces with radiation barriers to minimize emissivity. With assumed low values of emissivity and absorptivity for the spacecraft and the relatively low temperatures of these surfaces, radiation heat input to the spacecraft will be minimal.

FABRICATION: The insulation will be formed into a shape which will fit over the PCS with the foils applied to the material before shaping. The whole blanket will then be held with adhesive aluminum tape and ties. Effects of depressurization during launch will be negligible.

RELIABILITY: Reliability data is being generated on the material from its use in the Space Shuttle program.

2.5.2.9 FSCD Heat Source Heat Exchanger

The KIPS boiler is a once-through design, comprising three, series connected, stainless steel, helically wound tube coils attached to the outside of a cylindrical copper fin. They are radiantly heated by MHW isotope heat sources. The tubes are wound in a double spiral fashion, with a reverse "U" bend at the middle of the tube length, in order that the inlet and outlet can be at the same end of the HSA.

Another tube, used for auxiliary cooling in the absence of Dowtherm flow, is attached to the fin adjacent to the boiler tube in a similar manner.

The copper fin has an emissivity coating of iron titanate to increase the emissivity to 0.85. To ensure that MHW operating temperatures are sufficient to keep the iridium cladding of the fuel sphere assembly in the ductile range, an intermediate low emissivity radiation shield is placed between the fin surface and the HSA.

TRADE-OFFS

Both brazing and welding were considered for the attachment of the boiler tube and coolant tube to the boiler fin. The baseline approach selected is a welded construction, similar to the GDS configuration. It is estimated, however, that the development of the brazed configuration would lead to a total weight savings of 6 pounds. This will be pursued as an alternate approach in Phase II.

To simplify the loading of the isotope heat source into the HSA and to minimize the length of interconnecting plumbing between HSAs, it is preferable to have the Dowtherm and coolant tubes entering and leaving through the same end. It is desirable to interwind the two tubes to retain nearly the same temperature distributions that exist with the GDS. Two configurations were investigated and are presented in Figure 2.5.2.9-1. The simplest configuration, (a), currently presented as the baseline configuration, has the two tubes wound parallel to each other, with the coolant tube close to the Dowtherm tube as in the GDS configuration. This configuration does not require that the coolant tube cross the Dowtherm tube but has higher thermal gradients across the fin than the GDS, since alternate Dowtherm coils have no cooling coil between them. The second configuration, (b), has the nitrogen cooling coil crossing the Dowtherm tube so that two interlocking helices are formed. This allows the temperature distribution in the auxiliary cooling mode to be the same as the current GDS design. However, examination of the HSA assembly, as presented in subsection 2.5.1, shows limited space available for this crossover. It is felt that space could possibly be provided by locally removing the Min-K insulation and then installing the multifoil insulation from the other end, but this complicates the assembly procedures.

It is preferable to have the boiler tube on the inside of the fin, looking directly at the heat source, since this improves the heat transfer process. However, attaching the tube on the outside greatly simplifies the manufacturing process. The increased complexity of developing tube attachment on the inside outweighed the thermal benefits and, so, outside attachment was selected.

A similar trade-off was performed on selecting a continuously wound tube over a fin tube arrangement. The thermal efficiency of the continuous helix would be better than the finned tube, but the weight would be considerably greater, and so the finned tube was selected.

The advantages of a once-through boiler design compared to a multipass or recirculating design are that increased stability can be expected and also the fluid inventory at the high temperature and in the vicinity of the nuclear source is minimized. The selected boiler is a once-through design.

ANALYSIS

A computer program developed by Sundstrand was used to analyze the various heat transfer processes involved in the design of the boiler. The program models both heat transfer and fluid flow for subcooled, low quality bubbly flow, annular flow, drywall transition and superheated vapor regions. The effects of swirl wires, twisted tapes, and inner body flow blockage devices may be incorporated in the program, and induced flow accelerations calculated. The program allows the effect of tube diameter and length to be analyzed, thus determining the pitch of the helix of the tube on the fin.

The thermal analysis of the boiler is a twofold analysis. First, the external design is concerned with the efficiency with which heat is transferred from the heat source to the boiler by radiation; second,

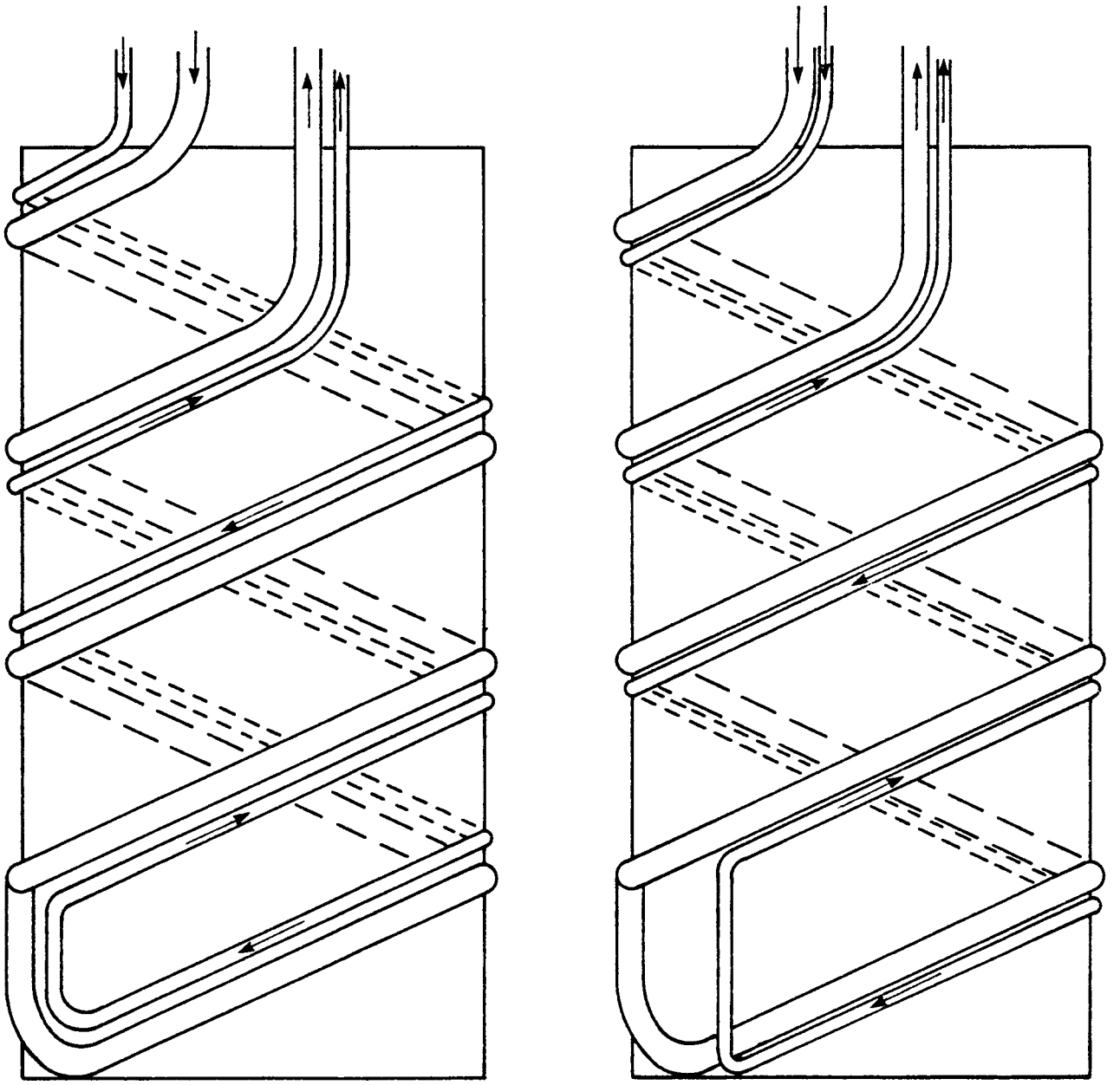

Figure 2.5.2.9-1 Boiler Tube Configuration

the internal heat transfer in the tubes is considered. In the latter portion, the tube geometry is optimized to ensure the working fluid is properly conditioned when passing through the boiler.

As described above, the outside of the boiler has radiation fins attached to it. Once the desired heat source temperature and heat flux are determined, it is then possible to size these radiation fins.

$$Q/A = \sigma F \eta (T_S^4 - T_B^4)$$

where
- Q/A - boiler heat flux
- σ - Stefan-Boltzmann constant
- η - fin effectiveness
- T_S - heat source temperatures
- T_B - average boiler temperature
- F - radiation heat parameter involving surface shape and emissivity

Once η has been calculated, the fin geometry can then be determined using a method proposed by Lieblein[1]. In that reference, fin effectiveness was presented as a function of a geometry parameter L.

where:
$$L = \left[\frac{N_s \epsilon \sigma L_f^2 T_F^3}{Kt}\right]^{.5}$$

where:
- N_s - number of radiating fin surfaces
- ϵ - fin emissivity
- σ - Stefan-Boltzmann constant
- L_f - fin length
- T_F - fin temperature
- K - fin thermal conductivity
- t - fin thickness

Now the boiler fin design is known as a function of the heat flux, therefore, a tube design can be obtained. The design of a boiler tube in a once-through boiler depends not only on the tube dimensions but also upon the working fluid thermodynamic properties.

Since typical system cycle analysis results in the turbine inlet or boiler exit being known, this point is used as a starting point for the computer program. Then the calculation system is that the boiler tubes are subdivided into an arbitrary number of increments. Next, by knowing boiler outlet conditions, the calculation can proceed from increment to increment throughout the boiler in a reverse direction with respect to flow. As this calculation proceeds, different flow regimes and conditions are encountered. For each specific regime, the appropriate set of correlations is used. Throughout the tube, the following regimes are encountered. Using the boiler outlet as a starting point, the first regime would be a superheated vapor region. This extends from the point of 100% quality to the boiler exit. Next, transition boiling would occur. This happens when there is a partial wetting of the tube wall. The annular flow evaporation regime extends from the point of partial wetting down to the beginning of the nucleate boiling region. Last, the subcooled liquid region is encountered from the inlet to the point of boiling initiation.

For an organic working fluid, the superheated vapor and the subcooled liquid regions are relatively

[1]Lieblien, S "Analysis of Temperature Distribution and Radiant Heat Transfer Along a Rectangular Fin." NASA TN D-196

simple to model. The bare tube pressure loss is calculated from the Blasius equation and heat transfer coefficients are calculated from the Dittus-Boelter equation.

$$h = 0.0243 \frac{K}{D_H} Re^{0.8} Pr^{0.4}$$

where:
- h - heat transfer coefficient
- K - fluid conductivity
- D_H - hydraulic diameter
- Re - Reynold's number
- Pr - Prandtl number

Since inserts are included in the tubes, the correlations proposed by Peterson[1] are combined in the pressure drop and heat transfer expressions.

Transition boiling and nucleate boiling regimes are calculated by using the Lockhart-Martinelli correlation to determine the particular flow pattern which is occurring. Once the type of flow encountered is determined (annular, dispersed, bubbling, etc.), the particular heat transfer coefficient for that flow pattern is calculated from the appropriate subroutine. When swirl inserts are included, this effect is then added to the heat transfer coefficient. In the two-phase regime, the artificial acceleration caused by inserts is:

$$A_R = \frac{2}{g_c d_i} \left[\frac{X G}{\rho_v \sqrt{\frac{\rho_i}{\rho_v}}} \frac{\pi di}{P} \right]^2$$

where:
- g_c - gravitational acceleration constant
- d_i - tube inside diameter
- x - mixture quality
- G - mass velocity
- ρ_v - density of vapor
- ρ_1 - density of liquid
- p - insert pitch

With the above analysis, the working fluid temperature, pressure and inventory, local tube wall temperature, and segment length are determined for each boiler increment. The working fluid degradation can be calculated using Sundstrand data correlations. The local degradation rate and the quantity of degradation products formed are determined from these calculations.

The output of the model is the boiler overall design parameters: tube length, boiler weight, working fluid inventory, and pressure drop.

Analyses were also performed to determine the expected temperature profiles for the fin tube using a finite difference thermal modeling computer program.

[1]Peterson, J.R. "Thermal Design Procedures for Space Rankine Cycle System Boilers, IECEC, 1968, Boulder, Colo

SIZING AND PERFORMANCE

The boiler tube design employs a 0.5 inch diameter stainless steel tube welded to the copper fin. The tube consists of three sections: the subcooled, two phase, and superheat sections. The lengths of the different heat transfer sections are: subcooled - 14.7 feet, two phase - 11.6 feet, and superheat - 1.35 feet. The subcooled and two phase sections contain a 0.3 inch diameter centerbody with a helically wound wire between centerbody and tube wall. The centerbody is discontinued after the point of critical quality (approximately 80%) but the helical wire is continued to the end of the two phase region and into the superheater. The centerbody is discontinued to ensure breakup of any rivulet type flow which may occur along the centerbody. The helical wire is wound to specified pitches to assure adequate induced acceleration levels on the fluid, ensuring that the liquid, when present, is centrifuged to the boiler walls. The variation of wire pitch with vapor quality is presented in Table 2.5.2.9-A.

The centerbody and helical wire increases the heat transfer coefficient, delays the onset of two phase flow and increases hydraulic stability by preventing plug-slug flow.

The temperature, quality, pressure, and induced acceleration fields within the boiler are presented in Figures 2.5.2.9-2 and 2.5.2.9-3.

Table 2.5.2.9-A Boiler Swirl Wire Pitch Summary

Vapor Quality	Swirl Wire Pitch (Feet)
0-.2	.152
.2-.6	.286
.6-1	.283
1	.283

The variation of fin and tube wall temperature is shown in Figure 2.5.2.9-4 as a function of distance from the tube centerline. Data are presented for both welded and brazed configurations.

MECHANICAL CONSTRUCTION

The boiler tube and centerbodies are fabricated from stainless steel because of their compatibility with Dowtherm while the fin is to be made from copper to increase the fin efficiency.

The boiler fin tube comprises a cylindrical copper fin with the boiler tube wrapped around the outside in a reversed double helical arrangement. The boiler auxiliary coolant coil is wrapped in a similar fashion adjacent to the Dowtherm tube.

A high emissivity coating is applied to the tubes and fin.

The cylindrical fin is located in the HSA by means of tabs at each end which are trapped by the Min-K insulation at each end of the heat source.

The boiler tube and coolant tube pass out through the end of the HSA and are sealed to the HSA by means of a bellows which allows the inside of the HSA to be isolated from external ambient conditions.

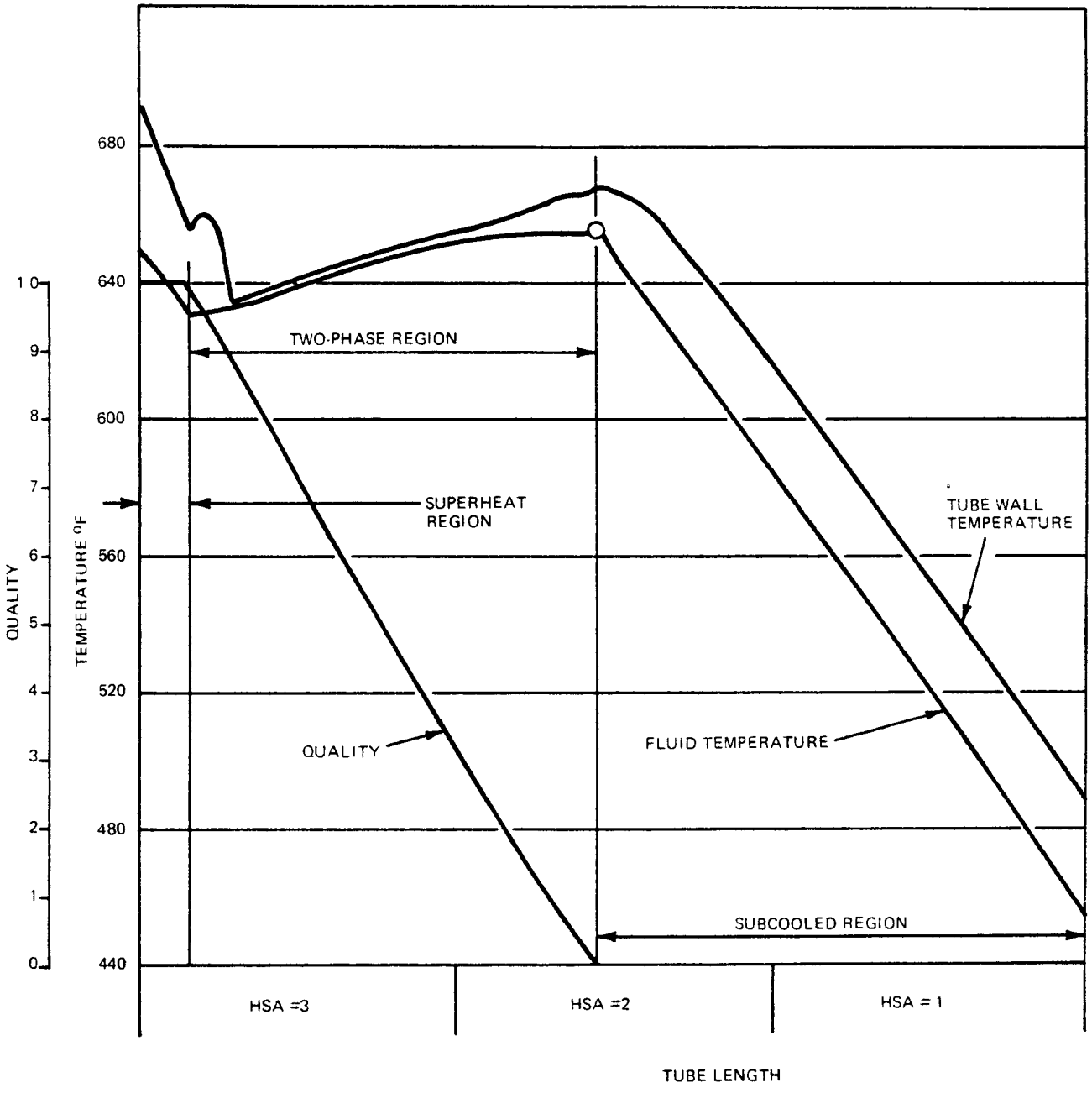

Figure 2.5.2.9-2 Quality and Temperature Profiles in Boiler Tube

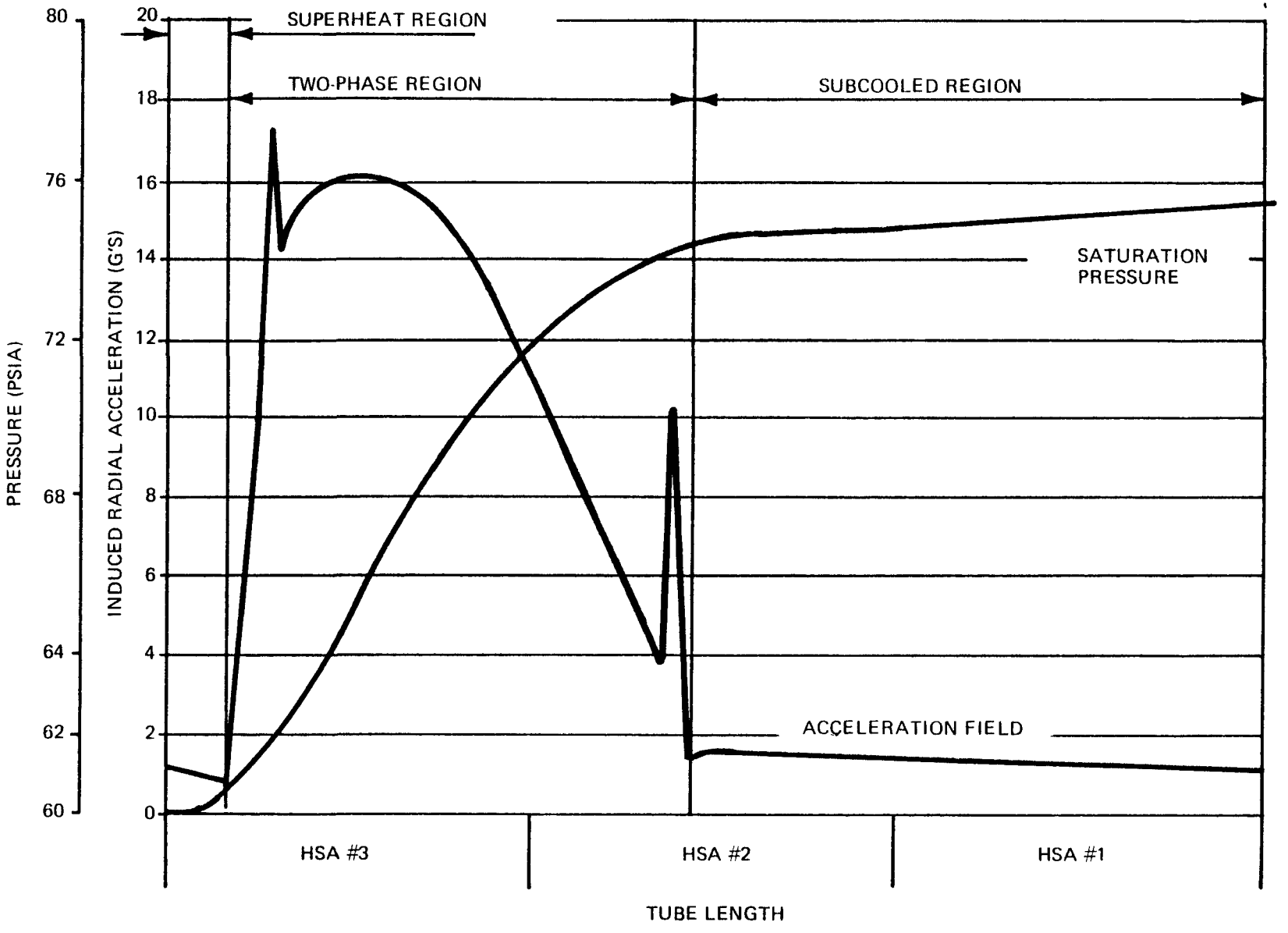

Figure 2.5.2.9-3 Pressure and Induced Radial Acceleration Profiles in Boiler Tube

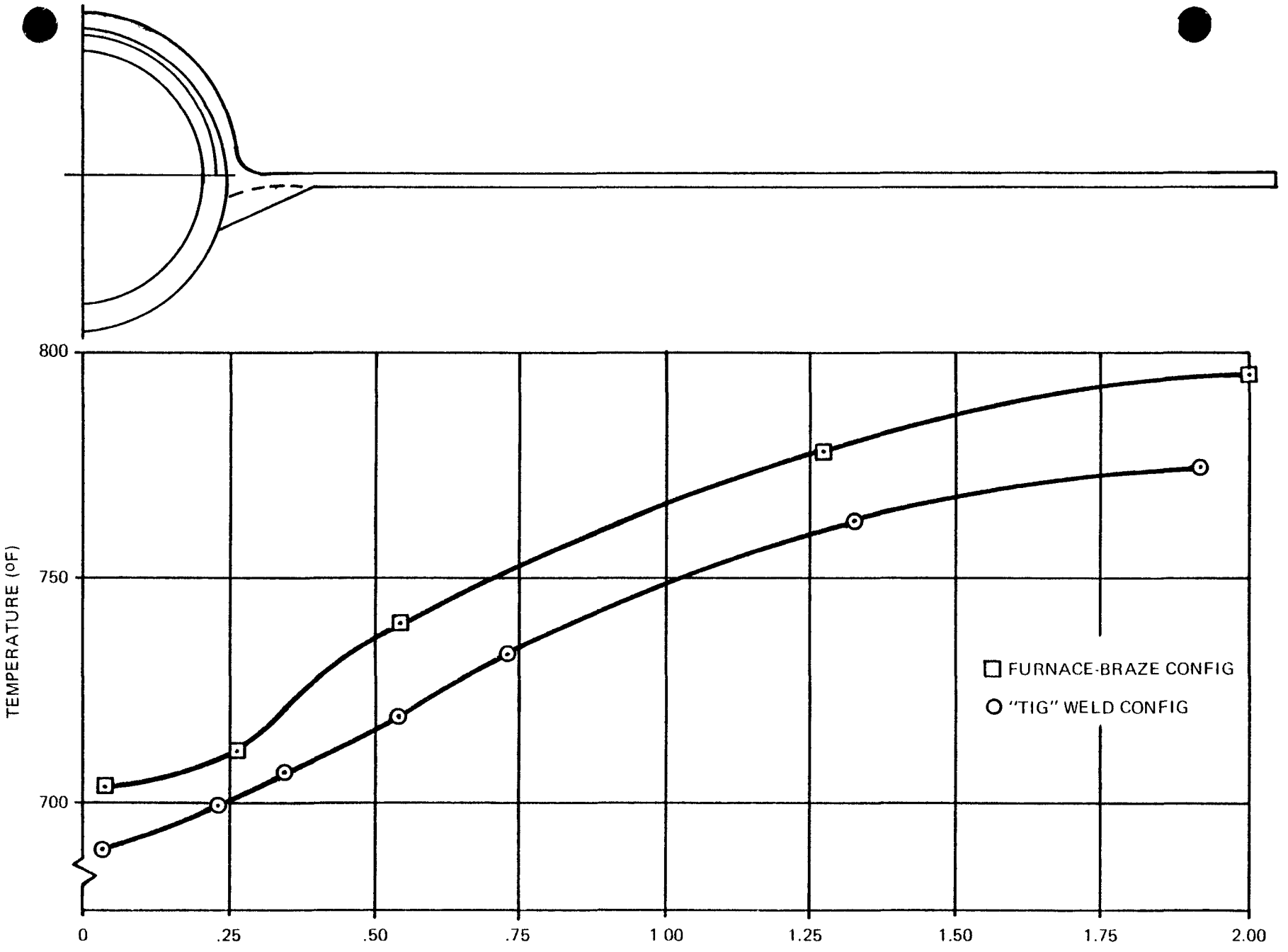

Figure 2.5.2.9-4 Boiler Fin and Tube - Wall Temperature

The boiler tube and fin expansion coefficients are essentially equal, so that during steady state operation, radial thermal stresses are very low and weld rupture is unlikely. Axial thermal gradients exist between adjacent Dowtherm tubes during steady state operation and between auxiliary coolant tubes during heatup. These gradients are not excessive as can be seen from Figure 2.5.2.9-4.

RELIABILITY AND STRESS

The boiler and coolant tubes are fabricated from seamless stainless steel and have no weld joints within the heat exchanger. Internal pressures are very low keeping stress levels in a perfectly safe regime.

The emissivity coating is designed for operation for seven years at 800°F, with the additional capability of withstanding 1550°F for one year. It is also capable of at least five thermal cycles from 800°F to ambient conditions. The heat source radiation shield allows some degradation in fin emissivity without performance degradation, since the radiation shield is the controlling thermal resistance.

The weld between tube and fin is very lightly stressed since the thermal expansion coefficients are essentially the same.

FABRICATION AND INSPECTION

The fabrication of the boiler fin-tube heat exchanger proceeds in four phases: insertion of centerbodies into the boiler tube and forming both boiler tube and coolant tube into double helices, forming the cylindrical copper fin, joining the tubes to the fin, and, finally, the application of the emissivity coating to the complete assembly.

The fabrication of the tube inserts involves winding the AISI 304 stainless steel swirl wire into a helical spring shape of the correct pitch. In the area where the wire has to be attached to the centerbody, the inner diameter of the helix is sized smaller than the centerbody outer diameter, while in the regime where there is no centerbody, the outer diameter of the helix is larger than the inner diameter of the tube. This ensures good contact both on the centerbody and on the inside of the tube. The swirl wire is then tack-welded in the AISI 304 stainless steel centerbody every six inches.

The centerbody comprises a hollow tube (for minimum weight) with a cap welded on one end to prevent through-flow.

The outside of both the boiler and coolant tubes is then copper plated with 0.010 inch of copper. To aid in winding, the boiler tube is filled with reagent grade biphenyl which freezes at 150°F. The complete boiler tube assembly and coolant tube are then wound in the spiral shape required for fitting the cylindrical fin and the biphenyl is removed. The inside diameter of the helix of the tubes is smaller than the cylindrical fin after spring-back and stress relieving to guarantee good contact between fin and tube.

Cross-sections of each boiler tube showing the respective inserts are shown in Figure 2.5.2.9-5.

The boiler fin is made from 0.020 inch thick OHFC copper sheet which is rolled into a cylindrical shape and seam welded. Helical grooves are then rolled into the outside surface of the cylinder to match the required tube helix.

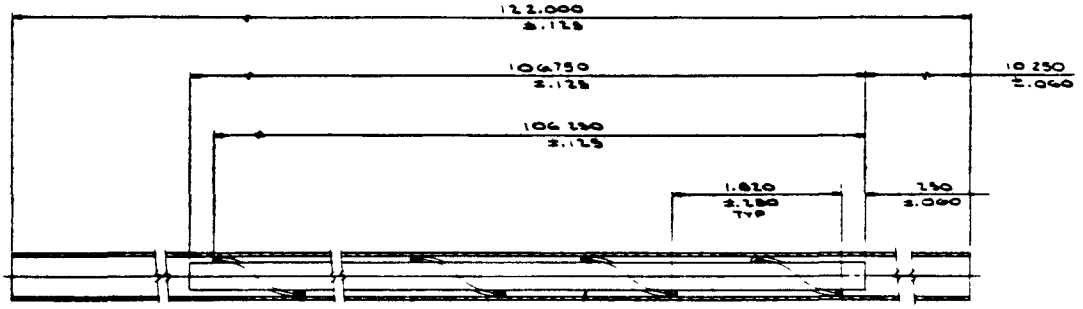

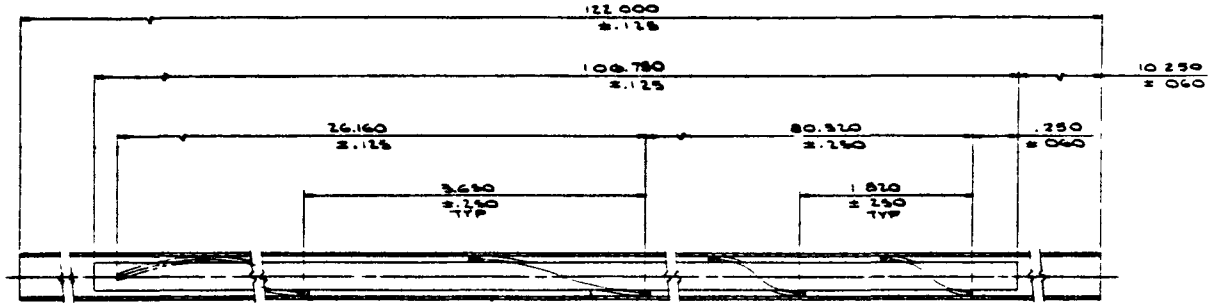

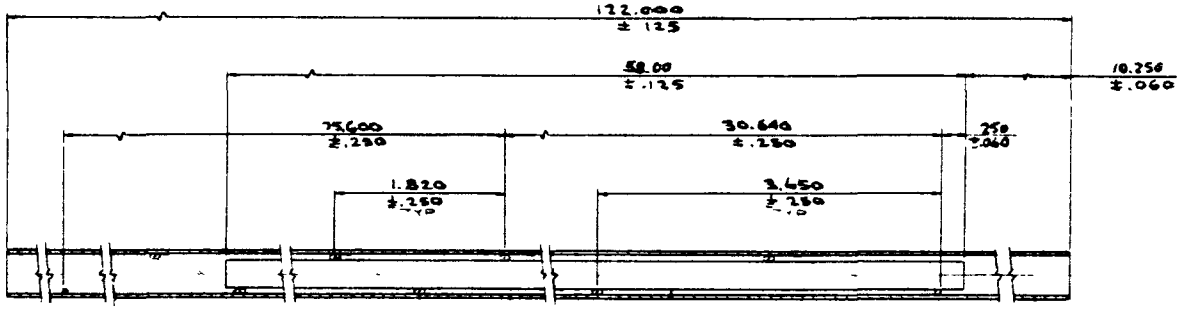

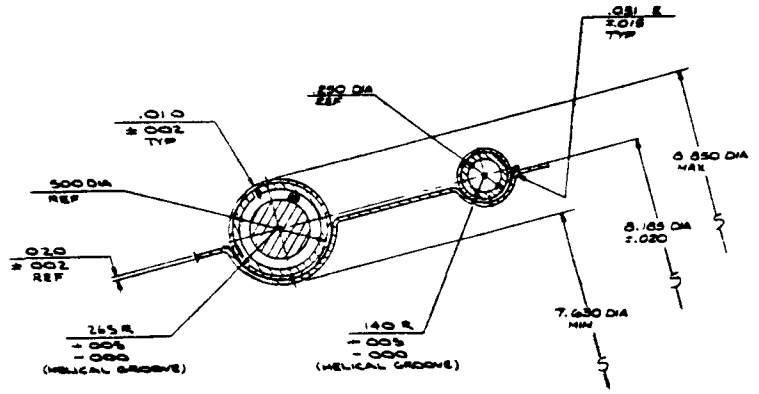

Figure 2.5.2.9-5 Boiler Tube Configurations

The copper plated tubes are then wound onto the fin and TIG welded to the fin in an inert atmosphere using pure copper filler to give a fillet of at least 0.125 inch. The welds are radiographically inspected. The only type of defect which could occur is a cold weld in which the filler is melted but not fused to the base metal. This would be shown by radiography. The minimum amount of penetration of copper into the stainless steel tubing precludes embrittlement of the stainless. Thermal cracking problems will not occur since material thicknesses and expansion coefficients are similar, and high temperatures are not required for welding.

The total assembly is then coated with the high emissivity coating.

CRITICAL CHARACTERISTICS

Characteristic	Location	Comment
Copper Plating	Boiler & Coolant Tubes	Good adhesion required for thermal contact
Tube-Fin Weld	Boiler & Coolant Tubes	Good bond required for thermal contact
Tube Helix Diameter	Boiler & Coolant Tubes	Smaller than fin cylindrical diameter to minimize weld stress

2.5.3 COMBINED ROTATING UNIT

2.5.3.1 Introduction

This section describes the Combined Rotating Unit (CRU). Its function in the KIPS is to extract useful work from the Dowtherm fluid and convert it into electric power from the alternator and hydraulic power from the system pump. The term CRU results from having the pump, alternator and turbine on a common shaft.

2.5.3.2 Summary

The CRU comprises three major components, the turbine, the alternator and the pump, mounted on a common shaft and supported on working fluid lubricated bearings.

The turbine extracts work from the high temperature, high pressure fluid leaving the boiler and converts it to useful shaft power. The KIPS turbine is a single stage, axial flow supersonic impulse type with a constant channel type shrouded blading. It uses multiple shock cancellation type nozzles.

The turbine directly drives the alternator rotor. The alternator is a homopolar induction type with four laminated poles on the shaft rotating within the stator windings. High efficiency is achieved by minimizing current density. The alternator waste heat is extracted by the working fluid flowing through a cooling coil. Thermal input from the turbine is minimized by thermal dams in the shaft and the turbine housings.

The system pump is at the end of the shaft away from the turbine. It is a six vaned, centrifugal type employing backward swept vanes and shrouds at both front and back. The flow exits from the impeller into a volute and is discharged through a diffuser for recovery of dynamic pressure. A floating close-clearance seal minimizes leakage into the bearing cavity. Sufficient inlet pressurization to prevent cavitation is provided by the jet condenser.

The rotating shaft is supported radially by two sets of tilting pad bearings, each comprised of four pads. Axial load, which is unidirectional, is supported by a set of tilting pad thrust bearings utilizing six pads with load equalizers. All bearings are lubricated by the liquid working fluid.

2.5.3.3 Turbine

The turbine selected for the flight system has the blade passage shape, blade height, and nozzle ring design experimentally determined to be most efficient of those tested during turbine rig testing. With the addition of a shroud on the turbine blades to reduce leakage losses and rim friction, a diffuser and close fitting side shrouds on the disc to reduce disc friction, it is predicted that the flight configuration will yield 69% efficiency at design conditions.

A cross-section showing the turbine arrangement for the flight system and the test rig are shown in Figures 2.5.3-1 and 2.5.3-2. A comparison of these figures indicate that the flight system turbine has side shrouds with smaller axial clearances than the test rig. The flight system has a shroud attached to the end of the turbine blades with two ridges that extend into honeycomb material that provide a labyrinth tip seal. The test rig turbine did not have a tip shroud attached to the blades. The flight version has a diverging diffuser compared to the straight annular passage used in rig testing.

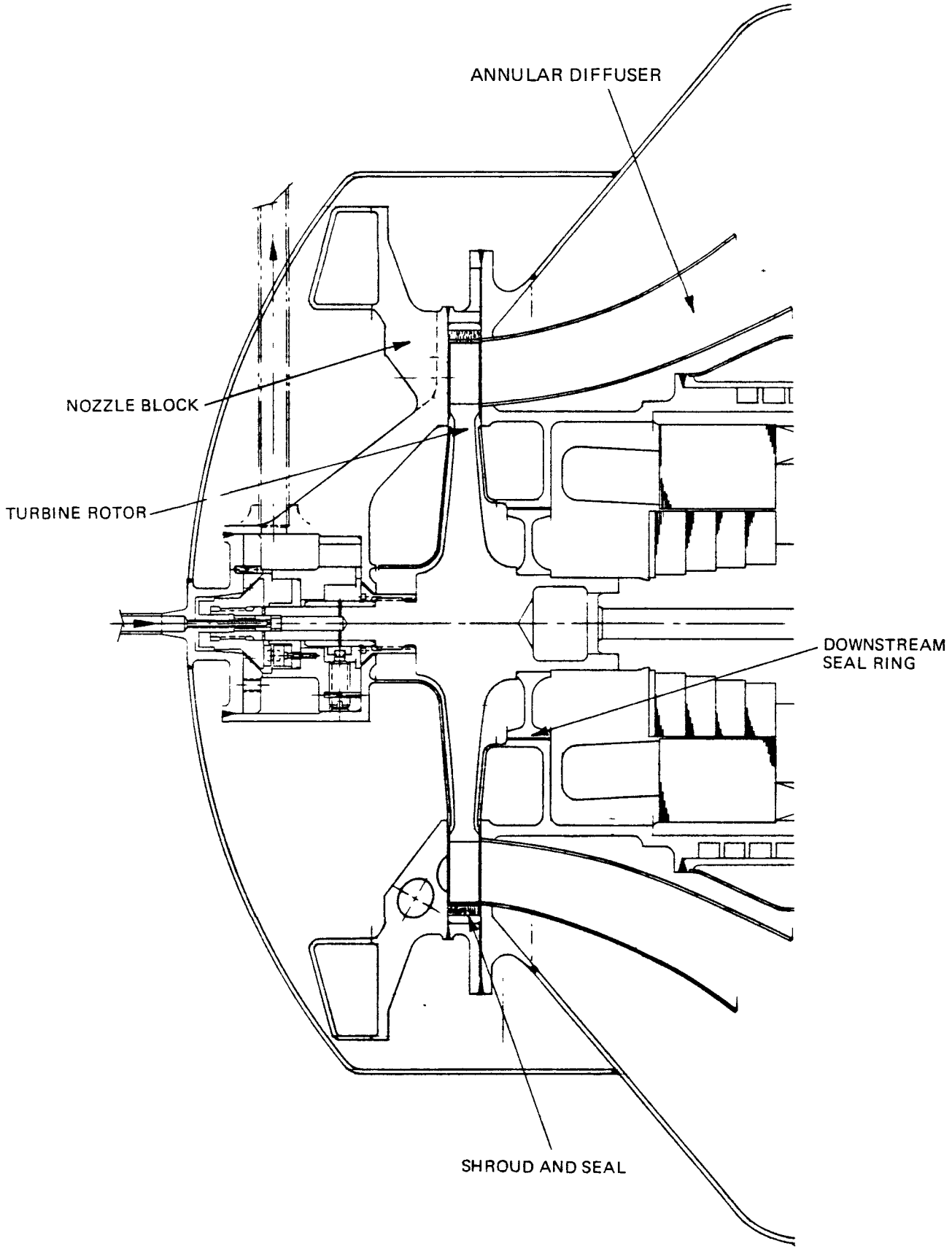

Figure 2.5.3-1 Flight System Turbine

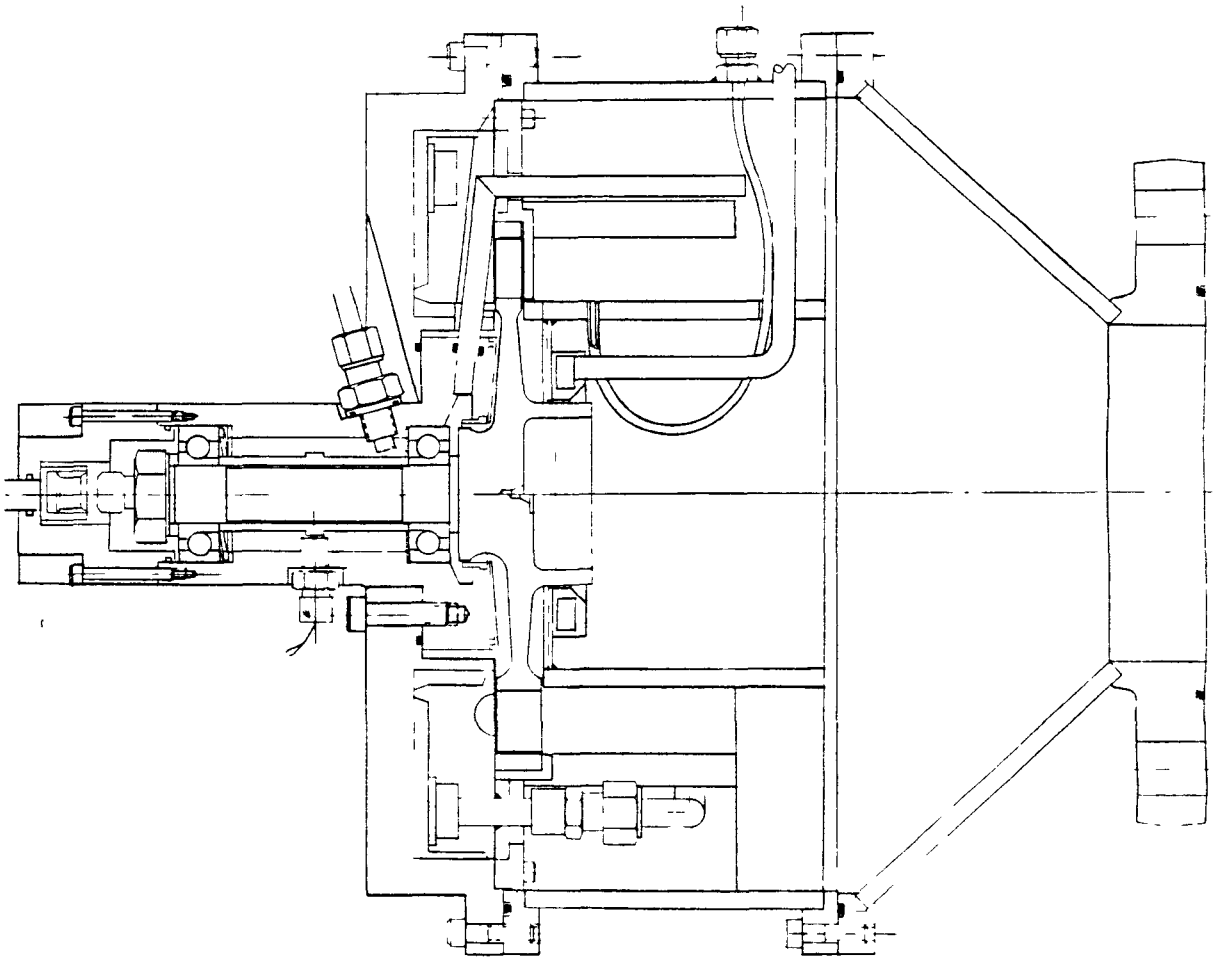

Figure 2.5.3-2 KIPS Turbine Test Rig

Test results (covered in subsection 3.5.3.3) indicated that the flight system geometry has a peak efficiency of 65% in the best rig configuration. An additional 4 points in turbine efficiency for the flight configuation are expected to result from the improved flight configuration; i.e. clearances, tip shroud and diffuser.

The diffuser has been conservatively estimated to result in an efficiency improvement of 1 percentage point.

The rig showed higher than expected drag losses (windage, pumping, and disc friction) in all tests indicating that the lack of close fitting side shrouds and the pumping losses between the blade tips and the unfilled honeycomb seal were contributing substantial drag. Reducing the test wheel drag to the predicted value for a closely shrouded wheel with a tip seal yields a predicted 4.7 percentage point improvement in test wheel efficiency.

A partial improvement of the rig hardware, substituting a solid ring for the honeycomb seal and adding a side shroud to the exit face of the wheel, resulted in a 2 percentage point improvement. Thus, it is reasonable to expect a 69% turbine efficiency when close fitting shrouds, a diffuser, and a tip seal are incorporated in the flight system design.

Additional improvements in the turbine efficiency are likely by continued experimental testing of variations of the constant area channel design for which only one configuration was tested in the GCS test program.

One obvious improvement is to decrease the blade wetted area and increase the hydraulic diameter of the blade channel. The blade Reynolds number based on hydraulic diameter will increase and the viscous friction loss will decrease. The improvement can be accomplished by reducing the number of blades in the wheel and the blade chord length. This modification also reduces the weight and inertia of the turbine wheel. Clearly, there is a tradeoff between minimizing viscous friction losses, maximizing blade Reynolds number (based on hydraulic diameter) and preventing flow separation due to increased blade loading. The turbine total to static efficiency is estimated to increase by 1 point if the chord of the constant channel width blade is reduced from 0.36 to 0.30 inches and the blade number reduced from 111 to 93.

An additional improvement in turbine efficiency of 1 point can be obtained by increasing the arc of admission from 66% to 100% since the blade pumping losses and scavenging losses are reduced for full admission. This would require a change in nozzle block for different power levels.

The contouring of the blade inlet angle to match the inlet gas angle (zero incidence) from hub to tip was analytically investigated. It was determined that it would only provide minute increases in turbine efficiency for constant channel blade geometry and the low Reynolds numbers experienced by the blades.

Experimental tests to further optimize the 0.30 inch chord blade designs and the low blade numbers are planned as part of the CRU advanced development testing of Phase II.

TURBINE DESIGN AND TRADE-OFFS

The turbine design includes the nozzles, the turbine blades and wheel and the diffuser between the turbine discharge and the entrance to the regenerator.

The turbine drives the alternator and feed pump and provides power for the mechanical, electrical and friction power losses in the CRU.

The vapor discharged from the exit of the turbine is diffused to a low Mach number by an annular diffuser. The diffuser exit then discharges the gas vapor into a larger annulus which is the inlet to the regenerator.

The KIPS turbine design was based on the performance requirements shown in subsection 2.6.4. The turbine speed selected was 33,680 rpm for nominal total inlet conditions of 57.0 psia and 650°F for superheated Dowtherm A vapor. The speed selection was based on an optimization of Combined Rotating Unit design. The inlet enthalpy is 396 BTU/lb for these conditions. The total to static pressure ratio and pitch diameter were specified as 558.3 and 5.95 inches. The ratio of the rotor speed (based on pitch diameter) to the spouting velocity U_p/C_o is 0.447, based on performance studies for maximum efficiency of an impulse rotor design.

The large pressure ratio results in supersonic Mach numbers at the nozzle exit and supersonic relative Mach numbers at the inlet to the rotor blading. A single-stage, partial admission, axial impulse turbine is used to satisfy the power requirements of the KIPS.

The convergent-divergent axisymmetric nozzles were designed using the real gas properties of Dowtherm A vapor. The nozzles are arranged to provide full admission when using 9 nozzles at the 2KW power level. The number of nozzles is reduced for other design power levels. Figure 2.5.3-3 shows the nozzle geometry and number of nozzles used for the reference power levels of 0.5, 1.3, and 2.0 Kilowatts.

The supersonic gas dynamic inlet conditions to the turbine rotor blade are governed by the nozzle exit conditions, the rotor speed, the rotor lap, and the wave systems propagating upstream due to the blockage of the blade row. The wave system, interacting with the geometry of the blades generates a unique incidence to align the inlet flow field with the blade suction surfaces.

A control volume analysis was developed to analyze these complex inlet flow conditions. The design technique used for the KIPS turbine is to balance the inlet flow field changes due to leading edge blade blockage with an increase in flow area by rotor-to-nozzle lap. The desired net effect is to maintain inlet flow conditions constant. Some trade-offs have to be made, however, to maintain a positive incidence angle on the blade suction surface at the tip and yet not exceed the blade starting margin at the hub.

The very low Reynolds number in the turbine blade passage must also be considered. While it is desireable to have long, gently curved passages and high blade solidity to minimize separation losses in the supersonic flow, these designs increase the wetted area and thus provide increased friction losses.

A detailed study and analysis of these effects led to a "supersonic"; i.e. converging-diverging blade passage shape with a 0.6 inch chord width for optimum performance. This design could be supported only by analysis as no test results for turbine of similar design were available. The blade profile for this design is shown in Figure 2.5.3-4.

Two alternate blades were also designed with a shorter chord of 0.360 inches to reduce viscous friction losses if the 0.60 inch chord did not perform up to expectation. All these blade designs were evaluated in the Sundstrand turbine inertia test rig to select the blade with the highest turbine efficiency.

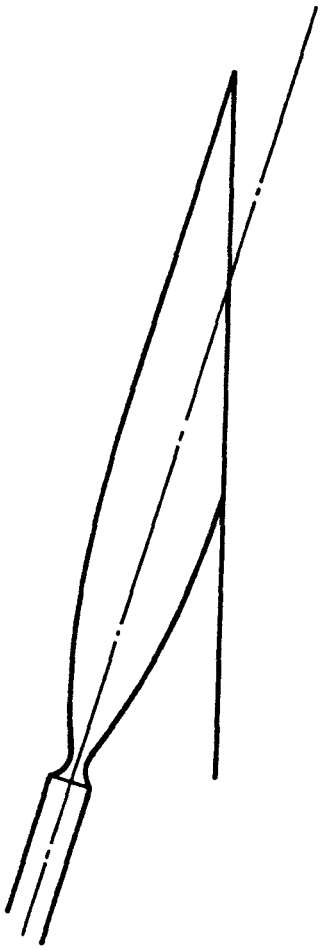

QUANTITY	0.5 KW	1.3 KW	2.0 KW
Nozzle Throat Area (Sq. In.)	.007547	.015093	.02264
Throat Diameter (In.)	.056594	.056594	.056594
Nozzle Exit Area (Sq. In.)	0.69197	1.38394	2.07590
Nozzle Exit Dia. (In.)	0.54192	0.54192	0.54192
Number of Nozzles	3	6	9
Nozzle Angle (Deg.)	15.0	15.0	15.0
Nozzle Total Pressure (psia)	53.2	57.0	61.0
Mass Flow (lbm/sec)	.0140	.030	.048
Arc of Admission	.320	.640	.960

Figure 2.5.3-3 Turbine Nozzle Configuration

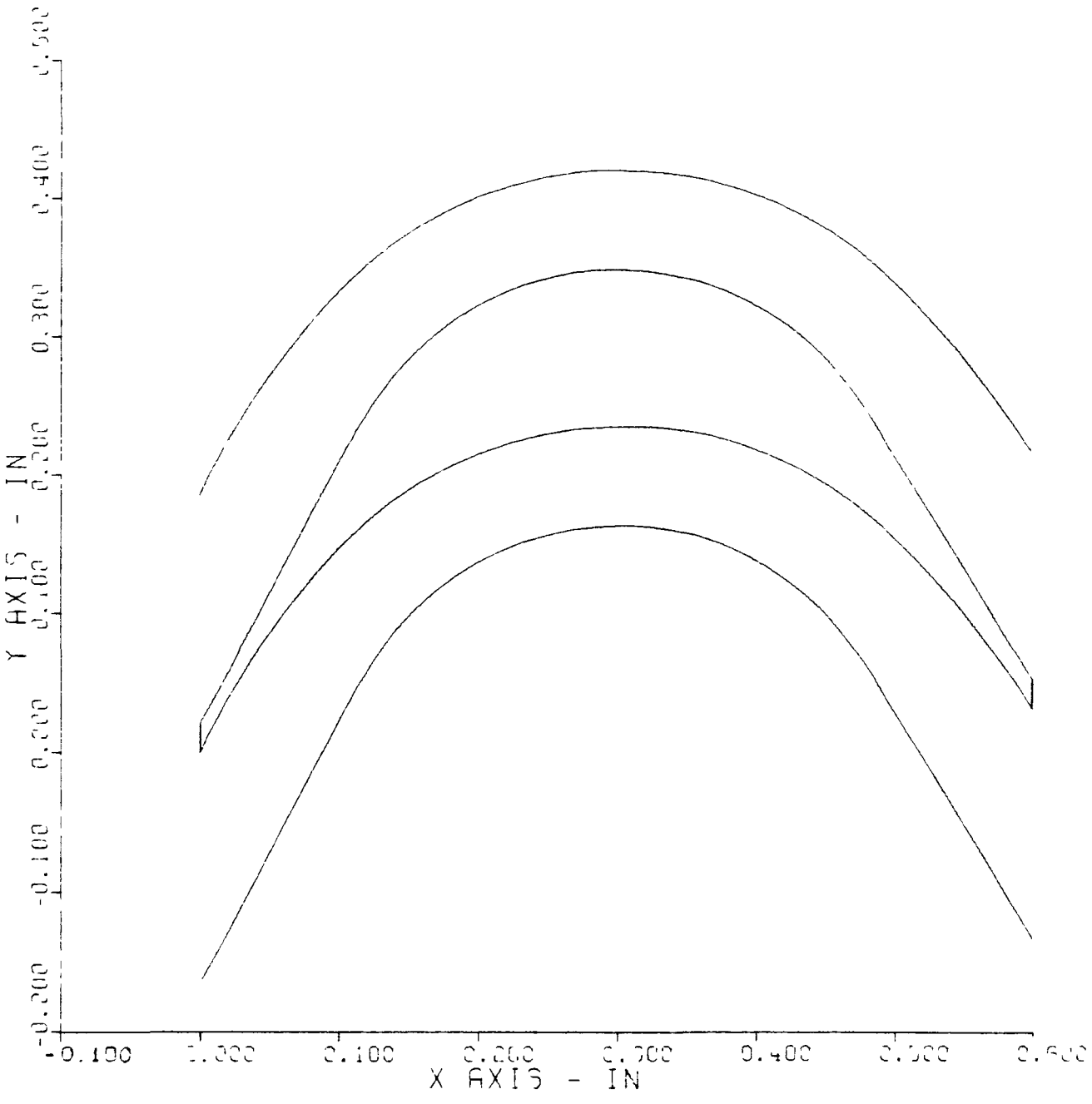

Figure 2.5.3-4 Supersonic Long Chord Blade

The same design system that was used to design the 0.60 inch chord supersonic blade was also used to design a "short chord" blade that had zero starting margin, a pressure surface contour that is on the verge of turbulent separation and an axial blade chord that results in the minimum machinable blade throat based on Sundstrand turbine blade experience. This blade has a chord of 0.36 inches. The blade profile for this short chord blade is shown in Figure 2.5.3-5.

The other alternate blade design considered a blade with the same chord; i.e. 0.36 inches, but a constant channel width rather than the varying channel width that was used for the two previous blade designs. This design permitted a direct comparison of the supersonic blading with constant channel (subsonic) blading. The constant channel width blade is shown in Figure 2.5.3-6.

The blade geometries of these three designs are summarized in Table 2.5.3-A. Note that the long chord blade has the largest length Reynolds number and hydraulic Reynolds number while the constant channel width short chord blade has the lowest length Reynolds number. The short chord with the varying channel width has the lowest hydraulic Reynolds number.

The trade-off of these designs could not be conclusively made analytically and therefore was performed by conducting tests of the three configurations. Other areas of uncertainty included the nozzle spacing and the rotor lap. These parameters were also varied on the test rig.

The blade height of each turbine rotor was reduced in four steps during the test program to determine the optimum blade-nozzle overlap. The optimum blade height is a function of the turbine hydraulic efficiency, mass flow rate, exit flow blockage, exit static pressure, exit relative flow angle and arc of admission.

In addition to evaluating rotor characteristics, two nozzle ring designs were evaluated to resolve conflicting data from previous experiments. The arc of admission was varied to produce an overlap, or spacing, between nozzles. The overlapped nozzles had an arc of admission of 64% for six axisymmetric nozzles and were referred to as merged nozzles. The merged nozzles were expected to result in higher turbine efficiencies since they minimized the wake systems between nozzles entering the turbine rotor. Some experimental data also indicated this conclusion. The spaced nozzles had an arc of admission of 66% for six axisymmetric nozzles. These nozzles were tested because other experimental data indicated they have higher turbine efficiencies than the merged nozzles. Figure 2.5.3-7 shows the two nozzle configurations.

The nozzle throat, contour and exit diameter were the same for both configurations.

The results of this trade-off study gave a clear indication that the spaced nozzles were superior to merged nozzles, that the constant area channel was superior to the "supersonic" design and that the blade nozzle overlap should be larger than analytically determined. Details of the testing and results are contained in subsection 3.5.3.3.

These results for the maximum efficiency turbine were incorporated into the FSCD.

MECHANICAL CONSTRUCTION

The turbine wheel consists of an Inconel 718 disc with integral impulse blading and a Hastelloy X shroud which is brazed to the blade tips. The disc is first rough machined and then blades are cut by an ECM process. The ECM process is controlled to obtain a smooth surface finish. The wheel OD is then machined and the shroud installed and brazed.

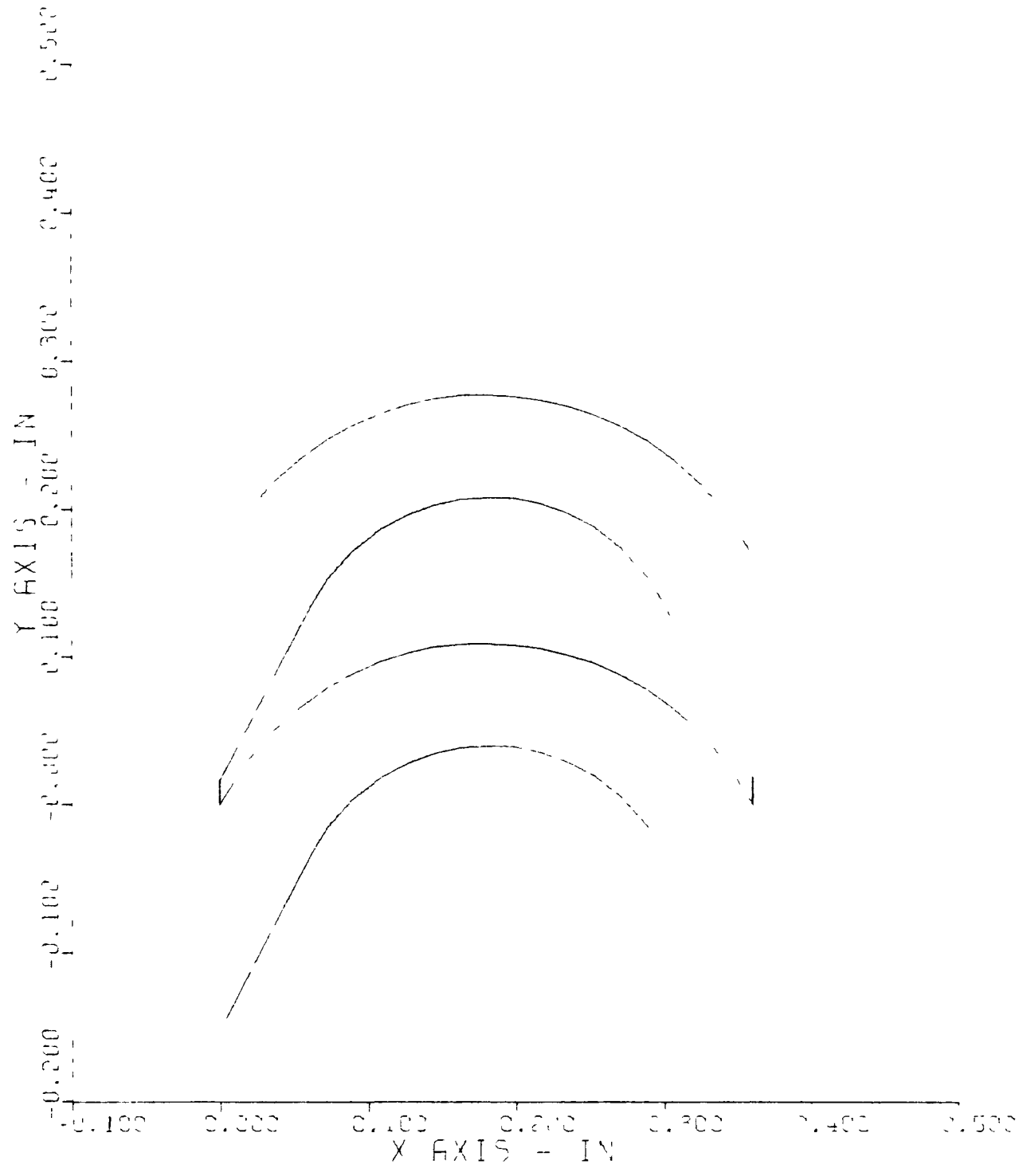

Figure 2.5.3-5 Supersonic Short Chord Blade

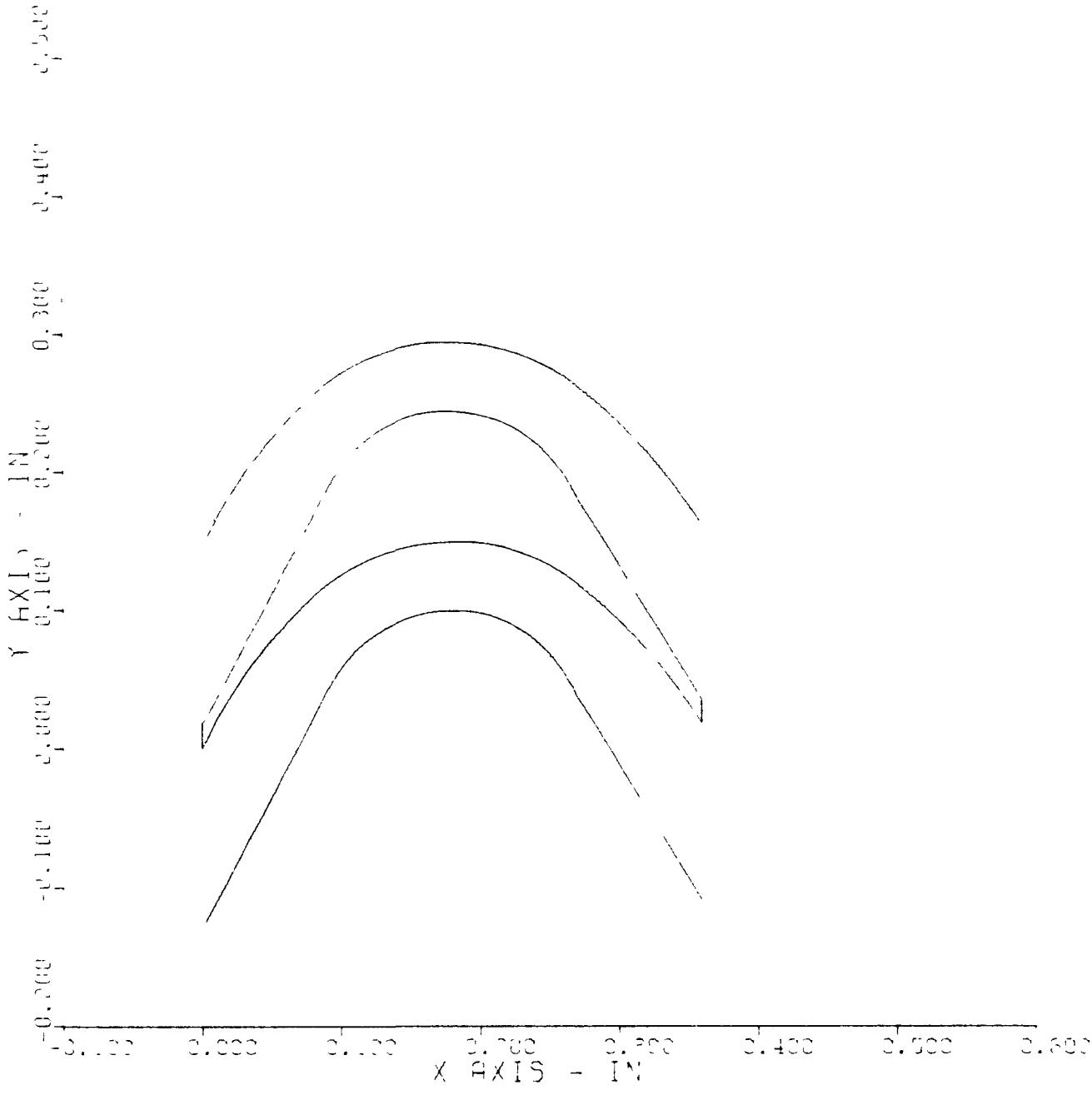

Figure 2.5.3-6 Constant Channel Width Blade

Table 2.5.3-A Blade Geometry at Pitch Line

PARAMETER	LONG CHORD	SHORT CHORD	SHORT CHORD
CHANNEL WIDTH	VARYING	VARYING	CONSTANT
AXIAL CHORD (IN)	0.60	0.36	0.36
ASPECT RATIO	1.083	1.806	1.806
MINIMUM BLADE THICKNESS (IN)	0.0095	0.0078	0.0080
MINIMUM THICKNESS TO CHORD	0.0158	0.0217	0.0222
MAXIMUM THICKNESS TO CHORD	0.1887	0.2631	0.275
LEADING EDGE BLOCKAGE	0.112	0.117	0.103
TRAILING EDGE BLOCKAGE	0.097	0.104	0.103
INLET AREA TO MINIMUM AREA	1.10	1.22	1.00
MINIMUM ROTOR AREA TO NOZZLE THROAT AREA	200	178	212
BLADE AREA (IN^2)	0.0467	0.0218	0.0258
BLADE PERIMETER (IN)	1.741	1.106	1.038
NUMBER OF BLADES	101	129	111
SOLIDITY	3.24	2.48	2.14
BLADE INLET ANGLE (DEG)	27.35	27.35	27.35
BLADE EXIT ANGLE (DEG)	31.79	31.34	27.35
BLADE TURNING ANGLE (DEG)	120.86	121.21	125.3
BLADE REYNOLDS NUMBER AT EXIT (LENGTH)	1.397×10^4	0.88×10^4	0.83×10^4
HYDRAULIC REYNOLDS NUMBER AT INLET	2900	2310	2687

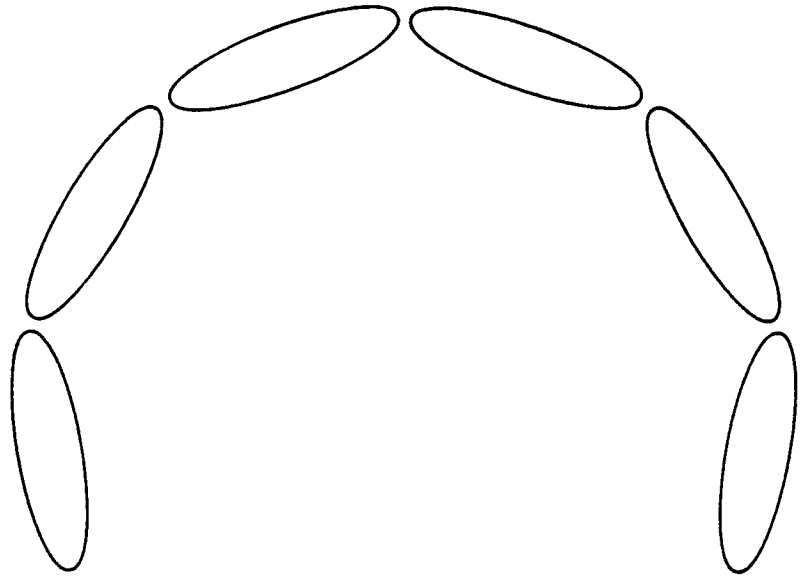

SPACED NOZZLES

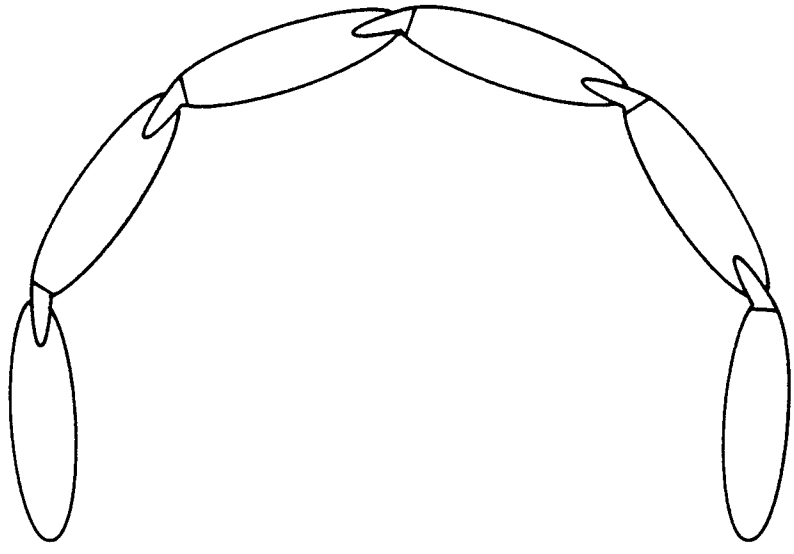

INTERSECTING OR MERGED NOZZLES

Figure 2.5.3-7 Nozzle Configurations

After assembly of the turbine wheel to the alternator assembly, all of the critical diameters are finish machined to size. The rotor is then balanced and given a final inspection to verify integrity.

A manufacturing flow diagram for the turbine assembly is shown in Figure 2.5.3-8.

RELIABILITY AND STRESS

To obtain a highly reliable design of the turbine wheel, the allowable stresses are derated both for temperature effects and by a stress ratio which reflects a maximum failure probability of 1×10^{-9}.

Several types of analysis were performed to determine the effects of rotation with superimposed temperature gradient and vibration in the disc, blades and shroud. Temperature distributions in the disc during startup and steady state conditions are shown in Figure 2.5.3-9.

The turbine disc stresses were obtained at normal operating speed, maximum normal speed during frequency wild operation and worst case conditions of maximum overspeed with a superimposed worst case temperature gradient. See curves a, b, and c respectively. The resulting margin of safety for each case was 2.56, 0.38 and 0.20 respectively.

Blade natural frequencies were then analyzed using a finite element approach (ANSYS). A typical model is shown in Figure 2.5.3-10. The results were plotted on the Campbell diagram of Figure 2.5.3-11. No resonance conditions occur in the operating speed range of the turbine. The blade root margin of safety at maximum worst case speed is 0.55. The blade has infinite fatigue life at normal rated speed.

Analysis of the shroud indicated that local yielding would occur under maximum speed conditions. This situation is normal for a shrouded design. The margin of safety based on ultimate strength is 1.63 at rated speed and 0.6 at maximum speed. Since the frequency wild mode occurs only during checkout, launch and orbital insertion of the KIPS, high speed operation would occur during only a small fraction of the seven year mission. The fatigue life of the shroud during speed excursions from design to overspeed is in excess of 10^5 cycles, far beyond what the system will experience during frequency wild operation.

2.5.3.4 System Pump

The system pump is located on the turbine shaft at the opposite end from the turbine wheel. Its function is to provide high pressure fluid through the regenerator and vaporizer to the turbine nozzles and through the radiator to the jet condenser.

TRADE-OFFS

Two types of pump impellers were considered for the KIPS. These were the swept vane type and drilled port type. The configurations are shown in Figure 2.5.3-12 and 2.5.3-13. The following rationale was used in selecting the swept vane type impeller.

SAFETY AND RELIABILITY

Both designs are of a one piece construction. Due to their sizes, the stress levels in the impellers are very low. Hence, both parts are equally acceptable.

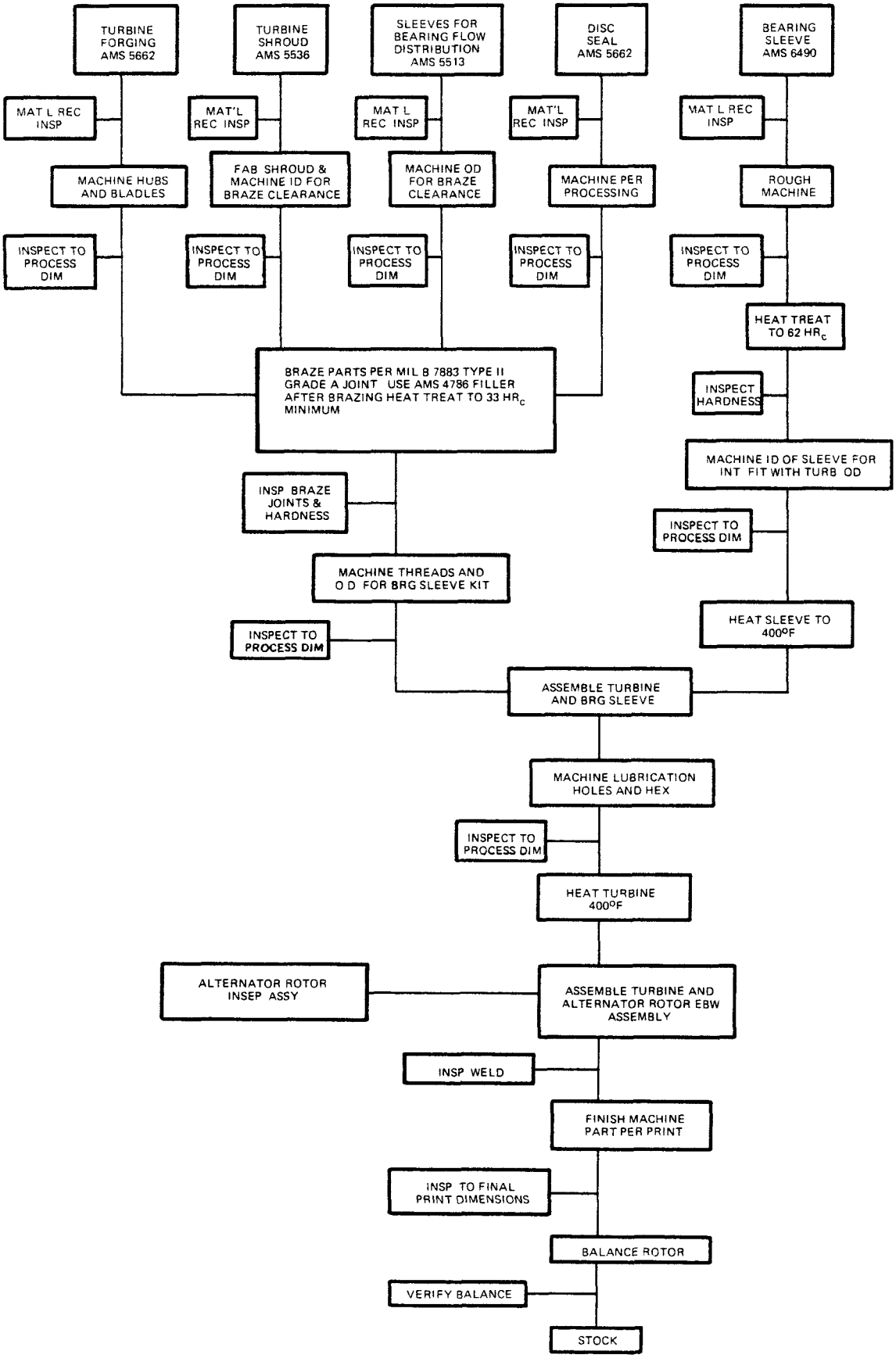

Figure 2.5.3-8 Turbine Manufacturing Flow Diagram

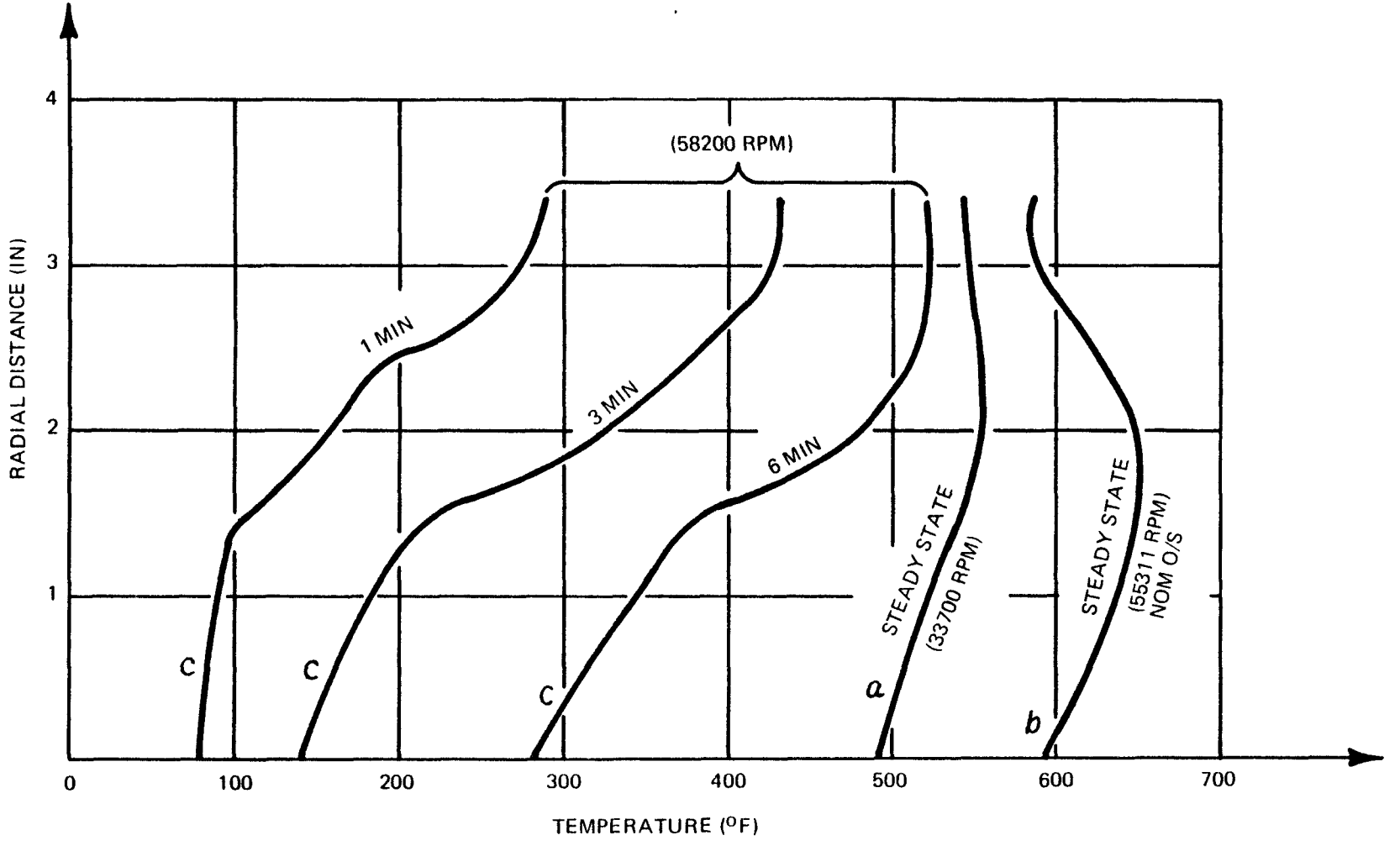

Figure 2.5.3-9 Temperature Distribution

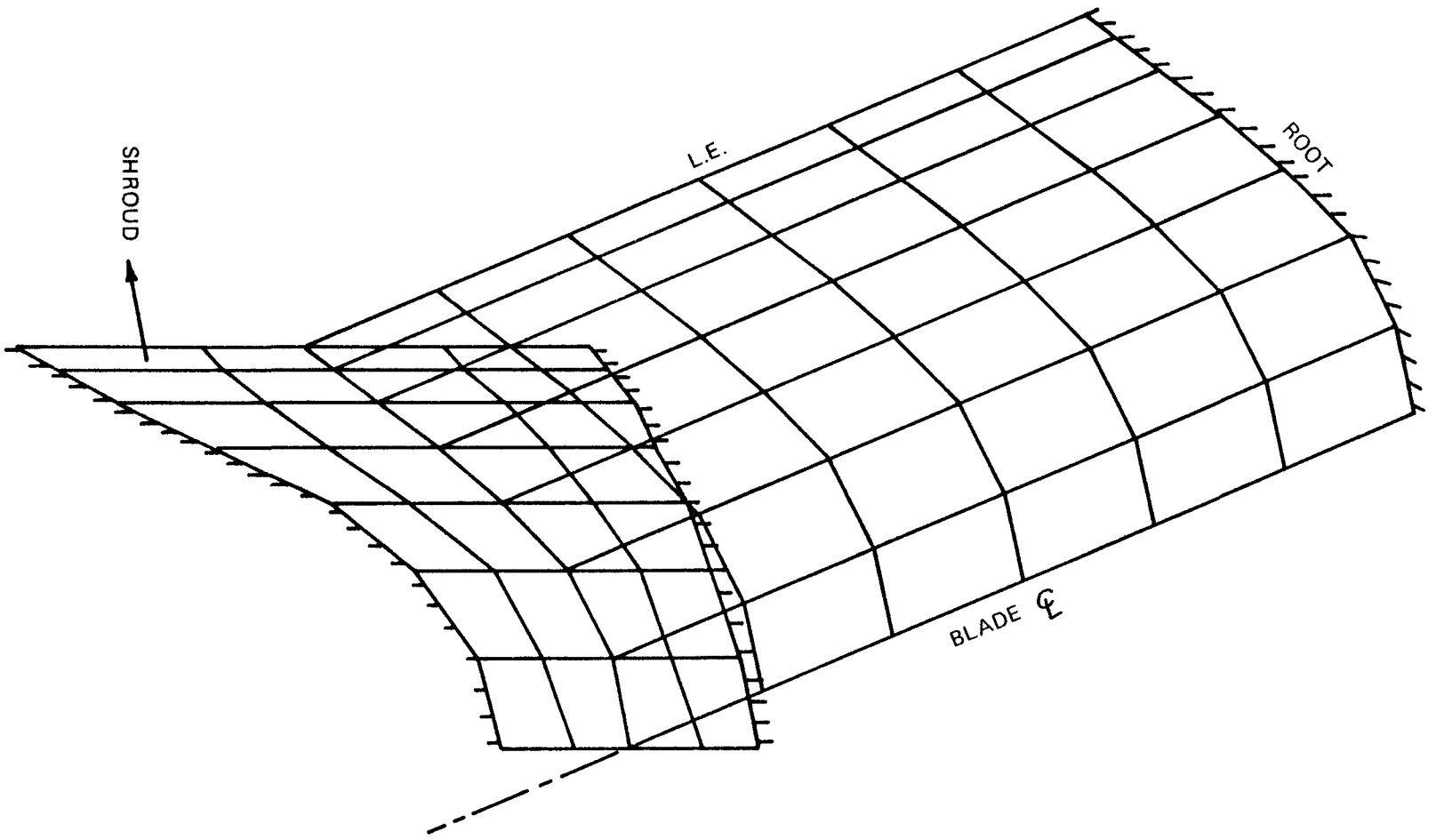

Figure 2.5.3-10 KIPS Turbine Finite Element Model

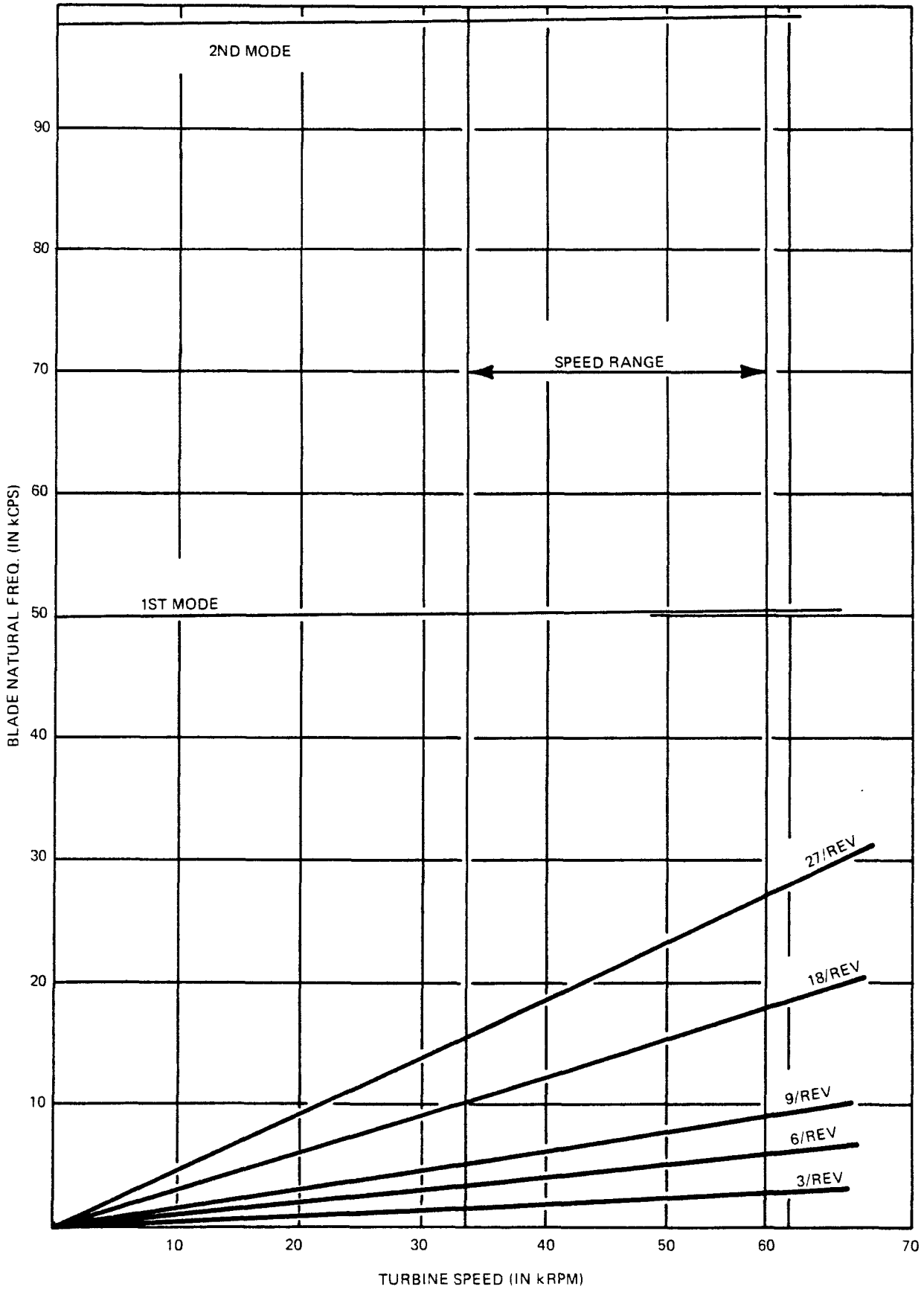

Figure 2.5.3-11 KIPS Turbine Blade Natural Frequencies

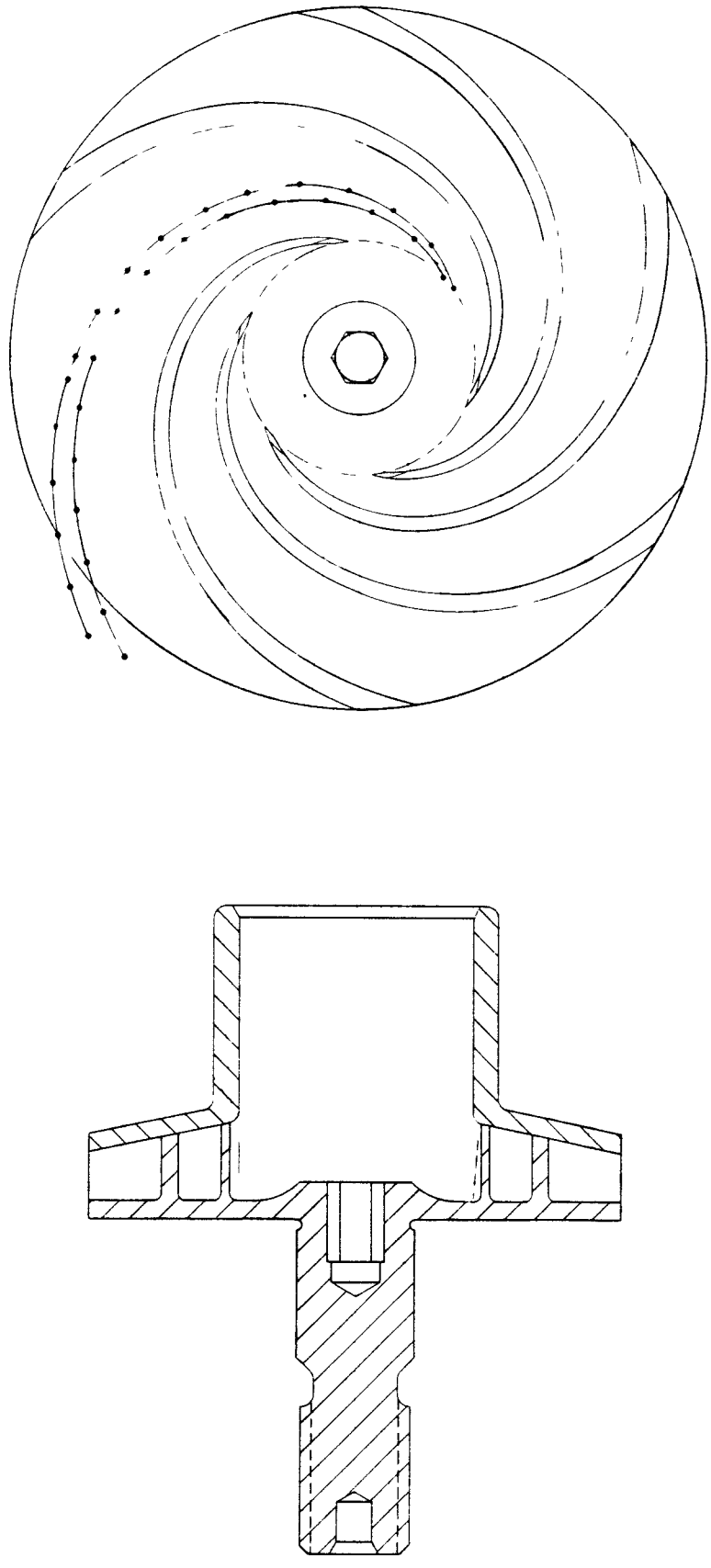

Figure 2.5.3-12 Swept Vane Impeller

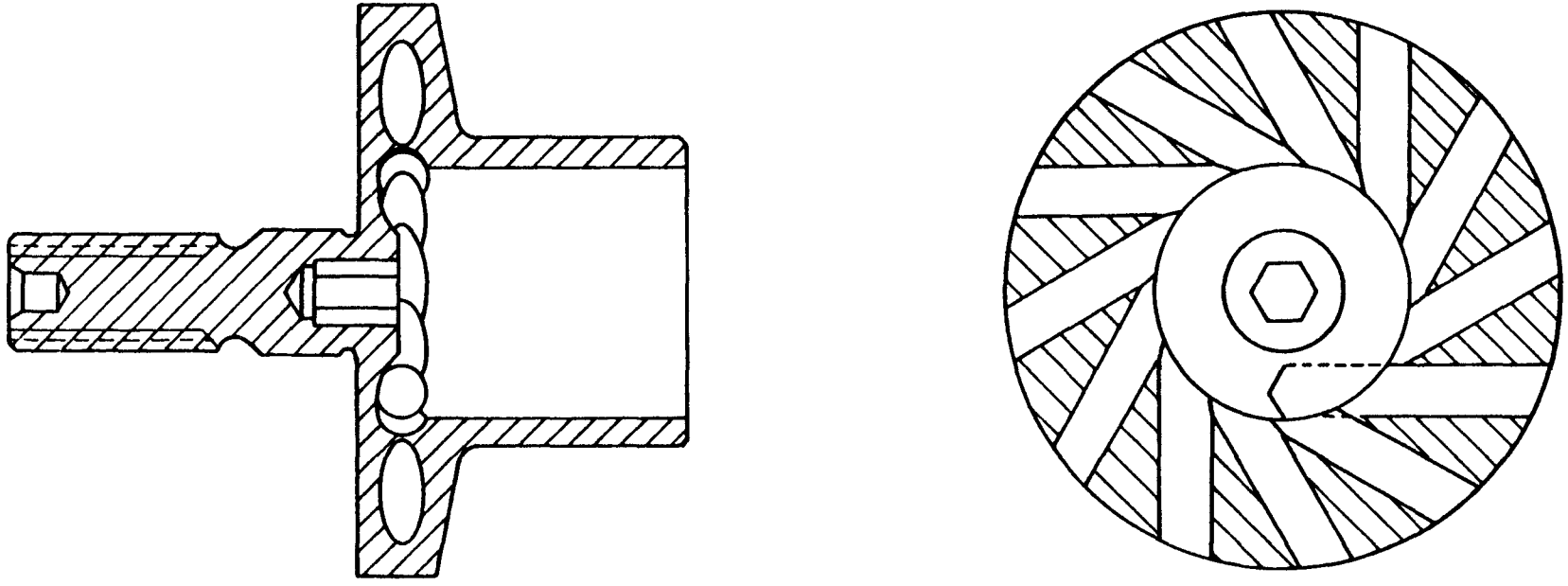

Figure 2.5.3-13 Drilled Port Impeller

PERFORMANCE

GDS component testing has shown the swept vane type impeller is more efficient than the drilled port type.

RISK AND PRODUCTABILITY

Both types of impellers are manufacturable and inspectable with present state of the art.

WEIGHT

Because of the small size of the pumps, weight was not considered as a factor in the tradeoffs.

DESIGN AND OPERATIONAL FLEXIBILITY

The drilled type impeller is easier to modify than the swept vane type impeller, should changes to the system be required, i.e. for the 500 or 2000 watt versions of the KIPS.

303 Stainless, 304 Stainless 6A1-4V Titanium, 6061-T6 Aluminum, Haynes 25 and 17-4PH were considered as materials for fabrication of the impeller. 17-4PH was selected based on the following rationale. The major considerations were as follows:

RELIABILITY AND EXPERIENCE

All of the materials are wrought products. Sundstrand has successfully made pump impellers out of all of the alloys listed; however, from a quality standpoint 17-4PH in a cast version has been the most widely used and the Haynes 25 and 304 least.

RISK

No difference in risk is seen in the various alloys which all have good material compatibility. The only possible exception is the Haynes 25 due to nuclear radiation effects.

JOINING

Due to the small size and intricate blade/vane shape, a precision brazement is called for. Titanium is difficult to braze. The aluminum alloy (6061) can be readily brazed; however, since the brazing is done so close to the melting point, it is more difficult to prevent distortion.

ANALYSIS

Figure 2.5.3-14 shows test results of the 0.668 inch diameter impeller. The figure also shows pump requirements for the FSCD. Based on the test results of the 0.668 diameter pump, the precise sizing of the swept vane impeller and volute for the FSCD unit could be defined.

Design requirements used were as follows:

Head = 65 PSI
Flow = 2.28 GPM
Speed = 33680 RPM

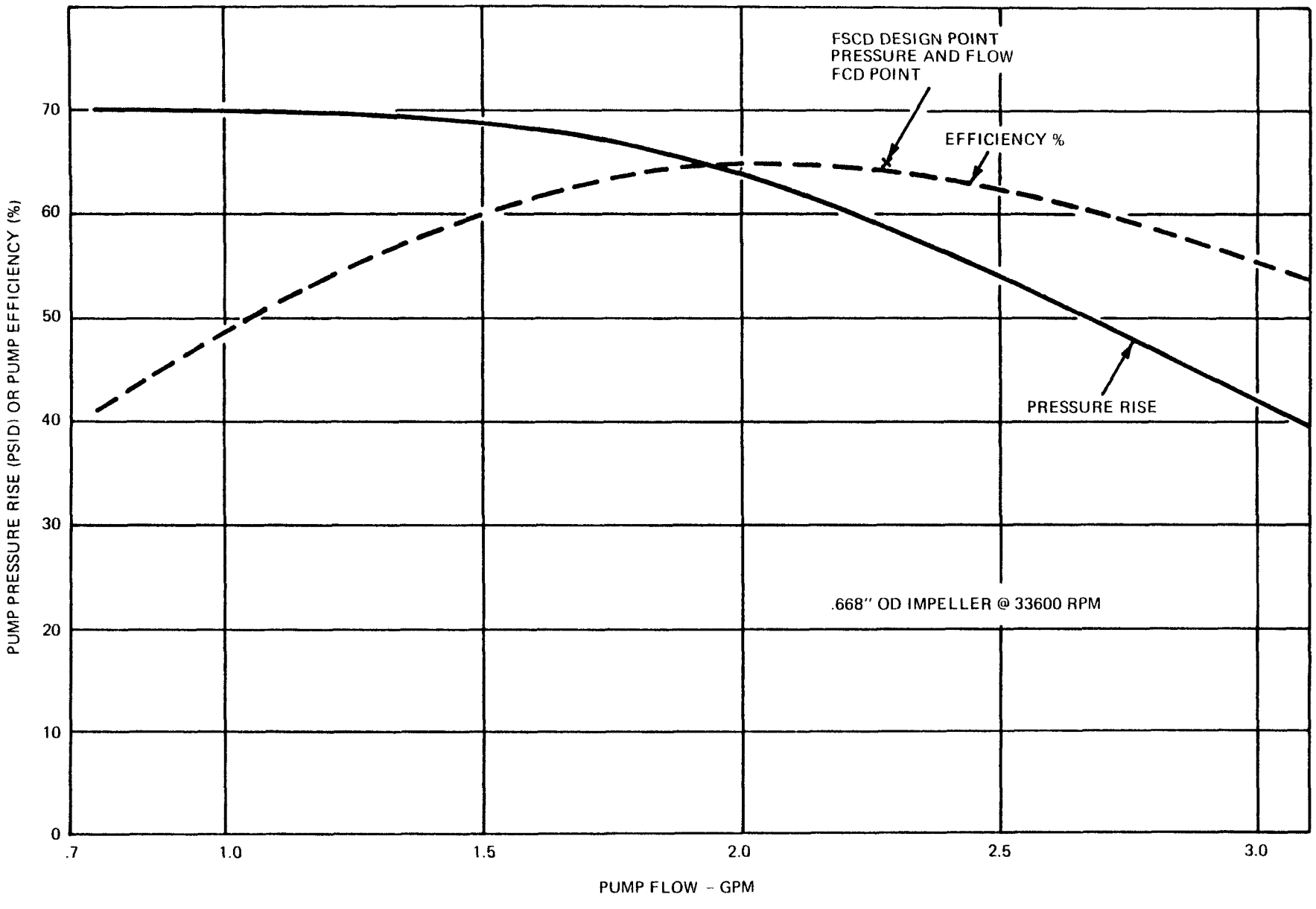

Figure 2.5.3-14 Pump Performance

The pump and volute size for the FSCD are as follows:

Impeller OD = 0.686 inches.
Impeller port width at OD = 0.0455 inches.
Volute throat size = 0.107 inches x 0.175 inches.
Recirculation flow = 0.004 GPM
Leakage flow = 0.002 GPM.
Axial thrust = 1.1 pounds.

STRESS ANALYSIS

Because of its physical size, the stresses in the impeller are quite low and result in more than adequate margin of safety required for 1×10^{-9} failure probability.

Critical Characteristic Selection

Characteristic	Location	Value	Comments
Tolerance	Volute throat	± .002	The size of volute throat in conjunction with impeller exit port width and O.D. determine where the peak efficiency will occur. By controlling these dimensions the variation in performance from unit to unit is minimized.
	Impeller OD	± .001	
	Impeller exit port width	± .001	
	Impeller OD at inlet	± .0001	Tight control minimizes recirculation and leakage losses and improves pump efficiency.
	Seal ID	± .00015	
	Impeller OD at mounting	± .0001	
Hardness		35-42 Rc	Gives high strength.

FABRICATION AND INSPECTION

The Manufacturing flow diagram for the pump is shown in Figure 2.5.3-15.

2.5.3.5 Alternator and Rotor

CONFIGURATION

The KIPS Flight System alternator is a four pole homopolar inductor device. Selection of this type of alternator was dictated by the high operating speed and long service life of this application. A homopolar inductor alternator contains no rotating electrical windings, slip rings, cages, magnets, etc. All electrical components are contained in the stator and are not subjected to rotational stresses and vibrations. This eliminates winding failures commonly associated with rotational loads.

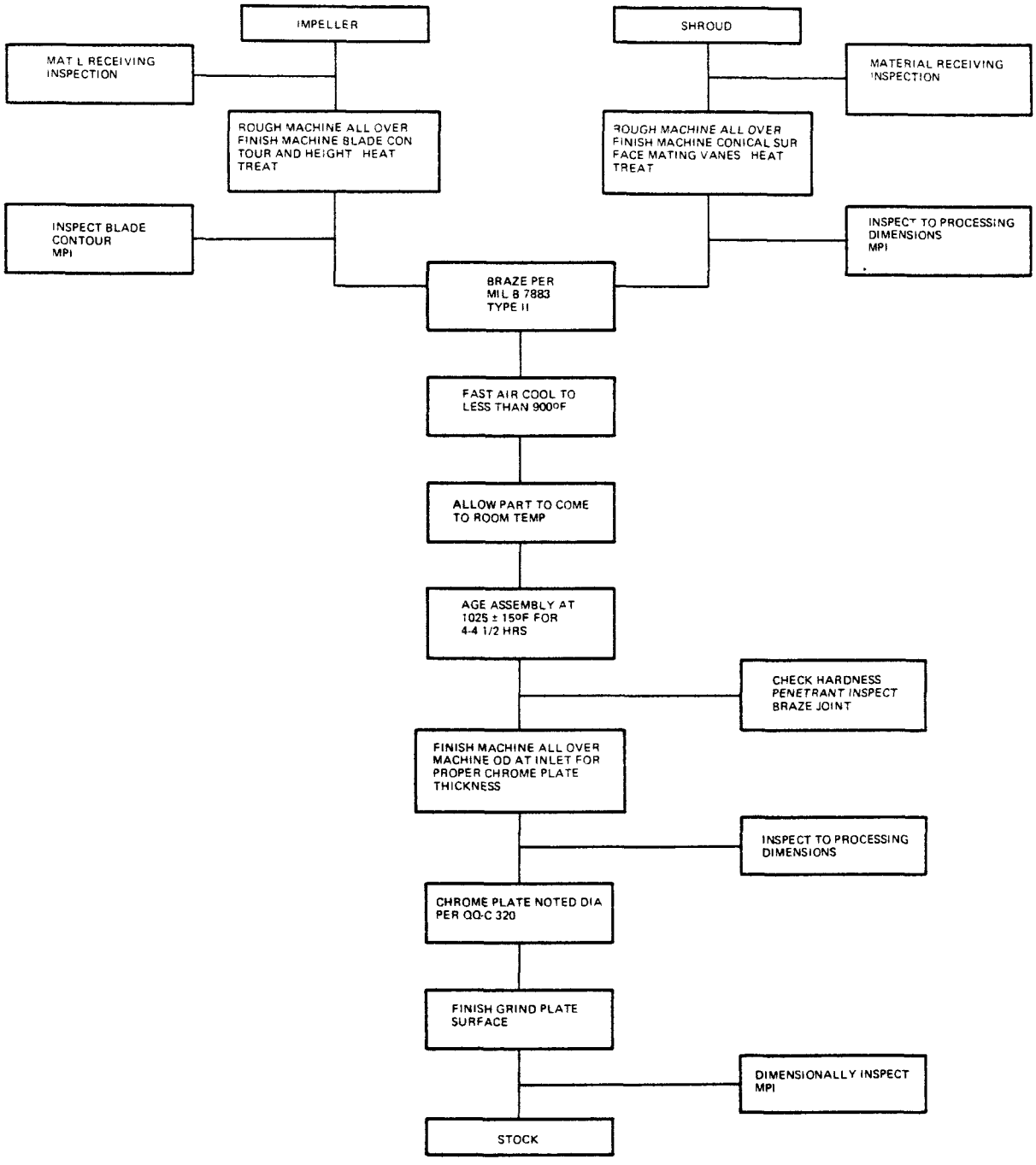

Figure 2.5.3-15 Fabrication and Inspection Process of System Pump

The rotor of the flight system alternator is an integral part of the combined rotating unit (CRU), as shown in Figure 2.5.3-16. The rotor configuration is a typical four pole, homopolar, inductor design with two poles of like polarity at each end, the ends displaced 90° (180 electrical degrees) from each other and connected by means of a magnetic shaft. To control pole face losses, the rotor is designed with laminated pole structures. Rotor laminations are made from fully processed AISI grade M-19 electrical steel sheet, 0.014" thick. They are electron beam welded to a shaft made from 8620 steel.

The stator assembly consists of a magnetic yoke containing the field coil sandwiched between two cores, which contain the armature windings. The yoke is a cylindrical piece of low carbon steel (1008) fully annealed to obtain maximum permeability. Each stator core is a stack of laminations containing 24 slots on its inner periphery. The laminations are made from 3% silicon sheet steel (Magnesil-N) and are 0.005" thick. This material was chosen for its high permeability, its low core loss characteristics, and its ability to produce a high resistance oxide surface coating which is essential to control eddy current iron losses and maintain high efficiency.

The stator winding is a conventional three phase, WYE connected, 60° phase belt winding. Because of the stringent efficiency requirements, the winding was designed for minimum losses. Current density was kept below 1620 amps/in^2 at rated load and measures were taken to minimize eddy losses. These can be considerable when the stator slot is relatively deep and the alternator output frequency is high. To reduce eddy losses, the stator conductors are made up of 31 strands of AWG No. 20 insulated wire each, and the strands are transposed (twisted) in the end turn area such that those located at the bottom of one slot will be at the top of the next slot. In this fashion, all strands have nearly equal reactances and the eddy current producing voltages are minimized. Because specific output voltage wave form requirements were not defined, the stator winding was designed with a full pitch and minimum distribution to obtain maximum possible output with minimum field excitation.

The field coil of the alternator is a simple toroid of 375 turns of DuPont HML insulated AWG No. 19 wire wound on an aluminum bobbin. As the coil is wound, DuPont ML varnish per MIL-L-24092B is brushed on each layer of wire and then is cured to hold the winding together during handling, prior to insertion into the magnetic yoke. The coil is insulated with double layers of 0.005" thick Kapton sheet. Once installed in the stator assembly, the coil is snugly held on both sides by the stator cores, the yoke on the O.D. and the aluminum bobbin on the I.D.

TRADE-OFF STUDIES

To meet the high efficiency requirements of the FSCD, in-depth studies were carried out to select the best materials for use in the alternator. For each magnetic component, several magnetic materials were considered. Considering all the desired features, the selections are described below.

For the rotor shaft and laminations, 8620 and M-19 steels, respectively, received the highest rating and these materials are being used.

For the stator yoke, ARMCO ingot iron would have been desirable; however, this material is no longer commercially available in the size and shape required, and the second choice 1008 steel is being used in the flight system and GDS alternators. The slight difference in magnetic properties is not enough to affect alternator performance appreciably.

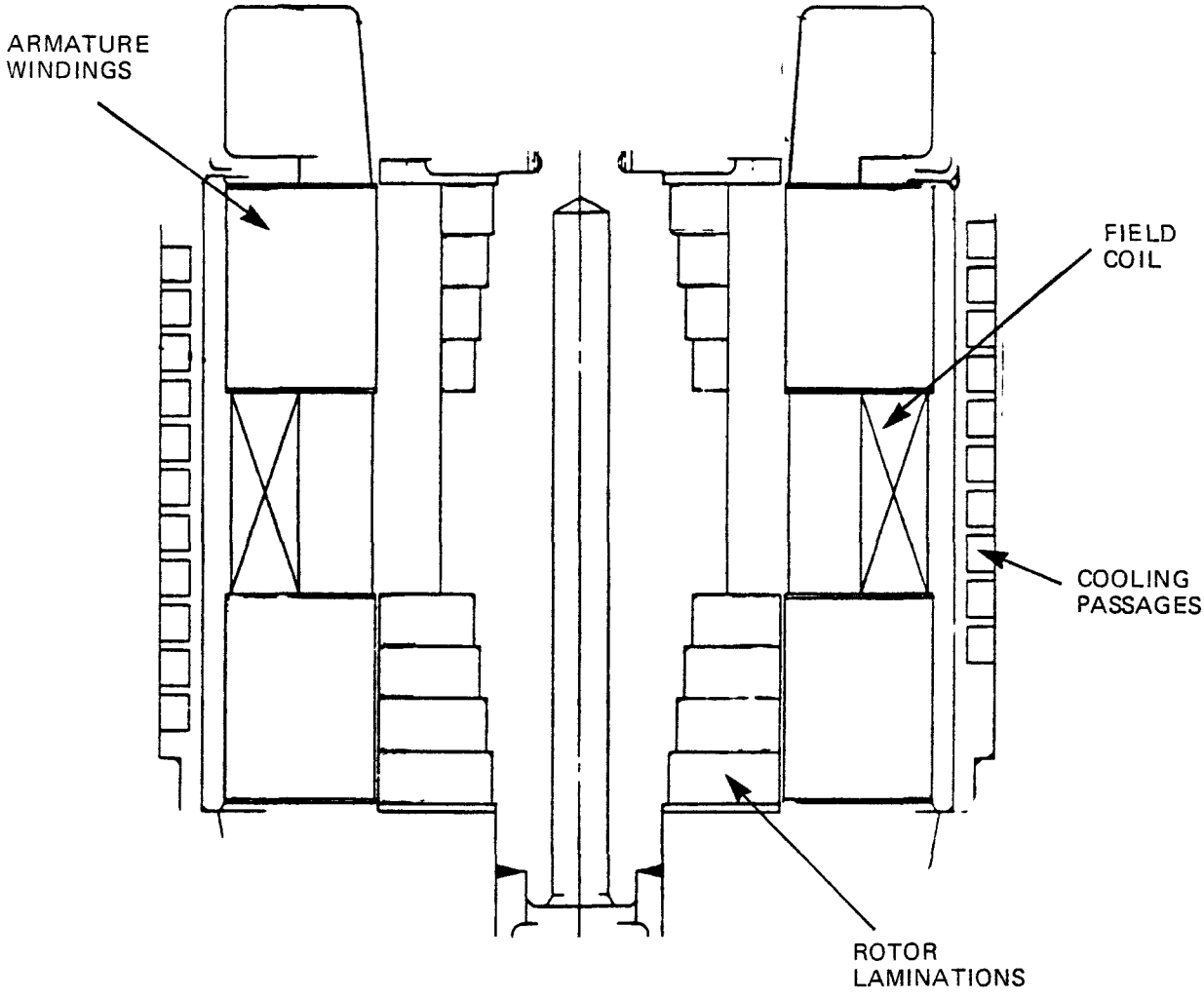

Figure 2.5.3-16 Alternator

For the stator lamination material, AL 4750 alloy was originally selected primarily for its high permeability at low induction levels and low core loss properties. However, the material's strong resistance to oxidation by conventional means resulted in excessive losses and low efficiency as demonstrated by component tests. Therefore, thin laminations of silicon steel (Magnesil-N), with an effective oxide coating were selected.

ELECTRICAL INSULATION

The materials for the FSCD alternator insulation system were selected on the basis of dielectric strength, long term compatibility with Dowtherm A and best life versus temperature characteristics.

With the exception of teflon sleeving and fiberglass tie cord, the entire KIPS alternator insulation system consists of polyimides in various forms (see Table 2.5.3-B). Polyimides possess the greatest dielictric strength and best life versus temperature rating of all known organic insulation materials.

SIZING AND PERFORMANCE

The flight system alternator is nominally rated at 1.56 KVA, 22.5 volts line-to-line, 40 amps, 0.93 to 1.0 power factor. It has a continuous thermal overload capability of 2.5 KVA; with added cooling, the electromagnetic capacity is well over 3 KVA.

The size and weight of the alternator were determined primarily by efficiency, thermal and service life considerations. These parameters are inherently interrelated: higher efficiency results in lower losses, lower losses result in lower operating temperatures, and lower temperatures result in longer insulation life.

A principal factor affecting alternator iron losses is the magnetic flux density. To maintain low iron losses, the flux density must be kept relatively low; this results in larger iron components and increased weight. Low flux densities also result in lower field excitation requirements, further increasing the efficiency. Table 2.5.3-C lists the calculated flux densities in the various magnetic components of the KIPS flight system alternator as compared with the typical flux densities at which the materials are often used in applications where efficiency is not a primary consideration. All calculations were made at rated load and nominal speed.

Alternator copper losses are also related to the amount of copper used in a particular winding design. In the flight system alternator, both the armature and field windings contain sufficient copper to maintain low current densities and therefore low copper losses. At rated load, the current densities are 1620 amps per square inch in the armature and 1980 amps per square inch in the field windings. In typical commercial applications, current densities of 3000 to 8000 amps per square inch are used, and in some aircraft applications, current densities well over 10,000 amps per square inch are common.

MECHANICAL CONSTRUCTION

The alternator rotor is assembled by welding and becomes an inseparable one piece assembly. It contains no mechanical fasteners or adhesives.

The stator laminations are assembled into cores using Scotchcast 265 epoxy adhesive. After grinding, the cores are fitted into the yoke with a 0.001" diametral interference fit.

Table 2.5.3-B KIPS GDS Alternator Insulation System

Component	Trade Name	Material
Magnet Wire	DuPont Heavy ML Film	Double Coat Polyimide Varnish
Slot Cells	DuPont Kapton Sheet .005" Thick	Polyimide Sheet (Flexible)
Field Coil Ins.	DuPont Kapton Sheet .005" Thick	Polyimide Sheet (Flexible)
Tie Cord	Varglas Non-Fray Sleeving	Braided Fiberglass Sleeving
Slot Wedges	Dixon Corp. Meldin P.I. 0.025" Thick	Polyimide Sheet (Rigid)
Impregnating Varnish	DuPont Pyre ML Varnish	Polyimide Varnish
End Leads	Teflon	

Table 2.5.3-C Alternator Flux Densities

	Flux Density	(K-lines/in^2)
Component	KIPS Alternator	Typical Values Used in Commercial Applications
Stator Teeth	45.4	90-100
Stator Core	19.2	80-90
Stator Yoke	43.3	70-90
Rotor Pole	21.9	80-90
Rotor Shaft	28.6	70-80

The field coil is wet wound, using a polyimide varnish. After curing, the varnish provides adhesion between wires and gives the coil rigidity. Once inserted in the yoke, the coil is supported by the two cores on the ends, the yoke on the O.D., and an aluminum bobbin on the I.D.

The armature windings are held within the cores by the semiclosed slot design. The conductor strands are larger than the slot openings so there is no possibility of a wire escaping out of the slot into the air gap. Because of this slot design, no slot wedges are needed. The armature winding end turns are given rigidity by dipping in polyimide varnish and curing.

The entire alternator stator assembly contains only one brazed connection -- the armature neutral where all three phase windings are joined together. The armature and field winding end leads contain no brazed joints since they are merely extensions of their respective windings.

The alternator stator is held in its housing by means of a shrink fit. No mechanical fasteners are used in the alternator assembly.

MAGNETIC FIELD

The KIPS alternator contains approximately 13.9 pounds of magnetic material (iron), parts of which are saturated to varying degrees of induction depending on the magnitude of the applied load and the operating speed of the alternator. Because of this magnetic field within the alternator iron structure, a weak leakage flux field will also exist outside the alternator structure. The pattern and intensity of this leakage field at any given point is greatly affected by the presence of magnetic structural parts of the KIPS system, making it difficult to calculate.

With proper instrumentation, it appears to be feasible to measure and map the leakage field. A test procedure will be established to accomplish this early in Phase II of the development program.

RELIABILITY AND STRESS

Maximum alternator efficiency, life and reliability can be achieved by designing the various components to operate at conservative thermal, electric and mechanical stress levels. This philosophy was adopted in the design of the FSCD alternator.

The most critical operating stress levels can be summarized as follows:

1. Mechanical:

Component	Rotor Laminations
Actual Maximum Stress	21,900 PSI
.2% Yield Strength	42,840 PSI
Margin of Safety	.956

(M.S. = .2% yield/Applied Stress - 1)

2. Electrical:

Component	Insulation
Actual Maximum Voltage	22.5 Volts RMS
Minimum Insulating Rating	10,000 Volts
Test Voltage	500 Volts RMS

3. Thermal:

Component	Insulation
Actual Maximum Temperature	141°C
Maximum Continuous Temperature for 60,000 Hours Life	230°C

FABRICATION AND INSPECTION

LAMINATIONS: The rotor and stator laminations can be produced either by punching or by means of a photochemical etch process. The latter produces parts having dimensional tolerances of ± 0.002" for the stator lamination (0.005" thick) and ± 0.005" for the rotor laminations (0.014" thick). Punched laminations are made to ± 0.002" tolerance regardless of thickness. Punched laminations were chosen for this reason.

After fabrication, the laminations are appropriately annealed and oxide coated to obtain the desired magnetic properties. Magnetic properties are tested using three sets of ring samples produced from the same material lot and annealed with the laminations. Magnetic saturation is tested per ASTM A596 and core losses are tested per ASTM A343. A set of three ring samples is produced and tested for each 200 pound lot of laminations.

STATOR CORES: Each stator core consists of a stack of approximately 300 laminations.

Laminations to be stacked into cores are degreased and coated with Scotchcoat 265 epoxy by immersion in a solution of the epoxy in acetone and allowing the acetone to evaporate. The laminations are then stacked on a specially designed stacking fixture, skewed to the proper angle and clamped together with a pressure of 400 to 500 PSI. The pressure is maintained during the cure cycle by means of compressed spring washers even when the epoxy softens and some compression of the stack occurs. The epoxy cure cycle is 1 to 2 hours at 330°F.

After stacking and bonding, the core O.D. and I.D. are ground to size and a slot is machined in those cores to be used at the lead end of the stator assembly. All excess epoxy is removed from the slots and the cores are then visually and dimensionally inspected.

FIELD COIL: A 0.030" thick aluminum sleeve is mounted on a special coil winding fixture and the coil I.D. and side insulation is installed. All adjoining surfaces are coated with a light coat of ML varnish by brushing. Two layers of AWG No. 19 insulated wire are then wound over the insulated sleeve (approximately 35 turns per layer). Each layer of wire is also covered with a very light coat of ML varnish and the varnish is thoroughly cured. Two more layers of wire are than wound over the first two, and the cure cycle is repeated. This process is repeated five times until a total of 375 turns of wire are wound.

Teflon sleeving is then placed over the end leads and the coil O.D. insulation installed. The last varnish cure cycle includes a post cure heat at 550°F.

The coil is then removed from the winding fixture, visually inspected, checked dimensionally, dielectric tested at 500 volts, and the resistance is measured at room temperature.

The entire coil winding is wound from a single continuous strand of wire. It contains no brazed or soldered connections. The end leads are merely extensions of the coil winding itself.

STATOR ASSEMBLY: The entire alternator stator assembly is contained within the stator yoke. The yoke is a tubular section of 1008 steel, annealed for best magnetic properties and machined to the proper wall thickness and tolerances to hold the two stator cores and to provide a good magnetic path between them.

The stator is assembled by heating the yoke to 400°F and chilling the "Lead End" core by soaking in liquid nitrogen. The core is placed into the yoke and a shrink fit is achieved as the temperature stabilizes at room temperature. The field coil end leads are then pushed through the slot in the core O.D. and the field coil is carefully placed in the center section of the yoke, flush against the core. This assembly is again heated to 400°F and the second core (having been chilled with liquid nitrogen) is inserted, trapping the field coil between the two cores. The yoke O.D. is ground to restore concentricity with the core I.D.s and to obtain proper dimensional fit with the CRU housing.

After dimensional inspection, slot cells are inserted into all slots and a piece of Kapton insulation is placed over the aluminum field coil support to separate it from the stator output windings. Stator conductors consisting of 31 strands of AWG No. 20 wire are precut to length and are inserted into the appropriate slots by means of "tunnel winding" (pulling of conductors through the slots). The slot cells are cuffed at both ends to keep them from slipping out of position during the "tunnel wind" process.

After the winding is completed, a dielectric test at 500 volts RMS is performed to insure that no damage was done to the insulation. The neutral connection is then brazed and insulated with Kapton sheet and teflon sleeving is placed over the end leads which are extensions of the winding conductors. All end turns are securely laced with fiberglass tie cord, dipped in ML varnish and thoroughly cured including a post cure heat at 550°F. The stator assembly is then subjected to a complete inspection: visual, dimensional, dielectric tests and resistance measurements of all windings, followed by a vacuum bake at 10^{-5} torr and 450°F. Figure 2.5.3-17 summarizes the alternator stator fabrication process.

ROTOR: The construction of the alternator rotor assembly is done by electron beam welding of laminations and windage rings to the rotor shaft. The rotor is carburized in the bearing area but not hardened prior to welding. The laminations are processed for optimum magnetic characteristics, oxidized and then electron beam welded to the rotor in 3/8" thick steps. After welding of each stack, the weld is ultrasonically inspected. The windage rings are welded after the laminations are in place. The welded assembly is stress relieved and then the carburized area is hardened to desired hardness. This assembly is now ready for welding to the turbine wheel and then final machining. Figure 2.5.3-18 summarizes the rotor fabrication process.

2.5.3.6 Bearings

The bearings for the Combined Rotating Unit (CRU) support both axial and radial loads under a variety of different operating conditions. The baseline operating point for which losses need to be minimized and hence performance maximized is the zero g condition when bearing loads are at a

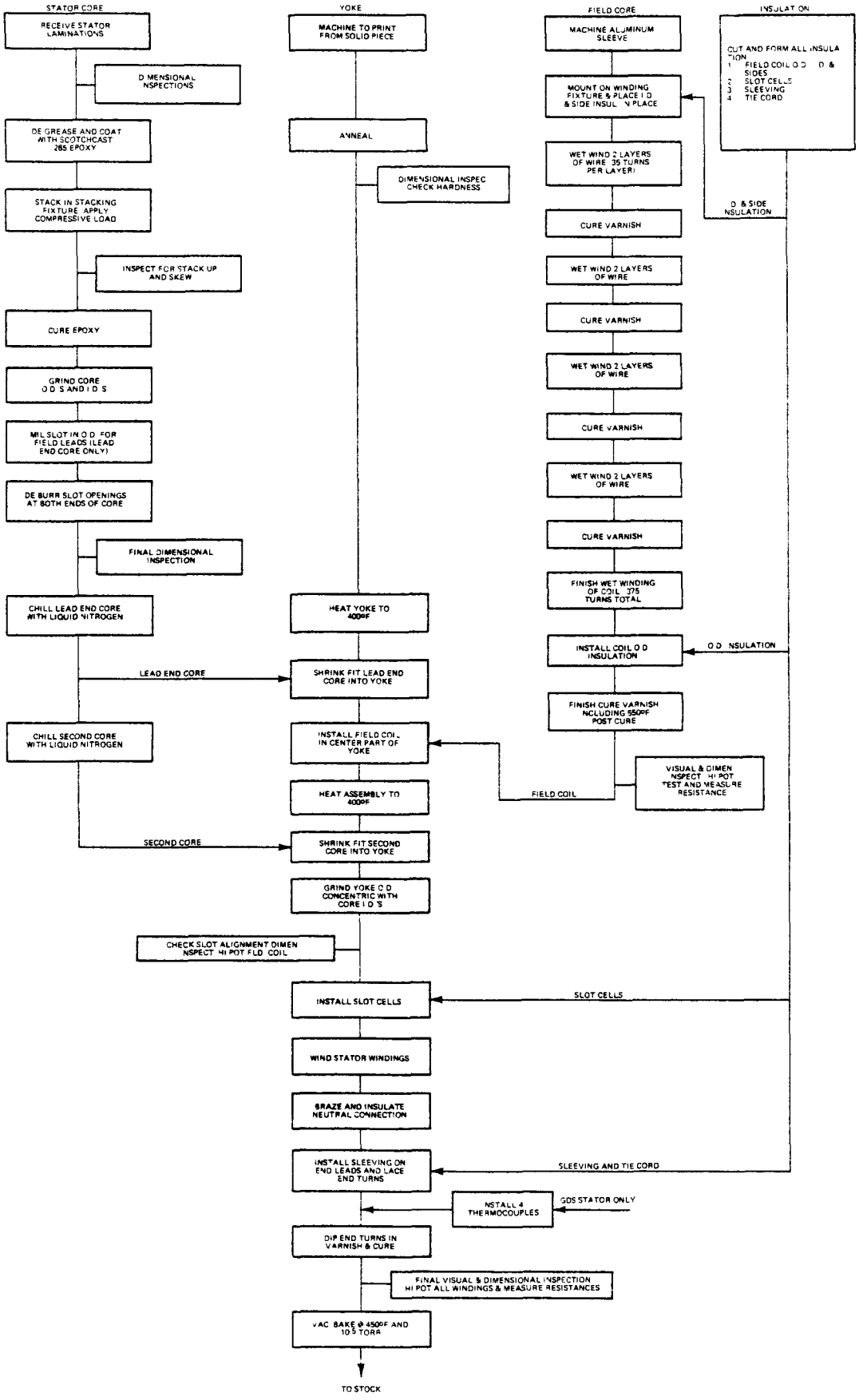

Figure 2.5.3-17 Stator Fabrication

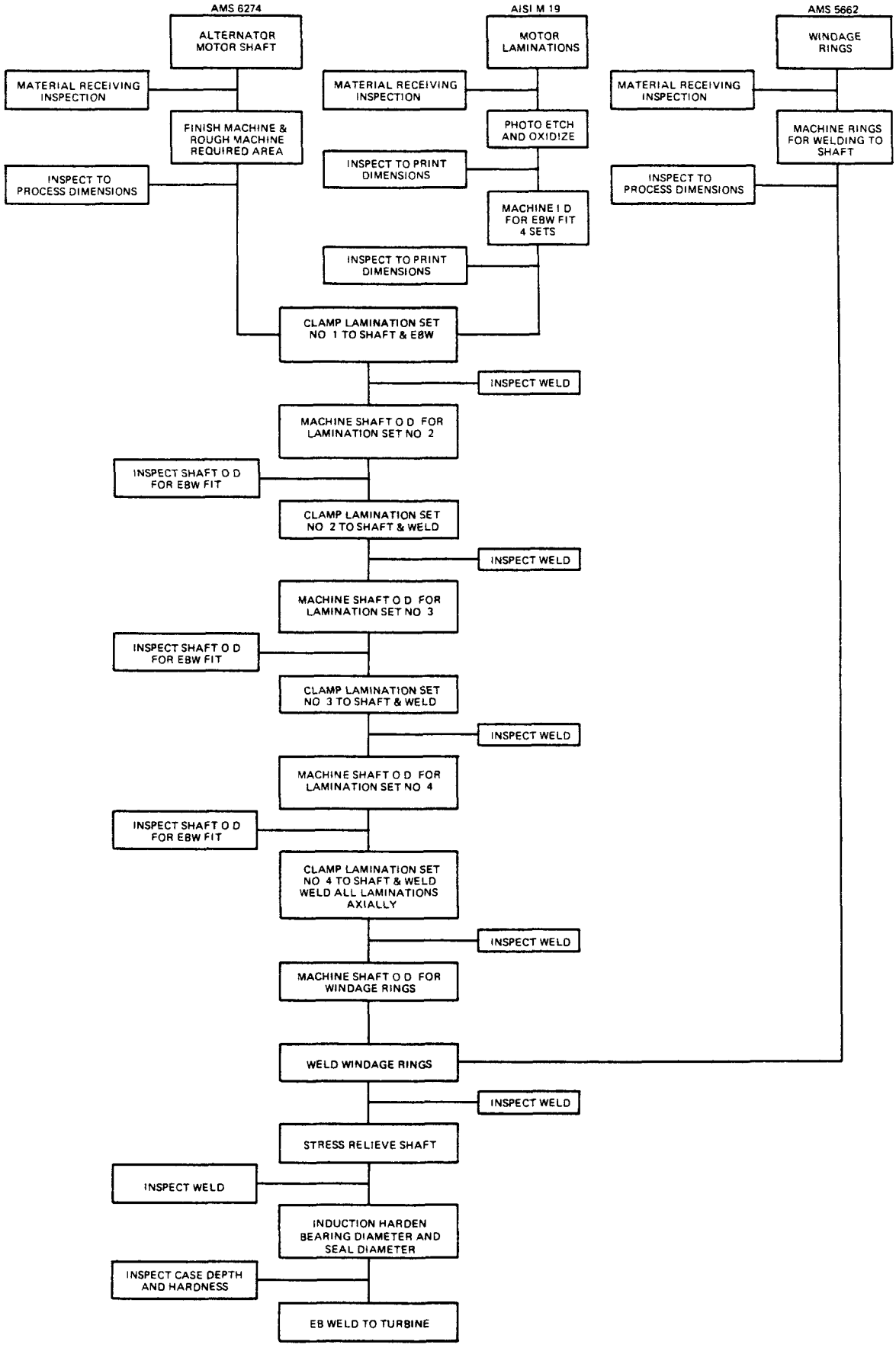

Figure 2.5.3-18 Rotor Fabrication

minimum and comprise only turbine, pump, alternator, and imbalance loads. The most stringent operating conditions will be during launch when either: (1) accelerations in the axial and radial directions reach nine and five g's respectively with superimposed vibration loads or (2) the short term shock loads are applied independently of the acceleration load. In addition, ground operation in the vertical direction will have one g axial load while horizontal operation would have one g radial load.

2.5.3.6.1 RADIAL BEARINGS

CONFIGURATION: The radial bearings consist of working fluid lubricated tilting pad bearings. Each set of bearings comprises four tilting pads of 80 degrees of arc pivoted at 44 degrees from the leading edge. The bearing pads are hardened M-50 tool steel with a thin electropolated silver coating. The coating enhances start stop characteristics.

TRADE-OFF STUDIES: Trade-off studies were peformed to determine the optimum type bearing for the application. Ball bearings were rejected from a reliability and life standpoint, while the large size and lack of backup data resulted in the rejection of vapor/gas bearings. The requirement of high stability against functional frequency whirl in zero g operation led to the investigation of several high stability bearings: lobed, tilted lobed, herringbone, and tilting pad. It was found that only the tilting pad configuration could meet the stability requirements. In addition, Sundstrand has considerable experience with this type of bearing.

The tilting pad bearing is inherently stable due to the fact that the shaft movement is essentially colinear with the applied load. The tilting pad bearing comprises a series of equally spaced shoes arranged circumferentially around the shaft. A pivot in the back side of the shoe allows it to tilt in the pitch direction in order to form a converging wedge for hydrodynamic pressure generation. Typically, instability only arises when pad pitch inertia is high enough to prevent adequate shaft tracking. This potential instability can be precluded by "preloading" the bearing and minimizing pad inertia. Preloading sets the bearing pads closer to the shaft than would be dictated by the machined clearance and thus has the same effect as applying an external load.

This preload technique can best be seen from Figure 2.5.3-19. Preloading has a stabilizing effect and can be used to increase the stiffness of the bearing (since the bearing stiffness increases with load). However, the power loss increases and minimum film thickness decreases with preload. The bearings were therefore designed to have sufficient preload with a minimum additional power loss.

An additional advantage of the tilting pad bearing is the self-aligning characteristic which eliminates alignment problems common with rigid bearings.

ANALYSIS: The selection of the bearing configuration considered the following factors:

- Minimum film thickness during launch loads
- Power loss at design point
- Critical speeds
- Pivot stresses
- Pad stability
- Maximum allowable shaft movement

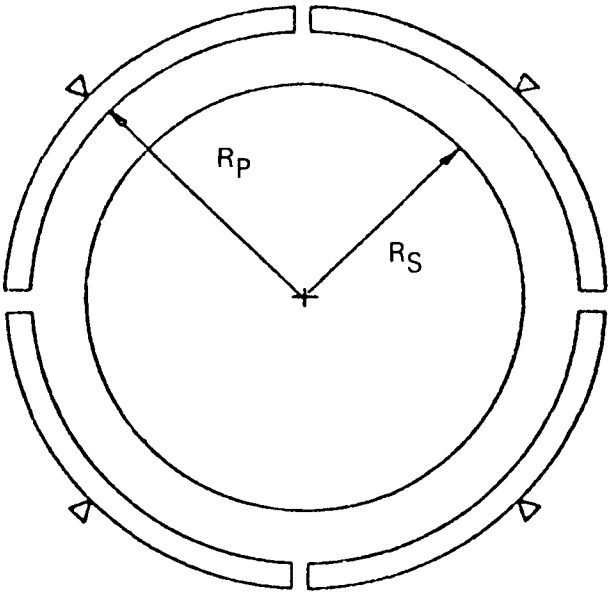

4 PAD BEARING
ZERO PRELOAD
(a)

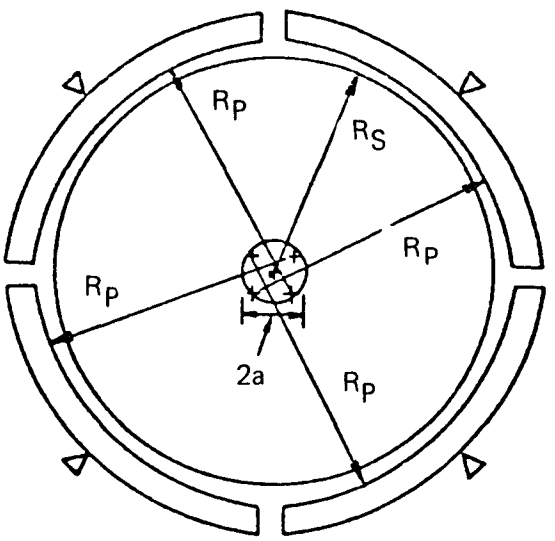

4 PAD BEARING
PRELOAD = a

$$\left(\text{PRELOAD COEFFICIENT} = \frac{a}{R_P - R_S}\right)$$

(b)

Figure 2.5.3-19 Geometrical arrangement of pads.

Radial bearing loads result from the combination of various static and dynamic forces existing in the CRU.

Imbalance load results from the residual imbalance left after subjecting the CRU rotor to standard balancing techniques. For this rotor, two plane subcritical balancing is employed, which is adequate since only rigid body critical speeds are encountered in the operating range.

The CRU rotor selected for the KIPS weighs 9.5 pounds and has a maximum residual imbalance of 0.0005 in/oz in each of two balance planes. This can result in a centrifugal loading of approximately 1.0 lb at design speed and 3.0 lb at overspeed. The actual bearing reactions are a function of bearing damping and the ratio of operating speed to critical speed which gives an appropriate amplification factor. The imbalance load is a rotating dynamic load which typically leads to a one-per-revolution synchronous vibration and benign synchronous whirl within the bearing.

Alternator magnetic loading is a static radial load which results from the rotor not being concentric within the stator. The value for the KIPS alternator has been calculated at 1.2 lb on each bearing with an estimated eccentricity of 0.002 in. The load direction is indeterminant.

Static pump load results from partial emission of the flow through the volute at flows other than design; i.e. as the rotor speeds up to overspeed. The maximum value at overspeed is 4.5 lb., directed away from the exit volute.

The static load due to the rotor weight is a function of local gravitational acceleration and rotor orientation. Vertical shaft orientation on the ground and during operation in space both lead to zero static radial bearing loading from rotor weight. Horizontal ground operation gives a total radial load of 9.5 lb. while maximum radial launch loads of five g's results in an equivalent rotor weight of 47.5 lb.

Shock and vibration dynamic loads occur during rocket staging and launch. The mounting structure and shock mounts reduce the values that are input from the launch vehicle from 775 g's and 15 g's for shock and vibration respectively to values less than 10 g's and five g's.

Table 2.5.3-D summarizes the bearing loading for different operating conditions. These comprise the sum of maximum static loads with imbalance loads superimposed which include appropriate magnification factors. Better balance, lower alternator eccentricity, and appropriate orientation of load vectors can reduce these values.

The bearing performance was analyzed using the Mechanical Technology, Inc. (MTI) Cadense 32 tilting pad bearing analysis program. This allows the number of pads, diameter, clearance, length/diameter (L/D) and preload to be varied and calculates film temperature rise, power loss, the stiffness and damping matrix and minimum film thickness.

SIZING AND PERFORMANCE: Different bearing sizes were analyzed to minimize losses and to best fit the critical speed map. The final bearing geometry selected is given in Table 2.5.3-E.

The KIPS bearings operate in the laminar flow regime throughout the operating range with Reynold's numbers of 544 and 920 at design point and maximum runaway speeds respectively.

Table 2.5.3-D - Radial Bearing Loads

ZERO G OR GROUND VERTICAL

KRPM	Turbine End Bearing (lb)	Pump End Bearing (lb)
10	2.4	1.4
20	2.6	0.9
30	3.5	0.3
40	3.0	0.6
50	2.4	3.3
60	2.4	7.2

MAXIMUM LAUNCH ACCELERATION

KRPM	Turbine End Bearing (lb)	Pump End Bearing (lb)
20	26.3	25.7
33.7	26.9	26.3
40	26.7	26.7
60	26.2	32.8

HORIZONTAL 1 G

KRPM	Turbine End Bearing (lb)	Pump End Bearing (lb)
20	6.7	6.5
33.7	7.3	7.9
40	7.7	7.7
60	6.9	7.1

Table 2.5.3-E - Radial Bearing Geometry

Number of pads:	4
Pad length:	0.275 ± 0.005
Shaft diameter:	0.5500 + .0000 − .0002
Pad I.D.:	0.5525 + 0.0002 − .0000
Machined clearance:	0.0025 ± 0.0002
Assembled clearance:	0.00175
Preload coefficient:	0.3
Pad thickness at pivot: (tapered towards leading and trailing edges)	0.150
Pad arc:	80°
Pivot point:	44° from leading edge
Leading edge radius:	0.05
Pad material:	M-50 with silver flash
Shaft material:	M-50 at turbine end AISI 8620 at pump end
Pivot spherical diameter:	0.666 inch
Socket spherical diameter:	1.00 inch
Design point power loss:	7.5 watts/bearing

The selected bearing configuration was analyzed to cover potential geometrical variations. Tolerances in manufacture result in a ± 0.0002 inches variation in diametral clearance and 0.0002 inches in setup clearance. This means the value of diametral clearance varies from 0.0023-0.0027 in. and the preload from 0.2-0.39.

The radial bearing minimum film thickness and power loss are presented in Figure 2.5.3-20 at varying operating conditions and speeds.

The bearing stability was checked for both the design point operation and runaway speed at zero g, using information available from Orcutt[1]. The criterion for stable pad operation is that the operating speed should be substantially less than the natural frequency of the spring-mass system of pad and film. A conservative value given in NASA CR-732 is $M_{crit}/M_{pad} > 4$.

where M_{crit} = critical pad mass

M_{pad} = effective pad mass

The pad pitch inertia was calculated for the selected pad geometry and the resulting effective pad mass calculated from:

$$M_{pad} = I/R_p^2$$

where I = pad pitch inertia

R_p = pivot point radius

The resultant ratios at design speed and overspeed are:

55,000 rpm: $M_{crit}/M_{pad} = 38$

33,700 rpm: $M_{crit}/M_{pad} = 48$

MECHANICAL CONSTRUCTION: The maintenance of bearing clearances is important to prevent excessive whirl orbit amplitudes and prevent the possibility of other components with close radial clearances from contacting. For this reason, special attention has been given to restraining the radial movement of the bearing pads.

The bearings are preassembled into steel support modules. The bearing clearance is set using an oversized mandrel by tightening a screw pivot pin which in turn is locked in place by drilling and inserting a roll pin. The whole assembly is then placed over the shaft and the steel housing is pressed into the housing. Removal of the bearing module is achieved by the use of threads which are used in conjunction with a puller.

The materials selected for the bearings comprise a hard-hard combination of M-50 pads versus either an M-50 sleeve at the turbine end or carburized AISI 8620 shaft at the pump end. A flash of silver plate is added to the pad inner surface to give additional bearing protection in the event of a high speed rub, and to enhance start-stop capability. The choice of M-50 was dictated by the selection of the pivot materials (see pivot design). The pivot pin is silver plated M-2 and is screwed into an AISI 8620 housing. The material selection was based on past Sundstrand experience in the 6 KWe and 1 KWe power systems.

[1]Steady State and Dynamics Properties of Tilting Pad Bearings, F. K. Orcutt, NASA, CR-732.

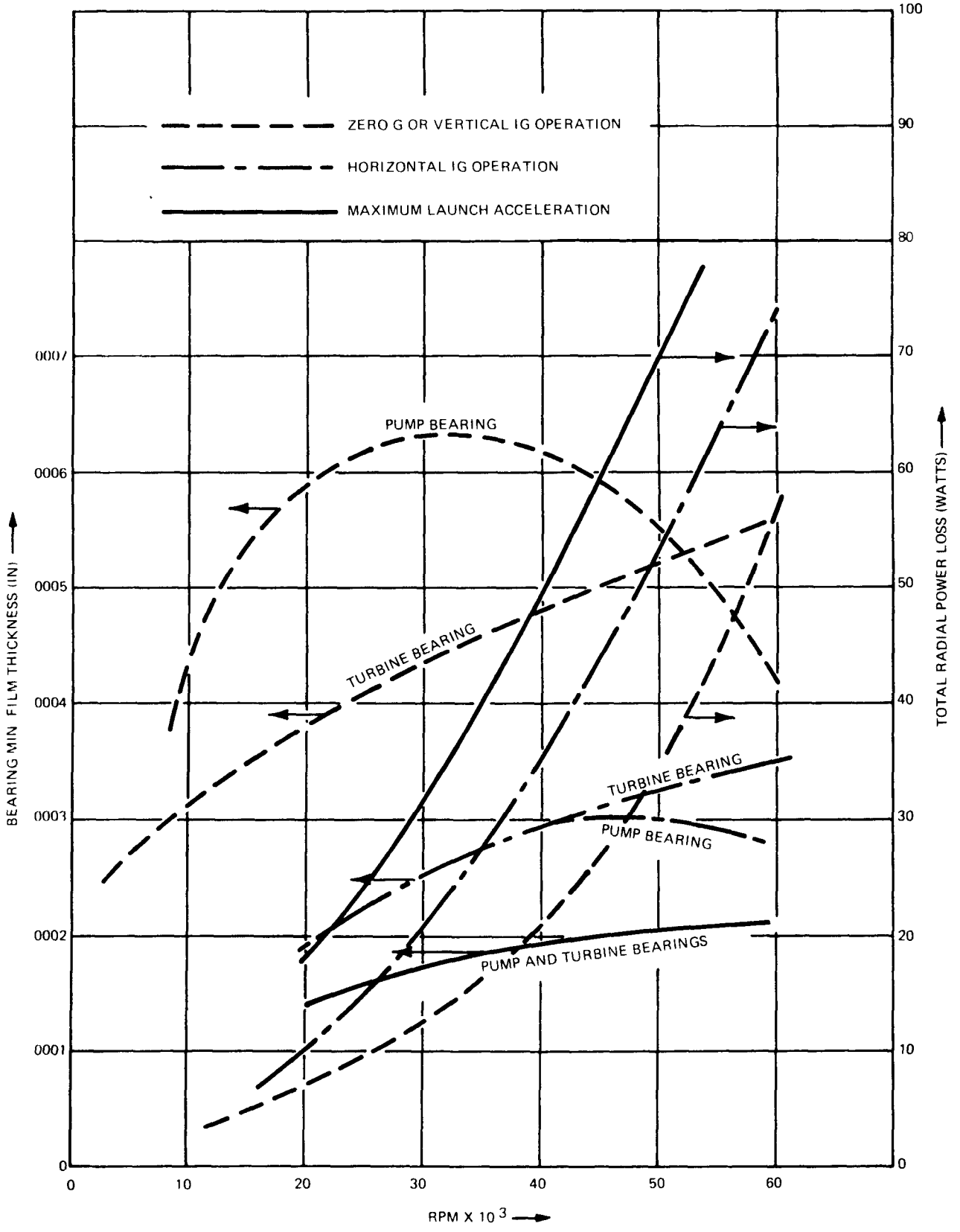

Figure 2.5.3-20 Radial Bearing Operating Characteristics

2.5.3.6.2 THRUST BEARINGS

The thrust bearing is designed for unidirectional thrust loading only, though short term reverse thrust loads resulting, for instance, from rocket staging, can be accommodated.

CONFIGURATION: The thrust bearing comprises a set of six AISI M-50 tilting pads pivoted at 60% from the leading edge and supported by two rows of six leveling pads.

TRADE-OFF STUDIES: Different rigid bearing configurations were investigated (such as a step bearing) but were rejected because satisfactory methods of load equalization were not possible. The large variation in load values presents problems in selecting an optimum size, while any wear can result in loss of load capacity. The large variation in load leads to the requirement that potential non-perpendicularity of the thrust runner and housing should not reduce the load capacity of the bearing.

The load equalized tilting pad bearing allows each pad to share the load equally and thus allows a minimum loss configuration for a given load. Trade-off studies were performed for selecting the number of pads to be used in the bearing. The simplest load equalized thrust bearing design would employ two pads and a simple tilting gimbal equalization technique. (See Figure 2.5.3-21(a). This is the configuration that was used on the Sundstrand 6 KWe ORC and the 1 KWe ORC.

When more than two pads are employed, the method of load equalization becomes more complex. The usual equalizer system employs two sets of equalizing pads distributing the load as shown in Figure 2.5.3-21 (b) or a double gimbal ring arrangement as shown in Figure 2.5.3-21(c) in which one ring gimbals against the other. Tilting pad bearings used by Sundstrand in the large Sundyne pumps use the former arrangement.

When the performance of a two pad bearing is compared to multipad configurations, the losses for the two pad bearing are less than the multipad bearing for a given film thickness, not accounting for losses between pads. However, for high loads associated with launch, the effect of increasing the number of pads is to decrease the pivot loading. For this reason, six pads were chosen and for the same reason, the multipad equalizer system was chosen over the double gimbal.

ANALYSIS: As with the radial bearings, the total thrust bearing load results from the sum of various loads in the system, namely, pump load, turbine load, rotor weight, and shock-vibration loads.

In zero g operation, the only thrust loading comprises the turbine and pump loads. Therefore, to minimize bearing losses, it becomes conceivable to use only one set of thrust bearings. This is also predicated on the preferred launch orientation being with the rotation axis vertical. To this end, the pump load was arranged to be in the same direction as the turbine load by appropriate selection of seal diameters. At the design point, this load is 1.9 lb. and varies approximately proportional to the square of the speed, since the seal pressures vary with the tip speed. The turbine thrust loads were calculated to be 0.2 lb. at design speed and 1.55 lb. at overspeed.

The rotor weight is 9.5 lb. For ground operation, the bearings will see this 9.5 lb., but during launch a 9 g acceleration load is applied. Table 2.5.3-F presents a summary of the expected loads for different operating conditions.

a SINGLE GIMBAL – TWO PADS

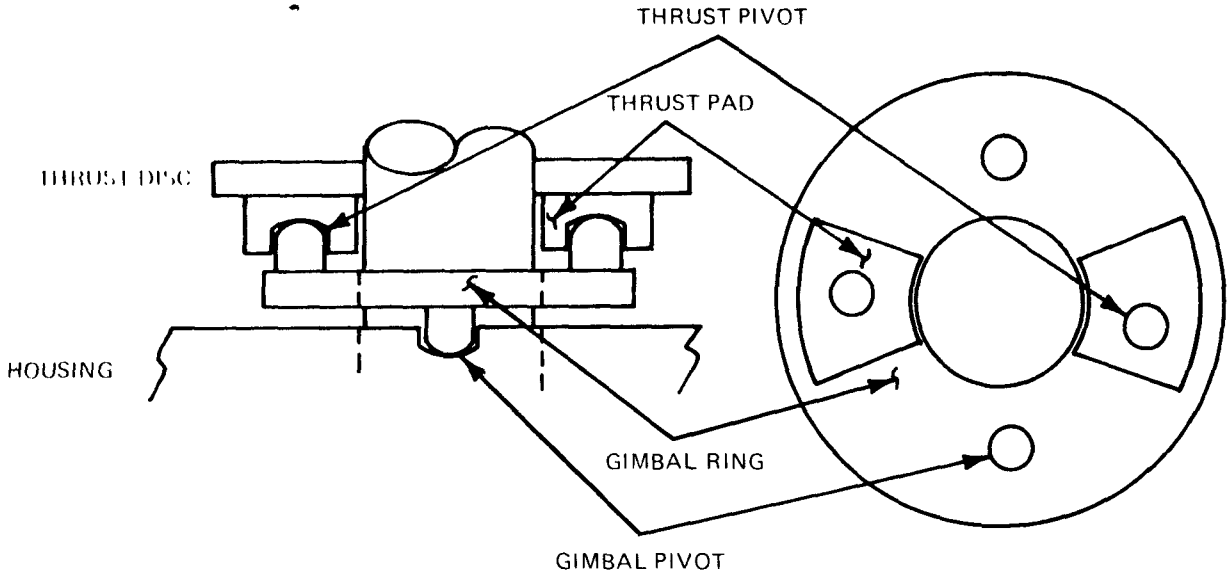

b LOAD EQUALIZER – MULTIPLE PADS (DEVELOPED DIAGRAM)

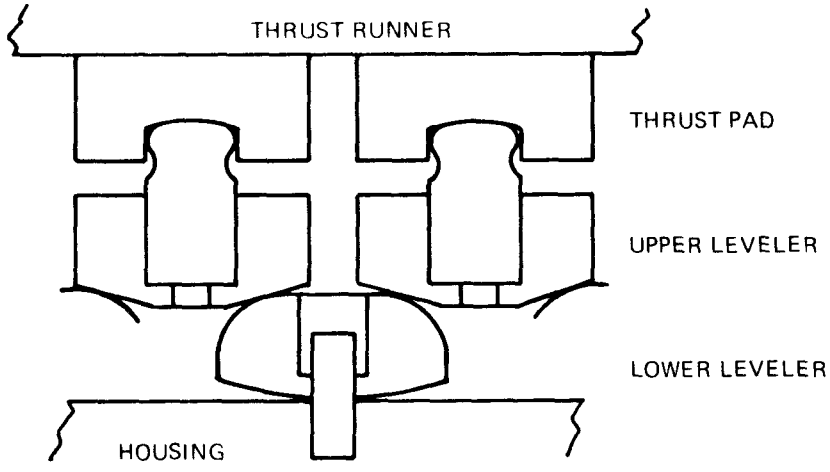

c DOUBLE GIMBAL - MULTIPLE PADS

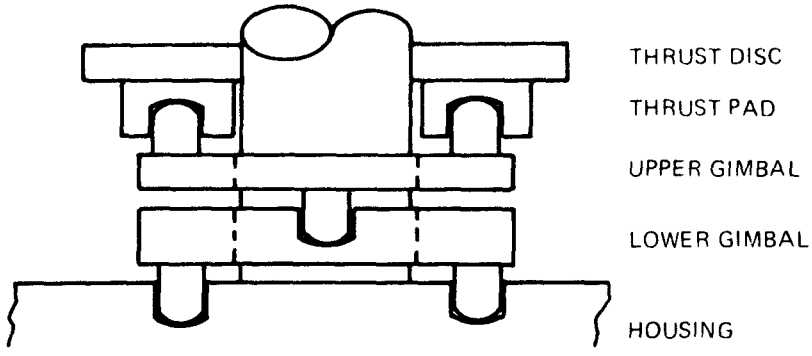

Figure 2.5.3-21 Thrust Bearing Load Equalizers

Table 2.5.3-F Thrust Bearing Loads (Total)

RPM	Zero "G" Operation (Lbs.)	Maximum Launch (Lbs.)	Ground Operation (Lbs.)
20,000	0.73	86.2	10.2
33,700	2.1	87.6	11.6
40,000	3.3	88.3	12.8
50,000	5.6	91.1	15.1
60,000	7.7	93.2	17.2

SIZING AND PERFORMANCE: The bearing analysis was performed using curves presented in Raimondi and Boyd[1] and Wilcock and Booser[2]. A pad aspect ratio; i.e. pad radial to circumferential width ratio, of unity was selected. This value maximizes load capacity for a given power loss with an optimum pivot position of 60% of the arc from the leading edge. Bearing operation is in the turbulent regime and appropriate corrections have been made to power loss calculations. Table 2.5.3-G presents a summary of the thrust bearing design.

The bearing design is based upon selecting an adequate film thickness for the launch condition load at overspeed. A value of 0.00015 inches has been chosen for the minimum film thickness under acceleration loads, to give some margin of safety for shock and vibration loads.

The minimum film thickness and power loss were calculated for the different load conditions and speeds. These are presented in Figure 2.5.3-22. An estimation was made of the effect of the shock loads on the thrust bearing film thickness, using information from Sternlicht [3].

Taking an average value of the load over the half sine shock leads to a minimum film thickness of approximately 50 micro inches. This means that metal-metal contact could occur for a very short period of time. Sundstrand experience has been that the selected bearing materials can withstand a short term contact of this nature without damage. Similar results have been presented by other authors[4].

MECHANICAL CONSTRUCTION: The thrust bearing configuration employs six M-50 pads with two rows of six leveling pads. A hemispherical pivot engages into a hemispherical socket in the pad. The pivot pin is mounted to the first leveler which, in turn, pivots on two of the second levelers by contact along radial lines. The bottom leveler pivots on an M-50 insert which doubles as a shim to set the turbine wheel clearance. The pin through the bottom leveler prevents circumferential motion while relatively tight radial clearances act as restraints in that direction. Similarly a tight clearance at the inner diameter of the thrust pads prevents windmilling of the pads about the pivots. The pad surface and the pivot surfaces have a flash of silver plate (0.0004"). The thrust runner is also made of M-50.

Although the preferred orientation of the power system axis precludes reverse thrust during normal operation and through launch, it is feasible that momentary reverse thrust loading could occur during orbit transfer or within the Space Shuttle bay. This can be accommodated by a bronze snubber which can withstand the surface speeds at which this occurs without lubrication and damage. This snubber also serves as a protection for the turbine wheel during handling and accommodates the initial reverse thrust load at start resulting from pump inlet pressurization by the start pump.

[1] "Applying Bearing Theory to the Analysis and Design of Pad Type Bearings", Raimondi and Boyd, ASME 53A-84.

[2] "Bearing Design and Application", Wilcock and Booser, McGraw Hill.

[3] "Theory of Hydrodynamic Lubrication, Pinkas and Sternlicht, McGraw Hill

[4] "Effects of Vibration and Shock on the performance of Gas Bearing Space Power Braytor Cycle Turbo Machinery", Spencer, Curner & Tyron, NASA CR 1762.

2.5.3.6.3 BEARING PIVOTS

In order to maintain the design point operating characteristics of the bearings throughout the operating life, it is necessary to preclude any possibility of pivot fretting type wear. The results of such wear are a decrease in the pad stability due to an increase in the pivot friction and an increase in the bearing clearance leading to a change in minimum film thickness. However, severe wear would be necessary before these effects manifested themselves.

The selection of the pivot design was based mainly on data presented by Peterson[5] which delineates the optimum geometry, materials and maximum loading to prevent fretting wear.

Table 2.5.3-G Thrust Bearing Geometry

Number of pads:	6
Active pad circumferential length:	0.25 inch
Active pad radial width:	0.25 inch
Pad thickness:	0.10 inch
Pivot location from leading edge:	0.15 inch
Pad material:	M-50 with silver flash
Thrust runner material:	M-50
Pivot spherical diameter:	0.666 inch
Socket spherical diameter:	1.00 inch
Number of upper load levelers:	6
Cylindrical pivot diameter:	0.125 inch
Cylindrical pivot diameter:	0.125 inch
Cylindrical pivot length:	0.125 inch
Number of lower load levelers:	6
Cylindrical pivot diameter:	1.00 inch
Cylindrical pivot length:	0.175 inch
Total axial clearance:	0.007 inch
Design point power loss:	25 watts

[5]"Analytical and experimental investigation of Gas Bearing Tilting Pad Pivots", Peterson, Geren etal. NASA CR 72609

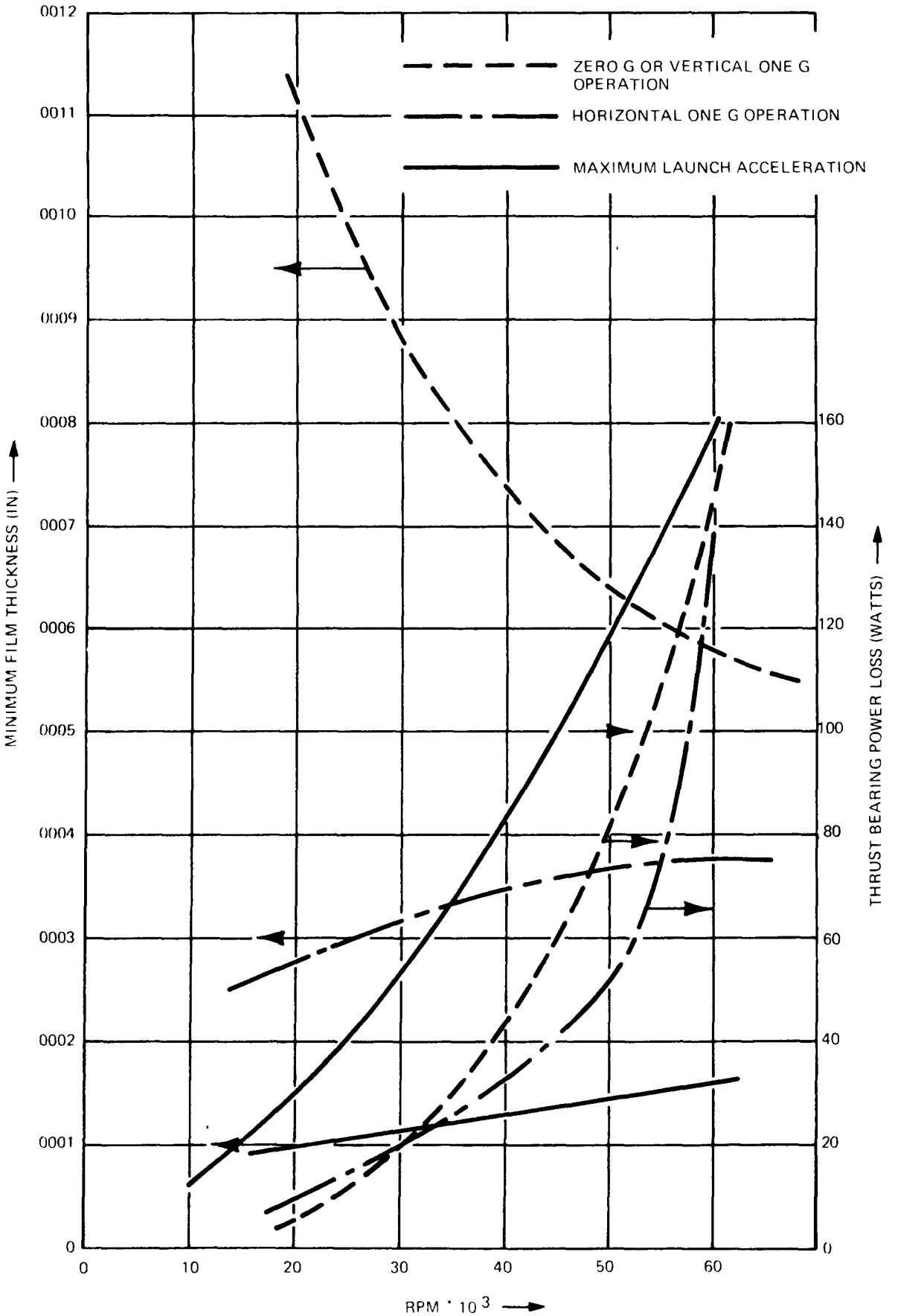

Figure 2.5.3-22 Thrust Bearing Characteristics

The pivot undergoes primarily rolling contact and the resultant material requirements are:

- High yield strength at maximum operating temperatures
- high hardness
- dimensional stability
- corrosion resistance
- good sliding compatibility
- relative ease of manufacture
- adequate shock resistance

The minimum hardness for rolling bearings is approximately R_c55 and this has been used for the minimum goal in the material selection. SAE 52100 steel and 440C stainless steel are recommended up to 450°F while the M series tool steels are good to 900°F. Since temperatures of the order of 450°F are conceivable due to a soakback after a system shutdown, M-50 tool steel with a hardness of R_c62 has been selected for the pivot-pad combination. Peterson considers the use of lubricating films to be of use only during a "break-in" period, but tests at Sundstrand have shown that a flash of silver applied to the pivot tip prevented any trace of fretting. In addition, a completely nonoxidizing atmosphere (i.e. leak tight system) prevents oxidation at the pivot surface.

The report deals specifically with gas bearings and it is recognized that oil lubricated tilting pad bearings have no pivot problems. Therefore, a design suitable for a gas bearing will present no problem with Dowtherm. The suggested design appraoch resulting from the investigation is a pivot radius ratio of 1.5 and a maximum Hertz stress of 220,000 psi.

The maximum loads that the bearings will see are shock loads, which are assumed not to occur at the same time as acceleration loads. This leads to a maximum load of approximately 21 lb. per pad for the thrust bearing and 46 lb. per pad for the radial bearing.

The load leveler design employs the same technique used in the Sundstrand Sundyne pumps with pivots which comprise a cylinder rolling on a flat surface with line contact as opposed to the point contact found with the tilting pads. The pivot designs are summarized in Table 2.5.3-H.

BEARING AND PIVOT STRESS LEVELS: Presented in Table 2.5.3-I is a summary of the operating stress levels and margins of safety for the critical bearing areas under different operating conditions. Margins of safety are based upon a maximum allowable Hertz stress of 220,000 psi and a minimum film thickness of 0.0001 in. Margin of safety (M.S.) is defined as M.S. = Actual/Allowable.

2.5.3.6.4 RELIABILITY

Tilting pad bearings are commonly used in the industry. Table 2.5.3-J specifically provides a summary of Sundstrand tilting pad bearing applications. Other similar bearings have accumulated over 30,000 hours on a Brayton cycle machine with gas bearings at NASA-Lewis and more than 5 million total hours operation of the ORMAT organic Rankine cycle using Dowtherm E as working fluid and lubricant.

Approximately 7.5 million hours of operation have been accumulated in Sundstrand Sundyne compressor gearboxes which use tilting pad bearings. The Sundyne product line is produced by the

Table 2.5.3-H Pivot Design

Pivot Location	Pivot Type	Pivot Diameter	Socket Diameter	Pivot Length
Thrust Pad	1	0.666	1.00	--
Upper Load Leveler	2	0.125	--	0.25
Lower Load Leveler	2	1.00	--	0.175
Radial Pad	1	0.666	1.00	--

(1) Spherical pivot in spherical socket.

(2) Cylinder on flat.

Table 2.5.3-I Summary of Bearing Safety Margins

Operating Condition	Ground	Space	Launch (Accel & Vib)	Launch (Shock)	Launch Shock Nonrotating
Radial load (lb)	2.0	2.0	42	46	43
Thrust load (lb)	11.2	1.7	107	123	123
Radial pivot stress (psi)	15600	15600	119,000	123,000	121,000
Margin of safety	14	14	1.8	1.8	1.8
Thrust pivot stress (psi)	19000	5400	90000	94,000	94,000
Margin of safety	12	41	2.4	2.3	2.3
Upper load leveler pivot stress (psi)	22000	8700	69000	74000	74000
Margin of safety	10	25	3.2	3.0	3.0
Lower load leveler pivot stress	8700	3000	37000	28000	28000
Margin of safety	25	73	5.9	7.9	7.9
Radial min. film thickness (in)	.00054	.00054	.00017	.00016	.00017
Margin of safety	5.4	5.4	1.7	1.6	1.7
Thrust min. film thickness (in)	.00033	.00086	.00014	.00013	.00013
Margin of safety	3.3	8.6	1.4	1.3	1.3
Thrust runner stress (psi)	—	—	—	510	510

Table 2.5.3-J Sundstrand Tilting Pad Bearings

Application	Bearing Load (LB)	Rotational Speed (RPM)	Bearing Diameter (IN)	Lubricant Viscosity (CPS)	Film Thickness (IN)	Hours Operation
Sundyne Petro-chemical Pump	610	19000	1.5	10.0	0.00062	> 7.5 million
Remcom 1.0 Kw ORC	6	55000	0.59	0.441	0.00049	~ 15000
Remcom 1.0 Kw ORC	180	85000	0.59	0.441	0.0001	~ 2
KIPS 1.3 Kw ORC	2	33700	0.55	1.0	0.00054	
KIPS 1.3 Kw ORC	43 (shock load)	55000	0.55	1.0	0.00017	
6 KW ORC	13	24000	1.10	1.0	0.00065	> 3000

Sundstrand Fluid Handling Division. The units which operate at speeds of 18,200 RPM and above contain tilting pad bearings. The Sundyne units are designed for industrial applications and contain bearings which are larger and built with much looser manufacturing tolerances than KIPS.

In addition, three Sundstrand 1.0 KW ORC Remcom units have operated for more than 13,000 hrs. to date and have not experienced any tilting pad bearing primary failures. During development, some instances of tilting pad bearing damage have occurred due to insufficient lubrication. These instances resulted from (1) boost pump problem (no accumulator was provided), and (2) lubricant starvation at shutdown. One set of bearings accumulated over 8,000 hours without damage. The Remcom unit uses the organic working fluid, toluene.

In another application, the Sundstrand 6 KW ORC machine, which uses Dowtherm A as its working fluid, accumulated 3,000 hours of test time with no detectable tilting pad bearing damage.

2.5.3.6.5 FABRICATION

The fabrication and inspection process is summarized in Figure 2.5.3-23 for the pads, pivots and load levelers, in Figure 2.5.3-24 for the bearing modules, and Figure 2.5.3-25 for the thrust runner.

2.5.3.6.6 BEARING LUBRICATION AND SCAVENGE

CONFIGURATION: In order to maximize bearing size for a given load capacity, the pump outlet flow is used for the source of lubricant since it is at a higher temperature (lower viscosity) than the radiator outlet temperature. The use of lower viscosity lubricant allows larger diameters for the same power loss. Individual Lee Visco jets are used to supply the correct bearing flows at each end of the rotor, allowing small flow rates to be metered without using small orifices. Bearing flow is filtered by the main filter in the system accumulator.

Simplification of the lubrication system is possible if the lubricant is introduced from the inside of the shaft. The method has been tested and operated successfully at Sundstrand and is especially beneficial at the turbine end where housing temperatures are relatively hot compared to saturation conditions. However, introduction of the fluid into the shaft becomes more difficult at the pump end than the turbine end. The fluid would have to pass through the eye of the impeller and filtration of this flow would be impossible before reaching the bearing.

The lubrication scheme, therefore, employs external lubrication at the pump end bearings and internal lubrication at the turbine end. The external lubrication is provided by an annular groove cut in the outside of the bearing module feeding four small feed tubes which carry the cool lubricant to each pad leading edge at the shaft. The annulus in turn is fed by an external tube. This method has been used successfully on the Sundstrand 1.0 KWe Remcom system. The internal lubrication scheme uses a small stationary feed tube which passes lubricant axially into the center of the rotating shaft. Orifices in the end and side inject the required flow split into two separate internal chambers, one for the thrust bearings and one for the radial bearings. The use of separate cavities prevents the lubricant from being removed by one bearing only or from leaking out of the end of the shaft. The centrifugal field pumps the liquid up through radial feed holes to the thrust disc face and to the radial bearing pads. The effects of launch loads on the distribution of the lubricant is minimized by keeping the feed orifices in the tube and the receiving chambers as close together axially as possible.

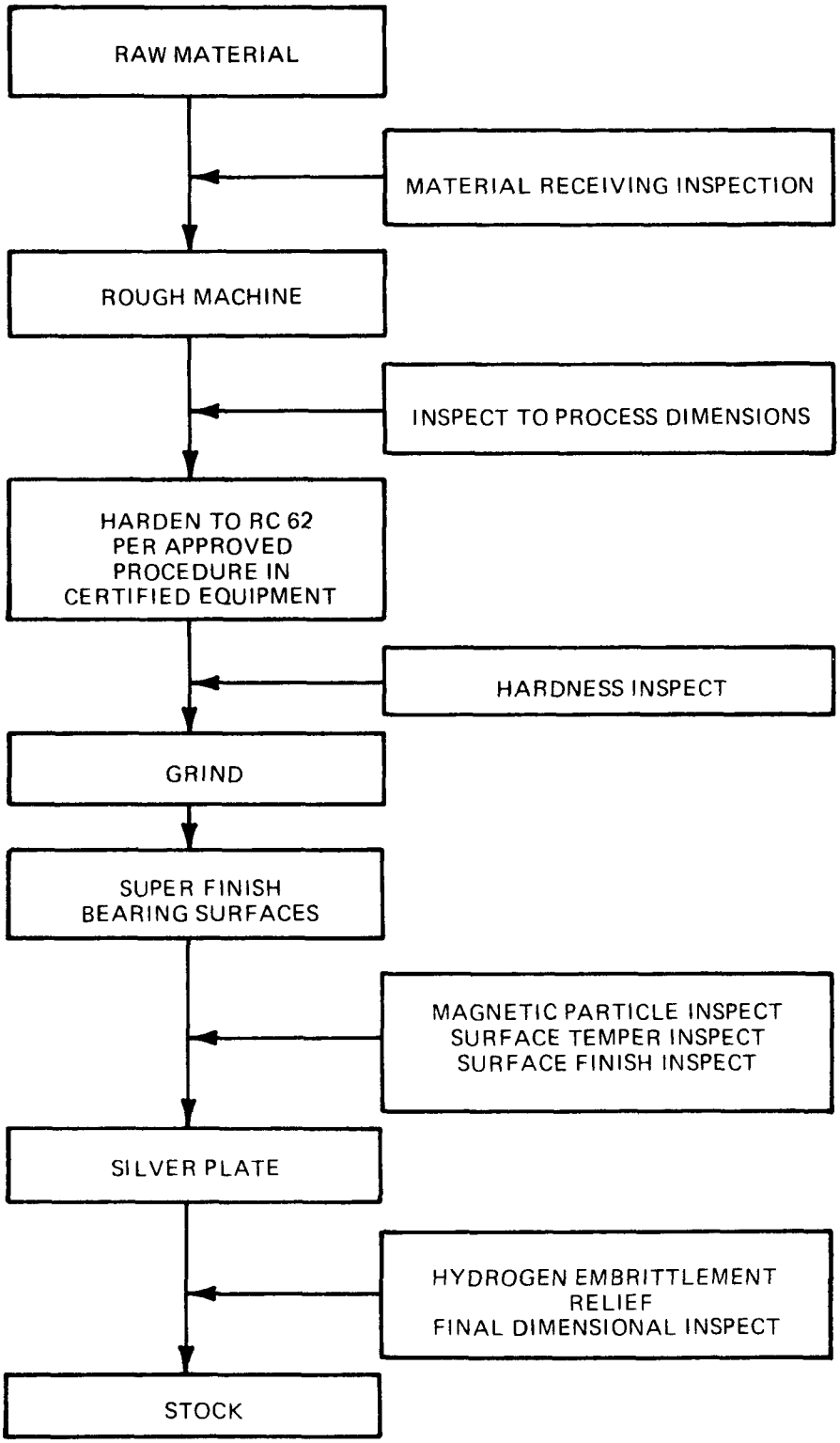

Figure 2.5.3-23 Bearing Radial and Thrust Pads, Pivot Pins, and Load Leveler Fabrication Process

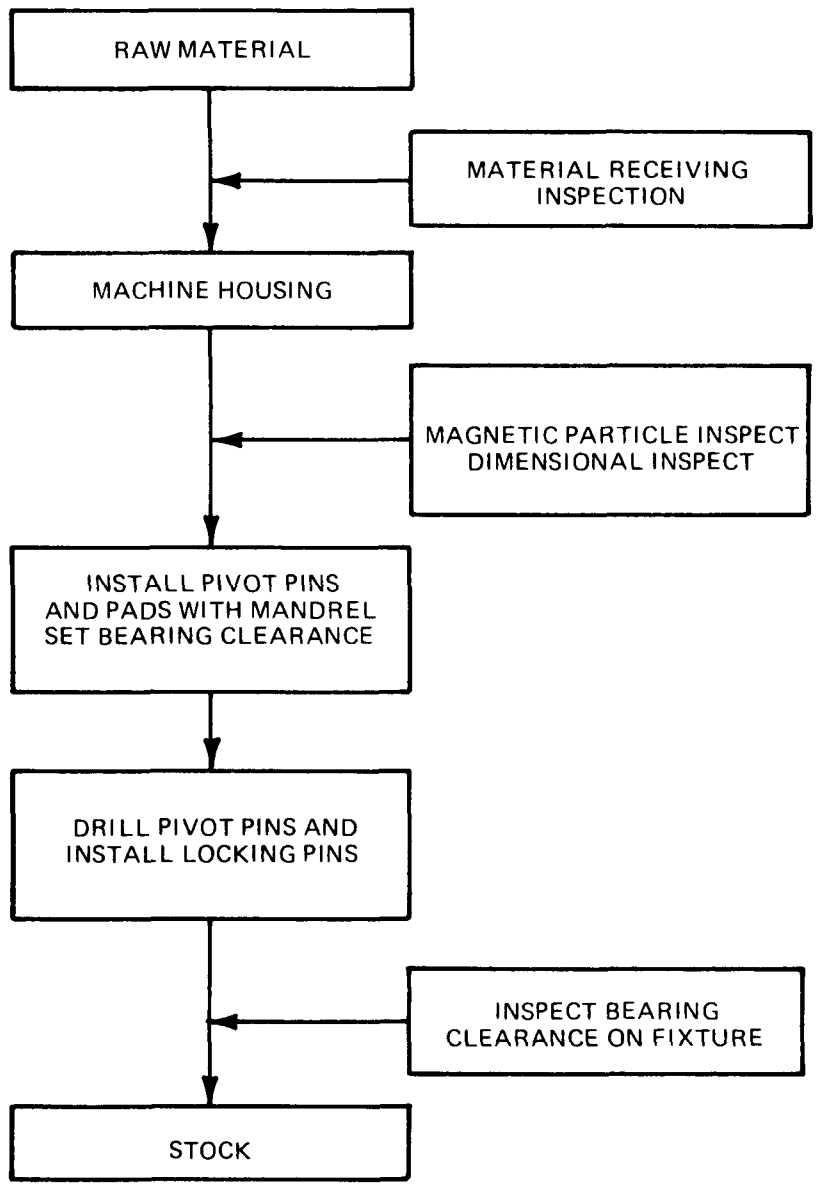

Figure 2.5.3-24 Bearing Module, Radial Pads Matched Set Fabrication Process

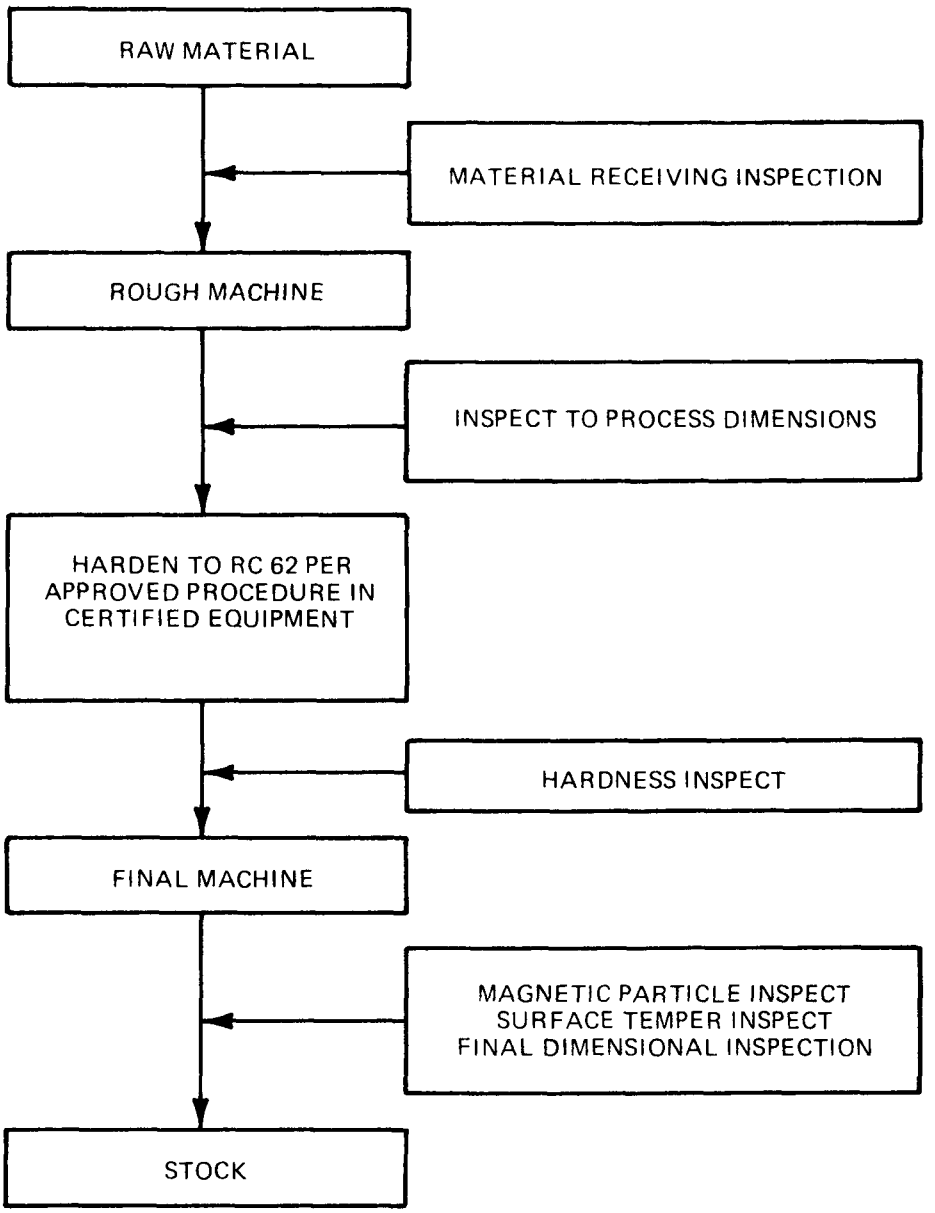

Figure 2.5.3-25 Thrust Runner Fabrication Process

Once the bearings have been lubricated with sufficient flow to remove the heat generated by liquid shear, the lubricant has to be removed from the cavity and returned to the system for heat rejection. For ground operation, this presents no problem because the gravitational field can be used to drive the liquid to the required location. In space, however, these forces are no longer available, and consequently, a flooded, pressurized bearing cavity is employed.

TRADE-OFF STUDIES: Several different scavenge schemes were considered. These include capillary pumping, dynamic slingers, centrifugal seals, and pitot type probes. Test results indicated that the first two methods were not viable, while the fourth is a very complicated configuration and has the tendency for liquid to splash around the pitot tube at higher speeds leading to potential leakage from the bearing cavity. Consequently, centrifugal seals were selected for KIPS.

SIZING AND PERFORMANCE: In order to drive the drainage flow back into the flowing liquid loop, a suitable injection location is required which will operate independent of gravity. The jet condenser throat has been selected for this purpose, where normal operating pressures at the wall are approximately 2 psia, as determined by test. In order to be able to inject the liquid flow into the throat at this pressure, the bearing cavities have to be pressurized to a level slightly above this value. The fluid is trapped within the bearing cavities by centrifugal dynamic seals, one on either side of the turbine cavity and one separating the pump bearing from the alternator cavity. The pressure generated by these seals is a function of the liquid level, which in turn determines the power loss. The back pressure at the jet condenser therefore determines the cavity pressure level and the seal power losses.

Additional power losses arise in the bearing cavities due to the flooded nature of the scavenge scheme. These are mainly churning losses from where the shaft passes through the cavities and also from the other faces of the centrifugal seals. Based on test results, the centrifugal seals will consume 4 watts each of power at design speed and 2.5 psia. The remaining losses are estimated to be approximately 28 watts, for a total scavenge/seal system loss of 40 watts.

MECHANICAL CONSTRUCTION: The two inboard centrifugal seals are both screwed onto the shaft, with a thread direction which precludes loosening during operation. The outboard seal doubles as the thrust runner, thereby reducing the total wetted surface. Fluid volume available for churning is minimized by keeping all housings closely conforming.

RELIABILITY: This type of seal is commonly used and has a high reliability due to the fact that there is no contact involved. The Sundstrand 1 KWe Remcom system employed a centrifugal seal, accumulating more than 13,000 hours operation before the units were shut down, with no sealing degradation.

FABRICATION: Fabrication and inspection procedures are summarized in Figure 2.5.3-26.

Figures 2.5.3-27 and 2.5.3-28 show turbine and pump end bearing and seal arrangements, respectively.

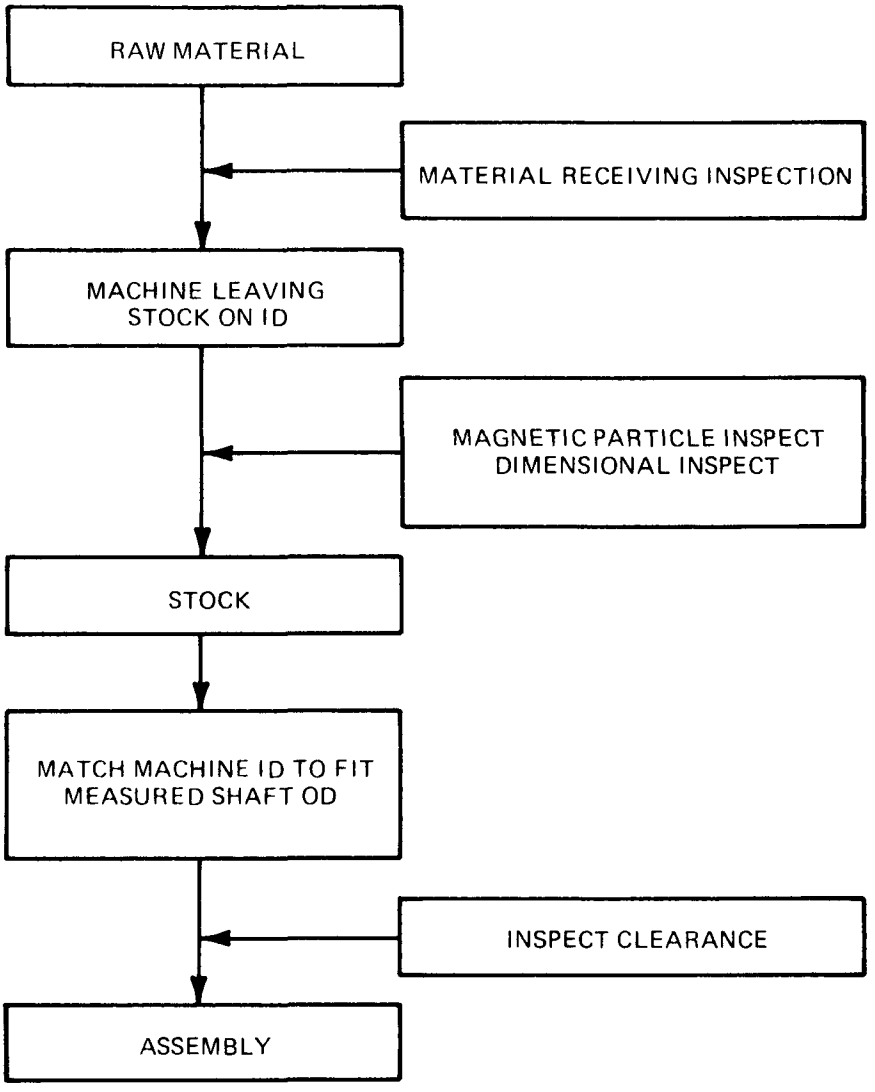

Figure 2.5.3-26 Centrifugal Seals Fabrication Process

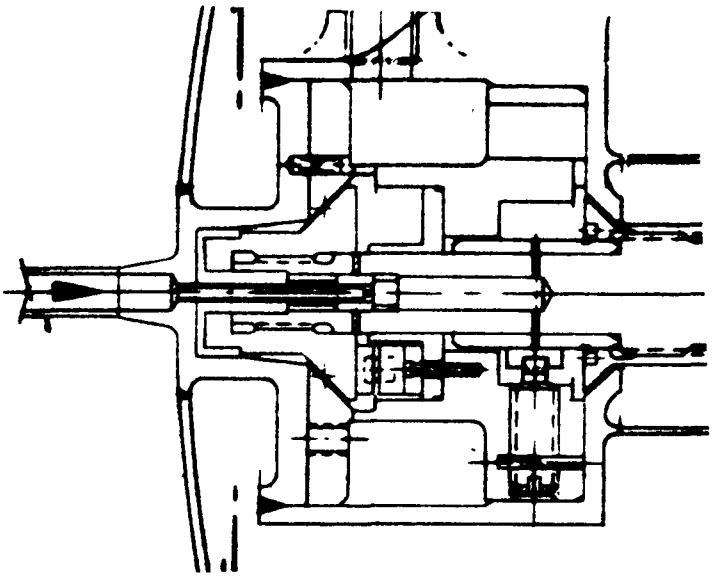

Figure 2.5.3-27 Turbine Bearing

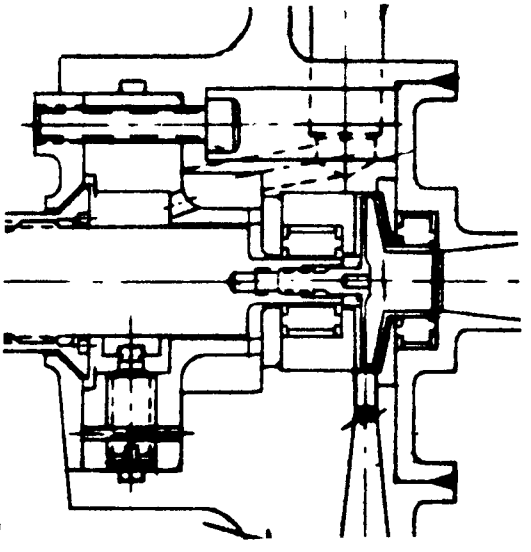

Figure 2.5.3-28 Pump Bearing

2.5.4 CONTROL SYSTEM

The KIPS control system must be designed to accommodate a wide variety of requirements. Some of these are fundamental control functions required on any organic Rankine cycle system, some are necessitated by the particular requirements of the changing thermal output of the isotope heat source used in the KIPS system, and additional functions are necessitated by spacecraft requirements.

The basic control functions include turbine loop flow control, turbine inlet temperature control, combined rotating unit (CRU) speed control, electrical overload protection, output voltage regulation, and system heat rejection control.

The control functions are performed by two separate modules: a valve pack and electronic controller. The "valve-pack" contains the turbine loop flow and temperature controls as well as the radiator bypass valve. The electronic controller provides voltage regulation, overload protection, and speed control.

The fluid loop controls are powered directly by mechanical and hydraulic forces and require no internal or external electrical power for operation. Because of this, the KIPS system can continue to operate safety under conditions of electrical overload.

The KIPS CRU is structurally designed to withstand continuous operation in a frequency wild (no speed control) mode which allows disabling the speed control system when desired. This capability provides the ability to run the CRU at higher speed during launch and orbital maneuvers resulting in added bearing load capability and jet condenser jet stiffness during periods of high shock and vibration.

A block diagram showing the location of the control components in the system is shown in Figure 2.5.4-1.

The flight system valve pack design, showing the fluid loop control components, is shown in Figure 2.5.4-2. The electrical controller circuit design and mechanical arrangement of electronic components are shown in Figures 2.5.4-3 and 2.5.4-4 respectively.

2.5.4.1 Fluid Loop Controls

2.5.4.1.1 TURBINE FLOW CONTROL

FUNCTION: A Rankine cycle system utilizes a control system to maintain turbine inlet conditions at the selected design point. Keeping turbine inlet conditions relatively close to the design point ensures that the system will be able to produce the required power and that the turbine will always be supplied with superheated vapor. This will avoid erosion damage from partially vaporized working fluid. The flow rate through the turbine nozzles is proportional to turbine inlet pressure and inversely proportional to the square root of temperature. Thus, for constant turbine nozzle area, only two of the three parameters: flow, temperature, and pressure, need to be controlled.

The function of the flow control can be illustrated by assuming that all other parameters of the system are held constant and noting the effects of a temperature perturbation on the system stability if no flow control is used. A slight decrease in turbine inlet temperature increases the vapor density at the turbine inlet and permits a greater mass flow rate through the turbine nozzles.

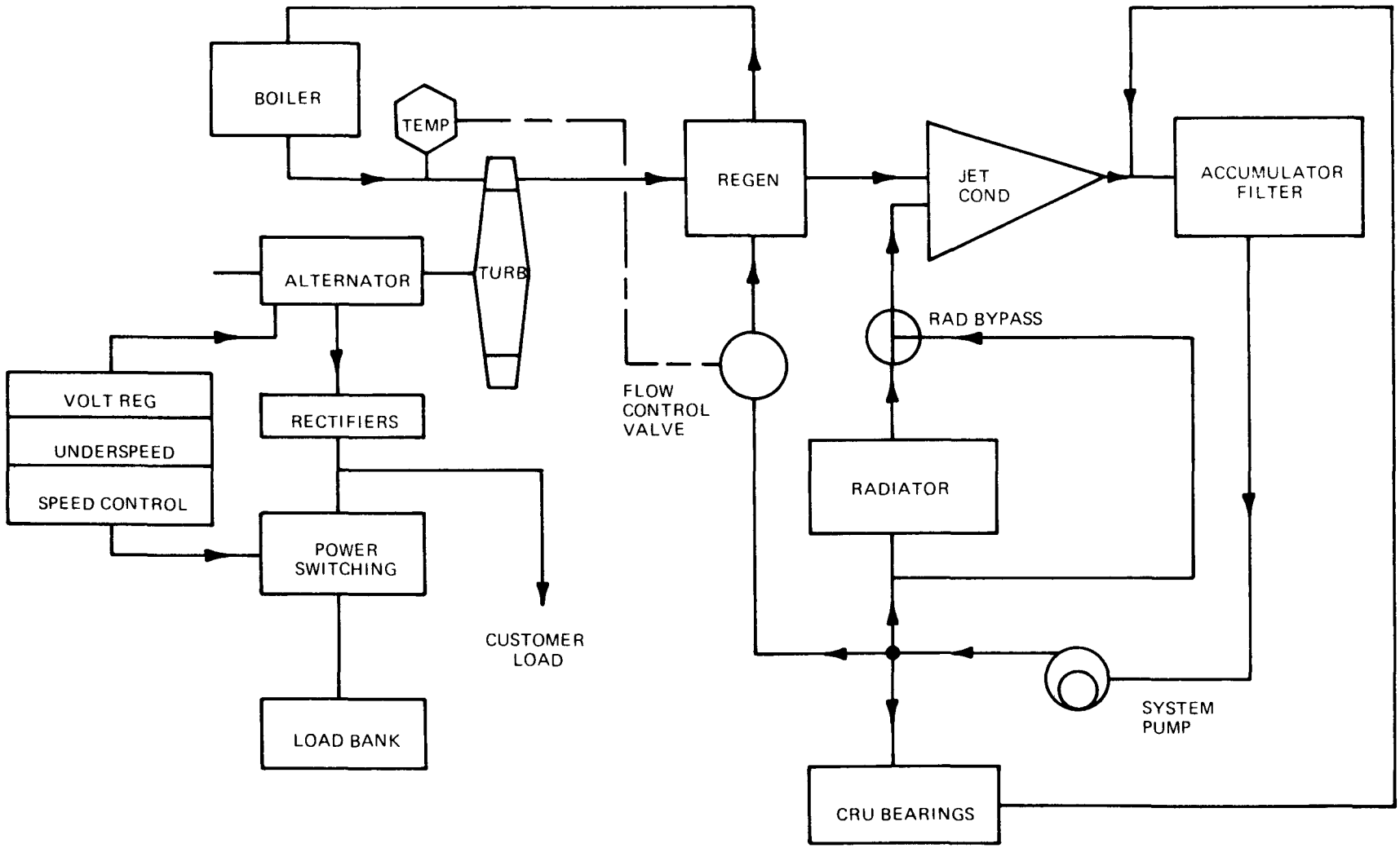

Figure 2.5.4-1 KIPS Block Diagram

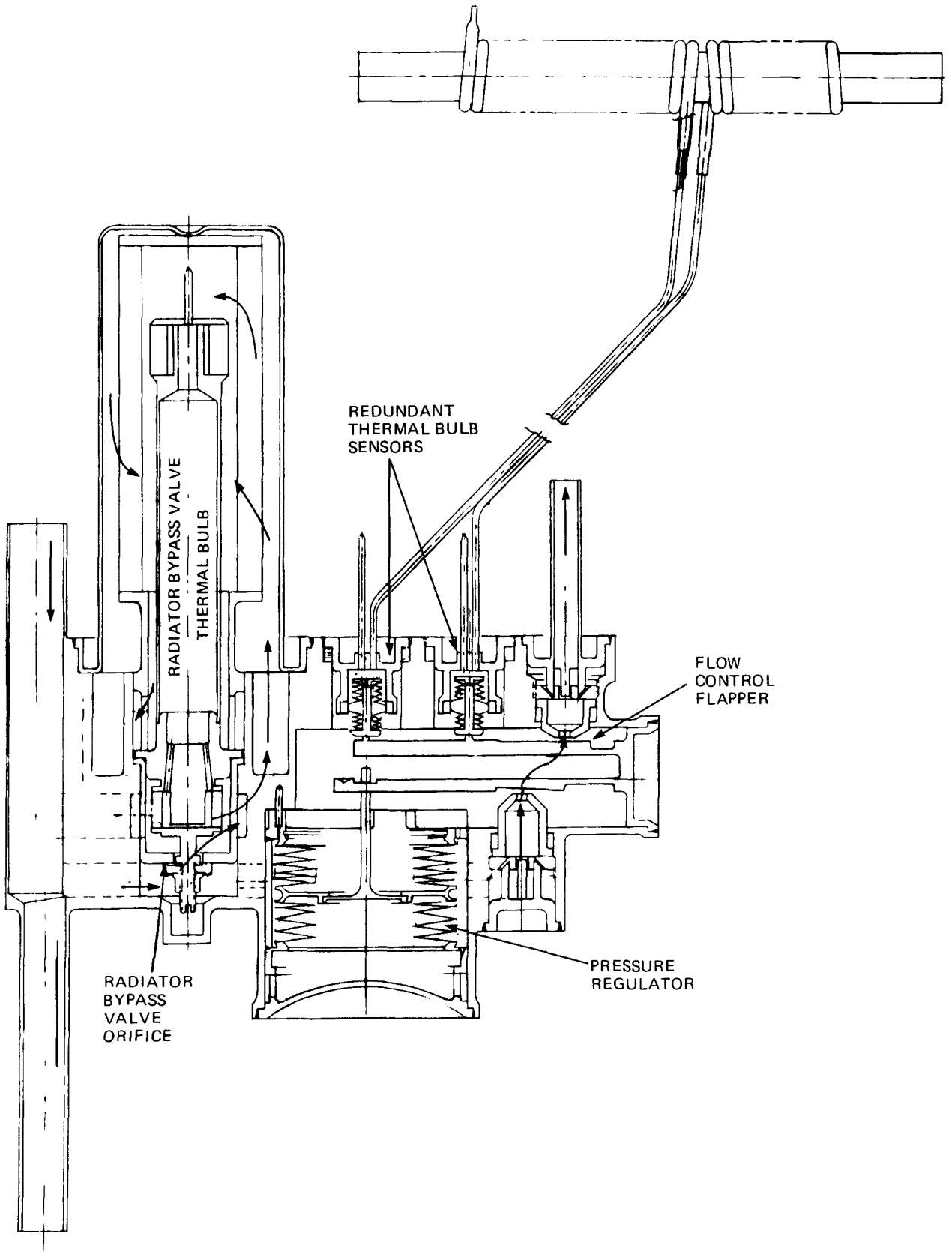

Figure 2.5.4-2 FSCD Fluid Loop Controls

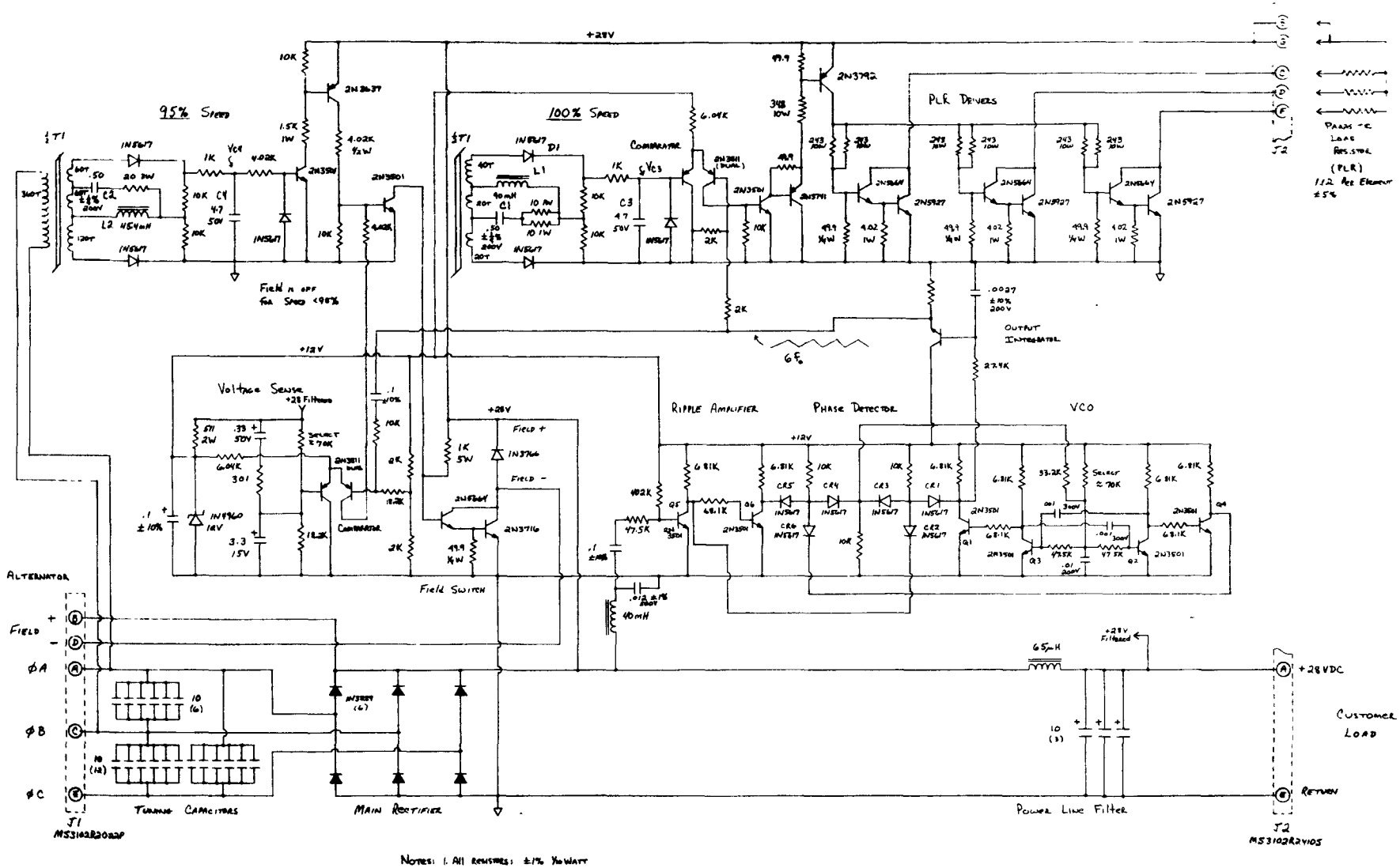

Notes: 1. All resistors: ±1% ¼ watt
2. All capacitors: Microfarads, ±5%, 100V

Figure 2.5.4-3 KIPS Alternator Controller

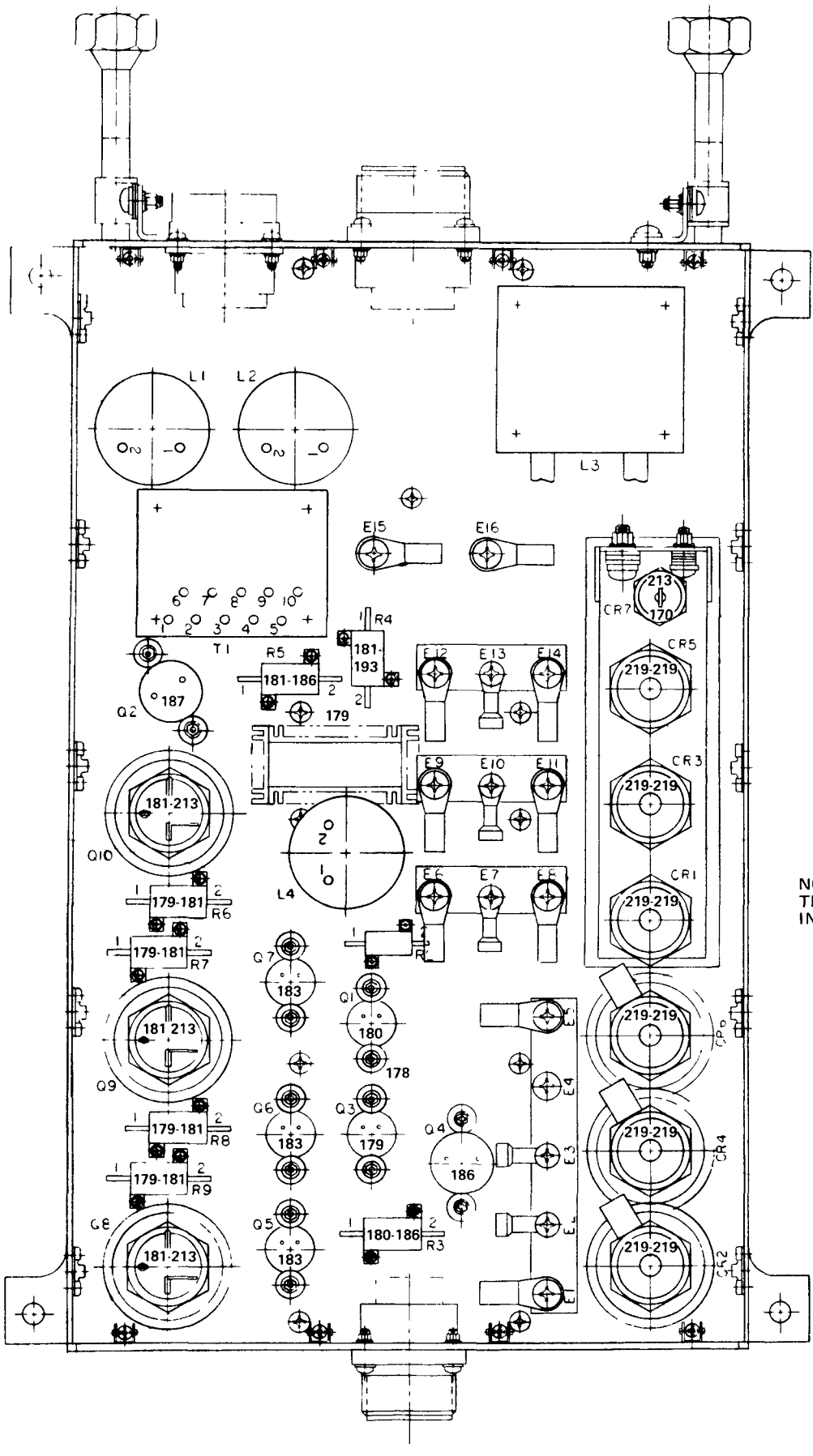

Figure 2.5.4-4 Mechanical Arrangement of KIPS FSCD Controller

Increased flow through the constant heat rate heater results in a further decrease of vapor temperature and even higher nozzle flow.

A positive temperature perturbation starts a cascading process in the opposite direction. The flow control valve adjusts the flow to compensate for any undesirable turbine inlet temperature variations.

For the KIPS organic Rankine cycle (ORC) system where there is only a small variation in system heat input due to isotope decay, sufficient control on turbine inlet conditions can be achieved by throttling flow and permitting the small corresponding change in pressure to occur. A pressure control or a flow limiter could provide constant flow rate, but would not provide adequate turbine inlet temperature control because the 7% decay in heat source input is of the same order of magnitude as the working fluid superheat. Small variations in heat input lead to large changes in temperature. Therefore, if a flow limiter or pressure regulator were used as the primary means of turbine inlet state property control, supplemental temperature control would also be required. This supplemental control could be achieved by using heat pipes or shutters to control heat input rate or by diverting working fluid within the loop to shunt excess heat to the radiator.

As the isotope heat source decays, less heat is delivered to the KIPS boiler. There are basically two approaches to maintain constant turbine inlet temperature as the isotope decays.

In the first approach, flow is kept constant and heat is diverted. It is possible to keep the flow rate constant at a value corresponding to the end of life condition and control turbine inlet temperature via shutters, thermal shunts, or heat pipes on the isotope heat source. This approach limits the power conversion system (PCS) output power to the end of life conditions even when additional heat is available. It also means that the isotope heat source will have additional thermal losses throughout the heat source life due to the presence of the thermal shunt device, further reducing PCS output power. An alternate method for dissipating excess heat at beginning of life condition is to shunt fluid around the regenerator. The regenerator connects the flow loop to the heat rejection loop so that excess heat can be dissipated through the regenerator/condenser interface. The regenerator can be shunted on either the liquid or vapor side to reduce its effectiveness and thus dissipate excess thermal input.

The second approach consists of using all of the available heat at all times and adjusting boiler flow rate as required to maintain constant turbine inlet temperature. This approach permits maximum possible power output at all times and is therefore preferred if it can be easily accomplished.

Various combinations of pressure regulators, regenerator bypass valves, and turbine inlet temperature sensors were investigated to determine their effect on system stability and recovery during output load changes, isotope decay and environmental changes. Direct control of temperature by throttling flow will inherently produce adequate control of turbine inlet pressure and can be designed to control temperature to any desired operating range. The other approach, using a flow limiter or pressure regulator for gross control during frequency wild operation and some means of shunting excess heat by use of a diverter valve, or shutter, provides distinctly inferior temperature control because of component thermal lags, and prevents the system from accepting full load immediately when operating at no load in the speed wild mode. Direct control of the flow in the turbine loop was therefore selected to control turbine inlet state point conditions.

COMPONENT TRADE-OFFS: Various flow control valve designs were investigated to determine which approach led to the highest reliability. Electrically operated valves were eliminated because of

the low reliability of the long chain of components required. The electrical valve requires redundant temperature sensors, electronic control circuits, an amplifier to produce valve drive current, and an electromechanical valve. With this valve, the temperature control function is also dependent on a continuous and uninterruptable supply of electrical power, requiring an additional alternator or an on-board battery.

A fluidic temperature control valve initially appeared to be quite attractive and within the state-of-the-art. The fluidic valve should require no moving parts if temperature sensing is accomplished via a fluid viscosity sensitive capillary tube. This approach was pursued in conjunction with Harry Diamond Laboratories. As the KIPS detailed model of the steady state operating points for the system was completed, an operating map of detailed requirements for the fluidic valve revealed that higher valve gain and faster response than originally anticipated were required. As additional amplifier stages were added, the valve passages became more complicated, heat losses through the temperature sensor increased and valve pressure drop increased. In addition, it was found that to properly start and shut down the system, a check valve must be added to the fluidic valve vent line.

Alternate valves were then investigated in which direct thermal expansion of bimetallic discs or hydraulic displacement of a liquid filled thermal bulb could be used to provide the temperature control signal to the flow control valve.

A bimetallic washer valve, a single stage thermal bulb driven valve and a two stage valve using a pressure regulating stage for basic flow control and a thermal bulb for temperature trim were evaluated as part of a formal trade-off and selection matrix study. These three concepts are shown in Figures 2.5.4-5 through 2.5.4-7.

The bimetallic washer valve was judged poorest of the three concepts. Bimetallic discs provide low force levels and small deflections per unit temperature change, requiring a stack of discs to achieve the required force and deflection levels to actuate a valve. A stack of discs suffers from a low spring rate which leads to potential oscillation problems. Relative movements at the disc control points gives a potential problem of wear and particle generation. Discs as well as other solid differential expansion devices provide an undesirable heat shunt, requiring higher boiler temperature. The relatively high thermal inertia of the disc pack necessitates the addition of a flow limiting or pressure regulating function to avoid transient flow problems during frequency wild operation.

The single stage thermal bulb driven valve represents a substantial improvement over the bimetallic washer valve design in that sliding friction and particle generation are eliminated by use of a flapper-nozzle throttling valve. Thermal shunting is minimized by the low conductivity of the tube connecting the sensor and the valve. Temperature sensitivity is improved by using a relatively large volume in the sensor and a small volume in the actuator bellows. This valve suffers from a slow response rate to temperature changes in the system and provides inadequate flow regulation during load changes in the frequency wild mode of operation.

The two stage valve retains the advantages of the single stage thermal bulb valve and overcomes the transient response problems by incorporating a flow limiting feature. Flow limiting is accomplished by regulating the pressure drop across an orifice via a second nozzle flapper which throttles turbine loop flow. The flow limiter maintains essentially constant flow during periods of rapid pressure change that occurs during frequency wild operation. The temperature sensor corrects the flow setting as required by changes in environmental conditions and gradual decay of the isotope heat source. The two stage valve, as finally configured, incorporates redundant thermal sensors and

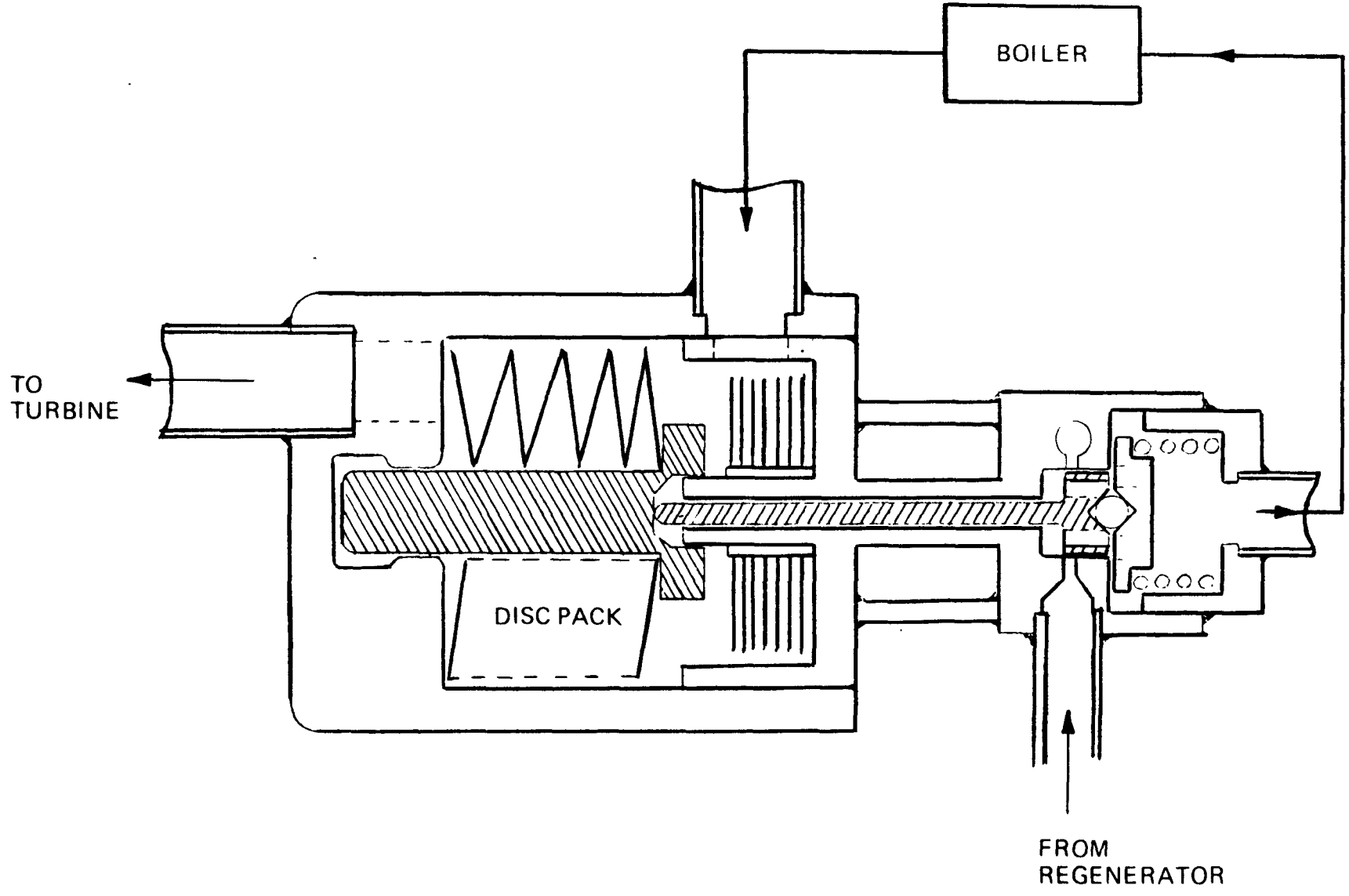

Figure 2.5.4-5 Candidate Bimetallic Flow Control Valve

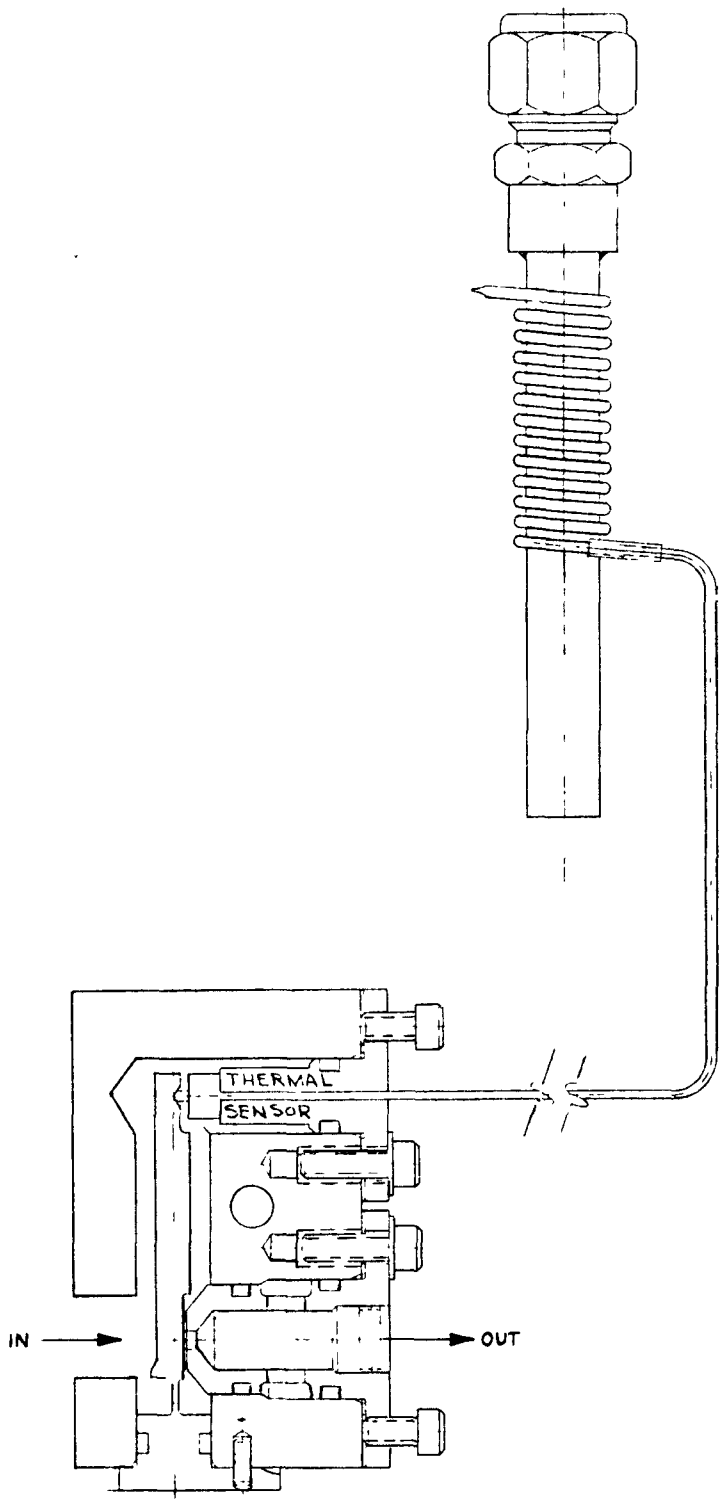

Figure 2.5.4-6 Candidate Single Stage Flow Control Valve

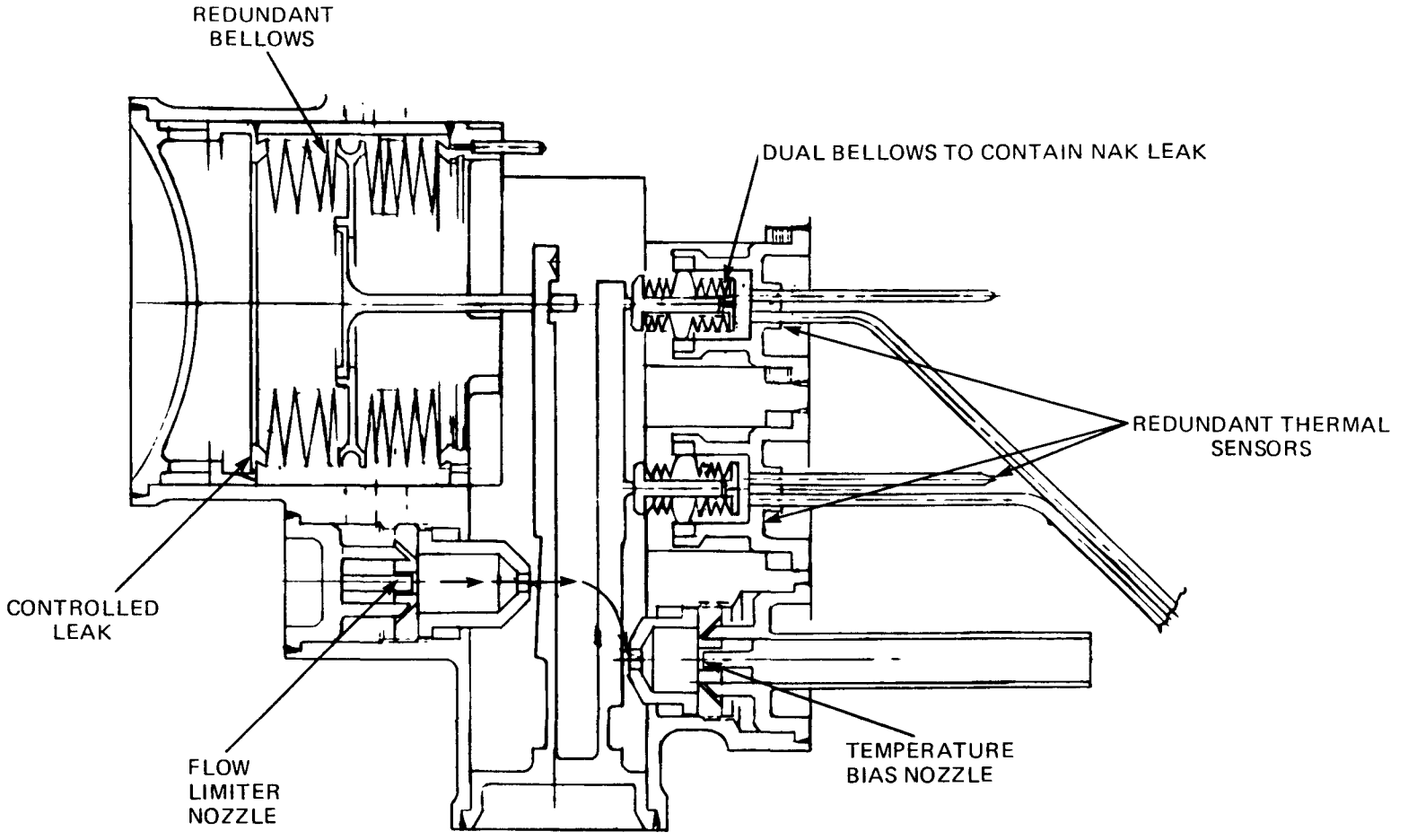

Figure 2.5.4-7 Baseline 2 Stage Flow Control Valve

redundant bellows in the flow limiter portion for added reliability.

A cross-section of the turbine loop flow control valve is shown in Figure 2.5.4-8. The inlet receives flow from the system pump and the regulated outlet flow enters the turbine loop. The pressure regulator bellows assembly senses valve chamber pressure on the side facing the valve chamber. The back of the bellows is connected via internal porting to the valve outlet. The bellows therefore moves in response to pressure drop across the temperature control orifice. When turbine inlet temperature is constant, the temperature control flapper remains in a fixed position and the effective orifice area of the temperature control orifice is constant. With the pressure regulator controlling the delta P across the orifice, system flow is kept constant regardless of inlet pressure. The pressure regulator performs this function by actuating the pressure regulator flapper which throttles inlet flow as required to keep the temperature control orifice delta P constant. Changes in valve inlet pressure are therefore prevented from affecting the flow rate through the valve.

The resulting valve performance characteristic curves are shown on Figure 2.5.4-9 where it can be noted that flow remains essentially constant (for constant turbine inlet temperature) as overall valve delta P varies from 20 to 160 psi.

As turbine inlet temperature increases, expansion of the NaK in the thermal sensor moves the temperature control flapper away from the temperature control orifice, thus increasing the area and the system flow rate. This effect is shown for several steady state temperatures on Figure 2.5.4-9. Superimposed on the figure is a map of required KIPS flows and pressure drops for frequency wild operation. It can be noted that the control valve keeps turbine inlet temperature between 645 and 658^{o}F under all operating conditions. When the speed control circuit is actuated and the system running at constant speed, variations in system pressure is very small and the system operates along the full load line. Under this condition, where the KIPS operates most of its life, the turbine inlet temperature range is 647 - 653^{o}F.

MECHANICAL CONSTRUCTION: The flow control valve was designed with redundant bellows in the pressure regulator assembly. These were sized such that a failure of either bellows would have only a minor effect on system operation. The effect of a cracked or failed bellows is a shift of turbine inlet temperature of less than 2^{o}F as shown in Figure 2.5.4-10. The figure also shows the effects on turbine inlet temperature of other failure modes including a plugged orifice and relaxation of the flapper spring. It can be noted that, in the worst case, the temperature shift is no more than $\pm$ 3^{o}F from the set point. Flexing components, flappers and bellows, were stress analyzed to assure that stresses were below the threshold for cyclic fatigue under worst case deflections.

Dual thermal sensor assemblies are utilized to provide complete redundancy in the temperature sensing portion of the valve.

Several fluids were considered for temperature sensor fluids. Dowtherm A was first considered because of its resistance to thermal breakdown and because Dowtherm A is the system working fluid. Closed capsule test data on the thermal breakdown was reviewed. It was concluded that the amount of gaseous products that could be expected to form over a seven year period was possibly sufficient to produce an unacceptable calibration shift in the unit. There was insufficient data on the solubilities of the gases to ensure that they would remain dissolved. Since Dowtherm A is at least as stable as any alternative organic fluid considered, metals were considered next.

Mercury was the first metal considered. The problem encountered with mercury was embrittlement

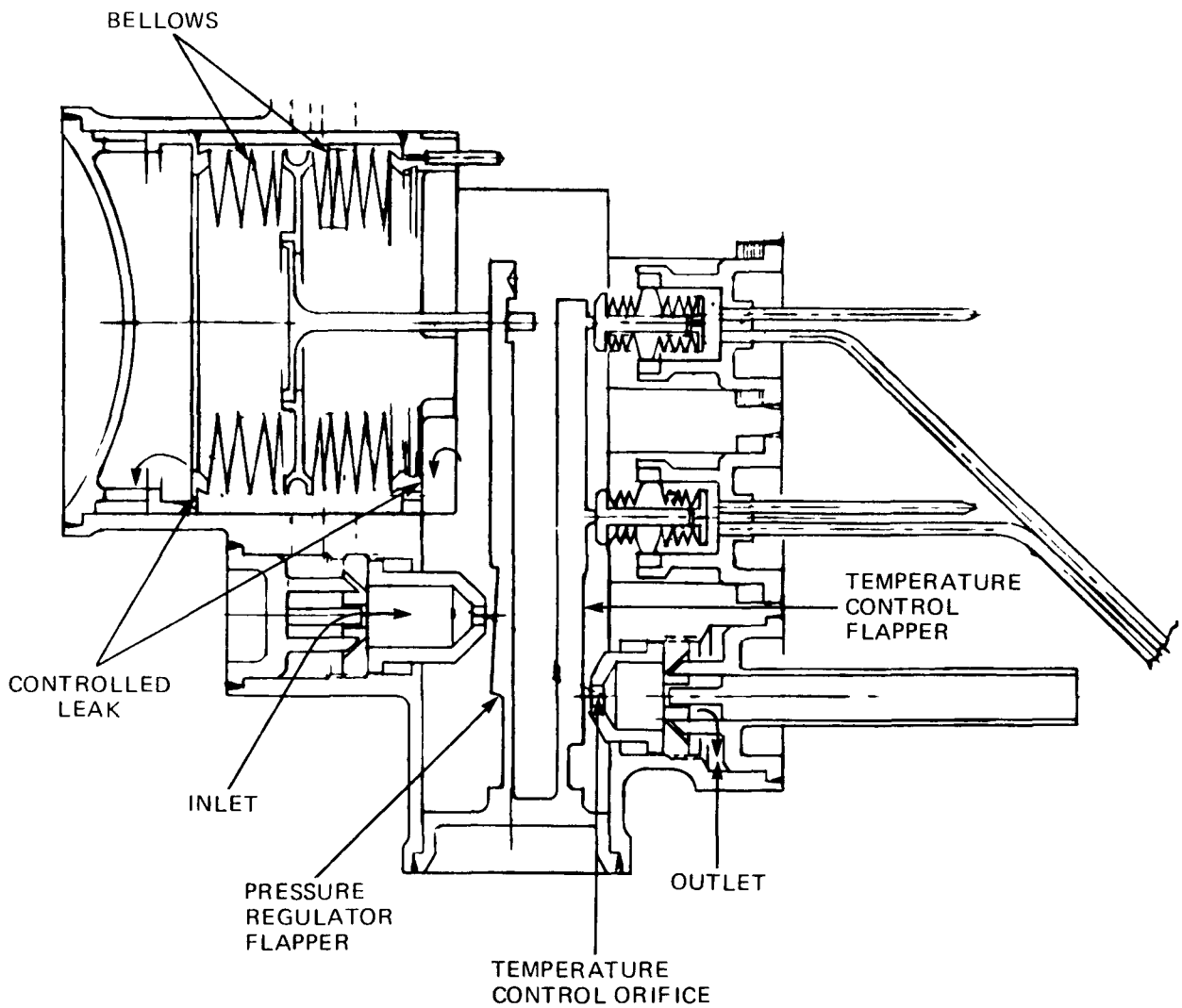

Figure 2.5.4-8 KIPS Flight System Flow Control Valve

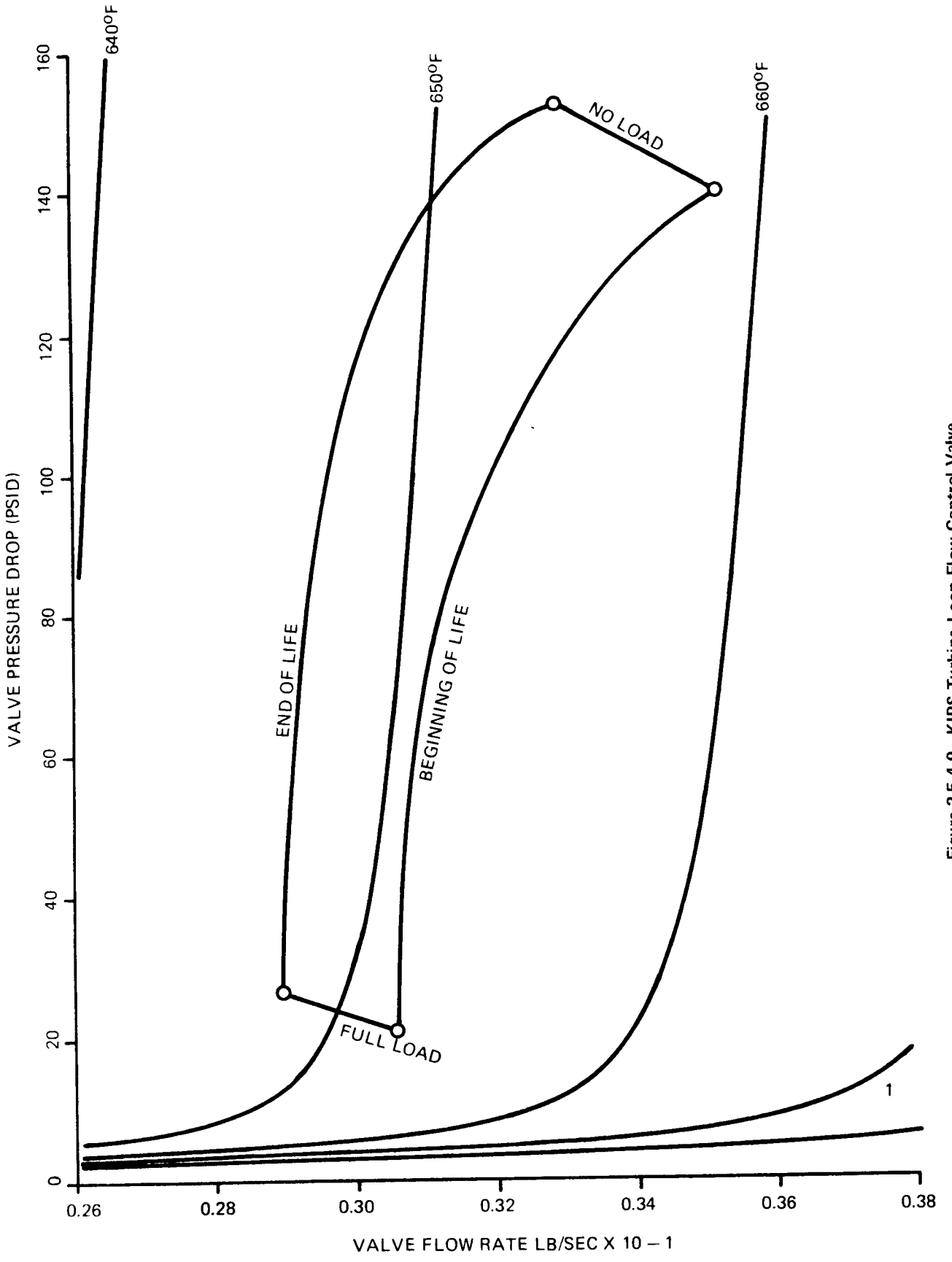

Figure 2.5.4-9 KIPS Turbine Loop Flow Control Valve

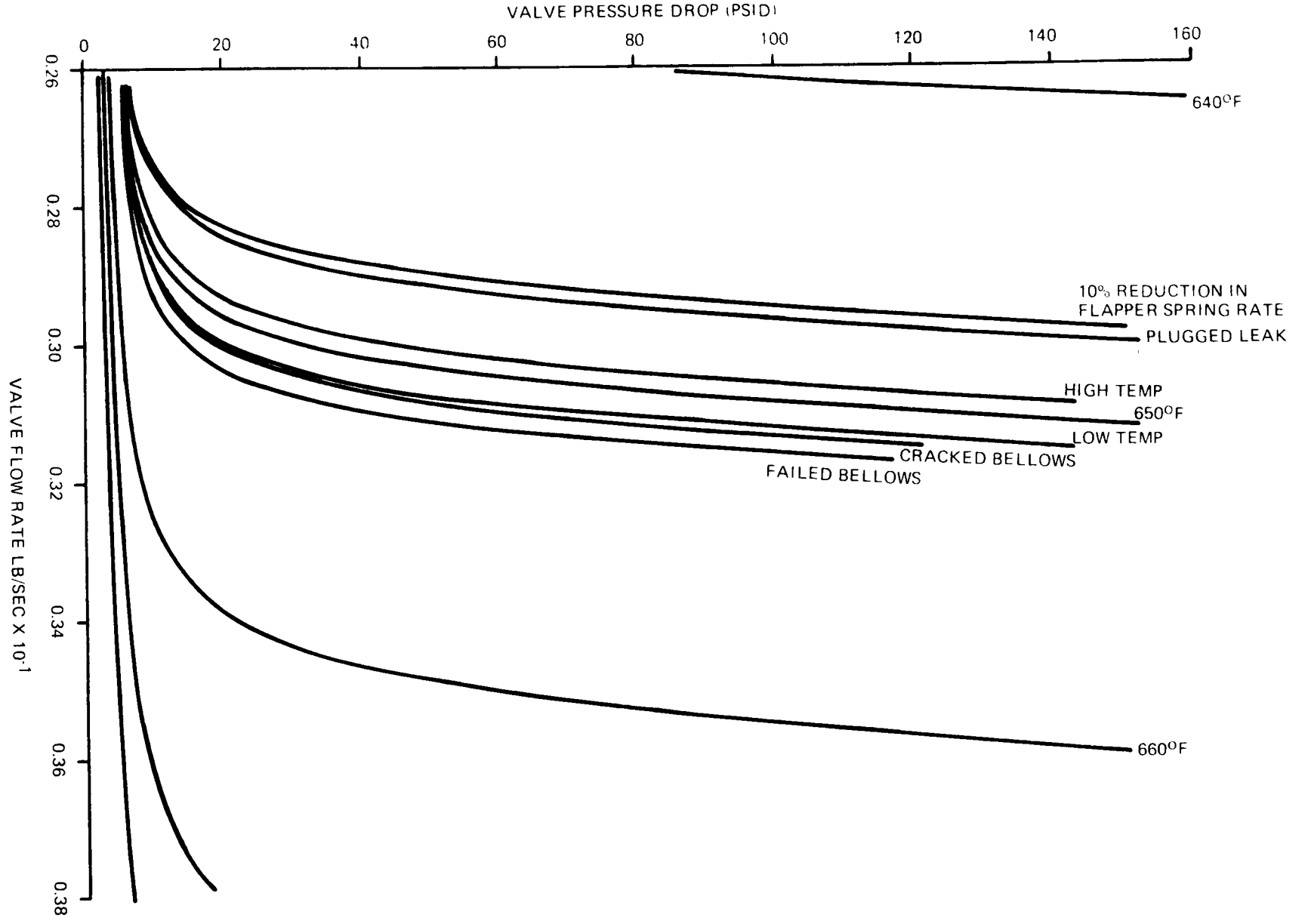

Figure 2.5.4-10 KIPS Turbine Loop Flow Control Valve

of the bellows material. The next metal considered was sodium. Sodium is commonly used in stainless steel containment in nuclear reactors and heat exchangers. Since Na has been extensively used, much data is available on its compatibility with stainless steel. The problem with sodium for the KIPS application is its high freezing point of 208°F. It is likely that a sodium temperature sensor would freeze during storage and might cause problems if melted nonuniformly. As an alternative to sodium, the eutectic NaK was considered. The freezing point of NaK is approximately 10°F and therefore the potential freezing problem should be obviated. The question of corrosion was investigated and found to present no problem if high purity NaK is used in all welded stainless steel assemblies. NaK filled temperature sensors were therefore designed to provide the required flapper deflections with temperature changes.

To ensure that reliable bellows and thermal sensor assemblies are constructed, the bellows assemblies are configured to allow cleaning and inspection from both sides prior to final assembly. The thermal sensor bellows, fitting and capillary tubing will all be cleaned as piece parts prior to assembly. After assembly, the helical bulb, transition capillary and actuator bellows will be leak-checked by helium mass spectrometer to 10^{-8} scc/sec. The containment bellows will be leak-checked to 10^{-8} scc/sec. Prior to filling with NaK, the helical bulb, transition capillary and actuator bellows will be vacuum baked at a pressure of 10^{-6} torr or lower and a temperature of 500°F or greater for a period of 48 hr. minimum. The area between the actuator bellows and the containment bellows will have the same vacuum baking process applied.

The flight system flow control valve pack utilizes an all welded assembly of stainless steel components to preclude internal or external leaks. This valve pack is fabricated from stainless steel.

2.5.4.1.2 RADIATOR BYPASS VALVE

FUNCTION: The primary means of PCS heat rejection is via the system radiator. The radiator must be large enough to reject beginning of life waste heat at full load and the highest heat sink temperature. At other operating conditions, the radiator is oversized and it is desirable to limit the heat rejected to maximize PCS efficiency; this capability is particularly desirable at end of life when the PCS output power is lowest.

It is also very desirable to have some means of controlling radiator outlet temperature when the radiator auxiliary cooling loop is used for system heat rejection when the PCS is installed in the Shuttle Bay. PCS control of the radiator temperature eliminates the need for active Shuttle control of the cooling temperature.

Another function of the radiator heat rejection control is to permit subcooling of the radiator metal to act as a heat sink if the KIPS system is launched using a Titan vehicle. This heat sink permits the KIPS system to continue running during the critical launch period when the radiator is shrouded.

Figure 2.5.4-11 illustrates the effect of radiator bypass function for hot and cold radiator sink temperatures and for both beginning of mission and end of mission heat input flow rates. The hot and cold sink temperature results from motion through space from positions where the radiator is in sunlight to positions where it sees deep space. It can be noted from the figure that it is very desirable to have the bypass valve fail closed (zero bypass). If the valve fails closed, the resulting reduction in power output is only 40 watts in the worst case while an open failure can greatly subcool the system, resulting in major power reductions.

TRADE-OFFS: As in the case of the turbine loop flow control valve, it is desirable to have the

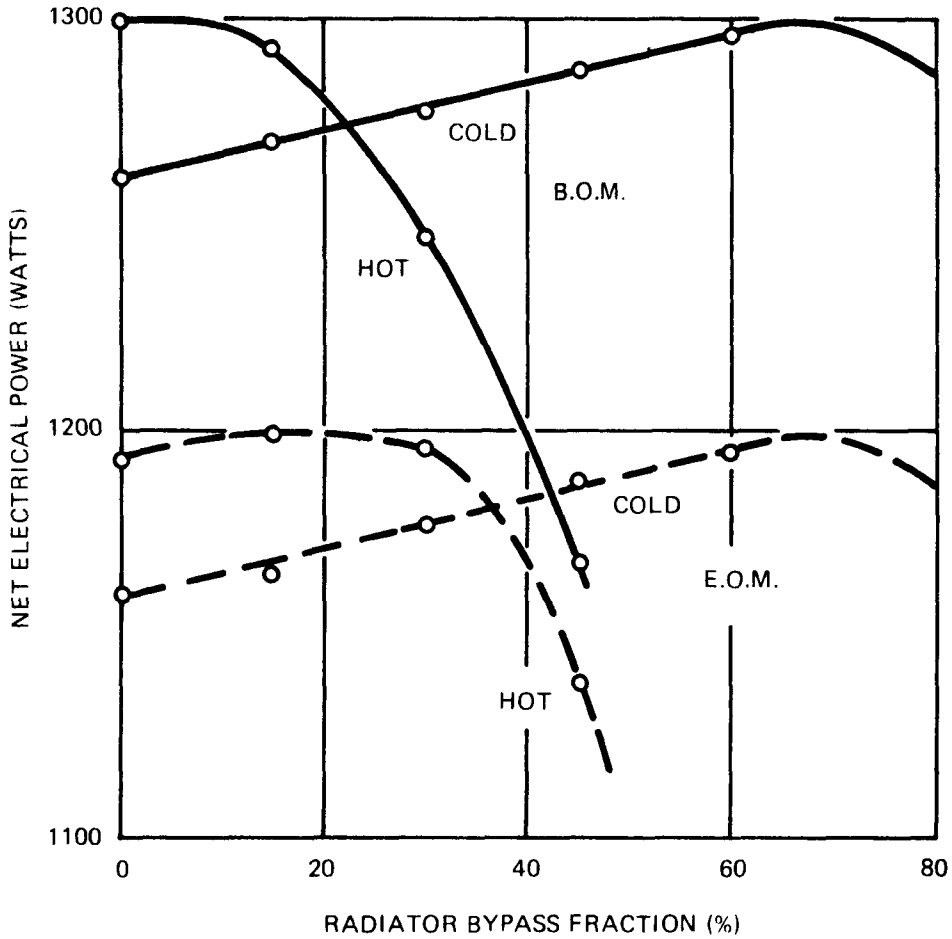

Figure 2.5.4-11 KIPS Performance as a Function of Radiator Bypass

bypass valve self-powered. Both bimetallic disc type valves and thermal bulb valves were investigated. The bimetallic valve has disadvantages similar to those of the bimetallic turbine loop flow control. The thermal bulb valve is ideally suited for use as a radiator bypass since the temperature level is relatively low in this location and the bulb can be filled with the system working fluid. A failure of the valve that creates a leak will permit the Dowtherm in the valve to enter the system with no ill effect and will also cause the valve to fail closed. This is the desirable failure mode from a system operation standpoint.

The thermal bulb valve was therefore selected for use as the radiator bypass valve. A cross-section of the valve is shown in Figure 2.5.4-12, integrated into the valve block and filter assembly.

OPERATION: Warm fluid from the pump passes through an orifice and mixes with cooler radiator outlet fluid. The mixed fluid is circulated around the thermal bulb and then exits to the jet condenser.

When the mixed fluid temperature is excessive, expansion of the fluid in the thermal bulb moves the valve seat closer to the orifice restricting the influx of warm fluid to reduce the mixed fluid temperature. The actuation bellows free length is shorter than its operating length so that a leak in the thermal bulb or bellows will cause the bellows to fully contract, thus pulling the auxiliary seat against the orifice to completely shut off the bypass flow.

MECHANICAL CONSTRUCTION: The radiator bypass valve has only one flexing part, the fluid containment bellows assembly. This bellows was designed such that cyclic fatigue would not occur, although a failure here is not critical to continued system operation. The working fluid in the thermal bulb is Dowtherm A, identical to the system working fluid, so there is no ill effect on the system of a leaking bellows. Redundancy was therefore not provided on the radiator bypass valve bellows.

The bypass valve components are cleaned and vacuum baked prior to welding. The assembly is helium leak checked to a level of 10^{-8} scc/sec prior to filling. A variation of ± 10% on resultant temperature gradient of the valve stroke is acceptable from a performance standpoint. Shims are provided to permit cracking point adjustment during assembly of the valve into the housing.

2.5.4.2 Electrical Controls

The controller provides output power conditioning, voltage regulation, speed control, and electrical overload protection. The controller is powered by the alternator. No external electrical power is required. Power conditioning includes rectifiers and an appropriate filter to achieve 0.1% rms ripple. The voltage regulator provides 28 VDC ± 2% voltage control through control of the alternator field. Speed control is achieved by applying a parasitic electrical load as required to keep the speed within ± 2% of the design speed. Electrical overload protection is provided by an underspeed detection circuit which removes alternator field current whenever the speed is less than 95% of rated speed.

2.5.4.2.1 BASELINE CONFIGURATION

Figure 2.5.4-13 shows a block diagram of the baseline control system.

SPEED CONTROL: Speed control is accomplished by a frequency discriminator which monitors the alternator output frequency, (which is proportional to speed) a comparator (pulse width modulator) and the parasitic load resistor.

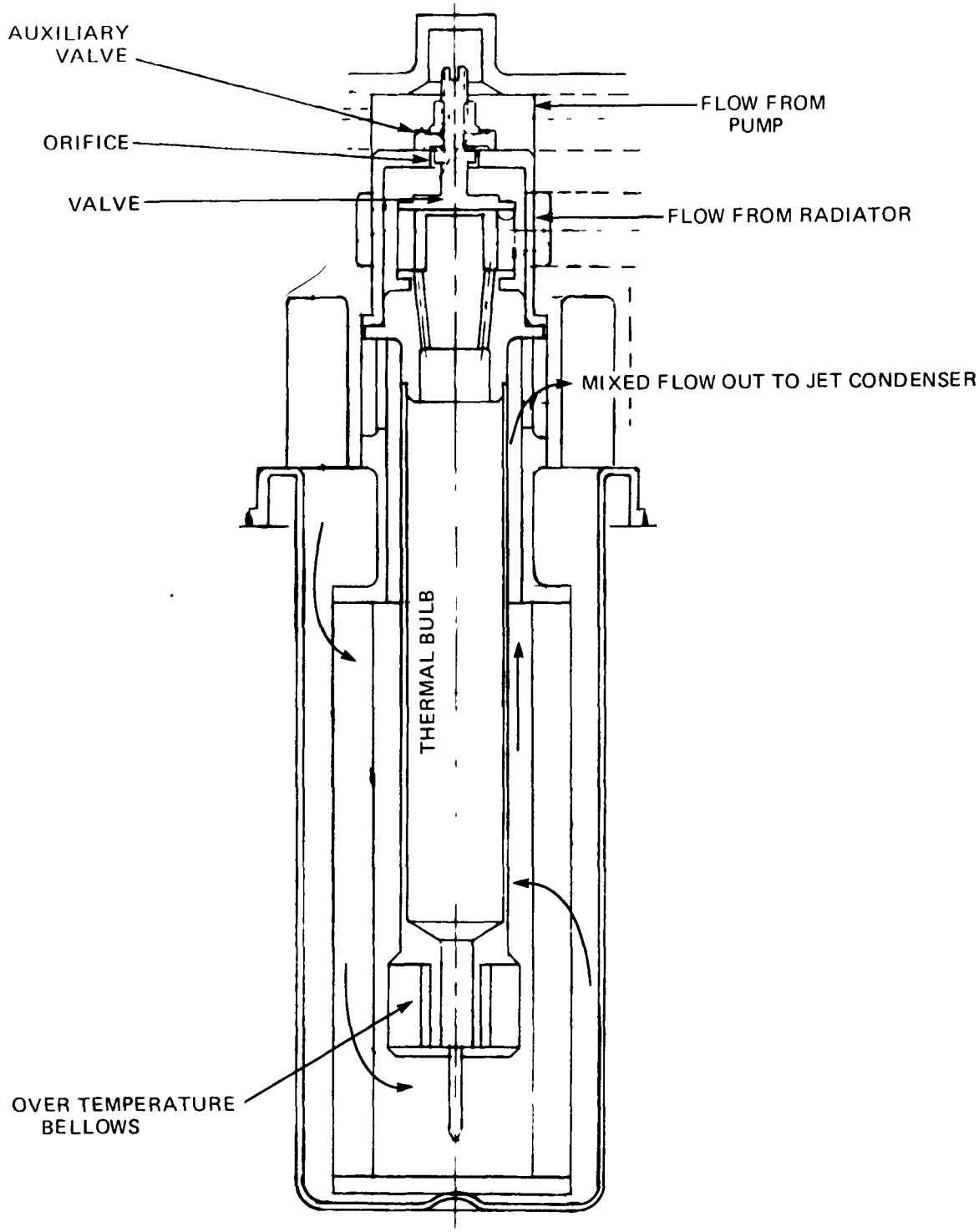

Figure 2.5.4-12 KIPS Radiator Bypass Valve

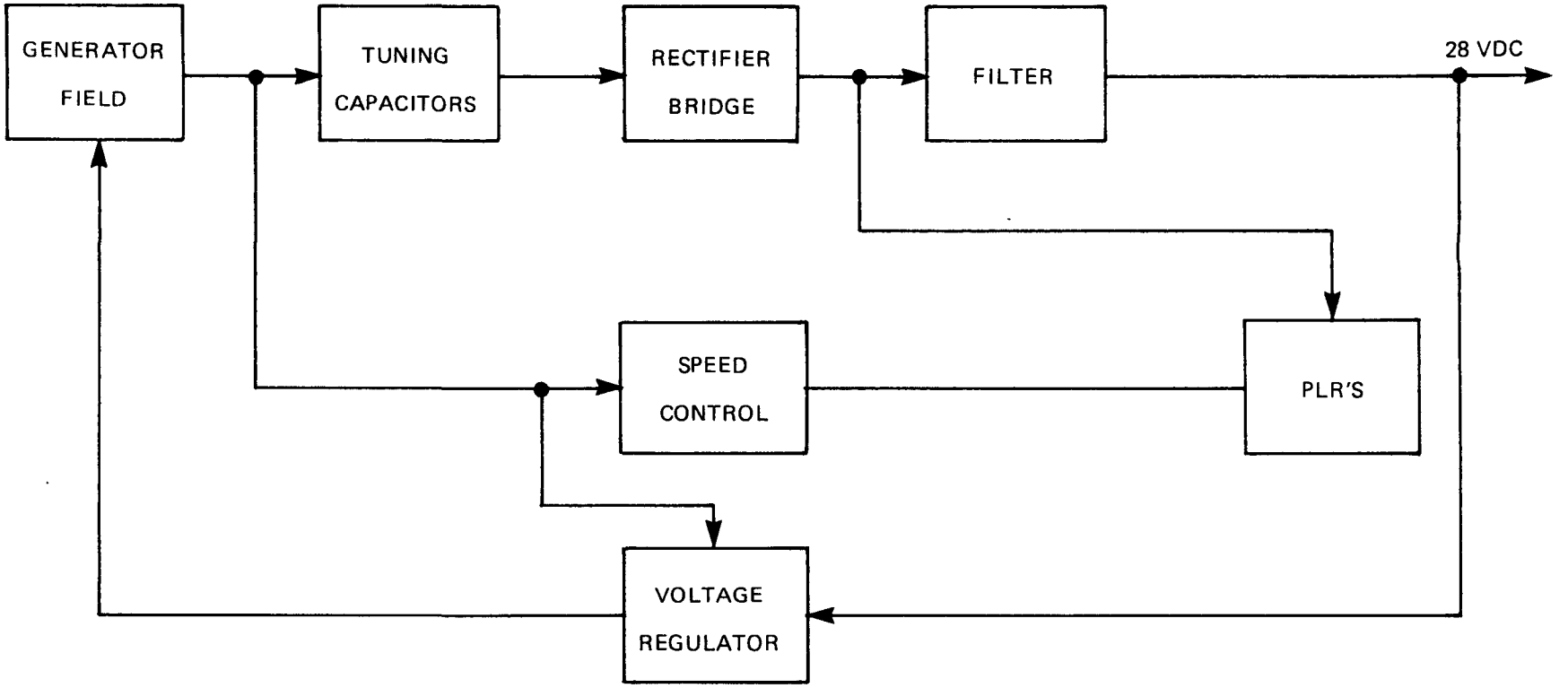

Figure 2.5.4-13 Control System Block Diagram

The parasitic load is comprised of three parasitic load resistors (PLRs) each capable of drawing 50% of the load. Thus, two PLRs are capable of providing full load. Having three PLRs with any two capable of handling full load greatly increases the reliability of the system.

The frequency discriminator consists of a passive tuned circuit which produces a DC output voltage proportional to system frequency near the resonant frequency of the tuned circuit.

The Pulse Width Modulator (PWM) comparator is set at a 50% duty cycle at a voltage proportional to 1122 Hz (33,700 RPM). The PWM rate is controlled by the carrier frequency which is the ripple frequency of the three phase, full wave bridge rectifier. The PWM comparator turns the power switches on or off, applying or removing power to the PLRs. Since the carrier frequency is high (6 x 1122 = 6732 Hz), the time averaged effect is a steady load determined by the PLR duty cycle. The duty cycle will change in response to system capability and customer loading.

VOLTAGE REGULATOR: The voltage regulator is pulse width modulated to minimize the regulating losses. The switching point of the PWM regulator is set at the 50% duty cycle of the carrier frequency. When the output voltage is low, the PWM duty cycle goes toward 100% causing maximum field current to flow in the field winding, increasing the generator voltage. When the output is high, the PWM duty cycle tends toward zero, allowing the field current and generator output voltage to decay.

OVERLOAD PROTECTION: The overload protection circuit uses a frequency discriminator similar to the speed control frequency discriminator and a comparator to detect when turbine speed falls below 95%. When this is detected, the switching amplifier is turned off, decreasing the generator output voltage and lowering the generator load. The generator output voltage will not decrease below a small residual voltage which is sufficient to operate the frequency discriminator, comparator and switching amplifier.

POWER CONDITIONING: The alternating current (AC) output of the alternator is converted to a DC voltage by a three phase full wave bridge rectifier assembly.

A low pass filter, consisting of an inductance and a capacitance, conditions the output voltage to a DC level having a 0.1% rms ripple content.

Alternator tuning capacitors are used to improve the power factor of the alternator, thus reducing the diode commutation overlap time of the full wave bridge rectifiers. Calculations indicate that the efficiency is improved by one percent using tuning capacitors. The tuning capacitors are sized to the load requirements for the particular mission.

When the turbine and alternator are operated in the frequency wild mode, the tuning capacitors can cause the alternator to operate self-excited. Self-excitation of the alternator results in excessive output voltage. To maintain proper voltage regulation, the signal which commands the frequency wild operation is also used to switch out the tuning capacitors from the alternator.

2.5.4.2.2 TRADE-OFF STUDIES

VOLTAGE CONTROL APPROACHES: A voltage regulator is required to maintain the output voltage within required limits. Voltage regulation is typically accomplished by controlling alternator field current. Several types of voltage regulator circuits can be used. These are described in the following paragraphs.

PROPORTIONAL VOLTAGE REGULATORS: Shunt and series regulators are simple with low parts count but have the major drawback since they are dissipative. High dissipation causes high junction temperatures in semiconductors and resistors, lowering their reliability. Therefore, dissipative proportional voltage regulators were eliminated because of their low reliability.

MAGNETIC AMPLIFIER REGULATOR: The magnetic amplifier acts as a phase controlled switch on the rectified AC field supply voltage to supply a variable DC voltage to the exciter field. The magnetic amplifier can be considered a switch in series with the exciter field that can be turned on at various phase angles of the rectified input voltage half sine waves, thus producing a variable DC. This regulator is simple with few parts; its drawback is the weight of the magnetic amplifier which must handle the total field current.

PULSE WIDTH MODULATED REGULATORS: The pulse width modulated regulators can be put into two classes: forced and bang-bang modulation.

- Pulse Width Modulation: In pulse width modulation, a switch in series with the field is operated at either the ripple frequency of the field power source or at a selected frequency derived from an oscillator. The duty cycle of the modulation frequency is varied by voltage error to maintain the output voltage.

- The pulse width modulation scheme operating at the ripple frequency has been determined to be the best in terms of stability, power dissipation and parts count, and was therefore selected for the baseline system.

- Bang-Bang Pulse Width Modulation: In the bang-bang system, the switch in series with the field is allowed to modulate at the system natural frequency and have a duty cycle dependent on the loop dynamics. This is a simple regulator with voltage regulation characteristics less refined than the forced pulse width modulation scheme. Experiments have shown unacceptable levels of voltage modulation with this approach.

SPEED CONTROL APPROACHES: Speed control is required to maintain the turbine within the required speed limits. Speed control is accomplished by applying a parasitic electrical load to the alternator. The control schemes considered are the two classes of the pulse width modulated regulator.

In the bang-bang pulse width modulation concept, the PLRs are turned on whenever the output frequency exceeds 1122 Hz (33,700 RPM). The added electrical load causes the CRU to slow down. The parasitic load is removed when the alternator frequency is less than the rated frequency of 1122 Hz. Experiments have shown unacceptable levels of speed modulation with this approach.

In the pulse width modulation approach, a switch in series with the parasitic load resistor is operated at the ripple frequency of the bridge rectifiers. The duty cycle of the modulation frequency is varied by the alternator frequency error voltage to maintain the turbine speed. Thus, the frequency of the pulses is much higher than in the bang-bang approach and speed can be more closely controlled. The pulse width modulation approach provides good speed control with low power dissipation and was therefore selected for the controller.

RELIABILITY STUDIES: Trade-offs were made between various controller configurations. The intent was to determine the least complex controller that has a probability of at least 0.986 of achieving the mission life of seven years.

The effect on circuit reliability of adding redundancy to various circuits was calculated and compared to the baseline approach to determine if significant improvement in overall reliability would result. It was determined that the PLR reliability was relatively low and that by adding redundancy in the PLR circuit, overall reliability met the design goal.

Added complexity and weight in other circuits yielded very low increases in reliability and were therefore not incorporated into the baseline controller.

SPEED CONTROL: Various speed control configurations that were reviewed are discussed below. The reliabilities (probability of seven year life) are summarized in Table 2.5.4-A. Version A has a single frequency discriminator, comparator, power switch, and PLR.

The baseline speed control, version B, has one frequency discriminator, one comparator, and a separate power switch for each of three PLRs. The PWM carrier is produced by a single circuit that also provides the carrier to the voltage regulator. Two of the three PLRs are required to dissipate the full load.

In version C, each PLR is driven by a separate frequency discriminator, comparator and power switch combination. Two PLRs are capable of handling the full load.

Version D is the same as C with an additional power switch to each of the three paths to provide additional reliability in the case of a power switch open circuit failure. Two PLRs are capable of full load.

The speed control of version E has three parallel connected frequency discriminators driving three sets of parallel connected comparators which control three sets of series connected power switches. Two PLRs are capable of full load.

It can be noted from the reliability comparison of these speed control concepts that adding PLR redundancy improves reliability significantly but that additional circuit redundancy yields little additional improvement in reliability.

VOLTAGE REGULATOR: The baseline voltage regulator with overload protection is described in subsection 2.5.4.2.1. The first alternate considered consisted of two of the baseline voltage regulators connected in parallel with only one regulator required for proper operation. The second alternate considered consisted of three baseline voltage regulators, with each one driving a separate field in the generator. Only two of the fields and associated circuitry are required for proper operation.

Reliabilities are:

Baseline	0.998345
Alternate 1	0.999998
Alternate 2	0.999994

It can again be noted that only minor improvements in reliability acrue from the more complex alternate circuits.

TUNING CAPACITOR: Figure 2.5.4-14 shows the baseline tuning capacitors and a tuning capacitor system that could be used for a no single point failure philosophy.

Table 2.5.4-A Reliability of Alternate Speed Control Circuits

VERSION	FREQUENCY DISCRIMINATORS	COMPARATORS	POWER SWITCHES	PLR's	RELIABILITY
A	1	1	1	Not Redundant	0.830451
B (Baseline)	1	1	3	3	0.991519
C	3	3	3	3	0.992223
D	3	3	6	3	0.992511
E	3	6	6	3	0.992515

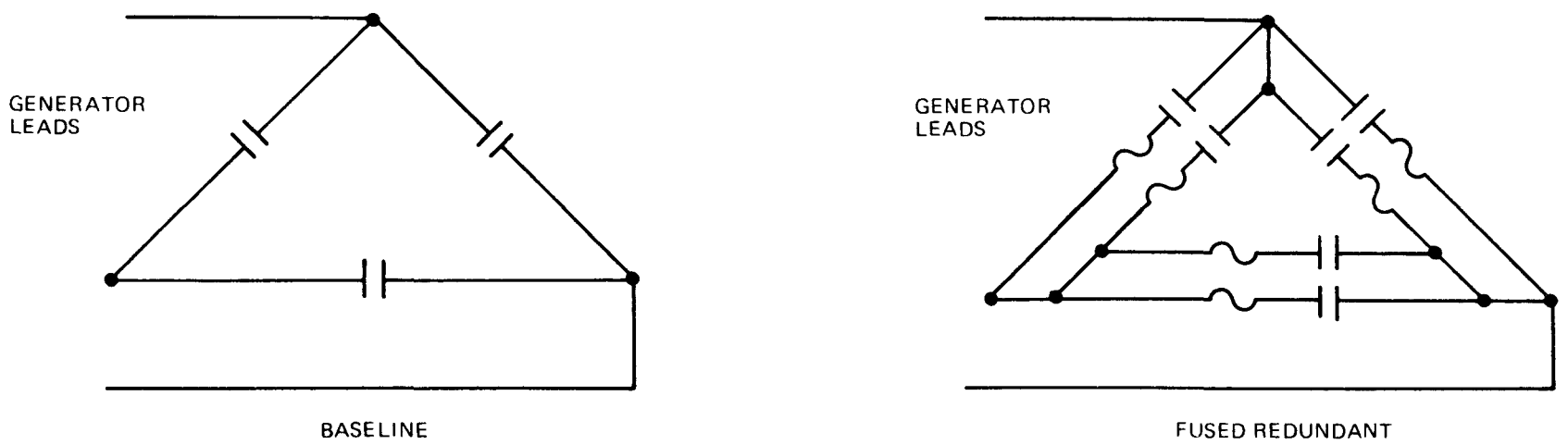

Figure 2.5.4-14 Tuning Capacitor Alternatives

Reliabilities are:

Baseline	0.999997
Fused Redundant	0.998756

In this example, the reliability is actually decreased by adding additional components to avoid single point failures.

RECTIFIER: The baseline rectifier and other rectifier configurations that could increase rectifier reliability are shown in Figure 2.5.4-15. The reliabilities are as follows:

Baseline	0.99909166
Redundant	0.99999961
Fused Redundant	0.99983158
Combination	0.99999185

A significant increase in weight and complexity yields only minor reliability improvement.

CONCLUSIONS: The allocated controller reliability for seven years was 0.986. Since the PLRs individually have the lowest reliability of all the controller components, the first step in increasing the baseline controller reliability is to choose the configuration where the PLRs are sized such that two PLRs are capable of full load. With this change, the baseline controller has a reliability of 0.982. Any additional changes that would significantly increase controller reliability would also significantly increase system weight. The achieved controller reliability is adequate to meet the overall KIPS reliability goal.

2.5.4.2.3 BASELINE CONTROLLER CIRCUIT DESCRIPTION

A functional schematic of the controller is given in Figure 2.5.4-16. The main circuit groups are:

Main Power Rectification, including tuning capacitors, rectifier diodes, and a power line filter

Voltage Regulation, including a 95% speed detector, a voltage sensing network, a comparator, and a field switch

Speed Control, including a 100% speed detector, comparator, and PLR driver stages

Synchronization, including a ripple amplifier, phase detector, and a voltage controlled oscillator (VCO)

Each of these sections is labeled on the schematic.

Key features of the design are the simplicity of the circuits, the use of components of the highest available reliability level and the low operating stress levels of the components.

The low power losses achieved provide a margin of compensation for parameter variations due to production tolerances and estimates of aging effects.

During breadboard testing, it was determined that the output ripple voltage decreases significantly when the PLR and field switches are synchronized with the ripple. To accomplish this, the ripple is

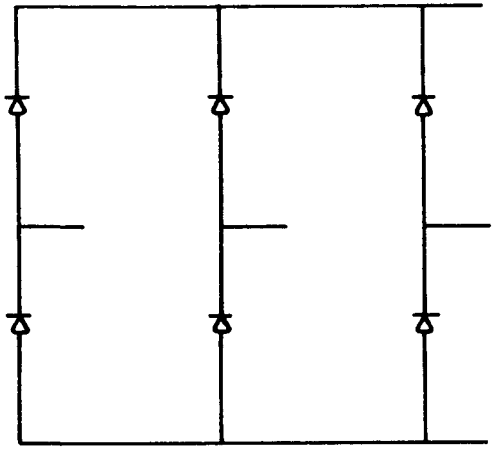

BASELINE

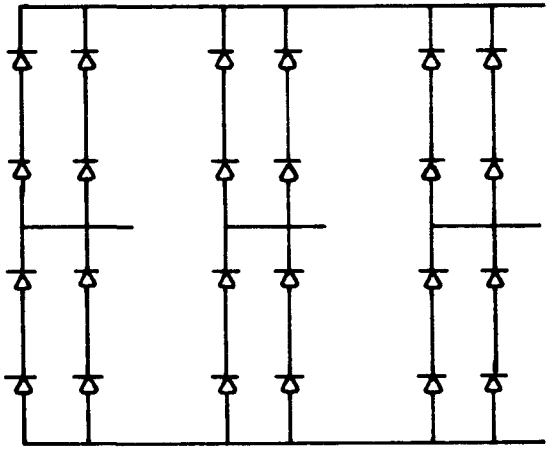

REDUNDANT

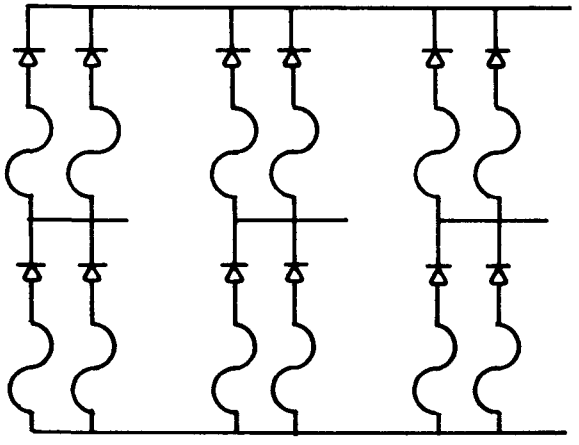

FUSED REDUNDANT

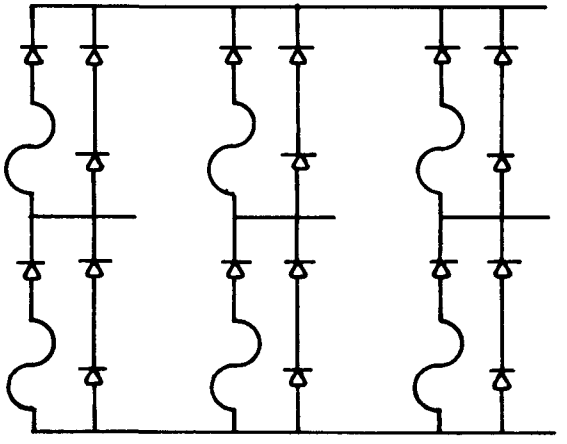

COMBINATION

Figure 2.5.4-15 Rectifier Alternatives

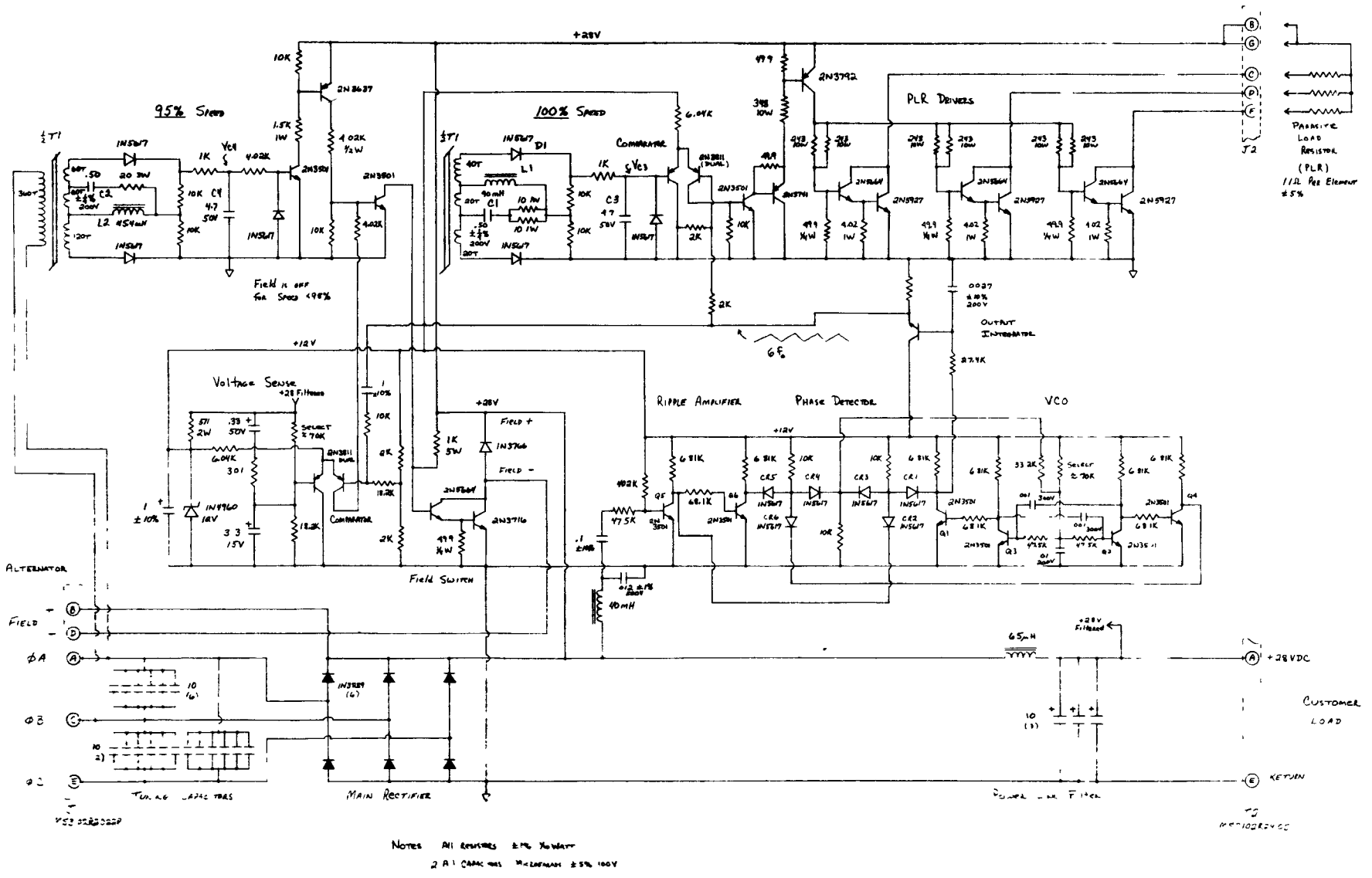

Figure 2.5.4-16 KIPS Alternator Controller

filtered, amplified and then used to vary the frequency of the voltage controlled oscillator so that its frequency is identical to the ripple frequency. This sets up a pulse width modulation that is synchronized to the ripple. The flight controller includes this synchronizing circuitry to minimize ripple.

2.5.4.2.4 MECHANICAL CONSTRUCTION

The controller is mounted by integral lugs protruding from the base casting. All components with large power dissipation are mounted on the chassis either by threaded studs or threaded fasteners in their bases. Insulation is used in these mountings where electrical isolation is required.

Heavy wound core components employ threaded fasteners cast into their encapsulation. Printed wiring boards provide mounting and interconnection of the small electronic components. The board assemblies are mounted by threaded fasteners to brackets attached to chassis side and end plates. Auxiliary support is provided by standoffs mounted to the chassis by threaded fasteners.

Wiring and bus bars are supported by standoffs and by clamps and the devices which they terminate. Electrical connectors are chassis supported by their shell flanges with threaded fasteners. To assure good thermal contact and reliability, while minimizing chassis weight, the cooling tube will be cleaned and sealed and then cast into the aluminum chassis.

The controller is protected against corrosion and malfunction in humidity and salt atmospheres as required by MIL-E-5400. Metals are protected by plating where required and the printed wiring boards protected by conformal coating.

CONTROLLER COOLING: The coldest fluid in the power conversion system, radiator outlet flow, is used as the heat sink for the waste heat from the electronic control package. A thermal model of the controller package was generated in order to optimize the location of the components on the plate and to design the plate to minimize component temperatures. The model resulted in the mounting being arranged so that those components with high electrical dissipation losses were thermally coupled as closely as possible to the coolant tube, while resistors and components with very low dissipation were mounted in the center of the plate. In order to keep thermal contact resistance between the component base and the plate to a minimum, an elastomeric interface material is employed; namely, Chotherm 1661. Special mounting nuts are employed for the rectification diodes and power switching transistors, both of which were high dissipation losses, to reduce the thermal resistance into the coolant fluid. The tube was sized to give a good liquid heat transfer coefficient with a low liquid side pressure drop.

The resultant component junction temperatures (^{o}F) are given in Figure 2.5.4-17. The first of the two temperatures, where two are listed, is the temperature that occurs during a 1300 watt customer load. The second is the temperature when no customer load is being provided. Maximum junction temperature is 219^{o}F (104^{o}C), well within the 125^{o}C limit for high reliability, long life operation of discrete components.

RELIABILITY AND COMPONENT STRESS: A stress analysis was made of the KIPS controls circuit. This analysis verified that all components have stress levels that are well below their rating. The maximum stress found for each component type is listed below:

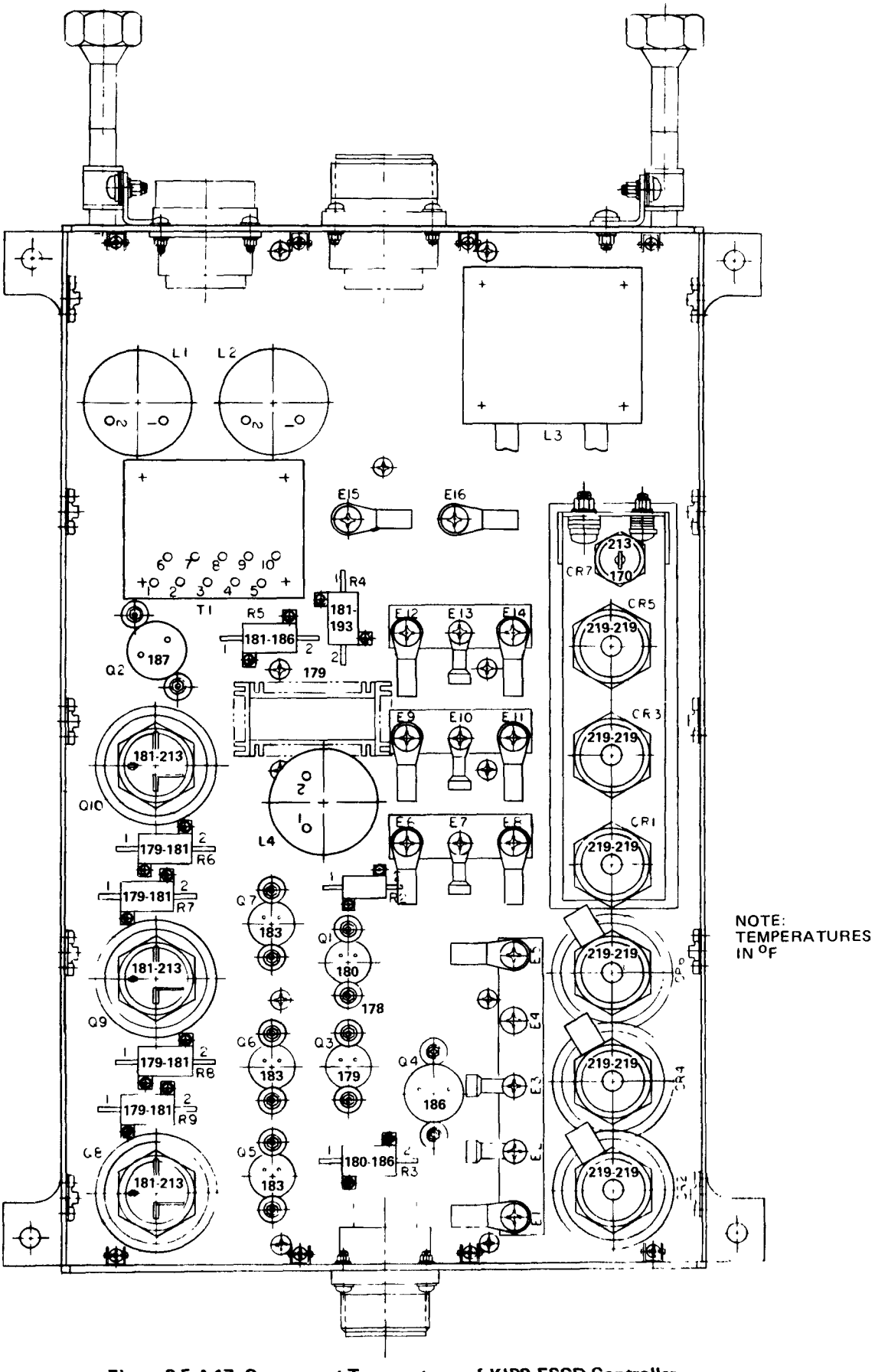

Figure 2.5.4-17 Component Temperatures of KIPS FSCD Controller

Component	Stress
Diode	Voltage .25, Current .22
Transistor	Voltage .35, Power .13
Resistor, Film	Power .24
Resistor, WW, Chassis	Power .21
Resistor, WW, Power	Power .25
Capacitor, Controller	Voltage .40
Capacitor, Ceramic	Voltage .05
Capacitor, Film	Voltage .32

These stress levels are the maximum values found in the circuit.

2.5.4.2.5 NO-SINGLE POINT FAILURE CONTROLLER OPTION

For some applications, a redundant controller may be desired which eliminates single point failures. In this section, two configurations of a no-single point failure (NSPF) controller are compared, one using discrete components and one using integrated circuits. Both configurations yield substantially heavier controllers than the baseline system (39 pounds versus 17.5 pounds). Reliability of the NSPF controller is .989 for the highest reliability, (discrete) version as compared to .982 for the baseline controller so system reliability will not be impaired if the NSPF configuration is used.

The NSPF discrete speed control is shown in Figure 2.5.4-18. The speed control drives each PLR from a separate frequency discriminator, comparator and two series power switches. The power switches are driven by two of the three redundant channels. Two PLRs are capable of handling the full load.

The integrated circuit version is the same except for the discriminator. The discrete discriminator is replaced by a shaping circuit which makes the generator output compatible with integrated logic, a one-shot that converts frequency to a constant volt-sec per unit frequency and a low pass filter.

Figure 2.5.4-19 shows the NSPF voltage regulator. The regulator is made up of three baseline regulators in parallel driving a matrix of six power switches which drives the generator field.

The block diagrams for the discrete and integrated circuit versions are the same.

The rectifier scheme selected for the no-single point failure scheme for both the discrete and integrated circuit version is the fused redundant approach shown in Figure 2.5.4-15.

The configuration selected for the no-single point failure is the fused redundant scheme of Figure 2.5.4-14.

The filter required to meet the no-single point failure criteria is as shown in Figure 2.5.4-20.

The discrete design is considered to be the better of the two options for an acceptable mission risk. The basis for selecting the discrete version versus integrated circuits is as follows:

Temperature – Typically discrete semiconductors are limited to a junction temperature of 200°C while integrated circuits are limited to 125°C. For operation at the same stress levels and junction temperatures, the discrete components are more reliable than the integrated devices because of the delta T margin.

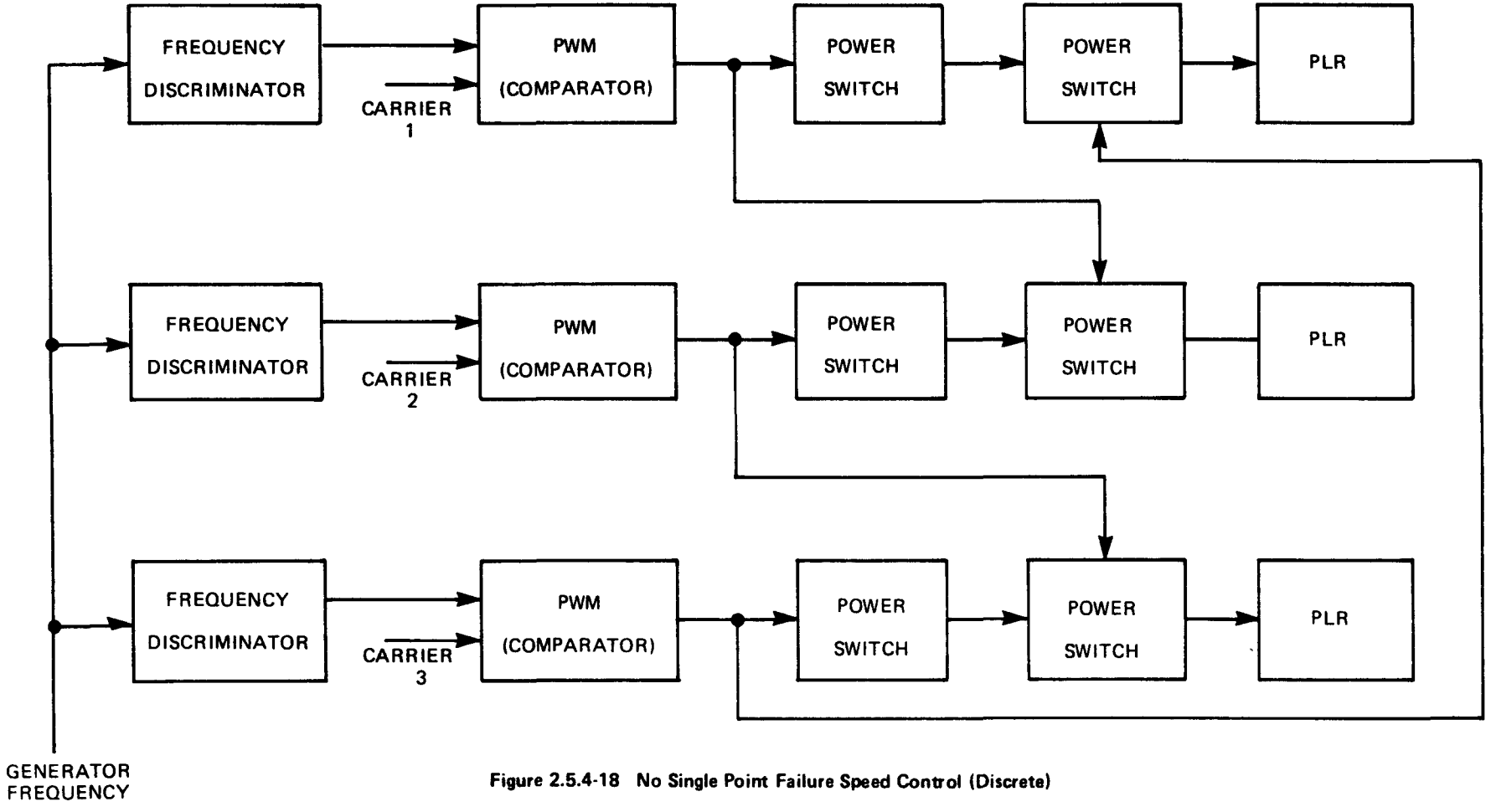

Figure 2.5.4-18 No Single Point Failure Speed Control (Discrete)

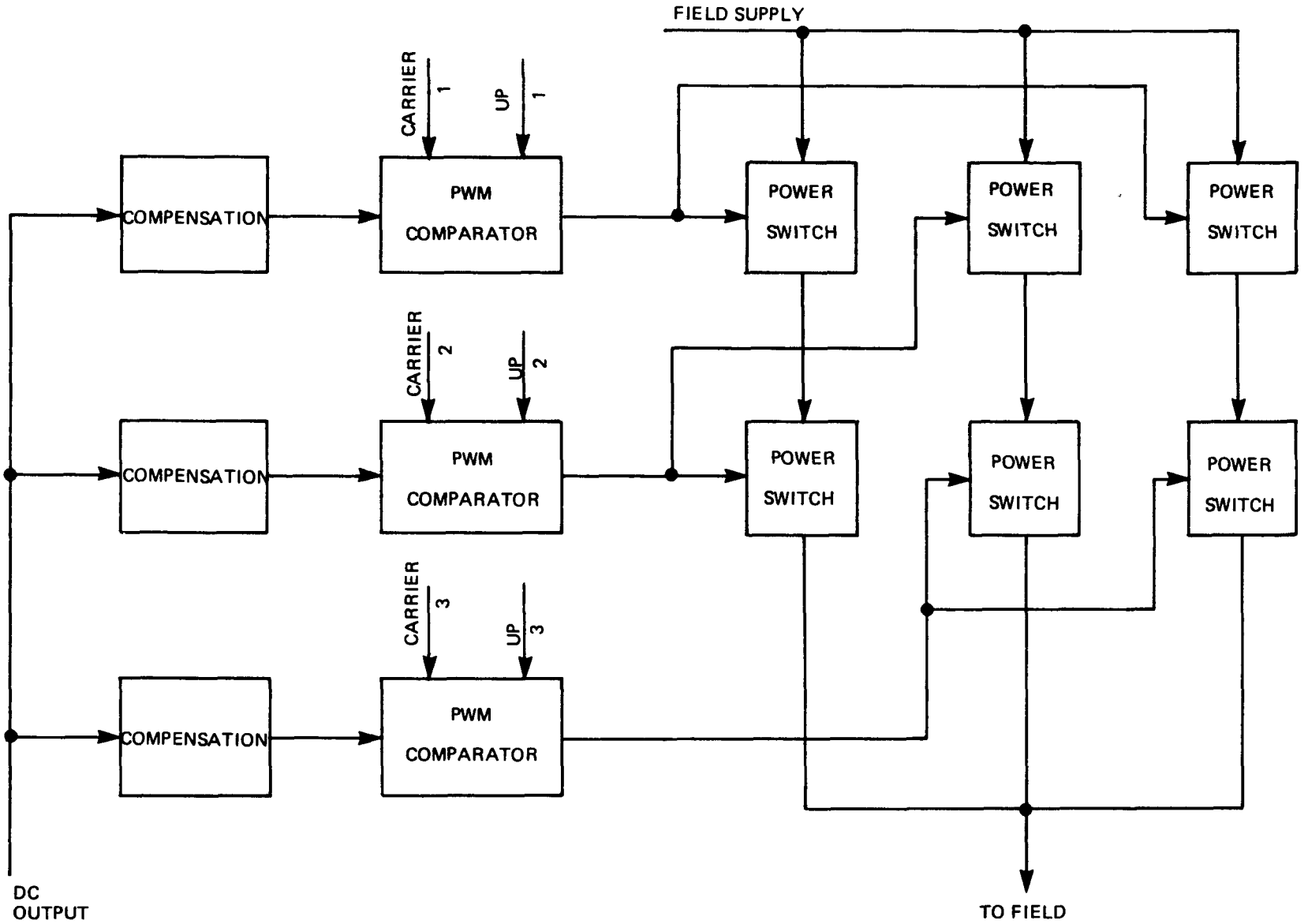

Figure 2.5.4-19 No Single Point Failure Voltage Regulator

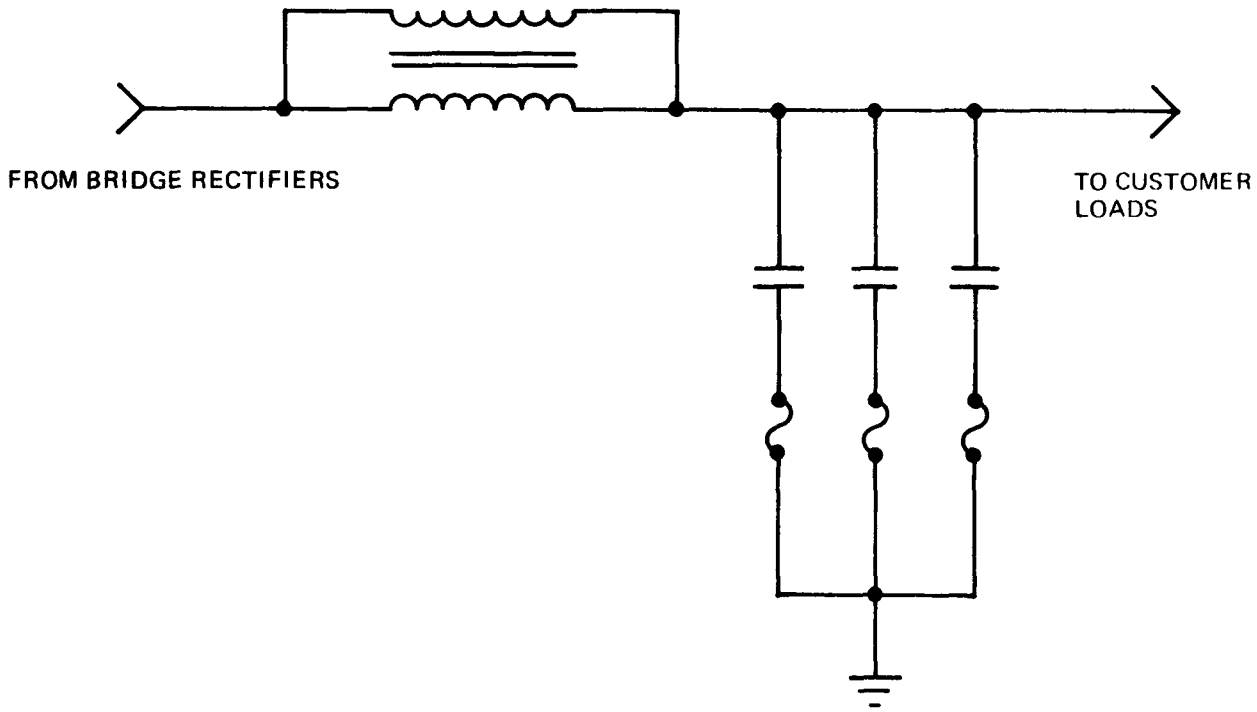

Figure 2.5.4-20 Filter

Nuclear Hardening – The range of available devices which are nuclear hardened and the level of hardening is greater for discrete components than for integrated circuits.

Reliability – The high component reliability and higher temperature margin of discrete components yields a higher controller reliability when discrete components are used.

It can be noted that the no-single point failure option is accomplished with no changes in the principles of operation of the circuits. The NSPF controller therefore functions identically to the baseline controller and no development risk is incurred if the NSPF controller is selected.

2.5.5 FSCD CONFIGURATION AND STRUCTURAL ANALYSIS

The total system comprises a cylindrical radiator, a PCS, three isotope HSAs, and several minor additional components. The three major components are configured so that they can all be mounted to the spacecraft through three mount points, a fully determinant mounting arrangement. An isometric drawing of the system mounting arrangement is shown in Figure 2.5.5-1.

Each HSA is mounted to one of the shock isolation mounts shown in Figure 2.5.5-2, through which the system is attached to the spacecraft. The PCS in turn is connected to each HSA via both a short linkage to the bottom of the HSA and direct attachment at the top of each HSA cylinder. The radiator is independently mounted to the three HSAs. This structural configuration results in high rigidity, in both bending and torsional modes, and light weight.

For shipping, ground checkout operation of the system with electric heat sources and for isotope fuel loading, the system will be mounted to a ground handling fixture which duplicates the spacecraft mounting locations and provides the necessary mount rigidity. In order to manipulate the system for the isotope fuel loading and for subsequent attachment to the spacecraft, three secondary mounting points are provided. These mount points are located in the top of each HSA and are accessible through the top of the radiator.

There are several major advantages to this system support configuration. The most important is that only three points of attachment are required to the spacecraft, allowing great flexibility in selection of mission. The fact that the components are mounted through the shock isolation mounts greatly reduces structural loading, particularly of the radiator, and means that no large differential motions occur between components. The use of the rigid HSA cylinders as load bearing members allows significant weight reduction from alternate mounting schemes.

Other system components, such as the electronic controller, parasitic load resistors, and radiator auxiliary heat exchanger are mounted to the radiator. All interfaces between the system and ground support equipment are located in one quadrant of the radiator. The electrical interface with the spacecraft is located in the same area. This location is flexible and can be varied to meet spacecraft requirements.

All component interconnecting and intraconnecting plumbing is appropriately supported to prevent vibration problems.

Tradeoff Studies

The use of a jet condenser and unidirectional thrust bearings requires that the system be mounted with the high axial launch acceleration vector passing along the jet condenser axis and in the same direction as the liquid jets. Three basic system spacecraft integration schemes were considered. These can best be understood by reference to Figure 2.5.5-3 which shows these three conceptual arrangements. Extensive trade-off studies were performed to select the current baseline approach. The baseline approach, shown in (a), is the lightest weight solution. The KIPS system is mounted directly to the spacecraft with the heavy components, i.e., PCS and HSA, directly connected to the mount points. Although lightweight, this configuration probably necessitates fuel loading while separated from the spacecraft before integration. Startup of the system can proceed either before or after integration.

Variations on this mounting scheme involve separate mounting of the radiator, HSAs and PCS to

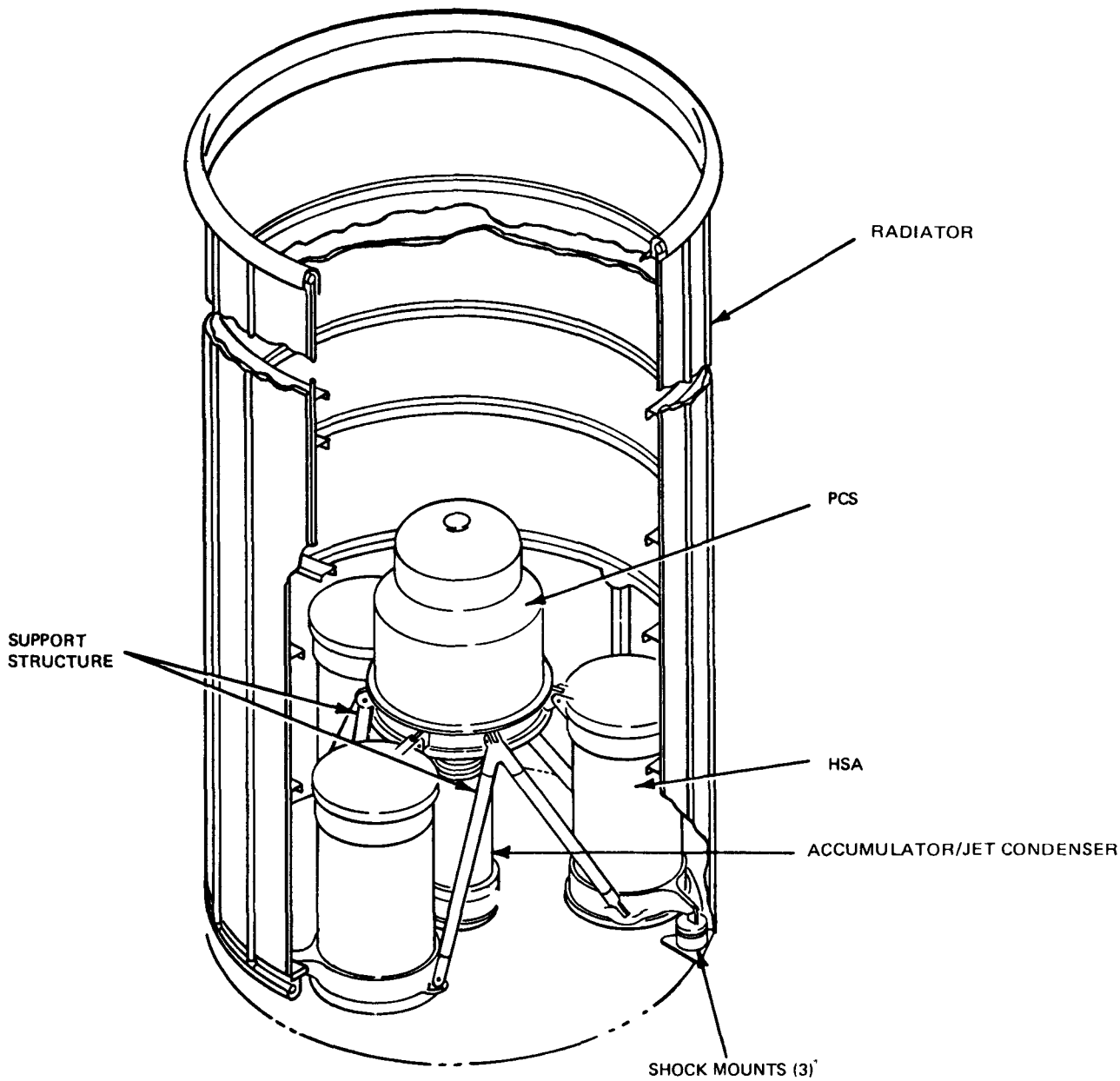

Figure 2.5.5-1 KIPS FSCD System Configuration

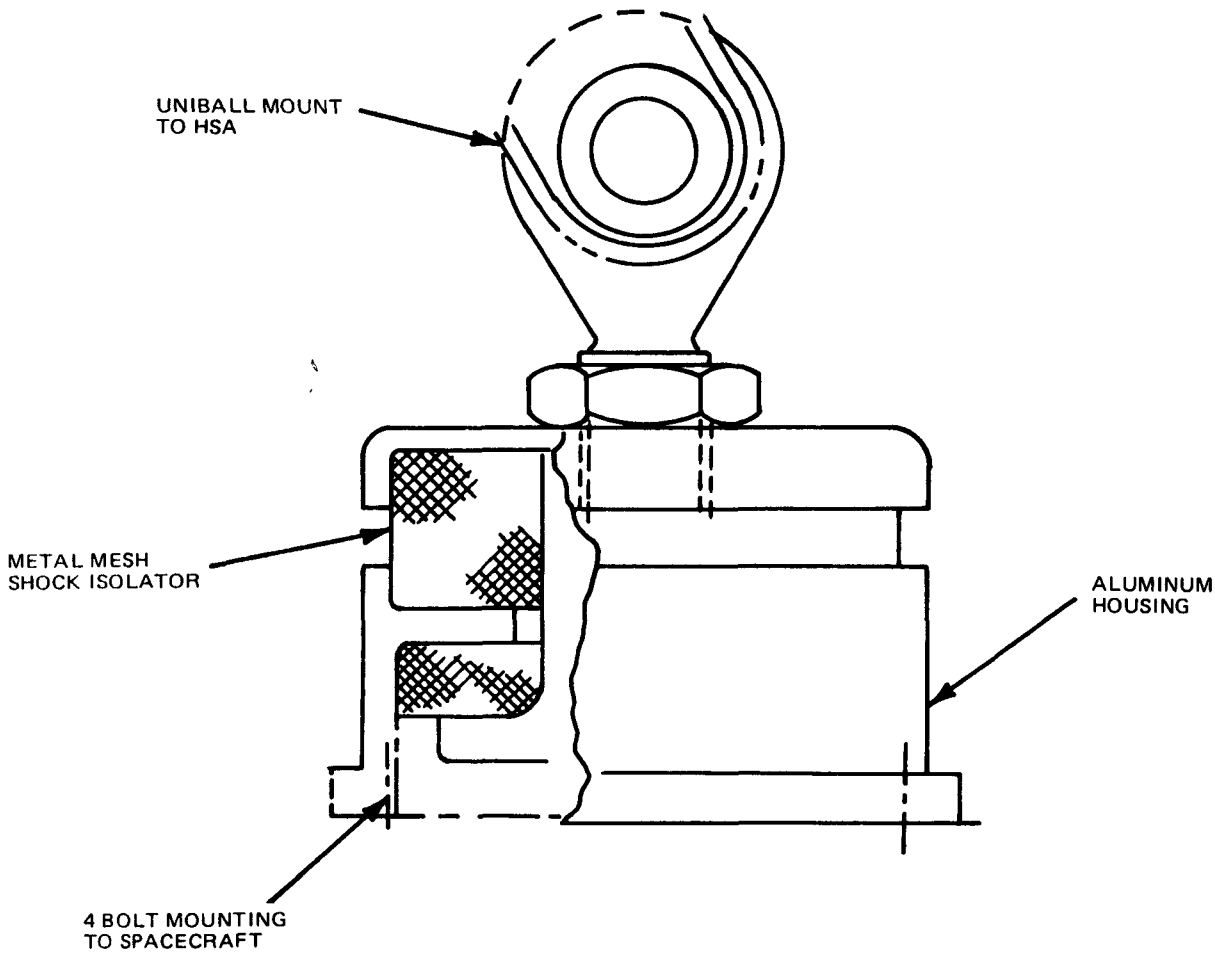

Figure 2.5.5-2 FSCD Isolation Shock Mounts

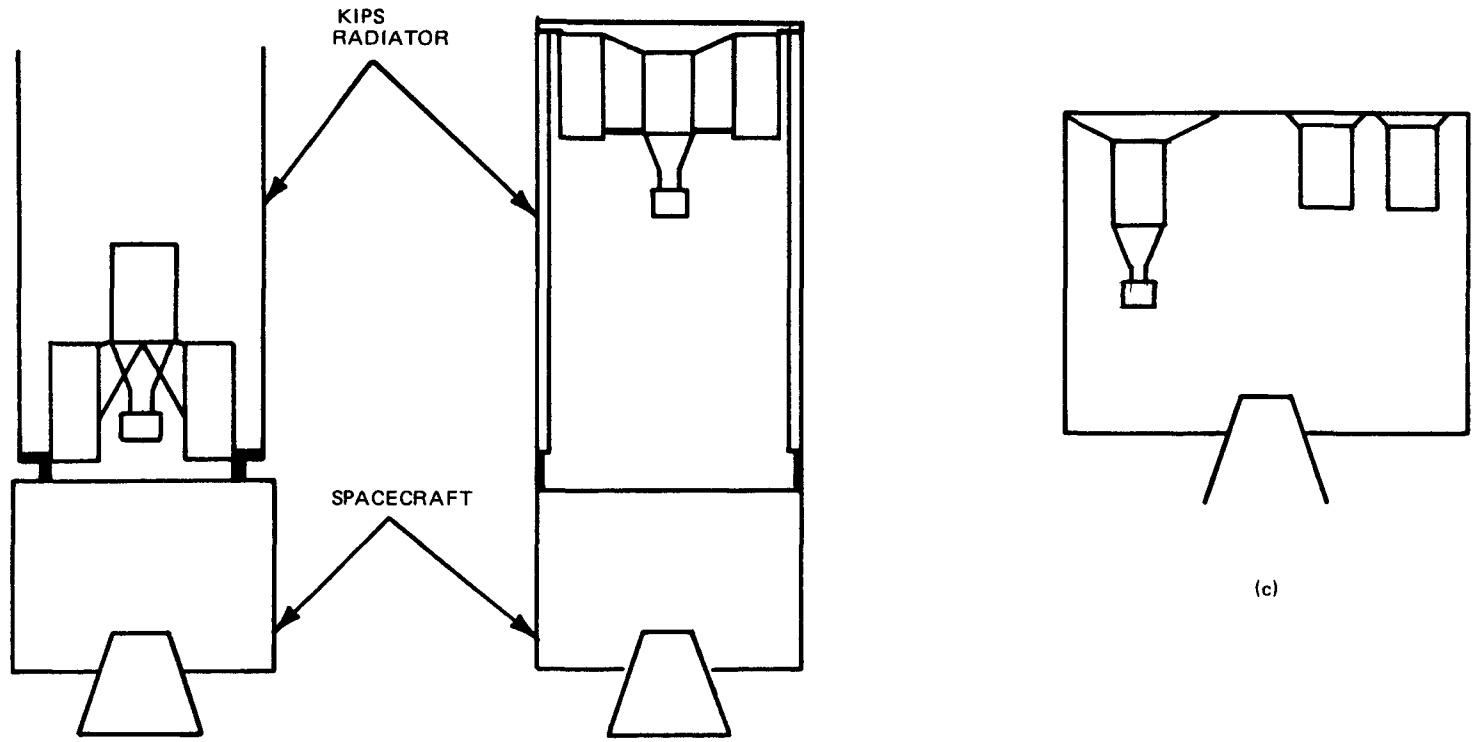

Figure 2.5.5-3 KIPS – Spacecraft Integration

the spacecraft, requiring a total of at least nine mounting locations, or alternatively these three components can be mounted to a lightweight intermediate structure which is, in turn, connected to the spacecraft. The latter was rejected because of excessive weight while the former suffers from lack of flexibility, though it may be suitable for configurations in which a larger diameter radiator is used.

An extension of the baseline approach can be considered for a system configuration which employs a radiator larger in diameter and shorter in length, such as might result from consideration of Space Shuttle payload considerations. This would use a spoked strut arrangement to connect the radiator to either the PCS or the HSAs.

In order to simplify the isotope loading and to enable it to proceed after integration of the KIPS and the spacecraft, configuration (b) was considered. This configuration requires that all launch loads be carried through the radiator. In order to meet this requirement, the radiator structure would need to be increased with considerable weight penalty.

Finally, the configuration shown in (c) embodies complete integration of the KIPS system with the spacecraft. This necessitates modularization of the KIPS components with separate mounting structures. This configuration is extremely inflexible and would have to be tailored to individual missions but could present an optimum weight or volume solution for certain mission requirements.

2.5.5.1 Thermodynamic Considerations

With a two phase closed loop thermodynamic cycle, inventory management is an important consideration. This becomes especially true in a zero g environment where gravitational forces are not available to drain liquid into the system accumulator if it should collect within the PCS. The purpose of the accumulator is to maintain the required back pressure on the jet condenser and to provide volume compensation for fluid temperature changes. In the event that fluid inventory is lost from the accumulator, insufficient pump inlet pressure would be available and system shutdown would occur. It is therefore critical to ensure that liquid cannot collect anywhere in the system other than within flowing lines and the system accumulator.

The potential mechanism by which liquid could collect within the PCS is condensation of the vapor on subcooled surfaces other than the jet condenser liquid streams. In order to preclude this possibility, all surfaces with temperatures below 230°F have been removed from contact with the vapor. This has been achieved in the following manner. The regenerator inner shell is arranged to form a vacuum vessel around the outside of the alternator stator and pump housings, both of which are cooled with relatively cold liquid. The plumbing lines feeding the pump, pump bearing and alternator are routed through ducts passing through the regenerator shells, such that all these cold surfaces are exposed to ambient (i.e., vacuum) conditions. This concept is shown diagramatically in Figure 2.5.5-4.

The potential for condensation on the regenerator inlet line is precluded by the use of a metallic block which shunts heat from the regenerator liquid outlet line to the inlet line to raise the temperature above the saturation value in the regenerator vapor exhaust region.

2.5.5.2 Dynamic Analysis

Reference: Design Review No. 3 Data Package 76-KIPS-49, Volume 2.

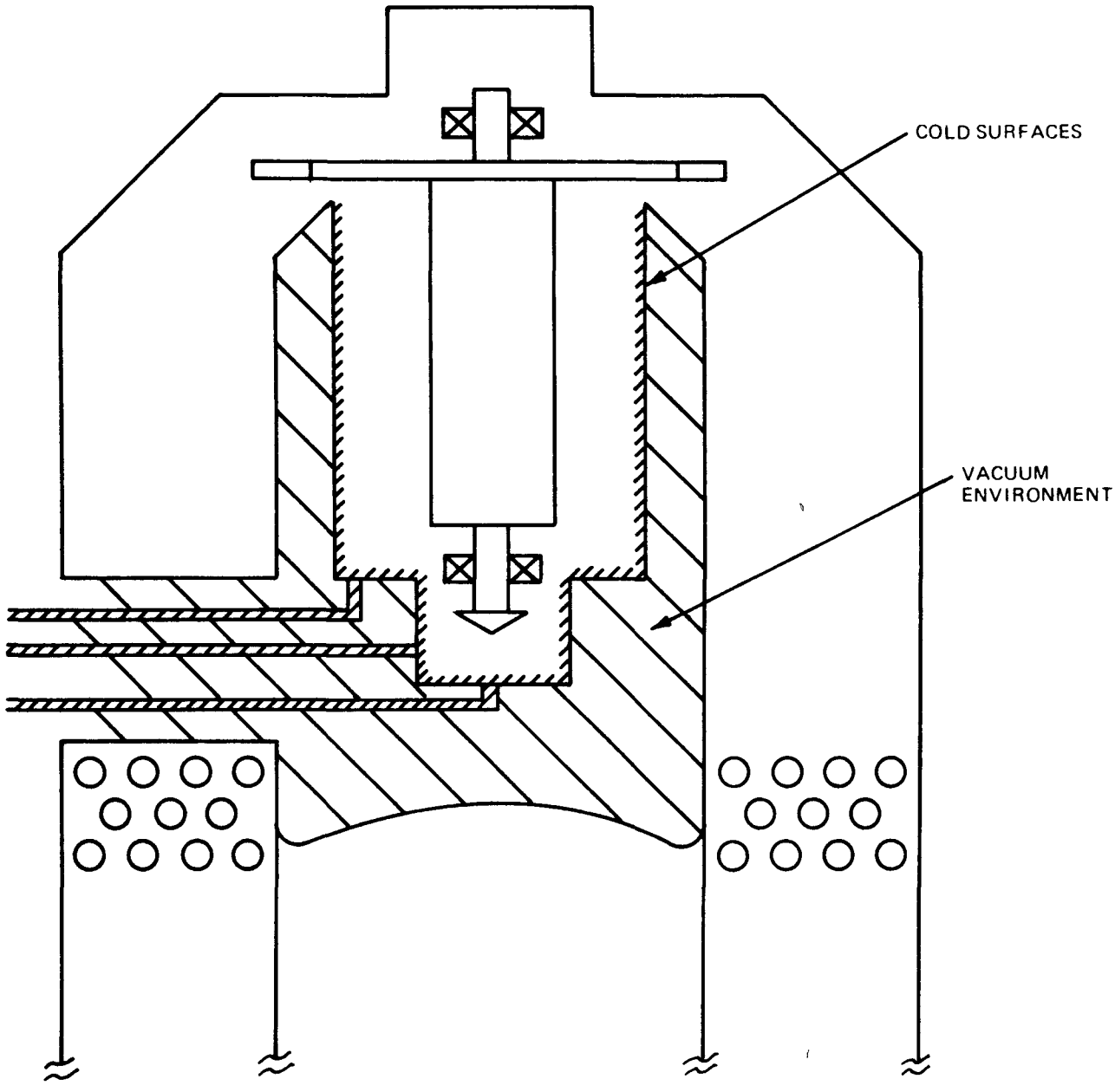

Figure 2.5.5-4 PCS Configuration – Isolating Cold Surfaces From Vapor

An extensive dynamic analysis of the original baseline KIPS was performed and updated as design changes dictated. These efforts were presented in the referenced documents. The following is presented to further update the analysis in the areas of major design changes (mounting configuration and jet condenser response) made since submittal of the referenced work.

ANALYSIS

The most severe operating environment that the KIPS system experiences is due to shock loads during launch. Considerable analysis has been performed on the effects of shock inputs through the shock isolation mounts on the relative motion of the system components and, in particular, the effect on the jet condenser.

The system dynamic response was analyzed using a computer program (SAP6, University of California) that generates a mathematical model of the system using beams to represent component attachments and strut work and humped masses located on the structure to represent actual weight distribution. Using the half sine-wave shock input, the first ten natural frequencies and mode shapes are determined, along with displacements and loading.

The lowest natural frequency is at 12.5 Hz. It is a torsional mode in which the radiator tips the HSAs back and forth while the PCS remains essentially stationary. This vibration mode is relatively insensitive to linear shock input.

The next two natural frequencies are mutually perpendicular at 16 Hz and 16.1 Hz. Lateral shocks excite these modes which are rocking motions on the shock mounts.

The next mode, at 34.4 Hz, is excited by the vertical shock input and results in a vertical motion with some torsion caused by the shock mounts noncentered on the HSAs.

Higher modes are harder to describe but have lower amplitudes than the first four described.

Representative system nodal points used for the shock response are presented in Figure 2.5.5-5. The response of some of these nodes to the 775 g shock input is presented in Tables 2.5.5-A and 2.5.5-B with shock isolation mount stiffnesses of 7000 lb-in in the vertical direction and 2333 lb-in in the lateral direction.

The effect of the shock loads on the jet condenser can be derived from the displacement-time output of the system shock analysis. Lateral jet condenser nozzle velocities angle and position can then be determined for each time step. With this information, the lateral position of the stream when it reaches the throat can be determined. This can be visualized with reference to Figure 2.5.5-6.

$$X' = X + \theta_y \cdot L + V_x \cdot dt$$

where:

- X' = lateral position of stream when it arrives at throat plane
- X = lateral nozzle position
- θ_y = angular position of nozzle plane
- L = nozzle to throat separation

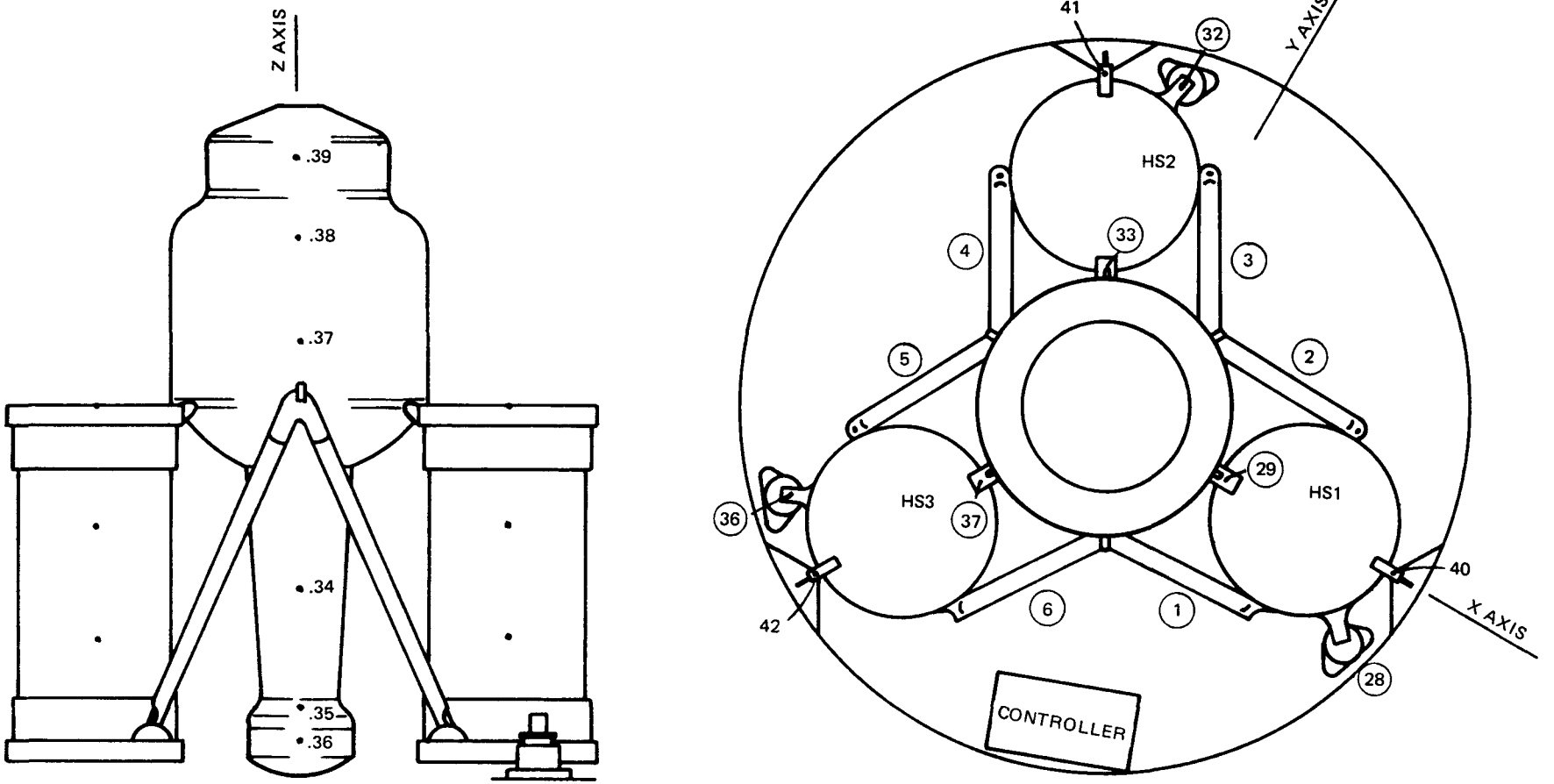

Figure 2.5.5-5 Dynamic Model Nodal Points for KIPS System

Table 2.5.5-A Component Loads Due to Shock Input

LOADS ON STRUTS DUE TO SHOCK (LB)

Strut #	1	2	3	4	5	6
X Shock	1250	790	1410	980	810	1000
Y Shock	1160	1140	690	750	1220	790
Z Shock	1170	1230	1040	1090	1280	1150

LOADS ON HSA DUE TO SHOCK (LB)

	HS_1–PCS (29)			HS_2–PCS (33)			HS_3–PCS (37)		
	Rad	Vert	Lat	Rad	Vert	Lat	Rad	Vert	Lat
X Shock	750	2130	660	500	1350	470	870	2090	560
Y Shock	640	1960	440	790	2230	660	580	1400	560
Z Shock	1330	2710	240	1200	2580	290	1320	2750	300

	HS_1–PAD (28)			HS_2–PAD (32)			HS_3–PAD (36)		
	Rad	Vert	Lat	Rad	Vert	Lat	Rad	Vert	Lat
X Shock	1190	3680	1270	400	1347	1380	1349	2460	290
Y SHock	830	890	990	1480	3500	640	590	2910	1580
Z Shock	500	2780	410	760	2650	370	570	2780	440

NOTE: Rad, Vert & Lat is radial, vertical and lateral with respect to the HSA CL.

Loads are in Lb. and are the peak absolute value.

Table 2.5.5-B Component Accelerations and Amplitudes

RADIATOR MOUNT

Node		40			41			42	
Direction	x	y	z	x	y	z	x	y	z
X Shock (G)	9.9	3.4	10.9	9.7	2.0	7.9	9.8	0.9	3.1
(IN)	.245	.066	.205	.250	.039	.1262	.258	.032	.065
Y Shock (G)	0.6	9.0	2.3	3.0	11.1	8.4	2.7	9.5	10.7
(IN)	.008	.259	.038	.035	.246	.160	.041	.240	.188
Z Shock (G)	0.7	8.1	12.7	7.0	4.5	13.8	7.2	4.7	12.6
(IN)	.009	.225	.135	.197	.123	.128	.203	.124	.135

JET CONDENSER (Acceleration in G's)

	NOZZLES			THROAT		
	x	y	z	x	y	z
X Shock	11.4	1.0	0.9	17.4	1.8	0.9
Y Shock	0.6	11.0	0.3	0.7	16.6	0.9
Z Shock	0.8	0.8	21.0	1.5	1.30	21.2

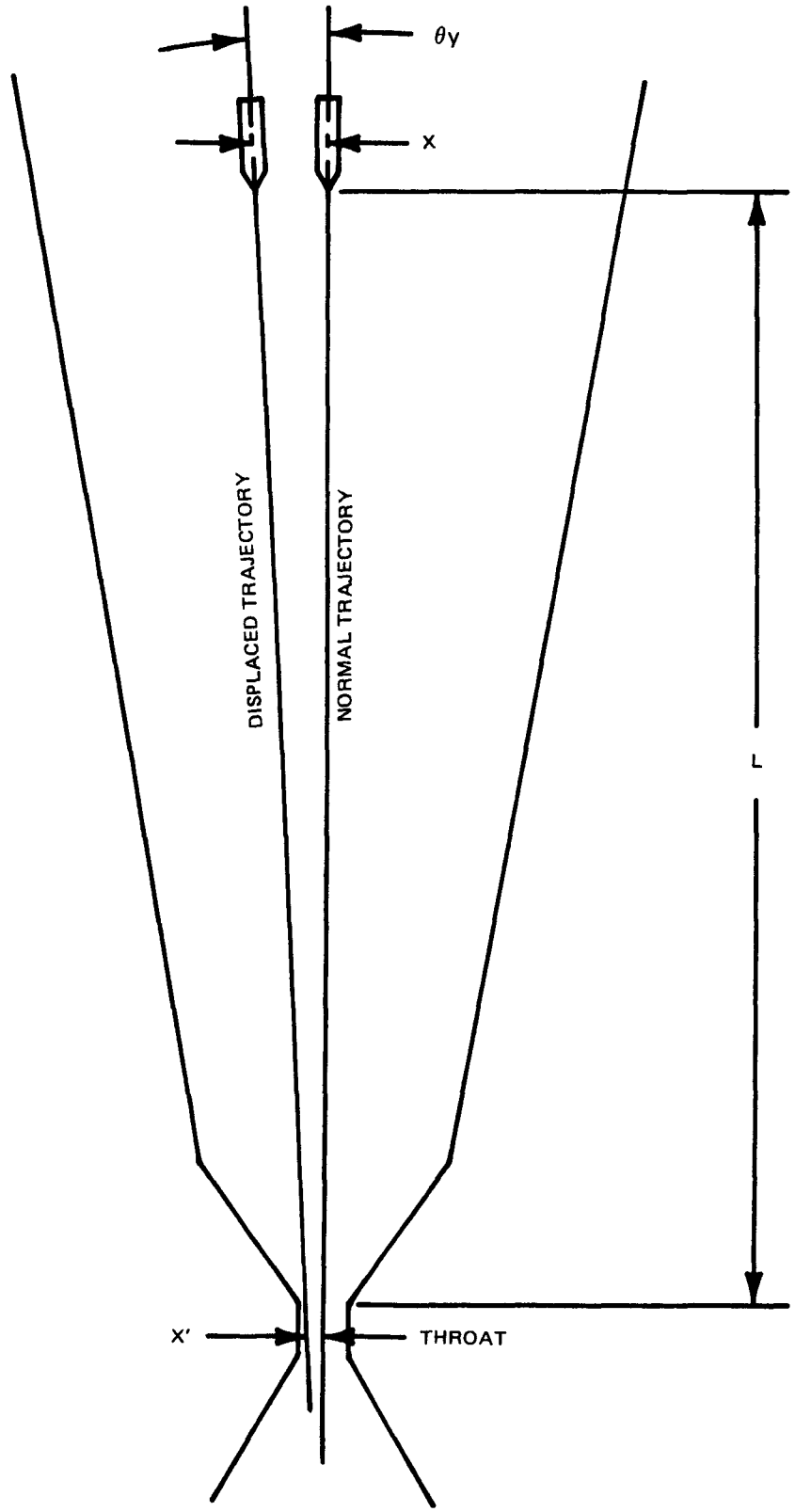

Figure 2.5.5-6 Jet Condenser Targeting – Shock Response

V_x = lateral velocity
dt = time of flight for liquid jet

By plotting the throat position of the stream as it reaches the plane of the throat, the targeting error can be determined. Lateral shock results in a target error of 0.086 inch as shown in Figure 2.5.5-7. Since this target error is of such a short duration (~ 2-3 milliseconds) only a minute amount of flow could be stopped by impinging the funnel wall. Rig tests have demonstrated that far in excess of this amount can easily be scavenged by the stream passing through the throat.

The dynamic analysis presented here accounts for the internal dynamics of the PCS as a lumped mass on the support structure. The FSCD PCS details do not differ significantly from the GDS and an analysis of the resonant frequencies of the GDS PCS are presented in 76-KIPS-49. The results of that analysis showed no problems with shaft speed excited natural frequencies.

It should be noted that with the entire system mounted on three shock isolation mounts, the system response to shock input can be changed depending on different inputs, thus leading to greater flexibility to accommodate different missions.

Stress analysis of the tubing showed that no expansion joints would be necessary for the system plumbing to compensate for thermal expansion or differential motion of components during vibration or shock. In addition, the accumulator support struts have been replaced with a cylinder to tie the accumulator to the housings at the jet condenser ejector head, both saving weight and leading to increased rigidity.

Bimetallic joints are used to connect the stainless steel plumbing from the PCS to the aluminum plumbing to the radiator and aluminum plumbing from the electronic cooler. These coextruded joints in 1/2 inch tubing are considered state-of-the-art.

FABRICATION AND INSPECTION

The fabrication of the total system consists of assembling the major subsystems; i.e., PCS, radiator, and HSAs together and onto the ground handling fixture. Each individual component will have previously been through its required inspections.

The HSAs are first mounted on the fixture and the PCS then attached. The radiator is then attached to the HSAs and all interconnecting plumbing joints are welded. Each joint is radiographically inspected.

After complete assembly, the total system is mass spectrometer leak checked. Bulk insulation is then applied to the PCS and the multifoil insulation to the plumbing lines. The system is evacuated and is then ready for qualification testing using electric heat sources, which were installed at the component assembly level.

The system is then hooked up to the various items of ground support equipment described in subsection 2.5.7 and the system started and operated for a period of time, as yet undefined, for acceptance testing. After being shut down and the fluid drained from the system into the start module, the system is ready for shipment to the launch facility.

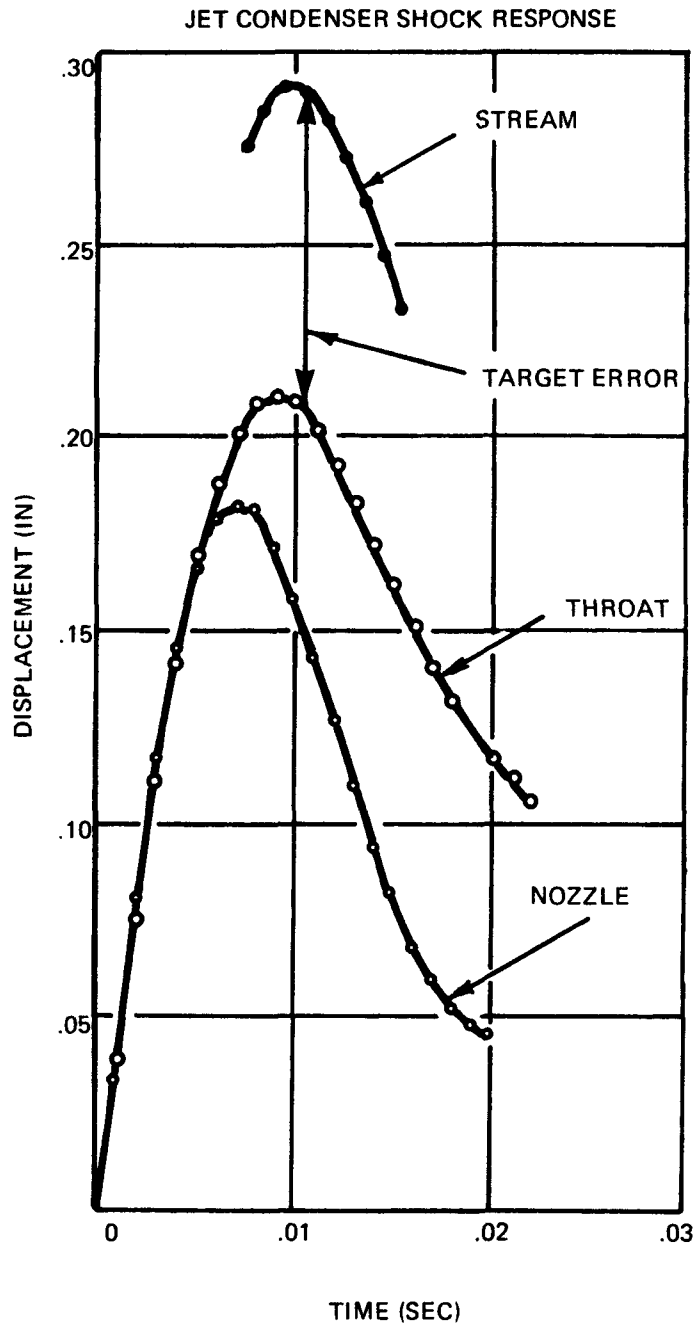

Figure 2.5.5-7 Jet Condenser Target Error — Lateral Shock

CRITICAL CHARACTERISTICS

The critical characteristics are listed below:

The shock isolation mounts must be tuned for a specific vehicle environment as a function of the anticipated shock inputs.

Mechanical integrity of welded tube joints is critical to ensure zero leakage of air into, or Dowtherm out of, the system.

Critical dimensions of the mount points must be maintained at assembly to prevent prestressing the support structure.

2.5.5.3 Stress

Reference: Design Review No. 3 Data Package

An extensive stress analysis of the original baseline KIPS was performed and updated as design changes dictated. These efforts were presented in the referenced document. Since submittal of the referenced work, design changes have been made in four major areas: (1) turbine wheel, (2) rotor housing, (3) accumulator, and (4) jet condenser. The following analysis updates the referenced document in these four areas.

ANALYSIS

MATERIAL PROPERTIES AND RELIABILITY: Strength properties are given as either "A-Basis" or "S-Basis". The "A-Basis" property is a statistical value above which at least 99 percent of the population is expected to fall, with a confidence of 95 percent. The "S-Basis" property is the specified minimum value of the applicable military specification not having a known statistical assurance. Fatigue endurance limit properties are usually given as mean, 50 percent, values.

Following is a list of the materials used and room temperature properties. The statistical basis is stated. In most cases, where data is used for an analysis, the properties are restated and given at the applicable temperature.

Material	F_{Tu}, ksi	F_{Ty}, ksi	Basis
Inconel 718	180	150	S
Hastelloy X, AMS 5536	100	45	S
M-19	–	42.84 @ 450°F	S
304L S.S.	75	30	S
17-4 PH, H1100	140	115	S
17-4 PH, H900	190	170	S
17-4 PH, H1150	135	111	S
321 S.S., SH & ST	90	30	S
321 S.S., AMS 5645	85	35	S
6061-T6 Al	42	35	A

To meet the requirement of a maximum failure rate of 1×10^{-9}, in design analysis it is necessary to use an allowable property reflecting this failure rate. For this purpose, the following table has been

assembled. The stress ratio, R, is the ratio of the allowable property to the given data. These data were obtained from "Probabilistic Design" by E.B. Haugen and P. H. Wirsching, 1975, MACHINE DESIGN.

Type of Property	A-Basis	S-Basis	Mean
Tensile Ultimate Strength	0.79	0.82	N/A
Tensile Yield Strength	0.69	0.73	N/A
Endurance Limit	N/A	0.68	0.52

The above considers uniform coefficients of variation for the properties listed. This is not precisely correct, as the coefficient of variation for the property is also affected by the specific material involved. The analysis will be refined during the initial design stage of Phase II using specific material data.

JOB KIPS PAGE
DATE
BY Y.E. REV.

Turbine Wheel

Material: [1]

Disk & Blades: Inconel 718

R.T. $\sigma_u = 180$ ksi
$\sigma_y = 150$ "
$E = 29.6 \times 10^6$ psi

550°F $\sigma_u = .93 \times 180 = 167.4$ ksi
$\sigma_y = .945 \times 150 = 142.$ "

For 1×10^{-9} failure rate

$\sigma_{u_{all}@550} = .82 \times 167.4 = 137.3$ ksi

$\sigma_{y_{all}@550} = .73 \times 142 = 103.7$ ksi

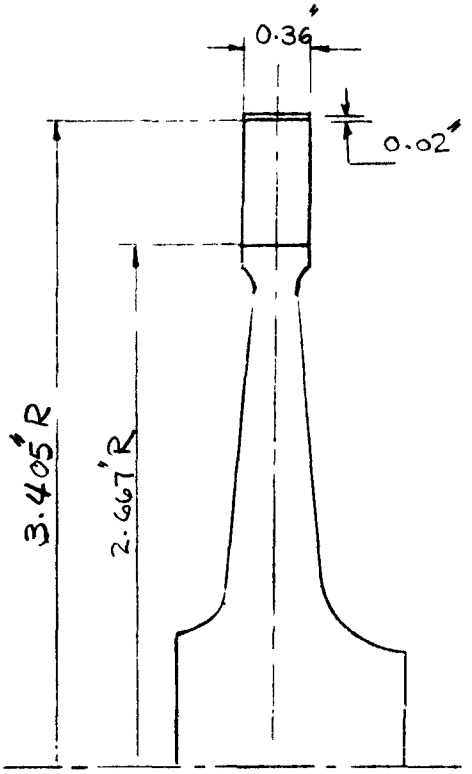

Fig. 1
Turbine disk

Method of Analysis

The turbine disk was analyzed using the inhouse computer program E-4 [4]. The disk was sized to guarantee a factor of safty of 1.2 at the worst operating condition (58200 rpm with 3-min. transient temperature distribution). The temperature distributions are shown in figure 2.

JOB KIPS

BY Y.E.

PAGE

DATE

REV.

The maximum stress in the disk was found to occur during the maximum over speed with a 3-minutes transient temperature profile.

σ_{eff}^{max} = 86,697 psi @ r = 1.4" from ℄.

M.S. (yield) = $\frac{103.7}{86.697} - 1 \cong$ 0.2

@ 1×10^{-9} failure Rate

@ 58200 rpm

The maximum stress at the Nominal overspeed (55311 rpm) with a Steady State temperature distribution is

$\sigma_{eff}^{max.}$ = 74,911 psi

M.S. (yield) = $\frac{103.7}{74.911} - 1 \cong$ 0.38

@ 1×10^{-9} failure Rate

JOB KIPS

BY Y.E.

PAGE

DATE

REV.

The maximum stress at the steady state operating speed 33,700 rpm is

$$\sigma_{eff_{max}} = 29{,}137 \text{ psi}$$

$$\text{M.S.(yield)} = \frac{103.7}{29.137} - 1 = \boxed{2.56}$$

$C \times 10^{-9}$ failure rate

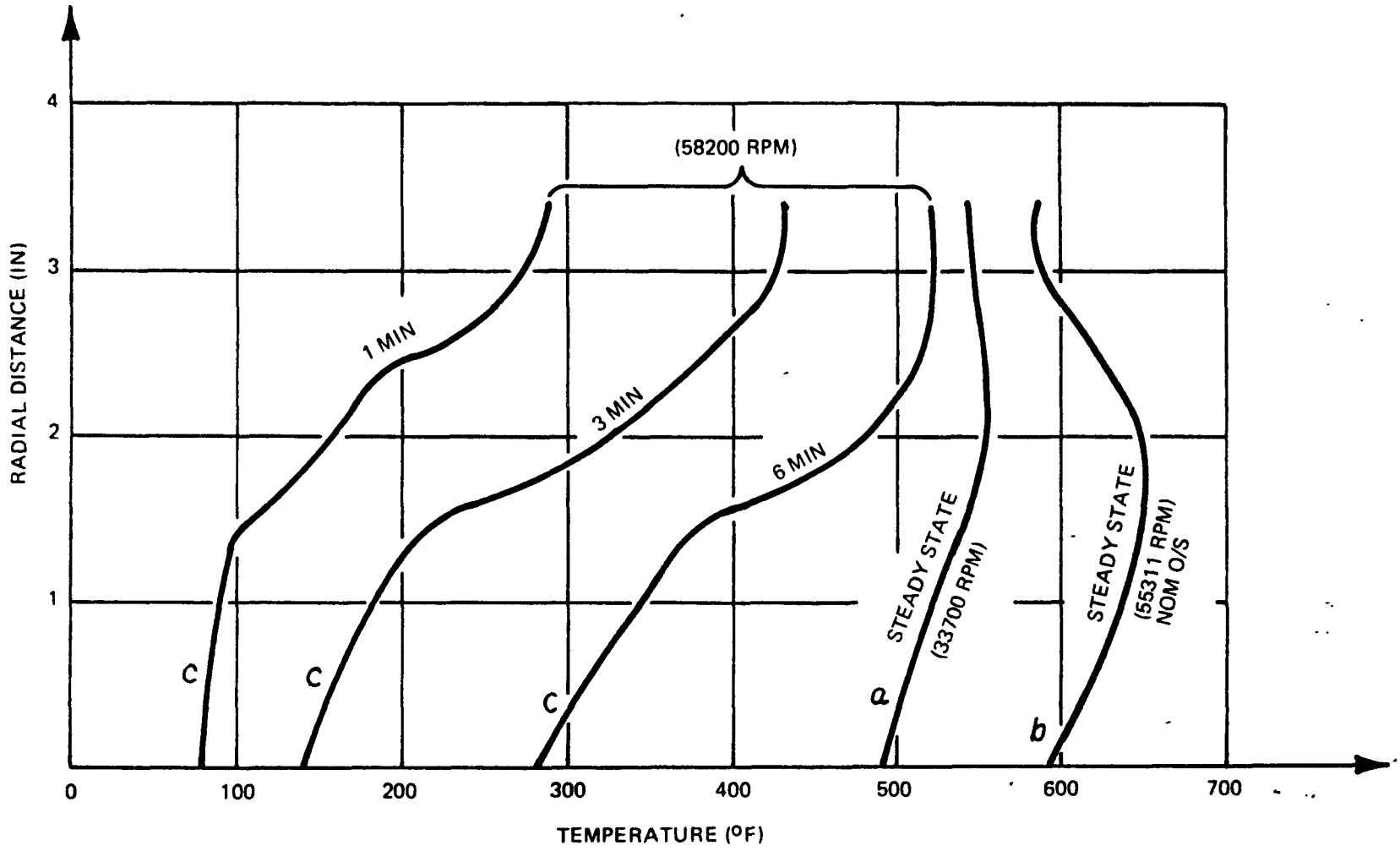

Figure 2 **Temperature Distribution**

REVISION C RUN START TIME(HR.MIN.SEC) 16.32.12 RUN DATE 02/01/78

KIPS TURBINE (33,700 RPM-STEADY STATE) 111 BLADES

DESIGN OF ROTATING DISKS WITH TEMP GRADIENT

INPUT

BLADE WIDTH AT DISK	NUMBER OF BLADES	BLADE AREA AT DISK	BLADE STRESS AT DISK	RPM
0.3600	111	0.025840	23209.	33700.

DENSITY	POISSONS RATIO	TEMP INNER DISK RADIUS	DISK OUTER RADIUS	BLADE OUTER RADIUS	SHROUD MEAN RADIUS
0.2970	0.3000	490.	2.6670	3.4050	3.4150

BOUNDARY CONDITION A11-A	BOUNDARY CONDITION A12-A	BOUNDARY CONDITION A13-A	BOUNDARY CONDITION C1-A	BLADE AREA AT TIP	SHROUD XSECT. AREA
0.0	1.000000	-1.000000	0.0	0.025840	0.007200

DISK RADIUS	DISK WIDTH	ELASTIC MODULUS AT STAT	EXPANSION COEF AT AT STAT	TEMP AT STATION	SIGMA YIELD	SIGMA ULTIMATE	SIGMA DESIRED
0.000	1.500	27800000.	0.0000076000	490.00			
0.250	1.400	27800000.	0.0000076000	500.00			
0.550	0.900	27800000.	0.0000076000	509.00			
0.600	0.700	27800000.	0.0000076000	510.00			
0.680	0.600	27700000.	0.0000076000	512.00			
0.740	0.570	27700000.	0.0000076000	515.00			
0.800	0.540	27700000.	0.0000076000	517.00			
1.000	0.490	27600000.	0.0000076000	523.00			
1.200	0.440	27600000.	0.0000076000	530.00			
1.400	0.380	27600000.	0.0000076000	533.00			
1.500	0.360	27500000.	0.0000076000	540.00			
1.600	0.340	27500000.	0.0000076000	544.00			
1.700	0.325	27500000.	0.0000076500	574.00			
1.800	0.310	27500000.	0.0000076500	550.00			
1.900	0.300	27500000.	0.0000076500	551.00			
2.000	0.280	27500000.	0.0000076500	552.00			
2.050	0.270	27500000.	0.0000076500	552.00			
2.100	0.260	27500000.	0.0000076500	552.00			
2.200	0.250	27500000.	0.0000076500	552.00			
2.300	0.240	27500000.	0.0000076500	553.00			
2.400	0.240	27500000.	0.0000076500	553.00			
2.450	0.240	27500000.	0.0000076500	554.00			
2.470	0.240	27500000.	0.0000076500	554.00			
2.500	0.260	27500000.	0.0000076500	552.00			
2.520	0.270	27500000.	0.0000076500	551.00			
2.540	0.290	27500000.	0.0000076500	550.00			
2.560	0.310	27500000.	0.0000076500	550.00			
2.580	0.340	27500000.	0.0000076500	549.00			
2.590	0.360	27500000.	0.0000076500	549.00			
2.600	0.360	27500000.	0.0000076500	548.00			
2.620	0.360	27500000.	0.0000076500	548.00			
2.630	0.360	27500000.	0.0000076500	548.00			
2.650	0.360	27500000.	0.0000076500	548.00			
2.667	0.360	27500000.	0.0000076500	548.00			

BLD ELASTIC MODULUS	EXPAN COEFF OF BLADE	TEMP AT BLADE TIP
27600000.	0.000007600	543.

Steady State @ Design Speed (33700 rpm)

OUTPUT

DISK RADIUS	DISK WIDTH	RADIAL STRESS (PSI)	TANGENTIAL STRESS (PSI)	EFFECTIVE STRESS (PSI)	DISK EXPANSION (IN)
0.0001	1.5000	17112.	17112.	17112.	0.0000004
0.2500	1.4000	16650.	15565.	16135.	0.0010103
0.5500	0.9000	22170.	17738.	20320.	0.0022329
0.6000	0.7000	27607.	19840.	24659.	0.0024462
0.6800	0.6000	30555.	21616.	27210.	0.0027944
0.7400	0.5700	30972.	22090.	27624.	0.0030504
0.8000	0.5400	31531.	22734.	28182.	0.0033115
1.0000	0.4900	31038.	23663.	28086.	0.0041786
1.2000	0.4400	30954.	23893.	28097.	0.0050254
1.4000	0.3800	32002.	24994.	29137.	0.0059030
1.5000	0.3600	31832.	24084.	28752.	0.0062778
1.6000	0.3400	31662.	23850.	28568.	0.0066057
1.7000	0.3250	30871.	18035.	26861.	0.0067588
1.8000	0.3100	30080.	23573.	27412.	0.0075343
1.9000	0.3000	28952.	23447.	26630.	0.0079676
2.0000	0.2800	28803.	23551.	26569.	0.0083978
2.0500	0.2700	28753.	23702.	26589.	0.0086200
2.1000	0.2600	28725.	23849.	26624.	0.0088422
2.2000	0.2500	27569.	23765.	25877.	0.0092843
2.3000	0.2400	26365.	23390.	25011.	0.0097051
2.4000	0.2400	24026.	22805.	23434.	0.0101375
2.4500	0.2400	22846.	22265.	22561.	0.0103319
2.4700	0.2400	22372.	22127.	22251.	0.0104167
2.5000	0.2600	19974.	21816.	20956.	0.0105803
2.5200	0.2700	18781.	21645.	20364.	0.0106820
2.5400	0.2900	17045.	21298.	19522.	0.0107828
2.5600	0.3100	15509.	20788.	18716.	0.0108832
2.5800	0.3400	13715.	20400.	18013.	0.0109621
2.5900	0.3600	12739.	20072.	17592.	0.0110013
2.6000	0.3600	12519.	20179.	17643.	0.0110601
2.6200	0.3600	12079.	19969.	17420.	0.0111378
2.6300	0.3600	11858.	19864.	17310.	0.0111766
2.6500	0.3600	11414.	19650.	17092.	0.0112539
2.6670	0.3600	11035.	19467.	16909.	0.0113193

MOMENT OF INERTIA (IN-LB-SEC**2) BLADE	SHROUD	DISK	TOTAL
0.0150705	0.0013849	0.0181245	0.0345798

BLADE EXPANSION FROM STRESS	BLADE EXPANSION FROM THERMAL	TOTAL EXPANSION (IN)
0.0005967	0.0026758	0.0145918

	SHROUD	BLADES	DISK	TOTAL
WEIGHT (LB)	0.046	0.629	2.511	3.186

Form G 7756

REVISION C RUN START TIME(HR.MIN.SEC) 15.06.52 RUN DATE 02/01/78

KIPS TURBINE (55311 RPM-STEADY STATE TEMP.) 111 BLADES

DESIGN OF ROTATING DISKS WITH TEMP GRADIENT

INPUT

BLADE WIDTH AT DISK	NUMBER OF BLADES	BLADE AREA AT DISK	BLADE STRESS AT DISK	RPM
0.3600	111	0.025840	62520.	55311.

DENSITY	POISSONS RATIO	TEMP INNER DISK RADIUS	DISK OUTER RADIUS	BLADE OUTER RADIUS	SHROUD MEAN RADIUS
0.2970	0.3000	595.	2.6670	3.4050	3.4150

BOUNDARY CONDITION A11-A	BOUNDARY CONDITION A12-A	BOUNDARY CONDITION A13-A	BOUNDARY CONDITION C1-A	BLADE AREA AT TIP	SHROUD XSECT. AREA
0.0	1.000000	-1.000000	0.0	0.025840	0.007200

DISK RADIUS	DISK WIDTH	ELASTIC MODULUS AT STAT	EXPANSION COEF AT AT STAT	TEMP AT STATION	SIGMA YIELD	SIGMA ULTIMATE	SIGMA DESIRED
0.000	1.500	27300000.	0.0000077000	595.00			
0.250	1.400	27240000.	0.0000077000	606.00			
0.550	0.900	27130000.	0.0000077300	618.00			
0.600	0.700	27100000.	0.0000077400	620.00			
0.680	0.600	27060000.	0.0000077400	624.00			
0.740	0.570	27020000.	0.0000077400	628.00			
0.800	0.540	27020000.	0.0000077400	629.00			
1.000	0.490	26970000.	0.0000077500	635.00			
1.200	0.440	26870000.	0.0000077500	640.00			
1.400	0.380	26840000.	0.0000077500	645.00			
1.500	0.360	26800000.	0.0000077500	647.00			
1.600	0.340	26800000.	0.0000077500	650.00			
1.700	0.325	26800000.	0.0000077500	650.00			
1.800	0.310	26830000.	0.0000077500	650.00			
1.900	0.300	26850000.	0.0000077500	648.00			
2.000	0.280	26870000.	0.0000077500	646.00			
2.050	0.270	26900000.	0.0000077500	644.00			
2.100	0.260	26950000.	0.0000077500	642.00			
2.200	0.250	27000000.	0.0000077500	637.00			
2.300	0.240	27060000.	0.0000077500	630.00			
2.400	0.240	27100000.	0.0000077400	624.00			
2.450	0.240	27110000.	0.0000077400	620.00			
2.470	0.240	27150000.	0.0000077400	619.00			
2.500	0.260	27180000.	0.0000077300	617.00			
2.520	0.270	27180000.	0.0000077300	615.00			
2.540	0.290	27190000.	0.0000077300	614.00			
2.560	0.310	27190000.	0.0000077300	613.00			
2.580	0.340	27200000.	0.0000077300	612.00			
2.590	0.360	27200000.	0.0000077300	611.00			
2.600	0.360	27200000.	0.0000077300	610.00			
2.620	0.360	27200000.	0.0000077300	610.00			
2.630	0.360	27200000.	0.0000077300	610.00			
2.650	0.360	27220000.	0.0000077300	608.00			
2.667	0.360	27260000.	0.0000077300	604.00			

BLD ELASTIC MODULUS	EXPAN COEFF OF BLADE	TEMP AT BLADE TIP
27320000.	0.000007700	586.

Steady State
&
Over Speed
(55311 rpm)

OUTPUT

DISK RADIUS	DISK WIDTH	RADIAL STRESS (PSI)	TANGENTIAL STRESS (PSI)	EFFECTIVE STRESS (PSI)	DISK EXPANSION (IN)
0.0001	1.5000	40805.	40805.	40805.	0.0000005
0.2500	1.4000	40715.	39306.	40029.	0.0012804
0.5500	0.9000	56053.	45466.	50940.	0.0028944
0.6000	0.7000	68524.	50621.	61627.	0.0031377
0.6800	0.6000	76019.	55114.	68020.	0.0036128
0.7400	0.5700	77106.	56822.	69230.	0.0039691
0.8000	0.5400	78572.	59072.	70864.	0.0043441
1.0000	0.4900	77643.	62585.	71316.	0.0055092
1.2000	0.4400	77775.	64794.	72165.	0.0067705
1.4000	0.3800	80670.	67229.	74860.	0.0079087
1.5000	0.3600	80389.	67832.	74904.	0.0085972
1.6000	0.3400	80190.	68181.	74911.	0.0091943
1.7000	0.3250	78850.	68657.	74280.	0.0098237
1.8000	0.3100	77498.	68999.	73617.	0.0104509
1.9000	0.3000	74941.	69154.	72166.	0.0110979
2.0000	0.2800	74705.	69915.	72429.	0.0117408
2.0500	0.2700	74701.	70547.	72704.	0.0120805
2.1000	0.2600	74753.	71172.	73028.	0.0124236
2.2000	0.2500	71994.	71603.	71800.	0.0131168
2.3000	0.2400	69134.	72248.	70742.	0.0138398
2.4000	0.2400	63312.	71535.	67798.	0.0145325
2.4500	0.2400	60382.	71259.	66491.	0.0148895
2.4700	0.2400	59206.	71074.	65946.	0.0150463
2.5000	0.2600	52968.	69466.	62862.	0.0152329
2.5200	0.2700	49874.	68774.	61541.	0.0153767
2.5400	0.2900	45331.	67431.	59541.	0.0155005
2.5600	0.3100	41312.	66196.	57913.	0.0156198
2.5800	0.3400	36598.	64743.	56228.	0.0157382
2.5900	0.3600	34026.	64035.	55493.	0.0158053
2.6000	0.3600	33473.	63928.	55384.	0.0158719
2.6200	0.3600	32362.	63289.	54815.	0.0159646
2.6300	0.3600	31803.	62968.	54533.	0.0160107
2.6500	0.3600	30682.	62780.	54373.	0.0161469
2.6670	0.3600	29726.	63142.	54714.	0.0163140

MOMENT OF INERTIA (IN-LB-SEC**2) BLADE	SHROUD	DISK	TOTAL
0.0150705	0.0013849	0.0181245	0.0345798

BLADE EXPANSION FROM STRESS	BLADE EXPANSION FROM THERMAL	TOTAL EXPANSION (IN)
0.0016240	0.0029892	0.0209271

	SHROUD	BLADES	DISK	TOTAL
WEIGHT(LB)	0.046	0.629	2.511	3.186

Form G 7756

REVISION C RUN START TIME(HR.MIN.SEC) 15.29.02 RUN DATE 02/01/78

KIPS TURBINE (58200 RPM-3 MIN) 111 BLADES.

DESIGN OF ROTATING DISKS WITH TEMP GRADIENT

INPUT

BLADE WIDTH AT DISK	NUMBER OF BLADES	BLADE AREA AT DISK	BLADE STRESS AT DISK	RPM
0.3600	111	0.021790	70198.	58200.

DENSITY	POISSONS RATIO	TEMP INNER DISK RADIUS	DISK OUTER RADIUS	BLADE OUTER RADIUS	SHROUD MEAN RADIUS
0.2970	0.3000	140.	2.6670	3.4050	3.4150

BOUNDARY CONDITION A11-A	BOUNDARY CONDITION A12-A	BOUNDARY CONDITION A13-A	BOUNDARY CONDITION C1-A	BLADE AREA AT TIP	SHROUD XSECT. AREA
0.0	1.000000	-1.000000	0.0	0.021790	0.007200

DISK RADIUS	DISK WIDTH	ELASTIC MODULUS AT STAT	EXPANSION COEF AT AT STAT	TEMP AT STATION	SIGMA YIELD	SIGMA ULTIMATE	SIGMA DESIRED
0.000	1.500	29600000.	0.0000071000	140.00			
0.250	1.400	29600000.	0.0000071000	146.00			
0.550	0.900	29600000.	0.0000071000	160.00			
0.600	0.700	29600000.	0.0000071000	162.00			
0.680	0.600	29600000.	0.0000071000	165.00			
0.740	0.570	29600000.	0.0000071000	168.00			
0.800	0.540	29600000.	0.0000071000	170.00			
1.000	0.490	29600000.	0.0000071000	180.00			
1.200	0.440	29300000.	0.0000071000	193.00			
1.400	0.380	29300000.	0.0000071000	210.00			
1.500	0.360	29200000.	0.0000071000	230.00			
1.600	0.340	29150000.	0.0000072000	260.00			
1.700	0.325	29100000.	0.0000073000	280.00			
1.800	0.310	29000000.	0.0000073500	300.00			
1.900	0.300	29000000.	0.0000074000	315.00			
2.000	0.280	29000000.	0.0000074000	330.00			
2.050	0.270	29000000.	0.0000074000	340.00			
2.100	0.260	29000000.	0.0000074000	350.00			
2.200	0.250	28700000.	0.0000074000	360.00			
2.300	0.240	28400000.	0.0000074000	366.00			
2.400	0.240	28400000.	0.0000074000	376.00			
2.450	0.240	28400000.	0.0000074000	376.00			
2.470	0.240	28400000.	0.0000074000	378.00			
2.500	0.260	28400000.	0.0000074000	390.00			
2.520	0.270	28200000.	0.0000074000	392.00			
2.540	0.290	28200000.	0.0000074500	394.00			
2.560	0.310	28200000.	0.0000074500	396.00			
2.580	0.340	28200000.	0.0000074500	398.00			
2.590	0.360	28200000.	0.0000074000	399.00			
2.600	0.360	28200000.	0.0000074000	400.00			
2.620	0.360	28000000.	0.0000074000	400.00			
2.630	0.360	28000000.	0.0000074000	400.00			
2.650	0.360	28000000.	0.0000074000	400.00			
2.667	0.360	28000000.	0.0000074000	400.00			

BLD ELASTIC MODULUS	EXPAN COEFF OF BLADE	TEMP AT BLADE TIP
28800000.	0.000007500	430.

3-min. Transient Temp. Distribution

Max O/S 58,200 rpm

OUTPUT

DISK RADIUS	DISK WIDTH	RADIAL STRESS (PSI)	TANGENTIAL STRESS (PSI)	EFFECTIVE STRESS (PSI)	DISK EXPANSION (IN)
0.0001	1.5000	46425.	46425.	46425.	0.0000084
0.2500	1.4000	46960.	46002.	46488.	0.0000954
0.5500	0.9000	64029.	52880.	59247.	0.0020045
0.6000	0.7000	79863.	58999.	71744.	0.0025161
0.6800	0.6000	88580.	64624.	79362.	0.0029048
0.7400	0.5700	89959.	66991.	80957.	0.0030643
0.8000	0.5400	91786.	69420.	82897.	0.0031303
1.0000	0.4900	91008.	73053.	83491.	0.0040168
1.2000	0.4400	91342.	74158.	84077.	0.0049342
1.4000	0.3800	94771.	75318.	86697.	0.0057631
1.5000	0.3600	94330.	72716.	85595.	0.0060425
1.6000	0.3400	93754.	67894.	83870.	0.0061796
1.7000	0.3250	91627.	64669.	81561.	0.0064088
1.8000	0.3100	89341.	61425.	79165.	0.0066213
1.9000	0.3000	85448.	58728.	75711.	0.0068854
2.0000	0.2800	84356.	56985.	74540.	0.0071467
2.0500	0.2700	83838.	55576.	73879.	0.0072336
2.1000	0.2600	83339.	54180.	73250.	0.0073166
2.2000	0.2500	79082.	52166.	69641.	0.0076071
2.3000	0.2400	74668.	50746.	66041.	0.0079450
2.4000	0.2400	67032.	47557.	59725.	0.0082135
2.4500	0.2400	63201.	46888.	56829.	0.0084266
2.4700	0.2400	61667.	46176.	55565.	0.0084731
2.5000	0.2600	54711.	41790.	49531.	0.0083708
2.5200	0.2700	51185.	40260.	46691.	0.0083952
2.5400	0.2900	46188.	38083.	42716.	0.0084004
2.5600	0.3100	41748.	36399.	39347.	0.0084344
2.5800	0.3400	36633.	34483.	35607.	0.0084650
2.5900	0.3600	33877.	33817.	33847.	0.0085127
2.6000	0.3600	33136.	33385.	33261.	0.0085462
2.6200	0.3600	31651.	32767.	32223.	0.0085756
2.6300	0.3600	30907.	32537.	31753.	0.0086077
2.6500	0.3600	29416.	32068.	30828.	0.0086711
2.6670	0.3600	28145.	31661.	30058.	0.0087243

MOMENT OF INERTIA (IN-LB-SEC**2)

BLADE	SHROUD	DISK	TOTAL
0.0127084	0.0013849	0.0181245	0.0322177

BLADE EXPANSION FROM STRESS	BLADE EXPANSION FROM THERMAL	TOTAL EXPANSION (IN)
0.0017057	0.0018970	0.0123270

	SHROUD	BLADES	DISK	TOTAL
WEIGHT(LB)	0.046	0.530	2.511	178 3.087

Form G 7756

JOB KIPS

BY Y. E.

PAGE

DATE

REV.

Natural frequency Analysis of KIPS Turbine Blades.

The KIPS turbine blades were analyzed to obtain their natural frequencies.

The analysis was Conducted by a finite Element approach, (The ANSYS program [3], Stiff 63).

The Campbell diagram was then constructed as shown in Fig. 1.

The Campbell diagram shows no resonance Conditions within the operating Speed range.

The F.E. Model of the blade and the first three mode Shapes are presented in Fig's 2, 3, 4 and 5.

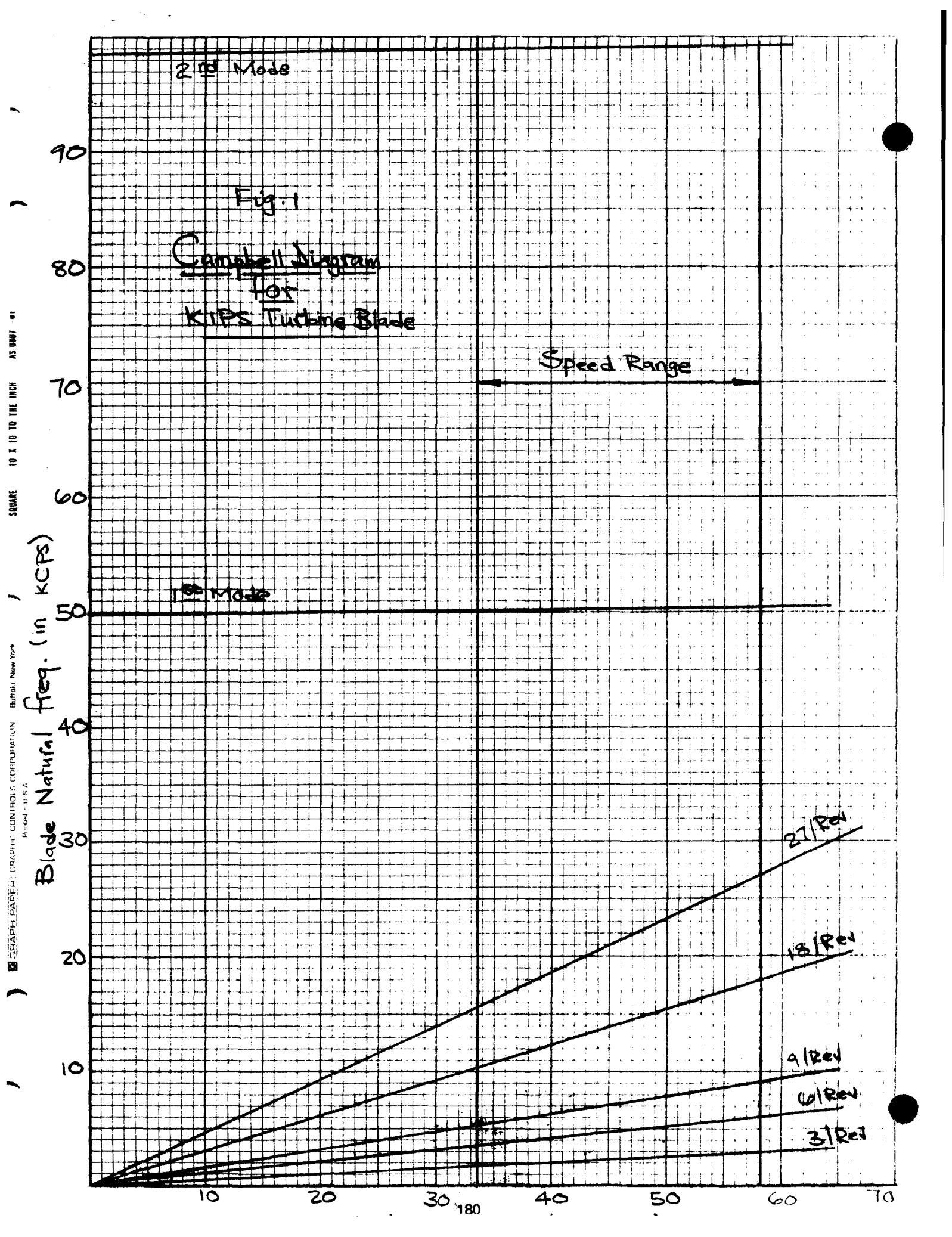
2nd Mode
Fig. 1
Campbell Diagram
for
KIPS Turbine Blade
Speed Range
1st Mode
Blade Natural Freq. (in KCPS)
27/Rev
18/Rev
9/Rev
6/Rev
3/Rev
90
80
70
60
50
40
30
20
10
10
20
30
40
50
60
70
180

JOB KIPS

BY Y.E.

PAGE

DATE

REV.

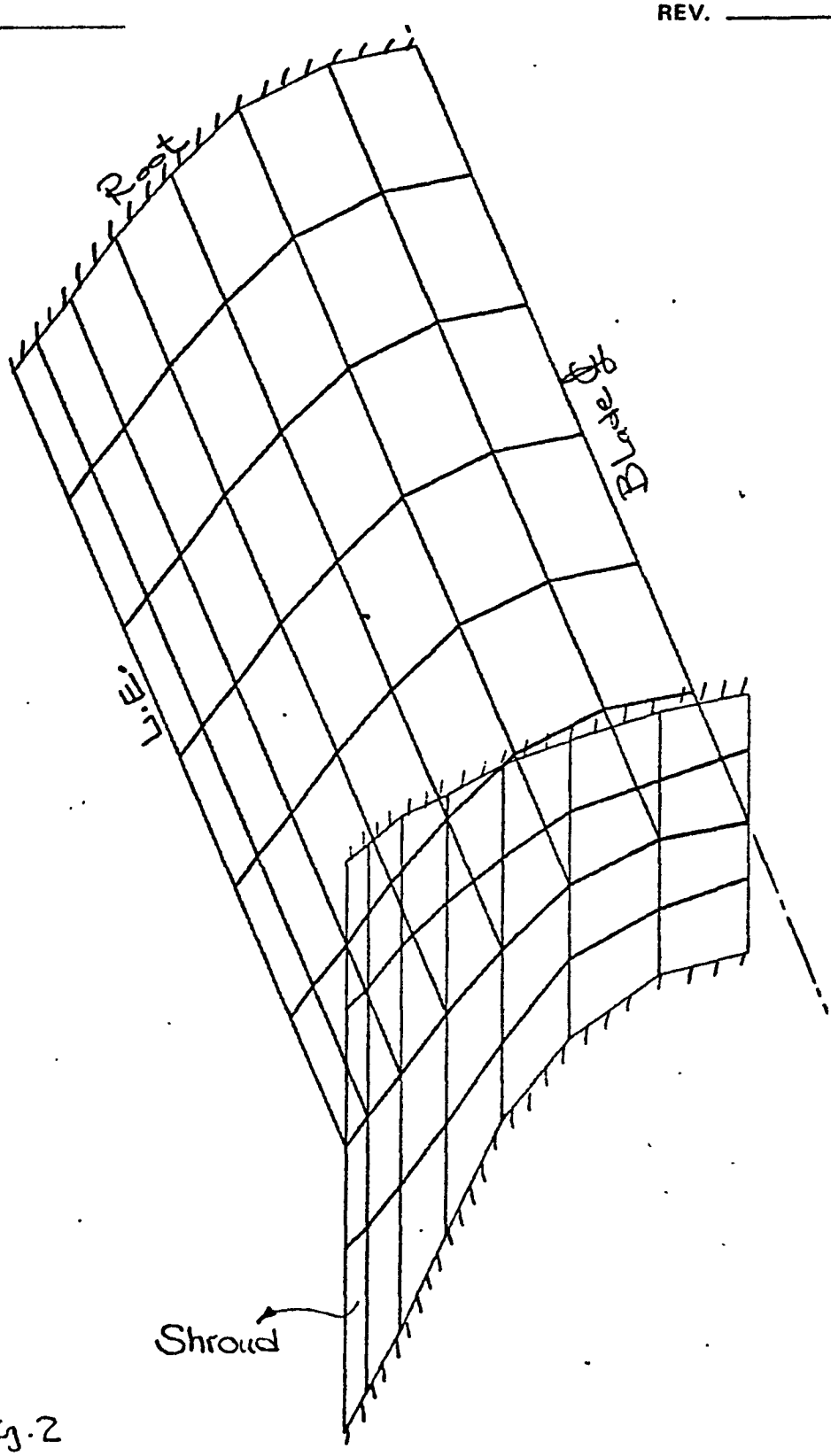

Fig.2

KIPS TURBINE BLADE-SHORT CHORD-111 BLADES.

Form G 7756

JOB KIPS

BY Y.E.

PAGE

DATE

REV.

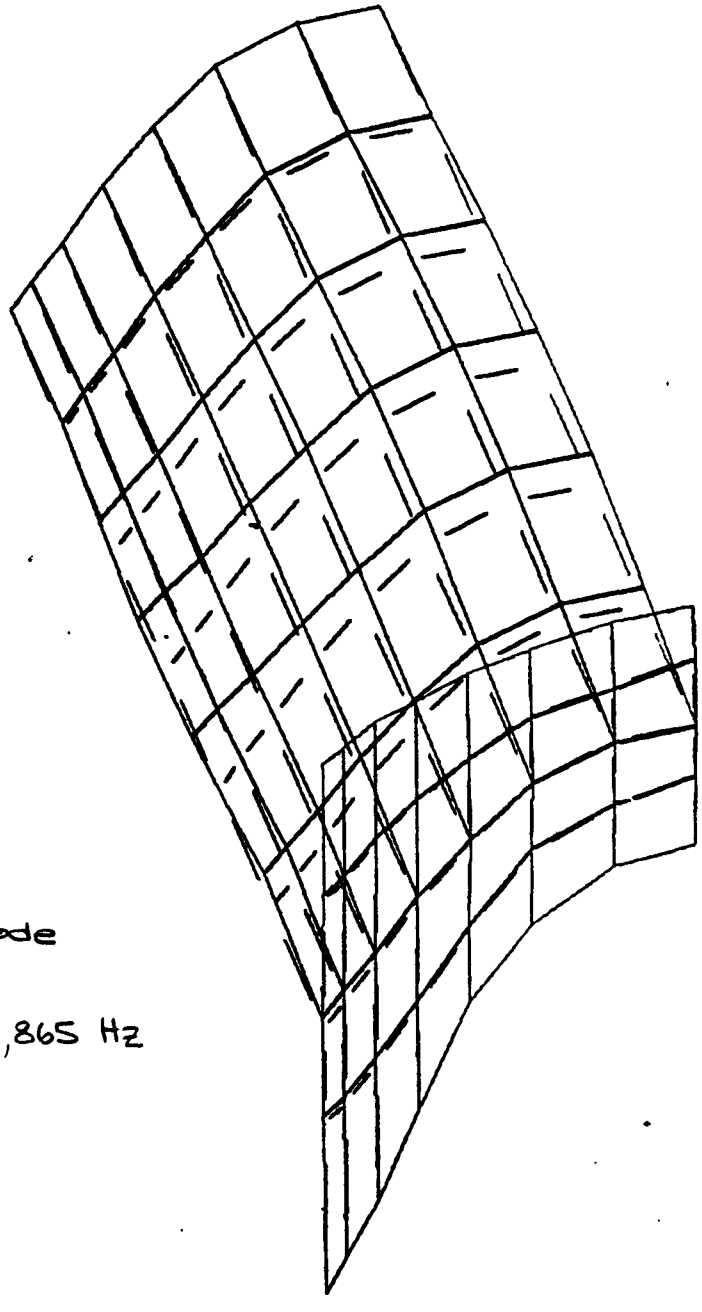

1st Mode

f_1 = 49,865 Hz

Fig. 3

KIPS TURBINE BLADE-SHORT CHORD-111 BLADES.

JOB kips

BY Y. E.

PAGE

DATE

REV.

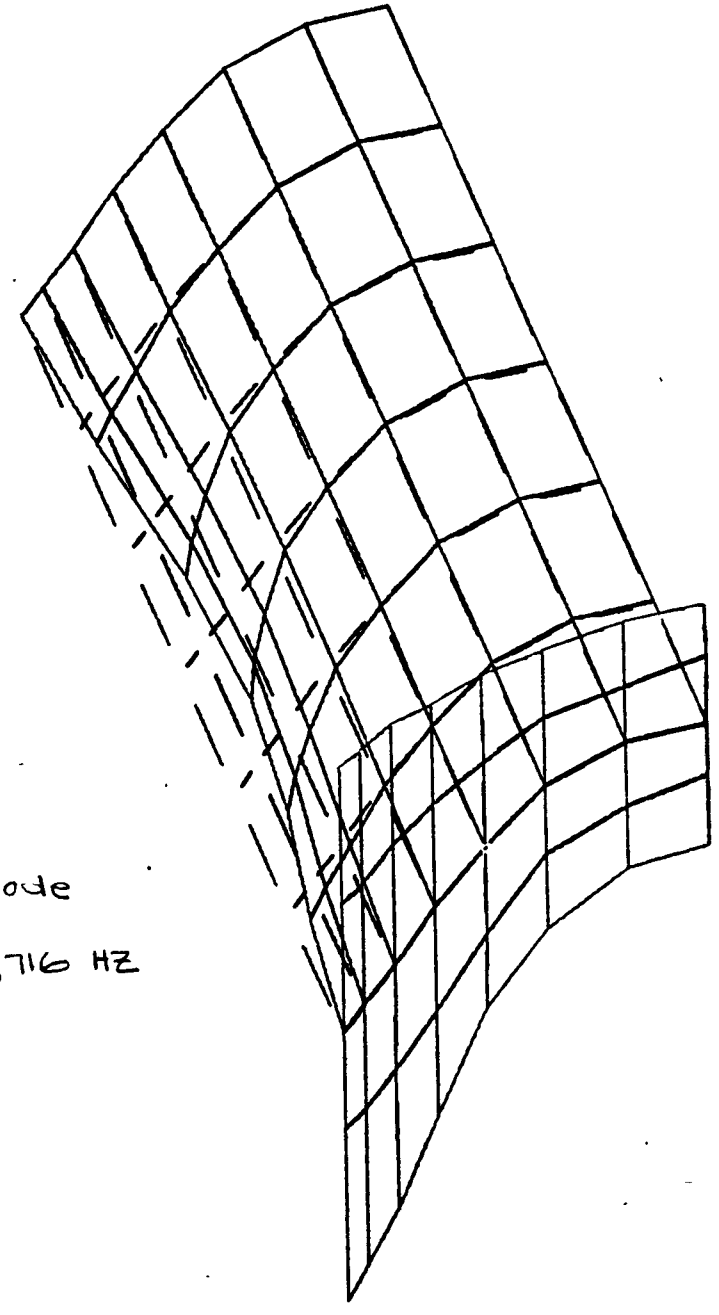

2nd Mode

f_2 = 98,716 HZ

Fig. 4

2 KIPS TURBINE BLADE-SHORT CHORD-111 BLADES.

JOB kips

BY Y.E.

PAGE

DATE

REV.

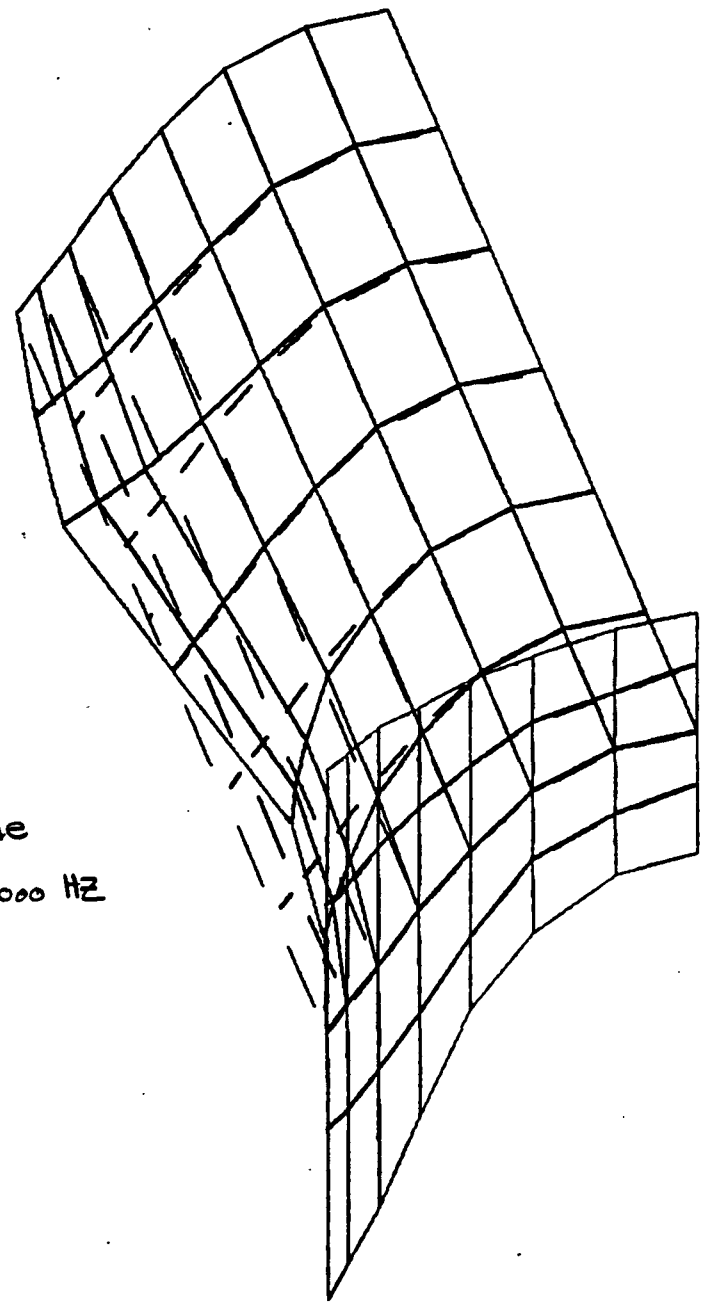

3rd Mode

F_3 = 108,000 HZ

Fig. 5

3 KIPS TURBINE BLADE-SHORT CHORD-111 BLADES.

JOB KIPS

BY Y.F.

PAGE

DATE

REV.

Effect of Partial Admission on Blade loading

$$\frac{\sigma_{dyn}}{\sigma_{st.}} \simeq \left(1 + \frac{2}{n\delta}\right)$$

where

n = no. of Cycles / rev.

$\delta = 2\pi\zeta \equiv$ Log decrement

ζ = damping Coefficient

Assume $\delta \simeq 0.001$

$$\frac{\sigma_{dyn}}{\sigma_{st.}} \simeq \left(1 + \frac{2000}{n}\right) \quad , \quad n = \frac{f_n}{(rps)} \quad , \quad f_n = 49{,}865\ Hz$$

RPM	Δp (psi)	n	D.M.F.	Δp_{dyn} (psi)
30,000	.094	99.73	21.05	1.97
40,000	.069	74.8	27.73	1.91
50,000	.044	59.8	34.44	1.51
60000	.019	49.87	41.1	0.78

The blade stresses due to the max. dynamic pressure loading is thus negligible.

JOB KIPS PAGE

DATE

BY J.E. REV.

Blade Centrifugal Stresses

The blade root stress at 58200 rpm is found from the E-4 program output.

$\sigma = 55{,}662$ psi

Assuming a stress concentration factor of 1.20 at the blade root

$\sigma_{max} = 1.20 \times 55{,}662 = 66{,}794$ psi

$\sigma_{min} = 66{,}794 \times \left(\frac{33}{58}\right)^2 = 21{,}623$ psi

for Inconel 718 @ 550°F ▷

$F_{tu} = 0.93 \times 180 = 167.4$ ksi (S-value)

$\sigma_e = 54 \times 0.86 = 46.44$ ksi (S-value)

for 1×10^{-9} failure probability

$F_{tu} = 0.82 \times 167.4 = 137.3$ ksi

$\sigma_e = 0.68 \times 46.44 = 31.6$ ksi @ 10^7 Cycles

σ @ 10^6 Cycles $= 0.86 \times 0.68 \times 59 = 34.5$ ksi @ 10^6 Cycles

σ @ 10^5 Cycles $= 0.86 \times .68 \times 65 = 38.0$ ksi @ 10^5 Cycle

JOB KIPS

BY Y.E.

PAGE

DATE

REV.

At the indicated stress levels, the fatigue life of the blade is Infinite.

The Goodman diagram for the material (Inconel 718) with a failure probability of 1×10^{-9} is shown in fig. 6.

M.S. Based on yield Strength @ 550°

with 10^{-9} failure Probability

$$F_{ty\ all} = (0.945 \times 150) \times 0.73 = 103.48 \text{ ksi}$$

$$\text{M.S.} = \frac{103.48}{66.794} - 1 = \boxed{0.549 \text{ on yield}}$$

Note: Creep effect @ 550° at maximum Stress is negligible for Inconel 718.

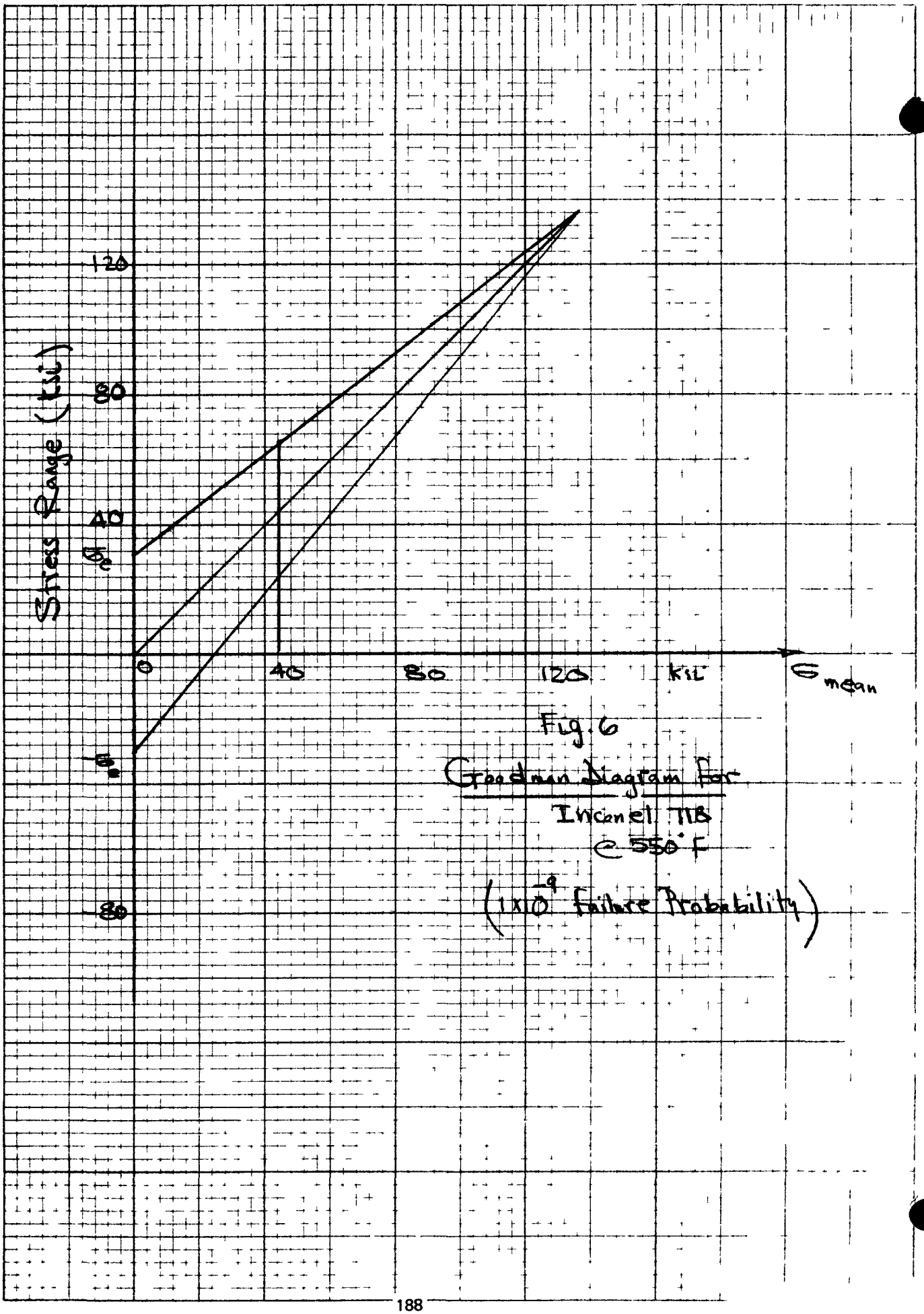

Fig. 6

Goodman Diagram For
Inconel 718
@ 550°F
(1×10^{-9} Failure Probability)

JOB KIPS

BY Y E.

PAGE

DATE

REV.

Shroud

MAT.: Hastelloy X

The membrane Stress & Strain of the shroud are computed from the turbine wheel growth data (E-4 output).

Table I- Membrane Stresses in Shroud

Operating Condition		Design Speed 33700 rpm Steady State	Overspeed 55311 rpm Steady State
Blade Growth (in)	Thermal	0.002676	0.0029892
	Centrifugal	0.0005967	0.0016240
Disk Growth (in) (Thermal + Centrifugal)		0.011319	0.0163140
Total Growth (in) ΔR (Disk + Blade)		0.014592	0.020927
Shroud Growth (in) $\delta_{th} = \alpha R \Delta T$		0.012357	0.01362
Net Shroud Disp. (in) $\Delta G = \Delta R - \delta_{th}$		0.002235	0.007305
Strain $= \epsilon = \frac{2\Delta G}{(R+\delta_{th})}$ (in/in)		0.00130	0.00426
Stress (psi)		28,000	44,000
Elastic or Plastic		Elastic	Plastic

JOB KIPS

BY Y E

PAGE

DATE

REV.

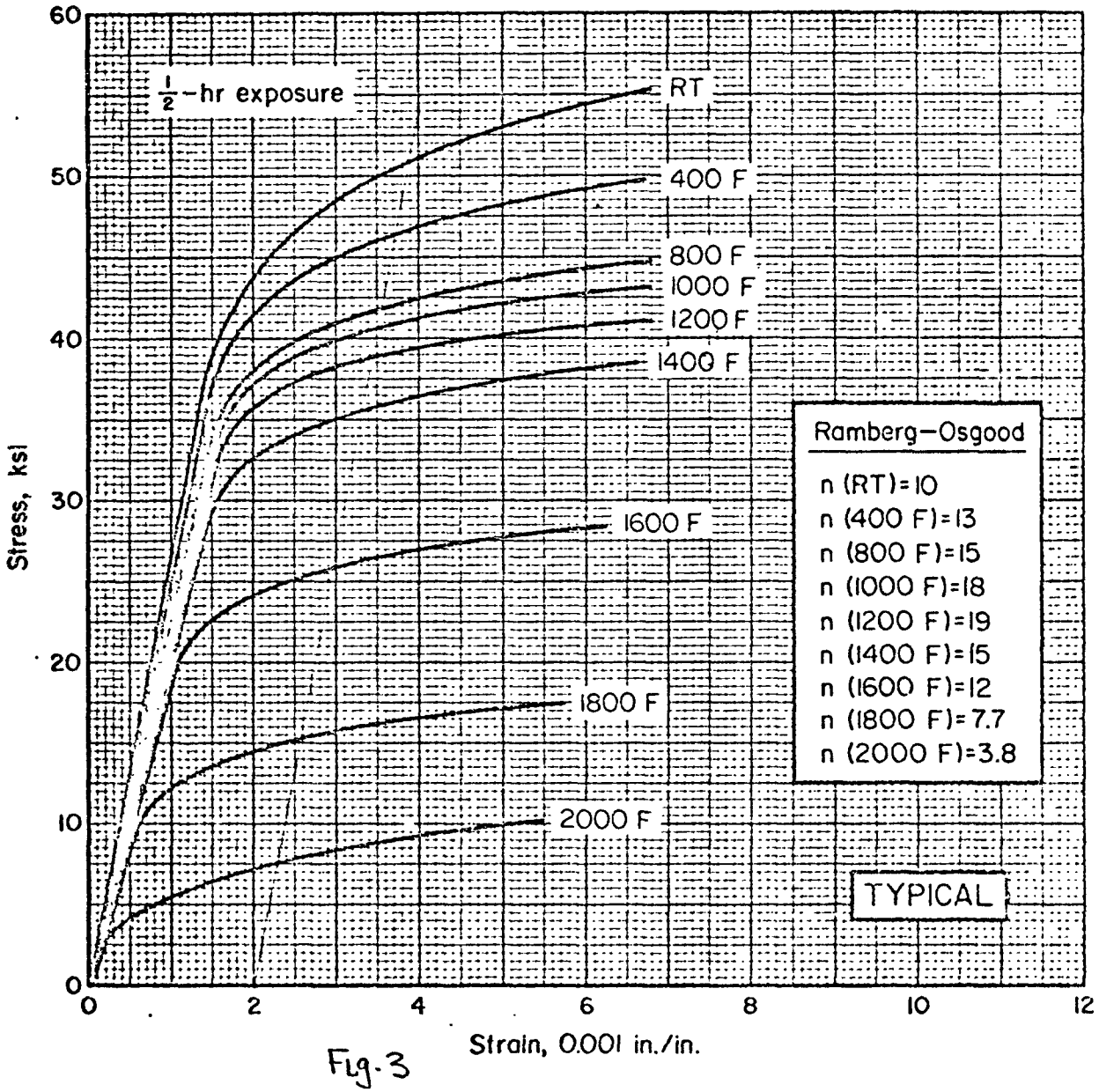

Fig. 3

FIGURE 6.3.2.1.6(a). *Typical tensile stress-strain curves for Hastelloy X (sheet) at room and elevated temperatures.*

JOB HPS

BY Y E.

PAGE

DATE

REV.

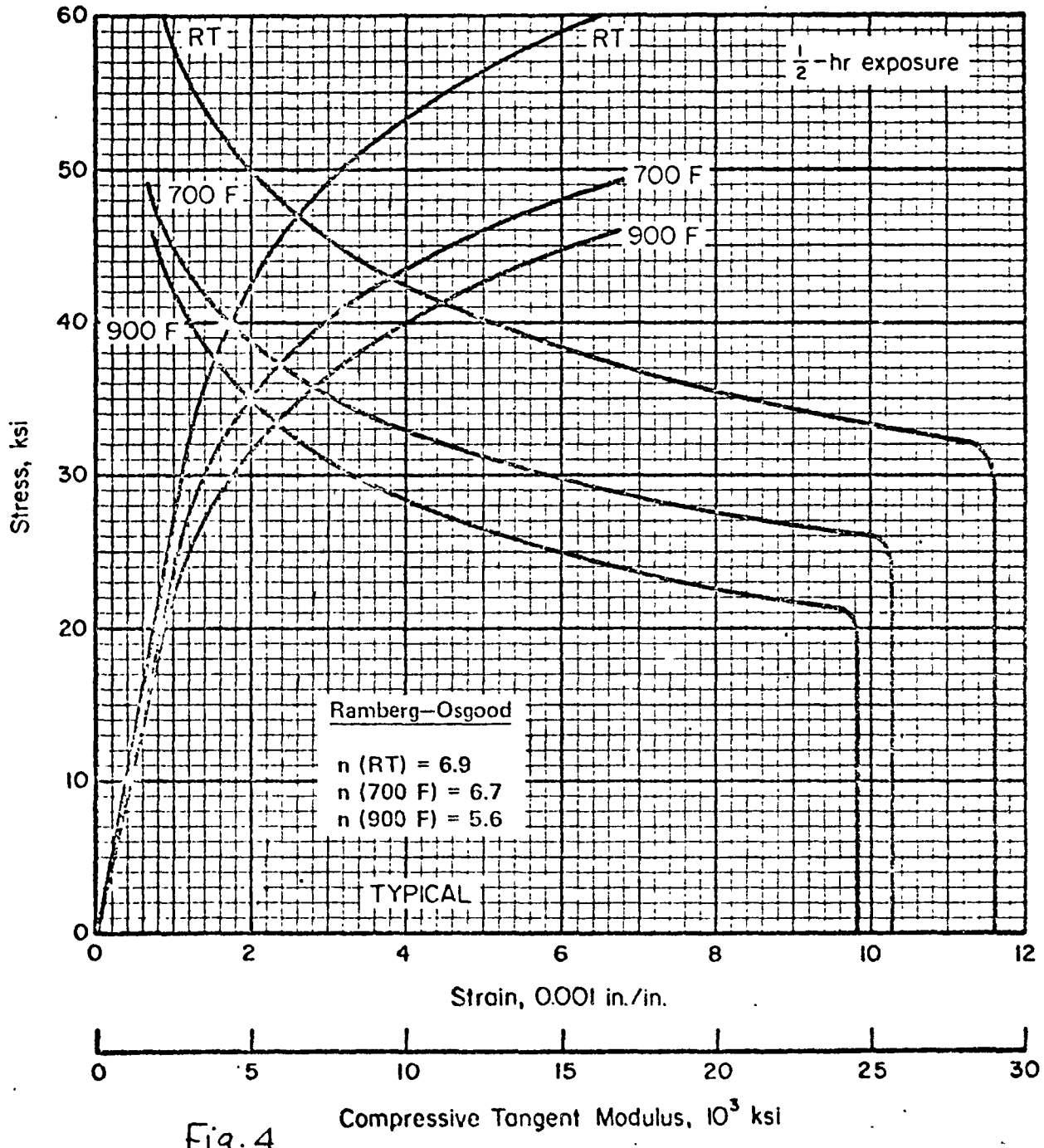

Fig. 4

FIGURE 6.3.2.1.6(b). *Typical compressive stress-strain and tangent modulus curves for Hastelloy X bar at room and elevated temperatures.*

JOB _____ PAGE _____

_____ DATE _____

BY _____ REV. _____

For Hastelloy X : ▷

@ 500°F :

$\sigma_u = 0.92 \times 100 = 92$ ksi

$\sigma_y = 0.85 \times 45 = 39.25$ "

@ 600°F :

$\sigma_u = 0.9 \times 100 = 90.$ ksi

$\sigma_y = 0.8 \times 45 = 36.$ "

M.S. @ Design Speed (33,700 rpm)

$M.S.(ult) = \frac{0.82 \times 90}{28.} - 1 =$ 1.63 @ 1×10^{-9} failure Rate

$M.S.(yield) = \frac{0.73 \times 39.25}{28} - 1 =$ 0.023 @ 1×10^{-9} failure Rate

M.S. @ over Speed (55,311 rpm)

$M.S.(ult) = \frac{90. \times .82}{46.} - 1 =$ 0.6

@ 1×10^{-9} failure Rate

NOTE: The fatigue life of the shroud under a maximum strain of 0.00426 in/in is larger than 1×10^5 cycles. Since this fatigue life is much larger than

JOB _____ PAGE _____

_____ DATE _____

BY _____ REV. _____

the actual number of occurences during the unit's life, the design is considered adequate.

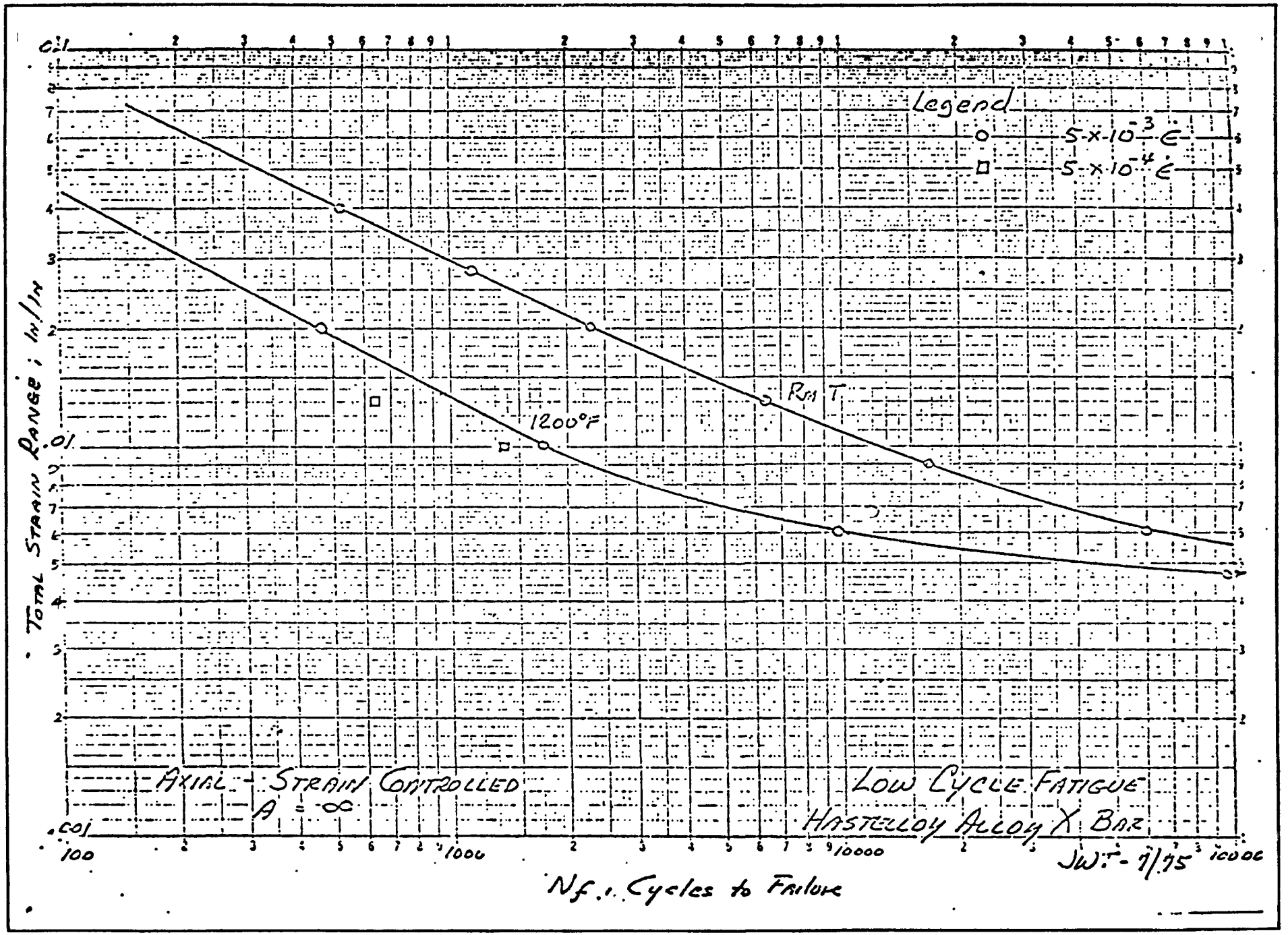

Fig. 5, Fatigue Data for Hastelloy X

JOB KIPS

BY Y.E.

PAGE

DATE

REV.

Shroud-Blade Braze Stresses

Blade Area = 0.02584 in^2

Mean radius of Shroud = 3.415"

Max. thickness of Shroud = 0.022"

Shroud width = 0.36"

No. Blades = n = 111

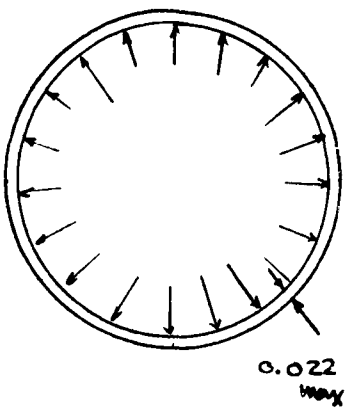

The braze stress is induced by two effects: I. Centrifugal forces; and II. Thermal growth.

$$\sigma_{braze} = \sigma_c + \sigma_{th}$$

where $\sigma_c = \frac{f}{A_B} = \frac{m\omega^2 R}{A_B} = \left(\frac{2\pi R \cdot A_s \cdot \rho}{n \cdot g}\right) \frac{R \cdot \omega^2}{A_B}$

A_s = Shroud Cross sectional area

n = no. of blades

ω = rotational speed (rad/sec.)

and A_B = braze area = 0.02584 in^2 (100% penetration)

$$\sigma_{th} = -\frac{2Et}{R^2}(\Delta G) \times \frac{S}{P}$$

where

$S = 2\pi \times 3.415 \times 0.36 = 7.7245\ in^2$

$P = 111 \times .02584 = 2.868\ in^2$

$E_{Cold} = 0.92 \times 29 \times 10^6 = 26.7 \times 10^6$ psi

JOB KIPS

BY Y. E.

PAGE

DATE

REV.

Operating Condition	Design Speed	Over Speed
	33,700 rpm	55311 rpm
	Steady State	Steady State
ΔG (in) Net Shroud disp	0.002235	0.007305
σ_{th} (psi)	−606.	−1982.
σ_c (psi)	1929.	5188.
$\sigma_{barge} = \sigma_{th} + \sigma_c$	1323.	3206.
M.S. (yield)	>>1	>>1

JOB KIPS

BY Y. E.

PAGE

DATE

REV.

Critical Speed Analysis of the KIPS Rotor Assembly

A Critical Speed analysis on the KIPS flight System rotor assembly was conducted using the F-10 inhouse Computer program.

A Summary of the Critical Speed picture is as follows:

Critical Speed (rpm)	Mode	Load Condition
10,000	1st Bending	Zero Vib & Zero Accel.
13,500	1st Bending	with Vib & Zero Accel.
22,000	2nd Bending	Zero Vib. & Zero Accel.
28,000	"	With Vib. & Zero Accel.
32,500	1st Bending	(Accel.) + Vib. or Shock

JOB KIPS

BY Y. E.

PAGE

DATE

REV.

It may appear that the 32,500 rpm critical speed is close to the lower bound of the speed range, however; the Acceleration + Vibration and Shock conditions occur at speeds close to the upper bound.

It is thus concluded that there is no danger of critical speeds within the speed range for the indicated load conditions.

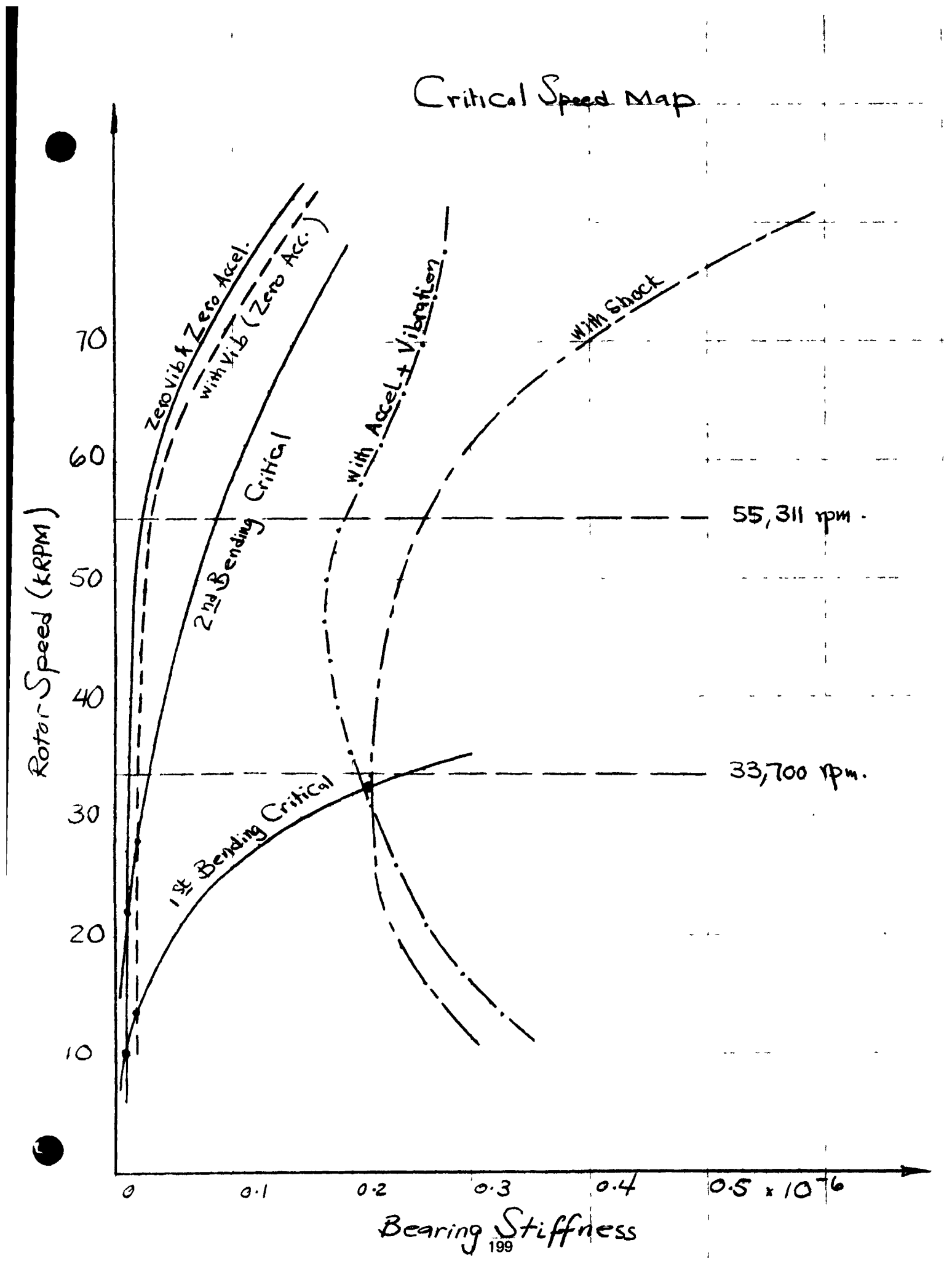
Critical Speed Map
Zero Vib & Zero Accel.
with Vib (Zero Acc.)
2nd Bending Critical
With Accel. + Vibration
With Shock
55,311 rpm.
33,700 rpm.
1st Bending Critical
Rotor Speed (kRPM)
70
60
50
40
30
20
10
0
0.1
0.2
0.3
0.4
0.5 x 10^6
Bearing Stiffness

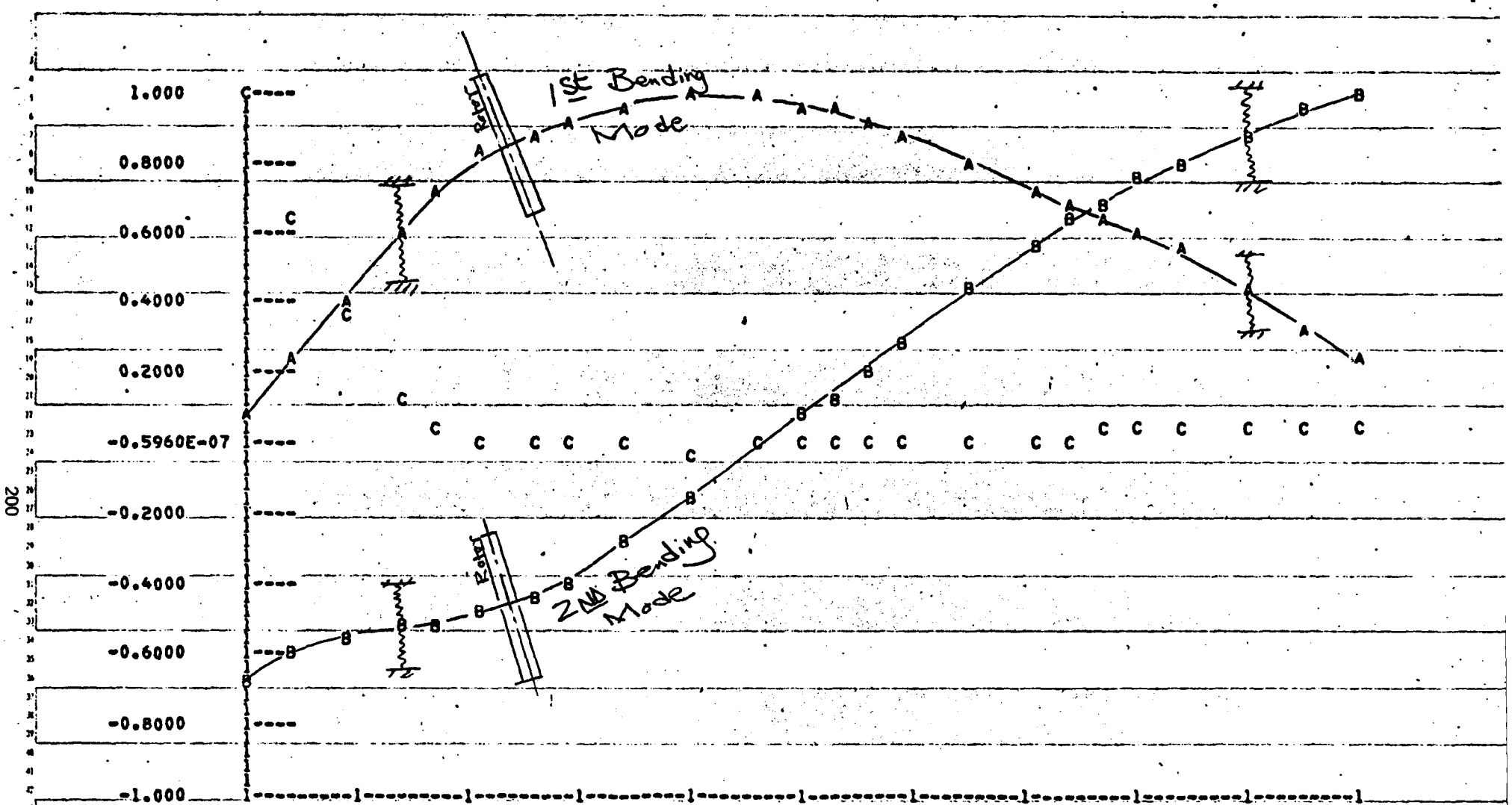

Bearing Stiffness = 130,000 lb/in

Typical Mode Shapes of KIPS Rotor

JOB Kit's Flight System

BY Y. E.

PAGE

DATE

REV.

Rotor Housing

The Kips rotor housing area and the corresponding finite element model are shown in Fig. 1.

The analysis was conducted by the ANSYS program [3]. Computer generated plots for the different areas are shown in figures 2 through 5.

The results shown are for the case of a steady state temperature distribution at the design speed, in addition to pressure loadings on the generator housing.

JOB KIPS

BY Y.E.

PAGE

DATE

REV.

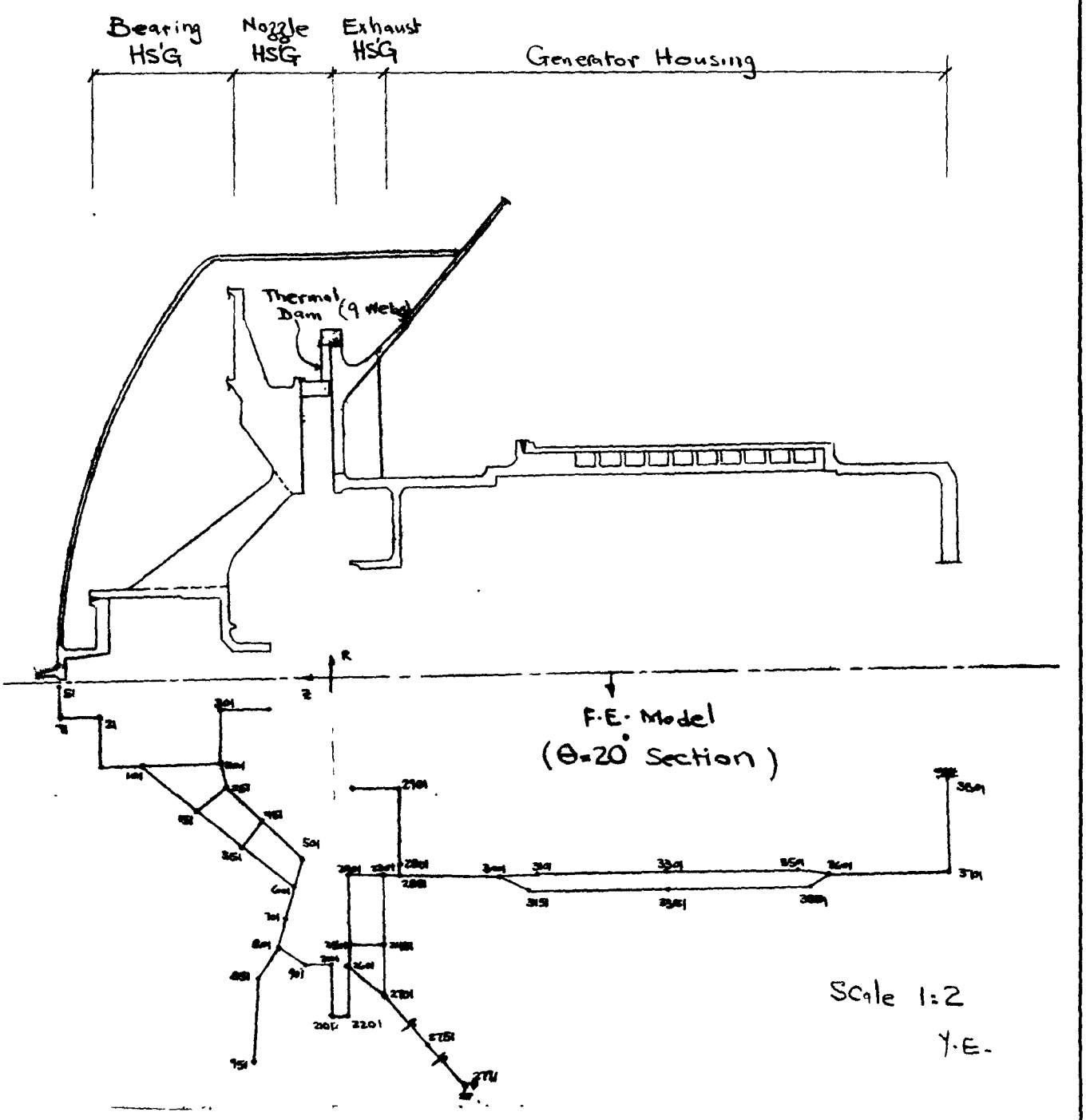

Fig. 1
Finite Element Model
for
KIPS rotor Housing

Form G 7756

Bearing Housing

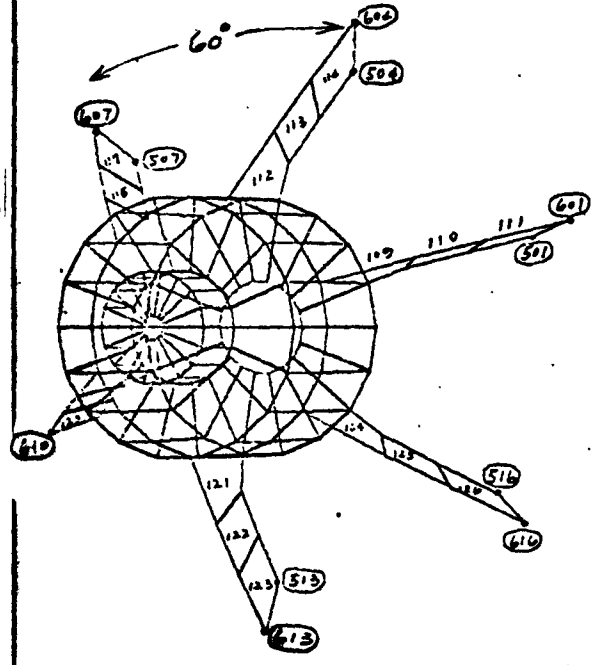

Fig. 2

Nozzle Housing

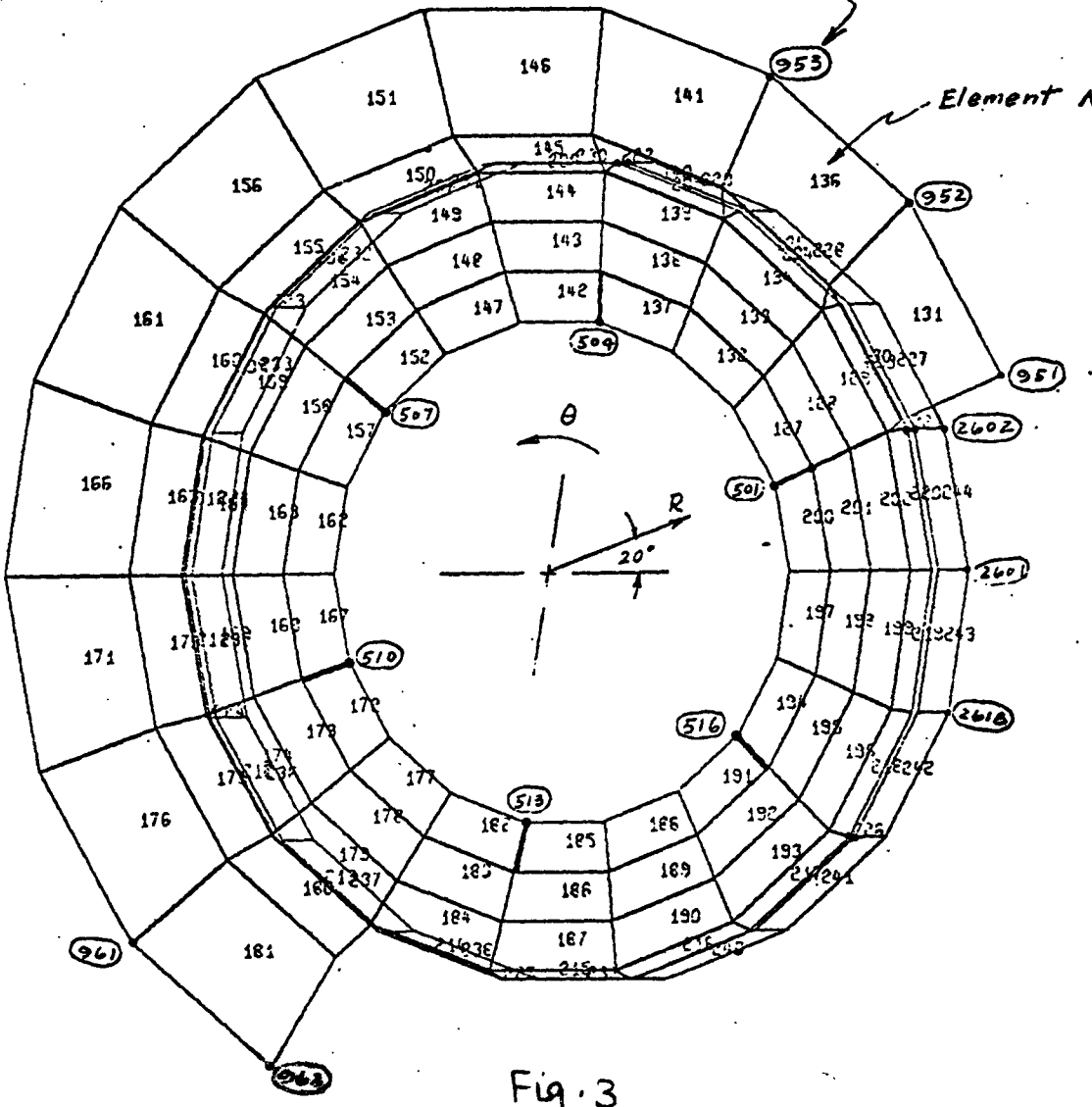

Fig. 3

JOB
BY
PAGE
DATE
REV.

203

Form G 7756

JOB KIPS

BY Y.E.

PAGE

DATE

REV.

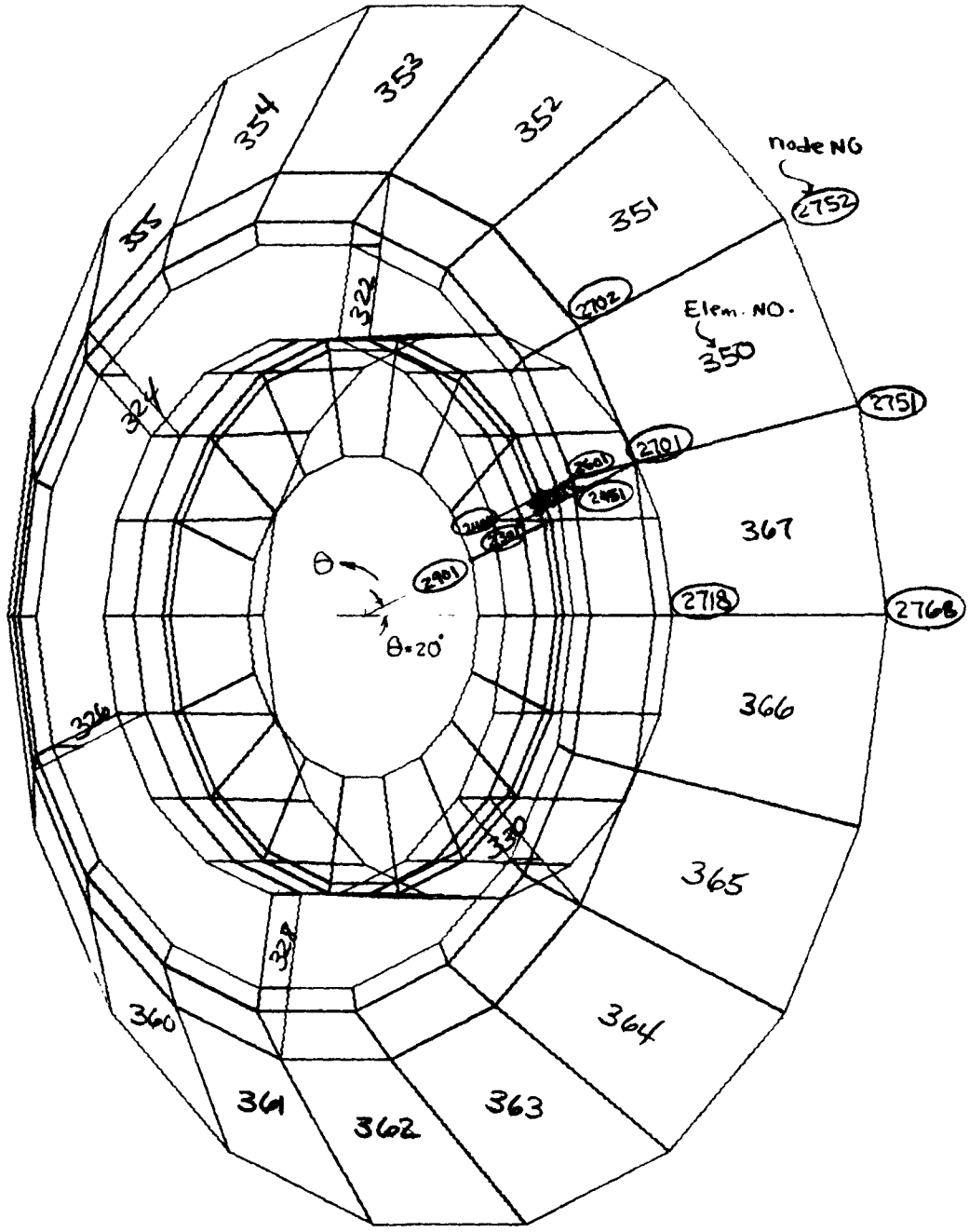

Fig. 4
Exhaust Housing

JOB KIPS

BY Y.E.

PAGE

DATE

REV.

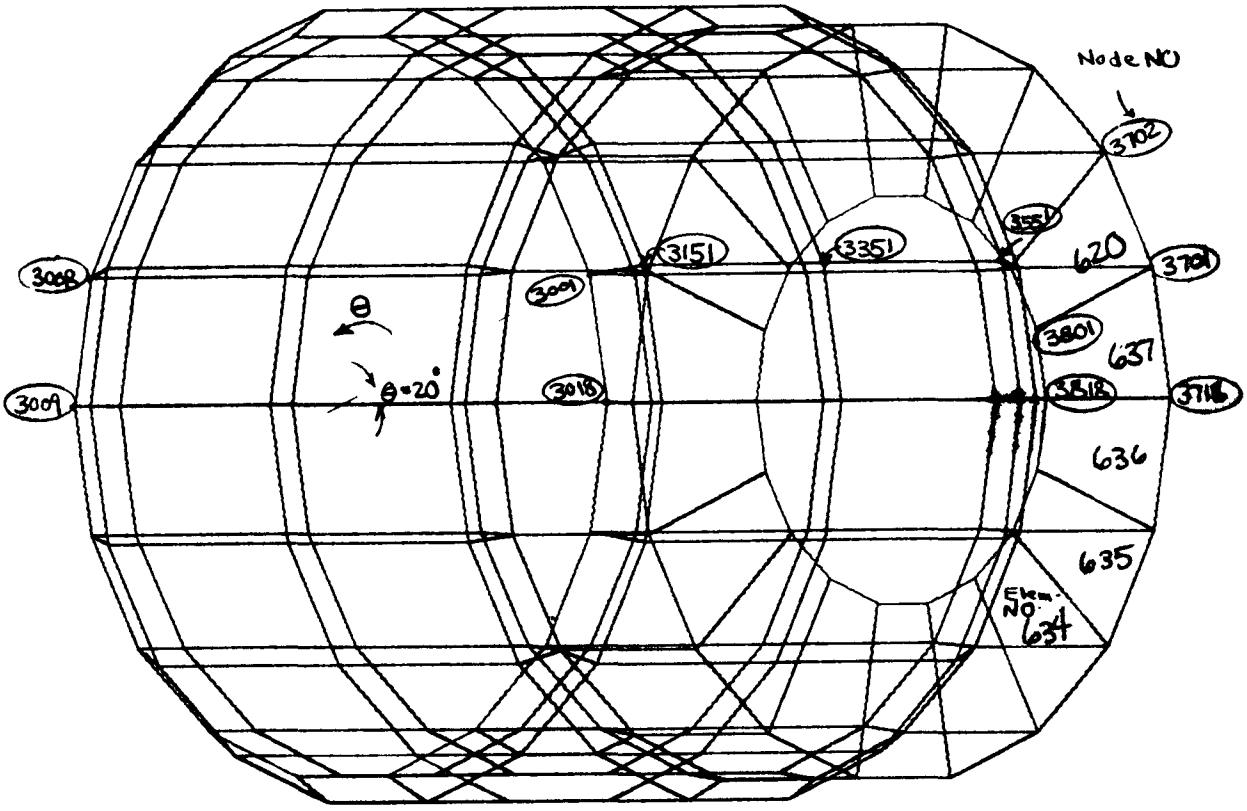

Fig. 5
Generator Housing.

JOB KIPS PAGE

DATE

BY Y.E. REV.

Summary of Maximum Stresses

Section	Max. Stress (psi)	M.S. (Yield)
Bearing Housing.	13,229	Large
Nozzle Housing.	30,854	1.26
Exhaust Housing.	10,660	0.75
Generator Housing	4,768	Large

Mat: 17-4 PH - H1150 (Bearing HSG, Nozzle HSG, Thermal Dam)

$\sigma_y = 111$ ksi

$\sigma_u = 135$ " @ R.T.

$\sigma_{all_{(y)}} = 69.7$ ksi

$\sigma_{all_{(u)}} = 95.2$ " @ (500° F, 1×10^{-9} failure rate)

304L S.S. (Exhaust HSG and Generator HSG)

$\sigma_y = 30$ ksi

$\sigma_u = 75$ " @ R.T.

$\sigma_{all_{(y)}} = 18.62$ ksi

$\sigma_{all_{(u)}} = 46.74$ " @ (500° F, 1×10^{-9} failure Rate)

JOB FIPs

BY Y.E.

PAGE

DATE

REV.

Close-up of Rotor Housing on turbine.

To avoid rubbing of turbine against housing, positive clearance should be maintained.

$$\Delta = u_{\delta_{2401}} - u_{\delta_{2601}}$$

$$= 0.0359 - 0.0357$$

$$\therefore \quad \underline{\Delta = 0.002''}$$

Thus, the amount of housing deflection is $0.002''$ which is less than the original clearance between the turbine and the housing.

JOB KIPS

BY Y.E.

PAGE

DATE

REV.

Deformation of KIPS Rotor Housing under S.S. Temperature and Pressure Loading.

ANSYS - ENGINEERING ANALYSIS SYSTEM UP190 REV 2 NUES-SC2E JAN 1 1972
SWANSON ANALYSIS SYSTEMS, INC. ELIZABETH, PENNSYLVANIA 15037 PHONE (412) 751-1940

STRESS AND THERMAL DISTORTION OF KIPS HOUSING (F.S.D.)

10:32:04 2/15/78
CP = 109.780 PP = 0.0

***** DISPLACEMENT SOLUTION ***** TIME = 0. LOAD STEP= 1 ITERATION= 1 CUM. ITER.=

NODE	UX	UY	UZ	ROTX	ROTY	ROTZ
1	.212770E-02	-.505148E-03	.394229E-01	.395849E-03	.650350E-03	.546119E-05
2	.194722E-02	-.551302E-03	.396244E-01	.441211E-03	.296605E-03	.111820E-03
3	.175599E-02	-.539505E-03	.397818E-01	.337370E-03	.153140E-03	-.111953E-03
4	.157671E-02	-.456144E-03	.398773E-01	.284252E-03	.232209E-03	-.127294E-04
5	.144806E-02	-.319169E-03	.400059E-01	.212936E-03	-.277484E-04	.940213E-04
6	.136778E-02	-.154872E-03	.400551E-01	.366243E-04	-.100629E-03	-.495896E-04
7	.134308E-02	.302074E-04	.400236E-01	-.792799E-04	.273833E-04	.886524E-06
8	.133951E-02	.211049E-03	.399926E-01	-.190258E-03	-.500680E-04	.884340E-04
9	.148911E-02	.365945E-03	.398857E-01	-.346871E-03	.846015E-04	-.106492E-03
10	.163306E-02	.488883E-03	.397093E-01	-.371382E-03	.408294E-03	.544355E-05
11	.182354E-02	.552456E-03	.395917E-01	-.368042E-03	.332577E-03	-.111854E-03
12	.201852E-02	.539479E-03	.394324E-01	-.414686E-03	.464185E-03	-.116270E-03
13	.219326E-02	.467494E-03	.392535E-01	-.316872E-03	.178930E-03	-.600436E-04
14	.234355E-02	.336821E-03	.391841E-01	-.167918E-03	.702045E-03	-.979404E-04
15	.243325E-02	.155586E-03	.391330E-01	-.818997E-04	.735434E-03	-.101973E-03
16	.244991E-02	-.398449E-04	.391080E-01	.891676E-04	.885683E-03	.151506E-06
17	.240672E-02	-.230341E-03	.392028E-01	.246521E-03	.668914E-03	.101676E-03
18	.229397E-02	-.397100E-03	.393136E-01	.294668E-03	.587783E-03	-.106387E-03
19	.210534E-02	-.458641E-03	.394853E-01	.376893E-03	.212636E-03	.617722E-05
20	.186282E-02	-.500718E-03	.395501E-01	.368775E-03	.981434E-04	.181389E-04
21	.168913E-02	-.489278E-03	.396175E-01	.345463E-03	-.343484E-04	-.277594E-04
22	.153910E-02	-.420504E-03	.396798E-01	.299178E-03	-.172129E-03	-.144402E-04
23	.140603E-02	-.302476E-03	.397196E-01	.157945E-03	-.226488E-03	.318234E-15
24	.132819E-02	-.148479E-03	.397399E-01	.675489E-04	-.250188E-03	-.227059E-04
25	.130944E-02	.220364E-04	.397393E-01	-.835998E-04	-.254612E-03	.134688E-05
26	.134007E-02	.190222E-03	.397114E-01	-.222088E-03	-.196822E-03	.241972E-04
27	.143589E-02	.337021E-03	.396665E-01	-.279713E-03	-.130462E-03	-.748834E-05
28	.157489E-02	.443451E-03	.396088E-01	-.381454E-03	-.425311E-04	.739064E-05
29	.173783E-02	.497244E-03	.395364E-01	-.430021E-03	.123262E-03	.183544E-04
30	.191099E-02	.491917E-03	.394683E-01	-.344624E-03	.268887E-03	-.281671E-04
31	.207886E-02	.425502E-03	.394131E-01	-.293410E-03	.370508E-03	-.149386E-04
32	.220622E-02	.306359E-03	.393679E-01	-.213198E-03	.485573E-03	-.533560E-05
33	.228664E-02	.149806E-03	.393462E-01	-.354834E-04	.534052E-03	-.237411E-04
34	.231414E-02	-.262013E-04	.393512E-01	.823655E-04	.517612E-03	.106658E-05
35	.227014E-02	-.198823E-03	.393744E-01	.191888E-03	.477597E-03	.244342E-04
36	.217287E-02	-.345806E-03	.394212E-01	.343563E-03	.367909E-03	-.967400E-05
37	.202592E-02	-.467372E-03	.404425E-01	.397614E-03	.602655E-04	.555439E-06
38	.216993E-03	-.729935E-03	.404565E-01	.400781E-03	-.111558E-04	-.221902E-05
39	-.357843E-04	-.704312E-03	.404699E-01	.355673E-03	-.215104E-03	-.340906E-05
40	-.264295E-03	-.594053E-03	.404809E-01	.269576E-03	-.325562E-03	-.550167E-05
41	-.441537E-03	-.412417E-03	.404884E-01	.156743E-03	-.404806E-03	-.656342E-05
42	-.546121E-03	-.181179E-03	.404919E-01	.374365E-04	-.441599E-03	-.410847E-05
43	-.569304E-03	.717234E-04	.404912E-01	-.748712E-04	-.434379E-03	-.112817E-05
44	-.497044E-03	.316077E-03	.404867E-01	-.179907E-03	-.388312E-03	-.140986E-05
45	-.349142E-03	.522435E-03	.404788E-01	-.279069E-03	-.304409E-03	-.248200E-05
46	-.134540E-03	.685959E-03	.404677E-01	-.360434E-03	-.187506E-03	-.114736E-05
47	.106219E-03	.729306E-03	.404539E-01	-.402254E-03	-.542476E-04	-.331965E-05
48	.359160E-03	.704403E-03	.404399E-01	-.389825E-03	.841437E-04	-.446211E-05
49	.588743E-03	.594999E-03	.404274E-01	-.322687E-03	.204195E-03	-.589166E-05
50	.766737E-03	.413146E-03	.404180E-01	-.210742E-03	.294296E-03	-.607394E-05
51	.871724E-03	.181330E-03	.404131E-01	-.664027E-04	.346263E-03	-.336015E-05
52	.891077E-03	-.725588E-04	.404135E-01	.910022E-04	.343101E-03	-.106778E-05
53	.822119E-03	-.317643E-03	.404193E-01	.235455E-03	.285736E-03	.855381E-06
54	.673649E-03	-.524162E-03	.404294E-01	.342102E-03	.186725E-03	.241356E-05
55	.111143E-02	-.667917E-03	.404420E-01	.373715E-03	.497486E-04	.101820E-05
56	.865274E-03	-.730499E-03	.404590E-01	.409933E-03	-.891393E-04	-.540397E-05
57	.612603E-03	-.705492E-03	.405546E-01	.360614E-03	-.228319E-03	-.577176E-06
58	.383769E-03	-.595146E-03	.406159E-01	.300459E-03	-.348435E-03	-.607706E-05
59	.207231E-03	-.413210E-03	.406608E-01	.206892E-03	-.456916E-03	-.104804E-04
60	.103469E-03	-.182065E-03	.406833E-01	.544587E-04	-.515874E-03	-.268236E-05
61	.843325E-04	.709209E-04	.406800E-01	-.839948E-04	-.509299E-03	-.102408E-05
62	.152432E-03	.315220E-03	.406547E-01	-.213210E-03	-.451622E-03	.298982E-06
63	.249237E-03	.521420E-03	.406069E-01	-.336942E-03	-.337117E-03	.725204E-05
64	.507936E-03	.605257E-03	.405434E-01	-.381549E-03	-.191574E-03	.488020E-06
65	.754359E-03	.728702E-03	.404768E-01	-.342586E-03	-.601216E-04	-.702551E-05
66	.100771E-02	.703607E-03	.404097E-01	-.275104E-03	.679140E-04	-.200578E-05
67	.123714E-02	.593757E-03	.403500E-01	-.219955E-03	.171577E-03	-.852329E-06

JOB KIPS

BY YE

PAGE

DATE

REV.

Deformation (Continued)

Node	U_x	U_y	U_z	Rotx	Roty	Rotz
97	.1271-1E-02	-.31F1R6F-03	.403174E-01	.212312E-03	.223514E-03	-.955573E-06
98	.132227E-02	-.524926E-03	.403623E-01	.291852E-03	.148754E-03	.655586E-05
101	.161890E-02	-.254954E-03	.383954E-01	.384437E-03	-.620564E-04	-.317458E-04
102	.193785E-02	-.266520E-03	.385364E-01	.450099E-03	.464255E-04	-.996986E-03
103	.184655E-02	-.314416E-03	.386938E-01	.334985E-03	-.945491E-04	.924430E-03
104	.135301E-02	-.262400E-03	.388470E-01	.311514E-03	-.448225E-03	.565957E-04
105	.163647E-02	-.169669E-03	.389223E-01	.235461E-03	-.328339E-03	-.931916E-03
106	.143424E-02	-.122899E-03	.389678E-01	.274278E-04	-.389745E-03	.637035E-03
107	.134049E-02	-.237340E-04	.389749E-01	-.886005E-04	-.596035E-04	-.201048E-04
108	.162934E-02	.757493E-04	.389040E-01	-.186746E-03	-.324909E-03	-.640759E-03
109	.160136E-02	.127780E-03	.388017E-01	-.367899E-03	-.209741E-03	.103125E-02
110	.126651E-02	.239381E-03	.386850E-01	-.396974E-03	-.304720E-03	-.502256E-04
111	.179206E-02	.315878E-03	.385040E-01	-.362070E-03	.753593E-04	-.103153E-02
112	.191519E-02	.278686E-03	.383433E-01	-.419272E-03	.207875E-03	.925753E-03
113	.162100E-02	.271341E-03	.382203E-01	-.310076E-03	.775904E-04	.402049E-04
114	.202022E-02	.236445E-03	.380978E-01	-.153166E-03	.385440E-03	-.928756E-03
115	.216670E-02	.107571E-03	.380444E-01	-.877753E-04	.418810E-03	.786190E-03
116	.180[illegible]E-02	.156045E-04	.380[illegible]E-01	-.[illegible]E-04	.175104E-03	-.106302E-04
117	.214442E-02	-.802435E-04	.381136E-01	.246266E-03	.367512E-03	-.785714E-04
118	.204696E-02	-.214310E-03	.382271E-01	.280470E-03	.287172E-03	.990555E-03
119	.197454E-02	-.176693E-03	.380995E-01	.189922E-03	-.473892E-03	-.430132E-03
120	.197040E-02	-.971014E-04	.387426E-01	.193973E-03	-.701154E-03	-.102097E-03
121	.197054E-02	-.704427E-04	.388290E-01	-.565059E-04	-.711722E-03	.151040E-04
122	.201436E-02	.2858-8E-04	.385515E-01	-.265594E-04	-.629570E-03	.134124E-03
123	.205590E-02	.214624E-03	.378063E-01	-.141221E-03	-.394218E-03	.347729E-03
124	.207434E-02	.799554E-04	.375342E-01	.893520E-04	-.350120E-03	.116609E-04
125	.202234E-02	.128594E-03	.367300E-01	.338657E-03	-.558163E-03	-.131432E-03
126	.197937E-02	.937835E-04	.368579E-01	.398672E-03	-.508999E-03	.760068E-03
127	.200952E-02	.899928E-04	.370109E-01	.384025E-03	-.630980E-03	-.719036E-03
128	.210995E-02	.324132E-04	.371723E-01	.276168E-03	-.911517E-03	-.542526E-04
129	.213487E-02	-.294409E-04	.372405E-01	.163226E-03	-.806945E-03	.705047E-03
130	.203076E-02	-.471174E-04	.372782E-01	.211863E-04	-.783889E-03	-.734739E-03
131	.233281E-02	-.105789E-03	.372839E-01	-.767692E-04	-.887086E-03	.745242E-05
132	.194101E-02	-.152219E-03	.372140E-01	-.173878E-03	-.738501E-03	.728988E-03
133	.190466E-02	-.133940E-03	.371230E-01	-.248139E-03	-.737538E-03	-.725537E-03
134	.213418E-02	-.140426E-03	.370164E-01	-.357570E-03	-.827166E-03	.610649E-04
135	.180738E-02	-.130010E-03	.368276E-01	-.434645E-03	-.497003E-03	.724590E-03
136	.177710E-02	-.620726E-04	.366672E-01	-.388610E-03	-.329733E-03	-.759836E-03
137	.204566E-02	-.300440E-04	.365573E-01	-.259461E-03	-.373095E-03	.104887E-03
138	.176173E-02	.449310E-05	.364342E-01	-.214778E-03	-.116113E-03	.696489E-03
139	.178491E-02	.805072E-04	.363780E-01	-.785784E-04	-.410997E-04	-.754227E-03
140	.211837E-02	.100790E-03	.363976E-01	.842326E-04	-.182033E-03	.743978E-06
141	.185550E-02	.108404E-03	.364439E-01	.245149E-03	-.106707E-03	.751662E-03
142	.184600E-02	.148862E-03	.365607E-01	.356545E-03	-.250734E-03	-.706902E-03
143	.186925E-02	.348085E-04	.369114E-01	.136110E-03	-.473892E-03	-.507451E-03
144	.337778E-02	.145934E-04	.374625E-01	.177876E-03	-.701154E-03	-.153906E-03
145	.337957E-02	-.104057E-03	.375580E-01	-.494996E-04	-.711722E-03	.304067E-04
146	.320707E-02	-.120391E-03	.372865E-01	-.243251E-03	-.629570E-03	.192277E-03
147	.304964E-02	.494019E-04	.366663E-01	-.825803E-04	-.394218E-03	.420437E-03
148	.316767E-02	.108791E-03	.364384E-01	.828393E-04	-.350120E-03	.797559E-05
149	.706016E-03	.123569E-03	.364372E-01	.405093E-03	-.241231E-03	-.391319E-04
150	.479248E-03	.992924E-04	.365038E-01	.516553E-03	-.462818E-03	.864542E-04
151	.911003E-03	.410530E-04	.366622E-01	.310777E-03	-.605365E-03	-.111909E-03
152	.799140E-03	.301599E-04	.366057E-01	.330192E-03	-.648472E-03	-.656338E-04
153	.941111E-03	-.155824E-04	.366535E-01	.326637E-03	-.812591E-03	.804609E-04
154	.934322E-03	-.523035E-04	.366784E-01	.256981E-04	-.873621E-03	-.112561E-03
155	.767194E-03	-.103034E-03	.366720E-01	-.955629E-04	-.803332E-03	.113131E-05
156	.486633E-03	-.141511E-03	.366520E-01	-.210205E-03	-.814426E-03	.109196E-03
157	.510317E-03	-.142840E-03	.366030E-01	-.486903E-03	-.694725E-03	-.877465E-04
158	.521980E-03	-.140658E-03	.365383E-01	-.412371E-03	-.486860E-03	.245423E-04
159	.709899E-03	-.119051E-03	.364897E-01	-.301659E-03	-.430331E-03	.113910E-03
160	.677550E-03	-.659402E-04	.364367E-01	-.450021E-03	-.299754E-03	-.914447E-04
161	.562730E-03	-.229814E-04	.363815E-01	-.309409E-03	-.102403E-03	.273163E-04
162	.[illegible]E-03	.210826E-04	.363[illegible]E-01	-.[illegible]E-04	-.934488E-04	.108966E-03
163	.[illegible]E-03	.[illegible]E-04	.363[illegible]E-01	-.129501E-03	-.548121E-04	-.117157E-03
164	.[illegible]E-03	.101840E-03	.363345E-01	.810334E-04	.184729E-04	-.685167E-06
165	.762161E-03	.114731E-03	.363515E-01	.276484E-03	-.111656E-03	.114122E-03
166	.[illegible]E-03	.134275E-03	.363956E-01	.207907E-03	-.196907E-03	-.117747E-03
167	.557102E-02	-.336047E-03	.384285E-01	.172596E-04	-.778457E-03	-.475186E-03
168	.571393E-02	-.563637E-04	.394969E-01	.532996E-04	-.740786E-03	-.156631E-03
169	.573187E-02	-.897057E-04	.395644E-01	-.186769E-04	-.655192E-03	.203136E-04
170	.553375E-02	-.393436E-06	.393301E-01	-.105164E-03	-.747985E-03	.192923E-03
171	.[illegible]E-02	.348606E-03	.384854E-01	.402371E-04	-.852557E-03	.364595E-03
172	.[illegible]E-02	.132844E-03	.382225E-01	.735025E-04	-.994596E-03	.181949E-04
173	.[illegible]E-02	-.173[illegible]E-03	.[illegible]E-01	-.812422E-04	-.778457E-03	-.500025E-03
174	.[illegible]E-02	-.140[illegible]E-04	.374100E-01	.225977E-04	-.740782E-03	-.190249E-03
175	.[illegible]E-02	-.102[illegible]E-03	.374795E-01	-.650301E-05	-.656192E-03	.318634E-04
176	.565221E-02	-.995174E-04	.372434E-01	-.657983E-04	-.747985E-03	.230155E-03
177	.547447E-02	.244826E-03	.366603E-01	.125111E-03	-.852557E-03	.416184E-03
178	.559683E-02	.147352E-03	.361766E-01	.702714E-04	-.994596E-03	.120433E-04
179	.815422E-02	-.220819E-03	.366986E-01	.579443E-03	-.144069E-02	-.354541E-04
180	.806489E-02	-.108217E-03	.372022E-01	.545488E-03	-.979612E-03	.203423E-03
181	.813589E-02	-.727074E-04	.374091E-01	-.578364E-04	-.894486E-03	-.142280E-03
182	.821054E-02	-.[illegible]E-04	.373420E-01	.675972E-04	-.115271E-02	-.993486E-04
183	.[illegible]E-02	-.743020E-04	.[illegible]E-01	.228975E-03	-.710744E-03	.126915E-03

JOB KIPS

BY Y.E

PAGE

DATE

REV.

Deformation (Continued)

Node	U_x	U_y	U_z	Rotx	Roty	Rotz
509	.811451E-02	-.964305E-04	.374408E-01	-.301044E-03	-.788102E-03	-.189893E-03
510	.806568E-02	-.646453E-04	.371922E-01	-.151295E-03	-.123507E-02	-.101795E-03
511	.794488E-02	-.289321E-05	.371968E-01	-.187093E-04	-.977555E-03	-.114326E-03
512	.786550E-02	.111457E-03	.369235E-01	-.615164E-03	-.106445E-02	-.652643E-03
513	.798579E-02	.306100E-03	.364132E-01	-.424148E-03	-.163983E-02	-.788606E-05
514	.811921E-02	.277936E-03	.363523E-01	-.413837E-04	-.139314E-02	-.711348E-04
515	.814371E-02	.211341E-03	.362945E-01	-.170114E-03	-.146681E-02	-.117758E-03
516	.824650E-02	.175151E-03	.361754E-01	.405853E-04	-.191323E-02	-.745147E-06
517	.829391E-02	.538071E-04	.361656E-01	.260113E-03	-.137207E-02	.193250E-03
518	.828342E-02	-.119476E-03	.365206E-01	.106010E-03	-.119573E-02	.192116E-04
601	.961933E-02	-.258536E-03	.376405E-01	.366315E-03	-.642354E-03	.157528E-03
602	.963619E-02	-.176838E-03	.379406E-01	.239073E-03	-.532436E-03	.127312E-04
603	.970748E-02	-.133760E-03	.381125E-01	.832005E-04	-.467576E-03	-.120245E-04
604	.974778E-02	-.112828E-03	.381631E-01	-.261760E-05	-.399916E-03	-.470044E-04
605	.980513E-02	-.108210E-03	.381454E-01	-.273861E-04	-.270302E-03	-.299837E-04
606	.981272E-02	-.107109E-03	.381293E-01	-.115861E-04	-.211435E-03	.178527E-06
607	.977204E-02	-.101548E-03	.381281E-01	-.632464E-05	-.238633E-03	-.196819E-04
608	.975944E-02	-.866550E-04	.381124E-01	-.806197E-05	-.254384E-03	-.443029E-04
609	.969758E-02	-.629035E-04	.380926E-01	-.210184E-04	-.343012E-03	-.942857E-05
610	.954428E-02	-.123042E-04	.380501E-01	-.691271E-04	-.473243E-03	.357107E-04
611	.951426E-02	.668046E-04	.379303E-01	-.151720E-03	-.517565E-03	.532419E-05
612	.942035E-02	.186234E-03	.377017E-01	-.279013E-03	-.599856E-03	-.811516E-04
613	.942437E-02	.334552E-03	.374466E-01	-.258306E-03	-.884432E-03	-.491487E-04
614	.956190E-02	.284551E-03	.372624E-01	-.362219E-04	-.982555E-03	-.566044E-04
615	.959729E-02	.232040E-03	.372534E-01	.857375E-04	-.111897E-02	.483718E-04
616	.961426E-02	.171218E-03	.373262E-01	.362667E-05	-.122667E-02	.129221E-04
617	.971397E-02	.283166E-04	.372669E-01	-.654229E-04	-.994212E-03	.666473E-05
618	.972795E-02	-.125402E-03	.373445E-01	.200322E-04	-.763663E-03	.126405E-03
701	.111904E-01	-.330549E-03	.384400E-01	.316930E-03	-.456649E-03	-.969330E-05
702	.112491E-01	-.248047E-03	.385361E-01	.183430E-03	-.464862E-03	-.508445E-04
703	.113187E-01	-.198572E-03	.386757E-01	.480901E-04	-.394028E-03	-.615366E-04
704	.113792E-01	-.156396E-03	.386797E-01	-.469966E-04	-.277148E-03	-.636047E-04
705	.114371E-01	-.138249E-03	.386181E-01	-.661950E-04	-.185968E-03	-.517324E-04
706	.114517E-01	-.120404E-03	.385763E-01	-.107137E-04	-.132372E-03	-.155071E-04
707	.114232E-01	-.103942E-03	.385733E-01	.411230E-05	-.121594E-03	-.170142E-04
708	.113937E-01	-.774735E-04	.385793E-01	.941651E-05	-.177447E-03	-.121273E-04
709	.113237E-01	-.345201E-04	.385987E-01	.299899E-04	-.262167E-03	.249206E-04
710	.112201E-01	.394165E-04	.386001E-01	-.194973E-04	-.351808E-03	.477456E-04
711	.112249E-01	.140201E-03	.385159E-01	-.118893E-03	-.441708E-03	.644663E-04
712	.110242E-01	.265901E-03	.383165E-01	-.213583E-03	-.486918E-03	.403812E-04
713	.109810E-01	.385193E-03	.381297E-01	-.140480E-03	-.637673E-03	.414782E-04
714	.110421E-01	.302512E-03	.380287E-01	-.540670E-04	-.878764E-03	.394603E-04
715	.110652E-01	.247185E-03	.380894E-01	.144665E-03	-.105719E-02	.311597E-04
716	.110900E-01	.173247E-03	.381573E-01	-.216975E-04	-.998206E-03	.152375E-04
717	.111604E-01	.173540E-04	.380411E-01	-.175417E-03	-.943751E-03	-.433613E-05
718	.112005E-01	-.148013E-03	.379944E-01	.121119E-03	-.650216E-03	.187961E-04
801	.127690E-01	-.422870E-03	.387949E-01	.318276E-03	-.431644E-03	-.177417E-03
802	.128639E-01	-.305811E-03	.391094E-01	.176339E-03	-.445728E-03	-.176276E-03
803	.129307E-01	-.257041E-03	.392134E-01	.138375E-04	-.366829E-03	-.102464E-03
804	.130059E-01	-.203299E-03	.391656E-01	-.649860E-04	-.248443E-03	-.138536E-03
805	.130723E-01	-.167120E-03	.390617E-01	-.831837E-04	-.151595E-03	-.742201E-04
806	.130957E-01	-.133549E-03	.389971E-01	-.123376E-04	-.101947E-03	-.398415E-04
807	.130706E-01	-.106507E-03	.389901E-01	.714952E-05	-.905744E-04	.384460E-05
808	.130324E-01	-.672976E-04	.390205E-01	.258641E-04	-.148243E-03	.175321E-04
809	.129544E-01	-.490310E-05	.390774E-01	.495141E-04	-.231134E-03	.785775E-04
810	.128422E-01	.887927E-04	.391206E-01	-.256237E-07	-.325617E-03	.121101E-03
811	.127327E-01	.215735E-03	.390754E-01	-.933475E-04	-.414727E-03	.122382E-03
812	.126347E-01	.365316E-03	.389934E-01	-.208947E-03	-.456200E-03	.204534E-03
813	.125362E-01	.427842E-03	.387582E-01	-.597407E-04	-.575905E-03	.135201E-03
814	.125180E-01	.333865E-03	.387610E-01	.693400E-05	-.859999E-03	.952943E-04
815	.125260E-01	.255167E-03	.388995E-01	.169107E-03	-.101271E-02	.493197E-04
816	.125506E-01	.179915E-03	.389581E-01	-.415821E-04	-.104632E-02	.272175E-04
817	.126035E-01	.218540E-04	.387916E-01	-.237412E-03	-.898977E-03	-.503317E-04
818	.126874E-01	-.183979E-03	.386180E-01	.341731E-04	-.620681E-03	-.108455E-03
851	.138719E-01	-.651448E-03	.402647E-01	.320914E-03	-.421434E-03	-.213591E-03
852	.139869E-01	-.447904E-03	.405839E-01	.155351E-03	-.419692E-03	-.180224E-03
853	.140048E-01	-.312742E-03	.406534E-01	-.121390E-04	-.320061E-03	-.164221E-03
854	.141817E-01	-.217001E-03	.405947E-01	-.103035E-03	-.210599E-03	-.143615E-03
855	.142830E-01	-.166017E-03	.404320E-01	-.861084E-04	-.109193E-03	-.940243E-04
856	.143241E-01	-.137871E-03	.403524E-01	-.303351E-04	-.643944E-04	-.349782E-04
857	.143045E-01	-.110445E-03	.403425E-01	.176404E-04	-.519738E-04	.331204E-05
858	.142434E-01	-.683965E-04	.403921E-01	.485453E-04	-.113535E-03	.406424E-04
859	.141365E-01	.535477E-05	.404762E-01	.672667E-04	-.192104E-03	.983176E-04
860	.139887E-01	.128046E-03	.405527E-01	.361328E-04	-.294850E-03	.140174E-03
861	.139499E-01	.254838E-03	.405376E-01	-.666342E-04	-.375861E-03	.152827E-03
862	.137271E-01	.541901E-03	.403677E-01	-.193873E-03	-.439055E-03	.231057E-03
901	.131804E-01	-.325210E-03	.380262E-01	.411276E-03	-.508021E-03	-.227727E-04
902	.132576E-01	-.308990E-03	.383165E-01	.866492E-04	-.310635E-03	-.184657E-03
903	.133040E-01	-.259476E-03	.384218E-01	.697758E-04	-.282494E-03	-.507247E-04
904	.133504E-01	-.242774E-03	.383569E-01	-.160826E-03	-.106124E-03	-.157487E-03
905	.133944E-01	-.197117E-03	.382493E-01	-.155517E-04	-.640384E-04	-.330934E-04
906	.134046E-01	-.143909E-03	.381751E-01	-.584127E-04	.417252E-04	-.554149E-04
907	.133815E-01	-.103033E-03	.381717E-01	.323559E-04	-.167617E-04	.229018E-05
908	.133523E-01	-.502506E-04	.382026E-01	.304370E-04	.391665E-05	.291080E-05
909	.132972E-01	.128821E-04	.382718E-01	.369350E-04	-.150174E-04	.584641E-04
910	.132076E-01	.961182E-04	.383198E-01	.418491E-04	-.197022E-04	.121154E-03

JOB KIPS

BY YE

PAGE

DATE

REV.

Deformation (Continued)

Node	U_x	U_y	U_z	Rotx	Roty	Rotz
951	.1302 8E-01	.3566 5E-03	.3803 1E-01	.1858 5E-03	-.8796 1E-03	.1226 8E-03
952	.1307 3E-01	.2821 6E-03	.3818 0E-01	.5095 9E-04	-.1075 9E-02	-.1455 7E-04
953	.1312 1E-01	.1749 2E-03	.3824 3E-01	-.2234 5E-04	-.1149 3E-02	.4233 1E-04
954	.1314 7E-01	-.2001 0E-03	.3786 7E-01	-.1504 1E-03	.9739 2E-03	.2420 5E-04
955	.1804 6E-01	-.9522 3E-03	.4128 6E-01	-.9780 5E-04	-.6471 2E-03	-.1096 9E-03
956	.1814 1E-01	-.7061 2E-03	.4159 3E-01	.2702 9E-03	-.4123 3E-03	-.1979 9E-03
957	.1826 7E-01	-.5920 2E-03	.4156 3E-01	.7789 3E-04	-.3961 5E-03	-.1901 3E-03
958	.1840 1E-01	-.3618 4E-03	.4133 4E-01	-.8161 0E-04	-.3017 2E-03	-.1661 9E-03
959	.1851 5E-01	-.2596 7E-03	.4108 6E-01	-.1471 9E-03	-.1687 1E-03	-.1378 3E-03
960	.1856 3E-01	-.1809 7E-03	.4094 7E-01	-.1116 5E-03	-.7203 7E-04	-.9461 1E-04
961	.1863 9E-01	-.1096 2E-03	.4093 4E-01	-.3966 8E-04	-.1785 7E-04	-.4268 2E-04
962	.1847 7E-01	-.2079 3E-04	.4104 7E-01	.2990 7E-04	-.1940 5E-04	.3126 3E-05
963	.1815 1E-01	.1078 0E-03	.4123 6E-01	.8193 6E-04	-.7344 0E-04	.4790 5E-04
964	.1819 4E-01	.2835 3E-03	.4142 4E-01	.1090 1E-03	-.1624 6E-03	.9814 2E-04
965	.1813 5E-01	.5246 2E-03	.4151 0E-01	.8631 9E-04	-.2673 9E-03	.1410 5E-03
966	.1790 9E-01	.8159 7E-03	.4138 6E-01	-.1347 1E-04	-.3599 2E-03	.1746 2E-03
2001	.1338 2E-01	-.2160 8E-03	.3709 1E-01	-.1372 7E-03	-.3955 7E-03	.1915 6E-03
2002	.1345 1E-01	-.2629 3E-03	.3738 2E-01	.2626 5E-03	-.6804 3E-03	-.1682 5E-04
2003	.1349 1E-01	-.2409 5E-03	.3749 5E-01	.2167 2E-03	-.3154 2E-03	-.1477 4E-03
2004	.1337 8E-01	-.2919 2E-03	.3740 7E-01	-.1701 4E-04	-.3778 1E-03	.1347 6E-05
2005	.1342 7E-01	-.1953 8E-03	.3727 9E-01	-.1161 7E-03	-.8617 3E-04	-.1442 1E-03
2006	.1314 6E-01	-.1584 2E-03	.3720 9E-01	-.7163 9E-04	-.1043 7E-03	-.1305 9E-04
2007	.1337 7E-01	-.9657 8E-04	.3720 4E-01	-.9728 2E-05	.7340 3E-04	-.5334 8E-04
2008	.1337 8E-01	-.4374 9E-04	.3723 9E-01	.2528 9E-04	-.1247 4E-03	.1209 1E-04
2004	.1335 6E-01	.2284 2E-04	.3730 5E-01	.4361 6E-04	-.2649 7E-04	-.1208 0E-04
2010	.1328 2E-01	.1061 7E-03	.3735 2E-01	.4360 5E-05	-.2666 9E-03	.3509 7E-04
2011	.1325 3E-01	.1609 5E-03	.3732 7E-01	-.3572 1E-04	-.4344 1E-03	.9872 6E-04
2012	.1315 3E-01	.2840 9E-03	.3713 6E-01	-.1941 7E-03	-.3723 7E-03	.2752 0E-04
2013	.1322 4E-01	.3545 1E-03	.3702 2E-01	-.1238 2E-03	-.8637 6E-03	.1766 3E-03
2014	.1336 1E-01	.3481 9E-03	.3705 5E-01	-.5866 4E-04	-.9144 5E-03	-.6194 6E-04
2015	.1347 3E-01	.2950 8E-03	.3720 3E-01	-.8222 8E-04	-.1236 3E-02	.9171 7E-04
2016	.1344 4E-01	.1849 3E-03	.3728 3E-01	-.1057 1E-04	-.1229 7E-02	-.5955 7E-04
2017	.1344 2E-01	.6051 7E-04	.3713 4E-01	-.5879 1E-04	-.1147 8E-02	.5136 3E-04
2018	.1339 7E-01	-.2114 5E-03	.3692 4E-01	.8816 9E-05	-.6897 2E-03	.7527 6E-04
2019	.1347 5E-01	.9410 6E-04	.4028 7E-01	.2288 5E-03	-.8477 1E-02	-.6967 5E-04
2102	.1550 4E-01	-.9761 9E-04	.4042 9E-01	.1201 4E-03	-.8441 4E-02	.1049 5E-03
2103	.1548 4E-01	-.9547 3E-04	.4037 9E-01	-.4948 5E-04	-.8047 9E-02	-.1648 9E-03
2104	.1551 6E-01	-.6481 2E-04	.4005 7E-01	-.2774 5E-03	-.8665 8E-02	.1328 1E-03
2105	.1551 2E-01	-.1195 1E-03	.4005 2E-01	.1387 7E-03	-.7560 7E-02	-.1963 3E-03
2106	.1552 5E-01	-.2894 3E-04	.4005 8E-01	-.2686 9E-03	-.7783 1E-02	.9885 5E-04
2107	.1544 3E-01	-.5207 4E-04	.4005 9E-01	.3143 4E-04	-.7513 3E-02	-.8266 5E-04
2108	.1544 3E-01	-.5797 0E-04	.4019 2E-01	.2488 7E-03	-.7870 6E-02	.5128 8E-04
2109	.1549 0E-01	.3184 2E-04	.4009 6E-01	-.1108 9E-03	-.7657 2E-02	-.9307 5E-05
2110	.1540 2E-01	.1501 9E-04	.4002 6E-01	.1267 7E-03	-.8112 1E-02	-.7595 7E-05
2111	.1534 5E-01	.5131 2E-04	.4026 2E-01	.1955 4E-04	-.7967 6E-02	.1315 0E-03
2112	.1535 8E-01	.1034 7E-03	.4036 7E-01	-.6204 7E-04	-.8347 3E-02	-.1125 4E-03
2113	.1529 6E-01	.2450 6E-03	.4022 7E-01	-.1363 8E-03	-.8319 6E-02	.2011 2E-03
2114	.1540 1E-01	.6842 6E-04	.4043 1E-01	.4213 2E-03	-.8343 7E-02	-.2047 2E-03
2115	.1557 5E-01	.1375 6E-03	.4051 0E-01	-.1628 2E-03	-.8200 5E-02	.1303 1E-03
2116	.1571 7E-01	.5707 9E-04	.4032 0E-01	.4367 7E-04	-.8397 6E-02	-.1976 3E-03
2117	.1554 3E-01	-.6348 9E-06	.4050 8E-01	.2819 7E-04	-.8383 7E-02	.7447 5E-04
2118	.1552 4E-01	-.4324 9E-05	.4041 0E-01	-.3355 8E-04	-.8473 5E-02	.1391 9E-03
2201	.1716 1E-01	-.6888 2E-04	.3983 5E-01	.2164 7E-04	-.8476 5E-02	-.8448 1E-04
2202	.1717 4E-01	-.8289 3E-04	.3997 9E-01	-.1811 9E-03	-.8163 3E-02	.1040 1E-03
2203	.1711 5E-01	-.1151 2E-03	.3992 8E-01	.9967 9E-04	-.8101 5E-02	-.1341 8E-03
2204	.1711 1E-01	-.1121 7E-03	.3960 4E-01	-.1954 6E-03	-.7740 1E-02	.1458 3E-03
2205	.1709 2E-01	-.7160 0E-04	.3960 2E-01	-.3827 2E-04	-.7591 3E-02	-.1684 8E-03
2206	.1705 5E-01	-.7613 6E-04	.3960 9E-01	.1360 7E-04	-.7515 9E-02	.1190 4E-03
2207	.1705 3E-01	-.4616 7E-04	.3940 8E-01	-.5113 6E-05	-.7277 0E-02	-.8722 1E-04
2208	.1703 7E-01	-.1469 2E-04	.3964 2E-01	.1606 5E-04	-.7583 0E-02	.4672 3E-04
2209	.1704 1E-01	-.9745 4E-05	.3964 6E-01	.9844 4E-05	-.7637 9E-02	-.1138 6E-04
2210	.1703 8E-01	.3418 7E-04	.3956 9E-01	-.1101 2E-03	-.7850 7E-02	-.2968 8E-04
2211	.1703 4E-01	.7778 4E-04	.3961 1E-01	-.3716 7E-04	-.8010 4E-02	.1135 9E-03
2212	.1702 7E-01	.9315 4E-04	.3991 0E-01	.1500 1E-03	-.8110 3E-02	-.1133 9E-03
2213	.1702 9E-01	.1134 7E-03	.3977 5E-01	-.6047 2E-05	-.8333 5E-02	.1758 9E-03
2214	.1701 2E-01	.1139 1E-03	.3998 1E-01	-.1238 3E-04	-.8099 3E-02	-.2013 7E-03
2215	.1723 4E-01	.8479 4E-04	.4006 0E-01	.7868 7E-04	-.8211 9E-02	.1468 3E-03
2216	.1738 1E-01	.6498 8E-04	.3986 9E-01	.5199 1E-04	-.8114 3E-02	-.2044 9E-03
2217	.1723 8E-01	.2945 6E-04	.4005 8E-01	-.1771 9E-03	-.8318 8E-02	.6269 2E-04
2218	.1720 1E-01	-.3816 3E-04	.3995 8E-01	.1108 4E-03	-.8179 5E-02	-.1415 9E-03
2301	.1075 5E-02	-.2445 3E-03	.3438 7E-01	-.1992 0E-03	.1486 7E-02	-.9857 6E-04
2302	.9960 1E-02	-.3961 5E-03	.3416 4E-01	-.1542 3E-03	.3016 7E-02	-.1503 3E-03
2303	.9847 5E-02	-.5813 9E-03	.3405 1E-01	-.5866 6E-04	.3404 8E-02	-.8119 7E-03
2304	.9857 4E-02	-.5367 7E-03	.3406 1E-01	-.5161 9E-04	.1873 1E-02	.4559 8E-03
2305	.9811 7E-02	-.4247 5E-03	.3391 9E-01	-.9410 3E-04	.3318 3E-02	.3664 9E-03
2306	.9840 2E-02	-.3771 2E-03	.3377 4E-01	-.1290 4E-03	.3652 6E-02	-.8699 6E-03
2307	.9840 0E-02	-.2351 5E-03	.3377 1E-01	-.6988 3E-04	.2104 5E-02	.3418 3E-03
2308	.9355 1E-02	-.7435 6E-04	.3366 0E-01	-.1950 1E-04	.3581 0E-02	.1216 7E-03
2309	.9344 5E-02	.1122 7E-04	.3360 2E-01	.2187 7E-04	.3591 5E-02	-.5662 0E-03
2310	.9355 7E-02	.1805 4E-03	.3377 5E-01	.7166 3E-04	.2122 4E-02	.5649 6E-03
2311	.9415 7E-02	.3401 1E-03	.3380 4E-01	.1277 8E-03	.3635 3E-02	-.9910 9E-04
2312	.9345 4E-02	.4092 4E-03	.3392 7E-01	.8762 5E-04	.3340 7E-02	-.3393 6E-03
2313	.9355 7E-02	.5394 0E-03	.3406 3E-01	.5700 4E-04	.1931 7E-02	.8220 2E-04
2314	.9355 1E-02	.6277 7E-03	.3405 8E-01	.1651 2E-03	.3885 7E-02	-.3471 2E-03

JOB KIPS

BY Y.E.

PAGE

DATE

REV.

Deformation (Continued)

Node	U_x	U_y	U_z	Rotx	Roty	Rotz
2317	.10[illegible]E-01	-.1[illegible]E-03	.3[illegible]E-01	-.3[illegible]E-03	.6[illegible]E-02	-.3[illegible]E-03
2318	.101[illegible]E-01	-.852[illegible]E-04	.344841E-01	-.116129E-03	.271371E-02	-.710245E-03
2401	.102659E-01	-.104974E-03	.339063E-01	-.242345E-03	.130286E-02	-.122774E-03
2402	.10092[illegible]E-01	-.339341E-03	.3366[illegible]E-01	-.559364E-03	.280635E-02	-.132312E-02
2403	.110696E-01	-.586326E-03	.356090E-01	-.173772E-03	.320059E-02	.871505E-03
2404	.991157E-02	-.500581E-03	.356605E-01	-.149703E-03	.119976E-02	.434[illegible]E-03
2405	.106202E-01	-.397259E-03	.355174E-01	-.508205E-03	.310321E-02	-.145111E-02
2406	.107970E-01	-.306[illegible]E-03	.353[illegible]E-01	.854115E-04	.346107E-02	.[illegible]E-03
2407	.992172E-02	-.204047E-03	.353643E-01	-.101103E-03	.106[illegible]E-02	.151[illegible]E-03
2408	.106495E-01	-.[illegible]E-03	.352579E-01	-.299925E-03	.337[illegible]E-02	-.113[illegible]E-02
2409	.106[illegible]E-01	.239647E-04	.3525[illegible]E-01	.300441E-03	.339340E-02	-.112[illegible]E-02
2410	.989[illegible]E-02	.147974E-03	.353647E-01	.103655E-03	.110511E-02	-.120[illegible]E-03
2411	.107276E-01	.269045E-03	.354000E-01	-.848403E-04	.344589E-02	-.[illegible]E-03
2412	.105726E-01	.383490E-03	.355264E-01	.485783E-03	.312744E-02	.138[illegible]E-02
2413	.997721E-02	.506703E-03	.356569E-01	.123811E-03	.127497E-02	-.431[illegible]E-03
2414	.112849E-01	.521820E-03	.356535E-01	-.211490E-03	.361865E-02	-.127[illegible]E-02
2415	.112542E-01	.384879E-03	.357975E-01	.649048E-03	.322722E-02	.167007E-02
2416	.108236E-01	.322708E-03	.359751E-01	.119572E-03	.129700E-02	-.166[illegible]E-03
2417	.111669E-01	.143566E-03	.360086E-01	-.222522E-03	.262085E-02	-.956[illegible]E-03
2418	.111070E-01	-.474955E-04	.360228E-01	-.223257E-03	.252949E-02	.110[illegible]E-02
2501	.135584E-01	-.105733E-03	.339353E-01	-.151729E-03	.[illegible]E-03	.144[illegible]E-03
2454	.135009E-01	-.199077E-03	.337510E-01	-.236295E-03	.275928E-03	.347[illegible]E-03
2457	.134944E-01	-.100553E-03	.335859E-01	-.122349E-03	.349[illegible]E-03	.[illegible]E-03
2460	.134567E-01	.671043E-04	.335647E-01	.166210E-03	.350[illegible]E-03	-.131[illegible]E-03
2463	.134721E-01	.229906E-03	.337147E-01	.197790E-03	.288985E-03	-.310311E-03
2466	.137446E-01	.145396E-03	.340106E-01	.157204E-03	.250949E-03	-.288[illegible]E-03
2501	.135597E-01	-.539213E-04	.354381E-01	-.100818E-03	.[illegible]E-02	.94[illegible]E-04
2502	.132579E-01	-.884759E-04	.348026E-01	-.978437E-03	.348060E-02	-.405[illegible]E-04
2503	.131916E-01	-.130170E-03	.348036E-01	-.978783E-03	.342931E-02	.119[illegible]E-03
2504	.132116E-01	-.119631E-03	.353283E-01	-.137764E-03	.127681E-02	.333[illegible]E-03
2505	.131348E-01	-.529212E-04	.348104E-01	-.756113E-03	.334099E-02	.[illegible]E-05
2506	.131175E-01	-.667939E-04	.347865E-01	.704243E-03	.339422E-02	.927[illegible]E-04
2507	.131358E-01	-.582054E-04	.351640E-01	-.856793E-04	.144527E-02	.150[illegible]E-03
2508	.130884E-01	-.901439E-06	.347248E-01	-.675576E-03	.351957E-02	-.274[illegible]E-04
2509	.130826E-01	-.280272E-04	.347210E-01	.667203E-03	.352115E-02	.484[illegible]E-04
2510	.130975E-01	.315388E-04	.351467E-01	.630277E-04	.149927E-02	-.118[illegible]E-03
2511	.130562E-01	.607603E-04	.346896E-01	-.826913E-03	.361662E-02	-.835[illegible]E-04
2512	.130622E-01	.681406E-04	.347063E-01	.866088E-03	.358414E-02	.924[illegible]E-06
2513	.131819E-01	.160593E-03	.352941E-01	.139968E-03	.128922E-02	-.307[illegible]E-03
2514	.132034E-01	.139167E-03	.348411E-01	-.866257E-03	.349605E-02	-.156[illegible]E-03
2515	.132841E-01	.120948E-03	.349178E-01	.100654E-02	.341588E-02	-.381[illegible]E-04
2516	.135018E-01	.928770E-04	.355702E-01	.899862E-04	.117498E-02	-.288[illegible]E-03
2517	.133[illegible]E-01	-.523811E-04	.349105E-01	-.113675E-02	.326001E-02	-.754[illegible]E-04
2518	.132442E-01	-.447996E-04	.348562E-01	.103862E-02	.355410E-02	-.867[illegible]E-04
2601	.[illegible]315E-01	-.486[illegible]E-04	.356[illegible]E-01	-.544307E-04	.282825E-02	-.171[illegible]E-04
2602	.[illegible]460E-01	-.634343E-04	.356244E-01	-.633654E-03	.422207E-02	-.426[illegible]E-03
2603	.142085E-01	-.131324E-03	.356160E-01	.641374E-03	.417703E-02	.410[illegible]E-03
2604	.142137E-01	-.868087E-04	.356314E-01	-.831597E-04	.267057E-02	.304[illegible]E-04
2605	.141694E-01	-.626518E-04	.355913E-01	-.452469E-03	.394348E-02	-.407[illegible]E-03
2606	.141554E-01	-.706242E-04	.355785E-01	.421175E-03	.401657E-02	.388[illegible]E-03
2607	.141403E-01	-.410465E-04	.355091E-01	-.526880E-04	.274752E-02	.305[illegible]E-04
2608	.141247E-01	-.105695E-04	.355438E-01	-.381928E-03	.411955E-02	-.412[illegible]E-03
2609	.141199E-01	-.167316E-04	.355377E-01	.376055E-03	.404608E-02	.431[illegible]E-03
2610	.141006E-01	.194557E-04	.354951E-01	.436330E-04	.280076E-02	-.133[illegible]E-04
2611	.140941E-01	.683719E-04	.355312E-01	-.511672E-03	.423875E-02	-.403[illegible]E-03
2612	.140976E-01	.747293E-04	.355493E-01	.540222E-03	.430191E-02	.435[illegible]E-03
2613	.141790E-01	.124090E-03	.356010E-01	.845494E-04	.275001E-02	-.758[illegible]E-04
2614	.142412E-01	.147674E-03	.356044E-01	-.534809E-03	.420938E-02	-.435[illegible]E-03
2615	.143221E-01	.108561E-03	.357287E-01	.654423E-03	.414406E-02	.351[illegible]E-03
2616	.144861E-01	.596028E-04	.358391E-01	.465291E-04	.257323E-02	-.588[illegible]E-03
2617	.143768E-01	-.698941E-05	.356947E-01	-.787678E-03	.410355E-02	-.305[illegible]E-03
2618	.142747E-01	-.620312E-04	.356514E-01	.686906E-03	.410443E-02	.412[illegible]E-03
2701	.[illegible]544E-01	-.544894E-04	.341624E-01	-.163212E-04	.871657E-04	.449[illegible]E-04
2702	.[illegible]345E-01	-.624583E-04	.347950E-01	.311208E-03	.145665E-02	-.248[illegible]E-03
2703	.[illegible]269E-01	-.106245E-03	.348217E-01	-.224313E-03	.158331E-02	.209[illegible]E-03
2704	.[illegible]794E-01	-.853959E-04	.342115E-01	-.625436E-04	.354152E-03	.850[illegible]E-04
2705	.[illegible]884E-01	-.583770E-04	.347667E-01	.349291E-03	.156224E-02	-.284[illegible]E-03
2706	.[illegible]908E-01	-.687153E-04	.347906E-01	-.293347E-03	.[illegible]E-02	.281[illegible]E-03
2707	.[illegible]75E-01	-.386063E-04	.341697E-01	-.362827E-04	.527547E-03	.[illegible]E-04
2708	.[illegible]59E-01	.724326E-05	.347856E-01	.372794E-03	.169536E-02	-.306[illegible]E-03
2709	.[illegible]27E-01	.162192E-04	.347731E-01	-.377867E-03	.168381E-02	.325[illegible]E-03
2710	.[illegible]40E-01	.221758E-04	.341586E-01	.347887E-04	.512861E-03	-.360[illegible]E-04
2711	.[illegible]18E-01	.653144E-04	.347836E-01	.288255E-03	.169604E-02	-.251[illegible]E-03
2712	.[illegible]33E-01	.720223E-04	.347859E-01	-.343061E-03	.162437E-02	.272[illegible]E-03
2713	.[illegible]47E-01	.109434E-03	.341941E-01	.612165E-04	.374622E-03	-.107[illegible]E-03
2714	.[illegible]32E-01	.132142E-03	.348665E-01	.283493E-03	.155862E-02	-.269[illegible]E-03
2715	.[illegible]47E-01	.886410E-04	.349276E-01	-.236083E-03	.156606E-02	.187[illegible]E-03
2716	.167907E-01	.554197E-04	.343695E-01	.454443E-04	.230031E-03	-.353[illegible]E-04
2717	.172054E-01	.103349E-05	.348508E-01	.913203E-04	.145946E-02	-.658[illegible]E-04
2718	.171101E-01	-.483941E-04	.347665E-01	-.226697E-03	.133815E-02	.211[illegible]E-03
2751	.182079E-01	-.218865E-04	.253767E-01	.783127E-05	.783898E-03	.142[illegible]E-04
2752	.184264E-01	-.740930E-05	.255746E-01	.913554E-04	.827995E-02	-.671[illegible]E-04
2753	.184662E-01	-.570644E-04	.256130E-01	-.351346E-04	.829830E-02	.753[illegible]E-04
2754	.182113E-01	-.351977E-04	.253754E-01	.543003E-05	.795138E-02	-.158[illegible]E-04
2755	.184500E-01	-.933351E-05	.255963E-01	.987573E-04	.829147E-02	-.755[illegible]E-04
2756	.184714E-01	-.444250E-04	.256125E-01	-.876335E-04	.831074E-02	.947[illegible]E-04

JOB KIPS

BY YE

PAGE

DATE

REV.

Deformation (Cont.)

Node	U_x	U_y	U_z	Rotx	Roty	Rotz
2700	.1884327E-01	-.2.8121E-04	.2557885E-01	-.991217E-04	.837890E-02	.980219E-04
2701	.1881044E-01	.112713E-04	.2553351E-01	-.704177E-05	.799567E-02	.269455E-05
2702	.1884327E-01	.452699E-04	.2558887E-01	.846517E-04	.832684E-02	-.946567E-04
2703	.1884327E-01	.1274.4E-04	.2553477E-01	-.102056E-03	.831644E-02	.744203E-04
2704	.1881704E-01	.1957.5E-04	.2553477E-01	-.999137E-05	.796318E-02	-.207794E-04
2705	.1881704E-01	.6784.0E-14	.2562.1E-01	.900695E-04	.832836E-02	-.115480E-03
2706	.1881704E-01	.1619.4E-04	.2565.4E-01	-.805698E-04	.835360E-02	.624367E-04
2707	.1882760E-01	.2040.0E-04	.2562.1E-01	-.142022E-04	.799102E-02	.140814E-04
2708	.1884784E-01	.1705.4E-04	.2561.6E-01	-.625382E-04	.827192E-02	-.445770E-04
2709	.1883926E-01	-.3493.4E-04	.2558.0E-01	-.661923E-04	.823158E-02	.834404E-04
2710	0.	0.	0.	.124776E-04	.154155E-01	.814751E-05
2711	0.	0.	0.	.505972E-04	.154150E-01	-.389729E-04
2712	0.	0.	0.	-.225757E-04	.154979E-01	.515602E-04
2713	0.	0.	0.	.781177E-05	.153713E-01	.134172E-04
2714	0.	0.	0.	.472748E-04	.154808E-01	-.354805E-04
2715	0.	0.	0.	-.249873E-04	.154919E-01	.491278E-04
2716	0.	0.	0.	.686848E-05	.153194E-01	.621039E-05
2717	0.	0.	0.	.406933E-04	.154782E-01	-.397930E-04
2718	0.	0.	0.	-.351340E-04	.154660E-01	.466387E-04
2719	0.	0.	0.	-.191671E-05	.153150E-01	-.267064E-05
2720	0.	0.	0.	.285006E-04	.154562E-01	-.503016E-04
2721	0.	0.	0.	-.493293E-04	.154667E-01	.352136E-04
2722	0.	0.	0.	-.142666E-04	.153370E-01	-.144623E-04
2723	0.	0.	0.	.246214E-04	.154945E-01	-.803248E-04
2724	0.	0.	0.	-.428279E-04	.155182E-01	.354226E-04
2725	0.	0.	0.	-.231655E-05	.154046E-01	.301669E-05
2726	0.	0.	0.	.354907E-04	.154079E-01	-.305310E-04
2727	0.	0.	0.	-.288313E-04	.155018E-01	.566442E-04
2728	.8678.5E-02	-.3285.3E-03	.333460E-01	-.166007E-03	.222659E-02	.199561E-04
2729	.8648.4E-02	-.4869.2E-03	.331760E-01	-.178753E-03	.256799E-02	.700957E-05
2730	.8626.7E-02	-.5672.7E-03	.330924E-01	.846108E-05	.272897E-02	.399796E-05
2731	.8606.1E-02	-.5655.1E-03	.330713E-01	-.670854E-04	.269391E-02	-.111.1E-04
2732	.7907.7E-02	-.4580.3E-03	.329457E-01	-.224282E-03	.265955E-02	-.314782E-04
2733	.7825.4E-02	-.348.16E-03	.328434E-01	.110464E-04	.261621E-02	-.294491E-04
2734	.7782.4E-02	-.2633.4E-03	.328104E-01	-.689013E-04	.259857E-02	-.201399E-04
2735	.7744.7E-02	-.1164.7E-03	.327177E-01	-.147716E-03	.249208E-02	-.905163E-05
2736	.7711.5E-02	.5390.6E-04	.327191E-01	.150222E-03	.231799E-02	.115590E-04
2737	.7741.9E-02	.2109.6E-03	.328145E-01	.718530E-04	.294767E-02	.222525E-04
2738	.7769.6E-02	.3514.2E-03	.328526E-01	-.150432E-05	.280926E-02	.293206E-04
2739	.7842.3E-02	.4710.3E-03	.329550E-01	.220471E-03	.267730E-02	.320401E-04
2740	.7999.4E-02	.5710.3E-03	.330817E-01	.815976E-04	.273057E-02	.110160E-04
2741	.8211.7E-02	.6056.7E-03	.331160E-01	.178521E-04	.288165E-02	-.390520E-05
2742	.8436.9E-02	.5384.5E-03	.332141E-01	.198484E-03	.271056E-02	-.215134E-05
2743	.8655.9E-02	.4004.7E-03	.333803E-01	.117944E-03	.293647E-02	-.124361E-04
2744	.8824.9E-02	.1776.6E-03	.334365E-01	.239607E-04	.213086E-02	-.844127E-05
2745	.8915.7E-02	-.4500.3E-04	.334490E-01	-.494354E-04	.260274E-02	.176432E-04
2746	.8977.4E-02	-.3248.1E-03	.331252E-01	-.186240E-03	.219730E-02	.110426E-03
2747	.8974.1E-02	-.4864.5E-03	.329171E-01	-.202520E-03	.267498E-02	-.136707E-03
2748	.8957.3E-02	-.5677.2E-03	.328176E-01	.970799E-05	.278392E-02	.126029E-03
2749	.8936.4E-02	-.5686.0E-03	.328039E-01	-.572641E-04	.270242E-02	.548041E-04
2750	.8920.4E-02	-.5018.7E-03	.326806E-01	-.230477E-03	.283888E-02	-.253775E-03
2751	.8912.5E-02	-.3957.1E-03	.326621E-01	-.241404E-05	.282033E-02	-.187680E-04
2752	.8905.0E-02	-.2670.4E-03	.325099E-01	-.712841E-04	.307161E-02	-.180748E-04
2753	.8923.6E-02	-.1154.5E-03	.324286E-01	-.143991E-03	.290895E-02	-.133308E-03
2754	.8911.2E-02	.5360.9E-04	.324282E-01	.147175E-03	.294778E-02	.137099E-03
2755	.8940.1E-02	.2137.4E-03	.325191E-01	.743521E-04	.306671E-02	.246472E-04
2756	.8964.9E-02	.3582.3E-03	.325721E-01	.105.8E-04	.281015E-02	-.158328E-04
2757	.9142.1E-02	.4644.9E-03	.326847E-01	.222305E-03	.285335E-02	.238132E-03
2758	.9299.1E-02	.5714.5E-03	.328075E-01	.648985E-04	.276622E-02	-.778364E-04
2759	.9514.5E-02	.5954.1E-03	.328274E-01	.122271E-04	.292970E-02	-.198801E-03
2760	.9736.7E-02	.5938.9E-03	.329447E-01	.225553E-03	.278848E-02	.205954E-03
2761	.9952.6E-02	.3974.1E-03	.331477E-01	.145962E-03	.232667E-02	-.135044E-03
2762	.9131.7E-02	.1744.1E-03	.332435E-01	.351146E-04	.213117E-02	-.190674E-03
2763	.9137.6E-02	-.9215.7E-04	.332410E-01	-.505810E-04	.208455E-02	.220664E-03
2764	.9272.2E-02	-.3537.7E-03	.329177E-01	.806235E-05	.241012E-02	.134409E-04
2765	.9071.2E-02	-.5677.5E-03	.325396E-01	.413176E-04	.248861E-02	.861505E-05
2766	.8853.4E-02	-.5678.1E-03	.325720E-01	.429361E-05	.251409E-02	-.123767E-06
2767	.8633.4E-02	-.5449.8E-03	.327410E-01	-.703606E-04	.258787E-02	-.125445E-04
2768	.8502.1E-02	-.4574.2E-03	.326977E-01	-.555509E-04	.271824E-02	-.236258E-04
2769	.8406.3E-02	-.3417.2E-03	.326905E-01	.690220E-05	.275905E-02	-.251361E-04
2770	.8346.6E-02	-.2242.4E-03	.326984E-01	-.254481E-04	.275230E-02	-.181747E-04
2771	.8312.6E-02	.1002.6E-03	.326690E-01	-.360453E-04	.285403E-02	-.608153E-05
2772	.8293.2E-02	.3341.0E-04	.326710E-01	.442399E-04	.285910E-02	.836963E-05
2773	.8308.9E-02	.1674.8E-03	.327063E-01	.422809E-04	.276911E-02	.199804E-04
2774	.8350.3E-02	.3332.1E-03	.327111E-01	.240.56E-04	.278930E-02	.261284E-04
2775	.8433.7E-02	.4413.7E-03	.327399E-01	.105629E-03	.276.52E-02	.238559E-04
2776	.8588.2E-02	.5540.7E-03	.328154E-01	.136785E-03	.264137E-02	.125946E-04
2777	.8795.1E-02	.5999.4E-03	.328688E-01	.485308E-04	.255239E-02	.155291E-05
2778	.9028.5E-02	.5574.3E-03	.328631E-01	-.530533E-04	.248343E-02	-.432738E-05
2779	.9247.5E-02	.4153.5E-03	.329133E-01	-.942225E-04	.241902E-02	-.687325E-05
2780	.9385.2E-02	.1752.2E-03	.329760E-01	-.834513E-04	.237025E-02	-.144718E-05
2918	.5393.5E-02	-.1094.9E-03	.327249E-01	-.439343E-04	.236437E-02	.986590E-05
3001	.6075.2E-02	-.6550.1E-03	.294946E-01	-.154111E-03	.142952E-02	.823337E-04
3002	.5901.1E-02	-.7755.7E-03	.293229E-01	-.132490E-03	.141120E-02	.215.28E-04
3003	.5743.6E-02	-.7869.1E-03	.292537E-01	-.104539E-03	.140555E-02	.215.28E-04
3004	.5811.7E-02	-.7869.1E-03	.291778E-01	-.197439E-04	.140555E-02	.274410E-04

JOB KIPS

BY Y.E.

PAGE

DATE

REV.

Deformation (Cont.)

Node	U_x	U_y	U_z	Rotx	Roty	Rotz
3007	.530294E-02	-.375466E-03	.288643E-01	-.826305E-04	.170217E-02	.560732E-03
3008	.518842E-02	-.153042E-03	.288170E-01	-.281161E-04	.175098E-02	.330428E-04
3009	.517814E-02	.982831E-04	.288197E-01	-.329476E-04	.174929E-02	-.322952E-04
3010	.527698E-02	.327578E-03	.288711E-01	.869968E-04	.169581E-02	-.108289E-04
3011	.542826E-02	.514525E-03	.289696E-01	.111905E-03	.162340E-02	-.245434E-05
3012	.563827E-02	.642653E-03	.290847E-01	.107116E-03	.156956E-02	.726725E-05
3013	.574726E-02	.701350E-03	.291814E-01	.100694E-03	.154931E-02	.281876E-03
3014	.585969E-02	.763688E-03	.292700AE-01	.120904E-03	.164860E-02	.404574E-03
3015	.584754E-02	.833614E-03	.293407E-01	.127484E-03	.174117E-02	-.247228E-03
3016	.666571E-02	.719629E-03	.295102E-01	.144994E-03	.137678E-02	-.813976E-03
3017	.742176E-02	.310377E-03	.296561E-01	.647507E-04	.879886E-03	-.419333E-03
3018	.743471E-02	-.241042E-03	.296496E-01	-.858331E-04	.901311E-03	.421796E-03
3101	.597156E-02	-.771173E-03	.285048E-01	-.191452E-03	.140544E-02	.135042E-02
3102	.483234E-02	-.864335E-03	.283502E-01	-.122466E-03	.229341E-02	.347464E-03
3103	.475497E-02	-.782237E-03	.282637E-01	-.620057E-04	.213569E-02	-.606253E-03
3104	.493369E-02	-.740246E-03	.281848E-01	-.101635E-03	.191377E-02	.326145E-03
3105	.479281E-02	-.717710E-03	.280846E-01	-.130512E-03	.192918E-02	.451917E-04
3106	.451618E-02	-.604440E-03	.277711E-01	-.115728E-03	.203861E-02	.381525E-04
3107	.431702E-02	-.413985E-03	.278754E-01	-.771184E-04	.212230E-02	.141321E-04
3108	.419698E-02	-.162650E-03	.278243E-01	-.271028E-04	.214915E-02	.310365E-04
3109	.418121E-02	.110269E-03	.278306E-01	.325698E-04	.213798E-02	-.306083E-04
3110	.429364E-02	.366321E-03	.278824E-01	.834603E-04	.211640E-02	-.220361E-04
3111	.448141E-02	.569353E-03	.279803E-01	.119710E-03	.202926E-02	-.351301E-04
3112	.473378E-02	.691527E-03	.280938E-01	.132684E-03	.192484E-02	-.175050E-04
3113	.485113E-02	.747376E-03	.281945E-01	.104778E-03	.190899E-02	.341218E-03
3114	.468489E-02	.814107E-03	.282771E-01	.655944E-04	.211770E-02	.585011E-03
3115	.480091E-02	.919097E-03	.283667E-01	.120968E-03	.225733E-02	-.367812E-03
3116	.596054E-02	.833511E-03	.285231E-01	.191476E-03	.139029E-02	-.134416E-02
3117	.717843E-02	.364841E-03	.286562E-01	.840779E-04	.320079E-03	-.699365E-03
3118	.718315E-02	-.259926E-03	.286503E-01	-.968051E-04	.376172E-03	.713127E-03
3151	.677703E-02	-.592638E-03	.285580E-01	-.133084E-03	.704549E-03	.535919E-03
3152	.613624E-02	-.776340E-03	.284677E-01	-.195894E-03	.168426E-03	-.169143E-03
3153	.592536E-02	-.804816E-03	.283532E-01	-.704729E-04	.401421E-03	-.271215E-03
3154	.590408E-02	-.775324E-03	.282230E-01	-.120516E-03	.795857E-03	-.188435E-03
3155	.573521E-02	-.712393E-03	.280996E-01	-.149488E-03	.607463E-03	.664028E-05
3156	.544626E-02	-.592273E-03	.279774E-01	-.115955E-03	.914270E-03	.461758E-05
3157	.531810E-02	-.401432E-03	.278780E-01	-.747111E-04	.948544E-03	.366721E-05
3158	.520101E-02	-.157955E-03	.278281E-01	-.295443E-04	.948144E-03	.227403E-04
3159	.519155E-02	.105112E-03	.278304E-01	.343299E-04	.945868E-03	-.224103E-04
3160	.529334E-02	.356862E-03	.278834E-01	.802177E-04	.945673E-03	-.787357E-05
3161	.545873E-02	.557403E-03	.279900E-01	.119785E-03	.911441E-03	-.149461E-05
3162	.567888E-02	.694277E-03	.281124E-01	.149959E-03	.891805E-03	.114261E-04
3163	.582944E-02	.785127E-03	.282388E-01	.120254E-03	.761735E-03	.205944E-03
3164	.585424E-02	.841047E-03	.283730E-01	.727366E-04	.371374E-03	.264314E-03
3165	.608926E-02	.829416E-03	.284879E-01	.105105E-03	.165230E-03	-.177423E-03
3166	.674966E-02	.656287E-03	.285737E-01	.125282E-03	.708134E-03	-.529307E-03
3167	.736604E-02	.274589E-03	.286230E-01	.482493E-04	.135753E-02	-.265194E-03
3168	.737693E-02	-.206960E-03	.286164E-01	-.562494E-04	.135945E-02	.264771E-04
3301	.503247E-02	-.957976E-03	.256092E-01	-.174340E-04	.245362E-03	.149435E-02
3302	.373968E-02	-.107527E-02	.253468E-01	-.400003E-04	.403935E-03	.201381E-03
3303	.383923E-02	-.990444E-03	.252226E-01	-.106617E-03	.408719E-03	-.684401E-03
3304	.399594E-02	-.971174E-03	.250841E-01	-.138499E-03	.209225E-03	-.431709E-03
3305	.378960E-02	-.935971E-03	.249583E-01	-.134173E-03	.132191E-03	-.436432E-05
3306	.341606E-02	-.801353E-03	.248469E-01	-.110839E-03	.116198E-03	.953221E-04
3307	.304911E-02	-.546413E-03	.247503E-01	-.743520E-04	.804926E-04	.596535E-04
3308	.293565E-02	-.206547E-03	.247120E-01	-.251091E-04	.302453E-04	.115792E-04
3309	.292945E-02	.163705E-03	.247144E-01	.304358E-04	.516653E-04	-.156671E-04
3310	.308304E-02	.507944E-03	.247657E-01	.791685E-04	.817234E-04	-.825431E-04
3311	.338571E-02	.770789E-03	.248566E-01	.115011E-03	.115012E-03	-.838225E-04
3312	.373180E-02	.921629E-03	.249704E-01	.137339E-03	.132665E-03	.687410E-04
3313	.391768E-02	.980754E-03	.250989E-01	.139859E-03	.212167E-03	.333292E-03
3314	.377710E-02	.103386E-02	.252376E-01	.105460E-03	.406817E-03	.694487E-03
3315	.371569E-02	.112455E-02	.253615E-01	.361504E-04	.394827E-03	-.226313E-03
3316	.503230E-02	.101040E-02	.254183E-01	-.238412E-04	.254072E-03	-.133701E-02
3317	.650031E-02	.435007E-03	.254378E-01	-.237104E-04	.999105E-03	-.775449E-03
3318	.649744E-02	-.342874E-03	.254245E-01	-.162313E-04	.995956E-03	.797983E-03
3351	.560541E-02	-.676963E-03	.254464E-01	-.597333E-04	.948836E-03	.366487E-03
3352	.506016E-02	-.926549E-03	.253641E-01	-.905934E-04	.101375E-02	.145634E-03
3353	.472088E-02	-.101816E-02	.252718E-01	-.119128F-03	.103463E-02	-.112372E-03
3354	.451273E-02	-.102201E-02	.251495E-01	-.142342E-03	.103202E-02	-.173110E-03
3355	.429409E-02	-.955785E-03	.249834E-01	-.141515E-03	.109281E-02	-.833323E-04
3356	.400346E-02	-.798175E-03	.248564E-01	-.114024E-03	.114048E-02	.259015E-04
3357	.372615E-02	-.538696E-03	.247620E-01	-.727132E-04	.117990E-02	.366250E-04
3358	.357940E-02	-.203236E-03	.247121E-01	-.239266E-04	.120132E-02	.449821E-05
3359	.357254E-02	.160247E-03	.247146E-01	.267507E-04	.121108E-02	-.664701E-05
3360	.370371E-02	.500441E-03	.247693E-01	.773807E-04	.117944E-02	-.341288E-04
3361	.396593E-02	.769867E-03	.248679E-01	.117902E-03	.114109E-02	-.152288E-04
3362	.423622E-02	.943948E-03	.249991E-01	.143870E-03	.109569E-02	.977791E-04
3363	.444488E-02	.103241E-02	.251474E-01	.142921E-03	.105602E-02	.174708E-03
3364	.466713E-02	.105352E-02	.252699E-01	.117971E-03	.104618E-02	.100019E-03
3365	.503097E-02	.973404E-03	.253995E-01	.872024E-04	.101111E-02	-.153424E-03
3366	.559583E-02	.730470E-03	.254570E-01	.542520E-04	.944856E-03	-.362975E-03
3367	.607682E-02	.492188E-03	.254732E-01	.163067E-04	.888072E-03	-.192482E-03
3368	.607667E-02	-.237019E-03	.254695E-01	-.225967E-04	.882361E-03	.210663E-03
3501	.455424E-02	-.758952E-03	.231418E-01	-.843256E-05	-.134467E-03	.641109E-04
3502	.417906E-02	-.108140E-02	.231254E-01	-.419534E-04	-.187040E-04	.526450E-04

JOB KIPS

BY Y.E

PAGE

DATE

REV.

Deformation (Cont)

Node	U_x	U_y	U_θ	Rotx	Roty	Rotz
	.3[illegible]E-02	-.1[illegible]E-02	.2271[illegible]E-01	-.1449[illegible]E-03	.[illegible]E-03	-.6[illegible]E-04
	.2760[illegible]E-02	-.9982[illegible]E-03	.2259[illegible]E-01	-.1123[illegible]E-03	.5014[illegible]E-03	.5058[illegible]E-04
	.2421[illegible]E-02	-.6719[illegible]E-03	.2251[illegible]E-01	-.7041[illegible]E-04	.4904[illegible]E-03	.5975[illegible]E-04
	.2222[illegible]E-02	-.2473[illegible]E-03	.2246[illegible]E-01	-.2258[illegible]E-04	.4835[illegible]E-03	.2027[illegible]E-04
	.2211[illegible]E-02	.2134[illegible]E-03	.2247[illegible]E-01	.2765[illegible]E-04	.4844[illegible]E-03	-.2281[illegible]E-04
	.2[illegible]E-02	.6[illegible]E-03	.2251[illegible]E-01	.7551[illegible]E-04	.4919[illegible]E-03	-.5721[illegible]E-04
	.2[illegible]E-02	.9757[illegible]E-03	.2260[illegible]E-01	.1171[illegible]E-03	.4989[illegible]E-03	-.4005[illegible]E-04
	.3[illegible]E-02	.1[illegible]E-02	.2273[illegible]E-01	.1481[illegible]E-03	.4572[illegible]E-03	.7439[illegible]E-04
	.3[illegible]E-02	.1272[illegible]E-02	.2288[illegible]E-01	.1561[illegible]E-03	.3075[illegible]E-03	.1899[illegible]E-03
	.3[illegible]E-02	.1[illegible]E-02	.2303[illegible]E-01	.1104[illegible]E-03	.1201[illegible]E-03	.7983[illegible]E-04
	.3[illegible]E-02	.1121[illegible]E-02	.2313[illegible]E-01	.3702[illegible]E-04	-.2024[illegible]E-04	-.6201[illegible]E-04
	.4[illegible]E-02	.5034[illegible]E-03	.2314[illegible]E-01	-.1419[illegible]E-04	-.1269[illegible]E-03	-.6040[illegible]E-04
	.4[illegible]E-02	.3093[illegible]E-03	.2311[illegible]E-01	-.1843[illegible]E-04	-.2013[illegible]E-03	-.3341[illegible]E-04
	.4[illegible]E-02	.[illegible]E-03	.2311[illegible]E-01	-.1267[illegible]E-04	-.2047[illegible]E-03	.4957[illegible]E-04
	.3[illegible]E-02	-.2441[illegible]E-03	.2311[illegible]E-01	-.1665[illegible]E-04	-.5817[illegible]E-03	.1489[illegible]E-04
	.3[illegible]E-02	-.7[illegible]E-03	.2311[illegible]E-01	-.7174[illegible]E-04	-.5567[illegible]E-03	.8552[illegible]E-04
	.3[illegible]E-02	-.1057[illegible]E-02	.2313[illegible]E-01	-.1426[illegible]E-03	-.4683[illegible]E-03	-.5221[illegible]E-04
	.3[illegible]E-02	-.1247[illegible]E-02	.2306[illegible]E-01	-.1426[illegible]E-03	-.4683[illegible]E-03	-.1184[illegible]E-03
	.3[illegible]E-02	-.1[illegible]E-02	.2298[illegible]E-01	-.1753[illegible]E-03	-.4468[illegible]E-03	-.4384[illegible]E-04
	.3[illegible]E-02	-.1213[illegible]E-02	.2279[illegible]E-01	-.1462[illegible]E-03	-.4823[illegible]E-03	-.2863[illegible]E-04
	.2[illegible]E-02	-.1[illegible]E-02	.2257[illegible]E-01	-.1063[illegible]E-03	-.4220[illegible]E-03	.3808[illegible]E-04
	.2[illegible]E-02	.6[illegible]E-03	.2244[illegible]E-01	-.6561[illegible]E-04	-.3735[illegible]E-03	.1338[illegible]E-04
	.2[illegible]E-02	-.2455[illegible]E-03	.2243[illegible]E-01	-.2183[illegible]E-04	-.3396[illegible]E-03	-.1439[illegible]E-04
	.2[illegible]E-02	.2120[illegible]E-03	.2243[illegible]E-01	.2618[illegible]E-04	-.3415[illegible]E-03	-.3552[illegible]E-04
	.2[illegible]E-02	.[illegible]E-03	.2[illegible]E-01	.7623[illegible]E-04	-.4[illegible]E-03	-.2065[illegible]E-04
	.2[illegible]E-02	.3[illegible]E-03	.2256[illegible]E-01	.1114[illegible]E-03	-.4345[illegible]E-03	.5352[illegible]E-04
	.2[illegible]E-02	.1[illegible]E-02	.2272[illegible]E-01	.1523[illegible]E-03	-.4847[illegible]E-03	.1219[illegible]E-03
	.2[illegible]E-02	.1[illegible]E-02	.2288[illegible]E-01	.1795[illegible]E-03	-.5047[illegible]E-03	.4741[illegible]E-04
	.3[illegible]E-02	.1[illegible]E-02	.2303[illegible]E-01	.1397[illegible]E-03	-.4981[illegible]E-03	.1338[illegible]E-04
	.3[illegible]E-02	.1095[illegible]E-02	.2314[illegible]E-01	.6599[illegible]E-04	-.5489[illegible]E-03	-.8997[illegible]E-04
	.4[illegible]E-02	.7596[illegible]E-03	.2317[illegible]E-01	.7366[illegible]E-05	-.5929[illegible]E-03	-.1459[illegible]E-03
	.4[illegible]E-02	.2[illegible]E-03	.2317[illegible]E-01	-.1028[illegible]E-04	-.6230[illegible]E-03	-.7482[illegible]E-04
	.4[illegible]E-02	-.2396[illegible]E-03	.2316[illegible]E-01	.6510[illegible]E-05	-.6186[illegible]E-03	.8565[illegible]E-04
	.4[illegible]E-02	-.1[illegible]E-03	.2[illegible]E-01	.1[illegible]E-04	-.5671[illegible]E-03	.1467[illegible]E-03
	.4[illegible]E-02	.1090[illegible]E-02	.2269[illegible]E-01	-.6[illegible]E-05	-.5[illegible]E-03	.9040[illegible]E-04
	.3[illegible]E-02	.1[illegible]E-02	.2258[illegible]E-01	-.1372[illegible]E-03	-.4663[illegible]E-03	-.5828[illegible]E-04
	.3[illegible]E-02	-.1330[illegible]E-02	.2243[illegible]E-01	-.1566[illegible]E-03	-.3575[illegible]E-03	-.1404[illegible]E-03
	.3[illegible]E-02	-.1[illegible]E-02	.2[illegible]E-01	-.1507[illegible]E-03	-.2[illegible]E-03	-.4833[illegible]E-04
	.2[illegible]E-02	-.1[illegible]E-02	.2221[illegible]E-01	-.1170[illegible]E-03	-.2050[illegible]E-03	.3640[illegible]E-04
	.2[illegible]E-02	-.[illegible]E-03	.2206[illegible]E-01	-.7[illegible]E-04	-.1[illegible]E-03	.4553[illegible]E-04
	.2[illegible]E-02	-.2943[illegible]E-03	.2202[illegible]E-01	-.2647[illegible]E-04	-.1907[illegible]E-03	.1601[illegible]E-04
	.2[illegible]E-02	.2223[illegible]E-03	.2202[illegible]E-01	.2742[illegible]E-04	-.1905[illegible]E-03	-.1728[illegible]E-04
	.2[illegible]E-02	.6[illegible]E-03	.2220[illegible]E-01	.7599[illegible]E-04	-.1931[illegible]E-03	-.4301[illegible]E-04
	.2[illegible]E-02	.1019[illegible]E-02	.2216[illegible]E-01	.1216[illegible]E-03	-.2085[illegible]E-03	-.2794[illegible]E-04
	.3[illegible]E-02	.1[illegible]E-02	.2229[illegible]E-01	.1538[illegible]E-03	-.2648[illegible]E-03	.5836[illegible]E-04
	.3[illegible]E-02	.1[illegible]E-02	.2244[illegible]E-01	.1566[illegible]E-03	-.3698[illegible]E-03	.1430[illegible]E-03
	.3[illegible]E-02	.1309[illegible]E-02	.2260[illegible]E-01	.1343[illegible]E-03	-.4731[illegible]E-03	.5184[illegible]E-04
	.3[illegible]E-02	.1[illegible]E-02	.2270[illegible]E-01	.6071[illegible]E-04	-.5096[illegible]E-03	-.9652[illegible]E-04
	.2[illegible]E-02	.7[illegible]E-03	.2272[illegible]E-01	-.1688[illegible]E-04	-.5[illegible]E-03	-.1420[illegible]E-03
	.2[illegible]E-02	.2919[illegible]E-03	.2270[illegible]E-01	-.1934[illegible]E-04	-.6090[illegible]E-03	-.7342[illegible]E-04
	.2[illegible]E-02	-.2[illegible]E-03	.2270[illegible]E-01	-.1420[illegible]E-04	-.6[illegible]E-03	.8678[illegible]E-04
	.2[illegible]E-02	-.7598[illegible]E-03	.2270[illegible]E-01	.7270[illegible]E-05	-.6[illegible]E-03	-.4169[illegible]E-05
	.2[illegible]E-02	-.1[illegible]E-02	.2[illegible]E-01	-.6458[illegible]E-04	-.6[illegible]E-03	.1087[illegible]E-05
	.2[illegible]E-02	-.1458[illegible]E-02	.2[illegible]E-01	-.1350[illegible]E-03	-.6587[illegible]E-03	.5831[illegible]E-05
	.2[illegible]E-02	-.1[illegible]E-02	.2[illegible]E-01	-.1721[illegible]E-03	-.5797[illegible]E-03	.4182[illegible]E-05
	.3[illegible]E-02	-.1465[illegible]E-02	.2[illegible]E-01	-.1567[illegible]E-03	-.4933[illegible]E-03	-.6327[illegible]E-06
	.3[illegible]E-02	-.1[illegible]E-02	.2[illegible]E-01	-.1129[illegible]E-03	-.4398[illegible]E-03	-.2734[illegible]E-05
	.2[illegible]E-02	-.7878[illegible]E-03	.2[illegible]E-01	-.6545[illegible]E-04	-.4178[illegible]E-03	-.1828[illegible]E-05
	.2[illegible]E-02	-.2825[illegible]E-03	.2[illegible]E-01	-.2017[illegible]E-04	-.4114[illegible]E-03	.4646[illegible]E-06
	.2[illegible]E-02	.2577[illegible]E-03	.2[illegible]E-01	.2461[illegible]E-04	-.4114[illegible]E-03	.3043[illegible]E-05
	.2[illegible]E-02	.7[illegible]E-03	.2[illegible]E-01	.7043[illegible]E-04	-.4187[illegible]E-03	.5103[illegible]E-05
	.3[illegible]E-02	.1[illegible]E-02	.2[illegible]E-01	.1180[illegible]E-03	-.4432[illegible]E-03	.5694[illegible]E-05
	.3[illegible]E-02	.1462[illegible]E-02	.2034[illegible]E-01	.1603[illegible]E-03	-.4997[illegible]E-03	.3219[illegible]E-05
	.4[illegible]E-02	.1565[illegible]E-02	.2050[illegible]E-01	.1721[illegible]E-03	-.5873[illegible]E-03	-.1648[illegible]E-05
	.4[illegible]E-02	.1478[illegible]E-02	.2065[illegible]E-01	.1320[illegible]E-03	-.6641[illegible]E-03	-.3087[illegible]E-05
	.5[illegible]E-02	.1[illegible]E-02	.2074[illegible]E-01	.5898[illegible]E-04	-.6[illegible]E-03	.1917[illegible]E-05
	.5[illegible]E-02	.7963[illegible]E-03	.2077[illegible]E-01	.2259[illegible]E-05	-.6246[illegible]E-03	.7314[illegible]E-05
	.5[illegible]E-02	.2[illegible]E-03	.2076[illegible]E-01	-.8511[illegible]E-05	-.5[illegible]E-03	.5231[illegible]E-05
	.5[illegible]E-02	.2494[illegible]E-03	.2075[illegible]E-01	.4731[illegible]E-05	-.5687[illegible]E-03	-.2011[illegible]E-05
	.3[illegible]E-02	-.7719[illegible]E-03	.1997[illegible]E-01	-.7416[illegible]E-04	-.6[illegible]E-03	-.1404[illegible]E-05
	.3[illegible]E-02	-.1[illegible]E-02	.1992[illegible]E-01	-.1127[illegible]E-03	-.6[illegible]E-03	.9844[illegible]E-06
	.2[illegible]E-02	-.1[illegible]E-02	.1985[illegible]E-01	-.1394[illegible]E-03	-.5779[illegible]E-03	.3466[illegible]E-05
	.2[illegible]E-02	-.1[illegible]E-02	.1978[illegible]E-01	-.1[illegible]E-03	-.5295[illegible]E-03	.2840[illegible]E-05
	.1[illegible]E-02	-.1[illegible]E-02	.1970[illegible]E-01	-.1408[illegible]E-03	-.4769[illegible]E-03	.2527[illegible]E-06
	.1[illegible]E-02	-.1198[illegible]E-02	.1964[illegible]E-01	-.1142[illegible]E-03	-.4311[illegible]E-03	-.1489[illegible]E-05
	.9[illegible]E-03	-.7882[illegible]E-03	.1959[illegible]E-01	-.7375[illegible]E-04	-.3982[illegible]E-03	-.1140[illegible]E-05
	.7[illegible]E-03	-.2835[illegible]E-03	.1957[illegible]E-01	-.2380[illegible]E-04	-.3812[illegible]E-03	.6290[illegible]E-06
	.7[illegible]E-03	.2546[illegible]E-03	.1957[illegible]E-01	.2950[illegible]E-04	-.3820[illegible]E-03	.2773[illegible]E-05
	.[illegible]E-03	.[illegible]E-03	.1960[illegible]E-01	.7895[illegible]E-04	-.4[illegible]E-03	.4356[illegible]E-05
	.1[illegible]E-02	.1181[illegible]E-02	.1965[illegible]E-01	.1184[illegible]E-03	-.4351[illegible]E-03	.4418[illegible]E-05
	.1[illegible]E-02	.1459[illegible]E-02	.1971[illegible]E-01	.1434[illegible]E-03	-.4822[illegible]E-03	.2444[illegible]E-05
	.2[illegible]E-02	.1562[illegible]E-02	.1979[illegible]E-01	.1504[illegible]E-03	-.5354[illegible]E-03	-.2355[illegible]E-06
	.2[illegible]E-02	.1478[illegible]E-02	.1986[illegible]E-01	.1377[illegible]E-03	-.5833[illegible]E-03	-.6933[illegible]E-06
	.3[illegible]E-02	.1216[illegible]E-02	.1992[illegible]E-01	.1084[illegible]E-03	-.6155[illegible]E-03	.1981[illegible]E-05
	.3[illegible]E-02	.8049[illegible]E-03	.1997[illegible]E-01	.6831[illegible]E-04	-.6[illegible]E-03	.4518[illegible]E-05
	.3805[illegible]E-02	-.2924[illegible]E-03	.1999[illegible]E-01	.2113[illegible]E-04	-.6354[illegible]E-03	.3352[illegible]E-05
	.3810[illegible]E-02	-.2563[illegible]E-03	.1999[illegible]E-01	-.2795[illegible]E-04	-.6345[illegible]E-03	-.1672[illegible]E-06

JOB kips

BY Y.E.

PAGE

DATE

REV.

Some Stresses on the Bearing Housing

```
ELEM 102 NODES= 212 312 313 213 MATERIAL= 1 AREA= .18715 TTOP,TBOT= 340. 340. PRESS= 0.
   NX,NY= 2. -0. MX,MY,MXY= 0. 1. 0. XC,YC,ZC= -.2560 -.7033 1.400
TOP STR SX,SY,SXY= 4857. 7154. -3442. SMAX,SMIN,TAUMAX= 9634. 2377. 3628. A=-35.8 VM= 8492.
MID STR SX,SY,SXY= 4370. 6237. -3333. SMAX,SMIN,TAUMAX= 8765. 1842. 3461. A=-37.2 VM= 7805.
BOT STR SX,SY,SXY= 3884. 5321. -3224. SMAX,SMIN,TAUMAX= 7906. 1299. 3303. A=-38.7 VM= 7343.

ELEM 103 NODES= 213 313 314 214 MATERIAL= 1 AREA= .18715 TTOP,TBOT= 340. 340. PRESS= 0.
   NX,NY= 2. -0. MX,MY,MXY= 0. 1. 0. XC,YC,ZC= .1145E-10 -.7485 1.400
TOP STR SX,SY,SXY= 7044. 4660. 3028. SMAX,SMIN,TAUMAX= 9107. 2598. 3255. A= 53.7 VM= 8125.
MID STR SX,SY,SXY= 6600. 3865. 3062. SMAX,SMIN,TAUMAX= 8604. 1861. 3372. A= 57.0 VM= 7841.
BOT STR SX,SY,SXY= 6155. 3069. 3136. SMAX,SMIN,TAUMAX= 8107. 1115. 3495. A= 58.1 VM= 7610.

ELEM 104 NODES= 214 314 315 215 MATERIAL= 1 AREA= .18715 TTOP,TBOT= 340. 340. PRESS= 0.
   NX,NY= 2. -0. MX,MY,MXY= 0. 0. 0. XC,YC,ZC= -.2560 -.7033 1.400
TOP STR SX,SY,SXY= -2392. 4569. 1048. SMAX,SMIN,TAUMAX= 4720. -2543. 3634. A= 0.4 VM= 4384.
MID STR SX,SY,SXY= -2426. 4415. 1096. SMAX,SMIN,TAUMAX= 4587. -2597. 3592. A= 0.9 VM= 4301.
BOT STR SX,SY,SXY= -2460. 4265. 1144. SMAX,SMIN,TAUMAX= 4454. -2650. 3552. A= 0.4 VM= 4218.

ELEM 105 NODES= 215 315 316 216 MATERIAL= 1 AREA= .18715 TTOP,TBOT= 340. 340. PRESS= 0.
   NX,NY= 2. 0. MX,MY,MXY= 0. 1. 0. XC,YC,ZC= .4811 -.5733 1.400
TOP STR SX,SY,SXY= 4869. 7019. -3737. SMAX,SMIN,TAUMAX= 9832. 2056. 3888. A=-37.0 VM= 8983.
MID STR SX,SY,SXY= 4482. 6215. -3604. SMAX,SMIN,TAUMAX= 9055. 1642. 3706. A=-38.2 VM= 8356.
BOT STR SX,SY,SXY= 4095. 5411. -3470. SMAX,SMIN,TAUMAX= 8265. 1221. 3532. A=-37.6 VM= 7747.

ELEM 106 NODES= 216 316 317 217 MATERIAL= 1 AREA= .18715 TTOP,TBOT= 340. 340. PRESS= 0.
   NX,NY= 2. -1. MX,MY,MXY= 0. 1. 0. XC,YC,ZC= .6482 -.3742 1.400
TOP STR SX,SY,SXY= 7354. 4549. 3282. SMAX,SMIN,TAUMAX= 9521. 2383. 3569. A= 56.6 VM= 8581.
MID STR SX,SY,SXY= 7001. 3694. 3301. SMAX,SMIN,TAUMAX= 9039. 1656. 3692. A= 58.3 VM= 8336.
BOT STR SX,SY,SXY= 6648. 2840. 3319. SMAX,SMIN,TAUMAX= 8571. 917. 3827. A= 59.9 VM= 8151.

ELEM 107 NODES= 217 317 318 218 MATERIAL= 1 AREA= .18715 TTOP,TBOT= 340. 340. PRESS= 0.
   NX,NY= 0. 1. MX,MY,MXY= 0. 0. -0. XC,YC,ZC= .7371 -.1300 1.400
TOP STR SX,SY,SXY= -2275. 4509. 1368. SMAX,SMIN,TAUMAX= 4775. -2540. 3657. A= 11.0 VM= 4431.
MID STR SX,SY,SXY= -2322. 4310. 1351. SMAX,SMIN,TAUMAX= 4573. -2586. 3581. A= 11.1 VM= 4341.
BOT STR SX,SY,SXY= -2369. 4110. 1335. SMAX,SMIN,TAUMAX= 4375. -2633. 3504. A= 11.2 VM= 6151.

ELEM 108 NODES= 218 318 301 201 MATERIAL= 1 AREA= .18715 TTOP,TBOT= 340. 340. PRESS= 0.
   NX,NY= 2. -2. MX,MY,MXY= 1. 1. 0. XC,YC,ZC= .7371 .1300 1.400
TOP STR SX,SY,SXY= 4799. 6974. -3292. SMAX,SMIN,TAUMAX= 9354. 2417. 3468. A=-35.8 VM= 8410.
MID STR SX,SY,SXY= 4275. 6145. -3231. SMAX,SMIN,TAUMAX= 8573. 1847. 3363. A=-36.9 VM= 7815.
BOT STR SX,SY,SXY= 3756. 5313. -3169. SMAX,SMIN,TAUMAX= 7798. 1272. 3263. A=-38.1 VM= 7246.

ELEM 109 NODES= 101 151 251 201 MATERIAL= 1 AREA= .38520 TTOP,TBOT= 342. 342. PRESS= 0.
   NX,NY= -0. 5. MX,MY,MXY= 2. 0. -0. XC,YC,ZC= 1.285 .4677 1.705
TOP STR SX,SY,SXY= -2. 4769. 1032. SMAX,SMIN,TAUMAX= 4982. -215. 2594. A= 11.7 VM= 5093.
MID STR SX,SY,SXY= -954. 4566. 854. SMAX,SMIN,TAUMAX= 4695. -1043. 2869. A= 8.6 VM= 5320.
BOT STR SX,SY,SXY= -1906. 4363. 677. SMAX,SMIN,TAUMAX= 4435. -1978. 3207. A= 6.1 VM= 5089.

ELEM 110 NODES= 151 351 451 251 MATERIAL= 1 AREA= .30690 TTOP,TBOT= 396. 396. PRESS= 0.
   NX,NY= -3. 1. MX,MY,MXY= 1. 0. 0. XC,YC,ZC= 1.701 .6191 1.955
TOP STR SX,SY,SXY= 2456. 5227. -4437. SMAX,SMIN,TAUMAX= 8490. -807. 4648. A=-36.3 VM= 7921.
MID STR SX,SY,SXY= 2099. 5133. -4233. SMAX,SMIN,TAUMAX= 8113. -880. 4496. A=-35.1 VM= 8547.
BOT STR SX,SY,SXY= 1743. 5039. -4029. SMAX,SMIN,TAUMAX= 7744. -962. 4353. A=-33.9 VM= 8267.

ELEM 111 NODES= 351 601 501 451 MATERIAL= 1 AREA= .33540 TTOP,TBOT= 546. 546. PRESS= 0.
   NX,NY= -5. -1. MX,MY,MXY= -2. -1. 0. XC,YC,ZC= 2.117 .7704 .5950
TOP STR SX,SY,SXY= 4591. -6947. -4295. SMAX,SMIN,TAUMAX= 4240. -8595. 6418. A=-69.0 VM= 11327.
MID STR SX,SY,SXY= 3983. -6294. -4243. SMAX,SMIN,TAUMAX= 5508. -7819. 6664. A=-70.2 VM= 11599.
BOT STR SX,SY,SXY= 5375. -5641. -4191. SMAX,SMIN,TAUMAX= 6788. -7054. 6921. A=-71.4 VM= 11988.

ELEM 112 NODES= 104 154 254 204 MATERIAL= 1 AREA= .38520 TTOP,TBOT= 342. 342. PRESS= 0.
   NX,NY= 0. 1. MX,MY,MXY= 1. -0. -0. XC,YC,ZC= .2375 1.347 1.705
TOP STR SX,SY,SXY= -399. 4576. 760. SMAX,SMIN,TAUMAX= 4689. -512. 2601. A= 8.5 VM= 4965.
MID STR SX,SY,SXY= -781. 4577. 726. SMAX,SMIN,TAUMAX= 4674. -878. 2776. A= 7.6 VM= 5169.
BOT STR SX,SY,SXY= -1164. 4579. 692. SMAX,SMIN,TAUMAX= 4661. -1246. 2954. A= 6.8 VM= 5393.

ELEM 113 NODES= 154 354 454 254 MATERIAL= 1 AREA= .30690 TTOP,TBOT= 400. 400. PRESS= 0.
   NX,NY= -1. 0. MX,MY,MXY= 0. 0. 0. XC,YC,ZC= .3143 1.783 1.955
TOP STR SX,SY,SXY= 2439. 4862. -4369. SMAX,SMIN,TAUMAX= 8197. -876. 4537. A=-37.2 VM= 8669.
MID STR SX,SY,SXY= 2150. 4871. -4273. SMAX,SMIN,TAUMAX= 7995. -974. 4484. A=-36.2 VM= 8524.
BOT STR SX,SY,SXY= 1860. 4880. -4177. SMAX,SMIN,TAUMAX= 7798. -1078. 4438. A=-35.1 VM= 8389.

ELEM 114 NODES= 354 604 504 454 MATERIAL= 1 AREA= .33540 TTOP,TBOT= 551. 551. PRESS= 0.
   NX,NY= -1. 1. MX,MY,MXY= -0. -0. 0. XC,YC,ZC= .3911 2.218 .6950
TOP STR SX,SY,SXY= 3957. -6448. -4404. SMAX,SMIN,TAUMAX= 5571. -8062. 6816. A=-69.9 VM= 11872.
MID STR SX,SY,SXY= 4088. -6311. -4339. SMAX,SMIN,TAUMAX= 5661. -7884. 6773. A=-70.1 VM= 11783.
BOT STR SX,SY,SXY= 4220. -6173. -4275. SMAX,SMIN,TAUMAX= 5752. -7707. 6729. A=-70.1 VM= 11696.

ELEM 115 NODES= 107 157 257 207 MATERIAL= 1 AREA= .38520 TTOP,TBOT= 342. 342. PRESS= 0.
   NX,NY= 0. -0. MX,MY,MXY= -0. 0. 0. XC,YC,ZC= -1.048 .8790 1.705
TOP STR SX,SY,SXY= 302. 4579. 639. SMAX,SMIN,TAUMAX= 4673. 209. 2232. A= 8.3 VM= 4572.
MID STR SX,SY,SXY= 401. 4576. 642. SMAX,SMIN,TAUMAX= 4673. 304. 2184. A= 8.5 VM= 4524.
BOT STR SX,SY,SXY= 499. 4574. 644. SMAX,SMIN,TAUMAX= 4673. 400. 2137. A= 8.8 VM= 4487.
```

JOB *KIPS* PAGE ______

______ DATE ______

BY *Y.E.* REV. ______

Bearing HSG Stresses (Cont.)

```
TOP STR  SX,SY,SXY= [illegible]  5030.  -4369.  SMAX,SMIN,TAUMAX=  8715.  -149.  4432.  A=-40.1  VM=  8790.
MID STR  SX,SY,SXY=  3603.  5030.  -4406.  SMAX,SMIN,TAUMAX=  8779.  -147.  4463.  A=-40.4  VM=  8854.
BOT STR  SX,SY,SXY=  3670.  5030.  -4443.  SMAX,SMIN,TAUMAX=  8844.  -144.  4494.  A=-40.6  VM=  8917.

ELEM 117  NODES=  357  607  507  457  MATERIAL=  1  AREA=  .33540  TTOP,TBOT=  549.  549.  PRESS=  0.
    NX,NY=  0.  -0.  MX,MY,MXY=  0.  0.  -0.  XC,YC,ZC=  -1.725  1.448  .6950
TOP STR  SX,SY,SXY=  5735.  -6536.  -4506.  SMAX,SMIN,TAUMAX=  7212.  -8113.  7612.  A=-71.9  VM=  13191.
MID STR  SX,SY,SXY=  5683.  -6574.  -4532.  SMAX,SMIN,TAUMAX=  7177.  -8068.  7622.  A=-71.8  VM=  13210.
BOT STR  SX,SY,SXY=  5631.  -6613.  -4558.  SMAX,SMIN,TAUMAX=  7142.  -8123.  7633.  A=-71.7  VM=  13229.

ELEM 118  NODES=  110  160  260  210  MATERIAL=  1  AREA=  .38520  TTOP,TBOT=  342.  342.  PRESS=  0.
    NX,NY=  -0.  -2.  MX,MY,MXY=  -1.  -0.  0.  XC,YC,ZC=  -1.285  -.4677  1.705
TOP STR  SX,SY,SXY=  -1587.  4624.  739.  SMAX,SMIN,TAUMAX=  4711.  -1674.  3192.  A=  6.7  VM=  5734.
MID STR  SX,SY,SXY=  -1132.  4541.  785.  SMAX,SMIN,TAUMAX=  4746.  -1237.  2991.  A=  7.6  VM=  5470.
BOT STR  SX,SY,SXY=  -676.  4658.  831.  SMAX,SMIN,TAUMAX=  4785.  -803.  2794.  A=  8.7  VM=  5233.

ELEM 119  NODES=  160  360  460  260  ATERIAL=  1  AREA=  .30690  TTOP,TBOT=  399.  399.  PRESS=  0.
    NX,NY=  1.  -1.  MX,MY,MXY=  -1.  -0.  -0.  XC,YC,ZC=  -1.701  -.6191  1.255
TOP STR  SX,SY,SXY=  1497.  4499.  -4193.  SMAX,SMIN,TAUMAX=  7724.  -1327.  4525.  A=-34.0  VM=  8466.
MID STR  SX,SY,SXY=  1426.  4921.  -4309.  SMAX,SMIN,TAUMAX=  7952.  -1205.  4579.  A=-35.1  VM=  8618.
BOT STR  SX,SY,SXY=  2155.  4942.  -4425.  SMAX,SMIN,TAUMAX=  8188.  -1091.  4639.  A=-36.3  VM=  8784.

ELEM 120  NODES=  360  610  510  460  MATERIAL=  1  AREA=  .33540  TTOP,TBOT=  549.  549.  PRESS=  0.
    NX,NY=  2.  -1.  MX,MY,MXY=  0.  0.  -0.  XC,YC,ZC=  -2.117  -.7704  .6950
TOP STR  SX,SY,SXY=  3990.  -6013.  -4326.  SMAX,SMIN,TAUMAX=  5609.  -7623.  6616.  A=-69.6  VM=  11503.
MID STR  SX,SY,SXY=  3774.  -6192.  -4400.  SMAX,SMIN,TAUMAX=  5439.  -7856.  6648.  A=-69.3  VM=  11577.
BOT STR  SX,SY,SXY=  3549.  -6371.  -4475.  SMAX,SMIN,TAUMAX=  5269.  -8091.  6680.  A=-69.0  VM=  11656.

ELEM 121  NODES=  113  163  263  213  MATERIAL=  1  AREA=  .38520  TTOP,TBOT=  342.  342.  PRESS=  0.
    NX,NY=  0.  -4.  MX,MY,MXY=  -1.  -0.  0.  XC,YC,ZC=  -.2375  -1.347  1.705
TOP STR  SX,SY,SXY=  -1392.  4469.  803.  SMAX,SMIN,TAUMAX=  4577.  -1500.  3038.  A=  7.7  VM=  5483.
MID STR  SX,SY,SXY=  -591.  4640.  929.  SMAX,SMIN,TAUMAX=  4801.  -750.  2775.  A=  9.8  VM=  5216.
BOT STR  SX,SY,SXY=  213.  4812.  1055.  SMAX,SMIN,TAUMAX=  5043.  -18.  2530.  A=  12.3  VM=  5051.

ELEM 122  NODES=  163  363  463  263  MATERIAL=  1  AREA=  .30690  TTOP,TBOT=  396.  396.  PRESS=  0.
    NX,NY=  1.  -1.  MX,MY,MXY=  -1.  -0.  -0.  XC,YC,ZC=  -.3143  -1.783  1.255
TOP STR  SX,SY,SXY=  2126.  4582.  -3929.  SMAX,SMIN,TAUMAX=  7471.  -763.  4117.  A=-36.3  VM=  7880.
MID STR  SX,SY,SXY=  2460.  4632.  -4137.  SMAX,SMIN,TAUMAX=  7823.  -731.  4277.  A=-37.6  VM=  8213.
BOT STR  SX,SY,SXY=  2793.  4683.  -4344.  SMAX,SMIN,TAUMAX=  8184.  -706.  4446.  A=-38.9  VM=  8550.

ELEM 123  NODES=  363  613  513  463  MATERIAL=  1  AREA=  .33540  TTOP,TBOT=  535.  535.  PRESS=  0.
    NX,NY=  4.  2.  MX,MY,MXY=  2.  1.  -0.  XC,YC,ZC=  -.3911  -2.218  .6950
TOP STR  SX,SY,SXY=  5553.  -4481.  -4433.  SMAX,SMIN,TAUMAX=  7231.  -6159.  6695.  A=-69.3  VM=  11608.
MID STR  SX,SY,SXY=  4459.  -4907.  -4461.  SMAX,SMIN,TAUMAX=  6244.  -6692.  6468.  A=-68.2  VM=  11204.
BOT STR  SX,SY,SXY=  3365.  -5333.  -4489.  SMAX,SMIN,TAUMAX=  5266.  -7234.  6250.  A=-67.0  VM=  10870.

ELEM 124  NODES=  116  166  266  216  MATERIAL=  1  AREA=  .38520  TTOP,TBOT=  342.  342.  PRESS=  0.
    NX,NY=  -0.  -0.  MX,MY,MXY=  -0.  -0.  0.  XC,YC,ZC=  1.048  -.8790  1.705
TOP STR  SX,SY,SXY=  131.  4711.  971.  SMAX,SMIN,TAUMAX=  4908.  -66.  2487.  A=  11.5  VM=  4942.
MID STR  SX,SY,SXY=  145.  4716.  987.  SMAX,SMIN,TAUMAX=  4920.  -59.  2489.  A=  11.7  VM=  4950.
BOT STR  SX,SY,SXY=  159.  4721.  1003.  SMAX,SMIN,TAUMAX=  4932.  -52.  2492.  A=  11.9  VM=  4958.

ELEM 125  NODES=  166  366  466  266  MATERIAL=  1  AREA=  .30690  TTOP,TBOT=  395.  395.  PRESS=  0.
    NX,NY=  0.  -0.  MX,MY,MXY=  0.  -0.  0.  XC,YC,ZC=  1.387  -1.163  1.255
TOP STR  SX,SY,SXY=  3457.  4718.  -4206.  SMAX,SMIN,TAUMAX=  8341.  -166.  4253.  A=-40.7  VM=  8425.
MID STR  SX,SY,SXY=  3442.  4720.  -4187.  SMAX,SMIN,TAUMAX=  8316.  -155.  4235.  A=-40.7  VM=  8394.
BOT STR  SX,SY,SXY=  3426.  4721.  -4167.  SMAX,SMIN,TAUMAX=  8291.  -144.  4217.  A=-40.6  VM=  8364.

ELEM 126  NODES=  366  616  516  466  MATERIAL=  1  AREA=  .33540  TTOP,TBOT=  529.  529.  PRESS=  0.
    NX,NY=  -0.  1.  MX,MY,MXY=  0.  -0.  0.  XC,YC,ZC=  1.726  -1.448  .6950
TOP STR  SX,SY,SXY=  5564.  -4846.  -4531.  SMAX,SMIN,TAUMAX=  7260.  -6541.  6901.  A=-69.5  VM=  11958.
MID STR  SX,SY,SXY=  5500.  -4819.  -4521.  SMAX,SMIN,TAUMAX=  7201.  -6519.  6860.  A=-69.4  VM=  11887.
BOT STR  SX,SY,SXY=  5436.  -4790.  -4512.  SMAX,SMIN,TAUMAX=  7142.  -6496.  6819.  A=-69.3  VM=  11816.

ELEM 127  NODES=  501  601  602  502  MATERIAL=  1  AREA=  .39208  TTOP,TBOT=  644.  644.  PRESS=  0.
    NX,NY=  231.  72.  MX,MY,MXY=  26.  7.  16.  XC,YC,ZC=  2.119  1.224  .3900
TOP STR  SX,SY,SXY=  2568.  1642.  -1738.  SMAX,SMIN,TAUMAX=  3904.  306.  1799.  A=-52.5  VM=  3760.
MID STR  SX,SY,SXY=  -692.  715.  198.  SMAX,SMIN,TAUMAX=  742.  -720.  731.  A=  7.9  VM=  1266.
BOT STR  SX,SY,SXY=  -3953.  -212.  2135.  SMAX,SMIN,TAUMAX=  755.  -4921.  2838.  A=  24.4  VM=  5339.

ELEM 128  NODES=  601  701  702  602  MATERIAL=  1  AREA=  .46308  TTOP,TBOT=  647.  647.  PRESS=  0.
    NX,NY=  -61.  -94.  MX,MY,MXY=  51.  22.  36.  XC,YC,ZC=  2.503  1.445  .4900
TOP STR  SX,SY,SXY=  691.  -454.  -461.  SMAX,SMIN,TAUMAX=  854.  -617.  735.  A=-70.6  VM=  1279.
MID STR  SX,SY,SXY=  -771.  -993.  410.  SMAX,SMIN,TAUMAX=  -457.  -1307.  425.  A=  52.6  VM=  1149.
BOT STR  SX,SY,SXY=  -2234.  -1531.  1281.  SMAX,SMIN,TAUMAX=  -554.  -3211.  1329.  A=  37.3  VM=  2973.

ELEM 129  NODES=  701  801  802  702  MATERIAL=  1  AREA=  .53408  TTOP,TBOT=  646.  646.  PRESS=  0.
    NX,NY=  -120.  -46.  MX,MY,MXY=  25.  18.  55.  XC,YC,ZC=  2.887  1.667  .5900
TOP STR  SX,SY,SXY=  -550.  -953.  -207.  SMAX,SMIN,TAUMAX=  -462.  -1040.  289.  A=-67.2  VM=  902.
MID STR  SX,SY,SXY=  -801.  -1126.  338.  SMAX,SMIN,TAUMAX=  -588.  -1338.  375.  A=  57.8  VM=  1162.
BOT STR  SX,SY,SXY=  -1052.  -1299.  883.  SMAX,SMIN,TAUMAX=  -284.  -2067.  892.  A=  49.0  VM=  1941.

ELEM 130  NODES=  801  851  852  802  MATERIAL=  1  AREA=  .64542  TTOP,TBOT=  648.  648.  PRESS=  0.
    NX,NY=  -33.  -4.  MX,MY,MXY=  3.  4.  9.  XC,YC,ZC=  3.224  1.861  .8200
TOP STR  SX,SY,SXY=  34.  -755.  -307.  SMAX,SMIN,TAUMAX=  283.  -1003.  643.  A=-63.9  VM=  1170.
MID STR  SX,SY,SXY=  [illegible]  [illegible]  [illegible]  SMAX,SMIN,TAUMAX=  -4.  -494.  490.  A=-74.8  VM=  922.
```

Max σeff (handwritten beside ELEM 117, VM= 13229.)

JOB LIPS

PAGE

DATE

BY Y.E.

REV.

Some Stresses in the thermal dam area (Nozzle HS'G)

```
ELEM  234  NODES=  914 2014 2015  915  MATERIAL=  1  AREA=    .38550      TTOP,TBOT=  594.  594.  PRESS=     0.
          NX,NY=     20.    0.  MX,MY,MXY=   -12.    -7.    -4.  XC,YC,ZC=    1.240          -3.424          .2500
TOP STR   SX,SY,SXY=  -1116.   3958.    339.   SMAX,SMIN,TAUMAX=   3981.  -1139.   2560.   A=  3.8  VM=   4656.
MID STR   SX,SY,SXY=     80.   4431.    -60.   SMAX,SMIN,TAUMAX=   4432.     79.   2277.   A= -5.8  VM=   4573.
BOT STR   SX,SY,SXY=   1275.   5305.   -459.   SMAX,SMIN,TAUMAX=   5356.   1223.   2066.   A= -5.4  VM=   4862.

ELEM  235  NODES=  915 2015 2016  916  MATERIAL=  1  AREA=    .38550      TTOP,TBOT=  594.  594.  PRESS=     0.
          NX,NY=     49.  -16.  MX,MY,MXY=   -12.    -1.    -1.  XC,YC,ZC=    2.342          -2.791          .2500
TOP STR   SX,SY,SXY=  -1553.   4450.   -117.   SMAX,SMIN,TAUMAX=   4452.  -1556.   3004.   A= -1.1  VM=   4401.
MID STR   SX,SY,SXY=   -440.   4551.   -187.   SMAX,SMIN,TAUMAX=   4558.   -447.   2502.   A= -2.1  VM=   4797.
BOT STR   SX,SY,SXY=    674.   4652.   -257.   SMAX,SMIN,TAUMAX=   4669.    657.   2006.   A= -3.7  VM=   4377.

ELEM  236  NODES=  916 2016 2017  917  MATERIAL=  1  AREA=    .38550      TTOP,TBOT=  579.  579.  PRESS=     0.
          NX,NY=     92.   16.  MX,MY,MXY=   -14.    -4.     2.  XC,YC,ZC=    3.156          -1.822          .2500
TOP STR   SX,SY,SXY=   -870.   4794.     58.   SMAX,SMIN,TAUMAX=   4794.   -870.   2835.   A=   .6  VM=   4528.
MID STR   SX,SY,SXY=    462.   5168.    258.   SMAX,SMIN,TAUMAX=   5168.    446.   2360.   A=  3.1  VM=   4930.
BOT STR   SX,SY,SXY=   1744.   5564.    457.   SMAX,SMIN,TAUMAX=   5564.   1738.   1913.   A=  6.9  VM=   4930.

ELEM  237  NODES=  917 2017 2018  918  MATERIAL=  1  AREA=    .38550      TTOP,TBOT=  579.  579.  PRESS=     0.
          NX,NY=      3.  -10.  MX,MY,MXY=   -13.    -7.     6.  XC,YC,ZC=    3.588          -.6327          .2500
TOP STR   SX,SY,SXY=  -1423.   5513.   -503.   SMAX,SMIN,TAUMAX=   5549.  -1459.   3504.   A= -4.1  VM=   5405.
MID STR   SX,SY,SXY=   -155.   6184.    109.   SMAX,SMIN,TAUMAX=   6186.   -157.   3171.   A=  1.0  VM=   6066.
BOT STR   SX,SY,SXY=   1113.   6955.    720.   SMAX,SMIN,TAUMAX=   6944.   1024.   2960.   A=  7.0  VM=   5492.

ELEM  238  NODES=  918 2018 2001  901  MATERIAL=  1  AREA=    .38550      TTOP,TBOT=  579.  579.  PRESS=     0.
          NX,NY=     20.   14.  MX,MY,MXY=   -15.    -3.     3.  XC,YC,ZC=    2.984          -.6327          .2500
TOP STR   SX,SY,SXY=  -1357.   7245.      8.   SMAX,SMIN,TAUMAX=   7245.  -1358.   4464.   A=  .1  VM=   6342.
MID STR   SX,SY,SXY=     59.   7895.    309.   SMAX,SMIN,TAUMAX=   7907.     47.   3930.   A=  2.1  VM=   7494.
BOT STR   SX,SY,SXY=   1468.   8204.    610.   SMAX,SMIN,TAUMAX=   8259.   1413.   3423.   A=  5.1  VM=   7451.

3-D BEAM  239   NODES 2001 2101   MAT  1   TEMP=  525.   TTOPZ,TBOTY= 525.0 525.0   DIR1,DIR2=  3356.  3356.
BZ1=-17414.  BY1=   930.  MAXI= 22296.  MINI=-14392.  BZ2=-17710.  BY2=  -383.  MAXZ= 22046.  MINZ=-14141.

3-D BEAM  240   NODES 2003 2103   MAT  1   TEMP=  525.   TTOPZ,TBOTY= 525.0 525.0   DIR1,DIR2=  3356.  3356.
BZ1=-16127.  BY1=  1005.  MAXI= 20191.  MINI=-14074.  BZ2=-18427.  BY2=  -412.  MAXZ= 21837.  MINZ=-17671.

3-D BEAM  241   NODES 2005 2105   MAT  1   TEMP=  540.   TTOPZ,TBOTY= 540.0 540.0   DIR1,DIR2=  3326.  3326.
BZ1=-17532.  BY1=   577.  MAXI= 20534.  MINI=-15883.  BZ2=-15450.  BY2=   -84.  MAXZ= 17859.  MINZ=-15408.

3-D BEAM  242   NODES 2007 2107   MAT  1   TEMP=  540.   TTOPZ,TBOTY= 540.0 540.0   DIR1,DIR2=  3310.  3310.
BZ1=-15227.  BY1=   248.  MAXI= 18785.  MINI=-14165.  BZ2=-16937.  BY2=   -72.  MAXZ= 19319.  MINZ=-14699.

3-D BEAM  243   NODES 2009 2109   MAT  1   TEMP=  540.   TTOPZ,TBOTY= 540.0 540.0   DIR1,DIR2=  3258.  3258.
BZ1=-16384.  BY1=  -103.  MAXI= 19345.  MINI=-14630.  BZ2=-16266.  BY2=   -91.  MAXZ= 18714.  MINZ=-13949.

3-D BEAM  244   NODES 2011 2111   MAT  1   TEMP=  540.   TTOPZ,TBOTY= 540.0 540.0   DIR1,DIR2=  2709.  2709.
BZ1=-16905.  BY1=  -886.  MAXI= 19599.  MINI=-14581.  BZ2=-17116.  BY2=   257.  MAXZ= 20082.  MINZ=-14547.

3-D BEAM  245   NODES 2013 2113   MAT  1   TEMP=  540.   TTOPZ,TBOTY= 540.0 540.0   DIR1,DIR2=  3432.  3432.
BZ1=-16575.  BY1= -1152.  MAXI= 21158.  MINI=-14294.  BZ2=-16867.  BY2=   511.  MAXZ= 20810.  MINZ=-13947.

3-D BEAM  246   NODES 2015 2115   MAT  1   TEMP=  540.   TTOPZ,TBOTY= 540.0 540.0   DIR1,DIR2=  3024.  3024.
BZ1=-15692.  BY1=   -793.  MAXI= 19523.  MINI=-13446.  BZ2=-15545.  BY2=   174.  MAXZ= 18757.  MINZ=-12680.

3-D BEAM  247   NODES 2017 2117   MAT  1   TEMP=  525.   TTOPZ,TBOTY= 525.0 525.0   DIR1,DIR2=  3602.  3602.
BZ1=-16950.  BY1=    179.  MAXI= 20761.  MINI=-13557.  BZ2=-15619.  BY2=   105.  MAXZ= 19326.  MINZ=-12122.

ELEM  248  NODES= 2101 2201 2202 2102  MATERIAL=  1  AREA=    .30562      TTOP,TBOT=  480.  480.  PRESS=     0.
          NX,NY=    300.   11.  MX,MY,MXY=    11.    0.     2.  XC,YC,ZC=    3.753          2.167          .2220E-15
TOP STR   SX,SY,SXY=   1766.  29259.   -391.   SMAX,SMIN,TAUMAX=  29265.   1761.  13752.   A=  -.8  VM=  28426.
MID STR   SX,SY,SXY=     80.  29225.   -122.   SMAX,SMIN,TAUMAX=  29226.     80.  14573.   A=  -.2  VM=  29186.
BOT STR   SX,SY,SXY=  -1606.  29191.    147.   SMAX,SMIN,TAUMAX=  29192.  -1606.  15399.   A=   .3  VM=  30027.

ELEM  249  NODES= 2102 2202 2203 2103  MATERIAL=  1  AREA=    .30562      TTOP,TBOT=  480.  480.  PRESS=     0.
          NX,NY=    468.  -17.  MX,MY,MXY=    15.    7.     2.  XC,YC,ZC=    2.785          3.319          .2220E-15
TOP STR   SX,SY,SXY=   2134.  30089.   -214.   SMAX,SMIN,TAUMAX=  30090.   2132.  13771.   A=  -.4  VM=  29043.
MID STR   SX,SY,SXY=    -77.  29005.     38.   SMAX,SMIN,TAUMAX=  29005.    -77.  14541.   A=   .1  VM=  29043.
BOT STR   SX,SY,SXY=  -2287.  27921.    289.   SMAX,SMIN,TAUMAX=  27924.  -2289.  15107.   A=   .5  VM=  29136.

ELEM  250  NODES= 2103 2203 2204 2104  MATERIAL=  1  AREA=    .30562      TTOP,TBOT=  480.  480.  PRESS=     0.
          NX,NY=    279.   19.  MX,MY,MXY=     8.   -1.     1.  XC,YC,ZC=    1.482          4.072          .2220E-15
TOP STR   SX,SY,SXY=   1354.  29408.    132.   SMAX,SMIN,TAUMAX=  29408.   1354.  13975.   A=  .3  VM=  28653.
MID STR   SX,SY,SXY=     90.  29500.    698.   SMAX,SMIN,TAUMAX=  29504.     87.  14708.   A=  .6  VM=  29460.
BOT STR   SX,SY,SXY=  -1180.  29693.    464.   SMAX,SMIN,TAUMAX=  29700.  -1187.  15444.   A=  .9  VM=  30311.

ELEM  251  NODES= 2104 2204 2205 2105  MATERIAL=  1  AREA=    .30562      TTOP,TBOT=  480.  480.  PRESS=     0.
          NX,NY=    239.  -17.  MX,MY,MXY=    10.    6.     3.  XC,YC,ZC=   -.2213E-10     4.333          .2220E-15
TOP STR   SX,SY,SXY=   1421.  30023.   -606.   SMAX,SMIN,TAUMAX=  30042.   1408.  14317.   A= -1.2  VM=  29363.
MID STR   SX,SY,SXY=    -70.  29137.   -222.   SMAX,SMIN,TAUMAX=  29139.    -72.  14566.   A=  -.4  VM=  29175.
BOT STR   SX,SY,SXY=  -1562.  28246.    163.   SMAX,SMIN,TAUMAX=  28246.  -1563.  14905.   A=   .3  VM=  29649.

ELEM  252  NODES= 2105 2205 2206 2106  MATERIAL=  1  AREA=    .30562      TTOP,TBOT=  480.  480.  PRESS=     0.
          NX,NY=    492.   17.  MX,MY,MXY=    14.    2.    -0.  XC,YC,ZC=   -1.482          4.072          .2220E-15
TOP STR   SX,SY,SXY=   2174.  30204.     55.   SMAX,SMIN,TAUMAX=  30204.   2174.  14015.   A=  .1  VM=  29174.
```

JOB KIPS

BY Y E.

PAGE

DATE

REV.

Stresses in thermal dam area (Continued)

```
ELEM  253  NODES= 2106 2206 2207 2107  MATERIAL=  1  AREA=   .30562     TTOP,TBOT=  480.  480.  PRESS=     0.
   NX,NY=   264.   -15.  MX,MY,MXY=      8.     4.     0.  XC,YC,ZC=   -2.785    3.319          .2220E-15
TOP STR  SX,SY,SXY=   1147.  29720.    185.  SMAX,SMIN,TAUMAX=  29721.   1146.  14288.  A=   .4  VM=  29165.
MID STR  SX,SY,SXY=    -26.  29176.     22.  SMAX,SMIN,TAUMAX=  29178.    -28.  14603.  A=   .4  VM=  29192.
BOT STR  SX,SY,SXY=  -1199.  28633.    272.  SMAX,SMIN,TAUMAX=  28636.  -1202.  14919.  A=   .5  VM=  29255.

ELEM  254  NODES= 2107 2207 2208 2108  MATERIAL=  1  AREA=   .30562     TTOP,TBOT=  480.  480.  PRESS=     0.
   NX,NY=   252.    13.  MX,MY,MXY=      9.     2.    -1.  XC,YC,ZC=   -3.753    2.167          .2220E-15
TOP STR  SX,SY,SXY=   1236.  29473.    -52.  SMAX,SMIN,TAUMAX=  29473.   1236.  14118.  A=  -.1  VM=  29475.
MID STR  SX,SY,SXY=      0.  29236.   -185.  SMAX,SMIN,TAUMAX=  29237.     -1.  14619.  A=  -.4  VM=  29238.
BOT STR  SX,SY,SXY=  -1236.  28999.   -317.  SMAX,SMIN,TAUMAX=  29003.  -1239.  15121.  A=  -.6  VM=  29642.

ELEM  255  NODES= 2108 2208 2209 2109  MATERIAL=  1  AREA=   .30562     TTOP,TBOT=  480.  480.  PRESS=     0.
   NX,NY=   430.   -17.  MX,MY,MXY=     13.     4.     0.  XC,YC,ZC=   -4.267    .7524          .2220E-15
TOP STR  SX,SY,SXY=   2031.  30263.     -6.  SMAX,SMIN,TAUMAX=  30263.   2031.  14116.  A=  -.0  VM=  29300.
MID STR  SX,SY,SXY=     24.  29731.      0.  SMAX,SMIN,TAUMAX=  29731.     24.  14853.  A=  .0  VM=  29719.
BOT STR  SX,SY,SXY=  -1482.  29199.      7.  SMAX,SMIN,TAUMAX=  29199.  -1982.  15591.  A=  .0  VM=  30239.

ELEM  256  NODES= 2109 2209 2210 2110  MATERIAL=  1  AREA=   .30562     TTOP,TBOT=  480.  480.  PRESS=     0.
   NX,NY=   244.   -17.  MX,MY,MXY=      9.     4.    -2.  XC,YC,ZC=   -4.267    .7524          .2220E-15
TOP STR  SX,SY,SXY=   1352.  29642.    623.  SMAX,SMIN,TAUMAX=  29655.   1339.  14154.  A=  1.3  VM=  29009.
MID STR  SX,SY,SXY=    -38.  29027.    282.  SMAX,SMIN,TAUMAX=  29030.    -41.  14534.  A=  .6  VM=  29050.
BOT STR  SX,SY,SXY=  -1429.  28413.    -58.  SMAX,SMIN,TAUMAX=  28413.  -1429.  14921.  A=  -.1  VM=  29154.

ELEM  257  NODES= 2110 2210 2211 2111  MATERIAL=  1  AREA=   .30562     TTOP,TBOT=  480.  480.  PRESS=     0.
   NX,NY=   253.   -17.  MX,MY,MXY=      9.     0.    -0.  XC,YC,ZC=   -3.753   -2.167          .2220E-15
TOP STR  SX,SY,SXY=   1391.  29214.   -303.  SMAX,SMIN,TAUMAX=  29266.   1338.  13939.  A=  -.6  VM=  28537.
MID STR  SX,SY,SXY=     56.  29238.   -324.  SMAX,SMIN,TAUMAX=  29242.     52.  14595.  A=  -.6  VM=  29216.
BOT STR  SX,SY,SXY=  -1280.  29274.   -345.  SMAX,SMIN,TAUMAX=  29278.  -1284.  15281.  A=  -.6  VM=  29940.

ELEM  258  NODES= 2111 2211 2212 2112  MATERIAL=  1  AREA=   .30562     TTOP,TBOT=  480.  480.  PRESS=     0.
   NX,NY=   250.   -17.  MX,MY,MXY=     14.     7.    -2.  XC,YC,ZC=   -2.785   -3.319          .2220E-15
TOP STR  SX,SY,SXY=   2052.  30174.    230.  SMAX,SMIN,TAUMAX=  30174.   2050.  14062.  A=  .5  VM=  29203.
MID STR  SX,SY,SXY=    -61.  29089.    -32.  SMAX,SMIN,TAUMAX=  29089.    -61.  14575.  A=  -.1  VM=  29119.
BOT STR  SX,SY,SXY=  -2174.  28907.   -294.  SMAX,SMIN,TAUMAX=  28907.  -2177.  15092.  A=  -.6  VM=  29157.

ELEM  259  NODES= 2112 2212 2213 2113  MATERIAL=  1  AREA=   .30562     TTOP,TBOT=  480.  480.  PRESS=     0.
   NX,NY=   244.   -13.  MX,MY,MXY=     10.     2.    -1.  XC,YC,ZC=   -1.482   -4.072          .2220E-15
TOP STR  SX,SY,SXY=   1625.  28984.    269.  SMAX,SMIN,TAUMAX=  28984.   1623.  13680.  A=  .6  VM=  26207.
MID STR  SX,SY,SXY=     77.  29215.    115.  SMAX,SMIN,TAUMAX=  29215.     77.  14569.  A=  .2  VM=  29177.
BOT STR  SX,SY,SXY=  -1471.  29449.    -40.  SMAX,SMIN,TAUMAX=  29449.  -1471.  15460.  A=  -.1  VM=  30211.

ELEM  260  NODES= 2113 2213 2214 2114  MATERIAL=  1  AREA=   .30562     TTOP,TBOT=  480.  480.  PRESS=     0.
   NX,NY=   244.    13.  MX,MY,MXY=      9.     6.     1.  XC,YC,ZC=   .4631E-10   -4.333          .2220E-15
TOP STR  SX,SY,SXY=   1244.  29494.   -461.  SMAX,SMIN,TAUMAX=  29491.   1240.  14126.  A=  -.9  VM=  28491.
MID STR  SX,SY,SXY=    -34.  29570.   -294.  SMAX,SMIN,TAUMAX=  29573.    -37.  14820.  A=  -.6  VM=  29597.
BOT STR  SX,SY,SXY=  -1416.  29617.   -129.  SMAX,SMIN,TAUMAX=  29617.  -1416.  14517.  A=  -.3  VM=  29352.

ELEM  261  NODES= 2114 2214 2215 2115  MATERIAL=  1  AREA=   .30562     TTOP,TBOT=  480.  480.  PRESS=     0.
   NX,NY=   -20.   -15.  MX,MY,MXY=     16.     4.     0.  XC,YC,ZC=    1.482   -4.072          .2220E-15
TOP STR  SX,SY,SXY=   2503.  29783.   -104.  SMAX,SMIN,TAUMAX=  29784.   2503.  13640.  A=  -.2  VM=  28614.
MID STR  SX,SY,SXY=     55.  29685.    -67.  SMAX,SMIN,TAUMAX=  29685.     55.  14815.  A=  -.1  VM=  29658.
BOT STR  SX,SY,SXY=  -2393.  29588.    -29.  SMAX,SMIN,TAUMAX=  29588.  -2393.  15990.  A=  -.1  VM=  30854.

ELEM  262  NODES= 2115 2215 2216 2116  MATERIAL=  1  AREA=   .30562     TTOP,TBOT=  480.  480.  PRESS=     0.
   NX,NY=   -17.   -17.  MX,MY,MXY=     11.     6.    -0.  XC,YC,ZC=    2.785   -3.319          .2220E-15
TOP STR  SX,SY,SXY=   1624.  30258.    224.  SMAX,SMIN,TAUMAX=  30258.   1622.  14318.  A=  .5  VM=  29481.
MID STR  SX,SY,SXY=    -64.  29356.    157.  SMAX,SMIN,TAUMAX=  29357.    -64.  14693.  A=  .3  VM=  29372.
BOT STR  SX,SY,SXY=  -1683.  28456.     85.  SMAX,SMIN,TAUMAX=  28456.  -1681.  15068.  A=  .2  VM=  29332.

ELEM  263  NODES= 2116 2216 2217 2117  MATERIAL=  1  AREA=   .30562     TTOP,TBOT=  480.  480.  PRESS=     0.
   NX,NY=   240.   -16.  MX,MY,MXY=     11.     4.    -1.  XC,YC,ZC=    3.753   -2.167          .2220E-15
TOP STR  SX,SY,SXY=   1694.  29958.    -15.  SMAX,SMIN,TAUMAX=  29958.   1694.  14132.  A=  -.0  VM=  29148.
MID STR  SX,SY,SXY=     26.  29385.   -161.  SMAX,SMIN,TAUMAX=  29388.     25.  14681.  A=  -.3  VM=  29374.
BOT STR  SX,SY,SXY=  -1643.  28812.   -308.  SMAX,SMIN,TAUMAX=  28815.  -1641.  15231.  A=  -.6  VM=  29673.

ELEM  264  NODES= 2117 2217 2218 2118  MATERIAL=  1  AREA=   .30562     TTOP,TBOT=  480.  480.  PRESS=     0.
   NX,NY=   -34.   -16.  MX,MY,MXY=     18.     2.     0.  XC,YC,ZC=    4.267   -.7524          .2220E-15
TOP STR  SX,SY,SXY=   2613.  29323.    -50.  SMAX,SMIN,TAUMAX=  29323.   2613.  13355.  A=  -.1  VM=  28108.
MID STR  SX,SY,SXY=    -14.  28996.      4.  SMAX,SMIN,TAUMAX=  28996.    -14.  14505.  A=  .0  VM=  29003.
BOT STR  SX,SY,SXY=  -2640.  28669.     58.  SMAX,SMIN,TAUMAX=  28670.  -2640.  15655.  A=  .1  VM=  30077.

ELEM  265  NODES= 2118 2218 2201 2101  MATERIAL=  1  AREA=   .30562     TTOP,TBOT=  480.  480.  PRESS=     0.
   NX,NY=   267.   -12.  MX,MY,MXY=      9.     5.    -1.  XC,YC,ZC=    4.267   -.7524          .2220E-15
TOP STR  SX,SY,SXY=   1244.  29117.    476.  SMAX,SMIN,TAUMAX=  29126.   1275.  13925.  A=  1.0  VM=  28509.
MID STR  SX,SY,SXY=    -56.  28445.    264.  SMAX,SMIN,TAUMAX=  28448.    -58.  14243.  A=  .5  VM=  28457.
BOT STR  SX,SY,SXY=  -1395.  27733.     52.  SMAX,SMIN,TAUMAX=  27733.  -1395.  14564.  A=  .1  VM=  28457.

ELEM  266  NODES= 2201 2601 2602 2202  MATERIAL=  2  AREA=   .96963     TTOP,TBOT=  516.  516.  PRESS=     0.
   NX,NY=   -21.   -15.  MX,MY,MXY=     33.    15.    -4.  XC,YC,ZC=    3.454    1.994          -.1000E+00
TOP STR  SX,SY,SXY=   9803.  -2356.   1053.  SMAX,SMIN,TAUMAX=   9894.  -2446.   6170.  A= 85.1  VM=  11317.
MID STR  SX,SY,SXY=  -2709.  -8066.   -638.  SMAX,SMIN,TAUMAX=  -2631.  -8140.   2755.  A=-83.3  VM=   7195.
BOT STR  SX,SY,SXY= -15215.  -13775.  -2330.  SMAX,SMIN,TAUMAX= -12057.  -16933.  2438.  A=-36.4  VM=  15098.

ELEM  267  NODES= 2202 2602 2603 2203  MATERIAL=  2  AREA=   .96963     TTOP,TBOT=  516.  516.  PRESS=     0.
```

Max Seff

JOB KIPS PAGE ______

DATE ______

BY Y.E. REV. ______

Some Stresses in the Exhaust HSG

```
      NX,NY=      73.        9.   MX,MY,MXY=       -0.          0.         -0.   XC,YC,ZC=   -2.657          -1.646          -.2900
TOP STR   SX,SY,SXY=     151.      621.     -104.   SMAX,SMIN,TAUMAX=     644.      129.      257.   A=-12.0   VM=     590.
MID STR   SX,SY,SXY=     193.      590.     -121.   SMAX,SMIN,TAUMAX=     624.      160.      232.   A=-15.6   VM=     562.
BOT STR   SX,SY,SXY=     235.      559.     -137.   SMAX,SMIN,TAUMAX=     609.      185.      212.   A=-20.1   VM=     541.

ELEM  327  NODES= 2460 2710 2610 2510  MATERIAL=  2  AREA=    .16910      TTOP,TBOT=   548.   548.   PRESS=     0.
      NX,NY=     -49.      -14.   MX,MY,MXY=        5.          1.          1.   XC,YC,ZC=   -3.479          -1.266          -.2900
TOP STR   SX,SY,SXY=    3009.     -115.      777.   SMAX,SMIN,TAUMAX=    3191.     -297.     1744.   A= 76.8   VM=    3350.
MID STR   SX,SY,SXY=    2334.     -283.      956.   SMAX,SMIN,TAUMAX=    2646.     -595.     1620.   A= 71.9   VM=    2988.
BOT STR   SX,SY,SXY=    1659.     -451.     1136.   SMAX,SMIN,TAUMAX=    2154.     -946.     1550.   A= 66.4   VM=    2752.

ELEM  328  NODES= 2313 2463 2513 2413  MATERIAL=  2  AREA=    .33440      TTOP,TBOT=   515.   515.   PRESS=     0.
      NX,NY=      23.       11.   MX,MY,MXY=        2.          0.         -2.   XC,YC,ZC=   -.5279          -2.994          -.2900
TOP STR   SX,SY,SXY=    -248.      522.     -250.   SMAX,SMIN,TAUMAX=     596.     -322.      459.   A=-16.5   VM=     807.
MID STR   SX,SY,SXY=    -527.      489.     -488.   SMAX,SMIN,TAUMAX=     685.     -723.      704.   A=-21.9   VM=    1220.
BOT STR   SX,SY,SXY=    -806.      455.     -726.   SMAX,SMIN,TAUMAX=     785.    -1137.      961.   A=-24.5   VM=    1675.

ELEM  329  NODES= 2463 2713 2613 2513  MATERIAL=  2  AREA=    .16910      TTOP,TBOT=   548.   548.   PRESS=     0.
      NX,NY=    -102.      -32.   MX,MY,MXY=       12.          2.          3.   XC,YC,ZC=   -.6429          -3.646          -.2900
TOP STR   SX,SY,SXY=    3717.     -155.      557.   SMAX,SMIN,TAUMAX=    3795.     -234.     2014.   A= 82.0   VM=    3917.
MID STR   SX,SY,SXY=    2273.     -427.      919.   SMAX,SMIN,TAUMAX=    2557.     -710.     1633.   A= 72.9   VM=    2976.
BOT STR   SX,SY,SXY=     830.     -699.     1282.   SMAX,SMIN,TAUMAX=    1558.    -1427.     1492.   A= 60.4   VM=    2586.

ELEM  330  NODES= 2316 2466 2516 2416  MATERIAL=  2  AREA=    .33440      TTOP,TBOT=   510.   510.   PRESS=     0.
      NX,NY=      24.       15.   MX,MY,MXY=       -3.         -0.         -1.   XC,YC,ZC=    2.329          -1.954          -.2900
TOP STR   SX,SY,SXY=   -1727.       84.     -771.   SMAX,SMIN,TAUMAX=     368.    -2011.     1189.   A=-20.2   VM=    2218.
MID STR   SX,SY,SXY=   -1330.      118.     -864.   SMAX,SMIN,TAUMAX=     522.    -1734.     1128.   A=-25.0   VM=    2045.
BOT STR   SX,SY,SXY=    -934.      152.     -957.   SMAX,SMIN,TAUMAX=     710.    -1492.     1101.   A=-30.2   VM=    1946.

ELEM  331  NODES= 2466 2716 2616 2516  MATERIAL=  2  AREA=    .16910      TTOP,TBOT=   542.   542.   PRESS=     0.
      NX,NY=     -78.       -5.   MX,MY,MXY=       13.          3.          2.   XC,YC,ZC=    2.836          -2.380          -.2900
TOP STR   SX,SY,SXY=    4357.      590.       77.   SMAX,SMIN,TAUMAX=    4359.      588.     1885.   A= 88.8   VM=    4097.
MID STR   SX,SY,SXY=    2765.      195.      358.   SMAX,SMIN,TAUMAX=    2814.      146.     1334.   A= 82.2   VM=    2744.
BOT STR   SX,SY,SXY=    1172.     -200.      639.   SMAX,SMIN,TAUMAX=    1423.     -451.      937.   A= 68.5   VM=    1695.

ELEM  332  NODES= 2401 2301 2302 2402  MATERIAL=  2  AREA=    .34313      TTOP,TBOT=   495.   495.   PRESS=     0.
      NX,NY=       8.       19.   MX,MY,MXY=        1.         -5.          5.   XC,YC,ZC=    2.217           1.280          -.2900
TOP STR   SX,SY,SXY=      85.    -7159.    -2479.   SMAX,SMIN,TAUMAX=     852.    -7926.     4389.   A=-72.8   VM=    8384.
MID STR   SX,SY,SXY=    -341.    -5071.     -635.   SMAX,SMIN,TAUMAX=    -258.    -5155.     2449.   A=-82.5   VM=    5031.
BOT STR   SX,SY,SXY=    -768.    -2984.     1209.   SMAX,SMIN,TAUMAX=    -236.    -3516.     1640.   A= 66.2   VM=    3404.

ELEM  333  NODES= 2402 2302 2303 2403  MATERIAL=  2  AREA=    .34313      TTOP,TBOT=   495.   495.   PRESS=     0.
      NX,NY=      29.       -1.   MX,MY,MXY=        4.          9.          1.   XC,YC,ZC=    1.646           1.961          -.2900
TOP STR   SX,SY,SXY=    2595.     -470.     -486.   SMAX,SMIN,TAUMAX=    2670.     -545.     1608.   A=-81.2   VM=    2980.
MID STR   SX,SY,SXY=     986.    -4065.      -82.   SMAX,SMIN,TAUMAX=     987.    -4067.     2527.   A=-89.1   VM=    4640.
BOT STR   SX,SY,SXY=    -623.    -7660.      323.   SMAX,SMIN,TAUMAX=    -609.    -7675.     3533.   A= 87.4   VM=    7390.

ELEM  334  NODES= 2403 2303 2304 2404  MATERIAL=  2  AREA=    .34313      TTOP,TBOT=   515.   515.   PRESS=     0.
      NX,NY=      42.       -6.   MX,MY,MXY=        5.          0.         -6.   XC,YC,ZC=    .8757           2.406          -.2900
TOP STR   SX,SY,SXY=     540.    -5461.     3057.   SMAX,SMIN,TAUMAX=    1823.    -6744.     4283.   A= 67.2   VM=    7817.
MID STR   SX,SY,SXY=   -1469.    -5530.      786.   SMAX,SMIN,TAUMAX=   -1322.    -5677.     2177.   A= 79.4   VM=    5145.
BOT STR   SX,SY,SXY=   -3477.    -5599.    -1486.   SMAX,SMIN,TAUMAX=   -2712.    -6364.     1826.   A=-62.8   VM=    5531.

ELEM  335  NODES= 2404 2304 2305 2405  MATERIAL=  2  AREA=    .34313      TTOP,TBOT=   515.   515.   PRESS=     0.
      NX,NY=      29.       16.   MX,MY,MXY=        3.         -6.          6.   XC,YC,ZC=   -.1308E-10       2.561          -.2900
TOP STR   SX,SY,SXY=    1110.    -8750.    -2951.   SMAX,SMIN,TAUMAX=    1926.    -9566.     5746.   A=-74.5   VM=   10660.
MID STR   SX,SY,SXY=    -226.    -6270.     -803.   SMAX,SMIN,TAUMAX=    -121.    -6375.     3127.   A=-82.6   VM=    6316.
BOT STR   SX,SY,SXY=   -1562.    -3790.     1345.   SMAX,SMIN,TAUMAX=    -930.    -4423.     1746.   A= 64.8   VM=    4039.

ELEM  336  NODES= 2405 2305 2306 2406  MATERIAL=  2  AREA=    .34313      TTOP,TBOT=   515.   515.   PRESS=     0.
      NX,NY=      35.       -1.   MX,MY,MXY=        4.          9.          1.   XC,YC,ZC=   -.8757           2.406          -.2900
TOP STR   SX,SY,SXY=    1541.    -1617.     -455.   SMAX,SMIN,TAUMAX=    1605.    -1682.     1643.   A=-82.0   VM=    2847.
MID STR   SX,SY,SXY=     -65.    -5242.     -130.   SMAX,SMIN,TAUMAX=     -62.    -5246.     2592.   A=-88.6   VM=    5215.
BOT STR   SX,SY,SXY=   -1672.    -8867.      196.   SMAX,SMIN,TAUM*X=   -1667.    -8873.     3603.   A= 88.4   VM=    8168.

ELEM  337  NODES= 2406 2306 2307 2407  MATERIAL=  2  AREA=    .34313      TTOP,TBOT=   515.   515.   PRESS=     0.
      NX,NY=      56.       -4.   MX,MY,MXY=        7.         -0.         -7.   XC,YC,ZC=   -1.646           1.961          -.2900
TOP STR   SX,SY,SXY=    2354.    -5715.     3416.   SMAX,SMIN,TAUMAX=    3605.    -6967.     5286.   A= 69.9   VM=    9309.
MID STR   SX,SY,SXY=    -328.    -5604.      786.   SMAX,SMIN,TAUMAX=    -213.    -5719.     2753.   A= 81.7   VM=    5615.
BOT STR   SX,SY,SXY=   -3009.    -5494.    -1845.   SMAX,SMIN,TAUMAX=   -2027.    -6476.     2224.   A=-62.0   VM=    5737.

ELEM  338  NODES= 2407 2307 2308 2408  MATERIAL=  2  AREA=    .34313      TTOP,TBOT=   515.   515.   PRESS=     0.
      NX,NY=      52.        8.   MX,MY,MXY=        6.         -3.          5.   XC,YC,ZC=   -2.217           1.280          -.2900
TOP STR   SX,SY,SXY=    2065.    -6970.    -3296.   SMAX,SMIN,TAUMAX=    3158.    -8062.     5600.   A=-72.0   VM=   10002.
MID STR   SX,SY,SXY=    -348.    -5834.     -307.   SMAX,SMIN,TAUMAX=    -231.    -5951.     2860.   A=-81.8   VM=    5838.
BOT STR   SX,SY,SXY=   -2780.    -4699.     1681.   SMAX,SMIN,TAUMAX=   -1804.    -5675.     1935.   A= 59.9   VM=    5022.

ELEM  339  NODES= 2408 2308 2309 2409  MATERIAL=  2  AREA=    .34313      TTOP,TBOT=   515.   515.   PRESS=     0.
      NX,NY=      37.       -0.   MX,MY,MXY=        4.          9.          0.   XC,YC,ZC=   -2.522           .4446          -.2900
TOP STR   SX,SY,SXY=    1555.    -1671.      -26.   SMAX,SMIN,TAUMAX=    1555.    -1671.     1613.   A=-89.5   VM=    2795.
MID STR   SX,SY,SXY=     -37.    -5176.       -5.   SMAX,SMIN,TAUMAX=     -37.    -5176.     2570.   A=-89.9   VM=    5159.
BOT STR   SX,SY,SXY=   -1628.    -8681.       17.   SMAX,SMIN,TAUMAX=   -1628.    -8681.     3526.   A= 89.9   VM=    7992.

ELEM  340  NODES= 2409 2309 2310 2410  MATERIAL=  2  AREA=    .34313      TTOP,TBOT=   515.   515.   PRESS=     0.
      NX,NY=      50.       -8.   MX,MY,MXY=        6.         -3.         -6.   XC,YC,ZC=   -2.522          -.4446          -.2900
TOP STR   SX,SY,SXY=    2039.    -6908.     3262.   SMAX,SMIN,TAUMAX=    3102.    -7971.     5536.   A= 71.9   VM=    9893.
```

JOB EIPS

BY YE

PAGE

DATE

REV.

Exhaust H&G
(Continued)

```
ELEM  341  NODES= 2410 2310 2311 2411  MATERIAL=  2  AREA=    .34313      TTOP,TBOT=  515.   515.  PRESS=     0.
     NX,NY=      34.      4.  MX,MY,MXY=       7.      -0.      7.  XC,YC,ZC=    -2.217      -1.280      -.2900
TOP STR  SX,SY,SXY=   2273.  -5782.  -3363.   SMAX,SMIN,TAUMAX=   3492.  -7002.   5247.   A=-70.1  VM=   9256.
MID STR  SX,SY,SXY=   -338.  -5610.   -791.   SMAX,SMIN,TAUMAX=    -222.  -5726.   2752.   A=-81.6  VM=   5619.
BOT STR  SX,SY,SXY=  -2949.  -5437.   1780.   SMAX,SMIN,TAUMAX=  -2021.  -6365.   2172.   A= 82.5  VM=   5633.

ELEM  342  NODES= 2411 2311 2312 2412  MATERIAL=  2  AREA=    .34313      TTOP,TBOT=  515.   515.  PRESS=     0.
     NX,NY=      35.      1.  MX,MY,MXY=       4.       9.      -1.  XC,YC,ZC=    -1.648      -1.961      -.2900
TOP STR  SX,SY,SXY=   1545.  -1678.    385.   SMAX,SMIN,TAUMAX=   1591.  -1724.   1657.   A= 83.3  VM=   2871.
MID STR  SX,SY,SXY=    -27.  -5187.    106.   SMAX,SMIN,TAUMAX=    -25.  -5188.   2579.   A= 81.8  VM=   5171.
BOT STR  SX,SY,SXY=  -1630.  -8885.   -173.   SMAX,SMIN,TAUMAX=  -1596.  -8690.   3547.   A=-88.6  VM=   6012.

ELEM  343  NODES= 2412 2312 2313 2413  MATERIAL=  2  AREA=    .34313      TTOP,TBOT=  515.   515.  PRESS=     0.
     NX,NY=      20.     -16.  MX,MY,MXY=       3.      -6.      -5.  XC,YC,ZC=    -.4757      -2.406      -.2900
TOP STR  SX,SY,SXY=    974.  -4516.   2878.   SMAX,SMIN,TAUMAX=   1782.  -9320.   5551.   A= 74.4  VM=  10327.
MID STR  SX,SY,SXY=   -342.  -6164.    794.   SMAX,SMIN,TAUMAX=    -255.  -6274.   3010.   A= 83.4  VM=   6151.
BOT STR  SX,SY,SXY=  -1731.  -3820.  -1290.   SMAX,SMIN,TAUMAX=  -1091.  -4430.   1669.   A=-64.7  VM=   3997.

ELEM  344  NODES= 2413 2313 2314 2414  MATERIAL=  2  AREA=    .34313      TTOP,TBOT=  515.   515.  PRESS=     0.
     NX,NY=      37.      1.  MX,MY,MXY=       5.       7.      -2.  XC,YC,ZC=    .3919E-10      -2.561      -.2900
TOP STR  SX,SY,SXY=   1371.  -6640.  -3429.   SMAX,SMIN,TAUMAX=   2659.  -7747.   5213.   A=-69.4  VM=   9383.
MID STR  SX,SY,SXY=   -415.  -5342.   -695.   SMAX,SMIN,TAUMAX=    -327.  -5430.   2801.   A=-82.8  VM=   5773.
BOT STR  SX,SY,SXY=  -2202.  -4204.   2039.   SMAX,SMIN,TAUMAX=  -1171.  -6235.   2532.   A= 63.2  VM=   5740.

ELEM  345  NODES= 2414 2314 2315 2415  MATERIAL=  2  AREA=    .34313      TTOP,TBOT=  515.   515.  PRESS=     0.
     NX,NY=      35.       4.  MX,MY,MXY=       5.      12.      -1.  XC,YC,ZC=    -.8757      -2.406      -.2900
TOP STR  SX,SY,SXY=   2049.   -167.    566.   SMAX,SMIN,TAUMAX=   2203.   -971.   1587.   A= 79.6  VM=   2817.
MID STR  SX,SY,SXY=    135.  -5667.    220.   SMAX,SMIN,TAUMAX=    193.  -5675.   2934.   A= 87.9  VM=   5774.
BOT STR  SX,SY,SXY=  -1730.  -10667.   -126.   SMAX,SMIN,TAUMAX=  -1728.  -10669.  4370.   A=-89.2  VM=   9721.

ELEM  346  NODES= 2415 2315 2316 2416  MATERIAL=  2  AREA=    .34313      TTOP,TBOT=  515.   515.  PRESS=     0.
     NX,NY=      12.     -21.  MX,MY,MXY=       2.      -7.      -6.  XC,YC,ZC=     1.046      -1.981      -.2900
TOP STR  SX,SY,SXY=   -414.  -3679.   3063.   SMAX,SMIN,TAUMAX=    524.  -10417.   5470.   A= 73.0  VM=  10688.
MID STR  SX,SY,SXY=  -1034.  -6880.    679.   SMAX,SMIN,TAUMAX=   -920.  -6957.   3015.   A= 83.5  VM=   6543.
BOT STR  SX,SY,SXY=  -1594.  -4281.  -1706.   SMAX,SMIN,TAUMAX=   -766.  -5108.   2171.   A=-64.1  VM=   4772.

ELEM  347  NODES= 2416 2316 2317 2417  MATERIAL=  2  AREA=    .34313      TTOP,TBOT=  500.   500.  PRESS=     0.
     NX,NY=      20.      13.  MX,MY,MXY=       2.      -2.       4.  XC,YC,ZC=     2.217      -1.280      -.2900
TOP STR  SX,SY,SXY=   1601.  -6183.  -2503.   SMAX,SMIN,TAUMAX=   2154.  -6735.   4545.   A=-73.3  VM=   8226.
MID STR  SX,SY,SXY=    443.  -5293.   -959.   SMAX,SMIN,TAUMAX=    667.  -5423.   3045.   A=-81.8  VM=   5765.
BOT STR  SX,SY,SXY=   -318.  -4414.    784.   SMAX,SMIN,TAUMAX=   -173.  -4559.   2193.   A= 79.5  VM=   4476.

ELEM  348  NODES= 2417 2317 2318 2418  MATERIAL=  2  AREA=    .34313      TTOP,TBOT=  500.   500.  PRESS=     0.
     NX,NY=      27.      -0.  MX,MY,MXY=       4.       9.      -0.  XC,YC,ZC=     2.522      -.4446      -.2900
TOP STR  SX,SY,SXY=   1277.   -619.     76.   SMAX,SMIN,TAUMAX=   1280.   -622.    951.   A= 87.7  VM=   1680.
MID STR  SX,SY,SXY=   -210.  -4094.    -37.   SMAX,SMIN,TAUMAX=   -209.  -4095.   1943.   A=-89.4  VM=   3994.
BOT STR  SX,SY,SXY=  -1697.  -7559.   -151.   SMAX,SMIN,TAUMAX=  -1693.  -7573.   2940.   A=-88.5  VM=   6885.

ELEM  349  NODES= 2418 2318 2301 2401  MATERIAL=  2  AREA=    .34313      TTOP,TBOT=  500.   500.  PRESS=     0.
     NX,NY=      17.     -14.  MX,MY,MXY=       2.      -4.      -1.  XC,YC,ZC=     2.522      .4446      -.2900
TOP STR  SX,SY,SXY=    141.  -5148.   2304.   SMAX,SMIN,TAUMAX=    928.  -5943.   3435.   A= 72.1  VM=   7450.
MID STR  SX,SY,SXY=   -417.  -4260.    713.   SMAX,SMIN,TAUMAX=   -367.  -4309.   2381.   A= 81.3  VM=   4923.
BOT STR  SX,SY,SXY=  -1015.  -3722.   -877.   SMAX,SMIN,TAUMAX=   -757.  -3981.   1612.   A=-73.5  VM=   3662.

ELEM  350  NODES= 2701 2751 2752 2702  MATERIAL=  2  AREA=    3.6247      TTOP,THOT=  447.   447.  PRESS=     0.
     NX,NY=      20.      1.  MX,MY,MXY=       2.       1.       0.  XC,YC,ZC=     4.200       2.425      -1.215
TOP STR  SX,SY,SXY=   4179.   4744.   -554.   SMAX,SMIN,TAUMAX=   5063.   3860.    622.   A=-31.5  VM=   4589.
MID STR  SX,SY,SXY=    429.   3139.   -254.   SMAX,SMIN,TAUMAX=   3162.    405.   1378.   A= -5.3  VM=   2880.
BOT STR  SX,SY,SXY=  -3321.   1533.     46.   SMAX,SMIN,TAUMAX=   1534.  -3322.   2428.   A=   .5  VM=   4299.

ELEM  351  NODES= 2702 2752 2753 2703  MATERIAL=  2  AREA=    3.6247      TTOP,THOT=  447.   447.  PRESS=     0.
     NX,NY=       1.       0.  MX,MY,MXY=       3.       1.       0.  XC,YC,ZC=     3.118       3.715      -1.215
TOP STR  SX,SY,SXY=   5136.   5656.   -330.   SMAX,SMIN,TAUMAX=   5817.   4978.    420.   A=-26.0  VM=   5446.
MID STR  SX,SY,SXY=    940.   3715.    -44.   SMAX,SMIN,TAUMAX=   3716.    939.   1388.   A=  -.9  VM=   3346.
BOT STR  SX,SY,SXY=  -3254.   1774.    243.   SMAX,SMIN,TAUMAX=   1785.  -3271.   2528.   A=  2.8  VM=   4441.

ELEM  352  NODES= 2703 2753 2754 2704  MATERIAL=  2  AREA=    3.6247      TTOP,THOT=  448.   448.  PRESS=     0.
     NX,NY=       2.      -0.  MX,MY,MXY=       2.       1.       0.  XC,YC,ZC=     1.659       4.558      -1.215
TOP STR  SX,SY,SXY=   4051.   4448.   -103.   SMAX,SMIN,TAUMAX=   4461.   4038.    412.   A= -7.2  VM=   4506.
MID STR  SX,SY,SXY=    177.   3182.    165.   SMAX,SMIN,TAUMAX=   3191.    168.   1511.   A=  3.1  VM=   3110.
BOT STR  SX,SY,SXY=  -3696.   1515.    432.   SMAX,SMIN,TAUMAX=   1551.  -3732.   2641.   A=  4.7  VM=   4703.

ELEM  353  NODES= 2704 2754 2755 2705  MATERIAL=  2  AREA=    3.6247      TTOP,THOT=  448.   448.  PRESS=     0.
     NX,NY=       2.       1.  MX,MY,MXY=       2.       1.       0.  XC,YC,ZC=    -.2477E-10       4.850      -1.215
TOP STR  SX,SY,SXY=   4122.   4638.   -517.   SMAX,SMIN,TAUMAX=   4957.   3802.    578.   A=-31.7  VM=   4493.
MID STR  SX,SY,SXY=    204.   3066.   -214.   SMAX,SMIN,TAUMAX=   3082.    276.   1402.   A= -4.4  VM=   2953.
BOT STR  SX,SY,SXY=  -3433.   1492.     88.   SMAX,SMIN,TAUMAX=   1494.  -3534.   2514.   A=  1.0  VM=   4473.

ELEM  354  NODES= 2705 2755 2756 2706  MATERIAL=  2  AREA=    3.6247      TTOP,THOT=  448.   448.  PRESS=     0.
     NX,NY=       1.       0.  MX,MY,MXY=       3.       1.       0.  XC,YC,ZC=    -1.659       4.558      -1.215
TOP STR  SX,SY,SXY=   5017.   5517.   -281.   SMAX,SMIN,TAUMAX=   5722.   4812.    455.   A=-28.4  VM=   5326.
MID STR  SX,SY,SXY=    764.   3522.    -49.   SMAX,SMIN,TAUMAX=   3525.    765.   1380.   A= -1.9  VM=   3212.
BOT STR  SX,SY,SXY=  -3481.   1528.    203.   SMAX,SMIN,TAUMAX=   1536.  -3489.   2513.   A=  2.3  VM=   4460.

ELEM  355  NODES= 2706 2756 2757 2707  MATERIAL=  2  AREA=    3.6247      TTOP,THOT=  448.   448.  PRESS=     0.
```

JOB KIPS

BY Y.E.

PAGE

DATE

REV.

Same Stresses in the Generator H's G

```
                NX,NY=    -38.      -2.   MX,MY,MXY=      1.       -.       1.   XC,YC,ZC=      .5570          1.5          -2.
TOP STR  SX,SY,SXY=     466.    -2495.    -2026.   SMAX,SMIN,TAUMAX=    1417.    -3447.    2932.   A=-66.4   VM=    4718.
MID STR  SX,SY,SXY=      27.    -1820.    -1220.   SMAX,SMIN,TAUMAX=     634.    -2427.    1530.   A=-63.6   VM=    2995.
BOT STR  SX,SY,SXY=    -412.     -745.     -415.   SMAX,SMIN,TAUMAX=    -132.    -1026.     447.   A=-55.9   VM=     967.

ELEM  459  NODES= 3002 3102 3103 3003  MATERIAL=  2  AREA=   .41415          TTOP,TBOT=  313.  313.  PRESS=     0.
                NX,NY=    -46.      4.   MX,MY,MXY=      2.       -1.       -0.   XC,YC,ZC=      1.676          1.999        -2.425
TOP STR  SX,SY,SXY=     654.    -3333.     -267.   SMAX,SMIN,TAUMAX=     672.    -3350.    2011.   A=-86.2   VM=    3732.
MID STR  SX,SY,SXY=    -500.    -2448.     -495.   SMAX,SMIN,TAUMAX=    -382.    -2567.    1092.   A=-76.5   VM=    2399.
BOT STR  SX,SY,SXY=   -1654.    -1964.     -722.   SMAX,SMIN,TAUMAX=    -885.    -2933.     724.   A=-43.2   VM=    2040.

ELEM  460  NODES= 3003 3103 3104 3004  MATERIAL=  2  AREA=   .41415          TTOP,TBOT=  313.  313.  PRESS=     0.
                NX,NY=    -50.      -1.   MX,MY,MXY=      2.        1.       -0.   XC,YC,ZC=      .6926          2.452        -2.425
TOP STR  SX,SY,SXY=    1118.    -2424.      129.   SMAX,SMIN,TAUMAX=    1122.    -2427.    1775.   A= 87.9   VM=    3144.
MID STR  SX,SY,SXY=    -201.    -3102.     -143.   SMAX,SMIN,TAUMAX=    -194.    -3109.    1457.   A=-87.2   VM=    3016.
BOT STR  SX,SY,SXY=   -1520.    -3780.     -415.   SMAX,SMIN,TAUMAX=   -1446.    -3854.    1204.   A=-79.9   VM=    3372.

ELEM  461  NODES= 3004 3104 3105 3005  MATERIAL=  2  AREA=   .41415          TTOP,TBOT=  313.  313.  PRESS=     0.
                NX,NY=    -39.      -1.   MX,MY,MXY=      2.        1.       -0.   XC,YC,ZC=    -.1333E-10       2.610        -2.425
TOP STR  SX,SY,SXY=    1525.    -2353.       65.   SMAX,SMIN,TAUMAX=    1526.    -2355.    1941.   A= 89.0   VM=    3886.
MID STR  SX,SY,SXY=     305.    -3171.       37.   SMAX,SMIN,TAUMAX=     305.    -3172.    1738.   A= 89.4   VM=    3334.
BOT STR  SX,SY,SXY=    -916.    -3989.        8.   SMAX,SMIN,TAUMAX=    -916.    -3989.    1536.   A= 89.8   VM=    3619.

ELEM  462  NODES= 3005 3105 3106 3006  MATERIAL=  2  AREA=   .41415          TTOP,TBOT=  313.  313.  PRESS=     0.
                NX,NY=    -31.      -0.   MX,MY,MXY=      2.        1.        0.   XC,YC,ZC=      .6926          2.452        -2.425
TOP STR  SX,SY,SXY=    1624.    -2589.      -22.   SMAX,SMIN,TAUMAX=    1624.    -2589.    2107.   A=-89.7   VM=    4060.
MID STR  SX,SY,SXY=     404.    -2906.       41.   SMAX,SMIN,TAUMAX=     404.    -2907.    1655.   A= 89.7   VM=    3184.
BOT STR  SX,SY,SXY=    -816.    -3223.      104.   SMAX,SMIN,TAUMAX=    -812.    -3227.    1208.   A= 87.5   VM=    2901.

ELEM  463  NODES= 3006 3106 3107 3007  MATERIAL=  2  AREA=   .41415          TTOP,TBOT=  313.  313.  PRESS=     0.
                NX,NY=    -42.       0.   MX,MY,MXY=      2.        1.        0.   XC,YC,ZC=     -1.678          1.999        -2.425
TOP STR  SX,SY,SXY=    1647.    -2621.      -79.   SMAX,SMIN,TAUMAX=    1649.    -2623.    2136.   A=-88.9   VM=    3731.
MID STR  SX,SY,SXY=     310.    -2961.      -31.   SMAX,SMIN,TAUMAX=     310.    -2964.    1637.   A=-89.5   VM=    3110.
BOT STR  SX,SY,SXY=   -1027.    -3305.       17.   SMAX,SMIN,TAUMAX=   -1027.    -3305.    1139.   A= 89.6   VM=    2930.

ELEM  464  NODES= 3007 3107 3108 3008  MATERIAL=  2  AREA=   .41415          TTOP,TBOT=  313.  313.  PRESS=     0.
                NX,NY=    -42.      -0.   MX,MY,MXY=      2.        1.        0.   XC,YC,ZC=     -2.260          1.305        -2.425
TOP STR  SX,SY,SXY=    1609.    -2614.      -28.   SMAX,SMIN,TAUMAX=    1609.    -2616.    2112.   A=-89.6   VM=    3693.
MID STR  SX,SY,SXY=     287.    -3006.      -16.   SMAX,SMIN,TAUMAX=     287.    -3006.    1646.   A=-89.7   VM=    3154.
BOT STR  SX,SY,SXY=   -1035.    -3396.       -8.   SMAX,SMIN,TAUMAX=   -1035.    -3396.    1180.   A=-89.8   VM=    3015.

ELEM  465  NODES= 3008 3108 3109 3009  MATERIAL=  2  AREA=   .41415          TTOP,TBOT=  313.  313.  PRESS=     0.
                NX,NY=    -41.      -0.   MX,MY,MXY=      2.        0.       -0.   XC,YC,ZC=     -2.570          .4532        -2.425
TOP STR  SX,SY,SXY=    1540.    -2681.        5.   SMAX,SMIN,TAUMAX=    1540.    -2681.    2110.   A= 89.9   VM=    3700.
MID STR  SX,SY,SXY=     306.    -2919.        5.   SMAX,SMIN,TAUMAX=     306.    -2919.    1613.   A= 89.9   VM=    3084.
BOT STR  SX,SY,SXY=    -928.    -3157.        5.   SMAX,SMIN,TAUMAX=    -928.    -3157.    1115.   A= 89.9   VM=    2811.

ELEM  466  NODES= 3009 3109 3110 3010  MATERIAL=  2  AREA=   .41415          TTOP,TBOT=  313.  313.  PRESS=     0.
                NX,NY=    -42.       0.   MX,MY,MXY=      2.        1.       -0.   XC,YC,ZC=     -2.570          -.4532       -2.425
TOP STR  SX,SY,SXY=    1605.    -2619.       33.   SMAX,SMIN,TAUMAX=    1606.    -2619.    2113.   A= 89.6   VM=    3694.
MID STR  SX,SY,SXY=     285.    -2998.       19.   SMAX,SMIN,TAUMAX=     285.    -2998.    1642.   A= 89.7   VM=    3151.
BOT STR  SX,SY,SXY=   -1035.    -3377.        6.   SMAX,SMIN,TAUMAX=   -1035.    -3377.    1171.   A= 89.8   VM=    2997.

ELEM  467  NODES= 3010 3110 3111 3011  MATERIAL=  2  AREA=   .41415          TTOP,TBOT=  313.  313.  PRESS=     0.
                NX,NY=    -42.      -0.   MX,MY,MXY=      2.        1.       -0.   XC,YC,ZC=     -2.260          -1.305       -2.425
TOP STR  SX,SY,SXY=    1660.    -2606.       81.   SMAX,SMIN,TAUMAX=    1662.    -2607.    2135.   A= 88.9   VM=    3727.
MID STR  SX,SY,SXY=     315.    -2965.       30.   SMAX,SMIN,TAUMAX=     316.    -2966.    1641.   A= 89.5   VM=    3136.
BOT STR  SX,SY,SXY=   -1029.    -3325.      -22.   SMAX,SMIN,TAUMAX=   -1029.    -3325.    1148.   A=-89.4   VM=    2947.

ELEM  468  NODES= 3011 3111 3112 3012  MATERIAL=  2  AREA=   .41415          TTOP,TBOT=  313.  313.  PRESS=     0.
                NX,NY=    -41.       0.   MX,MY,MXY=      2.        1.       -0.   XC,YC,ZC=     -1.678          -1.999       -2.425
TOP STR  SX,SY,SXY=    1639.    -2564.       32.   SMAX,SMIN,TAUMAX=    1639.    -2564.    2102.   A= 89.6   VM=    3669.
MID STR  SX,SY,SXY=     342.    -2921.      -28.   SMAX,SMIN,TAUMAX=     342.    -2921.    1656.   A=-89.5   VM=    3137.
BOT STR  SX,SY,SXY=    -856.    -3278.      -88.   SMAX,SMIN,TAUMAX=    -853.    -3291.    1214.   A=-87.9   VM=    2949.

ELEM  469  NODES= 3012 3112 3113 3013  MATERIAL=  2  AREA=   .41415          TTOP,TBOT=  313.  313.  PRESS=     0.
                NX,NY=    -39.       1.   MX,MY,MXY=      2.        1.        0.   XC,YC,ZC=     -.6926          -2.452       -2.425
TOP STR  SX,SY,SXY=    1514.    -2356.      -47.   SMAX,SMIN,TAUMAX=    1514.    -2356.    1935.   A=-89.3   VM=    3378.
MID STR  SX,SY,SXY=     253.    -3169.      -19.   SMAX,SMIN,TAUMAX=     253.    -3169.    1711.   A=-89.7   VM=    3303.
BOT STR  SX,SY,SXY=   -1008.    -3982.        8.   SMAX,SMIN,TAUMAX=   -1008.    -3982.    1487.   A= 89.8   VM=    3586.

ELEM  470  NODES= 3013 3113 3114 3014  MATERIAL=  2  AREA=   .41415          TTOP,TBOT=  313.  313.  PRESS=     0.
                NX,NY=    -41.      -1.   MX,MY,MXY=      2.        1.        0.   XC,YC,ZC=     .3994E-10       2.610        -2.425
TOP STR  SX,SY,SXY=    1126.    -2456.     -116.   SMAX,SMIN,TAUMAX=    1130.    -2459.    1795.   A=-88.1   VM=    3179.
MID STR  SX,SY,SXY=    -252.    -3104.      132.   SMAX,SMIN,TAUMAX=    -245.    -3110.    1432.   A= 87.4   VM=    2995.
BOT STR  SX,SY,SXY=   -1629.    -3752.      380.   SMAX,SMIN,TAUMAX=   -1563.    -3818.    1127.   A= 80.2   VM=    3324.

ELEM  471  NODES= 3014 3114 3115 3015  MATERIAL=  2  AREA=   .41415          TTOP,TBOT=  313.  313.  PRESS=     0.
                NX,NY=    -47.      -4.   MX,MY,MXY=      2.        1.       -0.   XC,YC,ZC=     -.6926          -2.452       -2.425
TOP STR  SX,SY,SXY=     782.    -3354.      256.   SMAX,SMIN,TAUMAX=     791.    -3364.    2083.   A= 86.5   VM=    3831.
MID STR  SX,SY,SXY=    -483.    -2494.      464.   SMAX,SMIN,TAUMAX=    -381.    -2595.    1107.   A= 77.6   VM=    2427.
BOT STR  SX,SY,SXY=   -1748.    -1634.      671.   SMAX,SMIN,TAUMAX=   -1017.    -2364.     674.   A= 42.6   VM=    2054.

ELEM  472  NODES= 3015 3115 3116 3016  MATERIAL=  2  AREA=   .41415          TTOP,TBOT=  313.  313.  PRESS=     0.
                NX,NY=    -36.       2.   MX,MY,MXY=      1.       -2.       -1.   XC,YC,ZC=      1.678          -1.999       -2.425
TOP STR  SX,SY,SXY=     624.    -2443.     2013.   SMAX,SMIN,TAUMAX=    1562.    -3380.    2474.   A= 85.6   VM=    4768.
```

Max Geff

JOB 21PS

BY YE

PAGE

DATE

REV.

Generator HSG
(Continued)

```
ELEM  473  NODES= 3016 3116 3117 3017  MATERIAL=  2  AREA=    .41415        TTOP,TBOT=  313.  313.  PRESS=  -90.
     NX,NY=     -5.    60.  MX,MY,MXY=     -1.     1.    -2.  XC,YC,ZC=    2.260    -1.305    -2.425
TOP STR  SX,SY,SXY=    350.   -794.   2291.   SMAX,SMIN,TAUMAX=   2138.   -2584.   2361.   A= 52.0  VM=   4096.
MID STR  SX,SY,SXY=   1019.  -1380.   1278.   SMAX,SMIN,TAUMAX=   1672.   -1938.   1755.   A= 66.6  VM=   3045.
BOT STR  SX,SY,SXY=   1687.  -1975.    266.   SMAX,SMIN,TAUMAX=   1707.   -1994.   1850.   A= 85.9  VM=   3208.

ELEM  474  NODES= 3017 3117 3118 3018  MATERIAL=  2  AREA=    .41415        TTOP,TBOT=  313.  313.  PRESS=  -90.
     NX,NY=     -1.     0.  MX,MY,MXY=     -2.     2.     0.  XC,YC,ZC=    2.570    -.4532    -2.425
TOP STR  SX,SY,SXY=    144.    307.    -14.   SMAX,SMIN,TAUMAX=    309.    147.     81.   A= -5.2  VM=    267.
MID STR  SX,SY,SXY=   1494.  -1015.      4.   SMAX,SMIN,TAUMAX=   1494.   -1015.   1254.   A= 89.9  VM=   2186.
BOT STR  SX,SY,SXY=   2839.  -2337.     22.   SMAX,SMIN,TAUMAX=   2839.   -2337.   2588.   A= 89.8  VM=   4490.

ELEM  475  NODES= 3018 3118 3101 3001  MATERIAL=  2  AREA=    .41415        TTOP,TBOT=  313.  313.  PRESS=  -90.
     NX,NY=     -5.     2.  MX,MY,MXY=     -1.     1.     2.  XC,YC,ZC=    2.570    -.4532    -2.425
TOP STR  SX,SY,SXY=    262.    -776.  -2306.   SMAX,SMIN,TAUMAX=    2107.   -2620.   2363.   A=-51.3  VM=   4101.
MID STR  SX,SY,SXY=    908.   -1362.  -1279.   SMAX,SMIN,TAUMAX=    1526.   -1919.   1723.   A=-56.3  VM=   2990.
BOT STR  SX,SY,SXY=   1674.   -1948.   -242.   SMAX,SMIN,TAUMAX=    1689.   -1963.   1826.   A=-86.3  VM=   3166.

ELEM  476  NODES= 3001 3151 3152 3002  MATERIAL=  2  AREA=    .38357        TTOP,TBOT=  313.  313.  PRESS=  -90.
     NX,NY=     -4.    -1.  MX,MY,MXY=     -4.    -1.    -1.  XC,YC,ZC=    2.345     1.354    -2.375
TOP STR  SX,SY,SXY=  -3512.   -1264.    455.   SMAX,SMIN,TAUMAX=   -1177.   -3601.   1211.   A= 11.0  VM=   3180.
MID STR  SX,SY,SXY=    -97.      31.    -79.   SMAX,SMIN,TAUMAX=      68.    -134.    101.   A=-25.4  VM=    179.
BOT STR  SX,SY,SXY=   3318.    1330.   -613.   SMAX,SMIN,TAUMAX=    3492.    1157.   1168.   A=-74.2  VM=   3081.

ELEM  477  NODES= 3002 3152 3153 3003  MATERIAL=  2  AREA=    .38357        TTOP,TBOT=  313.  313.  PRESS=  -90.
     NX,NY=     -2.    -3.  MX,MY,MXY=     -5.    -2.    -0.  XC,YC,ZC=    1.741     2.075    -2.375
TOP STR  SX,SY,SXY=  -4637.   -1333.    431.   SMAX,SMIN,TAUMAX=   -1277.   -4692.   1707.   A=  7.3  VM=   4202.
MID STR  SX,SY,SXY=   -313.     166.    275.   SMAX,SMIN,TAUMAX=     307.    -435.    371.   A= 23.9  VM=    646.
BOT STR  SX,SY,SXY=   4010.    1705.    118.   SMAX,SMIN,TAUMAX=    4016.    1699.   1159.   A= 87.1  VM=   3492.

ELEM  478  NODES= 3003 3153 3154 3004  MATERIAL=  2  AREA=    .38357        TTOP,TBOT=  313.  313.  PRESS=  -90.
     NX,NY=     25.     3.  MX,MY,MXY=     -3.    -0.     0.  XC,YC,ZC=    .9263     2.545    -2.375
TOP STR  SX,SY,SXY=  -3309.    -385.    175.   SMAX,SMIN,TAUMAX=    -375.   -3409.   1517.   A=  3.3  VM=   3238.
MID STR  SX,SY,SXY=   -459.      19.    144.   SMAX,SMIN,TAUMAX=      82.    -521.    301.   A= 18.8  VM=    566.
BOT STR  SX,SY,SXY=   2482.     423.    193.   SMAX,SMIN,TAUMAX=    2500.     405.   1047.   A= 84.7  VM=   2324.

ELEM  479  NODES= 3004 3154 3155 3005  MATERIAL=  2  AREA=    .38357        TTOP,TBOT=  313.  313.  PRESS=  -90.
     NX,NY=     14.     1.  MX,MY,MXY=     -2.    -0.    -0.  XC,YC,ZC=   -.133E-10    2.708    -2.375
TOP STR  SX,SY,SXY=  -2174.    -159.    -93.   SMAX,SMIN,TAUMAX=    -155.   -2183.   1014.   A= -2.5  VM=   2109.
MID STR  SX,SY,SXY=   -200.    -116.   -200.   SMAX,SMIN,TAUMAX=      46.    -363.    204.   A=-39.1  VM=    388.
BOT STR  SX,SY,SXY=   1778.     -73.   -310.   SMAX,SMIN,TAUMAX=    1829.    -124.    976.   A=-80.7  VM=   1894.

ELEM  480  NODES= 3005 3155 3156 3006  MATERIAL=  2  AREA=    .38357        TTOP,TBOT=  313.  313.  PRESS=  -90.
     NX,NY=     12.     0.  MX,MY,MXY=     -2.    -0.    -0.  XC,YC,ZC=    -.9263     2.545    -2.375
TOP STR  SX,SY,SXY=  -1817.    -341.     33.   SMAX,SMIN,TAUMAX=    -340.   -1818.    739.   A=  1.3  VM=   1674.
MID STR  SX,SY,SXY=    104.     -44.   -125.   SMAX,SMIN,TAUMAX=     175.    -115.    145.   A=-40.2  VM=    254.
BOT STR  SX,SY,SXY=   2025.     254.   -283.   SMAX,SMIN,TAUMAX=    2069.     210.    930.   A=-81.1  VM=   1972.

ELEM  481  NODES= 3006 3156 3157 3007  MATERIAL=  2  AREA=    .38357        TTOP,TBOT=  313.  313.  PRESS=  -90.
     NX,NY=     13.     1.  MX,MY,MXY=     -2.    -0.    -0.  XC,YC,ZC=   -1.741     2.075    -2.375
TOP STR  SX,SY,SXY=  -2044.    -481.    200.   SMAX,SMIN,TAUMAX=    -456.   -2069.    807.   A=  7.2  VM=   1883.
MID STR  SX,SY,SXY=     -4.    -157.     53.   SMAX,SMIN,TAUMAX=      13.    -174.     93.   A= 72.6  VM=    180.
BOT STR  SX,SY,SXY=   2035.     167.    -94.   SMAX,SMIN,TAUMAX=    2040.     162.    939.   A=-87.1  VM=   1964.

ELEM  482  NODES= 3007 3157 3158 3008  MATERIAL=  2  AREA=    .38357        TTOP,TBOT=  313.  313.  PRESS=  -90.
     NX,NY=     15.     1.  MX,MY,MXY=     -2.    -0.    -0.  XC,YC,ZC=   -2.345     1.354    -2.375
TOP STR  SX,SY,SXY=  -2197.    -547.    136.   SMAX,SMIN,TAUMAX=    -536.   -2208.    836.   A=  4.7  VM=   1995.
MID STR  SX,SY,SXY=    -42.    -212.    -31.   SMAX,SMIN,TAUMAX=     -37.    -216.     90.   A=-80.0  VM=    202.
BOT STR  SX,SY,SXY=   2112.     122.   -198.   SMAX,SMIN,TAUMAX=    2132.     103.   1015.   A=-84.4  VM=   2082.

ELEM  483  NODES= 3008 3158 3159 3009  MATERIAL=  2  AREA=    .38357        TTOP,TBOT=  313.  313.  PRESS=  -90.
     NX,NY=     12.     1.  MX,MY,MXY=     -2.    -0.    -0.  XC,YC,ZC=   -2.667     -.4703    -2.375
TOP STR  SX,SY,SXY=  -2218.    -564.    173.   SMAX,SMIN,TAUMAX=    -546.   -2236.    845.   A=  5.9  VM=   2019.
MID STR  SX,SY,SXY=     31.    -122.     14.   SMAX,SMIN,TAUMAX=      32.    -123.     78.   A= 84.8  VM=    142.
BOT STR  SX,SY,SXY=   2280.     320.   -144.   SMAX,SMIN,TAUMAX=    2290.     309.    991.   A=-85.8  VM=   2153.

ELEM  484  NODES= 3009 3159 3160 3010  MATERIAL=  2  AREA=    .38357        TTOP,TBOT=  313.  313.  PRESS=  -90.
     NX,NY=     14.     1.  MX,MY,MXY=     -2.    -0.    -0.  XC,YC,ZC=   -2.667     -.4703    -2.375
TOP STR  SX,SY,SXY=  -2210.    -524.    214.   SMAX,SMIN,TAUMAX=    -498.   -2237.    870.   A=  7.1  VM=   2034.
MID STR  SX,SY,SXY=    -55.    -187.     64.   SMAX,SMIN,TAUMAX=     -29.    -213.     92.   A= 67.9  VM=    200.
BOT STR  SX,SY,SXY=   2100.     150.    -86.   SMAX,SMIN,TAUMAX=    2104.     146.    979.   A=-87.5  VM=   2035.

ELEM  485  NODES= 3010 3160 3161 3011  MATERIAL=  2  AREA=    .38357        TTOP,TBOT=  313.  313.  PRESS=  -90.
     NX,NY=     13.     1.  MX,MY,MXY=     -2.    -0.    -0.  XC,YC,ZC=   -2.345     1.354    -2.375
TOP STR  SX,SY,SXY=  -2018.    -469.    144.   SMAX,SMIN,TAUMAX=    -456.   -2031.    788.   A=  5.3  VM=   1846.
MID STR  SX,SY,SXY=      2.    -158.     -8.   SMAX,SMIN,TAUMAX=       2.    -158.     80.   A=-87.1  VM=    159.
BOT STR  SX,SY,SXY=   2022.     154.   -160.   SMAX,SMIN,TAUMAX=    2035.     140.    948.   A=-85.1  VM=   1969.

ELEM  486  NODES= 3011 3161 3162 3012  MATERIAL=  2  AREA=    .38357        TTOP,TBOT=  313.  313.  PRESS=  -90.
     NX,NY=     12.     1.  MX,MY,MXY=     -2.    -0.    -0.  XC,YC,ZC=   -1.741     2.075    -2.375
TOP STR  SX,SY,SXY=  -1884.    -262.    285.   SMAX,SMIN,TAUMAX=    -213.   -1933.    860.   A=  9.7  VM=   1836.
MID STR  SX,SY,SXY=     27.      12.    149.   SMAX,SMIN,TAUMAX=     169.    -130.    149.   A= 46.4  VM=    259.
BOT STR  SX,SY,SXY=   1938.     286.     13.   SMAX,SMIN,TAUMAX=    1938.     286.    826.   A= 89.5  VM=   1812.

ELEM  487  NODES= 3012 3162 3161 3013  MATERIAL=  2  AREA=    .38357        TTOP,TBOT=  313.  313.  PRESS=  -90.
```

JOB KIPS PAGE
DATE
BY Y.E. REV.

Jet Condenser Accumulator

Material: 304 S.S. [1]

@ 250°F $\sigma_u = 65.3$ ksi.
$\sigma_y = 27.6$ " .

for 1×10^{-9} Failure Probability

$\underline{\sigma_u} = 0.82 \times 65.3 = \underline{53.55}$ ksi
$\underline{\sigma_y} = 0.73 \times 27.6 = \underline{20.15}$ ksi

Analytical Model:

A finite element model for the accumulator was constructed as shown in fig. 1.

The model consists of Conical Shell elements (Stiff. 11 of ANSYS [3]).

Deflections and Stresses were evaluated under max. pressure conditions. A Summary of the Stress Conditions is as follows:

JOB KIPS

BY Y.E.

PAGE

DATE

REV.

$$\sigma_{eff} = \sqrt{\sigma_{S_i}^2 + \sigma_{TH_i}^2 - \sigma_{S_i}\sigma_{TH_i}} \quad , \; i = 1,2$$

I- Outer Shell

Max. Stress occurs at elem. # 15 (Nodes 15-16)

$\sigma_S = 12,966$

$\sigma'_{TH_1} = -1,402$

$\sigma_{eff} = 13,720$ psi

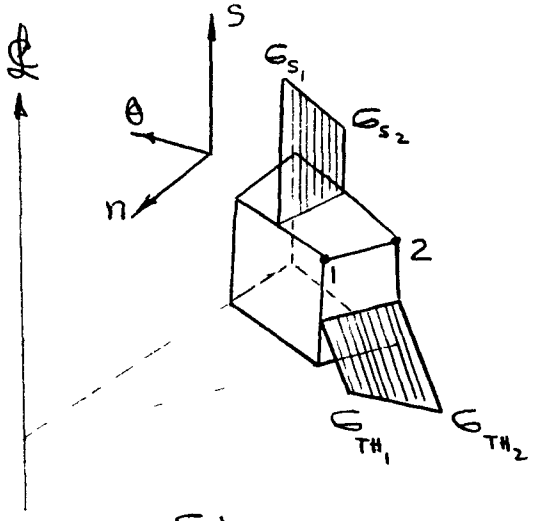

Stresses on a Conical Shell Element

$$M.S. = \frac{\sigma_y}{\sigma_{eff}} - 1$$

$$M.S. = \frac{20.15}{13,720} - 1 = \boxed{0.469 \text{ on yield}}$$

II- Inner Shell

Max. Stress occurs at elem. # 49 (Nodes 49,50)

$\sigma_{S_1} = -15,369$
$\sigma_{TH_1} = -9,381$ $\Rightarrow \sigma_{eff_1} = 13,417$ psi

$\sigma_{S_2} = 15,124$
$\sigma_{TH_2} = -1087$ $\Rightarrow \sigma_{eff_2} = 15,696$ psi

JOB KIPS PAGE
DATE
BY Y.E. REV.

$$M.S. = \frac{20.15}{15.696} - 1 = \boxed{0.284 \text{ on yield}}$$

III - Floating Piston

Max. Stress occurs at Element NO.

$\sigma_{S_2} = -12,456$ psi
$\sigma_{TH_2} = 376$ "

$\sigma_{eff_2} = 12,648$ psi

$$M.S. = \frac{20.15}{12.648} - 1 = \boxed{0.593 \text{ on yield}}$$

JOB KIPS

BY Y-E

PAGE

DATE

REV.

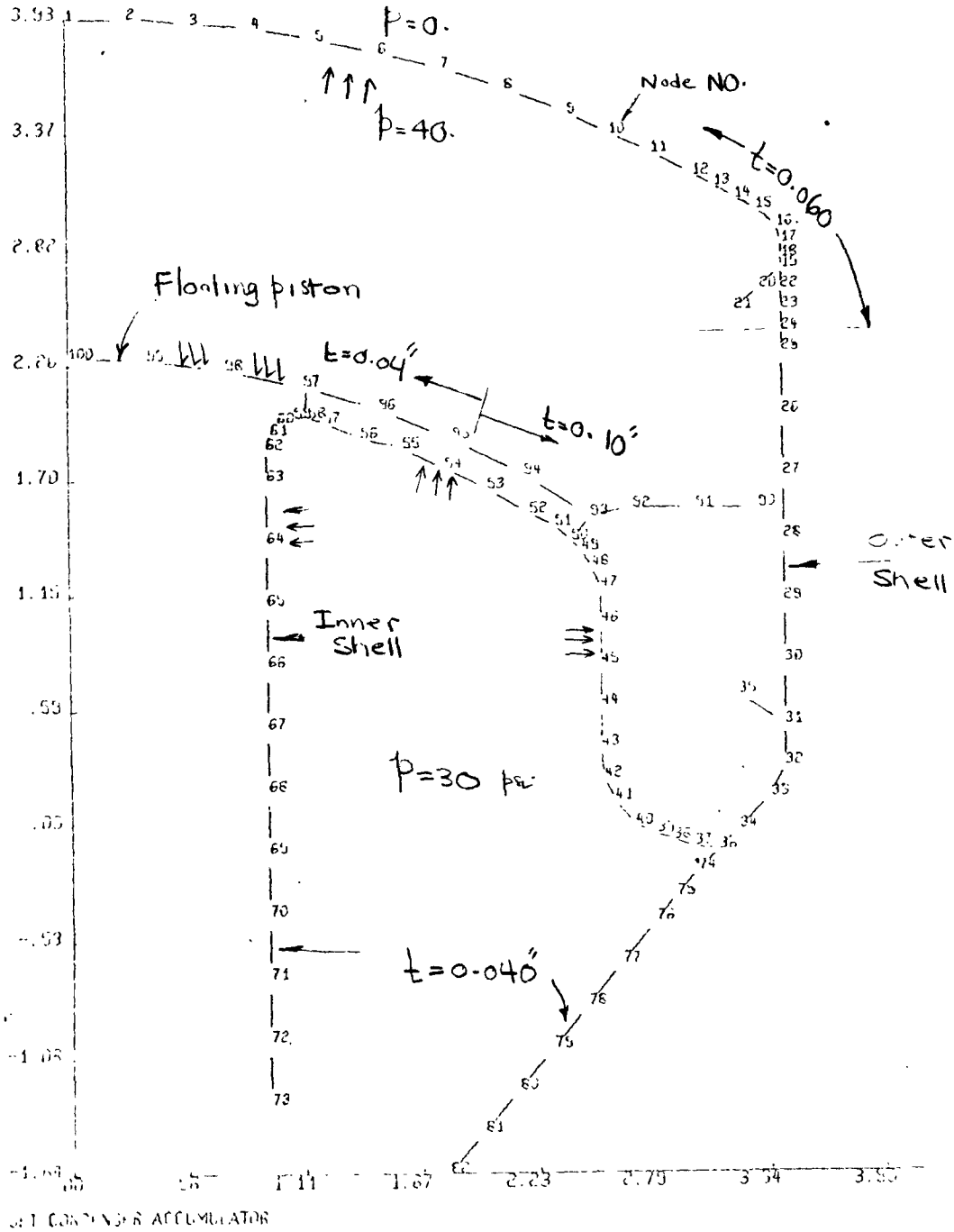

Fig. 1.

JOB KIPs

BY Y. E.

PAGE

DATE

REV.

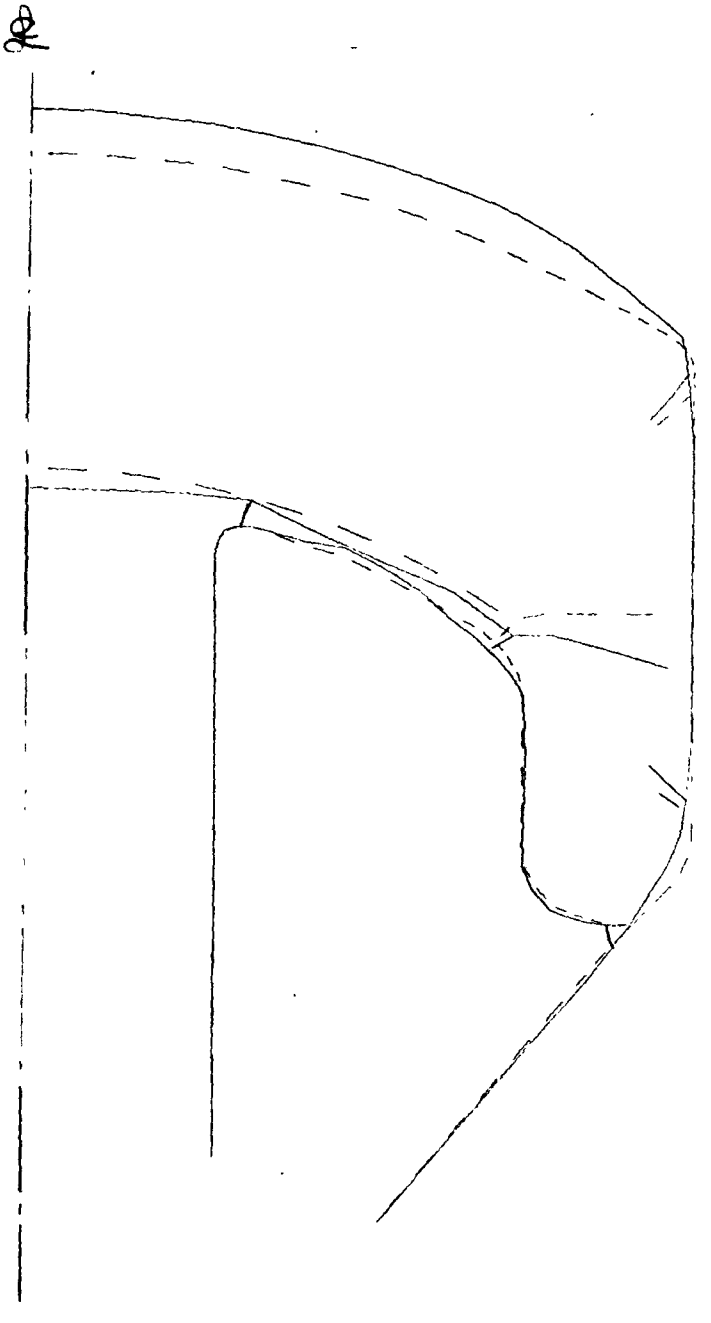

Fig. 2. Deformed Geomtry of Accumulator under max pressures

***** DISPLACEMENT SOLUTION ***** TIME = 0. LOAD STEP= 1 ITERATION= 1 CUM. ITER.= 1

NODE	UX	UY	ROTZ
1	0.	.303070E-02	0.
2	.253249E-04	.299643E-02	-.554042E-05
3	.472518E-04	.295996E-02	-.523838E-03
4	.607721E-04	.277477E-02	-.111964E-03
5	.108229E-03	.287692E-02	.322833E-03
6	.126054E-03	.284478E-02	-.409285E-03
7	.120655E-03	.271744E-02	-.131384E-03
8	.165174E-03	.276454E-02	.318948E-03
9	.214763E-03	.282043E-02	.618749E-04
10	.144744E-03	.274849E-02	-.983079E-03
11	.624461E-04	.239917E-02	-.222566E-02
12	-.194742E-03	.188243E-02	-.276175E-02
13	-.322244E-03	.160660E-02	-.262202E-02
14	-.458931E-03	.135829E-02	-.216935E-02
15	-.549743E-03	.117104E-02	-.135359E-02
16	-.597402E-03	.109560E-02	.922270E-04
17	-.590154E-03	.110022E-02	.992403E-03
18	-.462084E-03	.109477E-02	.147206E-02
19	-.283650E-03	.109121E-02	.164267E-02
20	-.215478E-03	.918517E-03	.174516E-02
21	-.403660E-04	.704017E-03	.177497E-02
22	-.234987E-03	.108548E-02	.133224E-02
23	-.116407E-03	.108041E-02	.104540E-02
24	-.237354E-04	.107697E-02	.819806E-03
25	.302249E-04	.107207E-02	.298038E-03
26	.140046E-04	.105801E-02	-.214525E-03
27	-.381867E-04	.104277E-02	-.935563E-04
28	-.597287E-04	.102688E-02	.778042E-04
29	-.135847E-05	.101148E-02	.139254E-03
30	-.110543E-04	.996766E-03	-.366503E-03
31	-.354620E-03	.978614E-03	-.213777E-02
32	-.736940E-03	.959779E-03	-.986292E-03
33	-.488055E-03	.915042E-03	.178962E-02
34	-.231122E-03	.459751E-03	.335335E-02
35	-.324242E-04	.145605E-02	-.219166E-02
36	.287268E-04	.154910E-03	.225732E-02
37	-.633945E-05	-.770756E-04	.173552E-02
38	-.487749E-04	-.224160E-03	.121931E-02
39	-.769245E-04	-.307445E-03	.857157E-03
40	-.102449E-03	-.368723E-03	.331017E-03
41	-.943802E-04	-.366442E-03	-.325627E-03
42	-.485584E-04	-.342526E-03	-.640374E-03
43	.635617E-04	-.337709E-03	-.713422E-03
44	.181434E-03	-.343296E-03	-.429176E-03
45	.227405E-03	-.350676E-03	-.344151E-05
46	.161067E-03	-.357954E-03	.748034E-03
47	-.479567E-04	-.361681E-03	.174463E-02
48	-.245362E-03	-.440337E-03	.207945E-02
49	-.397408E-03	-.532427E-03	.150386E-02
50	-.445765E-03	-.576176E-03	.183702E-03
51	-.386771E-03	-.499706E-03	-.177565E-02
52	-.252738E-03	-.216943E-03	-.262752E-02
53	.251679E-04	.260658E-03	-.187121E-02
54	.145776E-03	.504463E-03	-.543994E-03
55	.143189E-03	.493205E-03	.574827E-03
56	.963869E-04	.297439E-03	.132505E-02
57	-.724740E-05	.362009E-04	.135507E-02
58	-.381108E-04	-.505790E-04	.102709E-02
59	-.386227E-04	-.991460E-04	.279775E-03
60	-.405711E-04	-.900868E-04	-.295721E-03
61	-.539938E-04	-.815202E-04	-.186521E-03
62	-.591324E-04	-.789847E-04	.355570E-04
63	-.362718E-04	-.766836E-04	.174729E-03
64	-.142553E-04	-.696505E-04	.140693E-05
65	-.159119E-04	-.621094E-04	-.301965E-05
66	-.160860E-04	-.546630E-04	.316959E-06
67	-.160400E-04	-.472142E-04	.665535E-08
68	-.160418E-04	-.397642E-04	.346326E-07
69	-.159988E-04	-.323127E-04	.152581E-06

76	.312943E-03	-.147568E-03	-.217120E-03
77	.255520E-03	-.986916E-04	-.366004E-03
78	.170650E-03	-.617568E-04	-.190805E-03
79	.136702E-03	-.513924E-04	-.852151E-04
80	.108271E-03	-.464453E-04	-.132246E-03
81	.568942E-04	-.238156E-04	-.280889E-03
82	0.	0.	0.
90	.357950E-04	-.368952E-02	-.376039E-02
91	.368769E-04	-.255274E-02	-.376756E-02
92	.384627E-04	-.149417E-02	-.211538E-02
93	-.547133E-04	-.970340E-03	-.185547E-02
94	.964303E-04	-.732039E-03	-.443475E-04
95	-.101806E-03	-.110521E-02	.102410E-02
96	-.742468E-04	-.997963E-03	-.177630E-02
97	.162853E-03	-.219117E-03	-.641569E-03
98	.414962E-04	-.821604E-03	.218543E-02
99	-.107772E-04	-.132193E-02	.397273E-03
100	0.	-.135698E-02	0.

MAXIMUM VALUE

NODES	32	90	91
DISPL	-.736949E-03	-.368952E-02	-.376756E-02

4700 WORDS WRITTEN TO BLOCKS 1 AND 2
5904 WORDS WRITTEN TO BLOCK 3
269 ACTIVE DEGREES OF FREEDOM
10.0 R.M.S. WAVEFRONT

MATRIX SOLUTION TIME ESTIMATE(CDC7600) = .03 SECONDS.

KIPS JET CONDENSER-ACCUMULATOR CP = 0.7050 1/25/78
S.333 PP = 0.000

***** ELEMENT STRESSES ***** TIME = 0. LOAD STEP= 1 ITERATION= 1 CUM. ITER.= 1

SHELL ELEM 1 NODES= 1 2 MAT= 1 LENGTH= .2990 TEMPERATURES (1,2) = 70.0 70.0

I	X	Y	SIG S	SIG TH	S MOM	TH MOM	S BEND	SIG S1	SIG S2	TH BEND	SIG TH1	SIG TH2
1	.0010	3.9300	2558.	2691.	0.	0.	1367.	1191.	3925.	309.	322.	1060.
2	.0708	3.9305	3237.	3227.	0.	0.	1116.	2122.	4353.	1301.	1904.	4507.
3	.1406	3.9300	3243.	3228.	0.	0.	503.	2740.	3745.	814.	2333.	4122.
4	.2104	3.9300	3245.	3235.	-0.	0.	-111.	3356.	3134.	480.	2754.	3715.
5	.2802	3.9300	3246.	3236.	-0.	0.	-726.	3972.	2519.	65.	3174.	3303.
6	.3500	3.9300	3246.	3240.	-0.	-0.	-1342.	4588.	1905.	-352.	3592.	2888.

I	UN	US	ROT	UX	UY	EPS	EPTH	CURVE S	CURVE TH
1	-.003031	.0000000	-.0000000	.0000000	.003031	.0000847	.0000000	.0022632	.0000000
2	-.003027	.0000005	-.0000108	.0000005	.003027	.0000847	.0000833	.0017653	.0017844
3	-.003019	.0000010	-.0000163	.0000010	.003019	.0000847	.0000840	.0004675	.0013540
4	-.003009	.0000015	-.0000164	.0000015	.003009	.0000847	.0000842	-.0004304	.0009113
5	-.003000	.0000020	-.0000112	.0000020	.003000	.0000847	.0000843	-.0013283	.0004655
6	-.002996	.0000025	-.0000006	.0000025	.002996	.0000847	.0000844	-.0022261	.0000185

SHELL ELEM 2 NODES= 2 3 MAT= 1 LENGTH= .3015 TEMPERATURES (1,2) = 70.0 70.0

I	X	Y	SIG S	SIG TH	S MOM	TH MOM	S BEND	SIG S1	SIG S2	TH BEND	SIG TH1	SIG TH2
1	.3000	3.9300	3246.	3240.	-0.	-0.	-745.	3991.	2501.	-191.	3431.	3049.
2	.3600	3.9240	3249.	3252.	-0.	-0.	-48.	3298.	3201.	-65.	3317.	3187.
3	.4200	3.9180	3252.	3261.	0.	0.	681.	2571.	3933.	182.	3079.	3444.
4	.4800	3.9120	3247.	3243.	0.	0.	1430.	1817.	4677.	505.	2738.	3748.
5	.5400	3.9060	3231.	3192.	1.	0.	2194.	1037.	5424.	879.	2303.	4060.
6	.6000	3.9000	3200.	3069.	1.	0.	2966.	234.	6167.	1287.	1762.	4357.

I	UN	US	ROT	UX	UY	EPS	EPTH	CURVE S	CURVE TH
1	-.002984	-.0000273	-.0000006	.0000025	.002996	.0000847	.0000844	-.0012382	.0000184
2	-.002985	-.0000268	.0000033	.0000031	.002997	.0000847	.0000848	-.0009553	-.0000925
3	-.002987	-.0000263	.0000001	.0000036	.002998	.0000847	.0000851	.0011276	-.0000027
4	-.002988	-.0000103	-.0000041	.0000041	.002995	.0000847	.0000845	.0023105	.0002125
5	-.002973	-.0000253	-.0000278	.0000045	.002983	.0000847	.0000825	.0034935	.0005114
6	-.002948	-.0000247	-.0000524	.0000047	.002959	.0000847	.0000788	.0044764	.0008687

SHELL ELEM 3 NODES= 3 4 MAT= 1 LENGTH= .3007 TEMPERATURES (1,2) = 70.0 70.0

I	X	Y	SIG S	SIG TH	S MOM	TH MOM	S BEND	SIG S1	SIG S2	TH BEND	SIG TH1	SIG TH2
1	.6000	3.9000	3229.	3077.	1.	0.	2819.	410.	6047.	1249.	1828.	4326.
2	.6600	3.8940	3202.	2980.	0.	0.	1453.	1750.	4655.	1002.	1977.	3982.
3	.7200	3.8880	3175.	2883.	0.	0.	49.	3126.	3224.	617.	2261.	3494.
4	.7800	3.8820	3152.	2793.	-0.	0.	-1383.	4535.	1769.	125.	2668.	2918.
5	.8400	3.8846	3138.	2742.	-1.	-0.	-2835.	5977.	300.	-451.	3194.	2291.
6	.9000	3.8800	3137.	2738.	-1.	-0.	-4311.	7448.	-1174.	-1095.	3832.	1643.

I	UN	US	ROT	UX	UY	EPS	EPTH	CURVE S	CURVE TH
1	-.002956	-.0000150	-.0000524	.0000047	.002959	.0000856	.0000788	.0044314	.0008711
2	-.002948	-.0000145	-.0000721	.0000050	.002951	.0000856	.0000755	.0021109	.0010893
3	-.002939	-.0000139	-.0000778	.0000052	.002945	.0000856	.0000722	-.0001096	.0010778
4	-.002927	-.0000134	-.0000695	.0000054	.002929	.0000856	.0000674	-.0023301	.0008995
5	-.002921	-.0000129	-.0000473	.0000057	.002923	.0000856	.0000677	-.0044566	.0005623
6	-.002923	-.0000124	-.0000112	.0000061	.002925	.0000856	.0000675	-.0071711	.0001241

SHELL ELEM 4 NODES= 4 5 MAT= 1 LENGTH= .3070 TEMPERATURES (1,2) = 70.0 70.0

I	X	Y	SIG S	SIG TH	S MOM	TH MOM	S BEND	SIG S1	SIG S2	TH BEND	SIG TH1	SIG TH2
1	.9000	3.8800	2986.	2697.	-1.	-0.	-3817.	6803.	-832.	-963.	3659.	1734.
2	.9600	3.8760	2968.	2747.	-1.	-0.	-2681.	5670.	319.	-1488.	3595.	1900.
3	1.0200	3.8540	3039.	2855.	-0.	-0.	-1518.	4507.	1521.	-1286.	3534.	2257.
4	1.0800	3.8410	3069.	3000.	-0.	-0.	-335.	3424.	2754.	-350.	3431.	2730.
5	1.1400	3.8280	3137.	3255.	0.	0.	867.	2270.	4003.	4.	3251.	3260.
6	1.2000	3.8150	3171.	3381.	1.	0.	2063.	1087.	5254.	415.	2966.	3797.

I	UN	US	ROT	UX	UY	EPS	EPTH	CURVE S	CURVE TH
1	-.002725	-.0000528	-.0000112	.0000061	.002775	.0000806	.0000675	-.0063527	.0001216
2	-.002729	-.0000523	.0000217	.0000056	.002777	.0000806	.0000692	-.0043782	-.0002214
3	-.002749	-.0000518	.0000426	.0000076	.002796	.0000805	.0000741	-.0024037	-.0004078
4	-.002778	-.0000513	.0000547	.0000107	.002824	.0000806	.0000832	-.0004292	-.0004638
5	-.002809	-.0000508	.0000478	.0000098	.002853	.0000806	.0000860	.0014453	-.0004101
6	-.002835	-.0000503	.0000323	.0000108	.002877	.0000806	.0000902	.0034197	-.0002629

SHELL ELEM 5 NODES= 5 6 MAT= 1 LENGTH= .3070 TEMPERATURES (1,2) = 70.0 70.0

I	X	Y	SIG S	SIG TH	S MOM	TH MOM	S BEND	SIG S1	SIG S2	TH BEND	SIG TH1	SIG TH2
1	1.2000	3.8150	3119.	3357.	1.	0.	1950.	1169.	5069.	379.	2988.	3747.
2	1.2600	3.8020	3134.	3421.	0.	0.	1756.	1378.	4889.	417.	3005.	3838.
3	1.3200	3.7890	3132.	3411.	0.	0.	1556.	1577.	4688.	476.	2981.	3859.
4	1.3800	3.7760	3119.	3348.	0.	0.	1351.	1768.	4471.	435.	2930.	3806.
5	1.4400	3.7630	3097.	3246.	0.	0.	1143.	1964.	4240.	426.	2861.	3712.
6	1.5000	3.7500	3069.	3182.	0.	0.	932.	2137.	4000.	401.	2781.	3592.

I	UN	US	ROT	UX	UY	EPS	EPTH	CURVE S	CURVE TH

6	-.[illegible]2807	-.0000479	-.000040[illegible]	.0001[illegible]26	.0028[illegible]45	.[illegible]0000789	.0000840	.001[illegible]7[illegible]2	.0002667

SHELL ELEM 6 NODES= 6 7 MAT= 1 LENGTH= .3092 TEMPERATURES (1,2) = 70.0 70.0

I	X	Y	SIG S	SIG TH	S MOM	TH MOM	S BEND	SIG S1	SIG S2	TH BEND	SIG TH1	SIG TH2
1	1.5000	3.7500	3209.	3219.	0.	0.	1062.	2147.	4271.	435.	2785.	3654.
2	1.5600	3.7350	3174.	3088.	0.	0.	443.	2731.	3616.	287.	2801.	3375.
3	1.6200	3.7200	3128.	2955.	-0.	0.	-183.	3320.	2955.	115.	2840.	3070.
4	1.6800	3.7050	3106.	2838.	-0.	-0.	-814.	3920.	2792.	-73.	2917.	2758.
5	1.7400	3.6900	3083.	2752.	-0.	-0.	-1451.	4534.	1682.	-233.	3045.	2458.
6	1.8000	3.6750	3071.	2709.	-0.	-0.	-2093.	5154.	978.	-525.	3235.	2154.

I	US	POT	UX	UY	EPS	EPTH	CURVE S	CURVE TH
1	-.0002790	-.0005[illegible]68	-.0[illegible]0403	.0001[illegible]26	.0028[illegible]45	.0[illegible]000836	.0000840	.0014864	.0002647
2	-.0002763	-.0005[illegible]63	-.0[illegible]0482	.0001[illegible]24	.0028[illegible]15	.0[illegible]000836	.0000797	.0000524	.0002995
3	-.0002732	-.0000557	-.0004[illegible]90	.0001[illegible]22	.0027[illegible]86	.0[illegible]000836	.0000753	-.0003817	.0002934
4	-.0002703	-.0000552	-.0[illegible]50434	.0001[illegible]20	.0027[illegible]56	.0[illegible]000836	.0000714	-.0011457	.0002509
5	-.0002680	-.0006547	-.0003[illegible]15	.0001[illegible]19	.0027[illegible]32	.0[illegible]000835	.0[illegible]0685	-.0[illegible]24497	.0001756
6	-.0002664	-.0[illegible]05[illegible]2	-.[illegible]000131	.0001[illegible]21	.0027[illegible]17	.0[illegible]000836	.0000671	-.0034837	.0000708

SHELL ELEM 7 NODES= 7 8 MAT= 1 LENGTH= .3178 TEMPERATURES (1,2) = 70.0 70.0

I	X	Y	SIC S	SIG TH	S MOM	TH MOM	S BEND	SIG S1	SIG S2	TH BEND	SIG TH1	SIG TH2
1	1.8000	3.6750	3041.	2701.	-1.	-0.	-1899.	4940.	1142.	-474.	3175.	2227.
2	1.8600	3.6540	3041.	2703.	-0.	-0.	-1492.	4534.	1549.	-416.	3119.	2287.
3	1.9200	3.6330	3056.	2757.	-0.	-0.	-1081.	4137.	1975.	-342.	3069.	2415.
4	1.9800	3.6120	3079.	2843.	-0.	-0.	-666.	3745.	2413.	-252.	3035.	2591.
5	2.0400	3.5910	3107.	2945.	-0.	-0.	-247.	3[illegible].	2861.	-149.	3[illegible].	2[illegible].
6	2.1000	3.5[illegible]6	3135.	3049.	-0.	-0.	17[illegible].	2[illegible]9.	3311.	-33.	30[illegible].	3[illegible].

I	US	POT	UX	UY	EPS	EPTH	CURVE S	CURVE TH
1	-.0002605	-.0000784	-.000131	.000121	.002717	.0000826	.0000671	-.0031629	.0000689
2	-.0002[illegible]10	-.[illegible]000778	.000047	.0001[illegible]25	.002[illegible]13	.0000826	.0000672	-.0022[illegible]44	-.0000241
3	-.0002[illegible]10	-.0000773	.0[illegible]0182	.0001[illegible]32	.002[illegible]19	.0000826	.0000690	-.0017[illegible]58	-.0000894
4	-.0002625	-.0000768	.000272	.0001[illegible]42	.002[illegible]31	.0[illegible]0826	.0000718	-.0010[illegible]72	-.0001296
5	-.0002644	-.0000763	.000318	.0001[illegible]53	.002747	.0000826	.0000752	-.0003[illegible]87	-.0001470
6	-.0002664	-.0000757	.000319	.0001[illegible]65	.002[illegible]65	.0000826	.0000787	.0003[illegible]99	-.0001433

SHELL ELEM 8 NODES= 8 9 MAT= 1 LENGTH= .3231 TEMPERATURES (1,2) = 70.0 70.0

I	X	Y	SIG S	SIG TH	S MOM	TH MOM	S BEND	SIG S1	SIG S2	TH BEND	SIG TH1	SIG TH2
1	2.1600	3.5760	3011.	3015.	0.	-0.	156.	2655.	3367.	-37.	30[illegible].	2979.
2	2.2200	3.5460	3039.	3118.	0.	0.	279.	2760.	3318.	5.	3113.	3123.
3	2.2800	3.5220	3062.	3205.	0.	0.	403.	2859.	3465.	49.	3156.	3[illegible]4.
4	2.3400	3.4980	3081.	273[illegible].	0.	0.	527.	2953.	3608.	95.	3177.	3[illegible]9.
5	2.4000	3.4740	3093.	332[illegible].	0.	0.	652.	2441.	3745.	145.	3175.	3465.
6	2.4600	3.4500	3099.	3363.	0.	0.	778.	2521.	3877.	197.	3146.	3539.

I	US	POT	UX	UY	EPS	EPTH	CURVE S	CURVE TH
1	-.0002628	-.0000[illegible]73	.000319	.000165	.002765	.0000787	.0002[illegible]65	-.0001410
2	-.0002[illegible]43	-.0000[illegible]63	.0002[illegible]3	.0001[illegible]77	.002[illegible]81	.0000785	.0000821	.0004960	-.0001261
3	-.0002[illegible]46	-.0000[illegible]63	.000255	.0001[illegible]89	.002[illegible]96	.0000785	.0000849	.0006955	-.0001065
4	-.0002[illegible]81	-.0000[illegible]58	.0002[illegible]03	.0001[illegible]99	.002[illegible]08	.0000785	.0000872	.0008951	-.0000828
5	-.0002[illegible]02	-.0006[illegible]53	.000139	.0002[illegible]08	.002[illegible]16	.0000785	.0000887	.0010946	-.0000552
6	-.0002[illegible]8	-.0000848	.000062	.0002[illegible]15	.002[illegible]20	.0000785	.0000895	.0012941	-.0000239

SHELL ELEM 9 NODES= 9 10 MAT= 1 LENGTH= .2236 TEMPERATURES (1,2) = 70.0 70.0

I	X	Y	SIC S	SIG TH	S MOM	TH MOM	S BEND	SIG S1	SIG S2	TH BEND	SIG TH1	SIG TH2
1	2.4600	3.4500	3111.	3346.	0.	0.	509.	2602.	3620.	125.	3221.	3470.
2	2.5200	3.4300	3112.	3348.	0.	0.	1437.	1674.	4549.	390.	29[illegible]8.	3739.
3	2.5800	3.4100	3105.	3325.	1.	0.	2370.	736.	5479.	670.	2[illegible]5[illegible].	3995.
4	2.6400	3.3900	3088.	3200.	1.	0.	3306.	-218.	6394.	964.	22[illegible]6.	4224.
5	2.7000	3.3700	3055.	3[illegible]00.	1.	0.	4245.	-1189.	7301.	1271.	1[illegible]49.	4411.
6	2.7600	3.3500	3005.	2952.	1.	0.	5188.	-2163.	8192.	1590.	1361.	4542.

I	US	POT	UX	UY	EPS	EPTH	CURVE S	CURVE TH
1	-.0002[illegible]49	-.0001[illegible]69	.000062	.000215	.002820	.0000788	.0000895	.0006491	-.0000231
2	-.0002[illegible]17	-.000[illegible]66	-.0000[illegible]10	.0002[illegible]19	.002[illegible]20	.0000788	.0000886	.0023797	.0000338
3	-.0002[illegible]17	-.0001062	-.000151	.0002[illegible]20	.002[illegible]16	.0000788	.0000868	.0[illegible]0[illegible]84	.0000544
4	-.0002[illegible]05	-.0[illegible]01059	-.0000[illegible]69	.0002[illegible]18	.002[illegible]04	.0000788	.0000867	.0054380	.0001277
5	-.0002[illegible]45	-.0001055	-.0000[illegible]37	.0002[illegible]12	.002[illegible]83	.0[illegible]000788	.0000827	.0054677	.0002267
6	-.0002[illegible]68	-.0001052	-.000098[illegible]	.0001[illegible]99	.002[illegible]49	.0000788	.0000764	.0084973	.0003382

SHELL ELEM 10 NODES= 10 11 MAT= 1 LENGTH= .2193 TEMPERATURES (1,2) = 70.0 70.0

I	X	Y	SIC S	SIG TH	S MOM	TH MOM	S BEND	SIG S1	SIG S2	TH BEND	SIG TH1	SIG TH2
1	2.8[illegible]00	3.3[illegible]0	3271.	3[illegible]23.	1.	0.	5211.	-1940.	8482.	1600.	1423.	4623.
2	2.[illegible]400	3.[illegible]300	3207.	27[illegible].	1.	0.	6137.	-1329.	7745.	1483.	1307.	4276.
3	2.[illegible]800	3.[illegible]100	3128.	2[illegible]5[illegible].	1.	0.	7[illegible]9.	-7[illegible].	6[illegible]8.	1383.	1[illegible]44.	3[illegible]4.
4	2.[illegible]200	3.[illegible]900	3037.	2[illegible]07.	1.	0.	8[illegible]9.	-[illegible]42.	52[illegible].	1271.	9[illegible]5.	3[illegible]6.
5	2.[illegible]600	3.[illegible]700	2936.	2[illegible]44.	1.	0.	9[illegible]5.	4[illegible]1.	3[illegible]2.	1058.	7[illegible]5.	2[illegible]2.
6	2.[illegible]000	3.[illegible]500	2828.	3[illegible]8.	0.	0.	10[illegible].	1[illegible]2.	463[illegible].	894.	4[illegible]6.	2[illegible]9.

I	US	POT	UX	UY	EPS	EPTH	CURVE S	CURVE TH
1	-.0002[illegible]47	-.0[illegible]00983	.000[illegible]39	.0002[illegible]49	.0[illegible]0[illegible]877	.0[illegible]000764	.0008[illegible]38	.0[illegible]03448
2	-.0[illegible]53	-.[illegible]43	.000[illegible]1[illegible]1	.[illegible]97[illegible]1	.0[illegible]0[illegible]877	.0[illegible]000687	.0[illegible]07[illegible]66	.[illegible]0[illegible]6[illegible]2
3	-.[illegible]2	-.[illegible]48	.000[illegible]158	.[illegible]6[illegible]3[illegible]	.0[illegible]0[illegible]877	.[illegible]000[illegible]96	.0[illegible]0[illegible]203	.[illegible]0[illegible]5[illegible]2
4	-.[illegible]5	-.[illegible]55	.000[illegible]138	.[illegible]6[illegible]8[illegible]	.0[illegible]0[illegible]877	.[illegible]000[illegible]78	.0[illegible]0[illegible]2[illegible]	.[illegible]0[illegible]5[illegible]2
5	-.[illegible]5	-.[illegible]55	.000[illegible]138	.[illegible]6[illegible]8[illegible]	.0[illegible]0[illegible]877	.[illegible]000[illegible]78	.0[illegible]0[illegible]2[illegible]	.[illegible]0[illegible]5[illegible]2
6	-.0002[illegible]28	-.[illegible]0[illegible]2225	.000[illegible]62	.[illegible]2[illegible]4[illegible]	.0[illegible]0[illegible]877	.[illegible]000[illegible]23	.0[illegible]0[illegible]975	.[illegible]0[illegible]2[illegible]5

SHELL ELEM 11 NODES= 11 12 MAT= 1 LENGTH= .2253 TEMPERATURES (1,2) = 70.0 70.0

I	X	Y	SIC S	SIG TH	S MOM	TH MOM	S BEND	SIG S1	SIG S2	TH BEND	SIG TH1	SIG TH2

I	X	Y	SIG S	SIG TH	S MOM	TH MOM	S BEND	SIG S1	SIG S2	TH BEND	SIG TH1	SIG TH2
3	2.[illegible]800	3.21[illegible]	[illegible]	-4[illegible].	0.	0.	[illegible]	[illegible]	[illegible]	[illegible]	[illegible]	[illegible]
4	2.9200	3.1942	2[illegible]4.	-35.	0.	0.	1441.	1448.	4330.	825.	-860.	790.
5	2.96[illegible]0	3.1723	2744.	-572.	0.	0.	1234.	1510.	3977.	778.	-1352.	274.
6	3.0[illegible]	3.15[illegible]	2597.	-1117.	0.	0.	1025.	1572.	3623.	729.	-1845.	-338.

I	UN	US	ROT	UX	UY	EPS	EPTH	CURVE S	CURVE TH
1	-.002132	-.001101	-.002226	.000062	.002399	.0001035	.0000223	.0032173	.0006965
2	-.002027	-.001097	-.002365	.000016	.002305	.0001035	.0000057	.0024698	.0007295
3	[illegible]	[illegible]	[illegible]	-.000033	.002206	.0001035	-.0000115	.0025224	.0007569
4	[illegible]	[illegible]	[illegible]	-.000085	.002102	.0001035	-.0000291	.0021749	.0007787
5	[illegible]	[illegible]	[illegible]	-.000139	.001994	.0001035	-.0000470	[illegible]	.0007952
6	-.001556	[illegible]	[illegible]	-.000195	.001882	.0001035	-.0000649	.0014799	[illegible]

SHELL ELEM 12 NODES= 12 13 MAT= 1 LENGTH= .1118 TEMPERATURES (1,2) = 70.0 70.0

I	X	Y	SIG S	SIG TH	S MOM	TH MOM	S BEND	SIG S1	SIG S2	TH BEND	SIG TH1	SIG TH2
1	3.0000	3.1500	1998.	-1279.	0.	0.	262.	1736.	2261.	752.	-2041.	-516.
2	3.0200	3.1400	1932.	-1525.	-0.	0.	-217.	2148.	1715.	627.	-2152.	-897.
3	3.0400	3.1300	1866.	-1767.	-0.	0.	-695.	2563.	1170.	489.	-2256.	-1277.
4	3.0600	3.1200	1803.	-2004.	-1.	0.	-1177.	2979.	625.	348.	-2352.	-1655.
5	3.0[illegible]0	3.1100	1740.	-2234.	-1.	0.	-1658.	3399.	62.	204.	-2438.	-2030.
6	3.1000	3.1000	1680.	-2457.	-1.	0.	-2140.	3820.	-460.	58.	-2515.	-2399.

I	UN	US	ROT	UX	UY	EPS	EPTH	CURVE S	CURVE TH
1	-.001597	-.001016	-.002762	-.000195	.001882	.0000837	-.0000649	.0000671	.0008234
2	-.001535	-.001014	-.002757	-.000221	.001826	.0000837	-.0000731	-.0004596	.0008166
3	-.001473	-.001012	-.002741	-.000247	.001771	.0000837	-.0000811	-.0009863	.0008065
4	-.001412	-.001010	-.002713	-.000272	.001715	.0000837	-.0000889	-.0015130	.0007931
5	-.001352	-.001009	-.002674	-.000297	.001660	.0000837	-.0000965	-.0020397	.0007764
6	-.001293	-.001007	-.002622	-.000322	.001607	.0000837	-.0001039	-.0025664	.0007565

SHELL ELEM 13 NODES= 13 14 MAT= 1 LENGTH= .1166 TEMPERATURES (1,2) = 70.0 70.0

I	X	Y	SIG S	SIG TH	S MOM	TH MOM	S BEND	SIG S1	SIG S2	TH BEND	SIG TH1	SIG TH2
1	3.1000	3.1000	1883.	-2402.	-1.	0.	-2106.	3989.	-223.	41.	-2443.	-2362.
2	3.1200	3.0880	1812.	-2665.	-2.	-0.	-2543.	4355.	-731.	-96.	-2569.	-2762.
3	3.1400	3.0760	1744.	-2917.	-2.	-0.	-2980.	4724.	-1236.	-235.	-2682.	-3153.
4	3.1600	3.0640	1680.	-3157.	-2.	-0.	-3418.	5098.	-1739.	-377.	-2780.	-3534.
5	3.1800	3.0520	1619.	-3383.	-2.	-0.	-3857.	5475.	-2238.	-521.	-2862.	-3903.
6	3.2000	3.0400	1561.	-3594.	-3.	-0.	-4296.	5858.	-2735.	-667.	-2927.	-4261.

I	UN	US	ROT	UX	UY	EPS	EPTH	CURVE S	CURVE TH
1	-.001212	-.001103	-.002622	-.000322	.001607	.0000904	-.0001039	-.0024204	.0007253
2	-.001151	-.001101	-.002558	-.000352	.001554	.0000904	-.0001127	-.0029463	.0007030
3	-.001093	-.001099	-.002482	-.000380	.001502	.0000904	-.0001210	-.0034722	.0006779
4	-.001035	-.001097	-.002396	-.000407	.001452	.0000904	-.0001289	-.0039481	.0006501
5	-.000981	-.001094	-.002298	-.000434	.001404	.0000904	-.0001364	-.0044240	.0006197
6	-.000929	-.001092	-.002189	-.000459	.001358	.0000904	-.0001434	-.0049000	.0005867

SHELL ELEM 14 NODES= 14 15 MAT= 1 LENGTH= .1141 TEMPERATURES (1,2) = 70.0 70.0

I	X	Y	SIG S	SIG TH	S MOM	TH MOM	S BEND	SIG S1	SIG S2	TH BEND	SIG TH1	SIG TH2
1	3.2000	3.0400	1647.	-3571.	-3.	-0.	-4302.	5949.	-2654.	-658.	-2913.	-4229.
2	3.2200	3.0290	1600.	-3746.	-3.	-1.	-5154.	6754.	-3554.	-919.	-2827.	-4665.
3	3.2400	3.0180	1557.	-3906.	-4.	-1.	-6007.	7564.	-4450.	-1185.	-2721.	-5091.
4	3.2600	3.0070	1519.	-4047.	-4.	-1.	-6862.	8346.	-5343.	-1455.	-2592.	-5503.
5	3.2800	2.9960	1486.	-4170.	-5.	-1.	-7717.	9203.	-6232.	-1731.	-2439.	-5901.
6	3.3000	2.9850	1458.	-4271.	-5.	-1.	-8574.	10033.	-7116.	-2011.	-2260.	-6282.

I	UN	US	ROT	UX	UY	EPS	EPTH	CURVE S	CURVE TH
1	-.000969	-.001057	-.002189	-.000459	.001358	.0000933	-.0001434	-.0049096	.0005995
2	-.000920	-.001055	-.002067	-.000480	.001315	.0000933	-.0001492	-.0058399	.0005624
3	-.000875	-.001052	-.001923	-.000501	.001274	.0000933	-.0001545	-.0067703	.0005200
4	-.000833	-.001050	-.001758	-.000519	.001235	.0000933	-.0001592	-.0077006	.0004724
5	-.000795	-.001048	-.001571	-.000535	.001202	.0000933	-.0001632	-.0086309	.0004197
6	-.000761	-.001046	-.001364	-.000550	.001171	.0000933	-.0001666	-.0095613	.0003621

SHELL ELEM 15 NODES= 15 16 MAT= 1 LENGTH= .1312 TEMPERATURES (1,2) = 70.0 70.0

I	X	Y	SIG S	SIG TH	S MOM	TH MOM	S BEND	SIG S1	SIG S2	TH BEND	SIG TH1	SIG TH2
1	3.3000	2.9850	1492.	-4262.	-5.	-1.	-8480.	9972.	-6988.	-2025.	-2236.	-6287.
2	3.3200	2.9680	1453.	-4405.	-5.	-1.	-9092.	10546.	-7639.	-2242.	-2164.	-6647.
3	3.3400	2.9510	1426.	-4507.	-6.	-1.	-9705.	11131.	-8279.	-2461.	-2046.	-6967.
4	3.3600	2.9340	1410.	-4564.	-6.	-2.	-10319.	11729.	-8908.	-2683.	-1881.	-7246.
5	3.3800	2.9170	1408.	-4574.	-7.	-2.	-10933.	12341.	-9526.	-2908.	-1667.	-7482.
6	3.4000	2.9000	1418.	-4537.	-7.	-2.	-11548.	12966.	-10131.	-3135.	-1402.	-7672.

I	UN	US	ROT	UX	UY	EPS	EPTH	CURVE S	CURVE TH
1	-.000536	-.001177	-.001364	-.000550	.001171	.0000944	-.0001666	-.0094447	.0003148
2	-.000504	-.001175	-.001107	-.000569	.001145	.0000944	-.0001713	-.0101038	.0002541
3	-.000478	-.001172	-.000833	-.000584	.001124	.0000944	-.0001747	-.0107629	.0001901
4	-.000460	-.001170	-.000542	-.000593	.001108	.0000944	-.0001766	-.0114220	.0001229
5	-.000450	-.001167	-.000234	-.000598	.001099	.0000944	-.0001769	-.0120811	.0000526
6	-.000448	-.001165	.000092	-.000597	.001096	.0000944	-.0001757	-.0127402	-.0000207

Max. Stress at Element 15 (Outer Shell) ←

SHELL ELEM 16 NODES= 16 17 MAT= 1 LENGTH= .0825 TEMPERATURES (1,2) = 70.0 70.0

I	X	Y	SIG S	SIG TH	S MOM	TH MOM	S BEND	SIG S1	SIG S2	TH BEND	SIG TH1	SIG TH2
1	3.4000	2.9000	1230.	-4588.	-7.	-2.	-11640.	12869.	-10410.	-3148.	-1440.	-7736.
2	3.4040	2.8840	1240.	-4551.	-7.	-2.	-10944.	12184.	-9705.	-2973.	-1578.	-7523.
3	3.4080	2.8680	1257.	-4465.	-6.	-2.	-10249.	11506.	-8992.	-2796.	-1689.	-7282.
4	3.4120	2.8520	12[illegible]2.	-4394.	-6.	-2.	-9553.	10835.	-8271.	-2619.	-1774.	-7013.
5	3.4[illegible]0	2.8360	1313.	-4278.	-5.	-1.	-8857.	10170.	-7544.	-2441.	-1836.	-6719.
6	3.4200	2.8200	1351.	-4139.	-5.	-1.	-8161.	9511.	-6810.	-2263.	-1677.	-6402.

I	UN	US	ROT	UX	UY	EPS	EPTH	CURVE S	CURVE TH
1	[illegible]	-.001208	.000092	-.000597	.001096	.0000882	-.0001757	[illegible]	-.0000066

.000267	-.00[illegible]201	.000992	-.000550	.001100	.0000882	-.0001609	-.0089880	-.0000704

SHELL ELEM 17 NODES= 17 18 MAT= 1 LENGTH= .0700 TEMPERATURES (1,2) = 70.0 70.0

I	X	Y	SIG S	SIG TH	S MOM	TH MOM	S BEND	SIG S1	SIG S2	TH BEND	SIG TH1	SIG TH2
1	3.4200	2.8200	1042.	-4223.	-5.	-1.	-8198.	9240.	-7156.	-2213.	-2009.	-6436.
2	3.4200	2.8060	1077.	-4092.	-4.	-1.	-7402.	8479.	-6325.	-1999.	-2094.	-6091.
3	3.4200	2.7920	1116.	-3948.	-4.	-1.	-6606.	7722.	-5491.	-1794.	-2164.	-5732.
4	3.4200	2.7780	1158.	-3791.	-3.	-1.	-5811.	6969.	-4652.	-1569.	-2222.	-5360.
5	3.4200	2.7640	1204.	-3623.	-3.	-1.	-5015.	6218.	-3811.	-1354.	-2269.	-4977.
6	3.4200	2.7500	1252.	-3445.	-3.	-1.	-4219.	5471.	-2967.	-1139.	-2306.	-4584.

I	UN	US	ROT	UX	UY	EPS	EPTH	CURVE S	CURVE TH
1	.000550	-.001100	.000992	-.000550	.001100	.0000779	-.0001609	-.0091481	0.0000000
2	.000535	-.001099	.001113	-.000535	.001099	.0000779	-.0001565	-.0081698	0.0000000
3	.000519	-.001098	.001221	-.000519	.001098	.0000779	-.0001518	-.0072[illegible]4	0.0000000
4	.000501	-.001097	.001317	-.000501	.001097	.0000779	-.0001466	-.0064131	0.0000000
5	.000482	-.001096	.001401	-.000482	.001096	.0000779	-.0001410	-.0055347	0.0000000
6	.000462	-.001095	.001472	-.000462	.001095	.0000779	-.0001351	-.0046564	0.0000000

SHELL ELEM 18 NODES= 18 19 MAT= 1 LENGTH= .0500 TEMPERATURES (1,2) = 70.0 70.0

I	X	Y	SIG S	SIG TH	S MOM	TH MOM	S BEND	SIG S1	SIG S2	TH BEND	SIG TH1	SIG TH2
1	3.4200	2.7500	1048.	-3500.	-3.	-1.	-4258.	5306.	-3210.	-1150.	-2351.	-4550.
2	3.4200	2.7400	1084.	-3368.	-2.	-1.	-3791.	4875.	-2707.	-1024.	-2344.	-4392.
3	3.4200	2.7300	1120.	-3232.	-2.	-1.	-3325.	4445.	-2204.	-898.	-2335.	-4130.
4	3.4200	2.7200	1158.	-3094.	-2.	-0.	-2858.	4016.	-1700.	-772.	-2322.	-3865.
5	3.4200	2.7[illegible]	1196.	-2952.	-1.	-0.	-2392.	3588.	-1195.	-645.	-2306.	-3598.
6	3.4200	2.7000	1235.	-2808.	-1.	-0.	-1926.	3161.	-690.	-520.	-2288.	-3328.

I	UN	US	ROT	UX	UY	EPS	EPTH	CURVE S	CURVE TH
1	.000462	-.001095	.001472	-.000462	.001095	.0000712	-.0001351	-.0046992	0.0000000
2	.000447	-.001094	.001515	-.000447	.001094	.0000712	-.0001307	-.0041844	0.0000000
3	.000432	-.001093	.001556	-.000432	.001093	.0000712	-.0001262	-.0036696	0.0000000
4	.000416	-.001093	.001590	-.000416	.001093	.0000712	-.0001216	-.0031548	0.0000000
5	.000400	-.001092	.00161[illegible]	-.000400	.001092	.0000712	-.0001170	-.002[illegible]400	0.0000000
6	.000384	-.001091	.001643	-.000384	.001091	.0000712	-.0001122	-.0021252	0.0000000

SHELL ELEM 19 NODES= 19 20 MAT= 1 LENGTH= .1414 TEMPERATURES (1,2) = 70.0 70.0

I	X	Y	SIG S	SIG TH	S MOM	TH MOM	S BEND	SIG S1	SIG S2	TH BEND	SIG TH1	SIG TH2
1	3.4200	2.7000	-252.	-3209.	-3.	0.	-1599.	1347.	-1851.	44.	-3253.	-3166.
2	3.4[illegible]00	2.6800	-179.	-2939.	-2.	0.	-1339.	1159.	-1518.	126.	-3064.	-2813.
3	[illegible]	2.6[illegible]	-104.	[illegible]	-2.	0.	-1078.	974.	-1182.	206.	-2866.	-2453.
4	[illegible]	2.6400	-26.	-2373.	-1.	0.	-818.	792.	-845.	285.	-2659.	-2088.
5	[illegible]	2.6200	53.	-2090.	-1.	1.	-559.	611.	-500.	363.	-2443.	-1717.
6	[illegible]	2.6000	133.	-1781.	-0.	1.	-294.	433.	-156.	440.	-2221.	-1342.

I	UN	US	ROT	UX	UY	EPS	EPTH	CURVE S	CURVE TH
1	.00[illegible]643	-.000500	.001643	-.000384	.001091	.0000219	-.0001122	-.0011507	.0003396
2	.00[illegible]96	-.000500	.001673	-.000351	.001058	.0000219	-.0001032	-.0009803	.0003479
3	.00[illegible]43	-.000499	.001698	-.000318	.001023	.0000219	-.0000940	-.000[illegible]099	.0003553
4	[illegible]	-.000498	.001719	-.000284	.000[illegible]89	.0000219	-.000[illegible]845	-.000[illegible]395	[illegible]17
5	[illegible]	-.000498	.001734	-.000250	.00[illegible]54	.0000219	-.000[illegible]746	-.00[illegible]	[illegible]672
6	[illegible]	-.00[illegible]497	.001745	-.000215	.000919	.0000219	-.0000649	-.000[illegible]926	[illegible]

SHELL ELEM 20 NODES= 20 21 MAT= 1 LENGTH= .1562 TEMPERATURES (1,2) = 70.0 70.0

I	X	Y	SIG S	SIG TH	S MOM	TH MOM	S BEND	SIG S1	SIG S2	TH BEND	SIG TH1	SIG TH2
1	[illegible]	2.6000	-224.	-1878.	-1.	1.	-308.	84.	-532.	482.	-2360.	[illegible]
2	[illegible]	2.5[illegible]	-142.	-1574.	-0.	1.	-232.	90.	-374.	510.	-2043.	-1064.
3	[illegible]	2.5600	-58.	-1263.	-0.	1.	-157.	98.	-215.	537.	-1800.	-727.
4	[illegible]	2.5400	27.	-947.	-0.	1.	-81.	108.	-54.	564.	-1511.	-384.
5	[illegible]	[illegible]	114.	-625.	-0.	1.	-5.	119.	1[illegible]9.	5[illegible].	-1[illegible]5.	-3[illegible].
6	[illegible]	2.5[illegible]	202.	-29[illegible].	0.	1.	7[illegible].	132.	273.	616.	-914.	317.

I	UN	US	ROT	UX	UY	EPS	EPTH	CURVE S	CURVE TH
1	[illegible]	-.000423	.001745	-.000215	.000919	.0000101	-.0000649	-.0003[illegible]2	.0004038
2	[illegible]	-.000422	.001754	-.000181	.000876	.0000101	-.0000548	-.0002643	.0004089
3	[illegible]34	-.000422	.001762	-.000146	.000834	.0000101	-.000[illegible]446	-.000[illegible]153	.0004[illegible]36
4	[illegible]	-.000422	.001768	-.000[illegible]11	.000791	.0000101	-.0[illegible]341	-.0001664	.0004[illegible]81
5	[illegible]	-.000421	.001772	-.000076	.000747	.0000101	-.0[illegible]3[illegible]	-.000[illegible]174	.0004223
6	[illegible]	-.000421	.001775	-.000040	.000705	.0000101	-.0[illegible]26	-.000[illegible]684	.0004[illegible]5[illegible]

SHELL ELEM 21 NODES= 19 22 MAT= 1 LENGTH= .1000 TEMPERATURES (1,2) = 70.0 70.0

I	X	Y	SIG S	SIG TH	S MOM	TH MOM	S BEND	SIG S1	SIG S2	TH BEND	SIG TH1	SIG TH2
1	[illegible]	2.7000	814.	-2[illegible]2.	2.	[illegible]	2787.	-1973.	35[illegible].	753.	-3674.	-2159.
2	[illegible]	2.[illegible]	[illegible]	-2637.	2.	[illegible]	27[illegible]7.	-1906.	[illegible]	755.	-33[illegible]2.	-1881.
3	[illegible]	[illegible]	965.	[illegible]	2.	[illegible]	[illegible]	-1[illegible]2.	[illegible]	755.	-[illegible]21.	-1[illegible]5.
4	[illegible]	2.64[illegible]	1026.	[illegible]	2.	[illegible]	[illegible]	[illegible]	[illegible]	7[illegible]1.	[illegible]	[illegible]
5	[illegible]	2.[illegible]	1.[illegible]4.	[illegible]	2.	[illegible]	[illegible]23.	[illegible]	[illegible]3.	[illegible]64.	[illegible]2.	[illegible]
6	[illegible]	2.5[illegible]	1[illegible].	[illegible]	2.	[illegible]	[illegible]3.	-1[illegible].	[illegible]	7[illegible]5.	-3[illegible]4.	-[illegible]1.

I	UN	US	ROT	UX	UY	EPS	EPTH	CURVE S	CURVE TH
1	[illegible]	-.00[illegible]91	.0[illegible]1443	-.000384	.00[illegible]91	.0[illegible]73	-.[illegible]22	.00[illegible]751	0.[illegible]
2	[illegible]	[illegible]	[illegible]	[illegible]	[illegible]	[illegible]73	[illegible]	.003[illegible]874	0.[illegible]
3	[illegible]	[illegible]	[illegible]	[illegible]0	[illegible]84	[illegible]73	[illegible]	.003[illegible]987	0.[illegible]
4	[illegible]	[illegible]	[illegible]457	[illegible]1	[illegible]85	[illegible]73	[illegible]	[illegible]	0.[illegible]
5	[illegible]	[illegible]	[illegible]	[illegible]2	[illegible]7	[illegible]	[illegible]	[illegible]212	0.[illegible]
6	[illegible]	[illegible]	[illegible]	[illegible]	[illegible]	[illegible]3	[illegible]	[illegible]	[illegible]

SHELL ELEM 22 NODES= 22 [illegible] MAT= [illegible] LENGTH= .1000 TEMPERATURES (1,2) = 70.0 70.0

I	X	Y	SIG S	SIG TH	S MOM	TH MOM	S BEND	SIG S1	SIG S2	TH BEND	SIG TH1	SIG TH2
[illegible]	[illegible]	[illegible]	[illegible]	[illegible]	[illegible]	[illegible]	[illegible]	[illegible]	[illegible]	[illegible]	[illegible]	[illegible]

3	3.4200	2.5600	972.	-1244.	2.	0.	2543.	-1170.	3819.	716.	-1						
4	3.4200	2.5000	1022.	-1035.	2.	0.	2555.	-1326.	3884.	690.	-1						
5	3.4200	2.4400	1082.	-826.	1.	0.	2561.	-1389.	3950.	668.	-1						
6	3.4200	2.3800	1134.	-647.	1.	0.	2561.	-1247.	3514.	543.	-1						
	UN	US	ROT		UX	UY		EPS	EPTH	CURVE S	CURVE TH						
1	.0000116	-.0010	.0010		-.0001	.0010		.0000	-.0000	.0031	0.0000000						
2	.0000096	-.0010	.0009		-.0000	.0010		.0000	-.0000	.0031	0.0000000						
3	.0000077	-.0010	.0009		-.0000	.0010		.0000	-.0000	.0030	0.0000000						
4	.0000058	-.0010	.0009		-.0000	.0010		.0000	-.0000	.0029	0.0000000						
5	.0000041	-.0010	.0008		-.0000	.0010		.0000	-.0000	.0028	0.0000000						
6	.0000024	-.0010	.0008		-.0000	.0010		.0000	-.0000	.0027	0.0000000						

SHELL ELEM 23 NODES= 23 24 MAT= 1 LENGTH= .1000 TEMPERATURES (1,2) = 70.0 70.0

	X	Y	SIG S	SIG TH	S MOM	TH MOM	S BEND	SIG S1	SIG S2	TH BEND	SIG TH1	SIG TH2
1	3.4200	2.5000	863.	-715.	1.	0.	2384.	-1481.	3247.	638.	-1353.	-76.
2	3.4200	2.4400	932.	-534.	1.	0.	2396.	-1394.	3168.	604.	-1335.	69.
3	3.4200	2.3800	997.	-358.	1.	0.	2398.	-1339.	3096.	569.	-1322.	205.
4	3.4200	2.3200	1052.	-200.	1.	0.	2398.	-1298.	3042.	535.	-1315.	318.
5	3.4200	2.2600	1094.	-74.	1.	0.	2396.	-1268.	3002.	505.	-1311.	396.
6	3.4200	2.2000	1124.	24.	1.	0.	2394.	-1247.	2974.	481.	-1309.	439.
	UN	US	ROT		UX	UY		EPS	EPTH	CURVE S	CURVE TH	
1	.0000116	-.0010	.0010		-.0001	.0010		.0000	-.0000	.0026	0.0000000	
2	.0000096	-.0010	.0009		-.0000	.0010		.0000	-.0000	.0024	0.0000000	
3	.0000077	-.0010	.0009		-.0000	.0010		.0000	-.0000	.0023	0.0000000	
4	.0000058	-.0010	.0009		-.0000	.0010		.0000	-.0000	.0022	0.0000000	
5	.0000041	-.0010	.0008		-.0000	.0010		.0000	-.0000	.0021	0.0000000	
6	.0000024	-.0010	.0008		-.0000	.0010		.0000	-.0000	.0020	0.0000000	

SHELL ELEM 24 NODES= 24 25 MAT= 1 LENGTH= .1000 TEMPERATURES (1,2) = 70.0 70.0

	X	Y	SIG S	SIG TH	S MOM	TH MOM	S BEND	SIG S1	SIG S2	TH BEND	SIG TH1	SIG TH2
1	3.4200	2.4000	1422.	190.	1.	0.	3852.	-2429.	5274.	1040.	-850.	1230.
2	3.4200	2.3800	1459.	324.	1.	0.	3572.	-2113.	5030.	964.	-641.	1298.
3	3.4200	2.3600	1489.	436.	1.	0.	3292.	-1803.	4781.	889.	-452.	1325.
4	3.4200	2.3400	1514.	530.	1.	0.	3012.	-1497.	4525.	813.	-283.	1343.
5	3.4200	2.3200	1535.	606.	1.	0.	2732.	-1197.	4266.	738.	-131.	1344.
6	3.4200	2.3000	1551.	666.	1.	0.	2451.	-900.	4002.	662.	4.	1328.
	UN	US	ROT		UX	UY		EPS	EPTH	CURVE S	CURVE TH	
1	.0000024	-.0010	.0008		-.0000	.0010		.0000	-.0000	.0063	0.0000000	
2	.0000009	-.0010	.0006		-.0000	.0010		.0000	-.0000	.0059	0.0000000	
3	-.0000004	-.0010	.0005		.0000	.0010		.0000	.0000	.0054	0.0000000	
4	-.0000015	-.0010	.0004		.0000	.0010		.0000	.0000	.0049	0.0000000	
5	-.0000023	-.0010	.0003		.0000	.0010		.0000	.0000	.0045	0.0000000	
6	-.0000030	-.0010	.0002		.0000	.0010		.0000	.0000	.0040	0.0000000	

SHELL ELEM 25 NODES= 25 26 MAT= 1 LENGTH= .3000 TEMPERATURES (1,2) = 70.0 70.0

	X	Y	SIG S	SIG TH	S MOM	TH MOM	S BEND	SIG S1	SIG S2	TH BEND	SIG TH1	SIG TH2
1	3.4200	2.3000	1487.	649.	1.	0.	2230.	-743.	3717.	602.	47.	1251.
2	3.4200	2.2400	1515.	752.	0.	0.	1751.	-236.	3266.	473.	280.	1225.
3	3.4200	2.1800	1518.	764.	0.	0.	1272.	246.	2790.	343.	420.	1107.
4	3.4200	2.1200	1503.	708.	0.	0.	792.	711.	2295.	214.	494.	922.
5	3.4200	2.0600	1477.	611.	0.	-0.	313.	1163.	1790.	85.	526.	695.
6	3.4200	2.0000	1446.	497.	-0.	-0.	-166.	1612.	1280.	-45.	542.	452.
	UN	US	ROT		UX	UY		EPS	EPTH	CURVE S	CURVE TH	
1	-.0000030	-.0010	.0002		.0000	.0010		.0000	.0000	.0036	0.0000000	
2	-.0000042	-.0010	.0001		.0000	.0010		.0000	.0000	.0028	0.0000000	
3	-.0000043	-.0010	-.0000		.0000	.0010		.0000	.0000	.0021	0.0000000	
4	-.0000037	-.0010	-.0001		.0000	.0010		.0000	.0000	.0013	0.0000000	
5	-.0000026	-.0010	-.0002		.0000	.0010		.0000	.0000	.0005	0.0000000	
6	-.0000013	-.0010	-.0002		.0000	.0010		.0000	.0000	-.0002	0.0000000	

SHELL ELEM 26 NODES= 26 27 MAT= 1 LENGTH= .3000 TEMPERATURES (1,2) = 70.0 70.0

	X	Y	SIG S	SIG TH	S MOM	TH MOM	S BEND	SIG S1	SIG S2	TH BEND	SIG TH1	SIG TH2
1	3.4200	2.0000	1565.	529.	-0.	-0.	-45.	1610.	1521.	-12.	541.	517.
2	3.4200	1.9400	1535.	417.	-0.	-0.	-124.	1659.	1411.	-33.	451.	384.
3	3.4200	1.8800	1507.	312.	-0.	-0.	-203.	1710.	1304.	-55.	367.	257.
4	3.4200	1.8200	1481.	217.	-0.	-0.	-282.	1764.	1199.	-76.	294.	141.
5	3.4200	1.7600	1460.	138.	-0.	-0.	-362.	1821.	1098.	-98.	235.	-40.
6	3.4200	1.7000	1443.	77.	-0.	-0.	-441.	1884.	1002.	-119.	196.	-42.
	UN	US	ROT		UX	UY		EPS	EPTH	CURVE S	CURVE TH	
1	-.0000013	-.0010	-.0002		.0000	.0010		.0000	.0000	-.0000	0.0000000	
2	.0000000	-.0010	-.0002		.0000	.0010		.0000	.0000	-.0002	0.0000000	
3	.0000012	-.0010	-.0001		-.0000	.0010		.0000	-.0000	-.0003	0.0000000	
4	.0000022	-.0010	-.0001		-.0000	.0010		.0000	-.0000	-.0004	0.0000000	
5	.0000031	-.0010	-.0001		-.0000	.0010		.0000	-.0000	-.0005	0.0000000	
6	.0000038	-.0010	-.0000		-.0000	.0010		.0000	-.0000	-.0007	0.0000000	

SHELL ELEM 27 NODES= 27 28 MAT= 1 LENGTH= .3000 TEMPERATURES (1,2) = 70.0 70.0

	X	Y	SIG S	SIG TH	S MOM	TH MOM	S BEND	SIG S1	SIG S2	TH BEND	SIG TH1	SIG TH2
1	3.4200	1.7000	1509.	95.	-0.	-0.	-381.	1890.	1128.	-103.	198.	-8.
2	3.4200	1.6400	1498.	55.	-0.	-0.	-367.	1865.	1131.	-99.	154.	-44.
3	3.4200	1.5800	1493.	34.	-0.	-0.	-353.	1846.	1140.	-95.	130.	-61.
4	3.4200	1.5200	1492.	32.	-0.	-0.	-339.	1831.	1154.	-91.	124.	-59.
5	3.4200	1.4600	1497.	48.	-0.	-0.	-325.	1821.	1172.	-88.	136.	-39.
6	3.4200	1.4000	1505.	81.	-0.	-0.	-310.	1816.	1195.	-84.	165.	-3.
	UN	US	ROT		UX	UY		EPS	EPTH	CURVE S	CURVE TH	

6	.000040	-.001027	.000078	-.000040	.001027	.0000530	-.0000116	-.0005138	0.0000000

SHELL ELEM 28 NODES= 28 29 MAT= 1 LENGTH= .3000 TEMPERATURES (1,2) = 70.0 70.0

	X	Y	SIG S	SIG TH	S MOM	TH MOM	S BEND	SIG S1	SIG S2	TH BEND	SIG TH1	SIG TH2
1	3.4200	1.4000	1455.	68.	-0.	-0.	-358.	1813.	1097.	-97.	164.	-29.
2	3.4200	1.3400	1468.	117.	-0.	-0.	-264.	1733.	1204.	-71.	189.	46.
3	3.4200	1.2800	1486.	181.	-0.	-0.	-171.	1659.	1315.	-46.	227.	135.
4	3.4200	1.2200	1505.	254.	-0.	-0.	-77.	1582.	1428.	-21.	275.	233.
5	3.4200	1.1600	1526.	331.	0.	0.	17.	1509.	1543.	5.	326.	335.
6	3.4200	1.1000	1546.	406.	0.	0.	110.	1436.	1657.	30.	377.	436.

	UN	US	ROT	UX	UY	EPS	EPTH	CURVE S	CURVE TH
1	.000040	-.001027	.000078	-.000040	.001027	.0000513	-.0000116	-.0005922	0.0000000
2	.000034	-.001024	.000109	-.000034	.001024	.0000513	-.0000100	-.0004373	0.0000000
3	.000027	-.001021	.000130	-.000027	.001021	.0000513	-.0000079	-.0002823	0.0000000
4	.000019	-.001018	.000143	-.000019	.001018	.0000513	-.0000055	-.0001274	0.0000000
5	.000010	-.001015	.000146	-.000010	.001015	.0000513	-.0000029	.0000276	0.0000000
6	.000001	-.001011	.000139	-.000001	.001011	.0000513	-.0000004	.0001826	0.0000000

SHELL ELEM 29 NODES= 29 30 MAT= 1 LENGTH= .3000 TEMPERATURES (1,2) = 70.0 70.0

	X	Y	SIG S	SIG TH	S MOM	TH MOM	S BEND	SIG S1	SIG S2	TH BEND	SIG TH1	SIG TH2
1	3.4200	1.1000	1478.	388.	0.	0.	36.	1442.	1515.	10.	378.	398.
2	3.4200	1.0400	1497.	457.	0.	0.	429.	1068.	1926.	116.	342.	573.
3	3.4200	.9800	1510.	504.	0.	0.	822.	688.	2332.	222.	282.	726.
4	3.4200	.9200	1511.	508.	0.	0.	1215.	296.	2726.	328.	180.	836.
5	3.4200	.8600	1495.	447.	0.	0.	1608.	-118.	3102.	434.	13.	882.
6	3.4200	.8000	1455.	302.	1.	0.	2001.	-545.	3456.	540.	-238.	843.

	UN	US	ROT	UX	UY	EPS	EPTH	CURVE S	CURVE TH
1	.000001	-.001011	.000139	-.000001	.001011	.0000491	-.0000004	.0000597	0.0000000
2	.000006	-.001009	.000116	.000006	.001009	.0000491	.0000019	.0007102	0.0000000
3	.000012	-.001006	.000054	.000012	.001006	.0000491	.0000025	.0013606	0.0000000
4	.000017	-.001003	-.000047	.000012	.001003	.0000491	.0000036	.0020111	0.0000000
5	.000005	-.001000	-.000187	.000005	.001000	.0000491	.0000016	.0026615	0.0000000
6	.000011	-.000997	-.000367	-.000011	.000997	.0000491	-.0000032	.0033120	0.0000000

SHELL ELEM 30 NODES= 30 31 MAT= 1 LENGTH= .3000 TEMPERATURES (1,2) = 70.0 70.0

	X	Y	SIG S	SIG TH	S MOM	TH MOM	S BEND	SIG S1	SIG S2	TH BEND	SIG TH1	SIG TH2
1	3.4200	.8000	1801.	396.	1.	0.	2275.	-474.	4076.	614.	-218.	1010.
2	3.4200	.7400	1731.	137.	1.	0.	2791.	-1060.	4523.	754.	-615.	891.
3	3.4200	.6800	1622.	-268.	1.	0.	3308.	-1686.	4930.	893.	-1161.	625.
4	3.4200	.6200	1465.	-848.	1.	0.	3825.	-2359.	5290.	1033.	-1881.	185.
5	3.4200	.5600	1254.	-1629.	1.	0.	4341.	-3067.	5596.	1172.	-2801.	-457.
6	3.4200	.5000	982.	-2638.	1.	0.	4858.	-3876.	5840.	1312.	-3950.	-1327.

	UN	US	ROT	UX	UY	EPS	EPTH	CURVE S	CURVE TH
1	.000011	-.000997	-.000367	-.000011	.000997	.0000605	-.0000032	.0037659	0.0000000
2	.000040	-.000993	-.000618	-.000040	.000993	.0000605	-.0000118	.0046212	0.0000000
3	.000086	-.000990	-.000921	-.000086	.000990	.0000605	-.0000252	.0054766	0.0000000
4	.000152	-.000986	-.001275	-.000152	.000986	.0000605	-.0000444	.0063319	0.0000000
5	.000240	-.000982	-.001681	-.000240	.000982	.0000605	-.0000703	.0071872	0.0000000
6	.000355	-.000979	-.002138	-.000355	.000979	.0000605	-.0001037	.0080426	0.0000000

SHELL ELEM 31 NODES= 31 32 MAT= 1 LENGTH= .2000 TEMPERATURES (1,2) = 70.0 70.0

	X	Y	SIG S	SIG TH	S MOM	TH MOM	S BEND	SIG S1	SIG S2	TH BEND	SIG TH1	SIG TH2
1	3.4200	.5000	1999.	-2364.	1.	0.	2858.	-859.	4856.	772.	-3135.	-1592.
2	3.4200	.4600	1788.	-3142.	0.	0.	324.	1465.	2112.	87.	-3230.	-3055.
3	3.4200	.4200	1576.	-3929.	-1.	-0.	-2211.	3787.	-635.	-597.	-3332.	-4525.
4	3.4200	.3800	1378.	-4653.	-1.	-0.	-4745.	6122.	-3357.	-1281.	-3382.	-5944.
5	3.4200	.3400	1209.	-5267.	-2.	-1.	-7279.	8488.	-6069.	-1955.	-3221.	-7252.
6	3.4200	.3000	1087.	-5740.	-3.	-1.	-9813.	10900.	-8726.	-2549.	-3041.	-8389.

	UN	US	ROT	UX	UY	EPS	EPTH	CURVE S	CURVE TH
1	.000355	-.000979	-.002138	-.000355	.000979	.0000942	-.0001037	.0047309	0.0000000
2	.000443	-.000975	-.002243	-.000443	.000975	.0000942	-.0001295	.0059356	0.0000000
3	.000532	-.000971	-.002181	-.000532	.000971	.0000942	-.0001555	.0036897	0.0000000
4	.000615	-.000967	-.001950	-.000615	.000967	.0000942	-.0001798	.0076550	0.0000000
5	.000686	-.000964	-.001552	-.000686	.000964	.0000942	-.0002005	.0125504	0.0000000
6	.000737	-.000960	-.000986	-.000737	.000960	.0000942	-.0002155	.0182457	0.0000000

SHELL ELEM 32 NODES= 32 33 MAT= 1 LENGTH= .1655 TEMPERATURES (1,2) = 70.0 70.0

	X	Y	SIG S	SIG TH	S MOM	TH MOM	S BEND	SIG S1	SIG S2	TH BEND	SIG TH1	SIG TH2
1	3.4200	.3000	1713.	-5571.	-3.	-1.	-9958.	11670.	-8245.	-2757.	-2814.	-8328.
2	3.4200	.2700	1650.	-5802.	-3.	-1.	-10023.	11674.	-8373.	-2737.	-2945.	-8539.
[illegible]												
6	3.4200	.1500	1845.	-5248.	-3.	-1.	-10264.	12084.	-8465.	-2655.	-2998.	-7899.

	UN	US	ROT	UX	UY	EPS	EPTH	CURVE S	CURVE TH
1	.001074	-.000558	-.000986	-.000737	.000960	.0001149	-.0002155	.0174524	-.0012220
2	.001097	-.000554	-.000940	-.000752	.000965	.0001149	-.0002231	.0164744	-.0005486
[illegible]												
6	.001043	-.000534	-.001224	-.000686	.000915	.0001149	-.0002045	.0174473	.0012259

SHELL EL[illegible] 33 NODES= 33 34 MAT= [illegible] LENGTH= .2121 TEMPERATURES (1,2) = [illegible] 70.0

	X	Y	SIG S	SIG TH	S MOM	TH MOM	S BEND	SIG S1	SIG S2	TH BEND	SIG TH1	SIG TH2
1	[illegible]											

3	3.2900	.0900	1700.	-4199.	-1.	-0.	-5623.	7323.	-3923.	-1155.	-[illegible]	-5345.
4	3.2600	.0600	1913.	-3414.	-1.	-0.	-3239.	5146.	-1323.	-[illegible]	-[illegible]	-3890.
5	3.2300	.0300	2124.	-2543.	-0.	-0.	-953.	3[illegible].	1694.	1[illegible]6.	-[illegible]	-2[illegible].
6	3.2000	.0000	2331.	-1[illegible].	-0.	-0.	1523.	854.	3914.	83[illegible].	-[illegible]	-[illegible].

	UN	JS	ROT	UX	UY	EPS	EPTH	CURVE S	CURVE TH
3	-.0[illegible]22	-.[illegible]662	.001790	-.[illegible]	.[illegible]915	.0000[illegible]012	-.[illegible]2[illegible]2[illegible]	-[illegible]	.0003777
4	-.0[illegible]1[illegible]2	-.[illegible]588	.002[illegible]2	-.[illegible]	.[illegible]784	.0000[illegible]012	-.[illegible]1[illegible]83	-[illegible]	.0005201
5	-.0[illegible]3827	-.[illegible]153	.002928	-.[illegible]	.[illegible]764	.0000[illegible]012	-.[illegible]1[illegible]63	-[illegible]	.0006292
6	-.0[illegible]3796	-.[illegible]149	.[illegible]2945	-.[illegible]	.[illegible]750	.0000[illegible]012	-.[illegible]1[illegible]3	-[illegible]	.0007042
7	-.0[illegible]3764	-.[illegible]145	.[illegible]2961	-.[illegible]	.[illegible]736	.0000[illegible]012	-.[illegible]1[illegible]3	-[illegible]	.0007439
8	-.0[illegible]3731	-.[illegible]140	.[illegible]2977	-.[illegible]	.[illegible]721	.0000[illegible]012	-.[illegible]1[illegible]3	-[illegible]	.0007476

SHELL ELEM 34 NODES= 31 35 MAT= [illegible] LENGTH= [illegible].2663 TEMPERATURES (1,2) = 70.0 70.0

	X	Y	SIG S	SIG TH	S MOM	TH MOM	S BEND	SIG S1	SIG S2	TH BEND	SIG TH1	SIG TH2
1	3.4200	-.[illegible]50	-4[illegible].	-[illegible].	[illegible]	-1.	252.	-558.	-154.	-[illegible]55.	-[illegible].	-3668.
2	3.[illegible]00	-.[illegible]350	-2[illegible].	-[illegible].	[illegible]	-1.	1[illegible].	-446.	-78.	-6[illegible].	-[illegible].	-3171.
3	3.3620	-.0[illegible]60	-1[illegible].	-[illegible].	0.	-1.	118.	-230.	3.	-720.	-1216.	-2657.
4	3.2820	-.0[illegible]00	37.	-[illegible].	[illegible]	-1.	51.	-[illegible].	89.	-752.	-620.	-2123.
5	3.2440	-.02[illegible]	195.	-[illegible].	[illegible]	-1.	-15.	210.	179.	-783.	-5.	-1572.
6	3.2[illegible]	-.0[illegible]	357.	-[illegible].	[illegible]	-1.	-62.	[illegible]39.	278.	-814.	627.	-[illegible].

	UN	JS	ROT	UX	UY	EPS	EPTH	CURVE S	CURVE TH
1	.0[illegible]0609	.[illegible]0044	-.[illegible]2134	-.0003[illegible]55	.[illegible]0[illegible]979	.0000[illegible]146	-.0[illegible]01037	.0[illegible]0[illegible]662	-.0005165
2	.0[illegible]0723	.[illegible]0845	-.[illegible]2[illegible]3	-.0000291	.0[illegible]1073	.0000[illegible]146	-.0[illegible]0[illegible]662	.[illegible]0[illegible]647	-.0005269
3	.0[illegible]0832	.[illegible]0646	-.[illegible]2[illegible]5	-.[illegible]327	.0[illegible]1169	.0000[illegible]146	-.0[illegible]0[illegible]581	.0[illegible]0[illegible]232	-.0005371
4	.0[illegible]0954	.0[illegible]847	-.[illegible]2177	-.0[illegible]152	.0[illegible]1265	.0000[illegible]146	-.0[illegible]0[illegible]493	.0[illegible]01816	-.0005470
5	.0[illegible]1070	.0[illegible]847	-.[illegible]2[illegible]3	-.[illegible]0097	.0[illegible]1361	.0000[illegible]146	-.0[illegible]0[illegible]399	.0[illegible]01401	-.0005566
6	.0[illegible]1185	.0[illegible]848	-.[illegible]2192	-.[illegible]0032	.0[illegible]1456	.0000[illegible]146	-.0[illegible]0[illegible]101	.0[illegible]0[illegible]986	-.0005659

SHELL ELEM 35 NODES= 34 [illegible] MAT= [illegible] LENGTH= .1414 TEMPERATURES (1,2) = 70.0 70.0

	X	Y	SIG S	SIG TH	S MOM	TH MOM	S BEND	SIG S1	SIG S2	TH BEND	SIG TH1	SIG TH2
1	3.2000	-.0[illegible]0	15[illegible]	-[illegible]53.	0.	0.	1007.	541.	2605.	69[illegible]	-2[illegible]4.	-1163.
2	3.1800	-.0200	1762.	-1247.	1.	0.	2575.	-812.	4337.	1107.	-2[illegible]53.	-140.
3	3.1600	-.0400	1972[illegible]	-654.	1.	0.	4139.	-2217.	6061.	1513.	-2167.	859.
4	3.1400	-.0600	2074.	-91[illegible].	2.	1.	5702.	-3627.	7776.	1909.	-1909.	1818.
5	3.1200	-.0800	2215.	430.	2.	1.	7261.	-5046.	9476.	2294.	-1[illegible]65.	2724.
6	3.1000	-.1000	2339.	891.	2.	1.	8818.	-6478.	11157.	2669.	-1778.	3560.

	UN	JS	ROT	UX	UY	EPS	EPTH	CURVE S	CURVE TH
1	.0[illegible]0510	-.[illegible]140	.003383	-.000261	.000460	.0000750	-.0000816	.0[illegible]4651	.0007476
2	.0[illegible]0415	-.[illegible]138	.003305	-.0001[illegible]96	.000391	.0000750	-.0000615	.0[illegible]40638	.0007349
3	.0[illegible]0323	-.[illegible]136	.003153	-.0001[illegible]32	.000325	.0000750	-.0000415	.0[illegible]0625	.0007056
4	.0[illegible]0237	-.[illegible]134	.002928	-.0000[illegible]73	.000263	.0000750	-.0000232	.0[illegible]2613	.0006542
5	.0[illegible]0159	-.[illegible]132	.002630	-.0000[illegible]9	.000205	.0000750	-.0000060	.0[illegible]1600	.0005959
6	.0[illegible]0089	-.[illegible]130	.002257	.0000029	.000155	.0000750	.0000093	.0144588	.0005149

SHELL ELEM 36 NODES= 36 37 MAT= 1 LENGTH= .1217 TEMPERATURES (1,2) = 70.0 70.0

	X	Y	SIG S	SIG TH	S MOM	TH MOM	S BEND	SIG S1	SIG S2	TH BEND	SIG TH1	SIG TH2
1	3.1000	-.1000	-806.	42.	1.	0.	4736.	-5342.	3930.	1661.	-1639.	1723.
2	3.0760	-.0960	-827.	-34.	1.	0.	3917.	-4744.	3090.	1432.	-1467.	1398.
3	3.0520	-.0920	-846.	-106.	1.	0.	3099.	-3945.	2253.	1196.	-1295.	1084.
4	3.0280	-.0880	-864.	-173.	1.	0.	2283.	-3148.	1419.	953.	-1127.	780.
5	3.0040	-.0840	-882.	-238.	0.	0.	1469.	-2351.	587.	723.	-961.	485.
6	2.9800	-.0800	-899.	-302.	0.	0.	656.	-1555.	-243.	499.	-801.	197.

	UN	JS	ROT	UX	UY	EPS	EPTH	CURVE S	CURVE TH
1	.0[illegible]0458	-.[illegible]003	.002257	.0000029	.000155	-.0000292	.0000093	.0[illegible]4[illegible]0	.0007123
2	.0[illegible]0105	-.[illegible]004	.002088	.0000021	.000103	-.0000292	.0000067	.0[illegible]3039	.0006694
3	.0[illegible]0056	-.[illegible]004	.001951	.0000013	.000054	-.0000292	.0000044	.0[illegible]4[illegible]08	.0006304
4	.0[illegible]0010	-.[illegible]005	.001846	.0000007	.000009	-.0000292	.0000021	.0[illegible]3177	.0006014
5	-.0[illegible]0034	-.[illegible]005	.001775	-.0000000	-.000035	-.0000292	-.0000000	.0[illegible]2746	.0005827
6	-.0[illegible]0077	-.[illegible]006	.001736	-.0000006	-.000077	-.0000292	-.0000021	.0[illegible]4315	.0005745

SHELL ELEM 37 NODES= 37 38 MAT= 1 LENGTH= .1044 TEMPERATURES (1,2) = 70.0 70.0

	X	Y	SIG S	SIG TH	S MOM	TH MOM	S BEND	SIG S1	SIG S2	TH BEND	SIG TH1	SIG TH2
1	2.9800	-.0800	-485.	-190.	1.	0.	3467.	-3952.	2982.	1248.	-1439.	1058.
2	2.9600	-.0740	-512.	-290.	1.	0.	3306.	-3818.	2794.	1176.	-1477.	856.
3	2.9400	-.0680	-537.	-385.	1.	0.	3145.	-3682.	2607.	1125.	-1510.	740.
4	2.9200	-.0620	-561.	-474.	1.	0.	2984.	-3546.	2423.	1065.	-1539.	599.
5	2.9000	-.0560	-584.	-558.	1.	0.	2824.	-3408.	2239.	1005.	-1563.	447.
6	2.8800	-.0500	-606.	-638.	1.	0.	2663.	-3269.	2058.	946.	-1584.	309.

	UN	JS	ROT	UX	UY	EPS	EPTH	CURVE S	CURVE TH
1	-.0[illegible]0076	-.[illegible]0016	.001736	-.0000006	-.000077	-.0000155	-.0000021	.0[illegible]3868	.0005578
2	-.0[illegible]0111	-.[illegible]0016	.001622	-.0000016	-.000111	-.0000155	-.0000054	.0[illegible]3310	.0005247
3	-.0[illegible]0143	-.[illegible]0017	.001513	-.0000025	-.000142	-.0000155	-.0000086	.0[illegible]2733	.0004929
4	-.0[illegible]0174	-.[illegible]0017	.001410	-.0000034	-.000171	-.0000155	-.0000115	.0[illegible]2155	.0004624
5	-.0[illegible]0202	-.[illegible]0017	.001312	-.0000041	-.000199	-.0000155	-.0000143	.0[illegible]1578	.0004333
6	-.0[illegible]0229	-.[illegible]0018	.001219	-.0000049	-.000224	-.0000155	-.0000169	.0[illegible]1000	.0004055

SHELL ELEM 38 NODES= 38 39 MAT= 1 LENGTH= .0854 TEMPERATURES (1,2) = 70.0 70.0

	X	Y	SIG S	SIG TH	S MOM	TH MOM	S BEND	SIG S1	SIG S2	TH BEND	SIG TH1	SIG TH2
1	2.8300	-.0500	-496.	-608.	1.	0.	2694.	-3190.	2198.	949.	-1557.	841.
2	2.8640	-.0440	-516.	-684.	1.	0.	2663.	-3179.	2146.	929.	-1612.	745.
3	2.8480	-.0380	-536.	-756.	1.	0.	2632.	-3167.	2096.	908.	-1664.	652.
4	2.8320	-.0320	-554.	-824.	1.	0.	2600.	-3155.	2045.	887.	-1711.	564.
5	2.8160	-.0260	-572.	-888.	1.	0.	2569.	-3141.	1998.	867.	-1754.	481.
6	2.8000	-.0200	-588.	-948.	1.	0.	2538.	-3126.	1951.	846.	-1794.	402.

6	-.000316	-.000034	.000857	-.000079	-.000307	-.00001119	-.0000282	.0041250	.0002866		

SHELL ELEM 39 NODES= 39 40 MAT= 1 LENGTH= .1077 TEMPERATURES (1,2) = 70.0 70.0

I	X	SIG S	SIG TH	S MOM	TH MOM	S BEND	SIG S1	SIG S2	TH BEND	SIG TH1	SIG TH2
1	2.8000	-.0200	-487.	-921.	1.	0.	2483.	-2969.	1996.	829.	-1750.	-91.
2	2.7800	-.0120	-507.	-996.	1.	0.	2684.	-3191.	2177.	868.	-1864.	-128.
3	2.7600	-.0040	-525.	-1063.	1.	0.	2885.	-3410.	2359.	905.	-1968.	-158.
4	2.7400	.0040	-541.	-1123.	1.	0.	3065.	-3626.	2543.	940.	-2063.	-183.
5	2.7200	.0120	-555.	-1174.	1.	0.	3285.	-3840.	2730.	973.	-2147.	-201.
6	2.7000	.0200	-566.	-1215.	1.	0.	3484.	-4050.	2918.	1004.	-2220.	-211.

I	UN	US	ROT	UX	UY	EPS	EPTH	CURVE S	CURVE TH
1	-.000315	-.000041	.000857	-.000079	-.000307	-.00000085	-.0000282	.0040331	.0002842
2	-.000332	-.000041	.000767	-.000085	-.000324	-.00000085	-.0000307	.0043739	.0002560
3	-.000348	-.000041	.000669	-.000091	-.000338	-.00000085	-.0000329	.0047147	.0002250
4	-.000361	-.000041	.000563	-.000096	-.000351	-.00000085	-.0000349	.0050554	.0001909
5	-.000372	-.000042	.000451	-.000099	-.000361	-.00000085	-.0000366	.0053962	.0001539
6	-.000380	-.000042	.000331	-.000102	-.000369	-.00000085	-.0000379	.0057370	.0001138

SHELL ELEM 40 NODES= 40 41 MAT= 1 LENGTH= .1562 TEMPERATURES (1,2) = 70.0 70.0

I	X	SIG S	SIG TH	S MOM	TH MOM	S BEND	SIG S1	SIG S2	TH BEND	SIG TH1	SIG TH2
1	2.7000	.0200	-474.	-1191.	1.	0.	3296.	-3770.	2821.	934.	-2124.	-257.
2	2.6800	.0440	-495.	-1265.	1.	0.	2992.	-3486.	2497.	830.	-2096.	-435.
3	2.6600	.0680	-504.	-1299.	1.	0.	2689.	-3192.	2185.	729.	-2028.	-570.
4	2.6400	.0920	-503.	-1295.	1.	0.	2386.	-2889.	1884.	629.	-1924.	-665.
5	2.6200	.1160	-492.	-1256.	1.	0.	2084.	-2576.	1592.	532.	-1788.	-725.
6	2.6000	.1400	-474.	-1187.	0.	0.	1782.	-2256.	1309.	436.	-1624.	-751.

I	UN	US	ROT	UX	UY	EPS	EPTH	CURVE S	CURVE TH
1	-.000315	-.000218	.000331	-.000102	-.000369	-.00000055	-.0000379	.0056349	.0000785
2	-.000323	-.000218	.000169	-.000108	-.000374	-.00000055	-.0000404	.0049424	.0000404
3	-.000325	-.000218	.000022	-.000110	-.000376	-.00000055	-.0000415	.0044500	.0000053
4	-.000324	-.000218	-.000109	-.000109	-.000375	-.00000055	-.0000414	.0039575	-.0000265
5	-.000319	-.000218	-.000225	-.000105	-.000372	-.00000055	-.0000401	.0034650	-.0000550
6	-.000310	-.000219	-.000326	-.000098	-.000366	-.00000055	-.0000378	.0029726	-.0000802

SHELL ELEM 41 NODES= 41 42 MAT= 1 LENGTH= .1208 TEMPERATURES (1,2) = 70.0 70.0

I	X	SIG S	SIG TH	S MOM	TH MOM	S BEND	SIG S1	SIG S2	TH BEND	SIG TH1	SIG TH2
1	2.6000	.1400	-537.	-1204.	1.	0.	1923.	-2460.	1387.	490.	-1695.	-714.
2	2.5900	.1620	-512.	-1115.	0.	0.	1778.	-2290.	1266.	444.	-1559.	-670.
3	2.5800	.1840	-483.	-1006.	0.	0.	1633.	-2116.	1150.	399.	-1405.	-607.
4	2.5700	.2060	-449.	-879.	0.	0.	1488.	-1937.	1039.	354.	-1233.	-525.
5	2.5600	.2280	-410.	-736.	0.	0.	1343.	-1753.	933.	309.	-1045.	-427.
6	2.5500	.2500	-367.	-577.	0.	0.	1198.	-1566.	831.	265.	-843.	-312.

I	UN	US	ROT	UX	UY	EPS	EPTH	CURVE S	CURVE TH
1	-.000241	-.000293	-.000326	-.000098	-.000366	-.00000076	-.0000378	.0031981	-.0000518
2	-.000232	-.000293	-.000400	-.000090	-.000363	-.00000076	-.0000349	.0029608	-.0000639
3	-.000222	-.000293	-.000469	-.000081	-.000359	-.00000076	-.0000313	.0027235	-.0000752
4	-.000210	-.000293	-.000532	-.000070	-.000354	-.00000076	-.0000271	.0024862	-.0000856
5	-.000196	-.000294	-.000589	-.000057	-.000349	-.00000076	-.0000223	.0022489	-.0000952
6	-.000181	-.000294	-.000640	-.000044	-.000343	-.00000076	-.0000171	.0020116	-.0001039

SHELL ELEM 42 NODES= 42 43 MAT= 1 LENGTH= .1503 TEMPERATURES (1,2) = 70.0 70.0

I	X	SIG S	SIG TH	S MOM	TH MOM	S BEND	SIG S1	SIG S2	TH BEND	SIG TH1	SIG TH2
1	2.5500	.2500	-605.	-542.	0.	0.	1164.	-1769.	558.	305.	-947.	-337.
2	2.5460	.2800	-541.	-405.	0.	0.	814.	-1356.	273.	210.	-615.	-195.
3	2.5420	.3100	-473.	-253.	0.	0.	465.	-938.	-8.	115.	-268.	-38.
4	2.5380	.3400	-403.	108.	0.	0.	116.	-519.	-287.	20.	87.	128.
5	2.5420	.3700	-332.	371.	-0.	-0.	-233.	-99.	-565.	-74.	444.	297.
6	2.5400	.4000	-252.	630.	-0.	-0.	-582.	320.	-844.	-168.	798.	462.

I	UN	US	ROT	UX	UY	EPS	EPTH	CURVE S	CURVE TH
1	-.0000066	-.000339	-.000640	-.000044	-.000343	-.00000154	-.0000171	.0019310	-.0000167
2	-.0000046	-.000339	-.000690	-.000024	-.000342	-.00000154	-.0000092	.0013530	-.0000180
3	-.0000025	-.000340	-.000722	-.000002	-.000341	-.00000154	-.0000009	.0007749	-.0000189
4	-.0000003	-.000340	-.000736	.000020	-.000340	-.00000154	.0000077	.0001969	-.0000193
5	.0000019	-.000341	-.000734	.000042	-.000339	-.00000154	.0000164	-.0003812	-.0000192
6	.0000041	-.000341	-.000713	.000064	-.000338	-.00000154	.0000250	-.0004592	-.0000187

SHELL ELEM 43 NODES= 43 44 MAT= 1 LENGTH= .2000 TEMPERATURES (1,2) = 70.0 70.0

I	X	SIG S	SIG TH	S MOM	TH MOM	S BEND	SIG S1	SIG S2	TH BEND	SIG TH1	SIG TH2
1	2.5400	.4000	-640.	528.	-0.	-0.	-531.	-109.	-1171.	-143.	671.	385.
2	2.5440	.4400	-551.	858.	-0.	-0.	-662.	112.	-1213.	-179.	1037.	679.
3	2.5480	.4800	-467.	1166.	-0.	-0.	-796.	326.	-1260.	-214.	1382.	954.
4	2.5520	.5200	-389.	1452.	-0.	-0.	-934.	534.	-1314.	-249.	1705.	1203.
5	2.5460	.5600	-321.	1717.	-0.	-0.	-1055.	724.	-1376.	-285.	1992.	1423.
6	2.5400	.6000	-261.	1930.	-0.	-0.	-1186.	905.	-1447.	-326.	2255.	1609.

I	UN	US	ROT	UX	UY	EPS	EPTH	CURVE S	CURVE TH
1	.0000064	-.000338	-.000713	.000064	-.000338	-.00000279	.0000250	-.0004793	0.0000000
2	.0000041	-.000339	-.000674	.000041	-.000339	-.00000279	.0000360	-.0001961	0.0000000
3	.0000020	-.000340	-.000626	.000017	-.000340	-.00000279	.0000462	.0000872	0.0000000
4	-.0000001	-.000341	-.000569	-.000007	-.000341	-.00000279	.0000556	.0003705	0.0000000
5	-.0000022	-.000342	-.000504	-.000031	-.000342	-.00000279	.0000641	.0006538	0.0000000
6	-.0000043	-.000343	-.000429	-.000054	-.000342	-.00000279	.0000714	.0009371	0.0000000

SHELL ELEM 44 NODES= 44 45 MAT= 1 LENGTH= .2000 TEMPERATURES (1,2) = 70.0 70.0

I	X	SIG S	SIG TH	S MOM	TH MOM	S BEND	SIG S1	SIG S2	TH BEND	SIG TH1	SIG TH2

I	X	Y	SIG S	SIG TH	S MOM	TH MOM	S BEND	SIG S1	SIG S2	TH BEND	SIG TH1	SIG TH2
4	2.5400	.7200	-410.	2367.	-0.	-0.	-1335.	925.	-1745.	[illegible]	[illegible]	[illegible]
5	2.5400	.7600	-391.	2378.	-0.	-0.	-1433.	1042.	-1824.	-327.	2765.	1691.
6	2.5[illegible]	.8000	-354.	2403.	-0.	-0.	-1531.	1145.	-1925.	-413.	2816.	1990.

I	UN	US	ROT	UX	UY	EPS	EPTH	CURVE S	CURVE TH
1	.000181	-.000343	-.000429	.000181	-.000343	-.0000369	.0000714	-.0017227	0.0000000
2	.000197	-.000345	-.000357	.000197	-.000345	-.0000369	.0000776	-.0019450	0.0000000
3	.000210	-.000346	-.000278	.000210	-.000346	-.0000369	.0000826	-.0022473	0.0000000
4	.000219	-.000348	-.000193	.000219	-.000348	-.0000369	[illegible]	[illegible]	0.0000000
5	.000225	-.000349	-.000102	.000225	-.000349	-.0000369	.0000867	[illegible]	0.0000000
6	.000227	-.000351	-.000003	.000227	-.000351	-.0000369	.0000895	-.002[illegible]341	0.0000000

SHELL ELEM 45 NODES= 45 46 MAT= 1 LENGTH= .2000 TEMPERATURES (1,2) = 70.0 70.0

I	X	Y	SIG S	SIG TH	S MOM	TH MOM	S BEND	SIG S1	SIG S2	TH BEND	SIG TH1	SIG TH2
1	2.5400	.8000	-369.	2407.	-0.	-0.	-1534.	1165.	-1903.	-414.	2821.	1993.
2	2.5400	.8400	-376.	2363.	-0.	-0.	-1829.	1453.	-2204.	-494.	2877.	1839.
3	2.5400	.8800	-398.	2302.	-1.	-0.	-2123.	1725.	-2520.	-573.	2875.	1728.
4	2.5400	.9200	-438.	2153.	-1.	-0.	-2417.	1979.	-2854.	-653.	2806.	1500.
5	2.5400	.9600	-498.	1928.	-1.	-0.	-2711.	2213.	-3209.	-732.	2660.	1196.
6	2.5400	1.0000	-592.	1618.	-1.	-0.	-3005.	2423.	-3597.	-811.	2430.	807.

I	UN	US	ROT	UX	UY	EPS	EPTH	CURVE S	CURVE TH
1	.000227	-.000351	-.000003	.000227	-.000351	-.0000364	.0000895	-.0025403	0.0000000
2	.000225	-.000352	.000108	.000225	-.000352	-.0000364	.0000887	-.0030272	0.0000000
3	.000219	-.000354	.000239	.000219	-.000354	-.0000364	.0000860	-.0035142	0.0000000
4	.000206	-.000355	.000389	.000206	-.000355	-.0000364	.0000811	-.0040011	0.0000000
5	.000187	-.000356	.000559	.000187	-.000356	-.0000364	.0000737	-.0044880	0.0000000
6	.000161	-.000358	.000748	.000161	-.000358	-.0000364	.0000634	-.0049750	0.0000000

SHELL ELEM 46 NODES= 46 47 MAT= 1 LENGTH= .1700 TEMPERATURES (1,2) = 70.0 70.0

I	X	Y	SIG S	SIG TH	S MOM	TH MOM	S BEND	SIG S1	SIG S2	TH BEND	SIG TH1	SIG TH2
1	2.5400	1.0000	-145.	1736.	-1.	-0.	-3183.	3038.	-3328.	-860.	2596.	877.
2	2.5400	1.0340	-237.	1397.	-1.	-0.	-3326.	3090.	-3563.	-898.	2295.	499.
3	2.5400	1.0680	-349.	982.	-1.	-0.	-3469.	3121.	-3818.	-937.	1919.	45.
4	2.5400	1.1020	-482.	489.	-1.	-0.	-3613.	3131.	-4095.	-975.	1464.	-487.
5	2.5400	1.1360	-638.	-88.	-1.	-0.	-3756.	3118.	-4393.	-1014.	927.	-1102.
6	2.5400	1.1700	-816.	-749.	-1.	-0.	-3899.	3083.	-4715.	-1053.	304.	-1602.

I	UN	US	ROT	UX	UY	EPS	EPTH	CURVE S	CURVE TH
1	.000161	-.000358	.000748	.000161	-.000358	-.0000219	.0000634	-.0052701	0.0000000
2	.000133	-.000359	.000931	.000133	-.000359	-.0000219	.0000522	-.0055070	0.0000000
3	.000098	-.000359	.001123	.000098	-.000359	-.0000219	.0000394	-.0057439	0.0000000
4	.000056	-.000360	.001322	.000056	-.000360	-.0000219	.0000221	-.0059808	0.0000000
5	.000004	-.000361	.001529	.000004	-.000361	-.0000219	.0000030	-.0062176	0.0000000
6	-.000048	-.000362	.001745	-.000048	-.000362	-.0000219	-.0000189	-.0064545	0.0000000

SHELL ELEM 47 NODES= 47 48 MAT= 1 LENGTH= .1077 TEMPERATURES (1,2) = 70.0 70.0

I	X	Y	SIG S	SIG TH	S MOM	TH MOM	S BEND	SIG S1	SIG S2	TH BEND	SIG TH1	SIG TH2
1	2.5400	1.1700	-74.	-549.	-1.	-0.	-3887.	3813.	-3962.	-907.	358.	-1455.
2	2.5320	1.1900	-191.	-982.	-1.	-0.	-3064.	2873.	-3255.	-674.	-309.	-1655.
3	2.5240	1.2100	-316.	-1446.	-1.	-0.	-2241.	1925.	-2557.	-443.	-1003.	-1889.
4	2.5160	1.2300	-447.	-1931.	-0.	-0.	-1419.	971.	-1866.	-215.	-1716.	-2146.
5	2.5080	1.2500	-583.	-2432.	-0.	0.	-597.	14.	-1180.	11.	-2443.	-2422.
6	2.5000	1.2700	-720.	-2943.	0.	0.	224.	-944.	-497.	233.	-3176.	-2709.

I	UN	US	ROT	UX	UY	EPS	EPTH	CURVE S	CURVE TH
1	-.000179	-.000318	.001745	-.000048	-.000362	.0000026	-.0000189	-.0065047	.0002551
2	-.000218	-.000318	.001870	-.000084	-.000376	.0000026	-.0000332	-.0051463	.0002743
3	-.000259	-.000318	.001956	-.000123	-.000391	.0000026	-.0000486	-.0037880	.0002893
4	-.000302	-.000318	.002033	-.000163	-.000407	.0000026	-.0000647	-.0024296	.0003001
5	-.000347	-.000318	.002071	-.000204	-.000424	.0000026	-.0000813	-.0010712	.0003067
6	-.000391	-.000318	.002079	-.000245	-.000440	.0000026	-.0000981	.0002871	.0003089

SHELL ELEM 48 NODES= 48 49 MAT= 1 LENGTH= .0943 TEMPERATURES (1,2) = 70.0 70.0

I	X	Y	SIG S	SIG TH	S MOM	TH MOM	S BEND	SIG S1	SIG S2	TH BEND	SIG TH1	SIG TH2
1	2.5000	1.2700	-3.	-2749.	0.	0.	207.	-210.	205.	303.	-3052.	-2446.
2	2.4900	1.2860	-115.	-3166.	0.	0.	1627.	-1742.	1512.	684.	-3850.	-2482.
3	2.4800	1.3020	-226.	-3576.	1.	0.	3044.	-3271.	2818.	1059.	-4636.	-2517.
4	2.4700	1.3180	-333.	-3972.	1.	0.	4461.	-4794.	4128.	1429.	-5401.	-2543.
5	2.4600	1.3340	-433.	-4344.	2.	0.	5875.	-6309.	5442.	1792.	-6137.	-2552.
6	2.4500	1.3500	-525.	-4684.	2.	1.	7288.	-7813.	6763.	2150.	-6834.	-2534.

I	UN	US	ROT	UX	UY	EPS	EPTH	CURVE S	CURVE TH
1	-.000441	-.000243	.002079	-.000245	-.000440	.0000264	-.0000981	.0002243	.0004408
2	-.000481	-.000243	.002053	-.000279	-.000461	.0000264	-.0001119	.0025751	.0004370
3	-.000519	-.000242	.001982	-.000311	-.000480	.0000264	-.0001255	.0049259	.0004236
4	-.000555	-.000242	.001867	-.000342	-.000499	.0000264	-.0001387	.0072766	.0004006
5	-.000589	-.000241	.001708	-.000371	-.000517	.0000264	-.0001510	.0096274	.0003579
6	-.000619	-.000241	.001504	-.000397	-.000532	.0000264	-.0001622	.0119781	.0003253

SHELL ELEM 49 NODES= 49 50 MAT= 1 LENGTH= .0707 TEMPERATURES (1,2) = 70.0 70.0

I	X	Y	SIG S	SIG TH	S MOM	TH MOM	S BEND	SIG S1	SIG S2	TH BEND	SIG TH1	SIG TH2
1	2.4500	1.3500	69.	-4523.	2.	1.	7387.	-7318.	7457.	2238.	-6761.	-2285.
2	2.4400	1.3600	15.	-4724.	2.	1.	8963.	-8948.	8978.	2533.	-7357.	-2090.
3	2.4300	1.3700	-32.	-4900.	3.	1.	10537.	-10569.	10504.	3022.	-7922.	-1878.
4	2.4200	1.3800	-72.	-5047.	3.	1.	12109.	-12181.	12036.	3404.	-8451.	-1643.
5	2.4100	1.3900	-103.	-5160.	4.	1.	13679.	-13781.	13576.	3779.	-8939.	-1391.
6	2.4000	1.4000	-123.	-5234.	4.	1.	15247.	-15369.	15124.	4147.	-9381.	-1087.

Max. Stress on Inner Shell ←

I	UN	US	ROT	UX	UY	EPS	EPTH	CURVE S	CURVE TH
1	-.000657	-.000095	.001504	-.000397	-.000532	.0000461	-.0001622	.0121127	.0004340

5	-.000718	-.000093	.000522	-.000442	-.000573	.0000461	-.0001833	.0225043	.0031537
6	-.000723	-.000092	.000184	-.000446	-.000576	.0000461	-.0001857	.0252272	.0010541

SHELL ELEM 50 NODES= 50 51 MAT= 1 LENGTH= .1063 TEMPERATURES (1,2) = 70.0 70.0

I	X	Y	SIG S	SIG TH	S MOM	TH MOM	S BEND	SIG S1	SIG S2	TH BEND	SIG THI	SIG TH2
1	2.4000	1.4000	178.	-5153.	4.	1.	14922.	-14744.	15100.	4051.	-4214.	-1041.
2	2.3840	1.4140	168.	-5189.	4.	1.	13365.	-13217.	13553.	3558.	-3747.	-1631.
3	2.3680	1.4280	181.	-5142.	3.	1.	11850.	-11669.	12031.	3064.	-3296.	-2078.
4	2.3520	1.4420	214.	-5019.	3.	1.	10318.	-10104.	10532.	2579.	-2959.	-2446.
5	2.3360	1.4560	266.	-4828.	2.	1.	8788.	-8523.	9054.	2104.	-2932.	-2721.
6	2.3200	1.4700	333.	-4578.	2.	0.	7261.	-6928.	7594.	1638.	-3216.	-2861.

I	UN	US	ROT	UX	UY	EPS	EPTH	CURVE S	CURVE TH
1	-.000727	-.000144	.000184	-.000446	-.000576	.0000560	-.0001857	.0252886	-.0000576
2	-.000726	-.000343	-.000315	-.000445	-.000574	.0000560	-.0001869	.0221861	-.0000693
3	-.000714	-.000542	-.000760	-.000439	-.000565	.0000560	-.0001754	.0194836	-.0000814
4	-.000694	-.000740	-.001152	-.000426	-.000549	.0000560	-.0001613	.0171811	-.0000889
5	-.000666	-.000939	-.001490	-.000409	-.000527	.0000560	-.0001750	.0146786	-.0000901
6	-.000631	-.000038	-.001776	-.000387	-.000500	.0000560	-.0001657	.0121761	-.0000760

SHELL ELEM 51 NODES= 51 52 MAT= 1 LENGTH= .1342 TEMPERATURES (1,2) = 70.0 70.0

I	X	Y	SIG S	SIG TH	S MOM	TH MOM	S BEND	SIG S1	SIG S2	TH BEND	SIG THI	SIG TH2
1	2.3200	1.4700	120.	-4635.	2.	0.	7242.	-7122.	7363.	1572.	-4207.	-3054.
2	2.2960	1.4840	164.	-4399.	2.	0.	5815.	-5631.	5999.	1118.	-4517.	-3271.
3	2.2720	1.4980	261.	-4115.	1.	0.	4391.	-4130.	4652.	678.	-4793.	-3438.
4	2.2480	1.5120	348.	-3794.	1.	0.	2971.	-2623.	3318.	251.	-4044.	-3543.
5	2.2240	1.5260	443.	-3442.	0.	-0.	1555.	-1112.	1997.	-162.	-3280.	-3604.
6	2.2000	1.5400	543.	-3070.	0.	-0.	142.	401.	685.	-569.	-2510.	-3633.

I	UN	US	ROT	UX	UY	EPS	EPTH	CURVE S	CURVE TH
1	-.000520	.000122	-.001776	-.000387	-.000500	.0000490	-.0001667	.0121746	-.0004846
2	-.000568	.000124	-.002071	-.000365	-.000453	.0000490	-.0001589	.0097443	-.0005289
3	-.000605	.000165	-.002304	-.000340	-.000400	.0000490	-.0001495	.0073143	-.0005470
4	-.000645	.000126	-.002474	-.000312	-.000342	.0000490	-.0001388	.0051842	-.0005445
5	-.000377	.000128	-.002582	-.000283	-.000280	.0000490	-.0001272	.0029540	-.0005365
6	-.000307	.000129	-.002628	-.000253	-.000217	.0000490	-.0001149	.0005239	-.0005682

SHELL ELEM 52 NODES= 52 53 MAT= 1 LENGTH= .2332 TEMPERATURES (1,2) = 70.0 70.0

I	X	Y	SIG S	SIG TH	S MOM	TH MOM	S BEND	SIG S1	SIG S2	TH BEND	SIG THI	SIG TH2
1	2.2000	1.5400	25.	-3210.	-0.	-0.	-267.	292.	-243.	-646.	-2564.	-3356.
2	2.1600	1.5560	240.	-2415.	-0.	-0.	-1012.	1251.	-772.	-649.	-1566.	-3054.
3	2.1200	1.5720	495.	-1512.	-0.	-0.	-1752.	2208.	-1295.	-1039.	-573.	-2551.
4	2.0800	1.5880	670.	-821.	-1.	-0.	-2468.	3158.	-1819.	-1213.	392.	-2024.
5	2.0400	1.6040	875.	-63.	-1.	-0.	-3265.	4095.	-2346.	-1073.	1310.	-1435.
6	2.0000	1.6200	1064.	640.	-1.	-0.	-3948.	5012.	-2883.	-1519.	2155.	-875.

I	UN	US	ROT	UX	UY	EPS	EPTH	CURVE S	CURVE TH
1	-.000316	.000105	-.002628	-.000253	-.000217	.0000318	-.0001149	-.0001663	-.0010241
2	-.000194	.000107	-.002591	-.000191	-.000112	.0000318	-.0000686	-.0014969	-.0010286
3	-.000075	.000108	-.002497	-.000131	-.000009	.0000318	-.0000220	-.0028274	-.0010101
4	.000038	.000110	-.002346	-.000074	.000089	.0000318	.0000358	-.0038579	-.0009671
5	.000143	.000111	-.002137	-.000022	.000180	.0000318	.0000907	-.0050885	-.0009084
6	.000236	.000113	-.001871	.000025	.000261	.0000318	.0000126	-.0063190	-.0008023

SHELL ELEM 53 NODES= 53 54 MAT= 1 LENGTH= .2236 TEMPERATURES (1,2) = 70.0 70.0

I	X	Y	SIG S	SIG TH	S MOM	TH MOM	S BEND	SIG S1	SIG S2	TH BEND	SIG THI	SIG TH2
1	2.0000	1.5500	258.	422.	-1.	-0.	-3579.	3838.	-3321.	-1435.	1857.	-1013.
2	1.9600	1.5660	405.	964.	-1.	-0.	-3620.	4024.	-3215.	-1393.	2354.	-4264.
3	1.9200	1.5820	535.	1447.	-1.	-0.	-3660.	4194.	-3125.	-1341.	2788.	-106.
4	1.8800	1.5980	649.	1865.	-1.	-0.	-3698.	4346.	-3050.	-1288.	3154.	577.
5	1.8400	1.6140	742.	2215.	-1.	-0.	-3735.	4478.	-2993.	-1231.	3446.	983.
6	1.8000	1.6300	816.	2488.	-1.	-0.	-3772.	4588.	-2956.	-1171.	3658.	1318.

I	UN	US	ROT	UX	UY	EPS	EPTH	CURVE S	CURVE TH
1	.000244	.000094	-.001871	.000025	.000261	.0000052	.0000126	-.0056096	-.0008368
2	.000322	.000094	-.001614	.000060	.000330	.0000052	.0000305	-.0057939	-.0007366
3	.000389	.000095	-.001353	.000089	.000390	.0000052	.0000465	-.0059883	-.0006303
4	.000443	.000095	-.001084	.000114	.000439	.0000052	.0000604	-.0054827	-.0005174
5	.000484	.000095	-.000818	.000132	.000477	.0000052	.0000719	-.0060770	-.0003976
6	.000516	.000095	-.000544	.000146	.000504	.0000052	.0000810	-.0061714	-.0002703

SHELL ELEM 54 NODES= 54 55 MAT= 1 LENGTH= .2236 TEMPERATURES (1,2) = 70.0 70.0

I	X	Y	SIG S	SIG TH	S MOM	TH MOM	S BEND	SIG S1	SIG S2	TH BEND	SIG THI	SIG TH2
1	1.9600	1.5660	293.	2347.	-1.	-0.	-3630.	3923.	-3337.	-1132.	3478.	1215.
2	1.9200	1.5820	349.	2553.	-1.	-0.	-3384.	3733.	-3036.	-995.	3548.	1557.
3	1.8800	1.5980	383.	2681.	-1.	-0.	-3139.	3541.	-2737.	-856.	3542.	1877.
4	1.8400	1.6140	397.	2732.	-1.	-0.	-2894.	3351.	-2497.	-729.	3455.	2152.
5	1.8000	1.6300	390.	2706.	-1.	-0.	-2650.	3046.	-2260.	-598.	3304.	2370.
6	1.7600	1.6460	362.	2604.	-1.	-0.	-2406.	2768.	-2044.	-470.	3073.	2504.

I	UN	US	ROT	UX	UY	EPS	EPTH	CURVE S	CURVE TH
1	.000516	.000095	-.000544	.000146	.000504	-.0000122	.0000810	-.0059370	-.0002703
2	.000575	.000095	-.000267	.000155	.000521	-.0000122	.0000876	-.0056636	-.0001458
3	.000624	.000095	.000010	.000161	.000527	-.0000122	.0000931	-.0051492	-.0000214
4	.000662	.000095	.000287	.000164	.000524	-.0000122	.0000977	-.0044937	.0001168
5	.000690	.000095	.000562	.000162	.000513	-.0000122	.0001013	-.0037969	.0002611
6	.000708	.000095	.000833	.000156	.000493	-.0000122	.0001035	-.0030589	.0004215

SHELL ELEM 55 NODES= 55 56 MAT= 1 LENGTH= .2062 TEMPERATURES (1,2) = 70.0 70.0

I	X	Y	SIG S	SIG TH	S MOM	TH MOM	S BEND	SIG S1	SIG S2	TH BEND	SIG THI	SIG TH2

			104.	2421.	-1.	-0.	-2.66	2296.	-2080.	-246.	2685.		
			77.	2355.	-1.	-0.	-2.[illegible]	2077.	-1923.	-151.	2455.		
			36.	2153.	-0.	-0.	-1.[illegible]	1849.	-1777.	-35.	2101.		
			-15.	1964.	-0.	0.	-1.[illegible]	1611.	-1641.	75.	1880.		
	UN	US	ROT		UX	UY		EPS	EPTH	CURVE S	CURVE TH		
	.0000513	-.0000019	.0000575		.0001143	.0001493		-.0000195	.0000895	-.0004382	.0001345		
	[illegible]	-.0000020	.0000748		.0001137	.0001467		-.0000195	.0000881	-.0004586	.0001351		
	[illegible]	-.0000020	.0000969		.0001130	.0001433		-.0000195	.0000854	-.0004779	.0001350		
	[illegible]	-.0000021	.0001167		.0001121	.0001344		-.0000195	.0000795	-.0004993	.0001345		
	[illegible]	-.0000022	.0001198		.0001110	.0001246		-.0000195	.0000703	-.0005169	.0001332		
	[illegible]	-.0000023	.0001325		.0001098	.0001207		-.0000195	.0000703	-.0005469	.0001282		

SHELL ELEM 56 NODES= 56 57 MAT= 1 LENGTH= .1950 TEMPERATURES (1,2) = 70.0 70.0

	X	Y	SIG S	SIG TH	S MOM	TH MOM	S BEND	SIG S1	SIG S2	TH BEND	SIG TH1	SIG TH2
1	1.4400	1.9750	112.	1998.	-0.	0.	-1055.	1765.	-1540.	43.	1955.	2041.
2	[illegible]	1.9755	7.	1609.	-0.	0.	-1[illegible]	1614.	-1000.	266.	1343.	1476.
3	[illegible]	1.9300	-110.	1174.	-0.	0.	-[illegible]	255.	-415.	476.	498.	1145.
4	[illegible]	1.9450	-238.	706.	0.	0.	[illegible]	-510.	35.	669.	32.	1151.
5	[illegible]	1.9600	-372.	205.	0.	0.	[illegible]	-1277.	534.	846.	-641.	1551.
6	1.2200	1.9750	-509.	-304.	0.	0.	1553.	-2042.	1024.	1005.	-1309.	701.

	UN	US	ROT	UX	UY	EPS	EPTH	CURVE S	CURVE TH
1	.0000312	.0000024	.0001325	.0000098	.0000207	-.0000153	.0000703	-.0002717	.0008737
2	[illegible]	.0000023	.0001421	.0000078	.0000240	-.0000153	.0000574	-.0010267	.0009614
3	[illegible]	.0000022	.0001475	.0000057	.0000145	-.0000153	.0000430	-.0008816	.0010255
4	[illegible]	.0000022	.0001489	.0000035	.0000141	-.0000153	.0000273	.0001694	.0010641
5	[illegible]	.0000021	.0001493	.0000014	.0000088	-.0000153	.0000109	.0012085	.0010749
6	.0000031	.0000021	.0001395	-.0000007	.0000036	-.0000153	-.0000059	.0022535	.0010555

SHELL ELEM 57 NODES= 57 58 MAT= 1 LENGTH= .0743 TEMPERATURES (1,2) = 70.0 70.0

	X	Y	SIG S	SIG TH	S MOM	TH MOM	S BEND	SIG S1	SIG S2	TH BEND	SIG TH1	SIG TH2
1	1.2200	1.9750	-95.	-192.	0.	0.	1797.	-1892.	1702.	1088.	-1280.	896.
2	1.2060	1.9800	-142.	-365.	1.	0.	2341.	-2483.	2199.	1222.	-1587.	856.
3	1.1920	1.9850	-185.	-536.	1.	0.	2863.	-3071.	2694.	1348.	-1884.	812.
4	1.1780	1.9900	-233.	-702.	1.	0.	3423.	-3656.	3190.	1468.	-2178.	766.
5	1.1640	1.9950	-276.	-862.	1.	0.	3961.	-4237.	3684.	1580.	-2462.	718.
6	1.1500	2.0000	-317.	-1014.	1.	0.	4497.	-4814.	4180.	1685.	-2699.	672.

	UN	US	ROT	UX	UY	EPS	EPTH	CURVE S	CURVE TH
1	.0000032	.0000019	.0001395	-.0000007	.0000036	-.0000016	-.0000059	.0026840	.0010769
2	[illegible]	.0000019	.0001348	-.0000014	.0000017	-.0000016	-.0000117	.0030907	.0010530
3	[illegible]	.0000019	.0001288	-.0000021	-.0000002	-.0000016	-.0000173	.0034973	.0010178
4	[illegible]	.0000018	.0001215	-.0000027	-.0000021	-.0000016	-.0000229	.0039040	.0009711
5	[illegible]	.0000019	.0001128	-.0000032	-.0000035	-.0000016	-.0000281	.0043106	.0009123
6	-.0000040	.0000019	.0001027	-.0000038	-.0000051	-.0000016	-.0000331	.0072173	.0008411

SHELL ELEM 58 NODES= 58 59 MAT= 1 LENGTH= .0700 TEMPERATURES (1,2) = 70.0 70.0

	X	Y	SIG S	SIG TH	S MOM	TH MOM	S BEND	SIG S1	SIG S2	TH BEND	SIG TH1	SIG TH2
1	1.1500	2.0000	-49.	-941.	1.	0.	4503.	-4553.	4454.	1716.	-2657.	775.
2	1.1360	2.0000	-53.	-956.	1.	1.	5325.	-5379.	5272.	1890.	-2846.	933.
3	1.1220	2.0000	-53.	-972.	2.	1.	6145.	-6202.	6088.	2062.	-3023.	1100.
4	1.1080	2.0000	-62.	-988.	2.	1.	6961.	-7022.	6899.	2201.	-3169.	1254.
5	1.0940	2.0000	-66.	-1004.	2.	1.	7773.	-7839.	7707.	2338.	-3342.	1334.
6	1.0800	2.0000	-71.	-1020.	2.	1.	8582.	-8652.	8511.	2462.	-3483.	1442.

	UN	US	ROT	UX	UY	EPS	EPTH	CURVE S	CURVE TH
1	-.0000051	.0000038	.0001027	-.0000038	-.0000051	.0000073	-.0000331	.0072144	.0008931
2	[illegible]	.0000038	.0000916	-.0000038	-.0000064	.0000073	-.0000336	.0035990	.0008057
3	[illegible]	.0000038	.0000786	-.0000038	-.0000078	.0000073	-.0000341	.0000836	.0007008
4	[illegible]	.0000038	.0000637	-.0000038	-.0000086	.0000073	-.0000345	.0111642	.0005748
5	[illegible]	.0000039	.0000468	-.0000039	-.0000094	.0000073	-.0000352	.0127527	.0004278
6	-.0000099	.0000039	.0000280	-.0000039	-.0000099	.0000073	-.0000358	.0141373	.0002591

SHELL ELEM 59 NODES= 59 60 MAT= 1 LENGTH= .0838 TEMPERATURES (1,2) = 70.0 70.0

	X	Y	SIG S	SIG TH	S MOM	TH MOM	S BEND	SIG S1	SIG S2	TH BEND	SIG TH1	SIG TH2
1	1.0800	2.0000	-595.	-1162.	2.	1.	8604.	-9199.	8009.	2461.	-3623.	1299.
2	1.0640	1.9950	-592.	-1150.	2.	0.	6807.	-7399.	6215.	1871.	-3021.	722.
3	1.0480	1.9900	-596.	-1164.	1.	0.	5016.	-5612.	4420.	1305.	-2469.	140.
4	1.0320	1.9850	-605.	-1200.	1.	0.	3232.	-3837.	2627.	763.	-1962.	-437.
5	1.0160	1.9800	-619.	-1249.	0.	0.	1455.	-2074.	836.	246.	-1496.	-1023.
6	1.0000	1.9750	-634.	-1307.	-0.	-0.	-315.	-320.	-949.	-243.	-1064.	-1650.

	UN	US	ROT	UX	UY	EPS	EPTH	CURVE S	CURVE TH
1	-.0000083	.0000066	.0000280	-.0000039	-.0000099	-.0000101	-.0000358	.0141770	.0002473
2	[illegible]	.0000067	.0000167	-.0000038	-.0000102	-.0000101	-.0000354	.0112527	.0001598
3	[illegible]	.0000066	-.0000097	-.0000038	-.0000101	-.0000101	-.0000358	.0083264	-.0000868
4	[illegible]	.0000066	-.0000213	-.0000038	-.0000099	-.0000101	-.0000370	.0054041	-.0001966
5	[illegible]	.0000066	-.0000275	-.0000039	-.0000095	-.0000101	-.0000387	.0024798	-.0002618
6	-.0000074	.0000066	-.0000295	-.0000041	-.0000090	-.0000101	-.0000406	-.0004445	-.0002823

SHELL ELEM 60 NODES= 60 61 MAT= 1 LENGTH= .0626 TEMPERATURES (1,2) = 70.0 70.0

	X	Y	SIG S	SIG TH	S MOM	TH MOM	S BEND	SIG S1	SIG S2	TH BEND	SIG TH1	SIG TH2
1	1.0000	1.9750	-858.	-1368.	-0.	-0.	-356.	-502.	-1214.	-175.	-1192.	-1543.
2	[illegible]	1.9640	-885.	-1469.	-0.	-0.	-[illegible]43.	-242.	-1529.	-251.	-1218.	-1720.
3	[illegible]	1.9530	-912.	-1568.	-0.	-0.	-[illegible]30.	18.	-1842.	-324.	-1243.	-1892.
4	[illegible]	1.9420	-937.	-1661.	-0.	-0.	-1217.	280.	-2154.	-396.	-1265.	-2057.
5	.9760	1.9310	-960.	-1747.	-0.	-0.	-1502.	542.	-2463.	-466.	-1281.	-2213.
6	.9700	1.9200	-981.	-1823.	-0.	-0.	-1768.	807.	-2769.	-534.	-1289.	-2359.

	UN	US	ROT	UX	UY	EPS	EPTH	CURVE S	CURVE TH
1	[illegible]	[illegible]	[illegible]	[illegible]	[illegible]	[illegible]	[illegible]	[illegible]	[illegible]
2	[illegible]	[illegible]	[illegible]	[illegible]	[illegible]	[illegible]	[illegible]	[illegible]	[illegible]
3	[illegible]	[illegible]	[illegible]	[illegible]	[illegible]	[illegible]	[illegible]	[illegible]	[illegible]
4	[illegible]	[illegible]	[illegible]	[illegible]	[illegible]	[illegible]	[illegible]	[illegible]	[illegible]
5	[illegible]	[illegible]	[illegible]	[illegible]	[illegible]	[illegible]	[illegible]	[illegible]	[illegible]
6	[illegible]	[illegible]	[illegible]	[illegible]	[illegible]	[illegible]	[illegible]	[illegible]	[illegible]

	.000008	.000097	-.000187	-.000054	-.000082	-.00001174	-.0000557	-.0024351	-.0000921				

SHELL ELEM 61 NODES= 61 62 MAT= 1 LENGTH= .0728 TEMPERATURES (1,2) = 70.0 70.0

I	X	Y	SIG S	SIG TH	S MOM	TH MOM	S BEND	SIG S1	SIG S2	TH BEND	SIG TH1	SIG TH2
1	.9700	1.9260	-880.	-1796.	-0.	-0.	-1754.	874.	-2634.	-263.	-1293.	-2299.
2	.9660	1.9060	-901.	-1874.	-0.	-0.	-1791.	890.	-2692.	-506.	-1367.	-2380.
3	.9620	1.8920	-917.	-1933.	-0.	-0.	-1828.	911.	-2744.	-510.	-1423.	-2443.
4	.9580	1.8780	-928.	-1973.	-0.	-0.	-1865.	937.	-2792.	-512.	-1461.	-2486.
5	.9540	1.8640	-933.	-1994.	-1.	-0.	-1901.	968.	-2835.	-515.	-1479.	-2509.
6	.9500	1.8500	-933.	-1995.	-1.	-0.	-1938.	1005.	-2871.	-518.	-1477.	-2512.

I	UN	US	ROT	UX	UY	EPS	EPTH	CURVE S	CURVE TH
1	.000030	.000093	-.000187	-.000054	-.000082	-.00001141	-.0000557	-.0024895	-.0000528
2	.000032	.000093	-.000144	-.000056	-.000081	-.00001141	-.0000582	-.0025539	-.0000409
3	.000034	.000093	-.000101	-.000058	-.000080	-.00001141	-.0000602	-.0026183	-.0000287
4	.000035	.000093	-.000056	-.000059	-.000079	-.00001141	-.0000615	-.0026827	-.0000161
5	.000035	.000092	-.000011	-.000059	-.000079	-.00001141	-.0000622	-.0027471	-.0000031
6	.000035	.000092	.000036	-.000059	-.000079	-.00001141	-.0000622	-.0028114	.0000103

SHELL ELEM 62 NODES= 62 63 MAT= 1 LENGTH= .1500 TEMPERATURES (1,2) = 70.0 70.0

I	X	Y	SIG S	SIG TH	S MOM	TH MOM	S BEND	SIG S1	SIG S2	TH BEND	SIG TH1	SIG TH2
1	.9500	1.8500	-971.	-2005.	-0.	-0.	-1702.	731.	-2673.	-460.	-1545.	-2465.
2	.9500	1.8200	-952.	-1934.	-0.	-0.	-1246.	294.	-2197.	-336.	-1598.	-2271.
3	.9500	1.7900	-917.	-1805.	-0.	-0.	-789.	-128.	-1706.	-213.	-1592.	-2018.
4	.9500	1.7600	-872.	-1628.	-0.	-0.	-332.	-540.	-1204.	-90.	-1548.	-1727.
5	.9500	1.7300	-822.	-1415.	0.	0.	125.	-947.	-698.	34.	-1489.	-1421.
6	.9500	1.7000	-775.	-1278.	0.	0.	581.	-1356.	-193.	157.	-1435.	-1171.

I	UN	US	ROT	UX	UY	EPS	EPTH	CURVE S	CURVE TH
1	.000059	.000079	.000036	-.000059	-.000079	-.00001153	-.0000622	-.0028183	0.00000000
2	.000057	.000079	.000109	-.000057	-.000079	-.00001153	-.0000599	-.0027621	0.00000000
3	.000053	.000078	.000182	-.000053	-.000078	-.00001153	-.0000556	-.0013059	0.00000000
4	.000048	.000078	.000187	-.000048	-.000078	-.00001153	-.0000501	-.0000497	0.00000000
5	.000042	.000077	.000142	-.000042	-.000077	-.00001153	-.0000440	.0000065	0.00000000
6	.000036	.000077	.000175	-.000036	-.000077	-.00001153	-.0000382	.0000626	0.00000000

SHELL ELEM 63 NODES= 63 64 MAT= 1 LENGTH= .3000 TEMPERATURES (1,2) = 70.0 70.0

I	X	Y	SIG S	SIG TH	S MOM	TH MOM	S BEND	SIG S1	SIG S2	TH BEND	SIG TH1	SIG TH2
1	.9500	1.7000	-1019.	-1344.	0.	0.	526.	-1546.	-493.	142.	-1486.	-1202.
2	.9500	1.6400	-942.	-1059.	0.	0.	455.	-1398.	-487.	123.	-1182.	-936.
3	.9500	1.5800	-882.	-859.	0.	0.	384.	-1273.	-504.	104.	-963.	-755.
4	.9500	1.5200	-854.	-733.	0.	0.	314.	-1168.	-554.	85.	-847.	-648.
5	.9500	1.4600	-856.	-666.	0.	0.	243.	-1079.	-594.	65.	-781.	-606.
6	.9500	1.4000	-880.	-644.	0.	0.	172.	-1002.	-659.	45.	-691.	-598.

I	UN	US	ROT	UX	UY	EPS	EPTH	CURVE S	CURVE TH
1	.000036	.000077	.000175	-.000036	-.000077	-.00001234	-.0000382	.0000713	0.00000000
2	.000027	.000075	.000126	-.000027	-.000075	-.00001234	-.0000287	.0000539	0.00000000
3	.000021	.000074	.000084	-.000021	-.000074	-.00001234	-.0000221	.0000365	0.00000000
4	.000017	.000072	.000050	-.000017	-.000072	-.00001234	-.0000179	.0000190	0.00000000
5	.000015	.000071	.000022	-.000015	-.000071	-.00001234	-.0000157	.0000016	0.00000000
6	.000014	.000070	.000001	-.000014	-.000070	-.00001234	-.0000150	-.0000041	0.00000000

SHELL ELEM 64 NODES= 64 65 MAT= 1 LENGTH= .3000 TEMPERATURES (1,2) = 70.0 70.0

I	X	Y	SIG S	SIG TH	S MOM	TH MOM	S BEND	SIG S1	SIG S2	TH BEND	SIG TH1	SIG TH2
1	.9500	1.4000	-882.	-658.	0.	0.	66.	-947.	-816.	18.	-676.	-640.
2	.9500	1.3400	-862.	-661.	0.	0.	43.	-925.	-800.	12.	-673.	-649.
3	.9500	1.2800	-848.	-672.	0.	0.	20.	-906.	-789.	5.	-677.	-667.
4	.9500	1.2200	-844.	-695.	-0.	-0.	-2.	-897.	-792.	-1.	-696.	-698.
5	.9500	1.1600	-851.	-707.	-0.	-0.	-25.	-908.	-818.	-7.	-694.	-720.
6	.9500	1.1000	-866.	-711.	-0.	-0.	-48.	-928.	-844.	-13.	-698.	-724.

I	UN	US	ROT	UX	UY	EPS	EPTH	CURVE S	CURVE TH
1	.000014	.000070	.000001	-.000014	-.000070	-.00001251	-.0000150	.0000091	0.00000000
2	.000014	.000068	-.000044	-.000014	-.000068	-.00001251	-.0000151	.0000713	0.00000000
3	.000015	.000067	-.000087	-.000015	-.000067	-.00001251	-.0000155	.0001336	0.00000000
4	.000015	.000065	-.000088	-.000015	-.000065	-.00001251	-.0000162	.0001941	0.00000000
5	.000016	.000064	-.000087	-.000016	-.000064	-.00001251	-.0000167	.0002419	0.00000000
6	.000016	.000062	-.000088	-.000016	-.000062	-.00001251	-.0000167	.0002776	0.00000000

SHELL ELEM 65 NODES= 65 66 MAT= 1 LENGTH= .3000 TEMPERATURES (1,2) = 70.0 70.0

I	X	Y	SIG S	SIG TH	S MOM	TH MOM	S BEND	SIG S1	SIG S2	TH BEND	SIG TH1	SIG TH2
1	.9500	1.1000	-886.	-708.	-0.	-0.	-16.	-870.	-902.	-4.	-704.	-713.
2	.9500	1.0400	-897.	-713.	-0.	-0.	-12.	-879.	-915.	-3.	-709.	-716.
3	.9500	.9800	-911.	-717.	-0.	-0.	-8.	-891.	-931.	-2.	-712.	-720.
4	.9500	.9200	-925.	-719.	-0.	-0.	-5.	-904.	-947.	-1.	-714.	-723.
5	.9500	.8600	-938.	-719.	-0.	-0.	-3.	-917.	-960.	-1.	-715.	-723.
6	.9500	.8000	-950.	-719.	-0.	-0.	-1.	-929.	-972.	-0.	-715.	-723.

I	UN	US	ROT	UX	UY	EPS	EPTH	CURVE S	CURVE TH
1	.000016	.000062	-.000088	-.000016	-.000062	-.00001248	-.0000167	.0003245	0.00000000
2	.000016	.000061	-.000131	-.000016	-.000061	-.00001248	-.0000167	.0003713	0.00000000
3	.000016	.000059	-.000174	-.000016	-.000059	-.00001248	-.0000167	.0004181	0.00000000
4	.000016	.000058	-.000217	-.000016	-.000058	-.00001248	-.0000167	.0004649	0.00000000
5	.000016	.000056	-.000260	-.000016	-.000056	-.00001248	-.0000167	.0005117	0.00000000
6	.000016	.000055	-.000303	-.000016	-.000055	-.00001248	-.0000167	.0005585	0.00000000

SHELL ELEM 66 NODES= 66 67 MAT= 1 LENGTH= .3000 TEMPERATURES (1,2) = 70.0 70.0

I	X	Y	SIG S	SIG TH	S MOM	TH MOM	S BEND	SIG S1	SIG S2	TH BEND	SIG TH1	SIG TH2

4	.9500	.5200	-888.	-713.	0.	0.	1.	-888.	-887.	0.	-713.	-712.							
5	.9500	.5600	-888.	-712.	0.	0.	1.	-888.	-887.	0.	-713.	-712.							
6	.9500	.6000	-888.	-712.	0.	0.	1.	-888.	-887.	0.	-713.	-712.							
	UN	US	ROT		UX	UY		EPS	EPTH	CURVE S		CURVE TH							
1	.0000016	.0000055	.0000000		-.0000016	-.0000055		-.0000248	-.0000169	.0000012		0.0000000							
2	.0000016	.0000053	.0000000		-.0000016	-.0000053		-.0000248	-.0000169	.0000012		0.0000000							
3	.0000016	.0000052	.0000000		-.0000016	-.0000052		-.0000248	-.0000169	.0000012		0.0000000							
4	.0000016	.0000050	.0000000		-.0000016	-.0000050		-.0000248	-.0000169	.0000012		0.0000000							
5	.0000016	.0000049	.0000000		-.0000016	-.0000049		-.0000248	-.0000169	.0000012		0.0000000							
6	.0000016	.0000047	.0000000		-.0000016	-.0000047		-.0000248	-.0000169	.0000012		0.0000000							

SHELL ELEM 67 NODES= 67 66 MAT= 1 LENGTH= .3000 TEMPERATURES (1,2) = 70.0 70.0

	X	Y	SIG S	SIG TH	S MOM	TH MOM	S BEND	SIG S1	SIG S2	TH BEND	SIG TH1	SIG TH2
1	.9500	.5000	-888.	-712.	0.	0.	0.	-888.	-887.	0.	-713.	-712.
2	.9500	.4400	-888.	-712.	0.	0.	0.	-888.	-886.	0.	-712.	-712.
3	.9500	.3800	-888.	-712.	0.	0.	0.	-886.	-888.	0.	-712.	-712.
4	.9500	.3200	-888.	-713.	-0.	-0.	-0.	-888.	-888.	-0.	-712.	-712.
5	.9500	.2600	-888.	-713.	-0.	-0.	-0.	-887.	-888.	-0.	-712.	-713.
6	.9500	.2000	-888.	-712.	-0.	-0.	-0.	-887.	-886.	-0.	-712.	-713.
	UN	US	ROT		UX	UY		EPS	EPTH	CURVE S		CURVE TH
1	.0000016	.0000047	.0000000		-.0000016	-.0000047		-.0000248	-.0000169	.0000004		0.0000000
2	.0000016	.0000046	-.0000000		-.0000016	-.0000046		-.0000248	-.0000169	.0000002		0.0000000
3	.0000016	.0000044	-.0000000		-.0000016	-.0000044		-.0000248	-.0000169	.0000000		0.0000000
4	.0000016	.0000043	-.0000000		-.0000016	-.0000043		-.0000248	-.0000169	-.0000002		0.0000000
5	.0000016	.0000041	.0000000		-.0000016	-.0000041		-.0000248	-.0000169	-.0000004		0.0000000
6	.0000016	.0000040	.0000000		-.0000016	-.0000040		-.0000248	-.0000169	-.0000006		0.0000000

SHELL ELEM 68 NODES= 68 69 MAT= 1 LENGTH= .3000 TEMPERATURES (1,2) = 70.0 70.0

	X	Y	SIG S	SIG TH	S MOM	TH MOM	S BEND	SIG S1	SIG S2	TH BEND	SIG TH1	SIG TH2
1	.9500	.2000	-888.	-713.	-0.	-0.	-1.	-887.	-889.	-0.	-712.	-713.
2	.9500	.1400	-888.	-712.	-0.	-0.	-1.	-887.	-888.	-0.	-712.	-713.
3	.9500	.0800	-888.	-712.	-0.	-0.	-0.	-887.	-888.	-0.	-712.	-712.
4	.9500	.0200	-888.	-712.	-0.	-0.	-0.	-888.	-888.	-0.	-712.	-712.
5	.9500	-.0400	-888.	-711.	0.	0.	0.	-888.	-887.	0.	-712.	-711.
6	.9500	-.1000	-887.	-711.	0.	0.	0.	-888.	-887.	0.	-711.	-711.
	UN	US	ROT		UX	UY		EPS	EPTH	CURVE S		CURVE TH
1	.0000016	.0000040	.0000000		-.0000016	-.0000040		-.0000248	-.0000169	-.0000014		0.0000000
2	.0000016	.0000038	.0000000		-.0000016	-.0000038		-.0000248	-.0000169	-.0000010		0.0000000
3	.0000016	.0000037	.0000000		-.0000016	-.0000037		-.0000248	-.0000169	-.0000006		0.0000000
4	.0000016	.0000035	.0000000		-.0000016	-.0000035		-.0000248	-.0000169	-.0000002		0.0000000
5	.0000016	.0000034	.0000000		-.0000016	-.0000034		-.0000248	-.0000169	.0000002		0.0000000
6	.0000016	.0000032	.0000000		-.0000016	-.0000032		-.0000248	-.0000168	.0000006		0.0000000

SHELL ELEM 69 NODES= 69 70 MAT= 1 LENGTH= .3000 TEMPERATURES (1,2) = 70.0 70.0

	X	Y	SIG S	SIG TH	S MOM	TH MOM	S BEND	SIG S1	SIG S2	TH BEND	SIG TH1	SIG TH2
1	.9500	-.1000	-887.	-711.	0.	0.	1.	-886.	-886.	0.	-711.	-711.
2	.9500	-.1600	-887.	-711.	0.	0.	3.	-890.	-884.	1.	-712.	-710.
3	.9500	-.2200	-887.	-711.	0.	0.	6.	-893.	-881.	2.	-713.	-710.
4	.9500	-.2800	-888.	-713.	0.	0.	9.	-895.	-879.	2.	-715.	-711.
5	.9500	-.3400	-888.	-716.	0.	0.	12.	-900.	-877.	3.	-719.	-713.
6	.9500	-.4000	-890.	-722.	0.	0.	14.	-904.	-876.	4.	-726.	-718.
	UN	US	ROT		UX	UY		EPS	EPTH	CURVE S		CURVE TH
1	.0000016	.0000032	.0000000		-.0000016	-.0000032		-.0000248	-.0000168	.0000009		0.0000000
2	.0000016	.0000031	-.0000000		-.0000016	-.0000031		-.0000248	-.0000168	.0000055		0.0000000
3	.0000016	.0000029	-.0000001		-.0000016	-.0000029		-.0000248	-.0000169	.0000101		0.0000000
4	.0000016	.0000028	-.0000001		-.0000016	-.0000028		-.0000248	-.0000169	.0000147		0.0000000
5	.0000016	.0000026	-.0000002		-.0000016	-.0000026		-.0000248	-.0000170	.0000193		0.0000000
6	.0000016	.0000025	-.0000004		-.0000016	-.0000025		-.0000248	-.0000172	.0000238		0.0000000

SHELL ELEM 70 NODES= 70 71 MAT= 1 LENGTH= .3000 TEMPERATURES (1,2) = 70.0 70.0

	X	Y	SIG S	SIG TH	S MOM	TH MOM	S BEND	SIG S1	SIG S2	TH BEND	SIG TH1	SIG TH2
1	.9500	-.4000	-882.	-720.	0.	0.	45.	-928.	-837.	12.	-732.	-708.
2	.9500	-.4600	-885.	-730.	0.	0.	12.	-897.	-873.	3.	-733.	-727.
3	.9500	-.5200	-888.	-742.	-0.	-0.	-21.	-867.	-910.	-6.	-736.	-748.
4	.9500	-.5800	-891.	-750.	-0.	-0.	-55.	-836.	-945.	-15.	-736.	-765.
5	.9500	-.6400	-890.	-748.	-0.	-0.	-88.	-802.	-978.	-24.	-725.	-772.
6	.9500	-.7000	-885.	-730.	-0.	-0.	-121.	-764.	-1006.	-33.	-697.	-762.
	UN	US	ROT		UX	UY		EPS	EPTH	CURVE S		CURVE TH
1	.0000016	.0000025	-.0000004		-.0000016	-.0000025		-.0000246	-.0000172	.0000749		0.0000000
2	.0000017	.0000023	-.0000006		-.0000017	-.0000023		-.0000246	-.0000175	.0001199		0.0000000
3	.0000017	.0000022	-.0000006		-.0000017	-.0000022		-.0000246	-.0000179	-.0000352		0.0000000
4	.0000017	.0000020	-.0000002		-.0000017	-.0000020		-.0000246	-.0000182	-.0000903		0.0000000
5	.0000017	.0000019	.0000005		-.0000017	-.0000019		-.0000246	-.0000181	-.0001454		0.0000000
6	.0000017	.0000017	.0000015		-.0000017	-.0000017		-.0000246	-.0000175	-.0002004		0.0000000

SHELL ELEM 71 NODES= 71 72 MAT= 1 LENGTH= .3000 TEMPERATURES (1,2) = 70.0 70.0

	X	Y	SIG S	SIG TH	S MOM	TH MOM	S BEND	SIG S1	SIG S2	TH BEND	SIG TH1	SIG TH2
1	.9500	-.7000	-965.	-751.	-0.	-0.	-345.	-620.	-1310.	-93.	-658.	-845.
2	.9500	-.7600	-949.	-691.	-0.	-0.	-286.	-663.	-1235.	-77.	-614.	-769.
3	.9500	-.8200	-918.	-577.	-0.	-0.	-227.	-691.	-1145.	-61.	-516.	-639.
4	.9500	-.8800	-875.	-420.	-0.	-0.	-168.	-708.	-1043.	-45.	-375.	-466.
5	.9500	-.9400	-825.	-231.	-0.	-0.	-108.	-716.	-933.	-29.	-202.	-261.
6	.9500	-1.0000	-768.	-22.	-0.	-0.	-49.	-719.	-818.	-13.	-9.	-35.
	UN	US	ROT		UX	UY		EPS	EPTH	CURVE S		CURVE TH
1	.0000017	.0000017	.0000015		-.0000017	-.0000017		-.0000272	-.0000175	-.0005714		0.0000000

6	-.0000006	.0000009	.000113	-.0000006	-.0000009	-.00000272	.0000066	-.0000816	0.0000000

SHELL ELEM 72 NODES= 72 73 MAT= 1 LENGTH= .3000 TEMPERATURES (1,2) = 70.0 70.0

	X	Y	SIG S	SIG TH	S MOM	TH MOM	S BEND	SIG S1	SIG S2	TH BEND	SIG TH1	SIG TH2
1		.9500	-1.0000	-885.	-53.	0.	0.	1165.	-2050.	280.	315.	-368.	261.
2		.9500	-1.0600	-853.	64.	0.	0.	790.	-1644.	-63.	213.	-149.	277.
3		.9500	-1.1200	-862.	32.	0.	0.	415.	-1277.	-447.	112.	-81.	144.
4		.9500	-1.1800	-892.	-79.	0.	0.	41.	-933.	-851.	11.	-90.	-69.
5		.9500	-1.2400	-924.	-198.	-0.	-0.	-334.	-590.	-1258.	-90.	-108.	-288.
6		.9500	-1.3000	-939.	-254.	-0.	-0.	-709.	-230.	-1648.	-192.	-62.	-445.

	UN	US	ROT	UX	UY	EPS	EPTH	CURVE S	CURVE TH
1	-.0000006	.000009	.000113	.0000006	-.000009	-.00000311	.0000066	.0019290	0.0000000
2	-.0000010	.000007	-.000016	.0000010	-.000007	-.0000311	.0000105	.0013084	0.0000000
3	-.0000009	.000006	-.000044	.0000009	-.000006	-.0000311	.0000094	.0006877	0.0000000
4	-.0000005	.000004	-.000066	.0000005	-.000004	-.0000311	.0000058	.0000671	0.0000000
5	-.0000002	.000002	-.000052	.0000002	-.000002	-.0000311	.0000018	-.0005536	0.0000000
6	-.0000000	.000000	.000000	.0000000	-.000000	-.0000311	.0000000	-.0011742	0.0000000

SHELL ELEM 73 NODES= 74 37 MAT= 1 LENGTH= .1217 TEMPERATURES (1,2) = 70.0 70.0

	X	Y	SIG S	SIG TH	S MOM	TH MOM	S BEND	SIG S1	SIG S2	TH BEND	SIG TH1	SIG TH2
1	3.0000	-.2000	240.	2004.	-1.	-0.	-4403.	4642.	-4163.	-1140.	3144.	864.
2	2.9960	-.1760	132.	1603.	-1.	-0.	-2927.	3058.	-2795.	-737.	2340.	867.
3	2.9920	-.1520	16.	1173.	-0.	-0.	-1451.	1467.	-1439.	-336.	1509.	838.
4	2.9880	-.1280	-105.	726.	0.	0.	24.	-128.	-81.	64.	664.	792.
5	2.9840	-.1040	-225.	281.	0.	0.	1408.	-1723.	1273.	461.	-179.	742.
6	2.9800	-.0800	-342.	-152.	1.	0.	2972.	-3314.	2630.	856.	-1008.	704.

	UN	US	ROT	UX	UY	EPS	EPTH	CURVE S	CURVE TH
1	.0000198	-.0000074	.001588	.0000208	-.0000040	-.0000108	.0000692	-.0073120	.0000870
2	.0000158	-.0000074	.001737	.0000168	-.0000047	-.0000108	.0000560	-.0044708	.0000953
3	.0000114	-.0000074	.001825	.0000125	-.0000054	-.0000108	.0000418	-.0024296	.0001003
4	.0000069	-.0000074	.001855	.0000081	-.0000062	-.0000108	.0000270	-.0009116	.0001021
5	.0000025	-.0000075	.001825	.0000036	-.0000070	-.0000108	.0000122	.0024529	.0001005
6	-.0000019	-.0000075	.001735	-.0000006	-.0000077	-.0000108	-.0000021	.0048941	.0000957

SHELL ELEM 74 NODES= 36 74 MAT= 1 LENGTH= .1414 TEMPERATURES (1,2) = 70.0 70.0

	X	Y	SIG S	SIG TH	S MOM	TH MOM	S BEND	SIG S1	SIG S2	TH BEND	SIG TH1	SIG TH2
1	3.1000	-.1000	2487.	931.	1.	0.	4298.	-1810.	6785.	1449.	-518.	2380.
2	3.0960	-.1200	2598.	1341.	1.	0.	3749.	-1150.	6347.	1279.	63.	2620.
3	3.0920	-.1400	2761.	1723.	1.	0.	3200.	-499.	5962.	1112.	611.	2835.
4	3.0880	-.1600	2798.	2081.	1.	0.	2653.	145.	5451.	948.	1133.	3029.
5	3.0840	-.1800	2889.	2419.	1.	0.	2107.	782.	4996.	788.	1631.	3207.
6	3.0800	-.2000	2976.	2743.	0.	0.	1561.	1415.	4538.	631.	2111.	3374.

	UN	US	ROT	UX	UY	EPS	EPTH	CURVE S	CURVE TH
1	-.0000089	-.0000130	.002257	.0000029	.0000155	.0000799	.0000093	.0063758	.0005149
2	-.0000084	-.0000128	.002073	.0000070	.0000110	.0000799	.0000229	.0060774	.0004759
3	-.0000080	-.0000125	.001914	.0000109	.0000069	.0000799	.0000355	.0051790	.0004422
4	-.0000075	-.0000123	.001780	.0000144	.0000030	.0000799	.0000473	.0042805	.0004140
5	-.0000129	-.0000121	.001671	.0000177	-.0000006	.0000799	.0000585	.0033821	.0003913
6	-.0000175	-.0000119	.001588	.0000208	-.0000040	.0000799	.0000692	.0024837	.0003744

SHELL ELEM 75 NODES= 74 75 MAT= 1 LENGTH= .1562 TEMPERATURES (1,2) = 70.0 70.0

	X	Y	SIG S	SIG TH	S MOM	TH MOM	S BEND	SIG S1	SIG S2	TH BEND	SIG TH1	SIG TH2
1	3.2000	-.2000	2138.	2516.	2.	0.	6078.	-3939.	8216.	1831.	685.	4347.
2	3.1960	-.2240	2234.	2869.	1.	0.	5537.	-3303.	7771.	1650.	1219.	4520.
3	3.1920	-.2480	2312.	3198.	1.	0.	4996.	-2668.	7308.	1473.	1685.	4530.
4	3.1880	-.2720	2373.	3507.	1.	0.	4457.	-2084.	6831.	1298.	2084.	4485.
5	3.1840	-.2960	2421.	3792.	1.	0.	3919.	-1498.	6339.	1127.	2435.	4689.
6	3.1800	-.3200	2459.	3869.	1.	0.	3381.	-926.	5836.	959.	2730.	4643.

	UN	US	ROT	UX	UY	EPS	EPTH	CURVE S	CURVE TH
1	-.0000185	-.0000102	.001588	.0000208	-.0000040	.0000521	.0000692	.0019705	.0003390
2	-.0000135	-.0000101	.001291	.0000241	-.0000070	.0000521	.0000609	.0015914	.0002773
3	-.0000084	-.0000099	.001020	.0000268	-.0000094	.0000521	.0000505	.0042122	.0002207
4	-.0000037	-.0000097	.000778	.0000288	-.0000114	.0000521	.0000481	.0073331	.0001693
5	.0000015	-.0000096	.000562	.0000302	-.0000129	.0000521	.0001039	.0104540	.0001233
6	.0000063	-.0000094	.000374	.0000313	-.0000139	.0000521	.0001081	.0135749	.0000826

SHELL ELEM 76 NODES= 75 76 MAT= 1 LENGTH= .1502 TEMPERATURES (1,2) = 70.0 70.0

	X	Y	SIG S	SIG TH	S MOM	TH MOM	S BEND	SIG S1	SIG S2	TH BEND	SIG TH1	SIG TH2
1	[illegible]	-.3200	2282.	3634.	1.	0.	3340.	-1867.	5592.	948.	2666.	4582.
2	[illegible]	-.3440	2276.	3721.	1.	0.	2916.	-1623.	5194.	814.	2706.	4535.
3	[illegible]	-.3680	2267.	3787.	1.	0.	2493.	-1384.	4787.	684.	2707.	4454.
4	[illegible]	-.3920	2256.	3830.	1.	0.	2070.	-1148.	4371.	555.	2683.	4343.
5	[illegible]	-.4160	2243.	3850.	1.	0.	1648.	-913.	3949.	430.	2633.	4214.
6	[illegible]	-.4400	2230.	3846.	1.	0.	1226.	-680.	3522.	307.	2557.	4069.

	UN	US	ROT	UX	UY	EPS	EPTH	CURVE S	CURVE TH
1	[illegible]	[illegible]	[illegible]	[illegible]	[illegible]	.0000454	.0000081	[illegible]	[illegible]
2	[illegible]	[illegible]	[illegible]	[illegible]	[illegible]	.0000454	.0000169	[illegible]	[illegible]
3	[illegible]	[illegible]	[illegible]	[illegible]	[illegible]	.0000454	.0000126	[illegible]	[illegible]
4	[illegible]	[illegible]	[illegible]	[illegible]	[illegible]	.0000454	.0000132	[illegible]	[illegible]
5	[illegible]	[illegible]	[illegible]	[illegible]	[illegible]	.0000454	.0000128	[illegible]	[illegible]
6	[illegible]	[illegible]	[illegible]	[illegible]	[illegible]	.0000454	.0000116	[illegible]	[illegible]

SHELL ELEM 77 NODES= 76 77 MAT= 1 LENGTH= .2603 TEMPERATURES (1,2) = 70.0 70.0

```
  5    2.6667   -.6000   2158.   3233.      -0.      -0.    -144.    2303.    2014.     -91.    3324.    3141.
  6    2.6333   -.6400   2115.   3077.      -0.      -0.    -460.    2576.    1657.    -174.    3251.    2903.
  I      UN        US       ROT              UX       UY              EPS        EPTH      CURVE S    CURVE TH
  1   -.00       -.000087  -.000217        .000313  -.000148        .0000459   .0001118   .0014807  -.0000496
  2   -.000321  -.000085  -.000301        .000301  -.000141        .0000459   .0001088   .0013572  -.0000697
  3   -.000304  -.000082  -.000358        .000286  -.000131        .0000459   .0001047   .0004337  -.0000840
  4   -.000284  -.000080  -.000388        .000270  -.000121        .0000459   .0000998   .0003101  -.0000921
  5   -.000264  -.000077  -.000391        .000252  -.000110        .0000459   .0000946  -.0003134  -.0000938
  6   -.000244  -.000075  -.000365        .000236  -.000099        .0000459   .0000895  -.0007370  -.0000890

SHELL ELEM   78  NODES=    77      78  MAT=  1  LENGTH=      .2603  TEMPERATURES (1,2) =     70.0     70.0
  I      X        Y      SIG S   SIG TH    S MOM   TH MOM   S BEND   SIG S1   SIG S2  TH BEND  SIG TH1  SIG TH2
  1    2.6333   -.6400   2248.   3112.      -0.      -0.    -372.    2620.    1877.    -150.    3263.    2962.
  2    2.6000   -.6800   2208.   2965.      -0.      -0.    -390.    2599.    1818.    -151.    3115.    2813.
  3    2.5667   -.7200   2172.   2829.      -0.      -0.    -409.    2581.    1763.    -152.    2981.    2676.
  4    2.5333   -.7600   2138.   2705.      -0.      -0.    -427.    2566.    1711.    -153.    2858.    2552.
  5    2.5000   -.8000   2109.   2595.      -0.      -0.    -446.    2554.    1663.    -153.    2749.    2443.
  6    2.4667   -.8400   2083.   2502.      -0.      -0.    -464.    2547.    1620.    -153.    2655.    2349.
  I      UN        US       ROT              UX       UY              EPS        EPTH      CURVE S    CURVE TH
  1   -.000244  -.000075  -.000365        .000236  -.000099        .0000503   .0000895  -.0005913  -.0000890
  2   -.000226  -.000072  -.000334        .000220  -.000089        .0000503   .0000846  -.0006239  -.0000823
  3   -.000209  -.000070  -.000301        .000206  -.000080        .0000503   .0000801  -.0006566  -.0000751
  4   -.000195  -.000067  -.000265        .000193  -.000073        .0000503   .0000760  -.0006893  -.0000672
  5   -.000182  -.000065  -.000229        .000181  -.000067        .0000503   .0000724  -.0007220  -.0000587
  6   -.000171  -.000062  -.000191        .000171  -.000062        .0000503   .0000693  -.0007547  -.0000495

SHELL ELEM   79  NODES=    78      79  MAT=  1  LENGTH=      .2603  TEMPERATURES (1,2) =     70.0     70.0
  I      X        Y      SIG S   SIG TH    S MOM   TH MOM   S BEND   SIG S1   SIG S2  TH BEND  SIG TH1·SIG TH2
  1    2.4667   -.8400   2177.   2527.      -0.      -0.    -417.    2594.    1760.    -140.    2667.    2387.
  2    2.4333   -.8800   2156.   2447.      -0.      -0.    -350.    2506.    1805.    -118.    2565.    2329.
  3    2.4000   -.9200   2137.   2380.      -0.      -0.    -283.    2421.    1854.     -96.    2476.    2284.
  4    2.3667   -.9600   2122.   2323.      -0.      -0.    -217.    2339.    1905.     -75.    2399.    2248.
  5    2.3333  -1.0000   2109.   2274.      -0.      -0.    -151.    2260.    1958.     -55.    2330.    2219.
  6    2.3000  -1.0400   2097.   2230.      -0.      -0.     -85.    2182.    2012.     -36.    2267.    2194.
  I      UN        US       ROT              UX       UY              EPS        EPTH      CURVE S    CURVE TH
  1   -.000171  -.000062  -.000191        .000171  -.000062        .0000534   .0000693  -.0006767  -.0000495
  2   -.000162  -.000059  -.000158        .000162  -.000058        .0000534   .0000666  -.0005682  -.0000417
  3   -.000154  -.000056  -.000132        .000155  -.000055        .0000534   .0000644  -.0004598  -.0000351
  4   -.000148  -.000054  -.000111        .000148  -.000054        .0000534   .0000625  -.0003514  -.0000299
  5   -.000143  -.000051  -.000095        .000142  -.000052        .0000534   .0000609  -.0002429  -.0000261
  6   -.000138  -.000048  -.000085        .000137  -.000051        .0000534   .0000594  -.0001345  -.0000237

SHELL ELEM   80  NODES=    79      80  MAT=  1  LENGTH=      .2603  TEMPERATURES (1,2) =     70.0     70.0
  I      X        Y      SIG S   SIG TH    S MOM   TH MOM   S BEND   SIG S1   SIG S2  TH BEND  SIG TH1  SIG TH2
  1    2.3000  -1.0400   2155.   2246.      -0.      -0.     -74.    2230.    2081.     -33.    2280.    2213.
  2    2.2667  -1.0800   2144.   2204.      -0.      -0.      -2.    2146.    2142.     -13.    2217.    2190.
  3    2.2333  -1.1200   2132.   2160.       0.       0.      71.    2062.    2203.       5.    2154.    2165.
  4    2.2000  -1.1600   2119.   2111.       0.       0.     142.    1976.    2261.      23.    2088.    2134.
  5    2.1667  -1.2000   2103.   2054.       0.       0.     214.    1889.    2318.      39.    2014.    2093.
  6    2.1333  -1.2400   2085.   1994.       0.       0.     265.    1799.    2370.      55.    1929.    2039.
  I      UN        US       ROT              UX       UY              EPS        EPTH      CURVE S    CURVE TH
  1   -.000138  -.000048  -.000085        .000137  -.000051        .0000553   .0000594  -.0001167  -.0000237
  2   -.000134  -.000045  -.000082        .000132  -.000051        .0000553   .0000580   .0000033  -.0000232
  3   -.000129  -.000042  -.000085        .000126  -.000050        .0000553   .0000566   .0001233  -.0000245
  4   -.000125  -.000039  -.000095        .000121  -.000049        .0000553   .0000550   .0002433  -.0000277
  5   -.000119  -.000037  -.000111        .000115  -.000048        .0000553   .0000531   .0003633  -.0000328
  6   -.000113  -.000034  -.000133        .000108  -.000046        .0000553   .0000508   .0004833  -.0000399

SHELL ELEM   81  NODES=    80      81  MAT=  1  LENGTH=      .2603  TEMPERATURES (1,2) =     70.0     70.0
  I      X        Y      SIG S   SIG TH    S MOM   TH MOM   S BEND   SIG S1   SIG S2  TH BEND  SIG TH1  SIG TH2
  1    2.1333  -1.2400   2213.   2018.       0.       0.     341.    1871.    2554.      70.    1949.    2088.
  2    2.1000  -1.2800   2189.   1929.       0.       0.     338.    1851.    2526.      63.    1866.    1993.
  3    2.0667  -1.3200   2159.   1820.       0.       0.     334.    1825.    2493.      57.    1763.    1876.
  4    2.0333  -1.3600   2124.   1669.       0.       0.     331.    1793.    2455.      50.    1639.    1739.
  5    2.0000  -1.4000   2082.   1536.       0.       0.     327.    1755.    2410.      43.    1492.    1579.
  6    1.9667  -1.4400   2035.   1359.       0.       0.     324.    1711.    2358.      36.    1323.    1396.
  I      UN        US       ROT              UX       UY              EPS        EPTH      CURVE S    CURVE TH
  1   -.000113  -.000034  -.000133        .000108  -.000046        .0000596   .0000508   .0005759  -.0000399
  2   -.000105  -.000031  -.000163        .000100  -.000044        .0000596   .0000478   .0005729  -.0000496
  3   -.000096  -.000027  -.000193        .000091  -.000040        .0000596   .0000442   .0005698  -.0000597
  4   -.000085  -.000024  -.000222        .000081  -.000035        .0000596   .0000398   .0005667  -.0000700
  5   -.000073  -.000021  -.000252        .000070  -.000030        .0000596   .0000348   .0005637  -.0000805
  6   -.000059  -.000018  -.000281        .000057  -.000024        .0000596   .0000289   .0005606  -.0000914

SHELL ELEM   82  NODES=    81      82  MAT=  1  LENGTH=      .2603  TEMPERATURES (1,2) =     70.0     70.0
  I      X        Y      SIG S   SIG TH    S MOM   TH MOM   S BEND   SIG S1   SIG S2  TH BEND  SIG TH1  SIG TH2
  1    1.9667  -1.4400   2339.   1441.       0.       0.     531.    1808.    2869.      92.    1349.    1534.
  2    1.9333  -1.4800   2283.   1234.       0.      -0.      50.    2233.    2333.     -43.    1278.    1191.
  3    1.9000  -1.5200   2224.   1016.      -0.      -0.    -428.    2652.    1796.    -171.    1187.     846.
  4    1.8667  -1.5600   2169.    814.      -0.      -0.    -904.    3074.    1265.    -290.    1103.     524.
  5    1.8333  -1.6000   2126.    654.      -0.      -0.   -1378.    3504.     748.    -399.    1053.     255.
  6    1.8000  -1.6400   2103.    568.      -0.      -0.   -1849.    3952.     254.    -499.    1067.      69.
  I      UN        US       ROT              UX       UY              EPS        EPTH      CURVE S    CURVE TH
  1   -.000059  -.000018  -.000281        .000057  -.000024        .0000696   .0000289   .0007032  -.0000914
```

6	-.0000000	-.0001030	-.0000000	.0000000	-.0000000	.0000696	.0000029	-.0020842	-.0000484

SHELL ELEM 83 NODES= 90 91 MAT= 1 LENGTH= .3000 TEMPERATURES (1,2) = 70.0 70.0

I	X	Y	SIG S	SIG TH	S MOM	TH MOM	S BEND	SIG S1	SIG S2	TH BEND	SIG TH1	SIG TH2
1	3.3000	1.5500	-20.	298.	0.	-1.	220.	-240.	199.	-1218.	1516.	-920.
2	3.2400	1.5500	-18.	306.	-0.	-1.	-20.	1.	-38.	-1314.	1621.	-1008.
3	3.1800	1.5500	-16.	315.	-0.	-2.	-258.	242.	-274.	-1408.	1722.	-1093.
4	3.1200	1.5500	-14.	323.	-1.	-2.	-495.	482.	-509.	-1498.	1821.	-1175.
5	3.0600	1.5500	-11.	332.	-1.	-2.	-732.	721.	-743.	-1585.	1917.	-1252.
6	3.0000	1.5500	-9.	342.	-1.	-2.	-968.	959.	-976.	-1668.	2010.	-1326.

I	UN	US	ROT	UX	UY	EPS	EPTH	CURVE S	CURVE TH
1	-.0036900	-.0000036	-.0037637	.0000036	-.0036900	-.0000036	.0000108	.0004897	-.0011404
2	-.0034553	-.0000035	-.0037871	.0000036	-.0034634	-.0000036	.0000111	.0002994	-.0011688
3	-.0032357	-.0000036	-.0037997	.0000036	-.0032359	-.0000035	.0000114	.0001091	-.0011948
4	-.0030057	-.0000036	-.0038002	.0000036	-.0030074	-.0000036	.0000117	-.0000812	-.0012180
5	-.0027880	-.0000037	-.0037900	.0000037	-.0027880	-.0000036	.0000120	-.0002716	-.0012384
6	-.0025530	-.0000037	-.0037688	.0000037	-.0025530	-.0000036	.0000123	-.0004619	-.0012559

SHELL ELEM 84 NODES= 91 92 MAT= 1 LENGTH= .3000 TEMPERATURES (1,2) = 70.0 70.0

I	X	Y	SIG S	SIG TH	S MOM	TH MOM	S BEND	SIG S1	SIG S2	TH BEND	SIG TH1	SIG TH2
1	3.0000	1.5500	-59.	328.	-1.	-2.	-932.	872.	-991.	-1658.	1986.	-1330.
2	2.9400	1.5500	-56.	339.	-2.	-2.	-1777.	1720.	-1833.	-1897.	2236.	-1558.
3	2.8800	1.5500	-53.	350.	-3.	-2.	-2617.	2563.	-2670.	-2119.	2469.	-1769.
4	2.8200	1.5500	-50.	362.	-4.	-2.	-3452.	3402.	-3502.	-2323.	2685.	-1961.
5	2.7600	1.5500	-47.	374.	-5.	-3.	-4282.	4235.	-4329.	-2507.	2882.	-2133.
6	2.7000	1.5500	-43.	387.	-5.	-3.	-5107.	5063.	-5150.	-2671.	3058.	-2284.

I	UN	US	ROT	UX	UY	EPS	EPTH	CURVE S	CURVE TH
1	-.0025530	-.0000037	-.0037688	.0000037	-.0025530	-.0000053	.0000123	-.0004322	-.0012559
2	-.0023280	-.0000037	-.0037210	.0000037	-.0023280	-.0000053	.0000127	-.0011289	-.0012656
3	-.0021070	-.0000038	-.0036320	.0000038	-.0021070	-.0000053	.0000130	-.0018256	-.0012611
4	-.0018930	-.0000038	-.0035020	.0000038	-.0018930	-.0000053	.0000134	-.0025223	-.0012417
5	-.0016880	-.0000038	-.0033290	.0000038	-.0016880	-.0000053	.0000138	-.0032190	-.0012063
6	-.0014940	-.0000038	-.0031150	.0000038	-.0014940	-.0000053	.0000142	-.0039157	-.0011538

SHELL ELEM 85 NODES= 92 93 MAT= 1 LENGTH= .2082 TEMPERATURES (1,2) = 70.0 70.0

I	X	Y	SIG S	SIG TH	S MOM	TH MOM	S BEND	SIG S1	SIG S2	TH BEND	SIG TH1	SIG TH2
1	2.7000	1.5500	31.	407.	-6.	-3.	-5242.	5273.	-5212.	-2558.	3095.	-2280.
2	2.6590	1.5427	-35.	163.	-7.	-3.	-6201.	6166.	-6237.	-2839.	3052.	-2727.
3	2.6179	1.5353	-108.	-72.	-8.	-3.	-7155.	7057.	-7254.	-3074.	3002.	-3146.
4	2.5767	1.5280	-159.	-294.	-9.	-3.	-8105.	7946.	-8264.	-3241.	2947.	-3535.
5	2.5360	1.5206	-214.	-500.	-10.	-4.	-9049.	8835.	-9263.	-3384.	2889.	-3888.
6	2.4951	1.5133	-264.	-685.	-11.	-4.	-9988.	9724.	-10252.	-3517.	2831.	-4202.

I	UN	US	ROT	UX	UY	EPS	EPTH	CURVE S	CURVE TH
1	-.0014780	.0000225	-.0031150	.0000038	-.0014940	-.0000028	.0000142	-.0040328	-.0011358
2	-.0013520	.0000225	-.0029310	.0000016	-.0013700	-.0000028	.0000062	-.0048403	-.0010849
3	-.0012034	.0000225	-.0027120	-.0000004	-.0012540	-.0000028	-.0000015	-.0056477	-.0010198
4	-.0011126	.0000225	-.0024600	-.0000023	-.0011480	-.0000028	-.0000090	-.0064551	-.0009398
5	-.0010030	.0000225	-.0021750	-.0000040	-.0010530	-.0000028	-.0000158	-.0072626	-.0008441
6	-.0009046	.0000225	-.0018550	-.0000055	-.0009700	-.0000028	-.0000219	-.0080700	-.0007320

SHELL ELEM 86 NODES= 93 94 MAT= 1 LENGTH= .3795 TEMPERATURES (1,2) = 70.0 70.0

I	X	Y	SIG S	SIG TH	S MOM	TH MOM	S BEND	SIG S1	SIG S2	TH BEND	SIG TH1	SIG TH2
1	2.4951	1.5133	-134.	-650.	-11.	-4.	-9911.	9777.	-10044.	-3378.	2728.	-4028.
2	2.4310	1.5541	76.	125.	-9.	-3.	-8276.	8352.	-8201.	-2735.	2863.	-2613.
3	2.3670	1.5949	224.	677.	-7.	-2.	-6651.	6875.	-6426.	-2128.	2805.	-1452.
4	2.3030	1.6357	322.	1039.	-5.	-2.	-5034.	5355.	-4712.	-1553.	2591.	-514.
5	2.2390	1.6764	379.	1249.	-4.	-1.	-3427.	3806.	-3048.	-1013.	2262.	236.
6	2.1750	1.7172	407.	1351.	-2.	-1.	-1831.	2237.	-1424.	-514.	1665.	838.

I	UN	US	ROT	UX	UY	EPS	EPTH	CURVE S	CURVE TH
1	-.0008648	-.0000475	-.0018550	-.0000055	-.0009700	.0000015	-.0000219	-.0080343	-.0006272
2	-.0007220	-.0000475	-.0016295	.0000009	-.0008700	.0000015	-.0000037	-.0057296	-.0004493
3	-.0005849	-.0000475	-.0013834	.0000052	-.0007602	.0000015	.0000220	-.0034249	-.0002971
4	-.0004575	-.0000475	-.0011178	.0000078	-.0006761	.0000015	.0000340	-.0011202	-.0001728
5	-.0003575	-.0000475	-.0008329	.0000092	-.0006140	.0000015	.0000410	.0011845	-.0000765
6	-.0002566	-.0000475	-.0005344	.0000096	-.0005732	.0000015	.0000443	.0034892	-.0000172

SHELL ELEM 87 NODES= 94 95 MAT= 1 LENGTH= .3795 TEMPERATURES (1,2) = 70.0 70.0

I	X	Y	SIG S	SIG TH	S MOM	TH MOM	S BEND	SIG S1	SIG S2	TH BEND	SIG TH1	SIG TH2
1	2.1750	1.7172	642.	1415.	-2.	-1.	-7659.	8321.	-7017.	-2078.	3493.	-1663.
2	2.1110	1.7579	599.	1254.	-1.	-0.	-5921.	6572.	-5272.	-1622.	2953.	-1205.
3	2.0470	1.7987	469.	746.	-1.	-0.	-4260.	4771.	-3741.	-1144.	2384.	-723.
4	1.9830	1.8394	249.	-83.	-0.	0.	-2600.	2969.	-2204.	-644.	1784.	-214.
5	1.9190	1.8802	-58.	-1037.	1.	0.	-1980.	1946.	-2013.	-602.	1740.	64.
6	1.8550	1.9210	-171.	-1597.	1.	0.	-4335.	-4505.	4164.	1447.	-3044.	-150.

I	UN	US	ROT	UX	UY	EPS	EPTH	CURVE S	CURVE TH
1	-.0005575	-.0000475	-.0005344	.0000096	-.0005732	.0000093	.0000443	-.0126749	-.0000172
2	-.0004575	-.0000475	-.0002082	.0000092	-.0006140	.0000093	.0000410	-.0103811	-.0000765
3	-.0003575	-.0000475	.0001178	.0000078	-.0006761	.0000093	.0000340	-.0080774	-.0001728
4	-.0002566	-.0000475	.0004523	.0000052	-.0007602	.0000093	.0000220	-.0057736	-.0002971
5	-.0001566	-.0000475	.0007722	-.0000009	-.0008700	.0000093	-.0000037	-.0034698	-.0004493
6	-.0000566	-.0000475	.0010775	-.0000055	-.0009700	.0000093	-.0000219	-.0011660	-.0006272

SHELL ELEM 88 NODES= 95 96 MAT= 1 LENGTH= .3795 TEMPERATURES (1,2) = 70.0 70.0

5	1.6484	1.9505	573.	-2137.	1.	0.	4295.	-3722.	4867.	1159.	-3[illegible].	-[illegible].
4	1.6[illegible]	1.9[illegible]	563.	-2[illegible].	1.	0.	4560.	-4015.	5145.	1068.	-3232.	-1094.
3	1.5[illegible]	2.0[illegible]	646.	-1665.	1.	0.	4356.	-4211.	5502.	935.	-2[illegible].	-931.
2	1.4[illegible]	2.0377	833.	-1172.	1.	0.	5123.	-4240.	5956.	765.	-1937.	-4[illegible].

	UN	US	ROT	UX	UY	EPS	EPTH	CURVE S	CURVE TH
5	-.0011[illegible]	-.0005[illegible]	-.[illegible]024	-.0000102	-.001105	.0000411	-.0000554	.0053[illegible]	.0005147
4	-.0011[illegible]	-.0005[illegible]	-.[illegible]548	-.0001128	-.001159	.0000411	-.0000722	.0056479	.0002865
3	-.0011[illegible]	-.0005[illegible]	-.[illegible]30	-.0001139	-.001179	.0000411	-.0000[illegible]9	.0057[illegible]68	.0000164
2	-.0011[illegible]	-.0005[illegible]	-.[illegible]83.	-.0001135	-.001160	.0000421	-.0000[illegible]28	.0074636	-.0003010
1	-.0011[illegible]	-.0005[illegible]	-.[illegible]193	-.0001174	-.001191	.0000-11	-.0000[illegible]69	.0082214	-.0006720
6	-.0011[illegible]	-.0005[illegible]	-.[illegible]773	-.0000074	-.000998	.0000411	-.0000499	.0047792	-.0011043

SHELL ELEM 89 NODES= 93 97 MAT= 1 LENGTH= .3795 TEMPERATURES (1,2) = 70.0 70.0

	X	Y	SIG S	SIG TH	S MOM	TH MOM	S BEND	SIG S1	SIG S2	TH BEND	SIG TH1	SIG TH2
1	1.4878	2.0377	255.	-1334.	2.	0.	6937.	-6702.	7172.	1235.	-2569.	-99.
2	1.4[illegible]54	2.0[illegible]5	480.	-346.	1.	-0.	3281.	-2793.	3769.	-38.	-358.	-434.
3	1.3430	2.0[illegible]30	831.	871.	-0.	-0.	-332.	1163.	498.	-1152.	2023.	-280.
4	1.27[illegible]5	2.10[illegible]1	1211.	2282.	-1.	-1.	-3895.	5106.	-2684.	-2079.	4340.	203.
5	1.[illegible]12	2.1276	1568.	3603.	-2.	-1.	-7398.	8966.	-5830.	-2785.	4388.	313.
6	1.1259	2.1518	1822.	4542.	-3.	-1.	-10830.	12652.	-9009.	-3229.	7771.	1314.

	UN	US	ROT	UX	UY	EPS	EPTH	CURVE S	CURVE TH
1	-.0000974	-.0000229	-.001778	-.0000074	-.000998	.0000213	-.0000499	.0117926	-.0011399
2	-.0000811	-.0000228	-.002449	-.0000027	-.000842	.0000213	-.0000189	.0053774	-.0016501
3	-.0000514	-.0000226	-.002670	.0000031	-.000653	.0000213	.0000231	-.0000378	-.0018964
4	-.0000417	-.0000224	-.002443	.0000089	-.000405	.0000213	.0000698	-.0059530	-.0018338
5	-.0000254	-.0000223	-.001767	.0000136	-.000309	.0000213	.0001136	-.0114683	-.0014063
6	-.0000160	-.0000221	-.000642	.0000163	-.000219	.0000213	.0001447	-.0177835	-.0005435

SHELL ELEM 90 NODES= 97 98 MAT= 1 LENGTH= .3795 TEMPERATURES (1,2) = 70.0 70.0

	X	Y	SIG S	SIG TH	S MOM	TH MOM	S BEND	SIG S1	SIG S2	TH BEND	SIG TH1	SIG TH2
1	1.1259	2.1518	228.	4112.	-3.	-1.	-12684.	12912.	-12456.	-3736.	7848.	376.
2	1.0518	2.1682	319.	4448.	-2.	-1.	-9245.	9564.	-8926.	-2113.	6561.	2335.
3	.9777	2.1846	262.	4239.	-2.	-0.	-5841.	6103.	-5579.	-621.	4860.	3618.
4	.9036	2.2011	-82.	3573.	-1.	0.	-2482.	2564.	-2400.	707.	2656.	4279.
5	.8295	2.2175	-[illegible].	2571.	0.	0.	821.	-1009.	633.	1826.	745.	4397.
6	.7554	2.2339	-504.	1402.	1.	1.	4052.	-4555.	3548.	2676.	-1274.	4079.

	UN	US	ROT	UX	UY	EPS	EPTH	CURVE S	CURVE TH
1	-.0001179	-.0000206	-.000642	.0000163	-.000219	-.0000315	.0001447	-.0204488	-.0005563
2	-.0001185	-.0000209	.000737	.0000164	-.000226	-.0000315	.0001558	-.0154901	-.0006845
3	-.0002980	-.0000211	.001710	.0000146	-.000319	-.0000315	.0001489	-.0101315	-.0017074
4	-.0000434	-.0000214	.002275	.0000115	-.000470	-.0000315	.0001268	-.0047728	-.0024585
5	-.0000615	-.0000216	.002434	.0000078	-.000648	-.0000315	.0000936	-.0006859	-.0028551
6	-.0000743	-.0000218	.002186	.0000041	-.000822	-.0000315	.0000549	.0059445	-.0028259

Max Stress element on Floating piston

SHELL ELEM 91 NODES= 98 99 MAT= 1 LENGTH= .3795 TEMPERATURES (1,2) = 70.0 70.0

	X	Y	SIG S	SIG TH	S MOM	TH MOM	S BEND	SIG S1	SIG S2	TH BEND	SIG TH1	SIG TH2
1	.7554	2.2339	-623.	1370.	1.	1.	3003.	-3626.	2381.	2418.	-1048.	3788.
2	.6801	2.2438	-781.	782.	1.	1.	3102.	-3884.	2321.	2356.	-1575.	3139.
3	.6049	2.2537	-935.	212.	1.	1.	3191.	-4126.	2256.	2255.	-2043.	2467.
4	.5296	2.2636	-1079.	-322.	1.	1.	3265.	-4344.	2185.	2098.	-2420.	1775.
5	.4544	2.2735	-1206.	-792.	1.	0.	3315.	-4526.	2109.	1896.	-2648.	1064.
6	.3791	2.2834	-1302.	-1148.	1.	0.	3330.	-4632.	2028.	1481.	-2628.	333.

	UN	US	ROT	UX	UY	EPS	EPTH	CURVE S	CURVE TH
1	-.0003309	-.0001[illegible]48	.002186	.0000041	-.000822	-.0000354	.0000549	.0041969	.0028598
2	-.0003[illegible]53	-.0001[illegible]51	.001860	.0000024	-.000975	-.0000354	.0000354	.0044040	.0027115
3	-.0001091	-.0001[illegible]54	.001518	.0000010	-.001102	-.0000354	.0000166	.0045111	.0024980
4	-.0001193	-.0001[illegible]56	.001160	-.0000061	-.001203	-.0000354	-.0000011	.0045[illegible]22	.0021717
5	-.0001257	-.0001[illegible]59	.000787	-.0000098	-.001277	-.0000354	-.0000167	.0050[illegible]53	.0017162
6	-.0001312	-.0001[illegible]62	.000397	-.0000011	-.001322	-.0000354	-.0000284	.0052324	.0010389

SHELL ELEM 92 NODES= 99 100 MAT= 1 LENGTH= .3787 TEMPERATURES (1,2) = 70.0 70.0

	X	Y	SIG S	SIG TH	S MOM	TH MOM	S BEND	SIG S1	SIG S2	TH BEND	SIG TH1	SIG TH2
1	.3791	2.2834	-1213.	-1123.	0.	0.	1832.	-3045.	620.	1081.	-2204.	-42.
2	.3035	2.2868	-1231.	-1192.	0.	0.	1366.	-2597.	134.	765.	-1957.	-428.
3	.2278	2.2901	-1244.	-1238.	0.	0.	899.	-2143.	-345.	448.	-1686.	-790.
4	.1521	2.2934	-1250.	-1260.	0.	0.	433.	-1682.	-817.	132.	-1393.	-1128.
5	.0764	2.2967	-1249.	-1257.	-0.	-0.	-34.	-1215.	-1282.	-182.	-1075.	-1439.
6	.0008	2.3000	-981.	-265.	-0.	-0.	-394.	-586.	-1375.	-106.	-158.	-371.

	UN	US	ROT	UX	UY	EPS	EPTH	CURVE S	CURVE TH
1	-.0013[illegible]21	-.0000047	.000397	-.0000011	-.001322	-.0000325	-.0000284	.0027508	.0010469
2	-.0013[illegible]44	-.0000049	.000215	-.0000009	-.001345	-.0000325	-.0000307	.0020701	.0007068
3	-.0013[illegible]55	-.0000052	.000084	-.0000007	-.001356	-.0000325	-.0000322	.0013843	.0003670
4	-.0013[illegible]58	-.0000054	.000004	-.0000005	-.001359	-.0000325	-.0000330	.0007[illegible]56	.0000277
5	-.0013[illegible]57	-.0000057	-.000024	-.0000003	-.001358	-.0000325	-.0000328	.0000278	-.0003094
6	-.0013[illegible]56	-.0000059	-.000000	-.0000000	-.001357	-.0000325	.0000000	-.0006529	-.0000000

SHELL ELEM 93 NODES= 50 93 MAT= 1 LENGTH= .1479 TEMPERATURES (1,2) = 70.0 70.0

	X	Y	SIG S	SIG TH	S MOM	TH MOM	S BEND	SIG S1	SIG S2	TH BEND	SIG TH1	SIG TH2
1	2.4000	1.4000	-11857.	-8402.	0.	0.	9930.	-21787.	-1926.	2678.	-11080.	-5724.
2	2.4190	1.4227	-11750.	-8006.	0.	0.	6392.	-18141.	-5358.	1782.	-9788.	-6225.
3	2.4380	1.4453	-11455.	-6916.	0.	0.	2845.	-14300.	-8510.	857.	-7773.	-6059.
4	2.[illegible]	1.4640	-11082.	-5334.	-0.	-0.	-709.	-10373.	-11792.	-96.	-5438.	-5630.
5	2.[illegible]	1.49006	-10737.	-4254.	-0.	-0.	-4271.	-6466.	-15008.	-1076.	-3178.	-5330.
6	2.[illegible]	1.5133	-10521.	-3455.	-0.	-0.	-7840.	-2681.	-18360.	-2083.	-1371.	-5538.

	UN	US	ROT	UX	UY	EPS	EPTH	CURVE S	CURVE TH

6	.000582	-.000779	-.001855	-.000055	-.000970	-.0003424	-.0000219	-.1039592	.0004779

SHELL ELEM 94 NODES= 58 97 MAT= 1 LENGTH= .1586 TEMPERATURES (1,2) = 70.0 70.0

I	X	Y	SIG S	SIG TH	S MOM	TH MOM	S BEND	SIG S1	SIG S2	TH BEND	SIG TH1	SIG TH2
1	1.0800	2.0000	-11066.	-3989.	0.	0.	4021.	-15087.	-7044.	1081.	-5070.	-2909.
2	1.0892	2.0304	-10982.	-3680.	0.	0.	2595.	-13577.	-8387.	721.	-4401.	-2958.
3	1.0983	2.0607	-10655.	-2468.	0.	0.	1166.	-11821.	-9489.	350.	-2817.	-2118.
4	1.1075	2.0911	-10225.	-874.	-0.	-0.	-267.	-9958.	-10492.	-34.	-840.	-908.
5	1.1167	2.1214	-9827.	598.	-0.	-0.	-1703.	-8124.	-11530.	-430.	1027.	168.
6	1.1259	2.1518	-9594.	1460.	-0.	-0.	-3142.	-6452.	-12736.	-837.	2297.	623.

I	UX	UY	ROT	UX	UY	EPS	EPTH	CURVE S	CURVE TH
1	-.000008	-.000106	.000280	-.000039	-.000099	-.0003567	-.0000358	.0532799	-.0000749
2	.000006	-.000117	-.001109	-.000028	-.000114	-.0003567	-.0000255	.0342923	.0002944
3	.000056	-.000129	-.001895	.000016	-.000139	-.0003567	.0000146	.0153047	.0004991
4	.000120	-.000140	-.002079	.000075	-.000169	-.0003567	.0000674	-.0036829	.0005431
5	.000181	-.000151	-.001662	.000130	-.000197	-.0003567	.0001161	-.0226705	.0004304
6	.000219	-.000163	-.000642	.000163	-.000219	-.0003567	.0001447	-.0416581	.0001648

STEP 1 ITERATION 1 COMPLETE TIME= 0. KDIS= 1 KTEMP= -0

JOB FIPS, F-S.

BY Y.E.

PAGE

DATE

REV.

Accumulator Deflection Relative to Nozzle HSG.

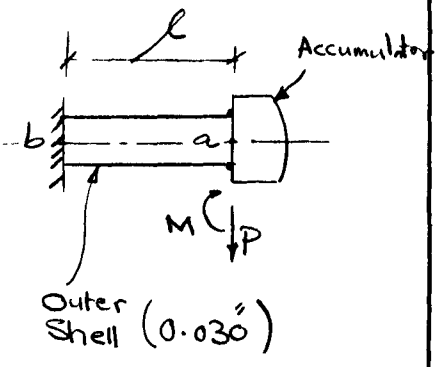

$P \simeq 12.\ \#$

$M \simeq 12 \times 1 \simeq 12.,\ \text{in-lb}$

$$\delta_{ab} = \left(\frac{Pl^3}{3EI} + \frac{Ml^2}{2EI} + \frac{Pl}{A_e G} \right)$$

$l \simeq 10".$

$E = 29 \times 10^6 \text{ psi}$

$G = \frac{E}{2(1+\nu)} = \frac{E}{2.6} = 11.15 \times 10^6 \text{ psi}$

$$H_e = \frac{2}{3} A = \frac{2}{3}\pi \left(R_o^2 - R_i^2 \right)$$

$$= \frac{2}{3}\pi \left(2.3^2 - 2.27^2 \right) = 0.2871 \text{ in}^2$$

$$I = \frac{\pi}{4} \left(R_o^4 - R_i^4 \right) = 1.1244 \text{ in}^4$$

$$\delta_{a\text{-}b} = \frac{12 \times (10)^3}{3 \times 29 \times 10^6 \times 1.1244} + \frac{12 \times (10)^2}{2 \times 29 \times 10^6 \times 1.1244} + \frac{12 \times 10}{.2871 \times 11.15 \times 10^6}$$

$$= 0.000179" \,/\, 1g$$

at 10 g

$$\delta_{a\text{-}b} = 0.00179"$$

(acceptable)

JOB KIPS

BY Y.E.

PAGE

DATE

REV.

Jet Condenser Deflection

The loads from the diffuser are replaced by a shear force F and a bending moment M at Sec. S-S.

The loads transmitted from the accumulator through the bellows are negligible.

$F = 0.22\ \#$

$M = 0.22 \times 1.0 = 0.22$ in-lb

The deflection of point "a" relative to point "b" due to bending is:

$$\delta_{a\text{-}b} = \int_a^b \left(\int_a^b \frac{M(x)\,dx}{EI(x)} \right) dx$$

The above double integral is evaluated numerically on the next page.

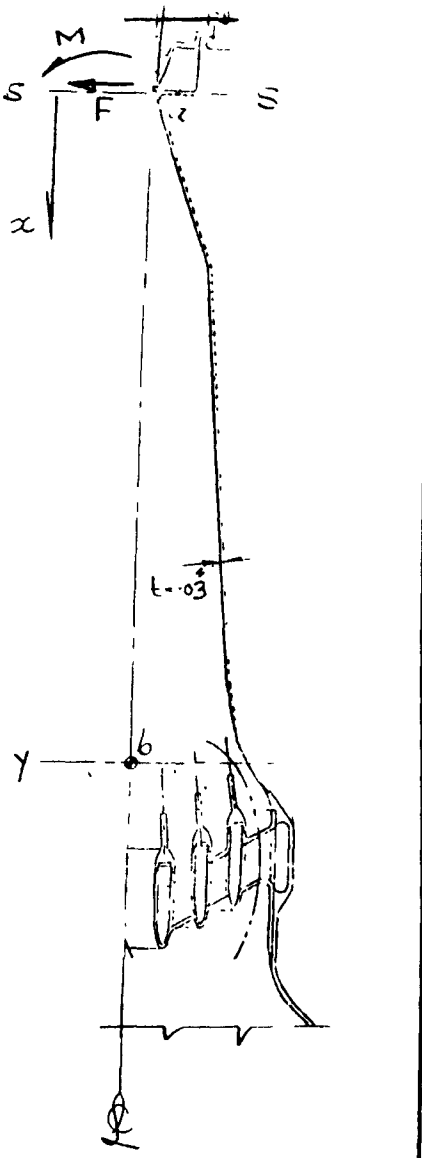

(Jet Condenser)

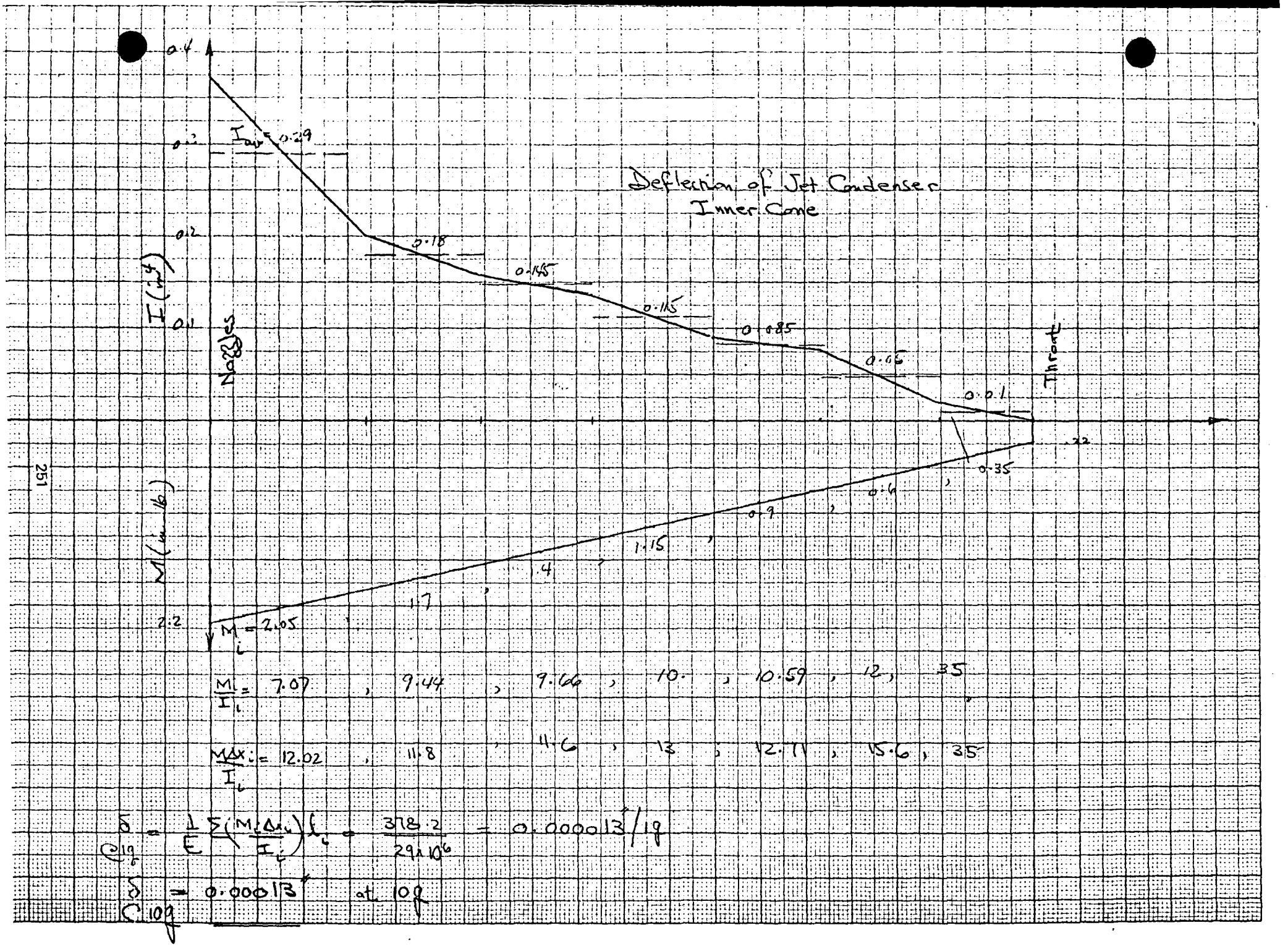
Deflection of Jet Condenser
Inner Cone
Nozzles
Throat
I (in⁴)
M (in-lb)
0.4
0.3
0.2
0.1
I_{av} = 0.29
0.18
0.145
0.145
0.085
0.05
0.01
.22
0.35
0.6
0.9
1.15
1.4
1.7
2.2
M_i = 2.05
$\frac{M}{I_i}$ = 7.07 , 9.44 , 9.66 , 10. , 10.59 , 12. , 35 ,
$\frac{M\Delta x}{I_i}$ = 12.02 , 11.8 , 11.6 , 13 , 12.11 , 15.6 , 35
$\delta_{C_{10^k}} = \frac{1}{E}\sum\left(\frac{M_i \Delta x_i}{I_i}\right)\Delta_i = \frac{378.2}{29 \times 10^6} = 0.000013''/1^k$
$\delta_{C_{10^k}} = 0.000113''$ at 10^k

JOB KIPS

PAGE

DATE

BY Y.E.

REV.

To account for the deflection due to the weight of the jet condenser core (wt. $\simeq$ 0.7 #), an upper bound on the deflection is:

$$\delta_{max} = \left(1 + \frac{0.8}{0.22}\right) \times .00013 \simeq 0.00006''/\#$$

at $\pm 10\#$

$$\delta_{@10\#} = 0.0006''$$ (acceptable)

JOB KIPS

BY Y.E.

PAGE

DATE

REV.

Internally Induced Dynamics of KIPS Accumulator

Influence of axial mode Vibrations on Pressure Recovery

let:

m_b = mass of bellows = 0.20 #

m_l = " " displaced fluid ≃ 0.79 #

m_p = " " piston = 0.613 #

k_b = axial stiffness of bellows, = 80 lbs/in

k_g = " " Compressed gas

k_p = " " due to nozzle pressure gradient

P_b = gas pressure at most deflected piston position (38.9 psiA)

S = piston area = 28.4 in^2

V_b = gas volume at most deflected position (90.2 in^3)

JOB KIPS

BY Y.E.

PAGE

DATE

REV.

Axial mode frequency

$$k_t = k_b + k_g + k_p$$

where $k_g = \dfrac{p_b S^2}{V_b}$

&

$$k_p = \left(\frac{dp}{dx}\right)_c \frac{S^2}{A_i}$$

where $\left(\frac{dp}{dx}\right)_c$ = pressure gradient of jet combustion at throat Section

Also

$$m_t = m_b + m_l + m_p$$

$$\omega_a = \sqrt{\frac{k_t}{m_t}}$$

Relative displacement resulting from input vibration $\Delta\ddot{u}$ is

$$\Delta x = \frac{\Delta \ddot{u}_i}{\omega_i^2 \left\| \left(1 - \dfrac{\omega_a^2}{\omega_i^2}\right) \right\|}$$

JOB KIPS

BY Y.E.

PAGE

DATE

REV.

where ω_i = frequency of input vibration;
System frequency.

$$m_t = 0.2 + 0.79 + 0.613 = 1.603 \#$$

$$k_g = \frac{P_b S^2}{V_b} = \frac{38.9 \times (28.4)^2}{90.2} = 347.8 \ \#/in$$

$$k_b = 80. \ \#/in.$$

$$k_p = \left(\frac{12.5}{0.4}\right) \times \frac{(28.4)^2}{\frac{\pi}{4} \times .25^2} = 513,472 \ \#/in.$$

$$k_t = 513,472 + 80 + 347.8 = 513,900 \ \#/in$$

$$f_a = \frac{1}{2\pi}\sqrt{\frac{k_t}{m_t}} = 1770 \ Hz$$

$$\Delta x = \frac{21.17 \times 386}{(11121)^2 - (217.8)^2} = 6.61 \times 10^{-5} \ in$$

$$\Delta V = S \Delta x = 28.4 \times 6.61 \times 10^{-5} = 0.00188 \ in^3$$

JOB KIPS PAGE

DATE

BY Y.E. REV.

Assuming isothermal condition.

$$pV = C$$

$$p\Delta V + \Delta p\, V = 0$$

$$|\Delta p| = \frac{p\Delta V}{V}$$

$$= \frac{38.9 \times .00188}{90.2} = \underline{\underline{0.0008}}\ psi$$

(Negligible)

Thus, the influence of the accumulator internal dynamics on pressure recovery is negligible.

Fig. Pressure Variation Along Jet Condenser

JOB KIPS

BY Y.E.

PAGE

DATE

REV.

REFERENCES

1) All Material References see Material Properties and Reliability Section.

2) Crose, J.G. and Jones, R.M., SAAS III Finite Element Stress Analysis of Axisymmetric and Plane Solids, The Aerospace Corp., June, 1971.

3) DeSalvo, G.J., and Swanson, J.A., ANSYS Engineering Analysis System, Swanson Analysis Systems, Inc., March, 1975.

4) Sundstrand Program Library, Program E-4, Design of Rotating Disk with Temperature Gradient.

5) Roark, R.J., and Young, W.C., Formulas for Stress and Strain, 5th Ed., McGraw Hill, 1975.

6) Griffel, W., Handbook of Formulas for Stress and Strain, Fred Ungar Publication Co., 1966.

7) Roark, R.J., Formulas for Stress and Strain, 3rd Ed., McGraw Hill

8) Peterson, R.E., Stress Concentration Design Factors, Wiley, 1974.

9) Rockwell International Corp., Space Division, Structures Manual.

10) Shanley, F.R., Strength of Materials, McGraw Hill, 1957.

NOTE: The number in the symbol ▷ used in the analyses is the number of the reference.

2.5.6 MISCELLANEOUS COMPONENTS

2.5.6.1 Introduction

In addition to the major subsystems discussed previously, several equally important, but less complex, components are utilized in the KIPS.

2.5.6.2 Summary

In order to maintain the proper condition of the working fluid over the seven year lifetime of the system, a noncondensable gas removal system and particle separators are used. The former statically removes the small amounts of free gas that may be evolved from or released to the Dowtherm. By continually removing any gas that may be produced, the thermodynamic cycle will be maintained constant. Filters and a centrifugal separator are used to remove any particulates or heavy droplets that may be self-generated or resulting from micrometeoroid impact on the fluid-carrying components.

Two other components are used which are not directly associated with flight operation of the KIPS. An auxiliary heat exchanger is incorporated into the radiator to provide system heat rejection, when the radiator is not used, during ground operation and launch. Quick disconnects are used to provide the necessary fluid connections to the ground support equipment.

2.5.6.3 Noncondensable Gas Removal System

The Dowtherm A organic working fluid undergoes a slight pyrolytic decomposition under long-term thermal cycling at high temperatures, forming gases and high molecular weight substances (liquid droplets) at the boiler outlet conditions. In addition, other system components may evolve gases at a low rate during operation. To assure continued reliable system performance over the mission duration in the presence of these factors, three components are utilized. A noncondensable gas separator and a palladium window are utilized to remove the gaseous degradation products, and a centrifugal separator is employed to remove the high molecular weight portion of the degradation products.

FUNCTION

Any noncondensables present in the working fluid will tend to be concentrated in the jet condenser by means of natural separation at that location. This is illustrated in Figure 2.5.6-1. Tests at Sundstrand have demonstrated that free stream noncondensable gas (air) concentrations in excess of 30 ppm will degrade performance and that concentrations in excess of 90 ppm can cause condenser failure. Refer to Figure 2.5.6-2. Performance degradation occurs because of the occulsion of the subcooled liquid jets by the noncondensable gas. At higher concentrations of gas in the liquid, the jet condenser floods out due to "brooming" of the liquid jets; i.e., the jets become unfocused due to the gas coming out of solution when the Dowtherm A is accelerated by the pressure drop through the jet condenser liquid nozzles.

A list of potential noncondensable gas sources is presented in Table 2.5.6-A. The magnitude of the gas evolution at many of these sources is very difficult to assess accurately. Because of this inability to accurately predict the noncondensable gas generation rate and the condenser's demonstrated sensitivity to gas concentration, a noncondensable gas removal system was incorporated to ensure the concentration was low enough to permit reliable operation.

X = FREE STREAM NONCONDENSABLE CONCENTRATION

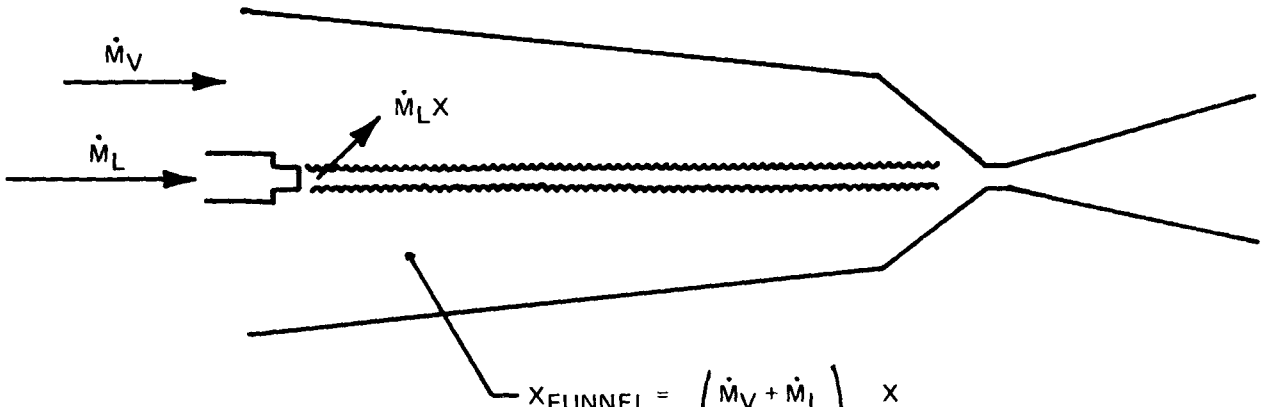

ASSUMING INSOLUBILITY OF NONCONDENSABLE IN LIQUID

Figure 2.5.6-1 Noncondensable Funnel Concentration

Table 2.5.6-A Potential Non-Condensable Gas Sources

PRIMARY SOURCES
1) Dowtherm Pyrolytic Degradation Products
2) Alternator Outgassing
OTHER POTENTIAL SOURCES
1) Carbon Pump Seals
2) Virtual Leaks
3) Gas dissolved in fluid charge
4) Residual gas from system evacuation prior to fill
5) Gas dissolved in metal matrix

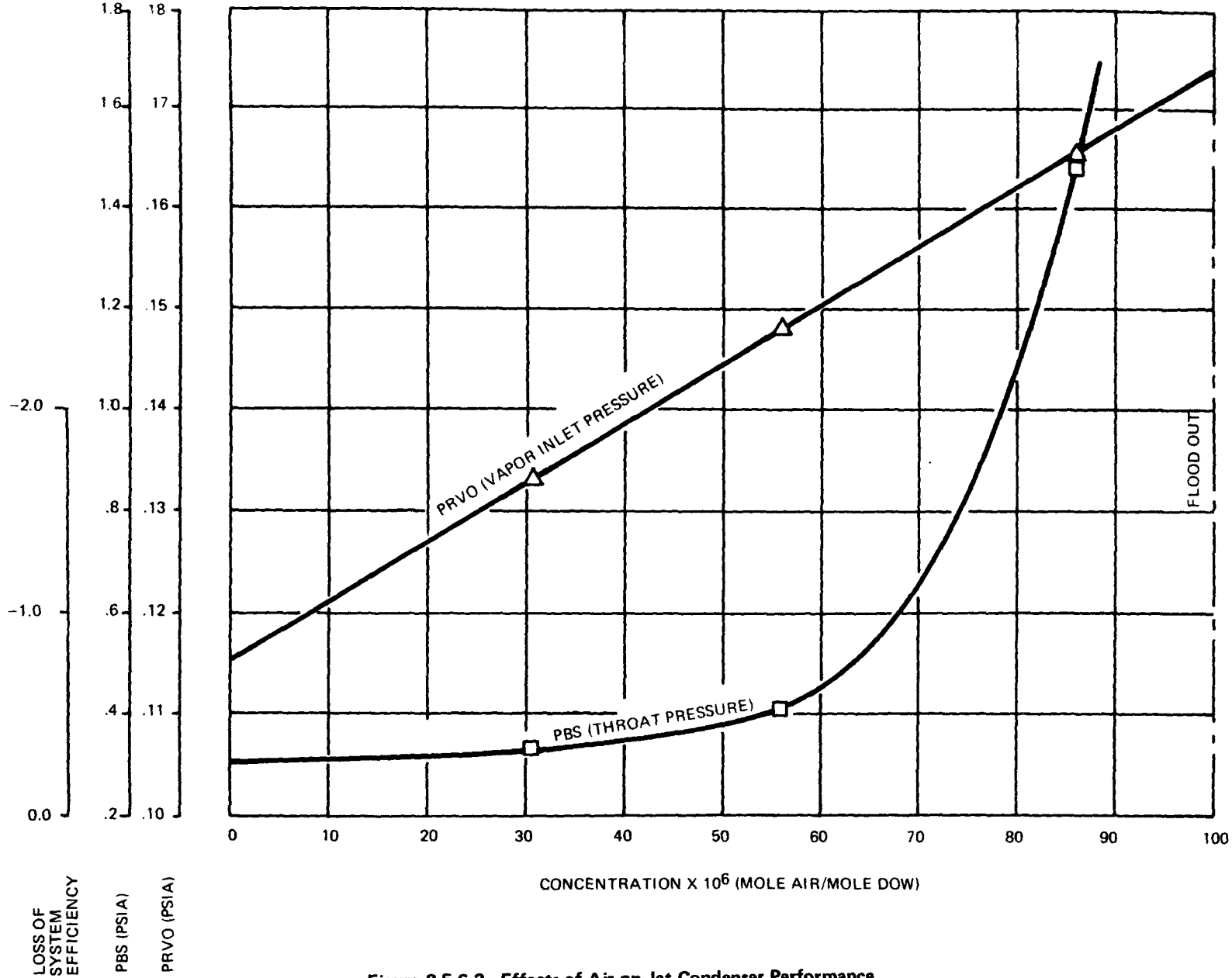

Figure 2.5.6-2 Effects of Air on Jet Condenser Performance

CONFIGURATION

The noncondensable gas removal system is comprised of a hydrogen diffusion cell made of palladium and a noncondensable gas separator (NCGS).

The diffusion cell consists of a palladium-silver diffusion material in the form of a tube, 0.062 inch OD x 0.003 inch wall thickness. The tube is 26 inches long with one end sealed and the other brazed to a nickel tube. The diffusion tube is coiled into a helix 1.125 inch diameter by 1.75 inch long and is supported by a "bird cage" constraint system. This constraint protects the diffusion tube from damage by handling or dynamic environment. The palladium diffusion cell assembly is placed at the regenerator vapor exit with the constraint welded to the wall interior and the nickel extension tube brazed through the wall.

The noncondensable gas separator is based on the gas controlled heat pipe principal (see Figure 2.5.6-3). Its two major sections are the condenser and the evaporator. The heart of the device is a 14 inch section of extruded ID grooved aluminum tube upon which the vapor condenses and is collected. It is then wicked through the grooves to the evaporator where the fluid is vaporized and returned to the flight system. At the aft end of the condenser the inlet to a capillary passage is located which collects and removes the noncondensable gases concentrated there.

The capillary passage is a 15 inch long section of tube 0.010 inch OD x 0.005 inch ID. The cooling fluid for the NCGS condenser is the jet condenser inlet flow. The heating fluid for the NCGS evaporator is the regenerator liquid outlet fluid (see Figure 2.5.6-4). The NCGS is integrated with the valve pack to minimize tube lengths, weight and number of joints, and, thus, assure high reliability.

2.5.6.3.1 PALLADIUM DIFFUSION CELL

ANALYSIS: The tolerance to any noncondensable gas is a function of its solubility in the working fluid. Since hydrogen is the most insoluble of the expected constituents and comprises the largest mole fraction of the pyrolytic degradation source term (which is the largest source term), it is of special concern.

It was noted in the AEC Organic Working Fluid Stability Program that the initial hydrogen generation rate for the first 2500 hours was approximately 50 times the asymptotic rate which prevailed after 2500 hours. In order to cope with this initial high generation rate, a palladium diffusion cell has been incorporated. The design of the noncondensable gas separator has conservatively allowed for a total gas generation of 10 times the asymptotic rate.

A palladium diffusion cell is a widely accepted method of removing hydrogen from process loops in industry. A palladium surface was incorporated in Sundstrand's Organic Working Fluid Thermal Stability Program. It was demonstrated to be compatible with Dowtherm and showed no contribution to the thermal degradation of the fluid.

Sundstrand has also run bench tests demonstrating the separation of hydrogen from a very low pressure Dowtherm A-hydrogen mixture with subsequent diffusion of the hydrogen through a palladium diffusion cell to the atmosphere. A calibrated hydrogen leak was leaked into the vapor space above a pool of Dowtherm A, kept a 0.2 psia saturated vapor temperature and the hydrogen was separated by a water cooled after condenser. A palladium hydrogen diffusion cell was on the downstream end of the after condenser.

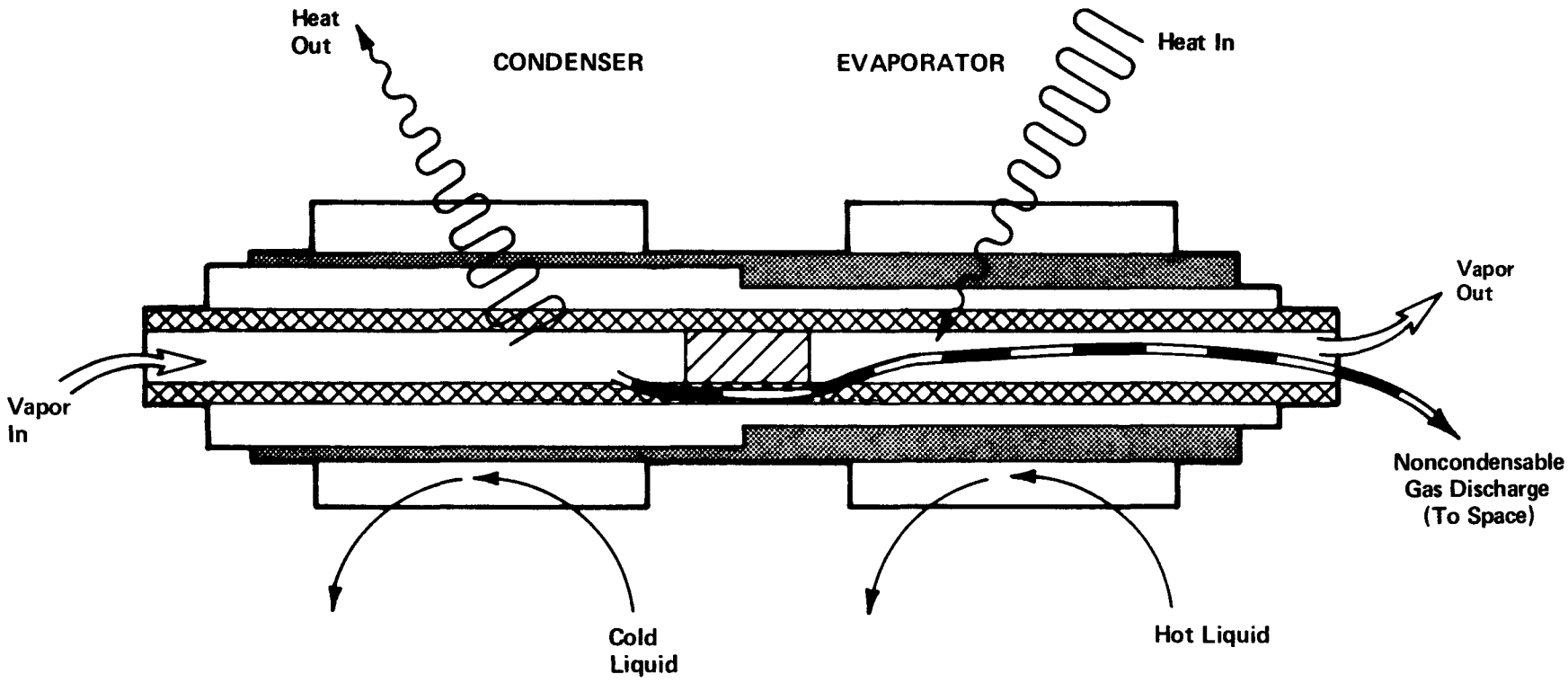

Figure 2.5.6-3 Noncondensable Gas Separator

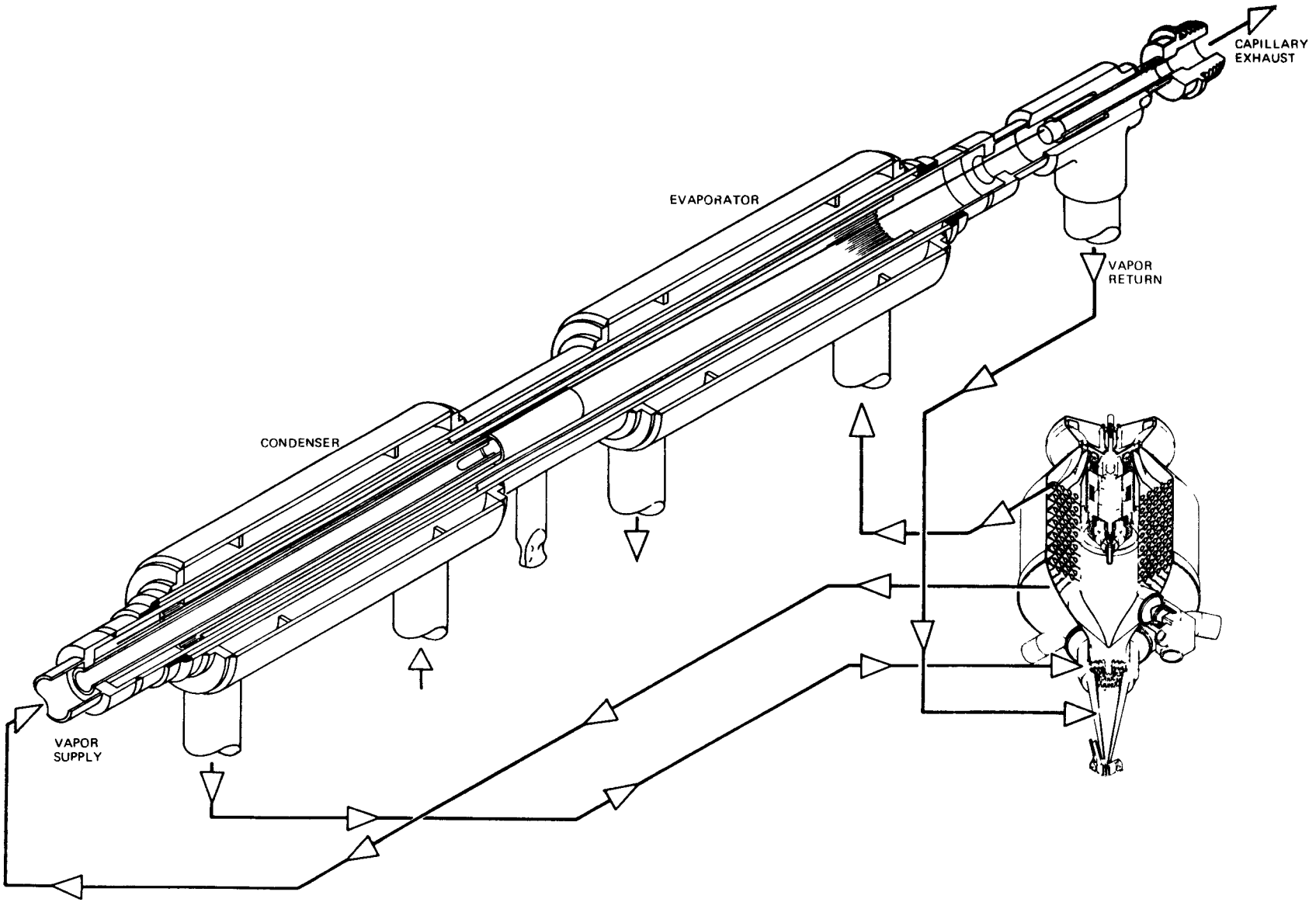

Figure 2.5.6-4 Noncondensable Gas Separator

The location of the diffusion cell in the system has an effect on the size required as the permeation rate is an exponential function of temperature, proportional to the square root of the partial pressure and inversely proportional to the membrane thickness. Although the diffusion cell should theoretically be placed in the high temperature and pressure region of the loop, such as in the boiler outlet line, the palladium at high temperatures may have a catalytic effect on the thermal degradation of Dowtherm. In the AEC loops, the palladium surface was placed in the hotwell, at moderate temperature and low pressure, and was found to not contribute measurably to the thermal degradation. Therefore, the KIPS diffusion cell has been placed at the regenerator vapor exit, at moderate temperature (240°F) and low pressure (0.10 psia).

The surface area of the diffusion cell was based on being capable of removing the entire hydrogen generation rate during the initial "burn-in" period. It was found that a surface area of 29 in^2 at 0.030 inch thick would be sufficient.

A vendor who makes palladium-silver diffusion material in the form of a tube with wall thickness of 0.003 inch was found. Since the thickness is 0.003 inch versus 0.030 inch, in the analysis, only 2.9 in^2 would be required. One commercial coil provides 5 in^2 and one coil placed in the regenerator vapor exit will be sufficient. Model analysis indicates that with one cell a maximum concentration of only 3% of the maximum tolerable level would occur. This would be reached at approximately 200 hours.

RELIABILITY STRESS: The tube has a very low stress level. The tube constraint system was checked to assure that no damage to the tube could occur under the dynamic environmental loading. The palladium diffusion cell has only one external joint which is essentially unstressed. Therefore, high reliability of this component is assured.

FABRICATION AND INSPECTION: The palladium tube is received brazed to a nickel tube and precoiled. The assembly consists of mounting the coil to the constraint system, welding the constraint to the wall and brazing the nickel tube through the wall. The only critical joint is in the wall braze which will be helium leak checked.

2.5.6.3.2 NONCONDENSABLE GAS SEPARATOR

ANALYSIS: To remove potential noncondensable gases other than hydrogen, a heat pipe NCGS, is used. The internal characteristics of the NCGS and its system integration are illustrated in Figure 2.5.6-4.

A small portion of the vapor from the regenerator outlet is circulated into the NCGS where the undesirable gases are removed and the vapor outlet is discharged to the jet condenser mixing chamber. This configuration provides a net "driving potential" of 0.017 psi through the separator to ensure continuous, steady flow. There is always a positive pressure gradient from the condenser to the evaporator sections. Thus, shunting or recirculation of the vapor is eliminated, even though no positive seal is incorporated between the condenser and evaporator.

Another important feature of the design is the use of a gas gap between heat pipe and fluid jackets for adjusting evaporator and condenser thermal conductances during NCGS testing. The selected wick, which consists of axial grooves, is basically a high conductance wick. By scaling previous test data with other low conductivity fluids such as methane, ethane, nitrogen, and oxygen, evaporator and condenser film coefficients of 160 and 540 BTU/hr-ft^2-°F are predicted. The corresponding temperature drops for a 6 inch evaporator and condenser in the present design are 3.5 and 1.1°F,

respectively. Similarly, the temperature drops associated with films in the heating and cooling jackets are small (20.9 and 3.4°F). These values are negligible compared to the temperature differences of 234 and 55°F, respectively, available from the various fluid temperatures.

Thus, most of the temperature drop occurs in the gas gap between heat pipe and cooling jackets. This gas gap (0.071 inch in the evaporator and 0.035 inch in the condenser) is filled with a mixture of helium and argon. By adjusting the concentration ratio, the mass flow through the separator can be varied from 0.108 lb-hr to 0.87 lb-hr. This will permit the NCGS to be adjusted to remove the gas at the most desirable rate. This important adjustment and optimization is made after the device is fabricated and during testing. The fill tube for the gas gap is then sealed after all optimization is completed. Gas gaps of this type are being used routinely in industry as part of calorimeters in low and high temperature heat pipes.

One of the more critical aspects of the device is the removal of the noncondensable gas from the separator. If the inlet vapor has a nominal gas concentration of 1 ppm, and a gas plug were allowed to build up in the condenser, as in a conventional variable conductance heat pipe (VCHP), the equilibrium mass concentration would be 29%, which corresponds to an enrichment of 3×10^6 (assuming CH^4 as the noncondensable). A capillary could be designed to bleed this equilibrium mixture of 29% (by mass) of CH^4 and 71% of Dowtherm A. However, such a design would have no performance margin since any excess gas generation would eventually flood the condenser with gas. The capillary was therefore designed to reject ten times the above minimum flow rate. Thus, the nominal gas concentration in the bleed stream will be only 3% and the gas enrichment will be 3×10^5. With this approach, the system has the capability of rejecting ten times as much gas as assumed. This design not only provides a performance margin, but it also can handle surges of gas generation. During surges, the total flow rate will remain unchanged but the fraction of gas could increase up to the theoretical maximum of 29%. Oversizing the capillary results, of course, in a larger loss of Dowtherm A, but the total amount will be only 9 grams in seven years which is negligible compared to the inventory.

The following sections describe the proposed design in greater detail.

The heat pipe proper will consist of a 14 inch long section of grooved tubing extruded from 6063 aluminum. The cross-section of this tubing is shown in Figure 2.5.6-5. This heat pipe material has been the workhorse of many NASA heat pipe applications. It is well characterized and has been space qualified. Its main advantage is the high film coefficient achievable with low conductivity fluids. As explained earlier, this feature places almost the entire temperature drop into the gas gap, where it can be accurately controlled and the mass flow optimized. The predicted heat transport capability for Dowtherm A is 500 watt-inches compared to 61 watt-inches required for this application. Evaporator and condenser lengths were chosen to be six inches each, with a two inch adiabatic section separating them. The six inch lengths were selected to yield adequate separation of noncondensable gas.

At the evaporator end, the heat pipe will be closed by a stainless steel end plug which is penetrated by the capillary. The latter consists of a 15 inch long tube with an inside diameter of 0.005 inch. Using the analytical model by Schock[2], this capillary will reject a volume flow rate of 6×10^{-8} ft^3/sec at the system pressure of 0.1 psia. This corresponds to a noncondensable gas flow rate of 3×10^{-12} lbm/sec and a Dowtherm flow rate of 1×10^{-10} lbs/sec passing through the capillary. The condenser end closure will be wicked with a single layer of wire mesh in order to return any liquid which condenses there to the grooves.

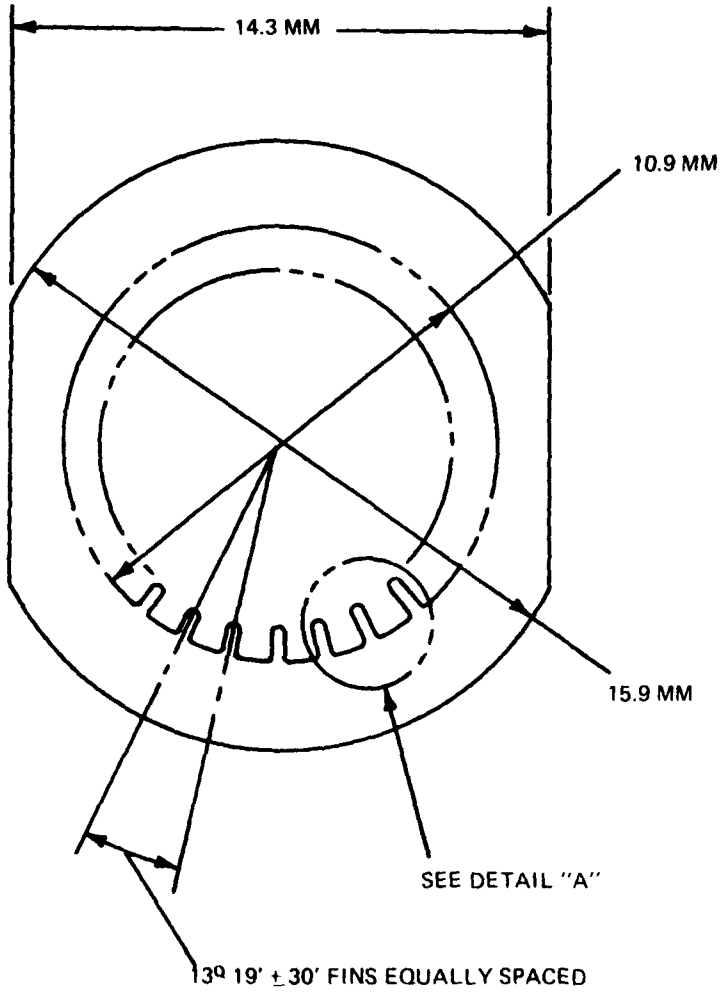

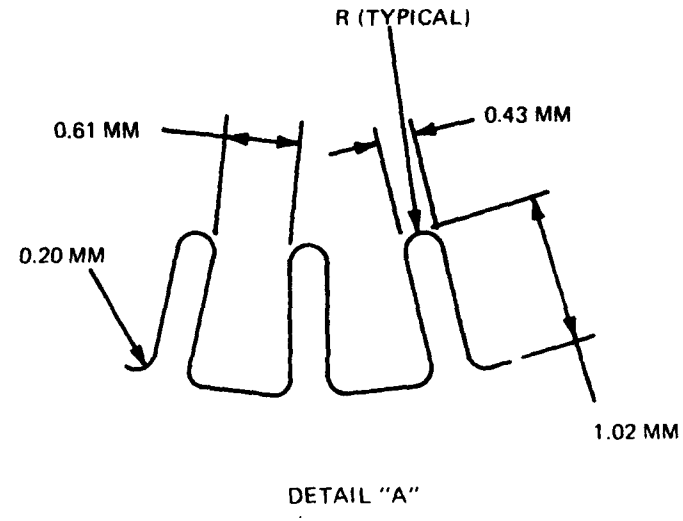

Figure 2.5.6-5 Cross Section of Extruded Grooved Tubing

The seal between condenser and evaporator will consist of a 1 inch long stainless steel plug which is interference fitted into the grooved aluminum tube. A 0.250 inch OD x 0.020 inch wall stainless tube will connect the condenser to the vapor source. The flow resistance of the tube (assuming a 6 inch length) is 0.023 psi-hr/lbm. Thus, for the nominal flow rate of 0.16 lbm/hr, the pressure loss in this tube will be 0.004 psi and the pressure drop across the seal between the condenser and evaporator will be 0.017–0.004 = 0.013 psi. The maximum delta P which the wick can sustain without blow-through is 0.015 psi which exceeds the existing pressure. Thus, in zero g, no vapor will bypass from the condenser to the evaporator. However, during vertical operation on the ground, the grooves will partially drain and some vapor can bypass the seal. The flow resistance of the seal is 0.288 psi hr/lbm. This will result in a bypass flow of approximately 15% of the nominal vapor flow rate. It should be noted that this bypass flow occurs in addition to the useful flow and does not detract from it.

The outside of the stainless steel tube which contains the aluminum heat pipe will be machined to different diameters in the evaporator and condenser. The resulting gas gaps between heat pipe and the surrounding stainless steel tube will be 0.071 inch and 0.035 inch at the evaporator and condenser, respectively. The gaps have been selected such that only 3.2 inches of the evaporator is needed to vaporize the liquid at the nominal flow rate. Thus, the evaporator has almost 100% excess capacity. A small, 0.125 inch OD tube will provide access to the gas gap for the purpose of adjusting the gas mixture. After completion of the tests, the tube will be sealed by heliarc welding.

The heat exchangers for the coolant and the heating fluid consist of simple jackets formed from 1.250 inch OD tubing. The film coefficients in the liquid were estimated to be 85 BTU/hr-^{o}F-ft^{2} in the condenser and 27 BTU/hr-^{o}F-ft^{2} in the evaporator. The corresponding delta T's (3.4 and 20.9^{o}F) are small compared to the available delta T's.

RELIABILITY AND STRESS: Only one joint in the NCGS has an appreciable stress level. That joint connects the tubes which form the inner and outer housing of the gas gap. Superimposing maximum thermal stress and pressure loading, the joint has a margin of safety in excess of 5.

Cleanliness is of special concern for this assembly as the capillary ID is small. In addition, the area of the shrink fit of the aluminum extrusion to its stainless housing is a potential contamination trap. Therefore, stringent process controls have been established to assure that all piece parts are adequately cleaned and maintained and assembled in a manner such that the cleanliness is not violated.

The design of the NCGS is such that the thermal load may be precisely established during the acceptance testing. Acceptance tests will also include calibration of the capillary discharge.

As previously described, the design is capable of removing 10 times more noncondensables than is predicted to be generated.

CRITICAL CHARACTERISTICS: The critical characteristics of the NCGS are the capillary discharge rate and the thermal load. The discharge rate is subject to two in-process checks as well as a final check at the time of the acceptance test. The thermal load is set by establishing the gas mixture in the gas gap at the time of acceptance test as described above.

2.5.6.4 Centrifugal Separator

The need for a centrifugal separator on the flight system was to be established in the Phase I system and capsule tests. These tests have not been completed at this time. The centrifugal separator is therefore included as part of the flight system.

FUNCTION

The Dowtherm A organic working fluid undergoes a slight pyrolytic decomposition under long-term thermal cycling at high temperatures forming high molecular weight substances (liquid droplets) at the boiler outlet conditions. It is desirable to separate these droplets from the vapor stream to prevent their deposit and subsequent buildup on the low pressure turbine nozzle surfaces. A centrifugal separator is located between the boiler and the turbine nozzle plenum. Its function is to prevent the buildup of any substance on the nozzle surfaces by swirling the vapor, causing foreign material to accumulate inside the swirl chamber.

CONFIGURATION

A cross-sectional view of the flight system centrifugal separator is presented in Figure 2.5.6-6. The separator consists of a rectangular-tangential inlet nozzle which accelerates the stream to a velocity of 50 ft/sec. The main body is comprised of three sections: an annular inlet and transition funnel, particle trap, and vapor exit nozzle.

The vapor enters the separator tangentially in the annular section and is forced in upon itself resulting in an axial acceleration toward the particle trap. This swirling axial motion continues through the straight section of the body and into the tapered section where the axial velocity is again accelerated to the throat. At the throat, a small carry-over of the vortex occurs, sweeping with it the separated particles and forcing them to the outer walls of the separator trap. At the throat, the primary vapor flow undergoes a reversal in axial direction and begins to swirl toward the vapor exit nozzle.

TRADE-OFF STUDIES

The long term thermal decomposition of Dowtherm A results in the generation of minute amounts of tarry, insoluble organic molecules in the system vaporizer. A mesh filter would require a relatively small pore size with a correspondingly large area to be capable of extracting this substance from the Dowtherm vapor without significant pressure drop. A centrifugal separator was selected to perform this task and placed between the boiler and the turbine nozzle.

ANALYSIS

Cyclone separators are widely used in industry for the separation of dust from process gases and, therefore, design guidelines are available. The centrifugal separator for the KIPS system was sized based on the guidelines established in "Cyclone Dust Collectors" by the American Petroleum Institute, New York, 1956. It was designed to have a minimum tangential velocity of 50 ft/sec for separating sticky or hygroscopic particles.

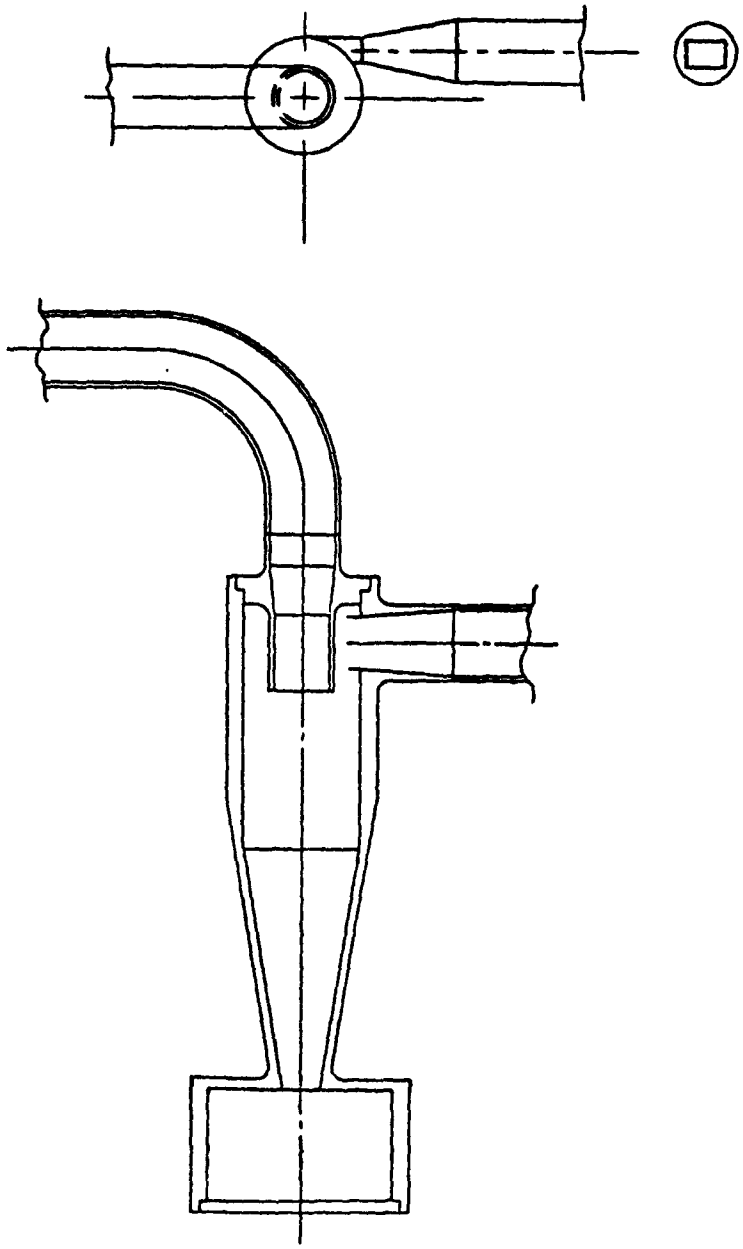

Figure 2.5.6-6 FSCD Centrifugal Separator

During Sundstrand's investigation of organic working fluid stability under contract to the AEC, the thermal decomposition of Dowtherm was measured. Extrapolation of this data indicates that 0.115% by weight of Dowtherm will be converted to high boiling point substances in the KIPS system over seven years of operation. This is equivalent to 0.44 in^3 to be trapped. The separator trap was sized to hold 0.88 in^3.

The separation efficiency of this device is predicted to be 95 to 100%. A pressure drop of 2.3 psi has been calculated. The final design was checked against the procedures outlined in "Votex Diodes", Fineblum, S.S., Bell Laboratories, Whippany, N.J., for presentation to HDL 1974 State-of-the-Art Symposium on Fluidics and "Investigation of the Effectiveness of Cyclone Separators on Fluidic Power Supplies", Westerman, W.J.; Wright, R.E.; and Roe, G.W., McDonnell Douglas Astronautics Company, Titusville, Florida, 21 December 1973, and the pressure drops were found to agree within a few percent.

RELIABILITY AND STRESS

The static operation of the centrifugal separator ensures a low failure probability. Reliability is further enhanced by an all stainless construction allowing for simple fabrication with 100% inspectability and easy incorporation into the KIPS system.

FABRICATION AND INSPECTION

The KIPS centrifugal separator will be constructed completely of 304 stainless steel procured per AMS 5639, 5513, and 5567. The end fitting covering the swirl chamber and end cap sealing the separator trap are electron beam welded to the separator housing and ultrasonically inspected. The centrifugal separator assembly is then TIG welded into the boiler to turbine nozzle line, which is also stainless, and the welds radiographically inspected. Prior to installing the centrifugal separator into the system, the inseparable assembly will be leak checked using a helium mass spectrometer.

CRITICAL CHARACTERISTICS

The critical characteristics of this device are the tangential velocity of the entering Dowtherm vapor, the size of the separator trap and the vapor pressure drop. The final design of the centrifugal separator involves a minimum vapor inlet tangential velocity of 50 ft/sec for separating sticky or hygroscopic particles, a trap volume of 0.88 cubic inches for an expected particle accumulation of approximately 0.44 cubic inches and a predicted pressure drop of 2.3 psi.

2.5.6.5 Quick Disconnect

FUNCTION AND NEED

There are five locations in the FSCD where quick disconnects will be used. Their locations are as follows:

Accumulator outlet line – This allows one of two connections to be made to the start module to start the system.

System pump outlet line – This allows the second connection required to be made to the start module.

System evacuation line – This allows the connection required to pump down the system prior to startup.

Auxiliary cooler coolant lines (2) – These allow connection of auxiliary cooler coolant lines to the system to allow the system to operate while on the launch pad or in the shuttle bay.

The functions of the quick disconnects are to: 1) allow hookup with a minimum amount of air inclusion (0.002 cubic inch maximum), 2) allow disconnect with a minimum amount of fluid spillage (0.003 cubic inch maximum), and 3) where system connections are made, to keep the system hermetically sealed (leak rate less than 1×10^{-8} standard cc/sec).

Investigations are being made to determine the proper means of making the final system hermetic closures after startup.

SELECTED CONFIGURATION

Two configurations are candidates for the FSCD:

CONFIGURATION A: This configuration is as shown in Figure 2.5.6-7. The nipple assembly is welded to the system. When the system is disconnected from the support equipment, the plunger moves to the closed position. The metal-to-metal seat is a lapped joint and thus keeps the system fluid and O ring isolated. After the system is started for launch, a cover can be placed on the nipple assembly to make the final closure and then welded or brazed in place.

CONFIGURATION B: This configuration is shown in Figure 2.5.6-8. In this version, all system start hookups are made in the same manner as Configuration A except that when the support module has to be disconnected just prior to launch, a plug assembly is installed in the hole and then the support equipment disconnected. This method eliminates the presence of an O ring but is somewhat cumbersome and risky.

The final configuration selected will be decided at a future date.

SELECTION RATIONALE

The following devices were considered for system and support equipment hookup:

Quick disconnects

Hand valves

Charge valves

Solenoid actuated valves

All but quick disconnects were rejected for the following reasons:

Valves are heavier.

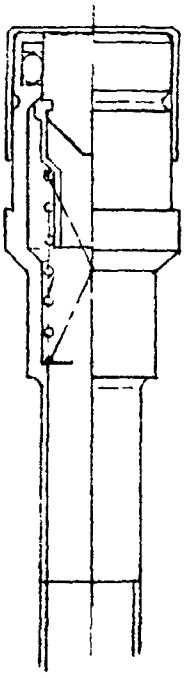

Figure 2.5.6-7 KIPS Baseline Quick Disconnect

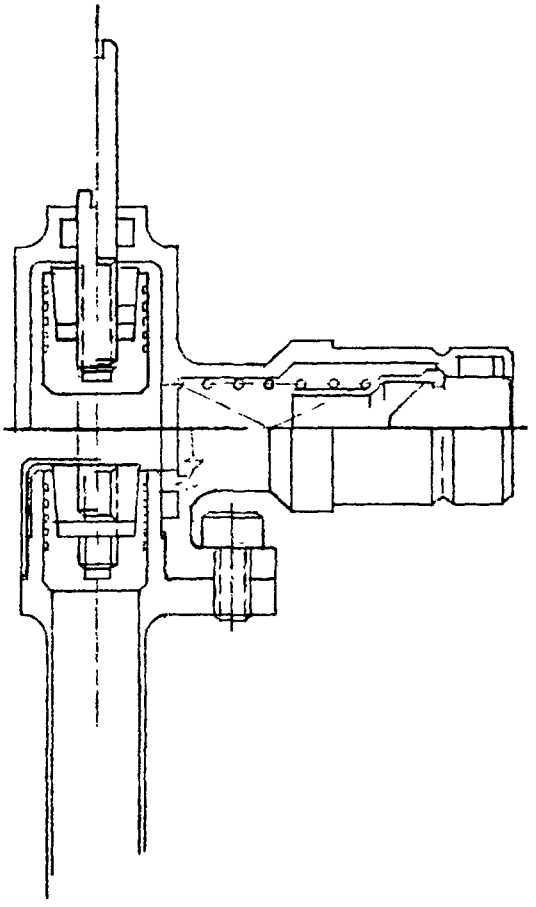

Figure 2.5.6-8 Candidate Quick Disconnect

Valves require a vacuum pump to be included in the start module to evacuate the trapped volume between the valves of the start module and the system.

Valves have to be manually closed prior to disconnecting the module from the system.

Fluid spillage from the support module lines is greater during disconnection.

FABRICATION AND INSPECTION

The quick disconnects are procured from Symmetrics, Inc. They have designed and fabricated numerous types of disconnects for many space applications. The final assembly is helium leak checked to verify it will meet a leak rate of less than 1×10^{-8} standard cc/sec of helium.

CRITICAL CHARACTERISTICS

AIR INCLUSION: If a large quantity of air inclusion takes place during system hookup, it may cause a system shutdown or fluid degradation.

FLUID SPILLAGE: If the nipple assembly does not seal when it is disconnected from the system after startup, it could result in loss of fluid and system shutdown.

LEAKAGE: If the assembly does not meet a helium leak rate of less than 1×10^{-8} standard cc/sec when the system is stored on ground between starts, air intake through the disconnect can take place. A large quantity of air can either degrade the fluid or cause system shutdown.

2.5.6.6 Filtration

The KIPS FSCD has two filters in its loop. Each has a specific function and need which is discussed below.

The jet condenser inlet filter is located between the radiator and the jet condenser. Its function is to prevent the jets of the condenser from being plugged should spallation products, by some chance, be generated from micrometeoroid strikes.

The system filter is located in the accumulator. Its function is to remove particles that may score the bearings.

CONFIGURATION

Both filter elements are of a conventional type made similar to AN 6235 configuration. The end is modified so that an O ring is not required.

SIZING AND PERFORMANCE

In space, due to potential micrometeoroid impact, some spallation at the inside diameter of radiator tubes may occur. A filter is therefore placed at the radiator outlet to preclude any spallation products from plugging nozzles in the jet condenser. Since the nozzles are approximately 0.010 inch in diameter, a 60 micron absolute filter was selected. The filter element selected has a nominal 6 gpm rating. The maximum radiator flow is 3.2 gpm. Therefore, the delta P is very low even if a substantial buildup of particulates occurs.

The filter element is located in the accumulator to save the weight required for a filter housing. During launch conditions, the minimum bearing film thickness is calculated to be approximately 0.00017 inch. The inner diameter of bearing pads are plated with 0.0004 minimum silver plating thickness, hence the absolute filtration level of retaining all particles larger than 0.00057 inch (14 micron) is desirable. The filter selected has a nominal rating of 2 microns and absolute rating of 10 microns. The filter area is equivalent to an AN 6235-3A element so, at normal operating conditions, the pressure drop through the filter will be low.

The Sundstrand 6 KW ORC system was tested for more than 3000 hours, and all hardware was visually inspected after termination of testing. No filter plugging was observed. The filter used had a nominal rating of 0.5 micron and absolute rating of 3 microns. Based on this experience, it is felt that no filter bypass is necessary.

MECHANICAL CONSTRUCTION

Both filters are of 304 stainless steel construction. The filter is welded to end rings via GTAW or EBW process. No epoxy patching of the part is allowed.

RELIABILITY AND STRESS

By the nature of the parts, the stress in these components is very low and will not affect the reliability of the system. The filters are substantially oversized to provide sufficient particle capacity.

FABRICATION AND INSPECTION

The welds and porosity of the filters will be inspected to ensure the integrity of the parts.

CRITICAL CHARACTERISTICS

The critical characteristic is the micron rating of the elements.

2.5.6.7 Radiator Auxiliary Heat Exchanger

FUNCTION

In order to reject the system waste heat both on the ground and in the Space Shuttle bay, an auxiliary waste heat rejection system will be incorporated. This system performs the function of the radiator.

CONFIGURATION

The heat exchanger is a simple, all aluminum, coaxial tube, counterflow device which is plumbed upstream and in series with the radiator. The system fluid passes through the center tube and the coolant passes through the outer tube. Placing the heat exchanger upstream of the radiator minimizes radiator temperature and, hence, minimizes heat rejection from the radiator to the Space Shuttle walls.

SIZING AND PERFORMANCE

The heat exchanger is sized to reject the complete power conversion system (PCS) heat input of 7200 watts thermal since the unit could be operating in the Space Shuttle in an overspeed with no requirements for any power output.

The following assumptions were made for the coolant supply from the Space Shuttle:

Fluid = Freon 21

$T_{in} = 45^{o}F$

$T_{out} = 130^{o}F$

Mass flow = 0.305 lb/sec

Max. pressure drop = 6 psia

Max. pressure = 200 psia

For ground operation, water will be used as coolant.

The constraints on the design of the Dowtherm side of the heat exchanger are: (1) minimize pressure drop and (2) keep the heat exchanger length less than the radiator length so that it can be attached to the inside wall of the radiator. With an overall radiator length of 8 ft, the auxiliary heat exchanger length is restricted to 7-1/2 ft to allow for fluid entrance and exit plumbing.

Different tube sizes were investigated to satisfy these requirements. Standard Dittus-Boelter type heat transfer correlations were used for the analysis, and the final configuration is given below:

Tube length = 7.46 ft

Outer tube OD = 0.750 in

Outer tube ID = 0.652 in

Inner tube OD = 0.500 in

Inner tube ID = 0.402 in

Freon side ΔP = 3.37 psia

Dowtherm side ΔP @ overspeed = 2.43 psi

Dowtherm side ΔP @ design speed = 1.25 psia

For system operation at different power levels, the heat exchanger length will vary in the same proportion as the radiator size.

FABRICATION AND INSPECTION

The heat exchanger is made up of two coaxial tubes. The outer tube has machined headers butt welded at each end for the coolant inlet and outlet lines. These headers, in turn, are welded to the outside of the inner tube as shown in Figure 2.5.6-9. These welds will be inspected radiographically.

MECHANICAL CONSTRUCTION

The Freon coolant is supplied to the heat exchanger via shut-off type quick-disconnects. This design prevents coolant from spilling from the unit or the coolant supply system when disconnected. After being disconnected, an evacuated storage bottle will be connected temporarily. This will be used to collect the residual Freon from the heat exchanger. The storage bottle serves two purposes: (1) it prevents an overpressure of the Freon due to temperature rise; (2) removal of the Freon precludes potential long term contamination problems and reduces orbit insertion weight. After a suitable time period, the storage bottle will be removed. A means will be developed for disconnecting the storage bottle.

RELIABILITY

The Dowtherm tube has low pressures and only two weld joints located where the heat exchanger is plumbed into the Dowtherm flow circuit. The coolant side of the heat exchanger has more joints, approximately 10, but the life requirements and, hence, reliability requirements are much lower for this circuit, since it is required to operate only up to orbit insertion. No Freon-Dowtherm joints exist.

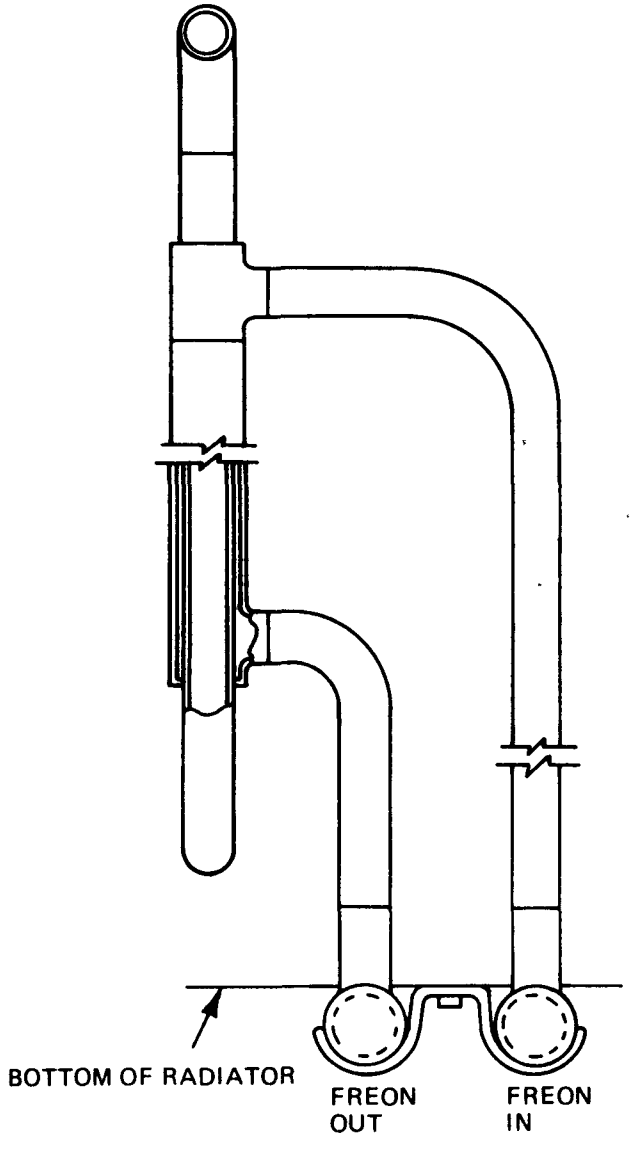

Figure 2.5.6-9 Auxiliary Heat Exchanger

2.5.7 FSCD GROUND SUPPORT EQUIPMENT

The KIPS will utilize ground support equipment (GSE) to enable it to be started and operated during installation and prelaunch operations. This GSE will provide the capability for (1) rejecting the heat from the electric or isotope heat sources prior to PCS starting and for emergency cooling, (2) starting, draining, and restarting the PCS, and (3) rejecting the radiator heat load when the KIPS is operating on the ground and in the launch vehicle prior to and during launch.

2.5.7.1 Start Module

The start module is used to provide liquid flow to the jet condenser, to the bearings, and to the boiler during startup. When turbine output shaft power is sufficient for the unit to be self-sustaining, the start module can be disconnected.

CONFIGURATION

The flight system start module will be an all welded, hermetic, hydraulic loop comprising a 28 VAC electrically driven start pump, an inverter, a spring loaded, nitrogen pressurized bellows accumulator and a 28 VDC solenoid valve. The Dowtherm loop will be connected to the Power Conversion System (PCS) through quick disconnects (QDs) with another quick disconnect being connected for accumulator charging. The loop schematic is shown in Figure 2.5.7-1.

Deaerated fluid will be prepared independently in a fluid deaerating facility and stored in evacuated containers to prevent introduction of air when filling the accumulator. The system and start module will be leak checked to better than 1×10^{-9} scc/sec of helium per joint and then evacuated prior to charging with Dowtherm. No further evacuation will be necessary even after storage for several months. However, the vacuum port will not be hermetically sealed until the fluid ports are sealed, prior to launch.

The fill quick disconnect allows the start accumulator to be evacuated and then filled with deaerated fluid. Filling will be accomplished by connecting a deaerated Dowtherm supply to the QD and relieving the N_2 pressure on the bellows, allowing the spring to force the bellows to the fully compressed condition; gravity will then fill the accumulator. The flight start system does not require a deaeration system since both the start system and PCS are hermetic and no leakage of air into the hydraulic circuit can occur.

The use of a spring in combination with the bellows allows the accumulator to be filled when draining the system, prior to a restart, without having to provide a vacuum on the nitrogen side of the bellows. On pressurization of the accumulator for start, the nitrogen pressure has to only be large enough to overcome the spring force, approximately 5 psia.

Pressure transducers are provided on the nitrogen side of the accumulator, the pump inlet, and pump outlet. The nitrogen pressure transducer allows the system accumulator pressure to be set at the proper value for starting the system and then at the required value for transferring the fluid inventory from the start accumulator to the system accumulator prior to disconnecting the start module. The transducers on the start pump inlet and outlet provide an indication of system pump operation.

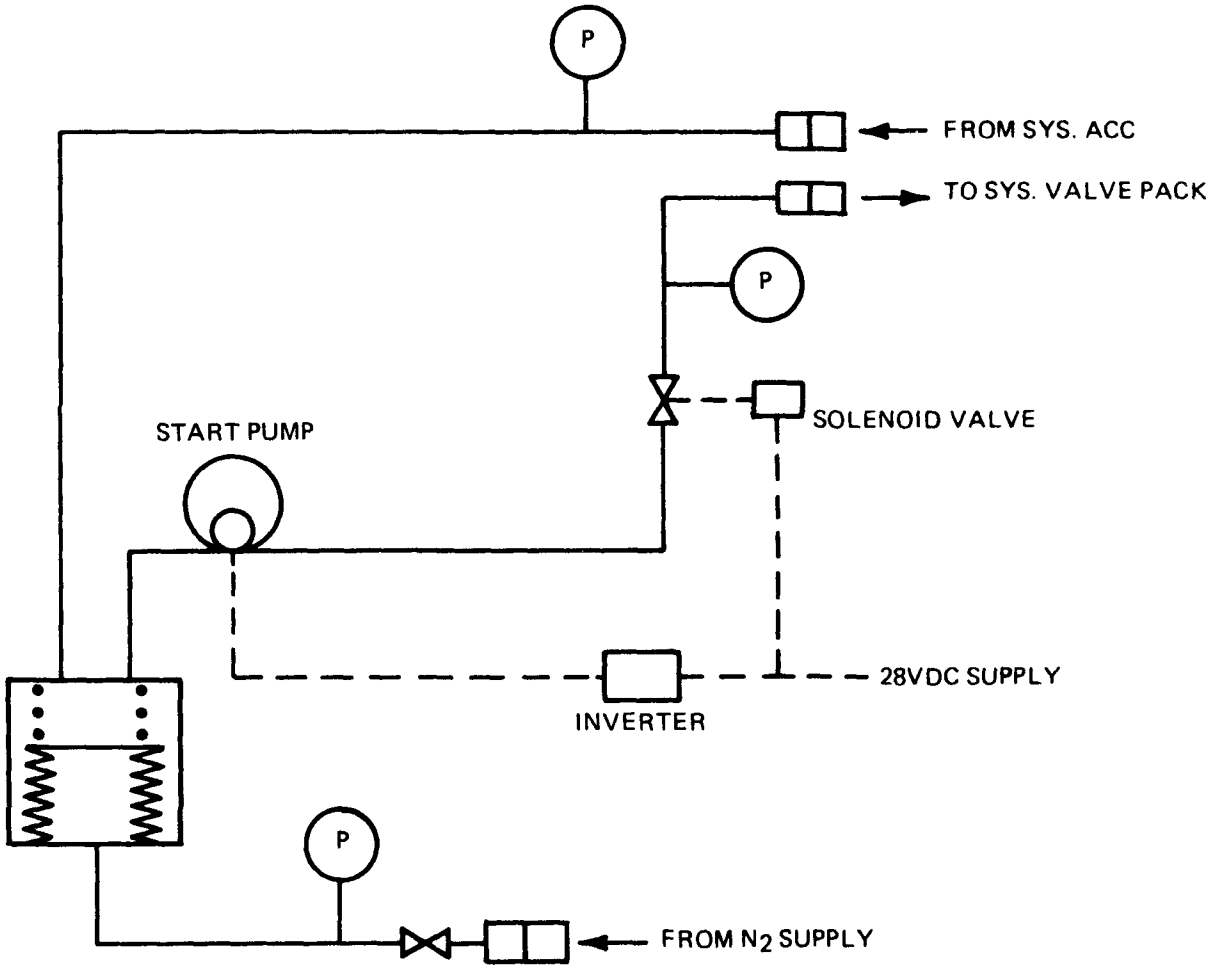

Figure 2.5.7-1 Flight System Start Module

ANALYSIS

The start pump must be capable of providing sufficient inlet pressure for the jet condenser while simultaneously filling the radiator. Knowing the flow resistance through the radiator bypass valve, the flow rate can be determined and, hence, the pump designed to have a flat enough head-flow curve to provide sufficient pressure to start the jet condenser. This pressure, currently being established using GDS test results, will be 80 psia or less.

The accumulator is sized to have an inventory sufficient to fill the KIPS. The filling is accomplished by increasing the start accumulator nitrogen pressure until the start accumulator pressure is slightly above the set point for the system accumulator. All hydraulic lines are designed to minimize pressure drop.

MECHANICAL CONSTRUCTION

The start pump is similar to those designed by Sundstrand for the Space Shuttle environmental and life support systems. The unit consists of an electric motor and pump sealed in one housing which is cooled by the working fluid. The unit is designed to deliver rated flow at minimum power input (20 volts) and maximum temperature (212^{o}F). The rated speed is 21,000 rpm, input power is 550 watts, and estimated weight is 2.78 pounds. The motor is a two phase, squirrel cage type designed for a nominal 28 volts, 440 Hz input. The pump uses a single stage, drilled radial passage impeller, which discharges through a multiple nozzle diffuser.

The start pump is supplied with 400 Hz, 28 volt power with an inverter. The inverter is a two phase, 4 transistor square wave power source, which supplies two center tapped motor windings displaced by 90 electrical degrees. The design uses a high current transistor switch that is JAN TX qualified. The logic circuit is an extremely simple design using CMOS gates to generate the waveforms.

The start accumulator is sized to supply the working fluid volume to the system. It consists of a cylindrical housing with a welded bellows accumulator compressed in its unpressurized state by a helical spring, sufficient to overcome the spring rate of the bellows itself.

The solenoid valve is a 28 volt DC, welded bellows type construction.

The quick disconnects are described in detail in subsection 2.5.6.5. The QD used for fluid return from the system will also be used for charging the start accumulator with deaerated fluid.

The start pump, inverter, solenoid valve and Dowtherm quick disconnects are mounted to the top of the accumulator, as shown in Figure 2.5.7-2.

RELIABLILITY AND STRESS

The start reliability will be at least 0.99. High reliability components are used for the inverter, and reliability data are being generated for pumps similar to the start pump. For a ground start system, high reliability is not a major requirement. If start in space were to become a requirement, it might be necessary to incorporate a redundant bellows configuration to minimize the probability of a bellows failure. However, it is expected that this will not be necessary because of the short life requirement of the start module for space starts.

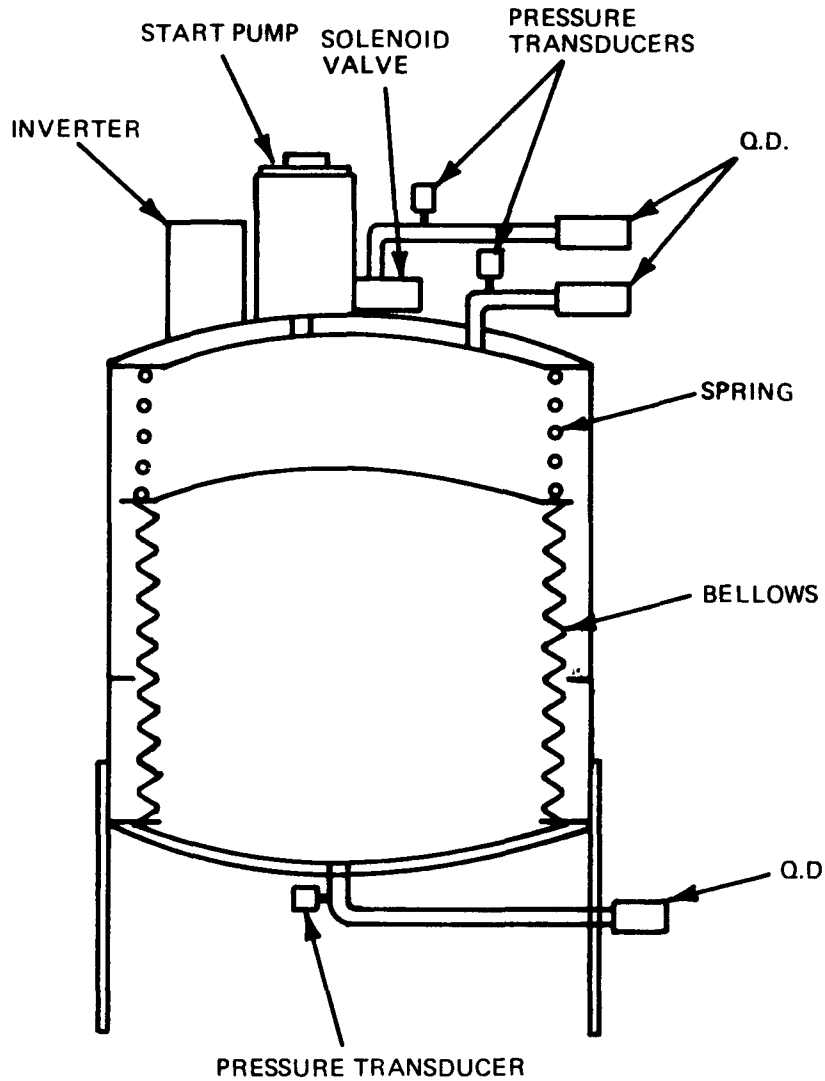

Figure 2.5.7-2 FSCD Start Module

FABRICATION AND INSPECTION

The start module will be fabricated from stainless steel and will be of all electron-beam welded construction. All welds can be radiographically inspected and the unit will be helium mass spectrometer leak checked. The bellows assembly will be of the welded convolution type. The start pump and valve will be flow checked prior to installation.

CRITICAL CHARACTERISTICS

In order to enable a successful start of the system to be obtained within the start reliability requirements, the start pump must be capable of achieving rated flow and pressure and the start valve must open when activated. These characteristics will be confirmed before the components are installed.

The start module must be completely hermetic since no deaeration capabilities are built into the system. Helium leak checking will guarantee this.

2.5.7.2 Heat Source Auxiliary Cooling

FUNCTION AND NEED

The auxiliary cooling system provides isotope heat rejection capability between isotope loading and system startup. The cooling loop is also available during the launch mode to prevent activation of the emergency heat dump system in the event of a fault requiring shutdown of the KIPS. The cooling system would also be used for ground checkout with electric heat sources before installation of the isotope heat sources.

The baseline start procedure provides for startup on the ground, prior to launch. Nitrogen coolant will be used for system checkout and for startup with the isotope heat sources. For emergency cooling capability in the Space Shuttle, flash evaporation cooling, using water, will be employed since the temperature will be too high for the freon system and a controlled temperature would not be required. If a space start of the KIPS system were to become a requirement, then temperature control would be necessary and a secondary loop employing Dowtherm with a Dowtherm-to-Freon heat exchanger would be used.

CONFIGURATION

Individual heat source assemblies incorporate a 0.25 inch diameter coolant tube welded to the fin adjacent to the Dowtherm tube, as described in subsection 2.5.2.9. Each HSA is connected in series with interconnecting tubes. The coolant inlet connection is made to the inlet end of HSA No. 1 and the outlet exits from HSA No. 3. Coolant passes in the same direction as the Dowtherm. By flowing in a series fashion, the resultant fin temperatures are close to actual operating temperatures, thus minimizing temperature changes during startup. Activation and control of the coolant loop is accomplished by a thermocouple sensing the outlet boiler tube/fin temperature on HSA No. 3. After the isotope is loaded, the fin temperature will rise and command coolant flow. HSA No. 3 will be the first to be loaded to ensure coolant flow while loading the other two.

During Shuttle launch, the cooling loop will be connected to the emergency water supply using quick disconnects. Just prior to deployment, these will be disconnected.

For a space start, the coolant lines will be connected to a support module employing Dowtherm as the circulating fluid. This will reject the isotope heat to the Space Shuttle cooling loop in a heat exchanger.

The schematics for the three configurations are given in Figure 2.5.7-3.

TRADE-OFF STUDIES

Water, nitrogen, and Dowtherm A were considered as candidate coolant loop fluids. Water was deemed unacceptable because of the high pressure required to keep it subcooled in a circulating system. Dowtherm was the most acceptable from a pressure standpoint but leads to the most complicated system. Nitrogen is most convenient for ground operation. Consequently, the coolant tube size was selected for both nitrogen and Dowtherm operation and was found to be acceptable for emergency cooling via flash evaporation of water also.

An investigation was performed on the advantages of parallel or series coolant flow through the HSAs. For parallel flow, all boiler fins would have the same temperature profile with an outlet temperature of approximately 710°F. This would lead to a significant thermal shock on HSA No. 1 when the cold working fluid is introduced. This thermal shock could possibly cause problems with the boiler fin emissivity coating. With series flow, in which the coolant loop runs parallel to the working fluid loop, the temperature profile through the three boilers approaches more closely the profile with working fluid cooling. Consequently, the thermal shock is minimized. The total nitrogen pressure drop will be significantly higher with a series connection, but is well within acceptable limits. Based on this study, the series flow configuration was selected.

ANALYSIS

Different tube sizes were investigated for the use of nitrogen, Dowtherm, and water as coolant fluids. The results of this investigation are presented in Table 2.5.7-A. It should be noted that these results are based on calculations for one HSA only with parallel flow. The results of the trade-off are equally applicable to series coolant flow.

The results of the analysis were that a 0.25 inch diameter tube could be used for Dowtherm or nitrogen, but that the high pressures required for circulating water (single phase) are unacceptable.

SIZING AND PERFORMANCE

The use of 0.25 inch diameter cooling tubes with 0.25 inch diameter interconnecting plumbing leads to relatively high total pressure drops for nitrogen. An inlet pressure of approximately 450 psi is required with a flow rate of about 250 lb/hr nitrogen. For Dowtherm, about 100 lb/hr flow is required with negligible pressure drop. If water is used for cooling the HSAs in an emergency mode, approximately 25 lb/hr will be needed.

When the isotopes are loaded, or the electric power of the electric heat sources activated, the boiler fin temperatures will increase. The temperature controller maintains the fin temperature at the design point by modulating the coolant flow. As working fluid flow increases, the coolant flow decreases preventing the fin temperature from exceeding the set point.

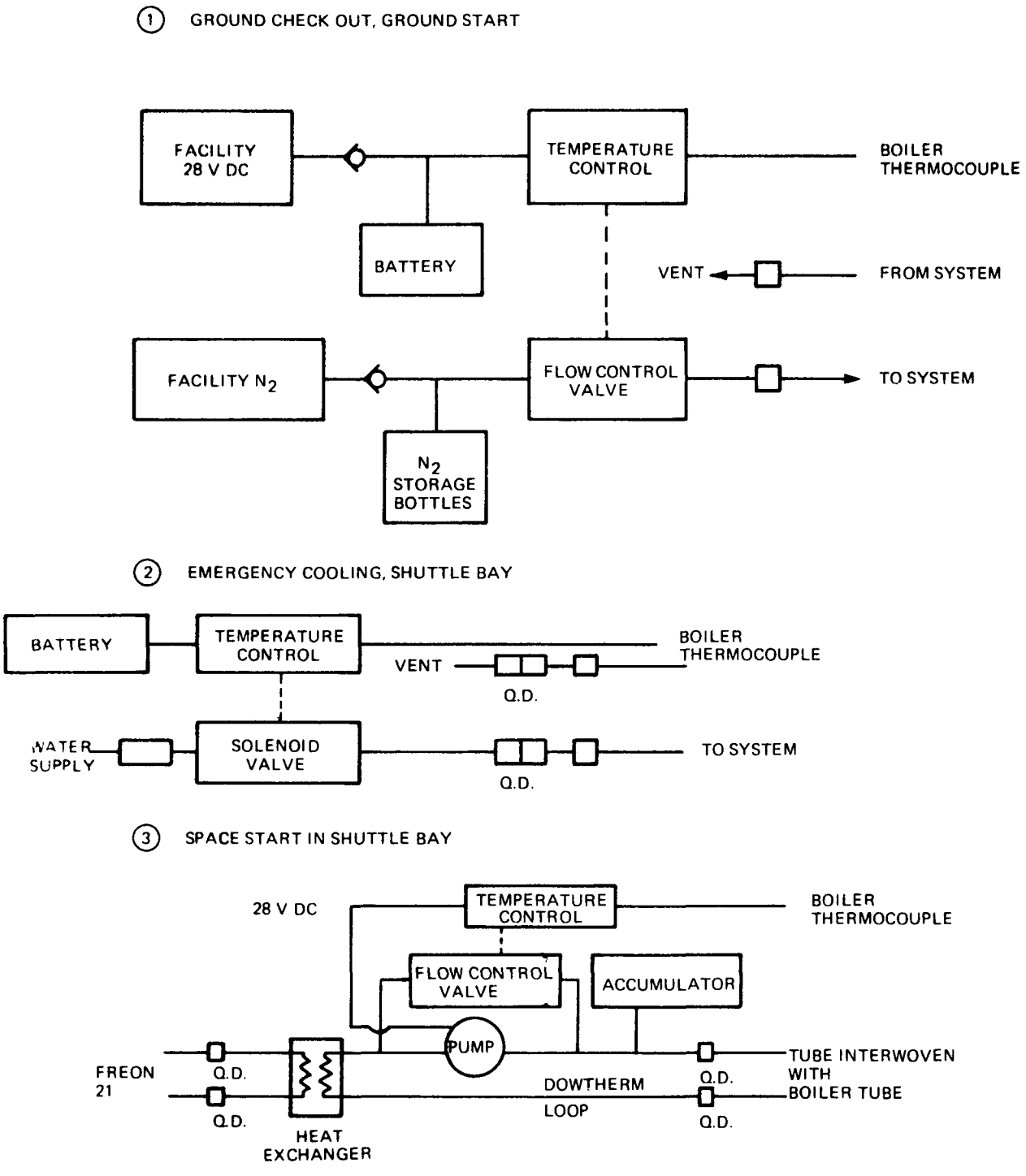

Figure 2.5.7-3 FSCD Boiler Temperature Control

Table 2.5.7-A Boiler Temperature Control Coolant Candidates

FLUID	FLOWRATE (lbm/hr)	DIA (in)	LENGTH (ft)	ΔP (psid)	P (psia)
Water	100	0.5	10	0.0064	2800
Nitrogen	50	0.125	10	4102	—
	100	0.5	10	6.17	—
	100	0.25	10	87	≈ 102
Dowtherm	100	0.25	10	0.66	≈ 30
	28	0.25	10	<0.66	>105

MECHANICAL CONSTRUCTION

All plumbing for the cooling circuit is stainless steel with an all welded construction. The flow control valve will be all stainless steel construction with solenoid actuation.

RELIABILITY AND STRESS

Stress levels in the 0.25 diameter tube are very low, less than 5000 psi at the inlet with nitrogen cooling.

Required reliability of the cooling circuit is extremely high, since loss of cooling could lead to heat source melt-down. The cooling circuit basically comprises a series of seamless tubes welded together with an overall reliability determined by the number of weld joints. The control valve will be a normally open type so that failure of controller or facility power leads to full flow.

A thorough reliability analysis will be performed to determine whether a redundant cooling tube is necessary, since failure of the cooling circuit could lead to HSA multifoil melt-down.

FABRICATION AND INSPECTION

All coolant tubes within the HSA are fabricated and coiled from a single piece of seamless tubing. All interconnecting plumbing joints will be welded, then radiographic inspected and helium mass spectrometer leak checked. The fabrication method for the coolant tube is covered in Paragraph 2.5.2.13.

CRITICAL CHARACTERISTICS

Characteristic	*Location*	*Comment*
mechanical integrity	tube joints	major coolant leak could lead to HSA overtemperature
temperature control		loss of flow could cause HSA melt-down

2.5.7.3 *Radiator Auxiliary Cooling*

This item of ground support equipment provides system heat rejection capability on the ground during checkout with electric heat sources and after startup with isotope heat sources. It also provides heat rejection in the Space Shuttle bay when the radiator is shrouded.

CONFIGURATIONS

For shuttle operation, the auxiliary heat exchanger described in subsection 2.5.6.7 is connected into the Space Shuttle closed loop freon coolant supply loop. For ground operation, water will be used as the coolant; this is obtained by connecting to an external, softened supply of city water and flowing in an open loop mode.

TRADE-OFF STUDIES

Closed loop cooling methods were investigated for ground operation, including the use of freon in a secondary loop and water glycol in a closed loop with a secondary heat exchanger. These were rejected in favor of open loop water because of the great simplicity of the water configuration. Overcooling the radiator allows sufficient time for disconnecting from the water supply, removing the residual water in the heat exchanger, and for reconnecting to the Space Shuttle freon supply.

SIZING AND PERFORMANCE

The sizing of the heat exchanger is covered in subsection 2.5.6.7. For ground operation where water is the coolant, the total system heat input can be rejected with 1 gpm water flow. The heat rejection coolant loop requires no temperature control, since the radiator bypass valve will compensate for coolant flow fluctuations.

MECHANICAL CONSTRUCTION

The auxiliary heat exchanger incorporates quick disconnects. These will be connected to a water source on the ground, with the outlet line vented, and into the coolant loop on the Space Shuttle.

RELIABILITY AND STRESS

Stress levels are very low since the maximum pressure encountered is 200 psia with the freon system. Reliability requirements are high since the system waste heat must be rejected through this equipment. A failure in the Space Shuttle could lead to a system shutdown if the radiator could not be used to reject the heat. This would necessitate activating the heat source emergency cooling system. The only reliability considerations are welded joints in the plumbing circuit and the mechanical integrity of the quick disconnects. It is assumed that the Space Shuttle heat rejection system has redundant flow circuits.

FABRICATION AND INSPECTION

All welded joints will be radiographic inspected and helium mass spectrometer leak checked.

CRITICAL CHARACTERISTICS

Characteristic	Location	Comment
mechanical integrity	tube joints	major leak could cause system failure
temperature control		loss of coolant would cause system failure

2.6 FLIGHT SYSTEM PERFORMANCE

This section describes the performance of the KIPS at typical design power levels and the provisions for fueling and handling. Table 2.6-A summarizes the important design characteristics of the system.

In addition to meeting the basic performance requirements of efficiency, speed control, quality of output power, weight and size, the KIPS is designed to accommodate Isotope Heat Source (IHS) cooling, spacecraft integration, and launch requirements on the Space Shuttle as well as the Titan IIIC. Appropriate cooling provisions have been designed into the IHS and the radiator to provide heat rejection to secondary fluids with both the system operating and nonoperating. After the system has been started, power conversion system (PCS) operation is completely self-controlling. If the constant speed mode of operation is selected, the electrical speed control system will automatically transfer excess electrical output capacity to the dissipative load bank as required to keep speed constant.

When the speed control circuit is disabled for launch, the combined rotating unit (CRU) operates at design point speed at maximum load and at a higher rotative speed at low load. In either mode of operation, a voltage regulator keeps output voltage constant at any customer applied load from zero to rated load.

The radiator can be excessively cooled without affecting system operation because system heat rejection is controlled by the radiator bypass valve. This feature permits auxiliary cooling of the radiator during system checkout or prelaunch operation.

Special features, such as frequency wild operation, use of the radiator bypass valve for subcooling of the radiator, and auxiliary cooling provisions of the boiler and radiator are discussed later in this subsection. Details of the location and function of these features are covered in subsection 2.5.

Performance characteristics in a space environment including torque effects, power degradation, and the effects of micrometeoroids on system life are covered in subsection 2.6.4.

2.6.1 FLIGHT SYSTEM SIZE AND WEIGHT

The flight system envelope dimensions are shown on Figure 2.6-1. Less than half of the space inside the radiator is occupied by the KIPS components, leaving space available for other spacecraft components in integrating the KIPS with a spacecraft.

The flight system radiator may easily be reconfigured to match specific spacecraft requirements. Radiator length and diameter can be varied as desired with radiator surface area being the only requirement for a given maximum power level.

For the baseline FSCD, the radiator diameter is 4.3 ft and the height is 8 ft.

The flight system weight breakdown showing major component weights is shown in Table 2.6-B.

2.6.2 FLIGHT SYSTEM EFFICIENCY

Sundstrand has developed comprehensive computer analysis programs to model the operation of the KIPS systems. One is a system design optimization program which can be used for optimizing a system with respect to weight or efficiency. The other is a system design program which can analyze

Table 2.6-A KIPS Characteristics

Rated Output Power	1300W(e) BOM
Optional Ratings	.500 to 2000W(e)
Input Power @1300W(e) BOM	.7200(t)
Overall Thermal Efficiency (1)	.18.1% rectified to 28 VDC
Peak Working Fluid Temperature	650°F
Total Weight(2)	475 pounds
Envelope Dimensions for 1300W(e) BOM(3)	.52 inches Diameter 96 inches Length
Design Point Output Voltage	28 VDC ± 2%
Response - Variable Output Power - 0 to 100%	Milliseconds
Partial Output Power Capability	.On Pad Launch to Parking Orbit Orbital Transfer to Final Orbit
Output Power Capability -0 to 100%	. Spin Stabilized Spacecraft
Lifetime	. 7 years

Capable of Stable Operation with Unbalanced Solar Input

Resistant to Natural & Induced Radiation

(1) With RTG topping, system efficiency can be increased to 22.1% or higher. See Appendix A of Volume IV.

(2) Based on updated flight system design utilizing conventional materials, weight reductions such as alternate radiator configuration and CPU housing machining, to approach the 450 pound goal will be studied in the Phase II design phase.

(3) Flexible in design for both size and shape to fit the specific spacecraft.

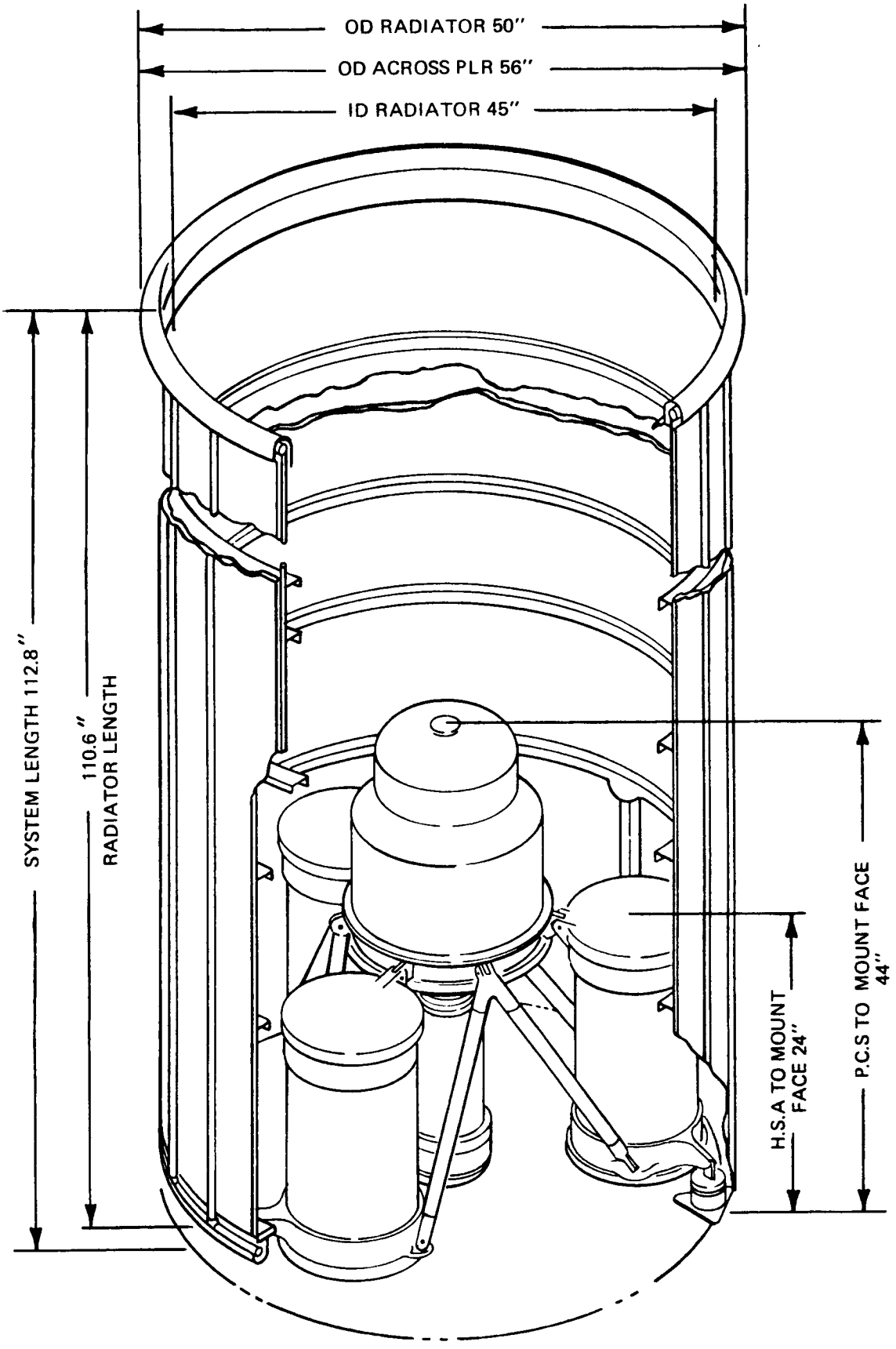

Figure 2.6-1 Flight System Envelope

Table 2.6-B Flight System Weight Breakdown

Component	F.C.D. Lbs.
Fluid Radiator	80.0
P.L.R.	8.6
H.S.A. (3 Loaded)	222.0
C.R.U.	56
P.C.S.	52
Valve Pack	6.5
Jet Condenser	5.1
Accumulator	5.0
Centrifugal Separator	0.4
Support Struts	3.1
Shock Mounts	2.5
Tubing	5.6
Controller	13.0
Electrical Harness	1.30
Insulation	3.0
Auxiliary Cooler	1.6
Fluid Weight	8.3
Total System Weight 474.0 Lb.	

the effects of environment or individual component performance on the system. The programs are updated as more complete design data, or measured component performance, becomes available.

System Design Optimization Program

For a given power level and operating environment, the performance and size of a Rankine cycle power system is primarily a function of the working fluid, the type of components making up the system, the thermal and hydraulic design of the components, and the cycle state points selected for system operation. To provide a means of integrating the multiple interactions which are in operation within the system, a comprehensive system mathematical model has been generated.

In a space power system, there may be as many as 20 variables which have a first order effect on the size, weight, and performance of the system. These variables include the heat rejection temperature and the pressure drops across the heat transfer components. The effectiveness of the regenerator and condenser and prime mover design variables, such as speed and thermodynamic state points, also affect the size, weight, and performance of the system.

The type of components can, to a large extent, be selected on the basis of packaging considerations and the overall objectives for the system such as life, duty, reliability, and cost effectiveness. However, component thermal and hydraulic design specifications and cycle state point selection require examination of the interrelated effect of these variables on the size and performance of the system as a whole. For instance, in Rankine cycle systems where minimization of condenser temperature for a given peak cycle temperature is desirable, increased efficiency has to be traded with increased component size. Similarly, the cycle performance improvements obtained with high effectiveness heat transfer equipment designed for low hydraulic resistance are achieved at the expense of system weight.

For a power system in which weight and volume along with system efficiency are important considerations, it is obvious that system design must be generated from an interaction between component design and thermodynamic cycle point selection. The optimum design will, therefore, be a compromise between efficiency, weight, and volume.

An efficient and tractable means to optimize the designs of Rankine cycle systems, considering the above trade-offs, has been developed by Sundstrand. It consists of a computerized mathematical model of the system, incorporating both cycle analysis and component design. The logic is arranged in the form of a mainline program which reads input data, performs a cycle analysis, and prints output. The mainline is the vehicle used to call subroutine elements which contain mathematical relationships describing working fluid properties, component design logic, and a multivariable optimization routine.

The operation of the program is illustrated by the flow chart shown in Figure 2.6-2.

Performance analysis involves the evaluation of the state points around the thermodynamic cycle from which the various heat loads and efficiency level are determined. State point definition requires knowledge of the thermal and hydraulic performance of each component together with the bounding thermodynamic state points of the cycles. For the inputs such as condenser temperature, regenerator effectiveness, heat transfer component pressure losses, prime mover design variables, and radiator component nonpuncture probabilities, a cycle analysis is undertaken and cycle efficiency and system weight calculated. A criterion function (PAOFF) defined as follows is then computed:

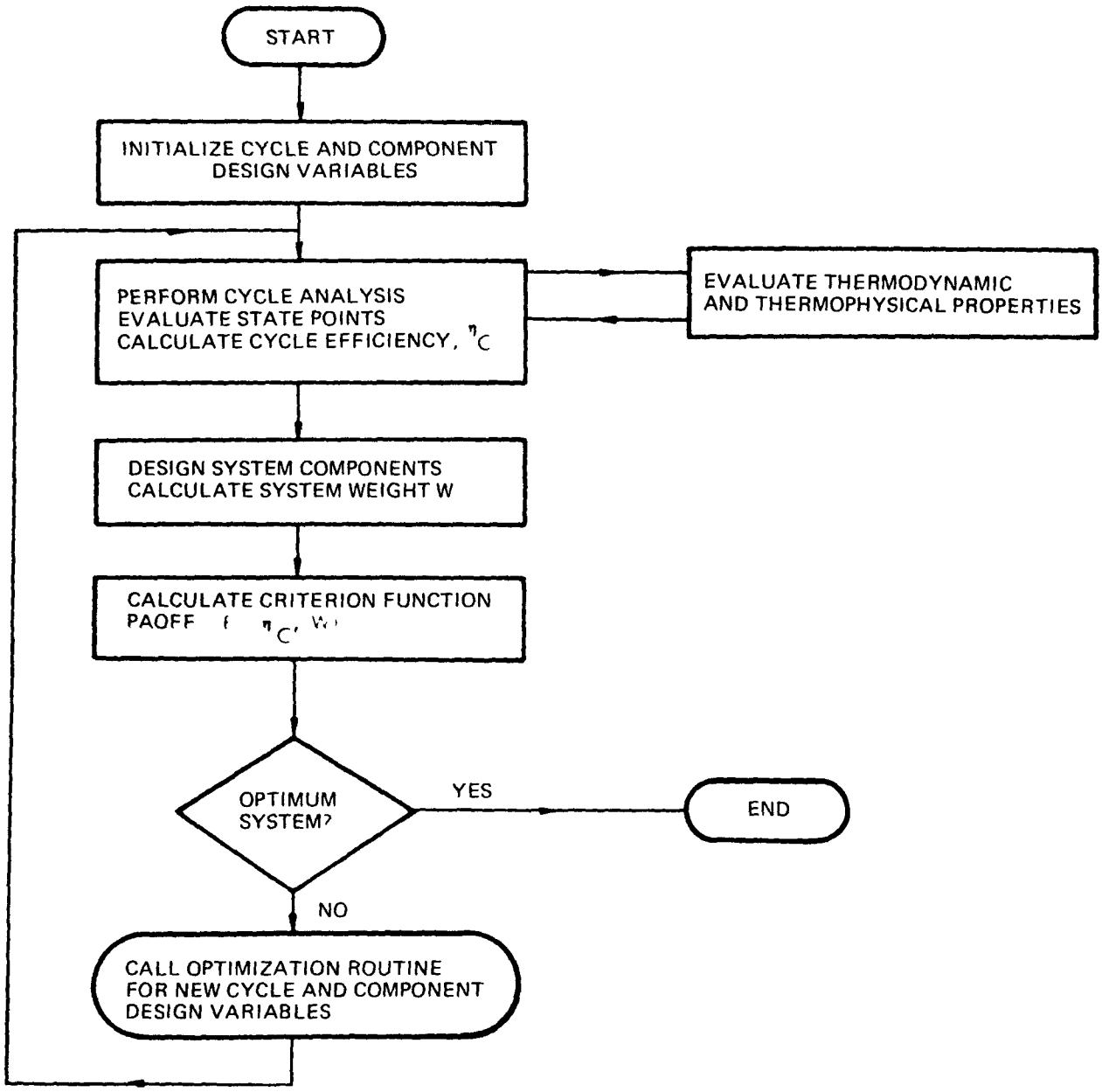

Figure 2.6-2 Flow Chart of Rankine Cycle System Design Optimization Program

$$PAOFF = \frac{(1-C)}{7} + (C)W$$

Where: C = weighting factor
η = system efficiency
W = system weight

The inputs to the program are then varied by the optimization subroutine and the cycle efficiency calculation and component design procedure repeated until PAOFF is minimized. By conducting the optimization with values of the weighting factors between zero and unity, a locus of optimum systems can be generated as a function of system weight and efficiency as shown by the general curve in Figure 2.6-3. Each point on the curve corresponds to a different optimum system design, the relative importance of efficiency and weight being different.

The modular construction of the program coupled with the generalized approach to optimization enables Sundstrand to optimize the design of Rankine cycle engines required for various applications in a very rapid manner. The basic mainline program is tailored to call the subroutines containing the logic for each component included in the particular system. Sundstrand has developed a comprehensive inventory of computer subroutines to support the overall system design optimization program. These include subroutines to design and analyze the performance of single and multistage axial turbines, single and multicylinder reciprocating expanders, wound and solid rotor alternators, plate-fin and tube-fin multipass regenerators, air and liquid cooled surface condensers, jet condensers, air heat rejectors, flat and cylindrical radiators with meteoroid protection modeled, and supercritical and subcritical vaporizers. Subroutines have also been developed to design and predict the performance of feed pumps, bearings, and seals incorporating, wherever possible, correlations based on an actual hardware test experience.

The optimizations have been performed for the system comprised of a turbo-alternator-feed pump combined rotating unit (CRU), a vapor-liquid regenerator, a jet condenser, and liquid radiator as illustrated in the basic system arrangement and block diagram shown in Figure 2.6-4.

By interconnecting detail design and evaluation subroutines for the various system components with the correct logical criteria, the mathematical model can be made to duplicate the operating characteristics of a real system. This technique is much more powerful than single parameter trade-offs. The information gained correctly reflects not just the first order variations, but, because the complete system is being studied, it also shows effects not available in single component parameter trade-offs.

System Off-Design Program

This program incorporates the basic cycle analysis outlined on the preceding pages, except that component performances are modeled according to their off-design conditions.

The procedure followed is similar to the design performance evaluation described in the preceding section. The parameters established during the design process now form the basis for off-design calculations. In contrast to the design analysis, off-design calculations must confine solutions to parameter ranges defined by component sizes and capacities. This basically requires a complete reversal of the design process and means starting the analysis with fundamental system characteristics. It is necessary to identify the system characteristics which change as functions of electrical load and environmental conditions. With knowledge of each parameter's functional

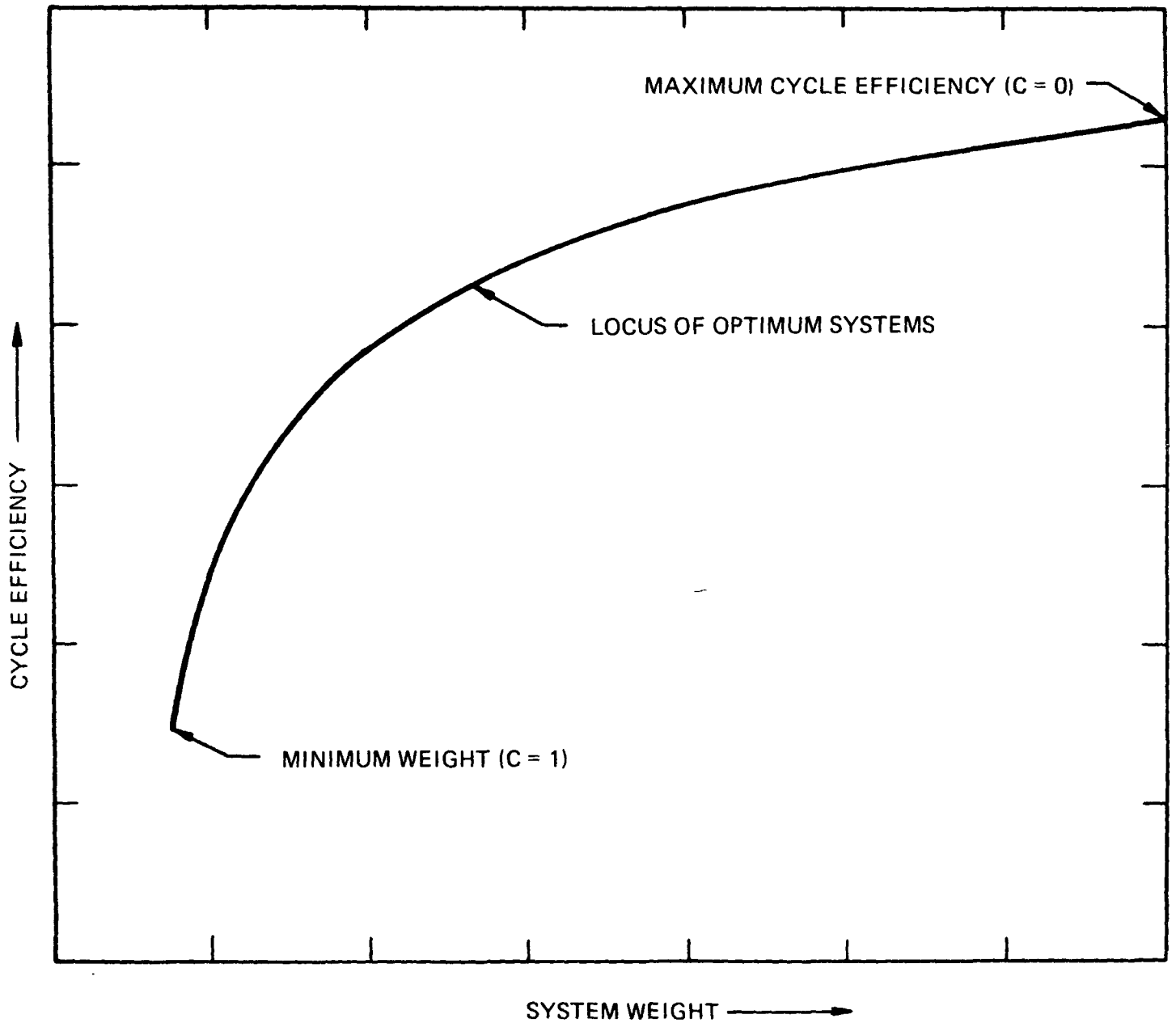

Figure 2.6-3 Typical Cycle Efficiency - Weight Relationship

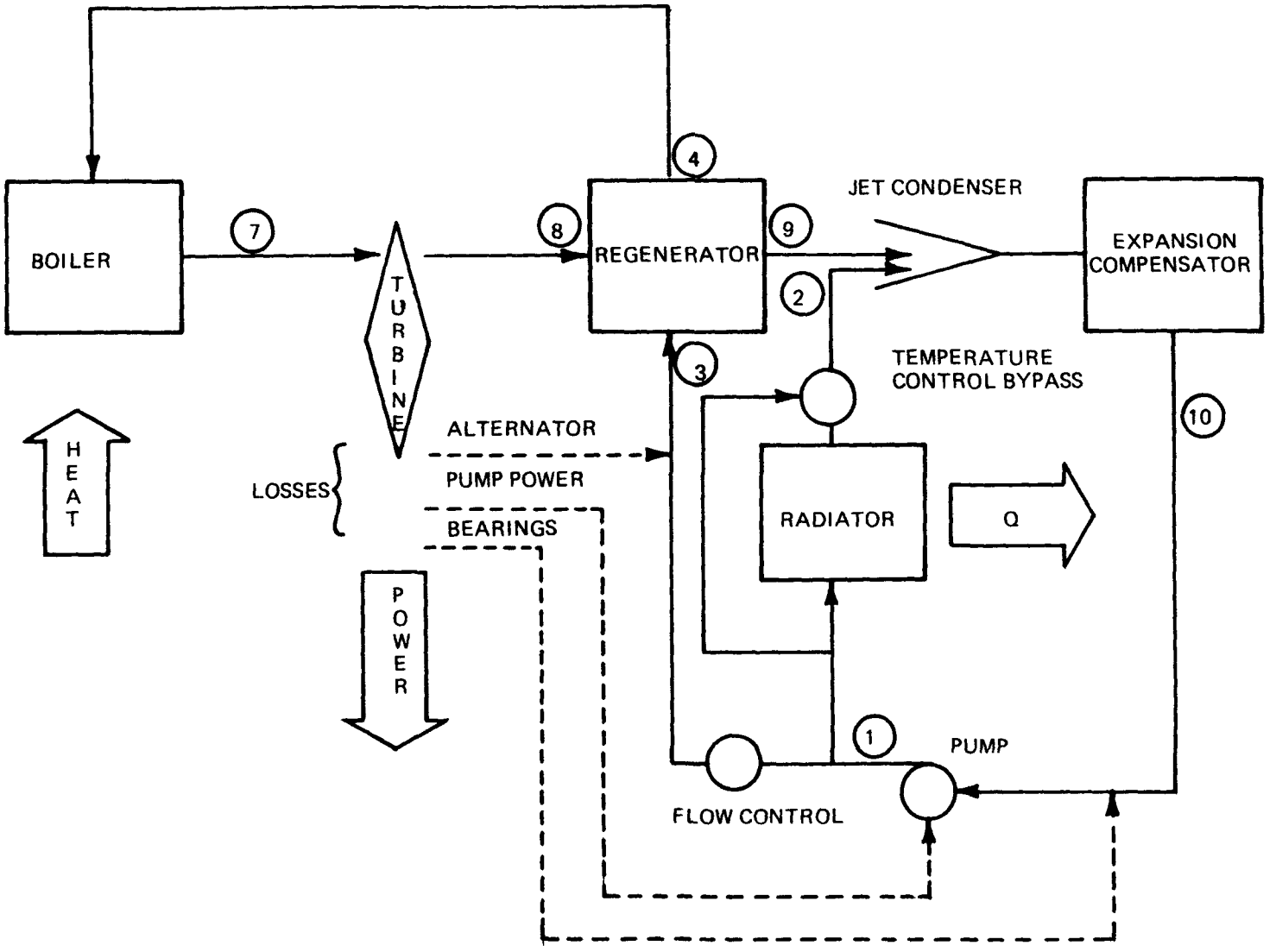

Figure 2.6-4 Basic System Configuration

dependence on other system characteristics, it is possible to determine cause and effect relations throughout the system. This is performed by careful analysis of all interconnections, followed by selection of a sequence of calculations which starts with a convenient point and proceeds to expand knowledge of the parameter variations in an efficient manner. This process results in a complex series of iterative calculations which must, in orderly fashion, all be satisfied in order to find the system parameters caused by the particular environment applied to the system.

Figure 2.6-5 shows the basic sequence followed in finding the off-design characteristics.

Design Point Efficiency

A schematic of the FSCD is presented in Figure 2.6-6. A breakdown of the electrical losses appears in Figure 2.6-7 and a hydraulic block diagram in Figure 2.6-8. The design point performance analysis has been performed using the data available from component testing, insofar as possible. Some parameters used were extrapolations of measured data. The model incorporates intrasystem heat losses and a detailed breakdown of system component pressure drops. A summary of the more important parametric assumptions in predicting the obtainable efficiency is as follows:

- Jet condenser: The jet condenser vapor pressure performance is based on Dowtherm test rig data, data from tests in which steam was condensed on individual water jets, and mathematical modeling of the thermodynamic process.

- The jet condenser is presumed to operate at a 40% recovery. Tests have shown 50% capability and this value allows a margin of safety and for a slight increase associated with recovery from overspeed operation.

- Alternator efficiency: Alternator rig testing has demonstrated that a slight increase in efficiency will result from an increase in air gap. Test data have been used to define the improvement to be expected for the flight system design.

- Rectifier losses: New technology is becoming available which will increase rectifier efficiency from 0.925 to 0.944.

- Turbine efficiency: As a result of turbine testing, it is anticipated that a turbine efficiency of can be obtained. Further turbine development could lead to watts additional system power.

The baseline system is based upon 7200 thermal watt input at the beginning of mission (BOM) and an effective sink temperature of 422°R. The heat absorbed by the fluid is less than this by the amount of the heat losses from the heat source assemblies. Most of this heat loss ends up in radiator through direct radiant heat transfer. The radiator is designed to reject the full heat loss, even though a small amount (discussed in subsection 2.6.3) is rejected to the spacecraft.

A computer printout of the design point performance is presented in Table 2.6-C.

A noncondensable separator allows removal of noncondensables resulting from thermal degradation of the working fluid and material outgassing. Performance benefits could be accrued by operating at slightly higher turbine inlet temperatures, while the slight increase in degradation at these temperatures could be accommodated by the noncondensable separator. These results are summarized in Table 2.6-D.

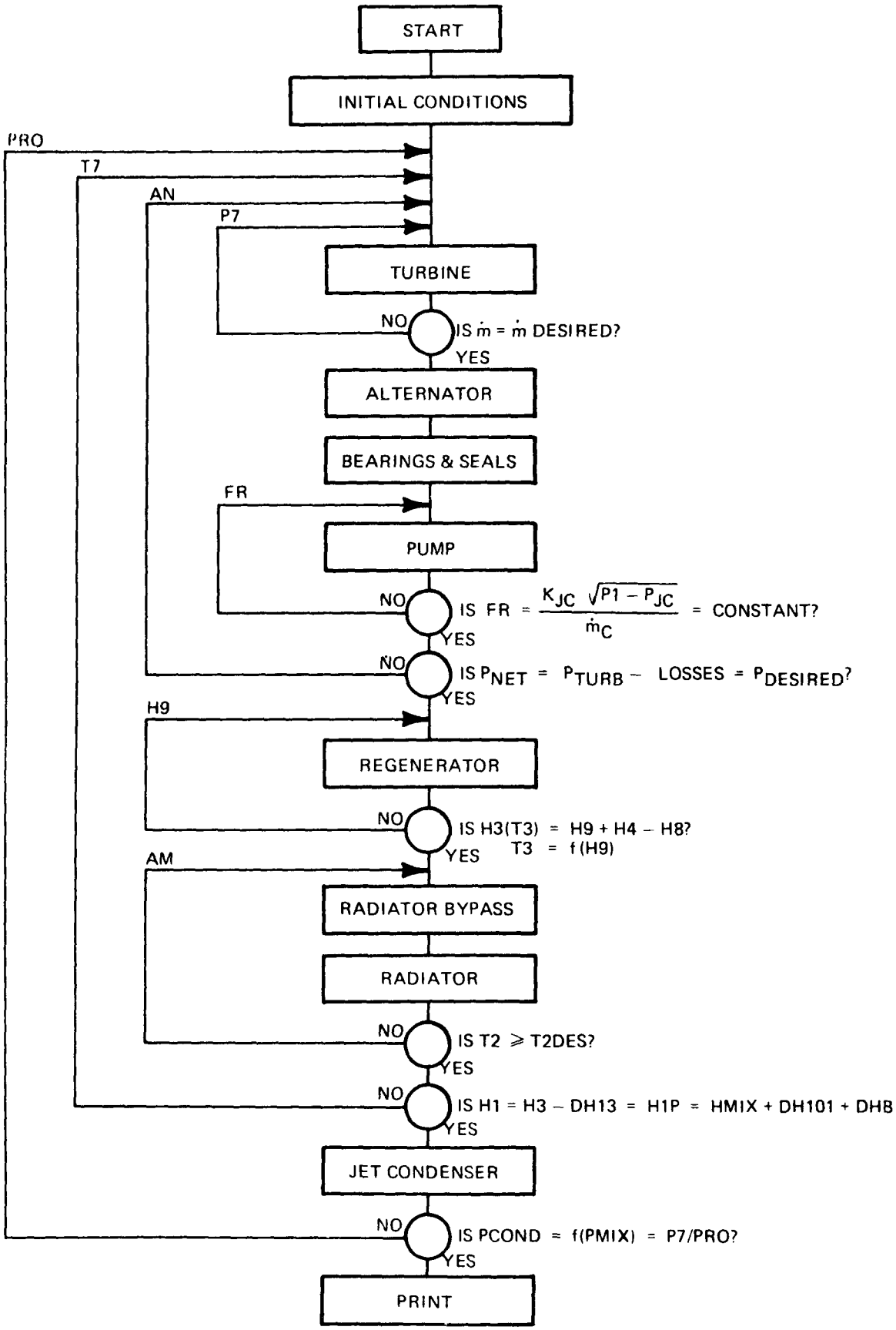

Figure 2.6-5 Off-Design Analysis Sequence

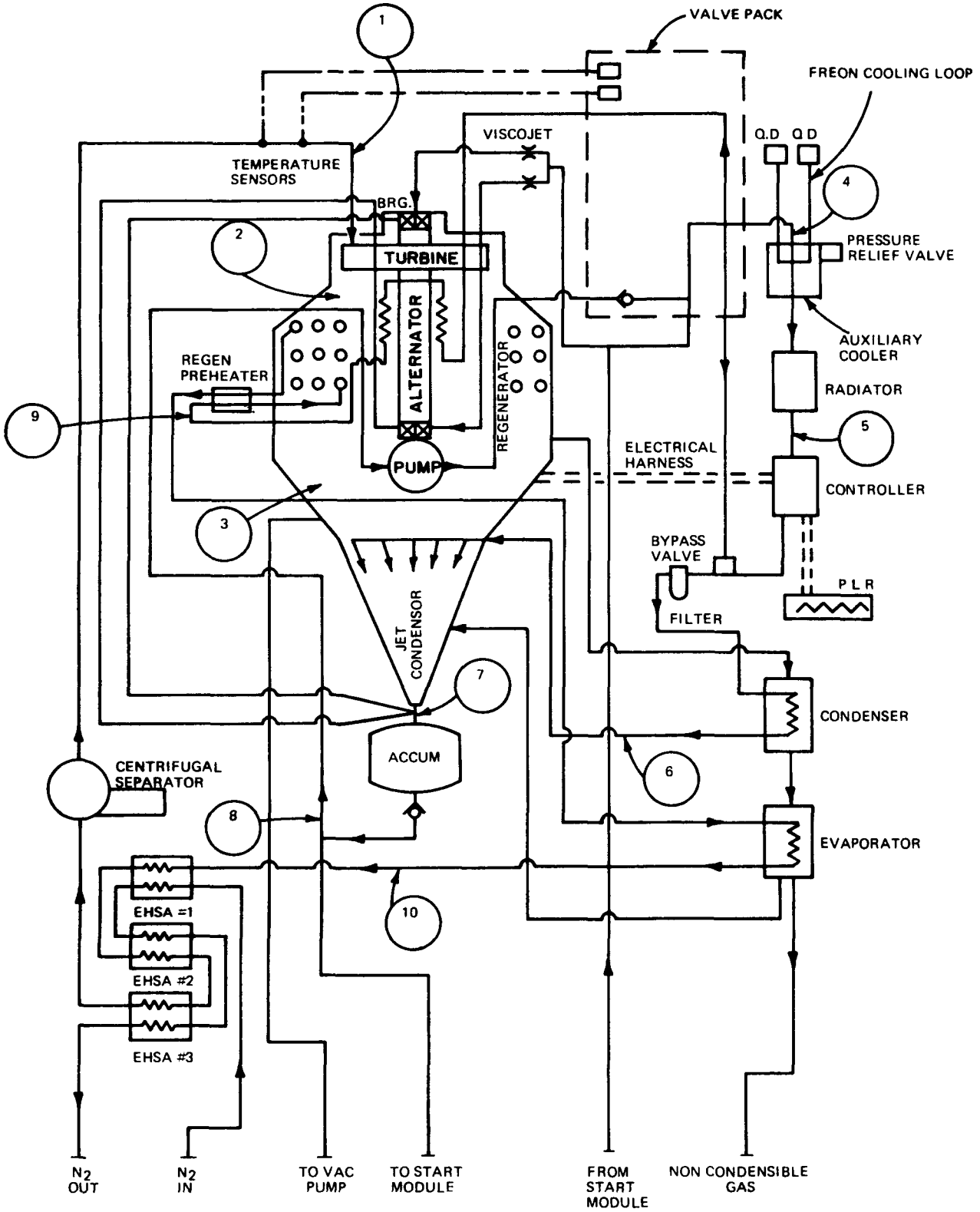

Figure 2.6-6 System Schematic

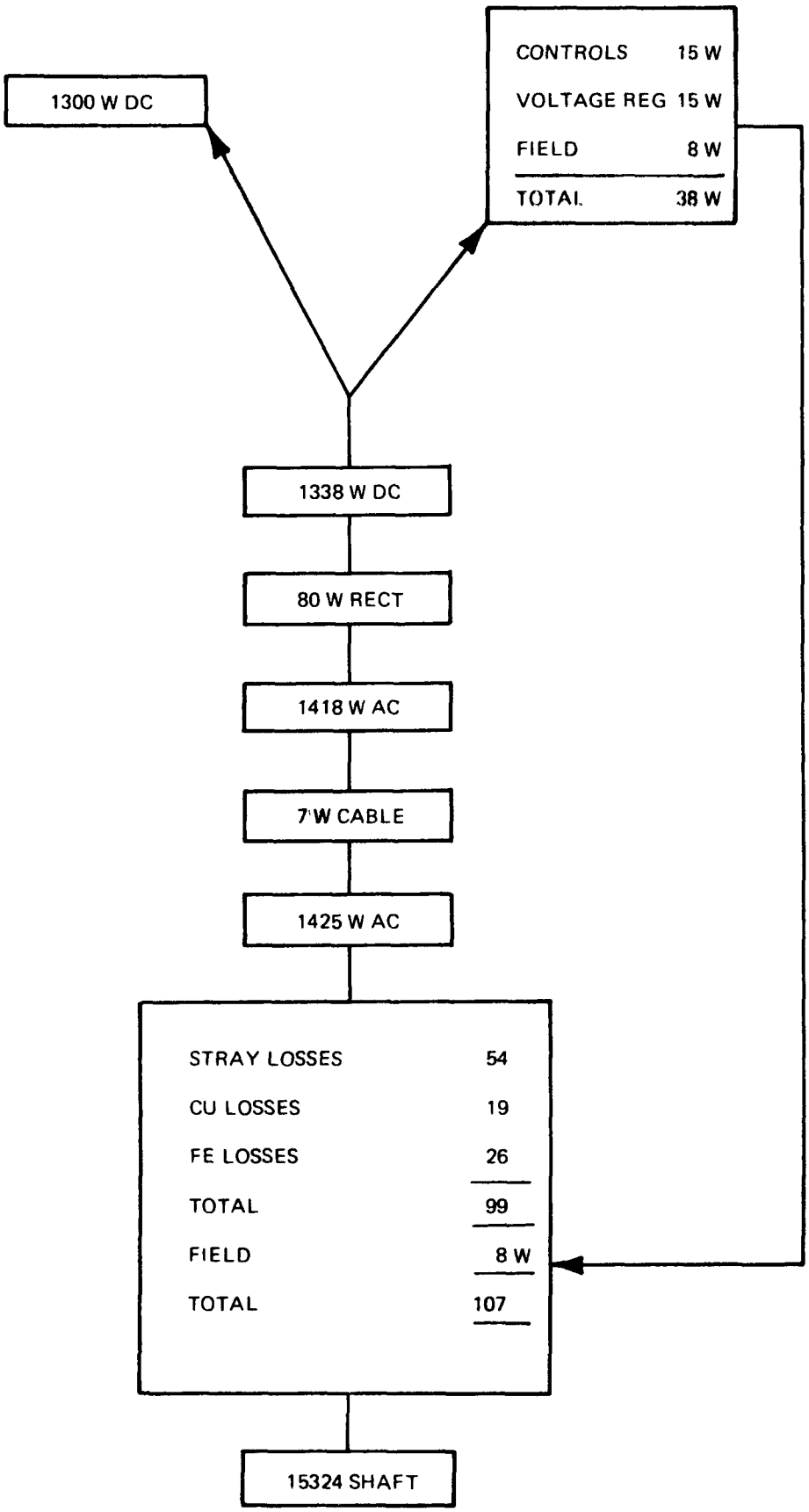

Figure 2.6-7 Electrical Losses

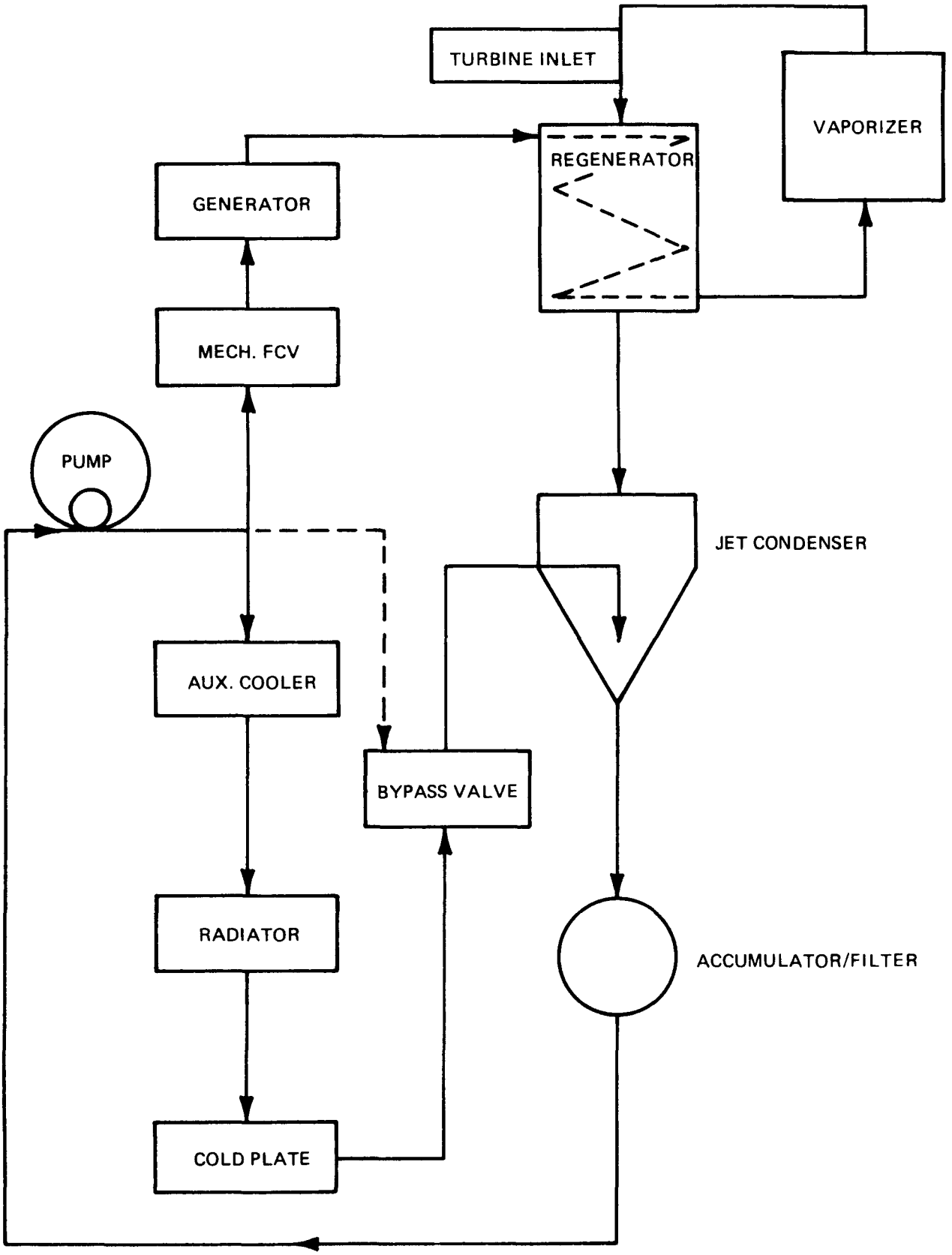

Figure 2.6-8 Hydraulic Block Diagram

Table 2.6-C Flight System Design Point

INPUT

TURB EFF	=	0.693	ALTERNATOR EFF	=	0.930
BEAR + SEAL LOSS	=	0.080	CONDITIONING EFF	=	0.944
REGEN EFFEC	=	0.950	J COND RECOVERY	=	0.400
CRU RPM	=	33700.	PUMP FLOW RATIO	=	10.000
NET O/P POWER	=	1.300	PARASITIC POWER	=	0.038
DES TURB IN PRES	=	57.000	TURB INLET TEMP	=	650.0
COND PRESS	=	0.0	BOILER HEAT LOSS	=	550.0
REGEN VAP P DROP	=	0.032	REGEN LIQ P DROP	=	4.40
BOILER PRES DROP	=	9.40	CENT SEP P DROP	=	2.50
RADIATOR P DROP	=	10.00	CON VALVE P DROP	=	23.10
CONTROL P DROP	=	6.40	ACCUM P DROP	=	1.30
DIFF PRES RISE	=	0.032	ALT WINDAGE	=	0.013
TURB HEAT LOSS	=	167.0	REGEN HEAT LOSS	=	175.0
TURB IN HT LOSS	=	22.0	REG HSG HT LOSS	=	12.0
PLUMBING HT LOSS	=	8.0			
RAD DES FLOW	=	0.0	J-COND DES PIN	=	80.0

OUTPUT

STATE POINT	PRESS(PSIA)	TEMP(F)	ENTHALPY(B/LB)
TURBINE PLENUM IN	57.000	650.000	396.266
TURB NOZ IN	57.000	646.464	394.550
TURB OUT	0.101	525.065	341.722
REGEN VAP IN	0.133	521.237	340.025
J COND VAP IN	0.101	239.387	229.432
J COND OUTLET	32.000	211.713	63.330
PUMP INLET	30.700	212.634	63.728
RAD+C VALVE IN	96.400	213.329	64.028
RAD OUTLET	86.400	167.333	44.603
J COND LIQ IN	80.000	167.993	44.874
REG LIQ IN	73.300	224.543	68.904
BOILER INLET	68.900	456.222	179.497
BOILER OUT	59.500	650.472	396.338

TURBINE CP	=	0.338	TURBINE GAMMA	=	1.037
PUMP SPEC SPEED	=	1160.	PUMP EFFICIENCY	=	0.650
TURBINE FLOW LB/SEC	=	0.03077	RADIATOR FLOW LB/SEC	=	0.277
TURBINE FLOW GPM	=	0.222	RADIATOR FLOW GPM	=	1.960
HEAT ADDED IN BOILER	=	24018.	HEAT REJ BY RADIATOR	=	20131.
ALT HEAT ADDED	=	540.0	CONTROLLER HEAT ADDED	=	270.9
OUTPUT KW	=	1.300	ALT INPUT KW	=	1.524
BEARING+SEAL LOSS KW	=	0.080	PUMP SHAFT KW	=	0.097
ALTERNATOR EFF	=	0.930	PUMP FLOW RATIO	=	10.00
RECTIFIER LOSS KW	=	0.079	BOILER HEAT LOSS	=	550.0
HEAT SOURCE WATTS	=	7198.3			

SYSTEM EFFICIENCY =18.05991 CYCLE EFFICIENCY =18.47346

Table 2.6-D System Performance as a Function of Turbine Inlet Temperature

Input Power Watt 1	Turbine Inlet Temperature (^{O}F)	Output Power (Watts)	System Efficiency(%)
7200	650	1300	18.1
7200	675	1325	18.4
7200	700	1350	18.7

Off-Design Performance

Overspeed protection is of major importance to the system operation. The system needs to operate in an overspeed mode during the launch phase in order to stiffen the jet condenser liquid jets and to provide additional load capacity for the bearings. During this overspeed requirement during launch, the need for output power of approximately 300 watts exists.

Analyses have been made to determine the system net power output as a function of operating speed. Power can be obtained in the active system by disabling the speed control, while retaining the voltage control function, thus allowing the system to run in the "frequency wild" mode and deliver useful power. The ultimate overspeed value, with zero net output, is important for determining the maximum stress levels that must be accommodated by the rotating hardware, and the maximum temperature levels that all hardware must experience. Information on power as a function of speed is given in subsection 2.6.4.

System Sensitivity to Component Performance

The effect of individual component performance on the overall system has been investigated. The analysis was performed using a baseline system with specific component performances and then reducing each component, one at a time by a given amount, to two lower levels of performance. Finally, the effect of the reduction of all parameters at once to the lower levels was investigated. The variables investigated and the performance values used are presented in Table 2.6-E.

The effect of all parameters varied at once, and one at a time are presented in Figures 2.6-9 through 2.6-11. The results have been plotted against a normalized cycle performance so that the effect on any system can be realized. As can be seen, certain parameters, namely turbine and alternator efficiency and jet condenser vapor inlet pressure (i.e., turbine outlet pressure), have large effects on the system, whereas other parameters represent secondary effects only.

The effect of pump flow ratio was analyzed separately. Figure 2.6-12 shows the effect of different design flow ratios on cycle performance for a given jet condenser inlet vapor pressure. As can be seen decreases in flow ratio yield increased cycle efficiency. The penalty for this is increased radiator size in order to obtain the required lower jet condenser liquid inlet temperatures. The benefit to the system performance results from reduced pump work.

System Performance with Variable Space Environment

The major variable in a space environment is the changing heat sink seen by the radiator as the spacecraft moves from a position of direct incidence of sunlight on the radiator to a position where the radiator sees deep space. These conditions correspond to radiator sink temperatures of 422°R and 25°R, respectively. The spacecraft may be oriented so that the entire radiator sees deep space or such that part of the radiator sees direct solar incidence. The radiator is capable of operating with this severe unbalance of solar input and maintains constant jet condenser inlet temperature via the radiator bypass valve. Only 4 watts difference in output power will exist between the extremes in temperature.

The radiator bypass valve maintains radiator outlet temperature by bypassing flow as required to keep the mixed radiator liquid outlet temperature up to 168°F. At worst case conditions, i.e., end of mission (EOM) with a 25°R heat sink, the bypass valve shunts 60% of the radiator loop flow around the radiator.

Table 2.6-E Parameters Investigated for Sensitivity Analysis

	Base	Level 1	Level 2
PCS Internal Heat Losses (Btu/hr)	300.0	450.0	600.0
Excess Seal Losses (Watts)	0.0	50.0	100.0
Alternator Efficiency (%)	93.0	90.5	88.0
Turbine Efficiency (%)	70.0	64.5	60.0
Pump Efficiency (%)	65.0	60.0	55.0
Regenerator Effectiveness (%)	95.0	92.5	90.0
Jet Condenser Back Pressure (Psia)	0.1	0.15	.20
Excess Liquid ΔP (Psi)	0	5.0	10.0

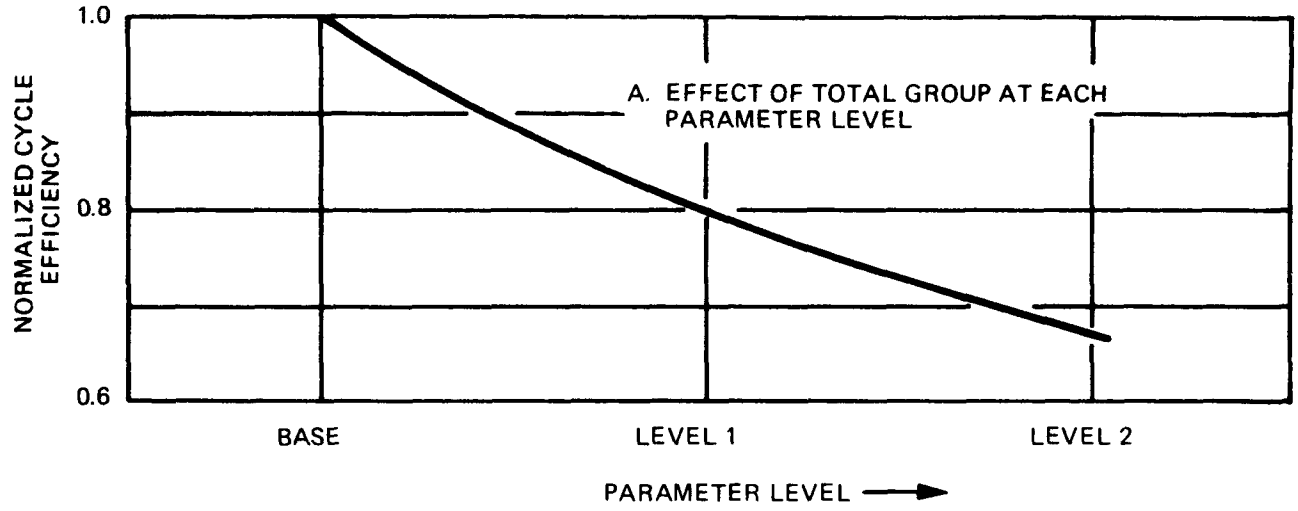

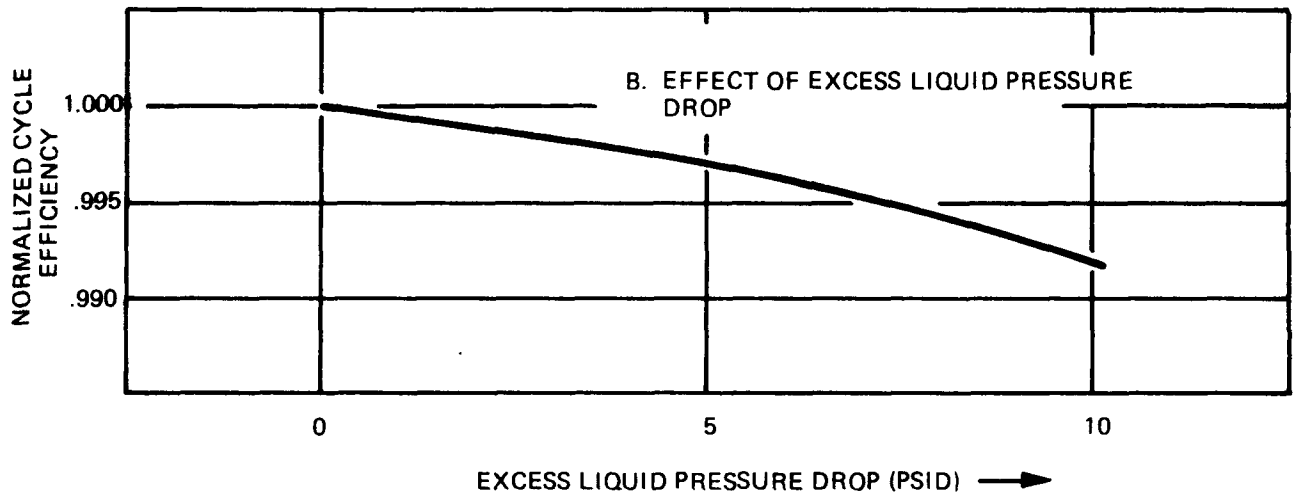

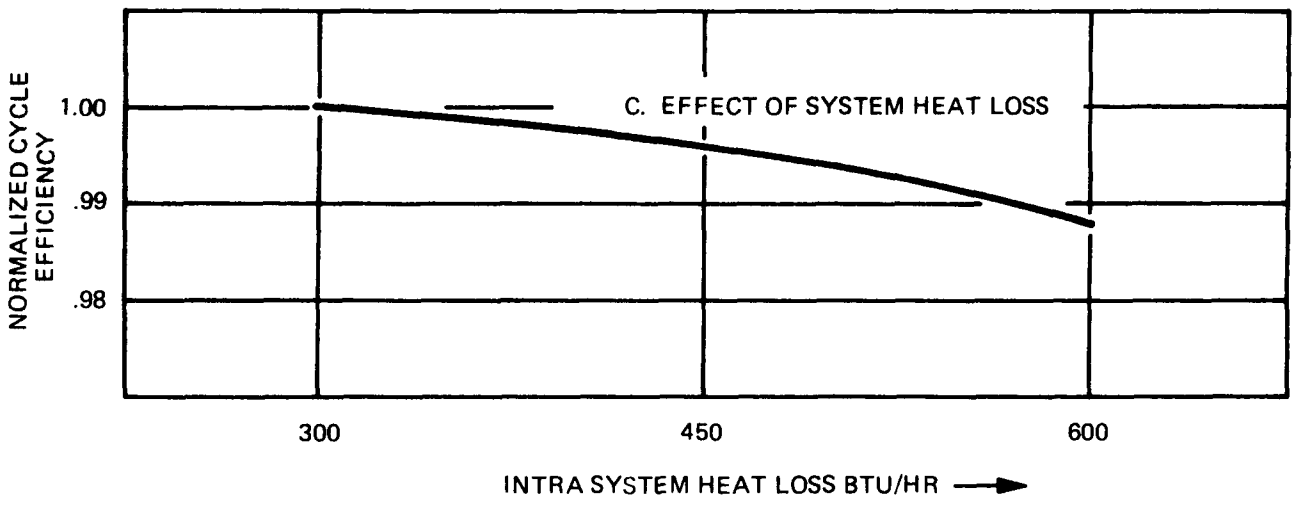

Figure 2.6-9 Results of Sensitivity Analysis

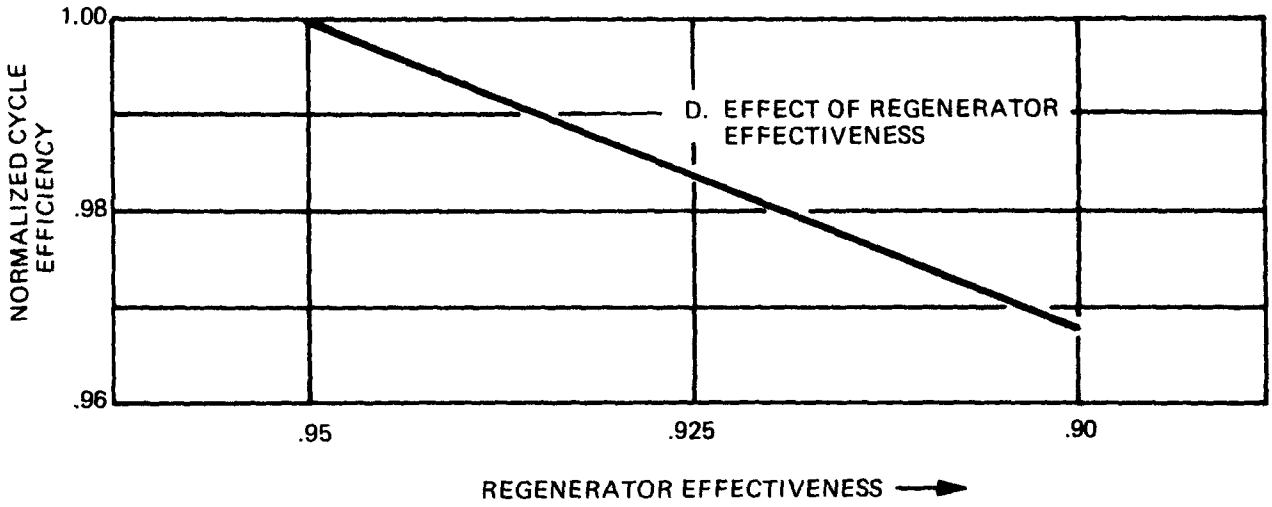

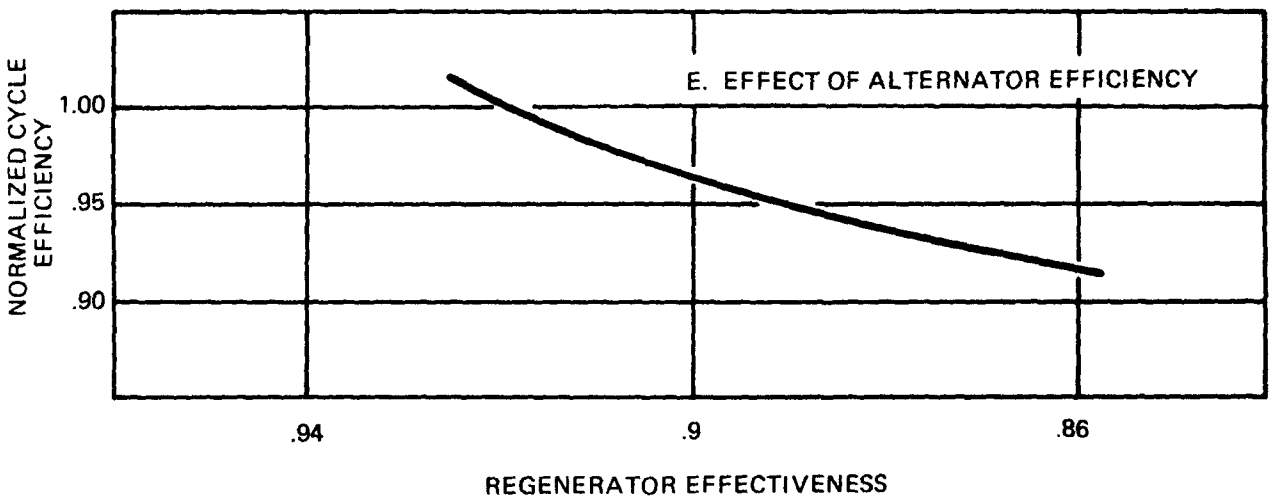

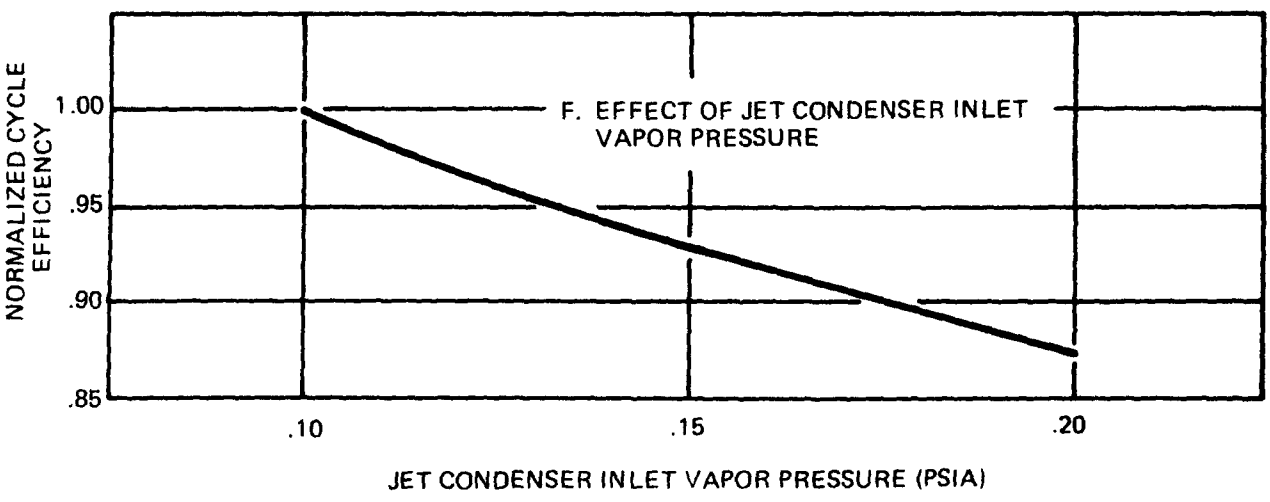

Figure 2.6-10 Result of Sensitivity Analysis (Contd)

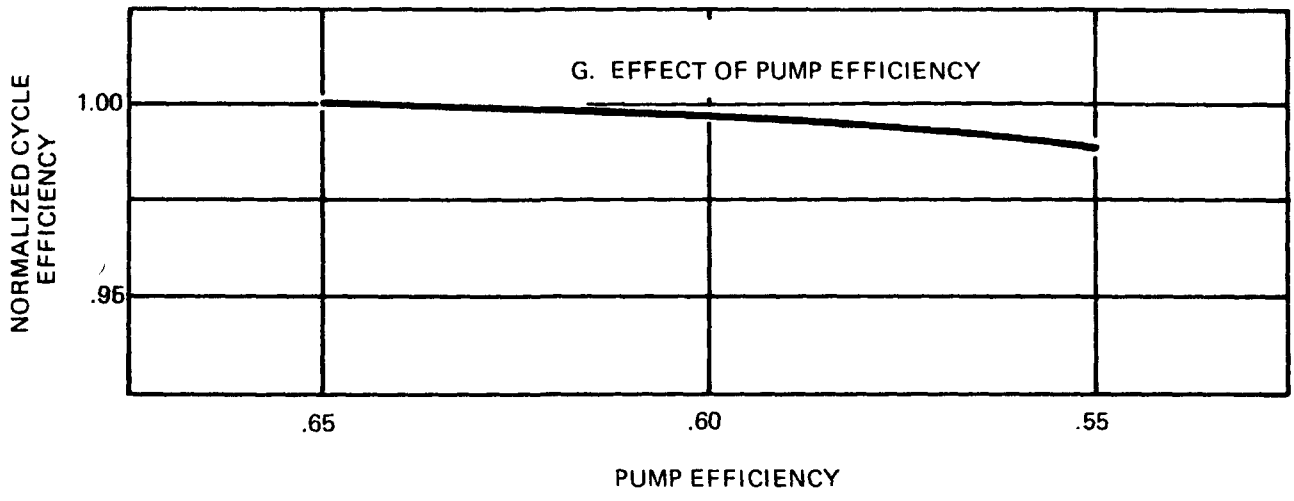

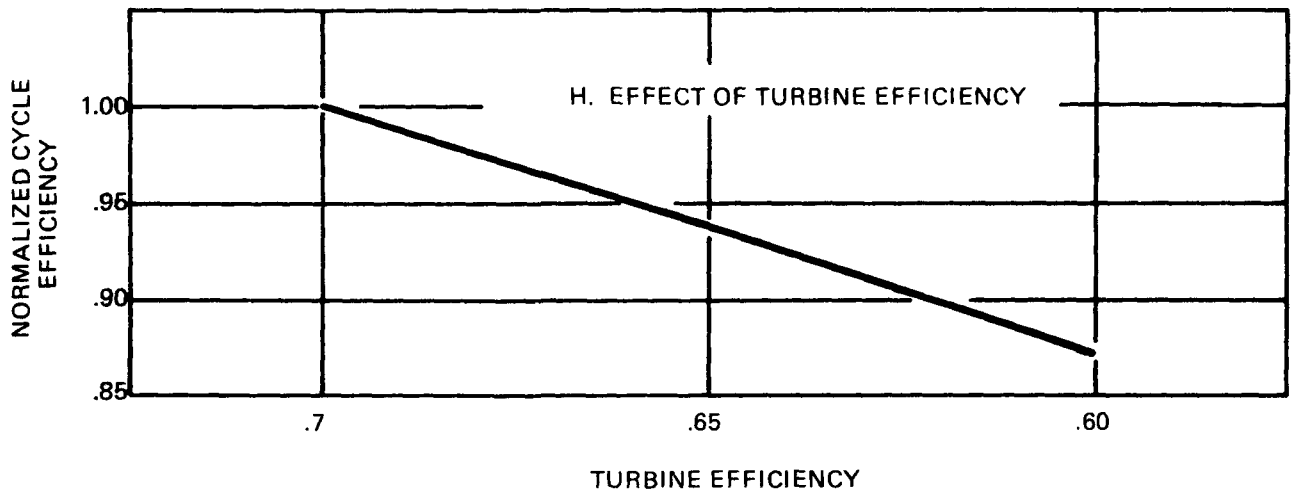

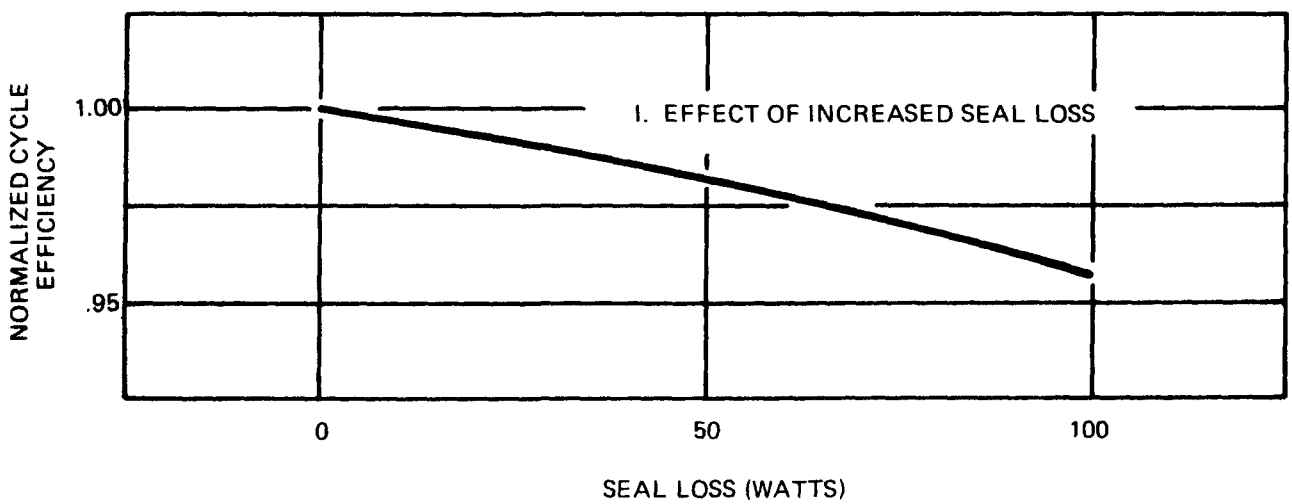

Figure 2.6-11 Result of Sensitivity Analysis (Contd)

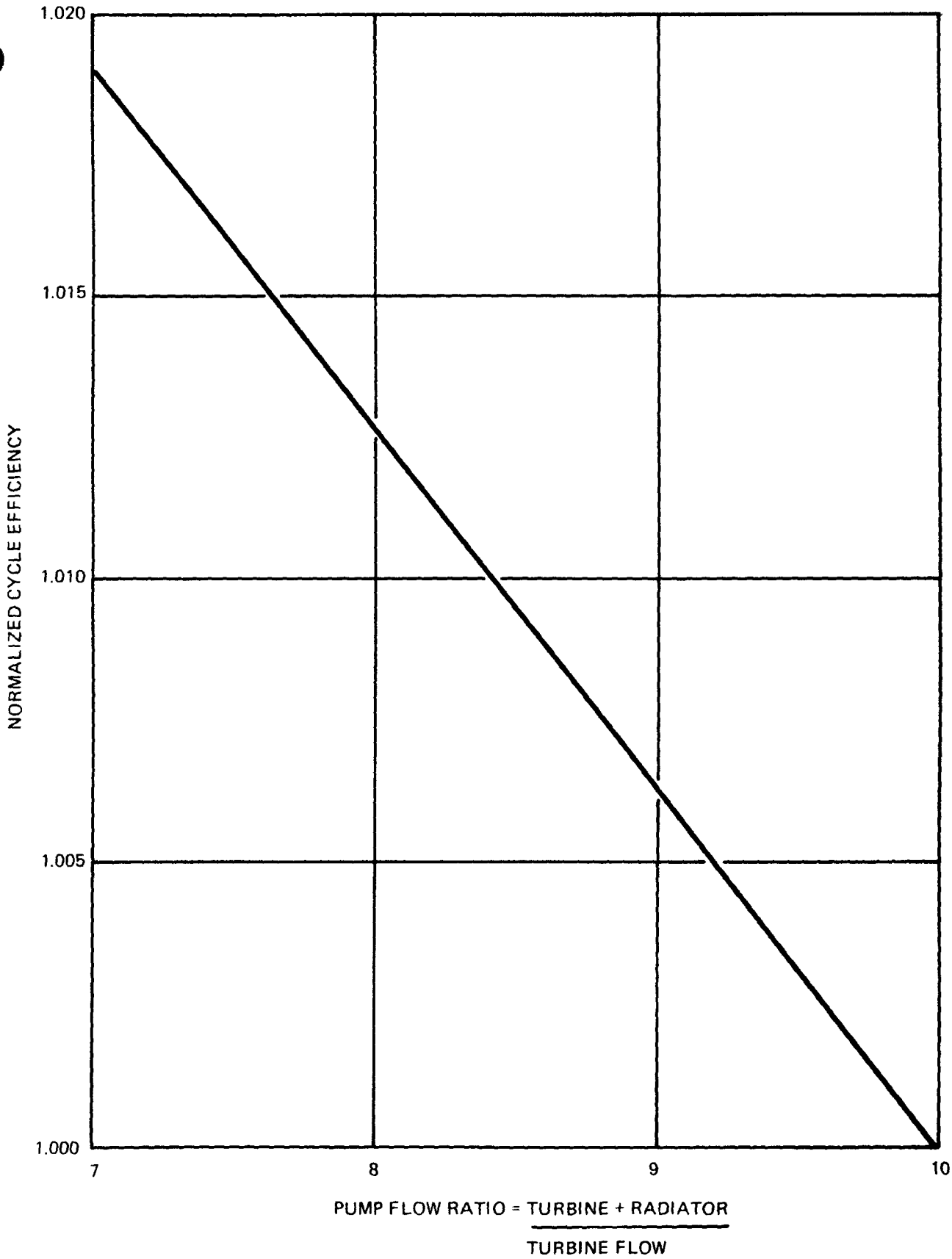

Figure 2.6-12 Effect of Pump Flow Ratio on Performance

The KIPS PCS can be used on either spin stabilized spacecraft or on nonrotating spacecraft, and will function in a zero g environment as well as a one g field. The PCS is configured to withstand launch loads and orbital transfer on a spinning vehicle while operating or nonoperating. The capability of of being launched while running is especially useful in that power can be produced during launch.

Multipower Performance

The system performance has been investigated at power levels other than design. The limits of investigation were 500 watts to 2000 watts. Component performances were investigated at these power levels and incorporated into the off-design performance analysis, with the assumption that modification to the system for power levels other than design must be performed with only minor component changes. Figure 2.6-13 summarizes the performance expected for the multipower operation. For power levels within the range of those defined, the system performance would fall between the limits.

2.6.3 PRELAUNCH HANDLING

2.6.3.1 Delivery and Loading

At some time prior to launch, the spacecraft, the KIPS PCS, and the IHSs must be integrated into a package and functionally checked. Various procedures and locations for performing this integration are discussed in the GSAR (subsection 6.2). It was determined that it is desirable to ship the spacecraft, PCS and IHS modules to the launch site after each component is assembled and checked out and perform the final integration at the launch site.

The spacecraft can be checked with a ground support 28 VDC power supply and the PCS operated with electrical heat sources to ensure integrity after shipping and storage. The IHS modules in their shipping containers are natural convection cooled and can be shipped and stored without the need for active cooling.

The present flight system design assumes that the KIPS will be attached to a spacecraft at one end of the specified 4.3' x 8' radiator. To minimize overhung weight and resulting high structural loads under shock and vibration, the KIPS boiler assemblies, including the IHS modules, are located as close as possible to the spacecraft. Access to the boilers for IHS loading is readily available from the spacecraft interface end of the radiator but difficult from the outboard end due to the length of the radiator. Loading from the "outboard" end is further complicated by the need for boiler and IHS inerting during loading. The present baseline approach, therefore, is to fuel and start the KIPS system prior to mounting to the spacecraft. This presumes the spacecraft is configured to prevent access for fueling from the KIPS/spacecraft interface end of the package.

The spacecraft configuration has not been defined, nor has the arrangement and location of the spacecraft and KIPS been defined with respect to the interim upper stage (IUS) and space shuttle for shuttle launched systems. For space shuttle usage, it may be desirable to reduce overall length by using a larger diameter and shorter radiator and installing both the KIPS and the spacecraft inside this envelope. In this case, fueling can easily be accomplished from either end and at any desirable point in the integration sequence.

For the baseline approach, the KIPS is tested with electrical heat sources after delivery to a fueling facility near the launch site. After checkout, the KIPS is shut down and the EHSs removed. The KIPS is then mounted to the loading and assembly station and the inerting chamber attached as

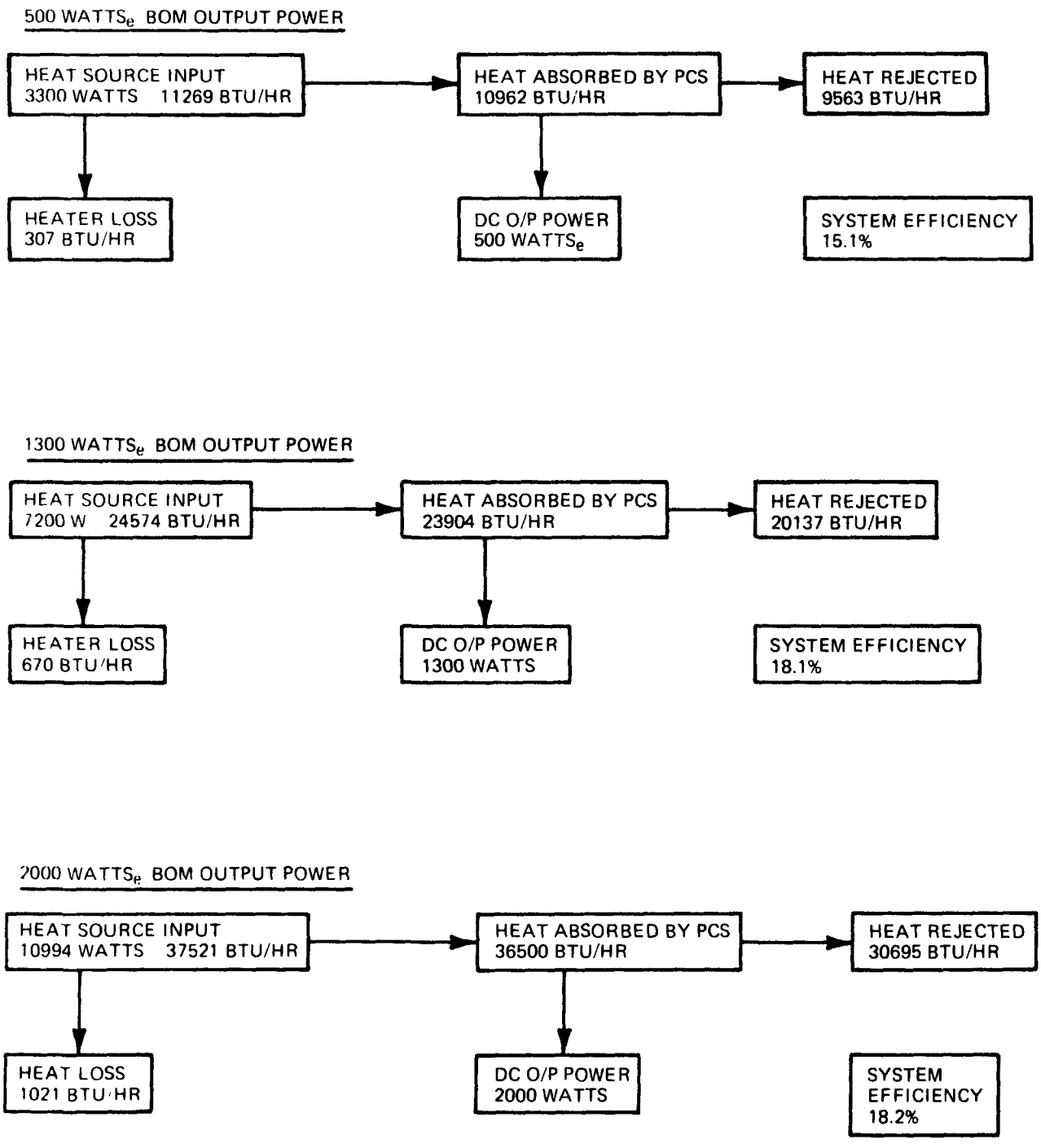

Figure 2.6-13 Performance Summary

shown in Figure 2.6-14. The KIPS boiler auxiliary cooling system and the isotope cooling coils inside the inerting chamber are attached to ground support cooling loops to maintain thermal control of the IHS during fueling. The chamber is then inerted and the boilers loaded as described in subsection 6.3. After the boilers are fueled and closed, the KIPS is removed from the loading and assembly station and attached to the start module. A facility nitrogen supply with nitrogen flow regulated to maintain the boiler fin at approximately 700°F is used to remove isotope heat until the start system is activated. Auxiliary cooling provisons of the KIPS are described in subsection 2.5.7.2. As Dowtherm enters the boiler tubes, the boiler fin is cooled by system working fluid and the nitrogen flow can be shut off. N_2 lines remain attached to provide emergency IHS cooling in the event of a KIPS shutdown. After the KIPS attains operating temperature, the start module is disconnected and disconnect points capped. The KIPS radiator has adequate heat rejection capability via natural convection on the ground so auxiliary cooling is not required if the building is ventilated. The radiator has an auxiliary cooling loop which can be used if desired. Control of coolant flow rate and temperature is not required as the KIPS radiator bypass valve will bypass fluid around the auxiliary cooler as required to maintain 170°F mixed radiator outlet temperatures.

When the spacecraft checkout is complete, the operating KIPS can be attached via the three shock absorbing mounts and electrically connected to the spacecraft.

The spacecraft/KIPS assembly is then mounted to the IUS, the shuttle or other launch vehicle and emergency cooling lines transferred to the vehicle.

A prelaunch performance test may be desirable to provide final assurance that the KIPS is operating properly and that integration and handling have not affected system operation.

In addition to tests of electrical output power, voltage regulation, transient response, and other electrical parameters of interest to the user, it is also easy to check the PCS at higher stress levels, pressures and flow rates than normally occur. This test can be conducted by shutting off the speed control system and permitting the system to run to maximum unloaded speed. The speed attained is controlled largely by bearing, seal and pump losses and provides a good indication of the condition of these components.

By applying successive load steps to the system, turbine speed versus load can be determined for comparison with acceptance test results to verify that system characteristics have not changed. The system can be left running in the frequency wild mode for launch after checking that the speed control system also functions properly at various loads.

2.6.3.2 Startup

The system start procedure requires the use of ground support equipment in the form of a start module, boiler temperature control module, and heat rejection module. This equipment supplies sufficient pressure and flow to start the jet condenser and then to supply turbine and bearing flow until the system is self-sustaining. It also provides cooling for the heat sources or radiator depending on whether the PCS is nonoperating or operating, respectively. The flight system ground support equipment is described in detail in subsection 2.5.7.

Prior to start, the boiler fin will be at temperature and controlled by nitrogen coolant. This will apply to both electric and isotope heat sources. The boiler temperature control will reduce the nitrogen flow as the working fluid starts circulating and will keep the fin at design temperature. By the time design system flow is passing through the tubes, there will be zero nitrogen flow.

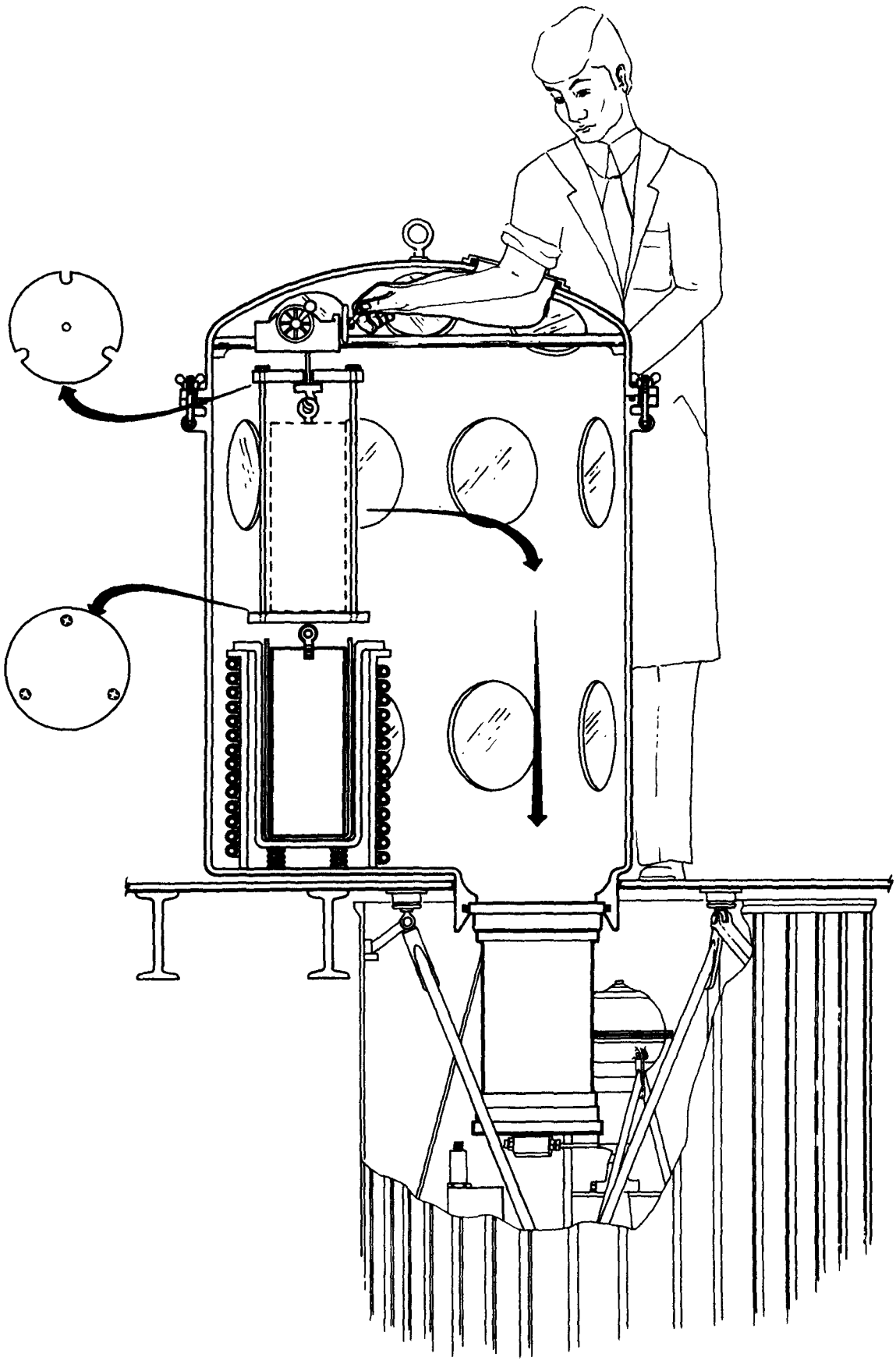

Figure 2.6-14 KIPS Loading and Assembly Station

On start initiation, the start valve will be opened and the system will start to fill. The start pump will be designed to have only a slight change in head capacity in the flow range expected between filling the system and flowing through the jet condenser. This ensures a high pressure jet will be maintained for proper operation of the jet condenser at all times. Therefore, as soon as the liquid reaches the jet condenser, the jet condenser will start and flow will be established through the radiator loop. Startup of the jet condenser will be performed with the system accumulator bellows at their operating pressure, so that the jet condenser recovery pressure will be determined by the start module accumulator pressure. The system will fill the radiator, within about 10 seconds from start initiation, and slowly fill the regenerator, at a low rate determined by the turbine flow control valve which will be at its minimum flow value, since the turbine inlet line will be cold. After approximately 5 minutes, hot vapor, at approximately 630°F, will start leaving the boiler and, as the boiler fills, the turbine inlet pressure will reach a value sufficient to start rotation.

The turbine exhaust will simultaneously heat the regenerator so that boiler inlet temperature will begin rising and the flow control valve will start increasing the flow to keep the turbine inlet temperature at the set point.

As the turbine accelerates, the system pump outlet pressure will reach a value which matches the start pump outlet pressure and the system pump outlet check valve will open, allowing the system pump to start sharing the flow with the start pump. By the time rated speed is reached, the system pump is supplying most of the flow.

As the system warms up to steady state, the parasitic load will automatically increase to keep speed constraint. When the sytem is operating at design speed, the start accumulator pressure is increased to a value slightly above the system accumulator design value and all the liquid left in the start accumulator is forced into the system, thus charging it with its correct inventory. The start pump is now deactivated and the quick disconnects are disconnected. For the final start, prior to launch, the final hermetic seal caps on the Dowtherm lines are applied. While operating on the ground prior to launch, the power system output will be slightly less than normal due to increased heat losses from natural convection but by no more than 150 watts.

The estimated times required to start are summarized in Table 2.6-F.

In the event that the system needs to be shut down (for instance, during the checkout phase with electrical heat sources), the heater power will be disabled. As the system begins to cool off, the flow control valve will reduce flow to maintain constant turbine inlet temperature as long as residual heat is available. The lower flows require the continual reduction of electrical load by the controller. Finally, the speed will start to drop and, at approximately 30,000 rpm, the jet condenser will stop operating. At this time, a high external field current will be applied, by the start module, to stop rotation. If the IHSs have previously been installed, the N_2 cooling flow will be introduced and increased to maintain proper heat source temperatures as the Dowtherm flow is decreased.

In order to accomplish a system restart, the fluid which has collected in the jet condenser when it stopped operating is drained through the jet condenser throat and accumulator back into the start module. As soon as the liquid level drops below the jet condenser throat, a restart will be possible, using the procedures previously stated.

It is possible to transport a fueled, nonoperating PCS in the Space Shuttle bay, using shuttle coolant through the boiler auxiliary cooling tubes to keep the isotope heat sources cool until the PCS is started. The start module must be carried along in the shuttle bay to provide system working fluid and pumping power for startup until the PCS is warmed up and self-sustaining.

Table 2.6-F Startup Times

Start Phase	Time from Start Initiation
Start Initiation	0
Jet Condenser Start	2 Seconds
Radiator Filled	10 Seconds
Hot Gas at Turbine Inlet	6 Minutes
Rotation	6.5 Minutes
100% Speed	10 Minutes
Full Power	3 Hours

Although the KIPS system can be started in a space environment, ground starting is the preferred mode for several reasons:

- A space start requires the additional payload of the start module and requires hermetic joints to be made after being disconnected.
- Only one start attempt is possible in space, so all phases of, and components needed for, the start procedure must have extremely high reliability. For ground start, this reliability requirement is minimized since a start module component failure could be repaired and the system could be restarted.
- In order to prevent the liquid freezing in the start module, or the system during the start phase, the complete system must be held at a temperature higher than 55°F. In addition, condensation which might occur on cold surfaces during startup could lead to inventory control problems. Hence, surface heating above local freezing or saturation conditions may be required during startup if the system is not operating.

2.6.3.3 Thermal Management

2.6.3.3.1 THERMAL INTERCHANGE

The KIPS system operates at relatively low temperatures, and, therefore, rejects heat to the spacecraft at low temperatures. Thermal interchange occurs by two processes only, conduction and radiation.

The conduction heat losses all pass through the three shock mounts by which the system is mounted to the spacecraft. These losses originate from the heat source assemblies only. The skin temperature at the heat source mount point is approximately 200°F which, with an assumed spacecraft temperature of 100°F and the high thermal resistance of the shock mounts, gives 11 watts due to conduction.

Heat is transferred by radiation from the bottom of the heat sources at a temperature of 200°F; from the system accumulator and cold end of the regenerator, both of which are thermally insulated and have skin temperatures of 150°F and 175°F; and finally from the inside of the radiator skin which is at an average temperature of 190°F but has a relatively low view factor to the spacecraft. A low emissivity surface, with a value of .04, is assumed for the spacecraft. With these assumptions, a total radiator loss of 35 watts is calculated.

2.6.3.3.2 THERMAL MANAGEMENT DURING LAUNCH

After the isotope heat sources are loaded into the boilers and thermally isolated, heat must be continually removed to prevent excessive IHS temperature rise. Auxiliary cooling coils on the boiler are used to keep the IHS cool prior to startup. After startup, when the IHS modules are cooled by system working fluid, emergency cooling must be provided to prevent overheating in the event of a KIPS shutdown.

For Space Shuttle launched missions, onboard cooling must be provided to keep the KIPS cool during the entire time that the KIPS is in the shuttle bay. If the KIPS is running, heat is extracted via the radiator auxiliary cooling coil. If the KIPS is not running, heat is extracted from auxiliary cooling coils on the boiler fin. This requirement for continuous cooling in the shuttle bay is present for any type of isotope fueled systems and applies whenever an IHS is carried in the shuttle bay.

The KIPS, with 3 IHS modules, has a beginning of mission heat input rate of 7200 thermal watts (24,600 BTU/hour). The shuttle cooling system, as described in JSC 07700, Volume XIV, consists of a freon or water coolant loop with 5200 BTU/hour heat rejection capability during the launch pahse of the orbiter when the bay doors are closed and up to 29,000 BTU/hour when in orbit with the bay doors open. There is, therefore, adequate cooling for the KIPS when the bay doors are open but supplemental cooling will be required during launch when the doors are closed. Supplemental cooling can be provided by a flash evaporator using excess water from the orbiter fuel cell power generating system or by additional water carried as part of the payload.

The shuttle cooling loop will normally be connected to the KIPS radiator auxiliary cooling coil when the KIPS is operating in the shuttle bay. In the event of a KIPS shutdown, the cooling fluid must be circulated through the boiler auxiliary coils. If stored water is used for emergency cooling, the flow rate can be set such that steam is generated in the auxiliary boiler coil and this steam dumped overboard directly, without using the shuttle flash evaporator.

For a Titan launched mission where onboard cooling system is available, the KIPS radiator can be subcooled prior to launch by circulating cold fluid through the radiator auxiliary heat exchanger. The bypass valve will then bypass working fluid around the radiator to maintain a constant mixed radiator outlet temperature, permitting the radiator to cool to ambient temperature. At launch when the ground support cooling is disconnected, the subcooled radiator provides a system heat sink until the radiator protective shroud is removed.

2.6.4 PERFORMANCE CHARACTERISTICS

2.6.4.1 Torque Effects

Changes in the rotative speed of the CRU produce torque reactions in the KIPS which are transmitted to the spacecraft. The magnitude, duration and repetition rate of these torque effects are all of interest to the spacecraft designer.

The moment of inertia of the flight system combined rotating unit (CRU) including all of the rotating components, is 0.00385 ft-lb-sec^2. At the design speed of 33,700 rpm (3529 rad/sec), the angular momentum of the CRU is 13.59 ft-lb-sec.

On the KIPS, there are four types of speed variations. These are speed shifts due to customer load change, long term speed change due to isotope decay, speed modulation at constant load caused by the interaction of the controller voltage regulator and speed control circuits, and speed changes which occur if a customer electrical overload is applied. Diurnal changes in heat sink capability are accommodated by the radiator bypass valve and have no effect on speed.

The speed shift due to customer load changes consists of a 2% drop in speed (from +1% to -1%) when customer load changes from zero to full load.

The initial torque when full load is added or dropped is 0.32 ft-lb. As the speed changes, the dissipative load is applied proportional to the speed error so that the average torque during the 1.7 second interval required to accomplish the 2% speed change is 0.16 ft-lb. For step load changes of less than 100%, the peak torque, average torque and speed change all decrease proportionally to the load change. These angular impulses occur only when load is changed and average out to zero when the load returns to the base load.

The second type of speed change occurs in input power decays due to isotope decay. This effect has been investigated on the KIPS alternator-controller test stand by changing the input power and noting the change in steady state speed. The expected speed change on the flight system based on these results is a reduction of 0.35% in CRU speed over the seven year mission. This speed change produces a miniscule but continuous torque of 2.15×10^{-10} ft-lb.

The third type of speed change occurs at the natural frequency of the integrated CRU-controller-load bank system. The magnitude of the speed excursions depends on the response of the voltage regulation and speed control circuits to changes in voltage and speed. For a worst case condition, speed variations of $\pm$ 0.05% at a frequency of 0.14 Hz have been predicted. This produces a fluctuating torque of $\pm$ 0.004 ft-lb.

Both the frequency and magnitude of this variation can be controlled by damping and tuning of the controller circuits.

The fourth type of speed variation occurs only in the event of a customer electrical overload; i.e., spacecraft demands exceed the power output capability of the KIPS. The KIPS control system will accommodate this condition without causing a PCS shutdown.

When excessive electrical load is demanded, the excess alternator torque causes the CRU to slow down. As the CRU passes through 95% speed, the KIPS controller removes all output power by shutting off the alternator field current. The CRU is then unloaded and speed increases until 95% speed is again attained, where alternator field is again applied. If the overload continues, the speed will then again fall and the cycle is repeated. In the case of a small overload (0 to 100 watts), the resulting torque pulses are $\pm$ 0.032 ft-lb at a rate of about 11 Hz. For an overload of 1300 watts (i.e., 2 x rated load), the torque pulse is $\pm$ 0.47 ft-lb at a rate of 21 Hz. The system returns to rated speed when the electrical overload is removed.

2.6.4.2 Hardenability

The evaluation criterion for hardenability is the effect on output power of the complete loss of the emissivity coating on 50% of the radiator. On the KIPS at BOL and maximum heat sink temperature, where the radiator has the least margin, this condition results in an output power reduction of 30%, based on the Z-93 coating applied to an anodized aluminum fin.

Other system components have been selected to minimize potential radiation damage. The electrical controller is built entirely of discrete components rather than integrated circuits. More discrete components are available in nuclear hardened versions and the levels of hardening are generally higher than for ICs.

2.6.4.3 Orbital Transfer Power – Launch Power

The PCS has designed-in capability to withstand the high shock and vibration loads of launch and orbital transfer without affecting the normal performance of the system. The areas of concern when operating through shock and vibration are the extra bearing loads and the deflection forces on the fluid jet streams in the jet condenser. Extra capability could have been provided by oversizing the bearings to carry the extra load and by increasing the design pressure of the system feed pump to supply extra jet velocity to minimize jet deflections. These solutions waste power in the normal mode of system operation and would have caused a reduction of system efficiency.

The solution adopted for the KIPS PCS is to let the CRU speed increase during periods when extra vibration loads are present. By switching off the speed control system, the CRU speed will vary inversely with electrical load, running at rated speed at maximum design load and at 175% rated speed at no load. As speed is increased, the tilting pad bearing film thickness increases and the bearing develops additional load carrying ability. The feed pump, attached to the CRU shaft, develops additional pressure as speed is increased to supply the jet condenser with additional jet velocity to resist jet deflection. The bearings and jet condenser can therefore be designed for low g operation and have capability for higher loads without reducing system design point efficiency.

The amount of spacecraft power which can be extracted during launch and orbital maneuvers depends on the vibration and shock levels which the CRU must withstand.

Should the system be launched on the Titan IIIC where shock and vibration loads are high, it is desirable to keep the PCS nearly unloaded so that maximum resistance to vibration and shock are retained.

For space shuttle launch and orbital transfer maneuvers where vibration and shock are less severe, the PCS can deliver more power.

During portions of the launch and orbital maneuvers where the PCS experiences no vibration, the speed can be permitted to drop to rated speed, so full electrical output is available.

Figure 2.6-15 shows the effects of customer load on CRU speed when operating in the frequency wild mode. A speed of 53,000 rpm is expected to be adequate for all shock and vibration loads which occur during launch, including orbital maneuvering loads. This figure shows that 320 watts are available under these worst case conditions (assuming Titan III launch).

The boiler and heat source assembly heat losses are greater than design when operating in the

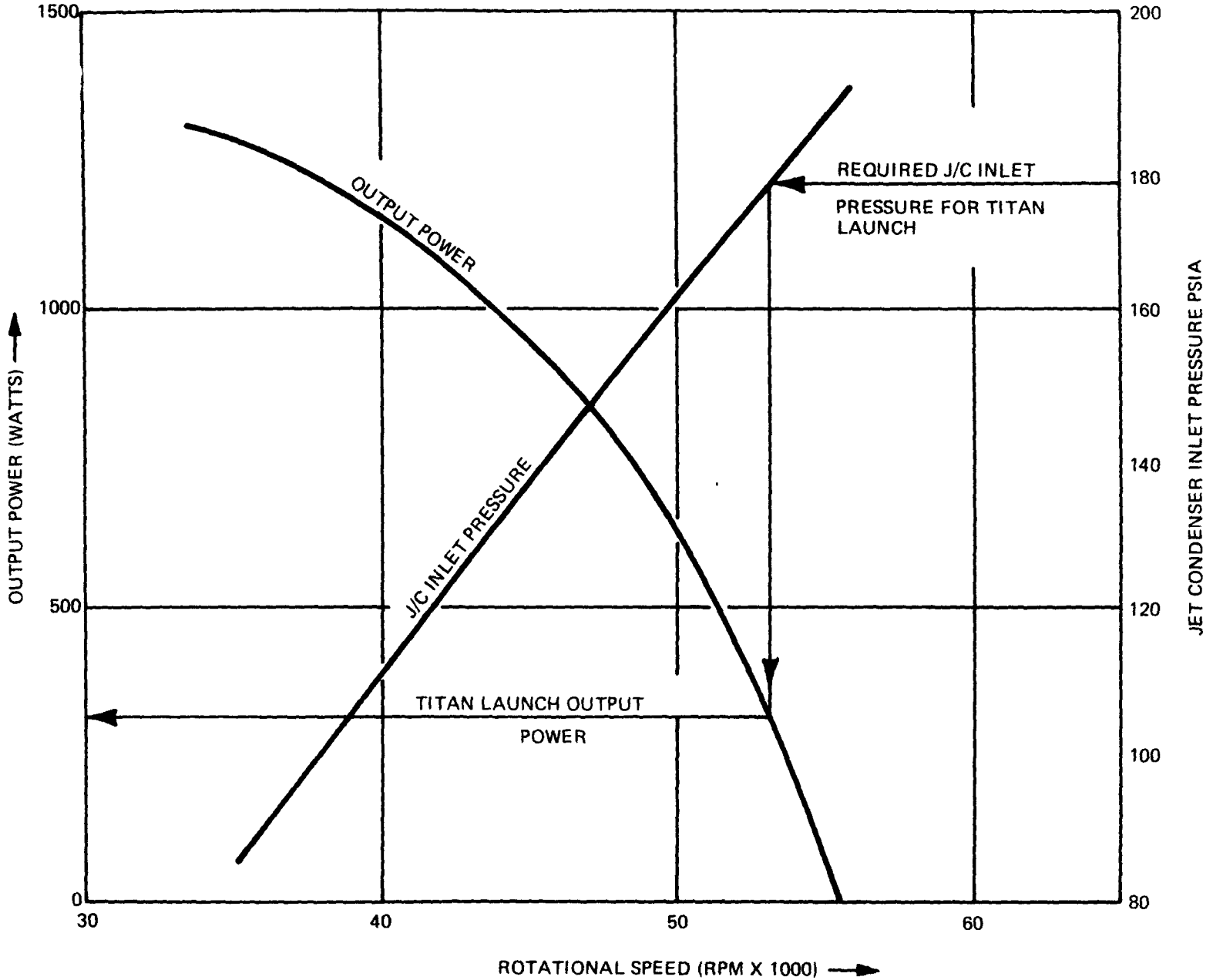

Figure 2.6-15 Output Power and Jet Condenser Inlet Pressure as a Function of Rotational Speed

atmosphere due to the presence of the inert gas in the HSA insulation. Under these conditions, allowable electrical load drops to 1170 watts for a 1300 watt system, when no vibration or shock loads are anticipated.

2.6.4.4 Power Degradation

The nuclear isotope heat sources produce heat by nuclear decay and, as such, the thermal output degrades with time. The thermal output of 7200 watts provides 1300 watts of electrical power at BOM. The electrical power decreases by 5.3% to 1196 watts after seven years.

2.6.4.5 Micrometeoroid Protection

The design goal for probability of nonpuncture of the fluid system by micrometeoroids is 0.99. Since puncture probability is a function of system wall thickness, it may be traded off with system weight as can be seen by reference to Figure 2.6-16 which represents radiator tube weight as a function of nonpuncture probability.

Protection against puncture falls into two categories: (1) direct impact and (2) secondary impact (resulting, for instance, from micrometeoroids passing through the radiator skin and then striking some part of the hydraulic system).

The first category covers the outside surface of the radiator tubes and all surfaces inside the radiator exposed to direct impact through the open end. This means the inside surface of the radiator tubes, the external skin of the turbine-radiator shell, certain parts of the plumbing and the heat source assemblies. Analysis of this type of impact has been made using information from Lieblein[1] which gives the required armor thickness as:

$$t_a = K_{\rho p}^{-1/3} \left(\frac{\rho p}{\rho t}\right)^{1/2} \left(\frac{V}{\sqrt{E_t/\rho t}}\right)^{2/3} \left[\frac{AT}{-\ln P}\right]^{1/3\beta}$$

where: t_a = required armor thickness

K and β are constants

ρp = meteoroid particle density
ρt = target material density
V = average meteoroid velocity
E_t = target Young's Modulus
A = effective target area
T = mission time
P = probability of non-puncture

The NASA model shows that 20% of the meteoroid particles in the near earth region travel together in common orbit, direction, and velocity. The remaining 80% are sporadic and, hence, treated using this probability relationship.

As can be seen, this is a function of effective area and, in the case of the PCS and other components buried within the cylindrical radiator, is reduced considerably by the shape factor as with radiant heat transfer.

[1] Loeffler, Lieblein and Clough "Recent Developments in Power Systems Meteoroid Protection, AIAA Paper, 64-759.

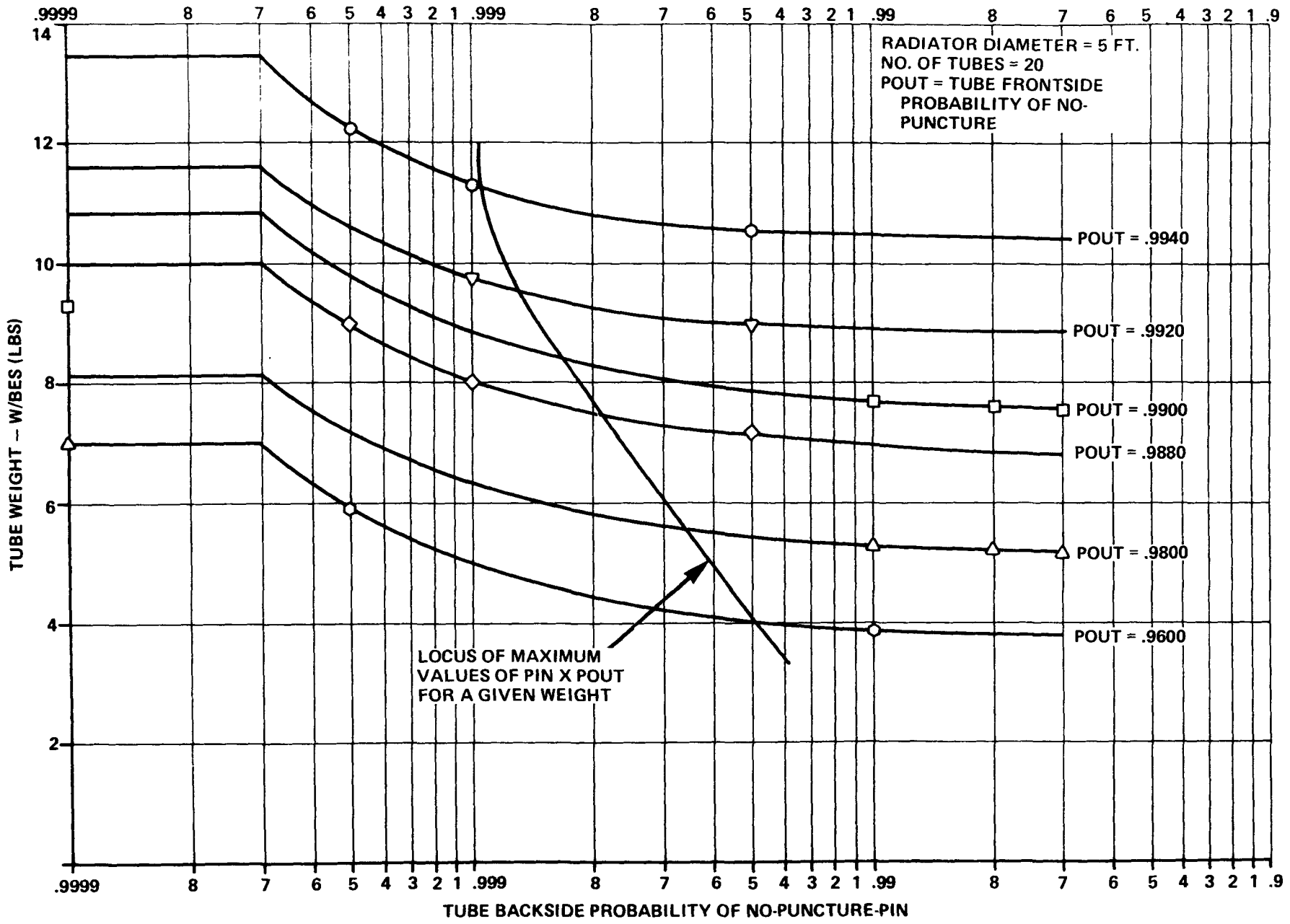

Figure 2.6-16 Relationship of Tube Weight to No-Puncture Probability

The outside surfaces of the radiator tubes are protected against these direct impacts by using a thick walled tube extrusion, while the inside surfaces are protected by a secondary thin aluminum bumper shield.

Analysis of the secondary category of impacts is more difficult. These result from micrometeorites passing through the radiator skin and subsequently striking the PCS, plumbing, or HSAs. Additional impacts of this nature result from particles passing through the bumper shields on the radiator headers or tube backside.

The analytical approach is based on the Cour-Polais[1] method which treats the secondary impact as a function of the condition of the particle after passing through the first wall and the separation between the target and the so-called "bumper" wall or shield.

The "critical particle mass"; i.e., required for penetration of the target material, is based on the standard Poisson probability of nonpuncture, i.e.,

$$m_c = \left(\frac{\alpha A T}{-\iota n P} \right)^{1/\beta}$$

where α and β are constant

A = effective area
T = mission time
P = probability of non-puncture

From this a critical particle diameter, d, may be calculated for an assumed average particle density. The required armor thickness then becomes a function of the ratio of the shield thickness to critical particle diameter ($t_{s/d}$) and the separation between the two, since these determine the condition of the particle on striking the target.

These fall into three general categories:

- The optimum range of $t_{s/d}$, in which the particle is completely vaporized upon passing through the shield, requires very little armor. This is, however, a dangerous regime in which to design since the presence of particles smaller than the critical value can cause spallation.

- Outside the optimum range of $t_{s/d}$, with the ratio of spacing to particle diameter less than 30, the required thickness shows an inverse square root dependence.

  $$t_a = K\,(\rho p - \rho t)^{1/6}\; m_c{}^{1/3}\; V/(S\sigma_y)^{1/2}$$

  where K is a constant

  ρp, ρt, m_c and V are as already defined
  S = spacing between shield and target
  σ_y = yield strength of target

- When the spacing ratio is greater than 30, Cour-Polais gives the required armor thickness independent of spacing. However, it is expected that the benefit of the spacing ratio of 30 should be incorporated as a constant to give

[1] B. G. Cour-Polais. "Meteoroid Protection by Multi-Wall Structures". NASA, Houston. Presented at AIAA Conference, Cincinnati, May, 1969.

$$t_a = C(\rho p - \rho t)^{1/6} \; m^{1/3} \; X \; V/(30d \; \sigma_y)^{1/2}$$

where C is a constant.

The results of the analyses for the various components of the system are presented in Table 2.6-G.

The resulting total system probability of nonpuncture is 0.977 for seven years. This can be improved with a slight weight penalty resulting from thicker tube walls.

2.6.4.6 Growth Potential and Flexibility

To provide different design power levels while maintaining high efficiency, system thermodynamic state points are kept constant and only the design flow rate is varied with design power level.

To accommodate the reduction in flow rate as design point power is decreased, components in the flow loops are designed to be easily modified or adjusted.

Turbine flow can be reduced by reducing the number of nozzles or by reducing the size of the nozzles and cropping the turbine blades. The CRU feed pump impeller and diffuser channels are designed so that channel heights can be changed for different power levels without affecting mating housings. The number of jet condenser nozzles is changed to adjust the radiator loop flow rate and the jet condenser throat diameter is changed to maintain essentially constant jet condenser recovery. The flow control valve is reset to the desired flow rate by adjusting the throttling orifice size. The values of the alternator tuning capacitors are changed to optimize alternator performance. Other controls including the speed control and voltage regulation remain unchanged. The basic combined rotating unit, bearings and alternator as well as the regenerator and associated housings are not changed for alternate design power levels.

The radiator size should be reduced to minimize weight as power level decreases although this is not required as the bypass valve will control system heat rejection if the radiator is oversized.

The number of HSAs can be adjusted in discrete steps to accommodate various power levels.

Since the system state points remain constant and the hardware is almost identical, control system response, stress levels, temperatures and pressures remain the same and qualification should not be necessary.

It may be desirable to run through a partial system requalification for each selected design power level to insure that components operate in the system as they do in the component development tests. These tests would include vibration, shock and performance to verify that all user requirements are met for a specific mission.

To provide for situations where it is desirable to rearrange the KIPS components for better spacecraft integration, the KIPS system is separable into modules. With no component design changes, the radiator, controller, load bank, boiler assemblies, and PCS can be moved to alternate locations. The radiator can easily be reconfigured with no weight penalty to a shorter and correspondingly larger diameter unit. The FSCD power conversion system includes the CRU, regenerator, jet condenser, and flow control valves. This PCS can be split into two modules, one containing the CRU and one containing the static components if desired for a particular application.

The low power conversion temperature of the KIPS will allow it to be "topped" by a thermoelectric generator without compromising any of the safety aspect of the MHW heat source. Topping will result in a desirable increase in total system efficiency. A detailed discussion of the topping concept is presented in Appendix A of Volume IV.

Table 2.6-G Summary of Non-Puncture Probabilities

Component	Thickness	Material	Direct Impact Puncture Probability	Secondary Impact Puncture Probability
Turbine Housing	0.062	17-4 PH	0.9995	--
Regenerator Shell	0.062	304 SS	0.99991	0.9995
Plumbing	0.035	304 SS	0.9986	0.995
HSAs	0.035	304 SS	--	0.995
Radiator Outside				
Radiator Inside		TOTAL	0.99	
Radiator Headers				
Auxiliary Hx	0.049	6061	--	0.9995

Total system non-puncture probability = 0.977.

2.7 GDS TEST RESULTS

At the time of writing this report, the development system is undergoing testing. Several components of this development system will be retrofitted in the early April time frame to achieve a higher efficiency system which is more prototypic of the FSCD.

Tests to date on the development system have resulted in over 480 hours of operation, including a single continuous run of 467 hours after which the system was purposefully shut down. Although the efficiency of the development system is low, as predicted, component tests have indicated that the retrofit to GDS configuration will yield 16% system efficiency. As discussed in Section 2.0, the next generation of hardware should readily achieve 18% plus of system efficiency.

For component efficiencies and performance, reference the KIPS GDS Component Test Reports which have been previously submitted to the evaluators.

Figures 2.7-1, 2.7-2, and 2.7-3 show respectively the development system after final assembly, the system being placed in the vacuum chamber for test, and the main console control panel in the KIPS test area.

During and after retrofit to the GDS configuration and subsequent to system tests, the evaluation team members will be kept informed of the results and furnished interim and final data for their evaluation.

NOTE: This section will be submitted in its entirety after GDS testing is completed.

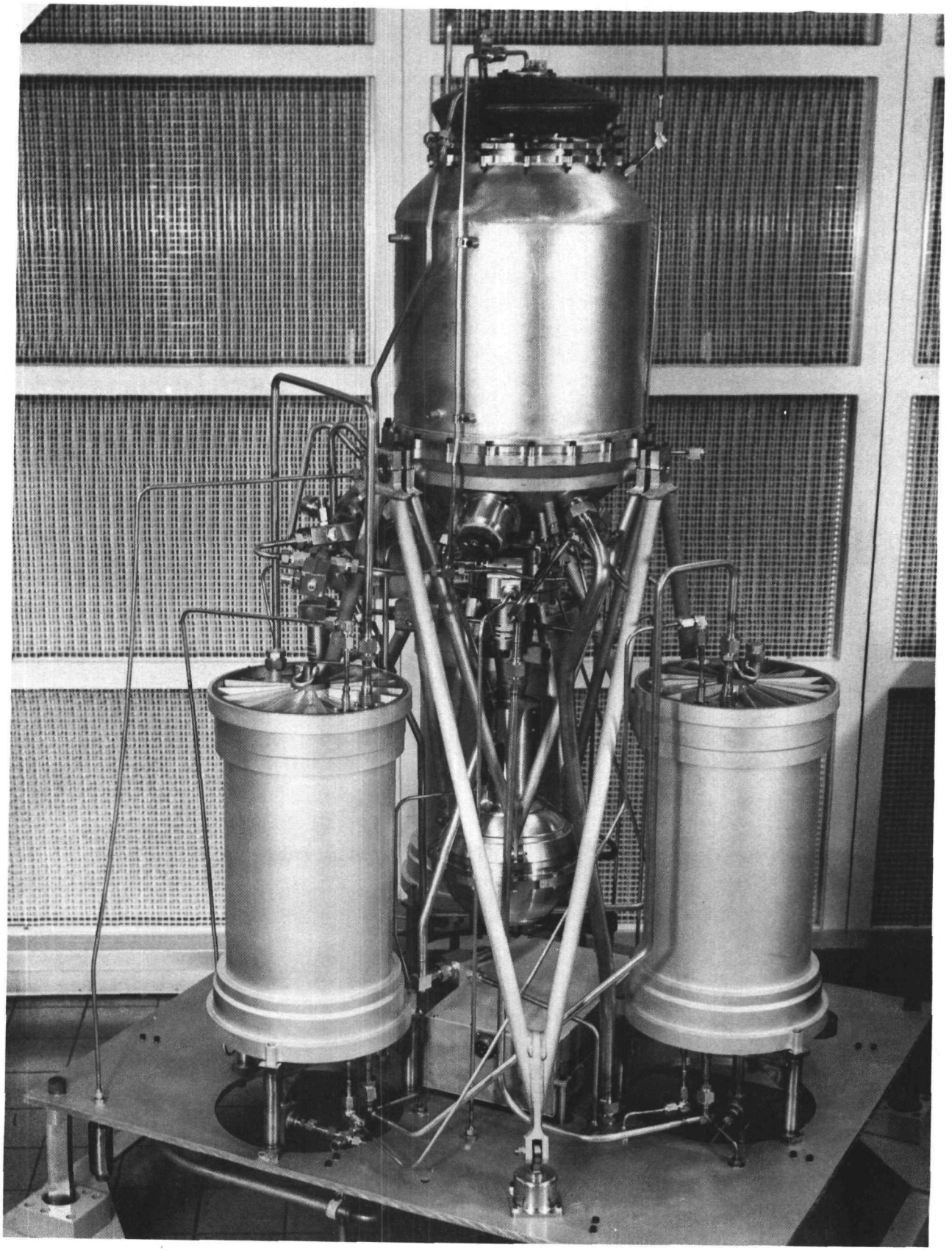

Figure 2.7-1 Development System

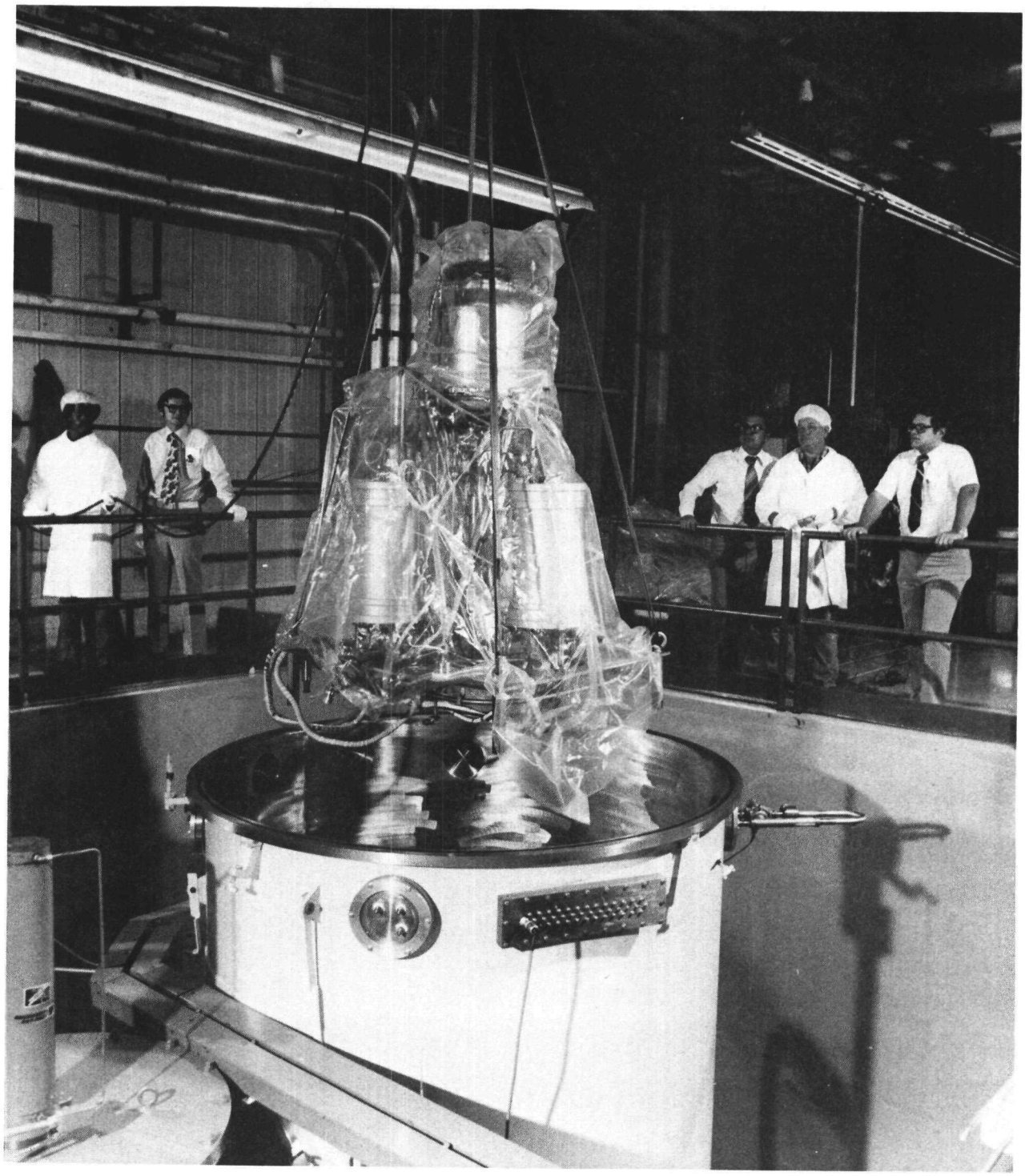

Figure 2.7-2 Development System Placement Vacuum Chamber

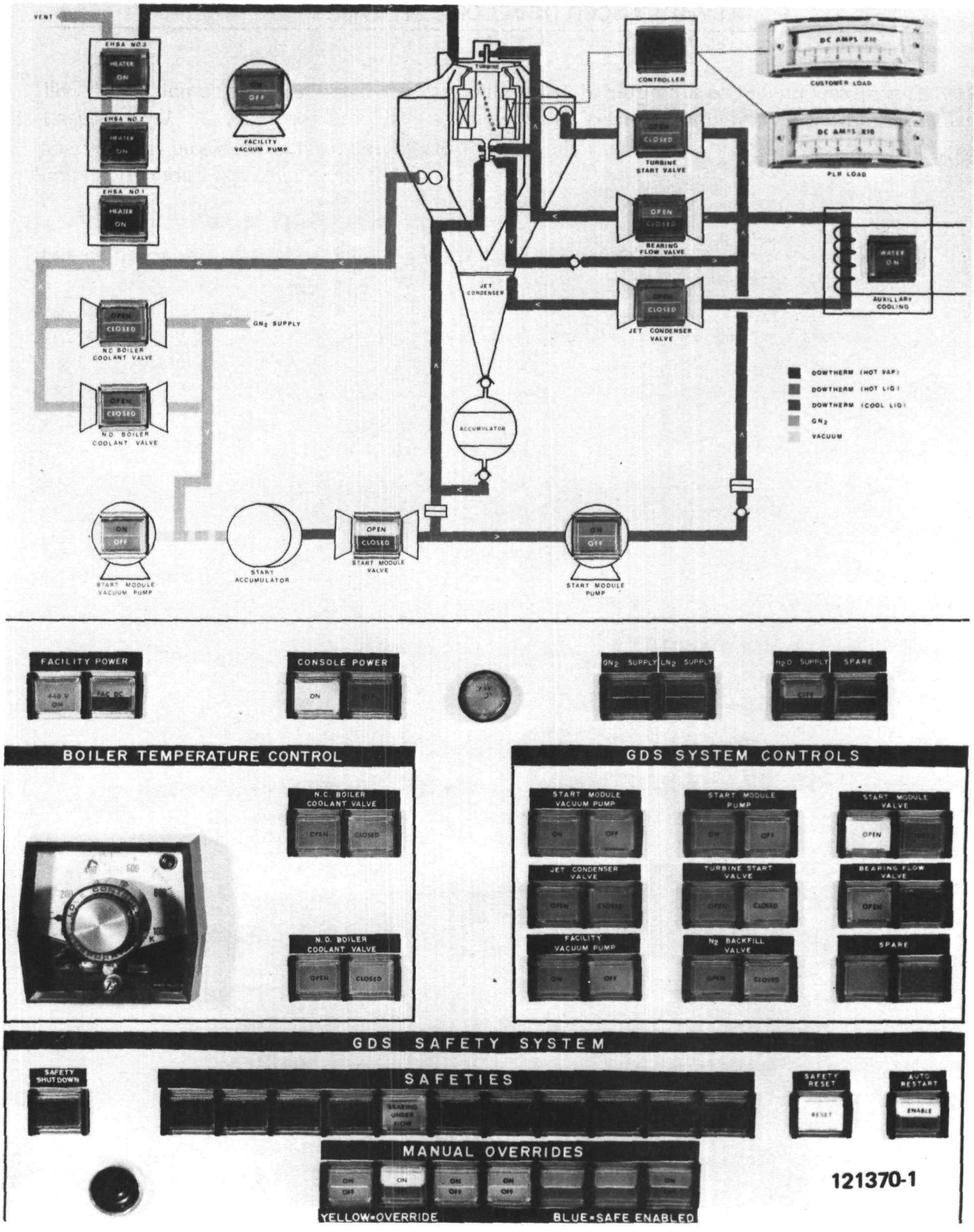

Figure 2.7-3 Master Control Panel

2.8 ADVANCED DEVELOPMENT TASKS

NOTE: This subsection will be submitted after the GDS and associated testing is completed. It will delineate the advanced development tasks which will be proposed for Phase II. While several specific tasks are recognized at this time, completion of the Phase I testing is required to determine all of the definitive efforts to be undertaken. These will include reliability, fabrication, and performance.

The tasks, together with the potential performers, known at this time that will be specified and proposed for the Phase II effort, are:

- Flow Control Valve (FCV) tests to assure demonstrated reliability of the valve assembly components. The thermal sensor is the critical component of the FCV and accelerated life tests and determination of failure modes will be proposed (Sandia/Sundstrand)
- Continuation and expansion of the working fluid tests currently being performed (Batelle)
- Evaluation of the boiler emissivity coating (Solar)
- Inspection (example: eddy current inspection of bellows welds) and welding techniques development and support (ORNL/Sandia/Sundstrand)
- Jet condenser single nozzle Dowtherm performance evaluation to complement the Phase I steam testing (Sundstrand)
- Alternate outgassing tests (Battelle)
- CRU testing to define parasitic losses and determine areas for performance improvement
- Component evaluation and sizing such as determination of effective conductivity of multifoil insulation and sizing of the system pump

The finalization and defining of the Phase II advanced development tasks will be submitted as GDS testing and further analysis dictates their need.

FSCD LAYOUT DRAWINGS

Five KIPS Flight System Conceptual Design Layout drawings, Numbers EP 2605-6101, 6201, 6301, 6401, and 6501, are included in reduced size on the following pages. Full size layouts have also been furnished separately.

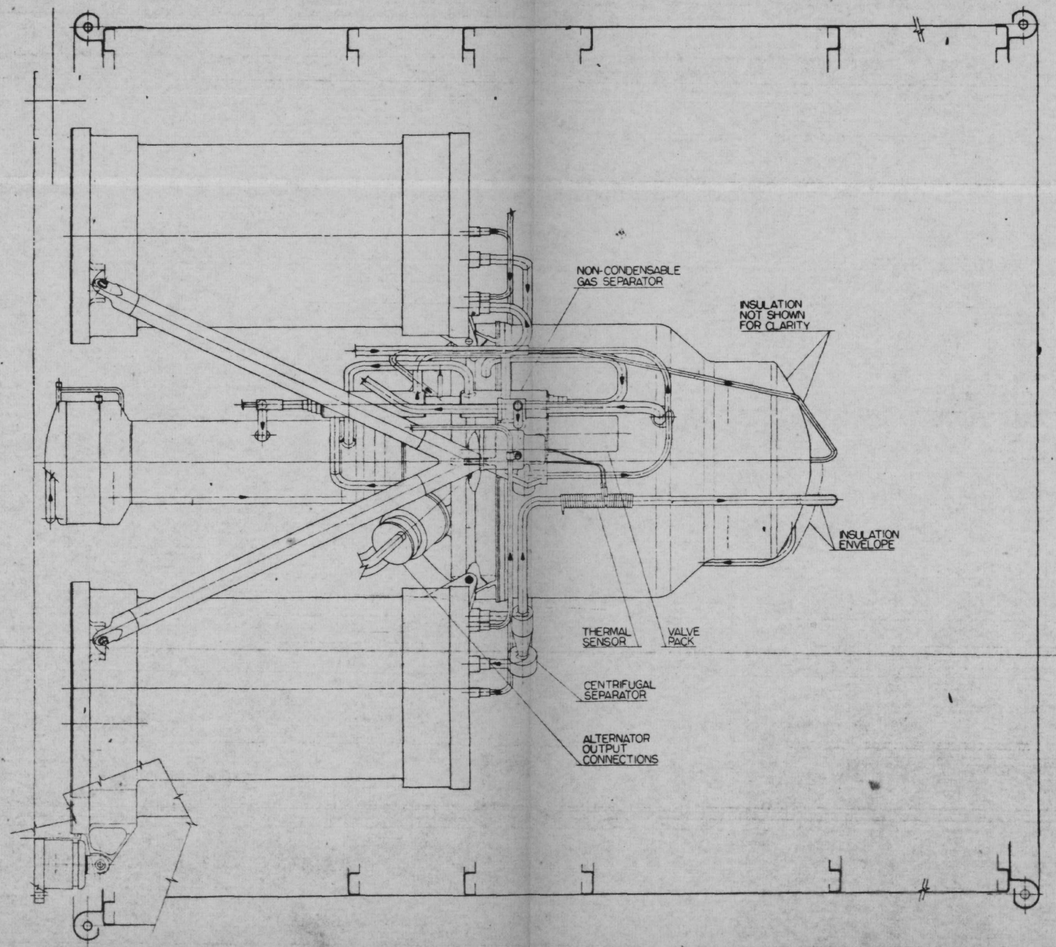

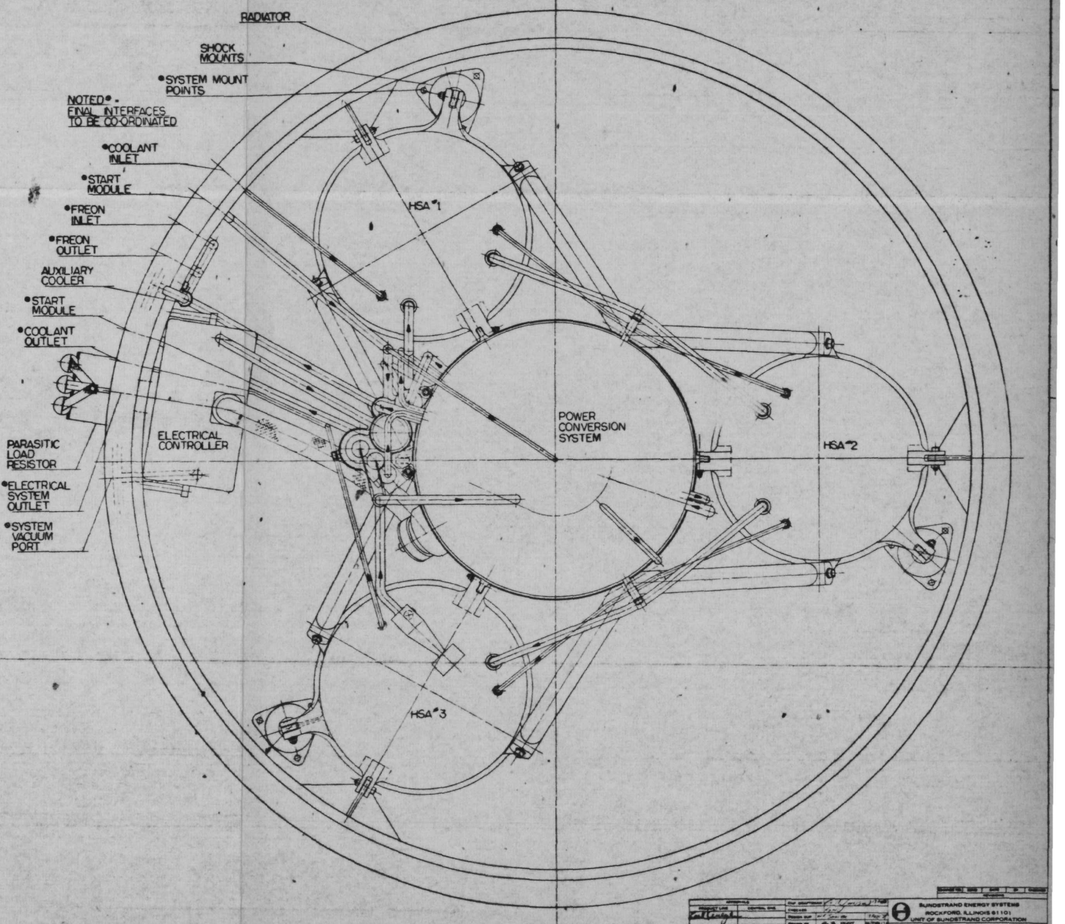

BUDD/STRAND ENERGY SYSTEMS
ROCKFORD, ILLINOIS 61101
A UNIT OF BUDD/STRAND CORPORATION

TITLE
LAYOUT, SYSTEM - KIPS
FLIGHT CONCEPTUAL DESIGN

SCALE HALF | SHEET 1 OF 1
WEIGHT LB
MATERIAL NO. 2605
KIPS

PART NO. 54664 | DRAWING NO. EP 2605-6101

REQUEST PER NO. 10175

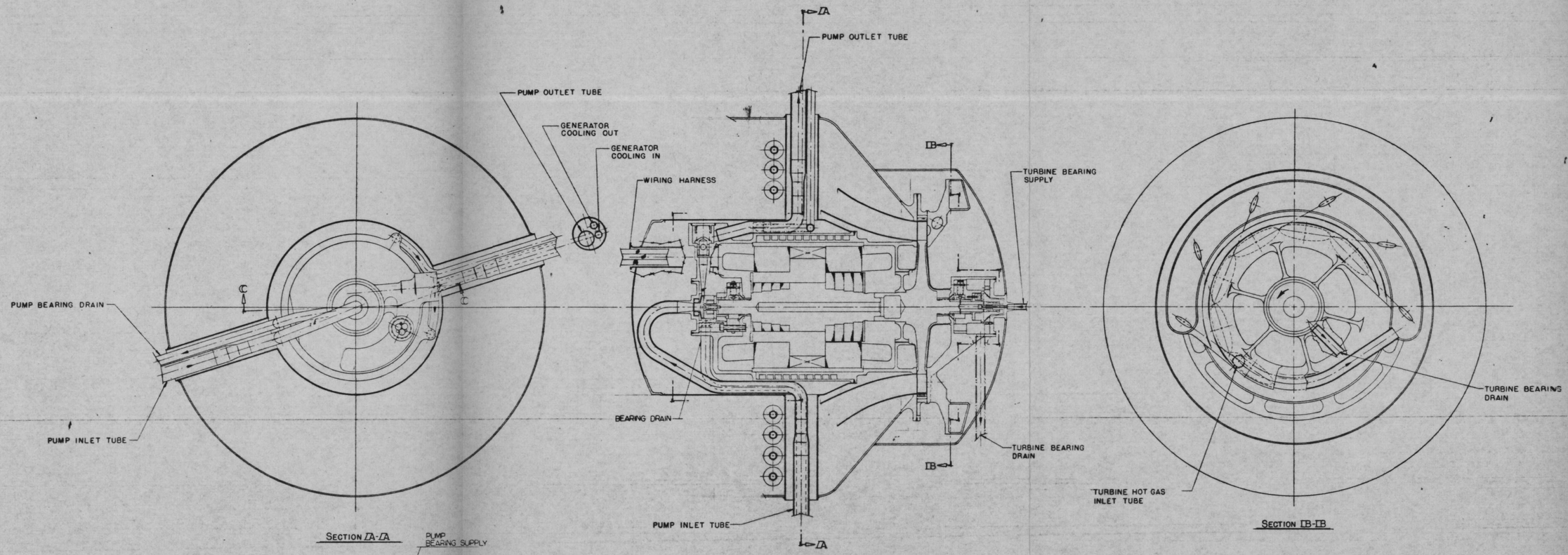

	BARBER-COLMAN COMPANY ROCKFORD, ILLINOIS 61101	
	TITLE LAYOUT— COMBINED ROTATING UNIT KIPS FLIGHT CONCEPTUAL DESIGN	
	SCALE FULL	SHEET 1 OF 1
	WEIGHT LB	
	KIPS	FSCM NO 54664 DRAWING NO EP2605-6201
		REQUEST DER NO 10179

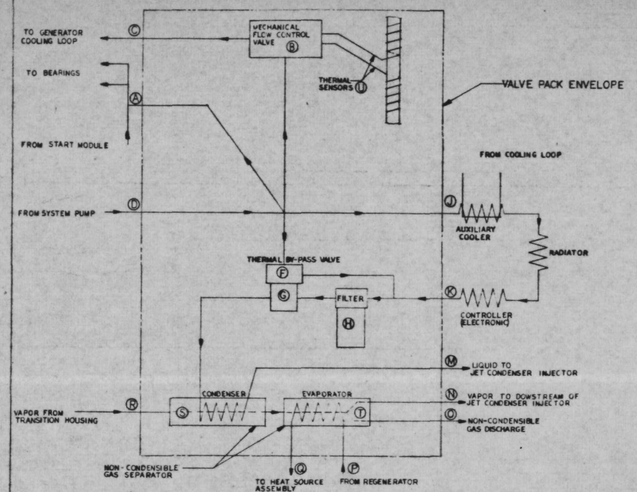

VALVE PACK SCHEMATIC

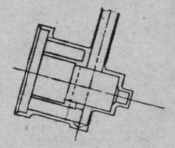

SECTION F-F

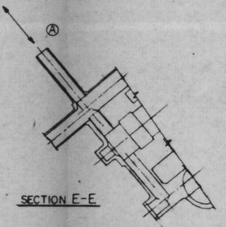

SECTION E-E

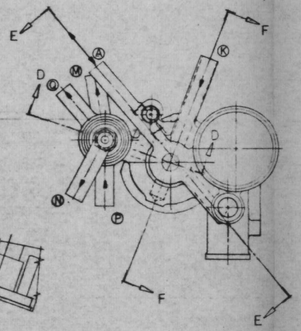

SECTION D-D

SECTION A-A

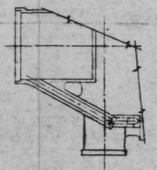

SECTION C-C

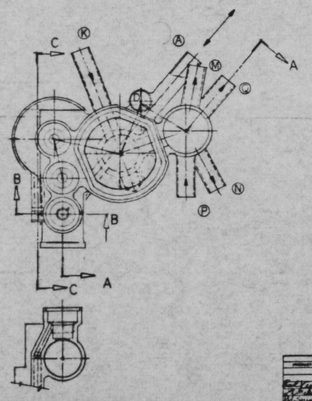

SECTION B-B

EP2605-6301

			SUNDSTRAND ENERGY SYSTEMS ROCKFORD, ILLINOIS 61101 A UNIT OF SUNDSTRAND CORPORATION	
		SCALE FULL	TITLE LAYOUT VALVE PACK KIPS FLIGHT CONCEPTUAL DESIGN	
		APPLICATION KIPS	CAGE NO. 54664	DRAWING NO. EP2605-6301

REQUEST REV NO. 1179

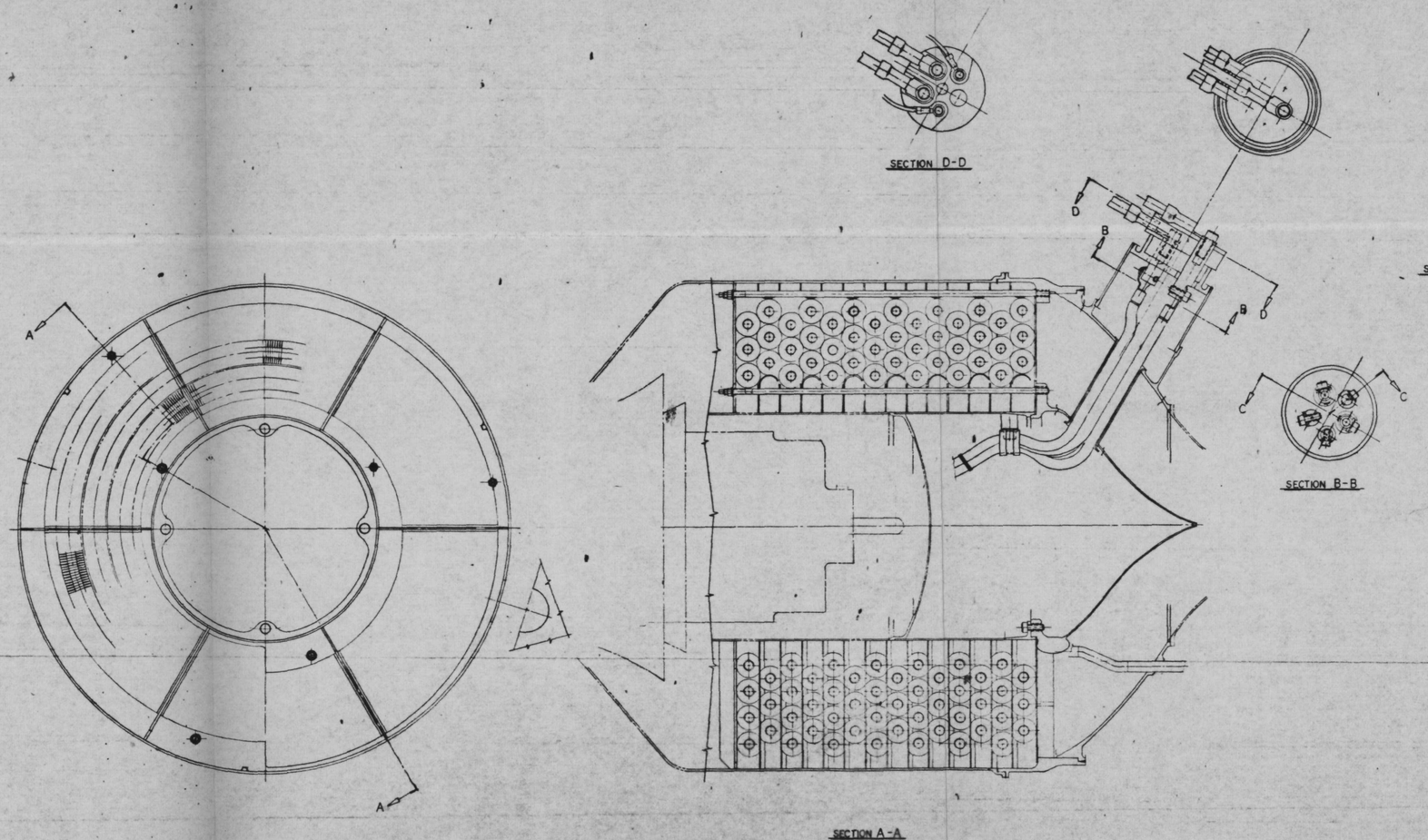

EP2605-6401

		BUNDSTRAND ENERGY SYSTEMS ROCKFORD, ILLINOIS 61101 UNIT OF BUNDSTRAND CORPORATION	
		TITLE LAYOUT, POWER-CONVERSION SYSTEM-KIPS-FLIGHT CONCEPTUAL DESIGN	
		SCALE FULL	
		KIPS	FSCM NO 54664
			DRAWING NO EP2605-6401

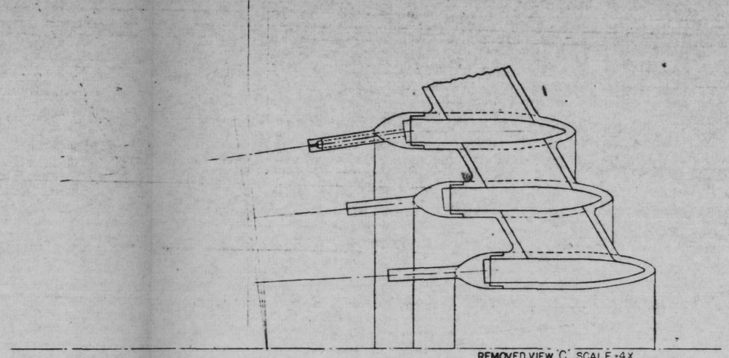

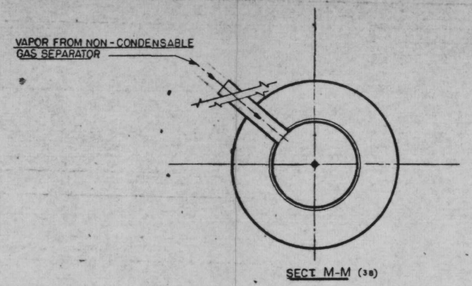

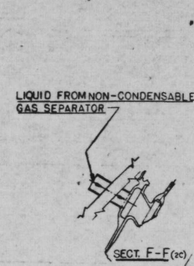

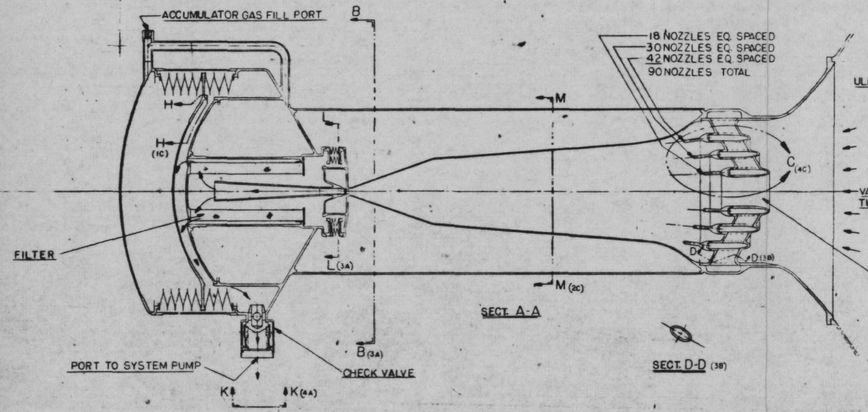

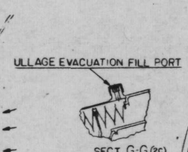

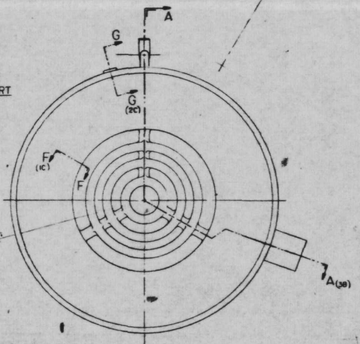

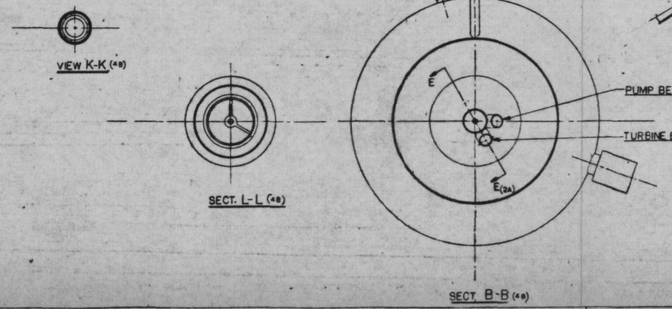

EP2605-6501

		SUNDSTRAND ENERGY SYSTEMS ROCKFORD, ILLINOIS 61101 UNIT OF SUNDSTRAND CORPORATION	
		TITLE LAYOUT - KIPS (EP-CONDENSER / ACCUM - FLIGHT	
		SCALE	
		WEIGHT LB	
	KIPS	PACK NO. 54664	DRAWING NO. EP2605-6501
		REQUEST SER NO.	